UNIVERSITÀ
DEGLI STUDI
DI PADOVA

Head Office: Università degli Studi di Padova

Padova Neuroscience Center

Ph.D. COURSE IN NEUROSCIENCE

XXXVI SERIES

Waves of Control:
Surfing Behavioral and EEG Uni/Multivariate Signatures to Map Proactive and Reactive Control

Coordinator: Prof. Antonino Vallesi

Supervisor: Prof. Ettore Ambrosini

Co-Supervisor: Prof. Antonino Vallesi; Prof. Livio Finos

Ph.D. student : Giada Viviani

Publications

Chapter 2 reports the work from the following publication, under License CC BY 4.0:

Viviani, G., Visalli, A., Montefinese, M., Vallesi, A., & Ambrosini, E. (2023). The Stroop legacy: A cautionary tale on methodological issues and a proposed spatial solution. *Behavior Research Methods*, 1-28. https://doi.org/10.3758/s13428-023-02215-0

Chapter 3 reports the work from the following publication, under License CC BY 4.0:

Viviani, G., Visalli, A., Finos, L., Vallesi, A., & Ambrosini, E. (2023). A comparison between different variants of the spatial Stroop task: The influence of analytic flexibility on Stroop effect estimates and reliability. *Behavior Research Methods*, 1-18. https://doi.org/10.3758/s13428-023-02091-8

Abstract

The overarching aim of this thesis was to explore cognitive control, a multifaceted construct. As outlined in the introduction (Chapter 1), this pursuit was not devoid of challenges, given the inherent complexity of cognitive control. Our research was guided by the Dual Mechanisms of Control (DMC) model, which highlights qualitative differences in control mechanisms rather than treating control as a single entity. Within this framework, we explored proactive and reactive control, for which evidence is still controversial about both their separability and signatures. To achieve this aim, we first laid the foundation of our work, emphasizing the importance of methodological (and statistical) rigor to effectively investigate cognitive control using the influential and widely used Stroop task. This not only marked the inception and fundamental tool for pursuing our goal but also emerged as a key aspect of the entire thesis, potentially extending its contribution beyond its main aim.

We indeed started our research journey by performing a methodological review focused on the measurement validity of the Stroop effects, providing researchers using this conflict task with clear methodological criteria (Chapter 2). This served us to design spatial Stroop tasks satisfying the criteria for yielding valid measures of Stroop performance, which were tested and validated in a behavioral study using multilevel modeling to obtain more precise and reliable Stroop measures (Chapter 3).

These methodological and statistical novelties, in turn, formed the foundation for our exploration of proactive and reactive control using a multimethod approach, combining behavioral and electrophysiological (EEG) investigations and then trying to bridge behavioral and EEG evidence.

We thus proposed a novel approach to manipulate the proxies of proactive and reactive control (LWPC and ISPC) simultaneously and at the trial level. The results of a two-experiment behavioral study suggested that our approach was indeed effective to explore more directly the DMC assumptions, overcoming limitations of previous approaches (Chapter 4).

We then turned to the EEG evidence for proactive and reactive control, using multiple complementary analytical approaches to scrutinize them from various angles, yielding a richer perspective on their neural dynamics. Using both univariate and multivariate analyses, we could indeed gain insights into both control processes and representations, respectively. Moreover, within each analytical approach we employed more than one analysis. As such, on the univariate side, we explored not only the temporal (ERP) but also the spectral (ERSP) aspects of control processes, enriching the understanding of how control processes are implemented (Chapter 5). On the multivariate side, our bidirectional exploration using both representational similarity analysis and ridge regression offered insights into how control-related

representations are encoded and whether their content can be decoded, respectively, shedding initial light on the informational patterns on which cognitive control relies (Chapter 6).

Finally, we concluded this thesis by returning to its origin, with two pre-registered behavioral experiments aimed to decompose the Stroop effect into its fundamental components (Chapter 7), which are only the first step of the next stage of our research journey.

The present thesis thus contributed to shedding further light on the existence of multiple control mechanisms, providing evidence for behavioral and EEG differences between proactive and (two forms of) reactive control. Nonetheless, the discussion of our findings (Chapter 8) unmistakably confirms the intricacies inherent in cognitive control, unveiling unresolved issues that warrant future studies and opening the door to numerous exciting avenues for further exploration.

Abstract in italiano

L'obiettivo principale di questa tesi era esplorare il controllo cognitivo, un tratto distintivo della cognizione umana. Come descritto nell'introduzione (Capitolo 1), questa ricerca non è stata priva di sfide, data l'intrinseca complessità di questo costrutto. La nostra investigazione è stata guidata dal modello del Meccanismo Duale di Controllo (DMC), che evidenzia le differenze qualitative nei meccanismi di controllo anziché trattare il controllo come un'entità unica. All'interno di questo quadro teorico, abbiamo esplorato il controllo proattivo e reattivo, poiché le evidenze sulla loro separabilità e le loro caratteristiche distintive rimangono ancora controverse. Per raggiungere il nostro obiettivo, abbiamo dapprima gettato le basi del nostro lavoro, sottolineando l'importanza del rigore metodologico (e statistico) per investigare efficacemente il controllo cognitivo usando il noto e ampiamente utilizzato compito di Stroop. Questo non solo ha segnato il punto di partenza e lo strumento fondamentale per i nostri scopi, ma è emerso come un aspetto chiave dell'intera tesi, potenzialmente estendendo il suo contributo oltre il suo obiettivo principale.

Abbiamo infatti iniziato il nostro percorso di ricerca eseguendo una revisione metodologica incentrata sulla validità di misurazione degli effetti Stroop, fornendo ai ricercatori che utilizzano questo compito di conflitto chiari criteri metodologici (Capitolo 2). Questo ci ha permesso di progettare compiti di Stroop spaziale che soddisfacevano i criteri per ottenere misure di prestazione valide, i quali sono poi stati testati e validati in uno studio comportamentale utilizzando tecniche di multilevel modeling per ottenere misure più precise e affidabili degli effetti Stroop (Capitolo 3).

Queste innovazioni metodologiche e statistiche hanno costituito la base per la nostra esplorazione del controllo proattivo e reattivo attraverso un approccio multimetodo, combinando studi comportamentali ed elettrofisiologici (EEG) e cercando poi di collegare le evidenze fornite da questi. Abbiamo quindi proposto un nuovo approccio per manipolare simultaneamente e a livello di trial le misure proxy del controllo proattivo e reattivo (LWPC e ISPC). I risultati di uno studio comportamentale multi-esperimento hanno suggerito che il nostro approccio era efficace per esplorare in modo più diretto le assunzioni del DMC, superando le limitazioni degli approcci precedenti (Capitolo 4).

Successivamente, ci siamo concentrati sulle evidenze EEG per il controllo proattivo e reattivo, utilizzando molteplici approcci analitici complementari per esaminarli da varie prospettive, ottenendo così una visuale più ricca sulla loro dinamica neurale. Utilizzando sia analisi univariate che multivariate, abbiamo potuto ottenere insight sia sui processi cognitivi, sia sulle rappresentazioni neurali di controllo, rispettivamente. Inoltre, all'interno di ciascun approccio analitico abbiamo utilizzato più di un tipo di analisi. Quindi, sul lato univariato, abbiamo esplorato non solo gli aspetti temporali (ERP) ma anche quelli spettrali (ERSP) dei processi di controllo, arricchendo la comprensione di come questi sono implementati (Capitolo 5). Sul lato

multivariato, la nostra esplorazione bidirezionale utilizzando sia la Representational Similarity Analysis che la regressione ridge ha offerto insight su come le rappresentazioni legate al controllo sono codificate nel cervello e se il loro contenuto può essere decodificato, iniziando così a chiarire i modelli informativi su cui si basa il controllo cognitivo (Capitolo 6).

Infine, abbiamo concluso questa tesi tornando alle sue origini, con due esperimenti comportamentali pre-registrati mirati a decomporre l'effetto Stroop nelle sue componenti fondamentali (Capitolo 7), che rappresentano solo il primo passo della prossima fase del nostro percorso di ricerca.

La presente tesi ha contribuito a gettare ulteriore luce sull'esistenza di molteplici meccanismi di controllo, fornendo evidenze per le differenze comportamentali ed EEG tra il controllo proattivo e (due forme di) controllo reattivo. Tuttavia, la discussione dei nostri risultati (Capitolo 8) conferma inequivocabilmente l’intrinseca complessità del controllo cognitivo, svelando questioni irrisolte che richiedono ulteriori approfondimenti e aprendo la porta a numerose affascinanti strade per ulteriori esplorazioni.

Table of contents

CHAPTER 1

General Introduction:

Project Rationale and Overview

1.1. Object of study of the current project

Cognitive control, a defining hallmark of human cognition, stands as a foundational element of adaptive and goal-directed behavior that allows us to flexibly pursue specific goals (Chiew & Braver, 2017; Cohen, 2017). This multifaceted construct encompasses a family of cognitive processes required to flexibly regulate, coordinate, and sequence our thoughts and actions in tandem with contextual demands and internal goals (Braver, 2012; Chiew & Braver, 2017). It becomes fundamental when automatic responses are not appropriate and thus give way to more flexible and complex behaviors driven by internal states and intentions (Miller & Cohen, 2001).

To comprehend the significance of cognitive control in daily life, envision a scenario, illustrated in Figure 1.1: you are behind the wheel, approaching a fork in the road. Your destination is Rome, and the road sign indicating Rome is positioned above the right-hand lane. Instinctively, you begin steering towards the right, driven by your automatic response to the visual cue. However, your attention is soon drawn to the arrow on the sign, which contradicts your automatic tendency by pointing towards the left. In this instant, you find yourself trying to resolve the interference generated by these conflicting pieces of information. Should you successfully navigate past this cognitive challenge and avoid taking the incorrect route, it serves as evidence of your brain's effective execution of cognitive control.

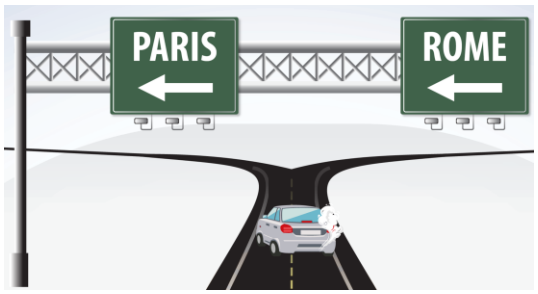

Figure 1.1.
Example of a real-life situation requiring cognitive control.

In everyday life, we continuously face similar kinds of interference, as we are constantly surrounded by an abundance of sensory stimuli and potential actions from which we have to select only the ones pertinent

to our objective in that particular moment (Gratton et al., 2018; Jiang et al., 2014; Nee et al., 2007). This is where cognitive control comes into play, and particularly its central component of interference resolution, enabling the selection of weaker but task-relevant information amidst more habitual but task-irrelevant competing information (Miller & Cohen, 2001; Nee et al., 2007; Tafuro et al., 2019).

At its core, cognitive control orchestrates the maintenance and updating of current goal representations to bias cognitive processes towards goal-relevant stimuli, processes, and actions while adapting to the changes of objectives and context (Botvinick et al., 2001; Chiew & Braver, 2017; Cohen, 2017; Diamond, 2013; Miller & Cohen, 2001). Indeed, as cognitive control molds behavior toward specific aims, a symphony of internal representations, containing multiple information, like the goals and the stimulus/response features, comes into play to influence individuals' perceptual, motor, and cognitive processes. Therefore, for successfully executing demanding tasks, cognitive control relies on such internal representations, which are encoded at the neural level (Cellier et al., 2022; D'Esposito, 2007; Kriegeskorte & Diedrichsen, 2019; Schumacher & Hazeltine, 2016). Given their pivotal role, representations form the bedrock upon which cognitive control theories are built. As such, as we will discuss profusely later, exploring such representations is necessary for bridging the cognitive and the neural domains to comprehensively understand cognitive control dynamics at the neural level (Freund et al., 2021; Kriegeskorte & Diedrichsen, 2019).

The ensuing chapters of this thesis undertake a comprehensive exploration of cognitive control, first delving into its behavioral signatures and then turning to its neural dynamics. This will be accomplished by adopting a specific theoretical framework, namely the dual-mechanism of control model (DMC; Braver, 2012; Braver et al., 2007). The field of cognitive control theories exhibits considerable heterogeneity, and this diversity leads to the interpretation of both behavioral signatures and the functional meanings of neural signatures of cognitive control strongly depending on the adopted framework. Hence, our selection of the theoretical framework, which was fundamental to ensure consistency throughout this work, was based on its capacity to be as comprehensive as possible and to facilitate the explanation of the phenomena commonly observed within the realm of experimental paradigms investigating cognitive control. Hence, we chose not to adopt the conflict monitoring model (Botvinick et al., 2001), the most influential network in cognitive control research; Indeed, despite its widespread recognition, it essentially conceptualizes cognitive control as a reactive adjustment enacted subsequent to conflict detection. In contrast to this account, the DMC, apart from being an equally influential model, holds the advantage of elucidating the intrinsic variability of cognitive control, regarding it as a core component rather than as an impediment to the understanding of its functioning. To capture such variability, the DMC accounts for the diverse temporal dynamics of cognitive control, that is, not only for reactive adjustments but also for proactive control implementations. The DMC indeed posits the existence of two qualitatively distinct cognitive control

modes: proactive control and reactive control. The former mode actively maintains task goals to bias cognitive processes in a goal-driven manner. By acting as a preparatory mechanism engaged in a sustained fashion even before encountering cognitively demanding events, it anticipates and reduces interference thanks to top-down attentional biases that favor the processing of the task-relevant information. In its most common definition, reactive control is instead mobilized transiently and on-demand, after detecting conflict, to resolve interference through a "late correction" mechanism relying on the bottom-up reactivation of task goals (see Figure 1.2). The DMC also implies (at least implicitly) a trade-off between proactive and reactive control modes, with the latter that is more essential when the former is not active (e.g., Braver et al., 2009, 2021; De Pisapia & Braver, 2006) but, to the best of our knowledge, clear evidence for this trade-off is still lacking.

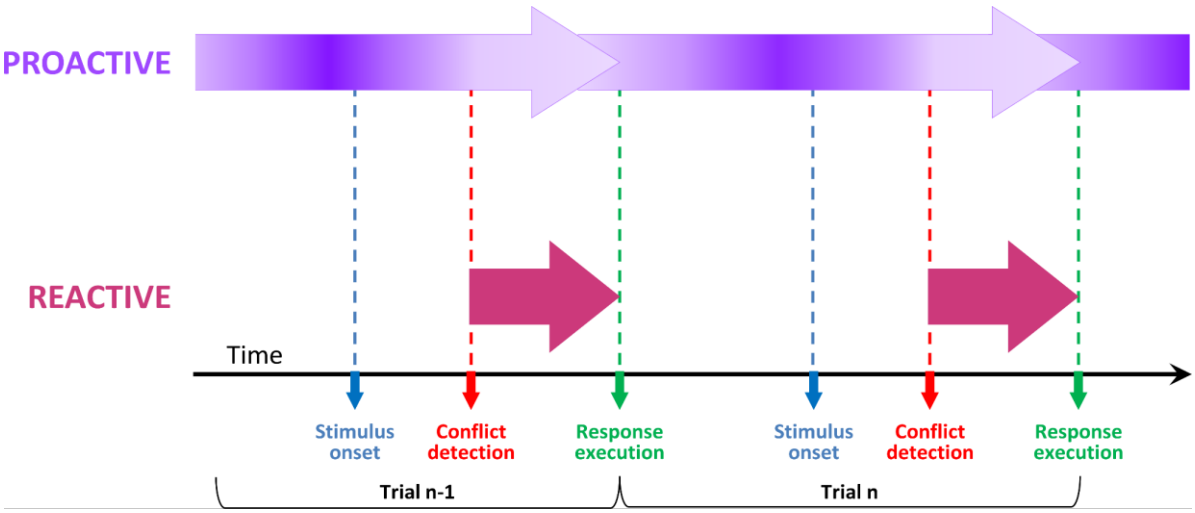

Figure 1.2.
Temporal dynamics of the involvement of proactive and reactive control modes in an exemplar task according to the DMC. The figure shows two trials of a hypothetical simple conflict task. The relative level of proactive engagement is reflected by the saturation of the lilac, while the reactive control, in fuchsia, does not show saturation nuances as it is postulated to be an all-or-none mechanism.

The DMC thus extends the single mechanism proposed by the conflict monitoring model and, assuming that cognitive control is characterized by two mechanisms, it more effectively maximizes information processing efficiency across a broad spectrum of scenarios (Braver, 2012). Moreover, by enabling the explanation of distinct time scales for control effects, it offers richer insights into two types of cognitive control adjustments that are frequently found in the context of cognitive control experimental tasks, namely conflict adaptation (CA) and proportion congruency (PC) effects. They reflect a short-term and reactive, and a long-term and proactive form of control regulation, respectively. In order to comprehend these two effects, it is essential to preface that tasks tapping cognitive control often manipulate the congruency between two features of the same stimulus, obtaining congruent stimuli when such features match, and incongruent stimuli when they do not. This congruency manipulation can then engender the conflict

adaptation effect, which is a diminished congruency effect in the current trial when following an incongruent trial, as opposed to a congruent one (Gratton et al., 1992), and/or the PC effect, which reflects fluctuations in the size of the congruency effect based on the varying likelihood of congruent trials within a given task block (Logan & Zbrodoff, 1979). Empirical evidence supports the DMC by emphasizing the necessity for multiple control mechanisms to comprehensively account for these two effects and their differences in terms of time scales (Torres-Quesada et al., 2013).

In addition to serving as a clear and efficient framework, the DMC offers an additional practical advantage as it inspired a large body of work that has employed specific manipulations to differentiate between the proactive and reactive control modes. These manipulations primarily focus on the variation of the PC at the list-wide (LWPC) and/or the item-specific (ISPC) levels, which will be expounded upon in subsequent sections. In brief, they embody the operationalization of the proactive and reactive control mechanisms, respectively, and are widely acknowledged within the literature (e.g., Bugg, 2012; Bugg & Crump, 2012).

With these foundations laid, the aim of the present project is to explore the DMC in a comprehensive manner, first investigating whether proactive and reactive control are characterized by specific signatures at the behavioral level and then focusing on their brain correlates by exploring them using an electroencephalographic multimethod approach, as we will explain in detail later. The rationale behind the necessity of inspecting both the behavioral and neural correlates of proactive and reactive control is that the available evidence in favor of the DMC, both in terms of behavioral manifestations and neural underpinnings, is not so strong and compelling, thus calling for further research efforts. As such, the still unanswered questions that will be mainly addressed in the present work will be: i) whether proactive and reactive control are separable mechanisms; ii) whether these two modes imply specific neural correlates, defining them in relation to both cognitive processes and representations.

In the following sections, how this aim is pursued will be clarified, elaborating on the rationale behind each step of the project. Hence, this introductory chapter will provide a general overview of the fundamental aspects of the project, deferring to the specific chapters that contain more elaborate theoretical discussions and the methodological details of each study.

1.2. How to study cognitive control: The Stroop task

To study cognitive control in the laboratory setting, interference tasks are commonly employed as they directly assess the resolution of interference arising by simultaneously presenting a weaker, task-relevant feature and a stronger yet task-irrelevant feature (Bugg & Crump, 2012; Gratton et al., 2018; Jiang et al., 2014). Among these, one of the most influential and widely employed is the Stroop task (Stroop, 1935). Its

original version is known as the color-word Stroop task and implies presenting words denoting a color printed in either the same or a different ink color and instructing participants to name the ink color of the word regardless of its meaning. The congruency between the ink color in which the word is displayed and the meaning of the same word is manipulated so to obtain congruent trials, in which the ink color and the meaning of the word match (e.g., GREEN displayed in green ink), and incongruent trials, in which the two features do not match (e.g., GREEN displayed in yellow ink). The typical behavioral measure is the so-called Stroop effect (SE), usually computed as the difference in the response time (RT) between incongruent and congruent trials (formally, SE = $RT_{Incongruent}$ - $RT_{Congruent}$), and characterized by a performance decline in incongruent as compared to congruent trials because interference must be resolved (MacLeod, 1991; Stroop, 1935) (see Figure 1.3).

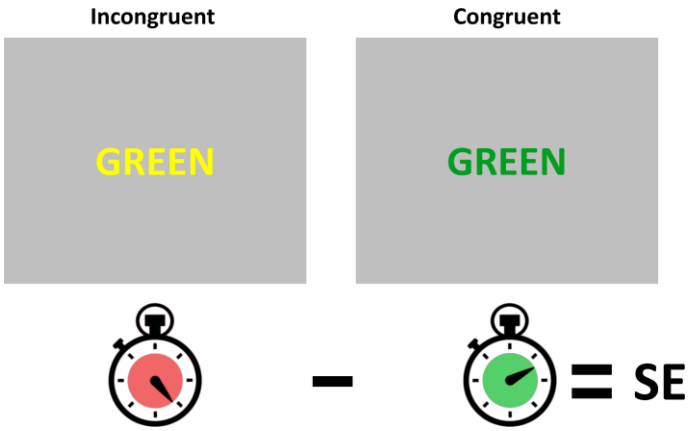

Figure 1.3.
Example of Incongruent and Congruent trials in the color-word Stroop task. The difference in performance (e.g., RT in the example) between them is the Stroop effect (SE).

Our selection of the Stroop task as the experimental paradigm is based on its long-standing history of nearly a century in assessing interference resolution. As such, this task, besides yielding an universal effect (Parsons, 2020), boasts an extensive body of literature, rendering it well-established for our purpose. Furthermore, the Stroop task accommodates the implementation of the previously alluded to PC manipulations, which satisfy our aim of exploring proactive and reactive control modes (but see the subsequent section for an elaborate discussion).

Despite these well-established advantages, prior to designing our Stroop paradigm, we had to decide which version to utilize because, since the original Stroop color-word task by the eponymous J. R. Stroop (1935), numerous variants of it have been devised. The fundamental prerequisite we considered in selecting our paradigm was the measurement validity of the yielded Stroop effect, that is, the extent to which such measure actually represents the variable it intends to measure, namely the Stroop performance decline due to interference (Flake & Fried, 2020). Indeed, although measurement validity should always be ensured as it

is the foundational prerequisite for any type of validity, including the validity of the statistical conclusions derived from experimental measurements, it is frequently overlooked (Flake & Fried, 2020).

Given the considerable heterogeneity of Stroop tasks in the literature and the absence of studies specifically ascertaining the validity of the measures obtained with each variant, we embarked on a methodological review of the literature. In this review, we initially outlined clear guidelines on how to design Stroop tasks ensuring measurement validity and subsequently examined whether original Stroop tasks and their main variants in the literature adhered to these criteria. The methodological criteria we employed to assess measurement validity relied on two seminal works that underscored the composite nature of the Stroop effect, that is, Parris and colleagues' work (2022), proposing that the Stroop effect emerges at distinct loci—stimulus, response, and task, where the first two entail both interference and facilitation and the latter involves only interference—, and Kornblum's (1992) work, showing that stimulus-stimulus and stimulus-response overlaps should be present to ensure the stimulus and response effects, respectively. As these constituent elements are originally inherent in the original Stroop task, they must be encompassed in any Stroop task (including variants), as it is the only means to ensure accurate comparisons of the evidence produced by individual studies. We then asserted whether the Stroop tasks in the literature fulfill such criteria, reaching the conclusion that the majority of Stroop task variants do not (but some color-word Stroop tasks were also not methodologically appropriate), as they did not comprehensively produce all the three required loci-related effects.

However, our methodological review was not solely intended to critically evaluate the existing literature. Indeed, with a constructive approach, we also suggested that an alternative version of the Stroop task already employed in the literature, namely the spatial Stroop task, has the potential to generate complete and methodologically valid Stroop effects. Moreover, we highlighted that, besides being methodologically similar, the spatial Stroop version offers some advantages over the classical color-word Stroop task. Such advantages, which stem from the inherent complexity and susceptibility to confounding effects typically associated with the classical Stroop paradigm, largely due to its linguistic nature, make the spatial Stroop paradigm more suitable for implementation in both online studies and neuroimaging research. This, in addition to ensuring methodological validity, significantly influenced our decision to adopt the spatial Stroop paradigm for the current project as our objective encompassed online behavioral studies as well as subsequent EEG studies. In the second part of the review, we thus overviewed the main spatial Stroop tasks used in the literature, showing that they did not always ensure a complete Stroop effect, highlighting that only purely spatial tasks were ideal spatial Stroop paradigms.

Overall, this methodological review, presented in its entirety in Chapter 2, constituted a fundamental starting point for the current project. It not only enabled us to identify the most suitable experimental paradigm for our objectives, but also allowed us to clarify the methodological principles that will recurrently

emerge throughout the entire project. In the final part of the review, we proposed six practical examples of spatial Stroop tasks to show that purely spatial Stroop variants can be created while still adhering to the proposed methodological criteria.

These six versions are the subject of a behavioral study, reported in Chapter 3, in which we first elaborated on the rationale used to create them and then examined which of the proposed spatial Stroop task variants yielded the most robust and reliable Stroop effect, with the ultimate aim of selecting the paradigm to use in our subsequent studies. In this study, we started from our Peripheral spatial Stroop version (Puccioni & Vallesi, 2012a, 2012b, 2012c), in which participants have to indicate the direction of an arrow, while disregarding the peripheral location in which it appears (the four corners of the screen). This version elicits a multiple-loci effect at the task, stimulus and response levels, while mitigating confounds inherent to the traditional color-word Stroop paradigm. However, its potential methodological limitations related to the peripheral presentation of the stimuli (such as large visuospatial attention shifts and a high amount of oculomotor artifacts) prompted us to propose five alternative versions. These tasks, while adhering to the required methodological criteria, could overcome such limitations by presenting the experimental stimuli at the center of the screen. Among these versions, there was the Perifoveal task, which is similar to the Peripheral version but with the arrow location manipulated inside the fixation stimulus in order for the stimulus to appear in perifoveal locations. To achieve this, we employed a partial outline of a square around the fixation cross, thus creating the impression of four small squares, presenting the arrows within one of the four apparent squares. The other four alternative versions were instead inspired by other interference paradigms (see Chapter 3 for a detailed description). In a within-subjects online study, the six spatial Stroop versions were evaluated based on three criteria: i) the magnitude of the effect, assessing which one showed the largest Stroop effect; ii) the robustness of the effect to analytical flexibility, assessing which one yielded the most stable Stroop effect across different analytical approaches; iii) the internal reliability of the effect, assessing which one produced the most reliable Stroop effect. While the latter aspect is often neglected, it holds paramount importance in correlational research, especially in light of the recently proposed reliability paradox, which posits that large effects, such as the Stroop, often exhibit low reliability (Hedge et al., 2018). Our evaluation was undertaken through an innovative approach, which not only employed the conventional general linear model, but also two multilevel modeling statistical techniques, which were crucial for providing a more precise estimation of the Stroop effect by explaining intra-subject, trial-by-trial variability. This comprehensive approach enabled us to assess the robustness of our results to analytic flexibility, thereby ensuring that the selection of the experimental paradigm was substantiated by robust and converging evidence.

Overall, our results indicated that the Peripheral and the Perifoveal spatial Stroop tasks produced the largest and more robust Stroop effects, with the highest and most robust internal reliability. These findings

thus point to the Perifoveal spatial Stroop task as the best one, as it not only has good statistical properties, but also offers methodological advantages over the Peripheral one, which will be crucial especially when the task will be used along with EEG, as it mitigates possible biases due to eye movements and (re)orienting of visuospatial attention. However, since in that study we manipulated only congruency and not the PC, in the subsequent behavioral study, where we explored proactive and reactive control (Chapter 4), we decided to employ both paradigms in order to examine whether the Perifoveal task maintains its advantages over the Peripheral task even with various PC manipulations. Additionally, adopting a multi-task approach enabled us to investigate proactive and reactive control behavioral signatures in a broader and less paradigm-specific manner.

Before moving on to the next section, where we will introduce the rationale behind the PC manipulations to measure proactive and reactive control, as well as the innovative approach we employed to do so, we need to make a specific clarification. In this section, we emphasized the importance of measurement validity, which in the case of the Stroop effect translates to the need for designing tasks that produce a Stroop effect encompassing task, stimulus, and response effects. By doing so, the resulting Stroop effect is composite, implying that in incongruent trials cognitive control is engaged to overcome interference not only at the task level, but also at the stimulus and response levels (Gonthier et al., 2016). Consequently, however, it is not possible to distinguish the weight of the three loci-specific components of the Stroop effect. This matter will be tackled in the final study included in the present thesis (Chapter 7) and introduced below.

1.3. How to tap proactive and reactive control with the Stroop task: PC manipulations

As anticipated in the preceding section, the Stroop task provides a means to distinctively engage proactive and reactive control by manipulating the PC (Bugg, 2017; Bugg & Crump, 2012), which is defined as the frequency, or likelihood, of congruent trials within the task (Gonthier et al., 2016; Logan & Zbrodoff, 1979). This manipulation is grounded on the assumption that the information regarding the likelihood of congruent trials is employed to adjust the level of cognitive control. When a higher degree of cognitive control is engaged, the magnitude of the Stroop effect is reduced, as it inversely reflects the efficacy of interference resolution. As such, when the PC is higher, being the frequency of incongruent trials relatively lower, it implies that cognitive control is less stringent and a large Stroop effect is observed mainly due to the poor performance in incongruent trials. When instead the PC is low, the higher probability of encountering incongruent trials and experiencing interference increases the cognitive control level, consequently improving performance especially in incongruent trials, yielding a smaller Stroop effect (Lindsay & Jacoby, 1994) (see Figure 1.4).

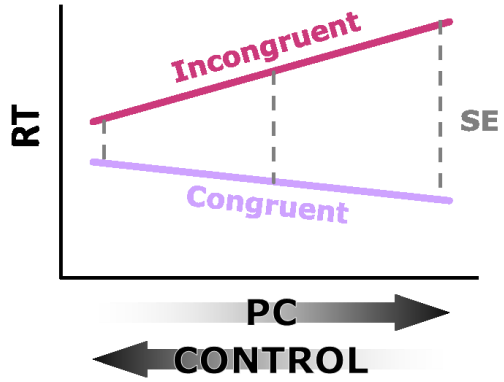

Figure 1.4.
The figure illustrates the PC-dependent modulation of cognitive control that, in turn, modulates the Stroop effect (SE). Of note, as assumed also in the text, PC should affect more Incongruent than Congruent trials, as reflected in the steeper slope for the Incongruent trials.

The differentiation between proactive and reactive control modes can be achieved by varying the PC at two distinct levels, referred to as list-wide (LWPC) and item-specific (ISPC), respectively (Bugg, 2012; Bugg & Crump, 2012) (see Figure 1.5). Despite yielding a comparable overarching pattern, each PC manipulation favors the adoption of one cognitive control mode over the other due to their distinct characteristics (Bugg, 2017). LWPC is postulated to emphasize the engagement of proactive control because, by varying the PC across blocks, individuals can gauge the overall likelihood of encountering congruent trials and then adjust their control level, implementing early preparatory strategies when this is instrumental to optimize performance (e.g., Braver et al., 2007; Bugg, 2017; Lindsay & Jacoby, 1994; Logan & Zbrodoff, 1979). Specifically, in blocks with low LWPC, proactive control is typically maximally engaged (Gonthier et al., 2016). In contrast, ISPC induces a reactive control modulation by varying the PC across a specific feature of the items (usually the task-irrelevant feature) within the same block. This enables individuals to learn the conflict likelihood associated with each item and adapt their control level on an item-by-item basis, but only after seeing the stimulus (Bugg et al., 2011; Bugg & Hutchison, 2013; Jacoby et al., 2003). Therefore, low-ISPC items trigger "stimulus-attention associations" rapidly after stimulus onset (Tafuro et al., 2020), typically engaging the highest degree of reactive control (e.g., Bugg, 2012, 2017; Bugg & Hutchison, 2013).

While LWPC and ISPC manipulations have been extensively employed in the literature, they are not exempt from limitations and criticism. Among the notable examples of criticism, the contingency hypothesis stands out (Schmidt, 2019; Schmidt et al., 2007; Schmidt & Besner, 2008), which posits that the PC effects can be more plausibly explained by contingency learning. This viewpoint proposes that responses can be modulated through implicit learning of contingencies (i.e., the tendency of specific stimuli to co-occur with specific responses), which are subsequently employed to predict and facilitate high-contingency responses. The contingency hypothesis strongly challenges the rationale underlying PC manipulations, as it posits that

performance modulation is primarily driven by simple stimulus-response associative learning processes. This implication suggests that what is elicited by LWPC and ISPC might not truly reflect the cognitive control modulations that we aim to explore. Indeed, the improvement in performance observed in low-PC incongruent trials compared to high-PC ones is explained by the contingency hypothesis without relying on cognitive control mechanisms: the incongruent responses are more frequent in low-PC vs. high-PC blocks/items (see Figure 1.5), so their facilitation can simply reflect stimulus-response association learning.

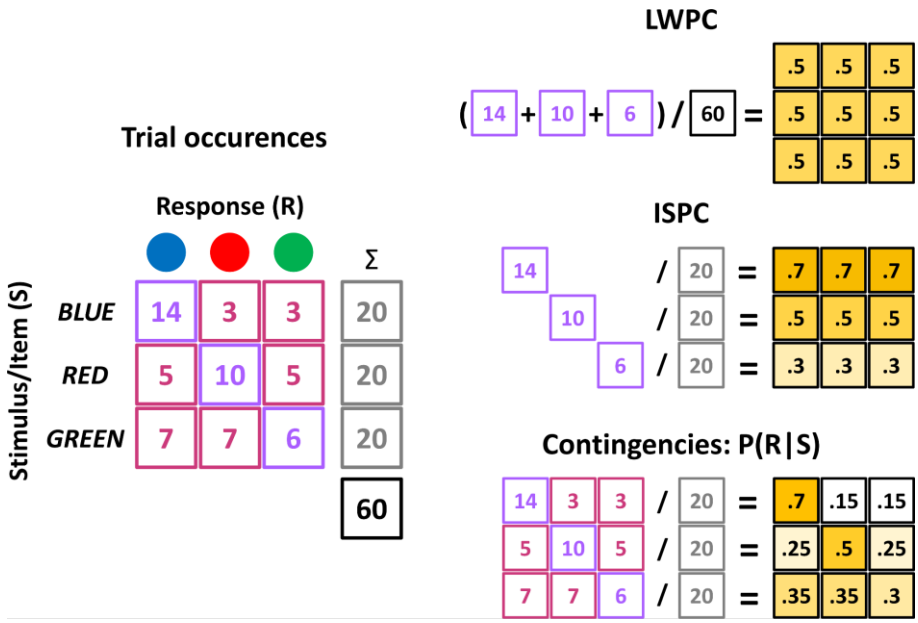

Figure 1.5.
The figure shows on the left an example of a block of trials of a color-word Stroop task involving three irrelevant stimulus features (Items or stimuli, S; here the words BLUE, RED, and GREEN) and three relevant stimulus features (corresponding to the responses, R; here the colors blue, red, and green). The trial occurrences are shown for both congruent (in lilac) and incongruent (in fuchsia) trials. The item-specific total occurrences are shown in gray, while the total number of trials is shown in black. Based on these trial occurrences at the block level, the figure shows how to compute the list-wide PC (LWPC), the item-specific PC (ISPC), and the contingency (or conditional probability of a response given a stimulus, P(R|S) or PRS) for all S-R combinations (the orange saturation level of the cells reflects the magnitude of LWPC, ISPC, and PRS values).

The effects of contingency learning are more likely to be confounded with those of ISPC, thus highlighting the necessity for methodologically sound designs that control for or reduce biases related to contingency. Some solutions have been proposed to address this issue, such as the use of "inducer" items where ISPC is manipulated, but its effect is then tested on a distinct set of items with balanced ISPC (called "diagnostic" items). For a comprehensive review on how to design cognitive control tasks while avoiding confounds, including those regarding LWPC, we refer to Braem and colleagues's work (2019) (summarized in the introduction of Chapter 4). However, the approaches recommended by this consensus paper have been rarely tested and, even more crucially, their implementation is generally inefficient. This inefficiency arises due to the impractical and time-consuming nature of these approaches, such as the need to create both

inducer items (those triggering adaptive control, having extreme PC values) and diagnostic items (those measuring adaptive control effects without confounds) while analyzing only the diagnostic ones. Additionally, some of these approaches may not always be feasible, especially when a limited number of potential items is available, as in classical color-word Stroop tasks, and/or rely on assumptions (e.g., within-category transfer) that might not always be assured.

Due to these limitations, the majority of the proposed solutions, which share the fact that they address confounders at the level of the experimental design (thus referred to as design-level control approaches), are insufficient, particularly if utilized exclusively. The alternative approach that we propose, which involves controlling for confounding effects at the analysis level (thus referred to as analysis-level control), could instead be potentially more efficient and flexible. A more comprehensive discussion regarding the PC manipulations and their constraints can be found in the introduction of the behavioral study (Chapter 4). Here, albeit briefly, we still addressed these topics with the specific intent of elucidating the reasons that prompted us to adopt the novel approach that we employed, for the first time, in that behavioral study. Specifically, this study emerged from the need to address the limited evidence in the literature concerning the actual separability at the behavioral level of the two control mechanisms postulated by the DMC (which derives, at least in part, from the limits of the design-level control approach). Our alternative approach was thus devised to achieve this goal, and we leveraged the behavioral study to validate it.

In brief, our novel approach implied manipulating simultaneously the proxy variables for proactive and reactive control (i.e., the LWPC and ISPC, respectively), but also those related to low-level confounders, including contingency. Moreover, all these variables were manipulated at the trial-level to obtain more fine-grained estimates of their effects. Subsequently, we used multilevel modeling analytical techniques that not only ensured more accurate and reliable estimations of all the effects, but also allowed us to assess them at the same time, that is, to assess their specific weight while controlling for all the other (experimental and confounding) effects.

The first important novelty of our approach thus lies in the simultaneous manipulation of both LWPC and ISPC, thereby affording the benefit of directly evaluating whether proactive and reactive control are indeed separable mechanisms as proposed by the DMC. This separability would gain support if we observe the effects of both modes, implying that each mode exists per se while also the other is engaged. The previous study by Gonthier and colleagues (2016) addressed the same question in a within-subject design but, as they implemented the LWPC and ISPC manipulations in two separate blocks, they provided only indirect evidence for such separability. Thanks to the use of a simultaneous manipulation, we could also test how the interaction between LWPC and ISPC affects Stroop effect resolution, which would offer additional support for their separability, as their interaction would only be possible if they are distinct mechanisms. Moreover, it is important here to note that the DMC assumes the interaction between the two modes of

control (e.g., Braver et al., 2009; Braver et al; 2021), albeit this assumption has been rarely tested empirically in the methodologically appropriate way, that is, by manipulating both control modes simultaneously.

A second difference from all previous studies is that we did not operationalize LWPC and ISPC using their block-level estimates, as they are instead more realistically estimated and updated trial-by-trial by the cognitive system of individuals. For example, the operationalization of the LWPC at the block level (i.e., considering all the trial occurrences of a given block) assumes that LWPC has the same value for all the trials within each block. However, since participants are typically not aware of the PC manipulations, it is much more realistic to assume that participants continuously update their PC estimations based on the history of previous trials. Therefore, to assess such dynamic modulations, we computed trial-by-trial estimates of LWPC and ISPC using an ideal Bayesian observer (Mathys et al., 2011). As such, our fine-grained manipulations allowed us to more accurately account for the dynamic modulations of cognitive control, by taking into account the actual recent history of trial congruency that participants experienced.

The third significant innovation pertains to our utilization of multilevel modeling techniques, a statistical methodology that enabled us to manage variables that were beyond our control at the methodological level. Specifically, in our experimental design we tried to orthogonalized contingency as much as possible with respect to LWPC and ISPC and then, by including also contingency in our statistical model, we obtained the effects of LWPC and ISPC regardless of contingency. Moreover, the use of multilevel modeling techniques played a pivotal role in the simultaneous examination of the effects of proactive and reactive control.

The same approach was adopted employing both the Peripheral and Perifoveal spatial Stroop tasks, in two separate experiments, as detailed in Chapter 4. This study offered compelling evidence for the presence of a LWPC-dependent proactive control mechanism, which modulated the Stroop effect regardless of either contingency or ISPC-dependent reactive control. Furthermore, although explicit evidence for the existence of an ISPC-dependent reactive control effect was not identified, ISPC interacted with LWPC in modulating the Stroop effect, providing evidence for the interplay between proactive and reactive control modes.

In essence, this behavioral study not only provided valuable insights into the distinctive behavioral signatures of proactive and reactive control, but also established the groundwork for the subsequent EEG study. Indeed, we successfully validated the effectiveness of our novel approach which, with a few adjustments (such as employing shorter blocks to enhance PC variability), was then employed in the EEG study. Furthermore, our findings confirmed the methodological advantages of the Perifoveal task over the Peripheral one, enabling us to discontinue the latter in favor of the former.

1.4. Proactive and reactive control processes and representations: how to explore them and their relationship

Over the past decades, extensive research has been dedicated to exploring how cognitive control functions in our brain; nevertheless, numerous inquiries persist regarding the underlying neural mechanisms, and this holds even truer for the neural mechanisms of proactive and reactive control.

Regarding the evidence derived from EEG studies, our understanding of cognitive control neural correlates primarily revolves around event-related potentials (ERPs). Specifically, the N2, N450 and LP ERP components have been commonly reported (Heidlmayr et al., 2020; Larson et al., 2014). However, while ERP components exhibit a certain degree of consistency across studies, the interpretation of their functional significance strongly depends on the adopted theoretical framework, and this has been done mainly within the context of the conflict monitoring model (Botvinick et al., 2001). As a result, conclusive evidence concerning the specific ERP components linked to proactive and reactive control remains lacking. Of note, this is not solely due to the limited number of studies on this matter (for a brief overview of existing studies, see Chapter 5), but also to the highly heterogeneous paradigms and manipulations employed in these few studies, which have rarely systematically integrated the PC manipulations outlined above.

More recently, the spectral information of EEG has also become a subject of interest, leading to investigations of process-dependent changes in spectral power across distinct frequency bands using event-related spectral perturbations (ERSPs). Just as with ERPs, although certain ERSP correlates of cognitive control have been consistently reported (e.g., Cavanagh & Frank, 2014; Engel & Fries, 2010; Gutteling et al., 2022), specific studies investigating cognitive control ERSPs from the DMC perspective are extremely scarce, and even nonexistent when it comes to the utilization of the Stroop task (see Chapter 5 for more details).

Therefore, while fMRI studies have presented evidence for anatomical and functional dissociation between proactive and reactive control (for an overview see Braver, 2012; see also Braver et al., 2021), there is currently not equally compelling evidence for the distinction of these two mechanisms at the electrophysiological level. However, the utilization of EEG holds promise in providing valuable insights, given its potential to offer the required finer temporal resolution to test the predictions of the DMC.

Based on these considerations, the necessity of delving into the EEG correlates of proactive and reactive control becomes evident. Additionally, it is clear that, in EEG studies, there is a requirement for a more systematic use of PC manipulations. This is precisely what we delve into in Chapter 5 and Chapter 6 of this thesis. Specifically, we conducted an EEG study to specifically explore the electrophysiological correlates of proactive and reactive control, assessing whether they are distinguishable at the neural level, and we did this by employing the same novel approach that had been validated in the preceding behavioral study

(Chapter 4). Hence, we leveraged the advantages of our approach to respond to the same research inquiries addressed before, specifically, whether proactive and reactive control mechanisms co-exist and simultaneously influence the Stroop performance, as well as their interplay at the neural level. We introduced only minor modifications to our experimental approach, maximizing the variation of both LWPC and ISPC in order to more effectively explore the corresponding dynamic changes in neural activity. These modifications and the experimental design in general, were planned in advance to ensure that the study would be suitable for both traditional univariate analyses (Chapter 5) and more innovative multivariate analyses (Chapter 6). Indeed, the potential of multivariate approaches is maximized by increasing the variability of the manipulated variables, as we will discuss later on. Lastly, as previously mentioned, we employed the perifoveal spatial Stroop task which, aside from its good statistical attributes, also ensures minimal artifacts during EEG recording.

In Chapter 5, we examined the univariate EEG correlates of proactive and reactive control. Specifically, along with presenting a brief overview of the existing literature and its aforementioned gaps, we utilized two classical univariate analysis approaches: event-related potentials (ERPs) and event-related spectral perturbations (ERSPs). These analyses showed the specific ER(S)P correlates of proactive control, revealing how LWPC manipulation modulated EEG Stroop effects. Furthermore, they contributed to shedding initial light on the modulations of reactive control, revealing that the effect of reactive control induced by ISPC was not so strong and independent, consistent with our behavioral findings. It appeared instead that an alternative form of reactive control was likely engaged when the other control mechanisms failed. In summary, the results presented in Chapter 5 had the merit of demonstrating that proactive control relies on distinct neural mechanisms as compared to (some form of) reactive control, but further investigation was needed to better understand the ISPC-induced reactive control neural mechanism.

Overall, the findings of this study gave rise to the following consideration. It is possible that by using classical univariate approaches, we might be missing something that, although more evident in the case of ISPC-induced reactive control, holds true for cognitive control in general: investigating cognitive control processes alone might not be sufficient, and it is essential to explore the underlying neural representations for proactive and reactive control as well.

As previously mentioned, representations constitute the central aspect of cognitive control, as they play a fundamental role in encoding the diverse information necessary for goal-directed behavior (Cellier et al., 2022; D'Esposito, 2007; Kriegeskorte & Diedrichsen, 2019; Schumacher & Hazeltine, 2016). Consequently, cognitive control theories frequently delineate cognitive control in terms of representations, directly describing the information encoded by the activity of neural units (e.g., Badre et al., 2021; Braver, 2012; Cohen et al., 1990; Freund et al., 2021; Kriegeskorte & Diedrichsen, 2019). Representations, to be effectively employed, are encoded at the neural level and, in turn, are assumed to be utilized by downstream cognitive

processes to successfully guide behavior. As such, the representational perspective has the potential of directly linking cognition and brain activity, providing valuable insights into cognitive control dynamics (Diedrichsen & Kriegeskorte, 2017; Kriegeskorte & Diedrichsen, 2019; Kriegeskorte & Kievit, 2013; see also Chapter 6 for a more detailed discussion).

Understanding cognitive control hinges on representations, but they have been largely overlooked and the predictions of cognitive control theories have rarely been tested directly. This gap likely prevents a comprehensive grasp of cognitive control mechanisms (Freund et al., 2021). The analytical methods used in neuroimaging studies, mainly mass-univariate approaches aimed to reveal correlates of cognitive processes, have described brain activity based on few abstract conditions, neglecting the richness of neural signals and providing only process-level measures that are indirect proxies of control representations. This univariate analytical approach allows only assessing the overall level of activation and changes in activity elicited by experimental manipulations, for example by revealing which condition elicits a higher control demand, and this is taken as the hallmark of the underlying process (Cheng et al., 2021). This limits their ability to identify representational content because, by revealing overall activation levels, they lack insight into how information is represented (Freund et al., 2021; Gluth et al., 2012; Kriegeskorte & Diedrichsen, 2019; Popal et al., 2019). Therefore, while such studies offer some empirical contribution, they leave gaps in fully understanding the phenomena under study. Given cognitive control reliance on representations, and given that representations are encoded as distributed patterns of activity in the brain (e.g., Etzel et al., 2020), there is a need for methods sensitive to such complex encoding (Badre et al., 2021). Multivariate approaches, like multivariate pattern analysis (MVPA), are thus crucial to measuring distributed patterns of information, revealing the representational content (Davis et al., 2014; Popal et al., 2019). As a result, researchers are increasingly turning to MVPA to overcome these limitations and have confirmed its advantages in cognitive control studies (see Chapter 6 for a brief overview). However, although previous functional studies have used MVPA to study the neural underpinnings of cognitive control with the Stroop task (Freund et al., 2021), to the best of our knowledge, no existing work has specifically explored proactive and reactive control using the LWPC and ISPC manipulations. Therefore, given their potential, we incorporated multivariate analytical methods to enhance our grasp of proactive and reactive control, while using the experimental approach explained above.

This topic will be extensively addressed in Chapter 6. Briefly, we adopted a multimethod approach, employing two common multivariate techniques, namely Representational Similarity Analysis (RSA) and ridge regression decoding (see Chapter 6 for an extensive description of such techniques and the rationale behind using them). This allowed us to first explore the encoding of proactive and reactive control representations by using RSA to directly test the DMC predictions and finely characterize proactive and reactive control representational geometry. We could then test the decoding of such representations by

using ridge regression to determine whether the previously identified information patterns could be decoded, which would mean that they were truly available to be used by downstream neurons.

Thus, by using also MVPA, we could attain a more holistic perspective beyond the process-level insights obtained from the ER(S)P analyses, uncovering the underlying representational content encoded within these processes. By using both univariate and multivariate approaches, we could also glean valuable insights into the interaction between cognitive processes and their associated representations, as these aspects are inherently interconnected (Cheng, 2021). Moreover, by using MVPA along with EEG, the inherent dynamic nature of representations was more effectively captured, thanks to the high temporal resolution of EEG (Badre et al., 2021; Cellier et al., 2022).

Our findings confirmed the hypothesized benefits of employing MVPA techniques. They indeed revealed clear encoding patterns for both proactive and reactive control modes, demonstrating their discernibility at the neural level, and offering a detailed characterization of their respective encoding patterns. Therefore, the findings presented in Chapter 6 extend the current body of knowledge regarding proactive control by providing evidence of the representations that underlie its previously identified processes. However, the implications are even more profound for reactive control, as our findings showed preliminary yet substantial evidence for the existence of ISPC-induced reactive control representations at the neural level, affirming its intricate multivariate nature that can solely be unveiled through multivariate approaches.

1.5. Going beyond the composite Stroop effect: the weight of the loci

The multivariate analyses presented in Chapter 6 constitute the logical conclusion of this thesis work, achieving the overarching goal of comprehensively exploring the neural correlates of both proactive and reactive control. However, despite the evidence reported here, the landscape of proactive and reactive control neural correlates remains complex, clearly indicating the need for future studies. Furthermore, in addressing this research question, we encountered, and started to address, various methodological issues. The emphasis we placed on these methodological aspects was not merely an end in itself; it proved to be both the starting point and the necessary means to achieve our aim.

Hence, each step of this thesis, as in any scientific journey, has given rise to additional open questions that potentially provide fertile ground for years of further investigation, not only regarding proactive and reactive control but also concerning more basilar methodological issues. These open questions will be discussed in the concluding remarks, outlining future directions in greater detail. Nevertheless, one of these open questions emerged early on, and our curiosity to gain a better understanding has driven us to embark on an additional study to begin addressing it. This study, outlined in Chapter 7, simultaneously serves as

both the natural continuation and development of the present project, starting from the findings of the previous studies, and the initial step for all future studies that will stem from it.

Indeed, since the outset of this project, we have emphasized the composite nature of the Stroop effect, highlighting that it is imperative to employ adequate experimental tasks to ensure its measurement validity. Consequently, in this project, we have been attentive to ensure that our experimental paradigm generated a Stroop effect encompassing at the same time task, stimulus, and response effects, in alignment with the multiple-loci account (see Chapter 2 and 3, and Parris et al., 2022). While this approach has allowed us to obtain a valid measurement of the Stroop effect, it has also resulted in the impossibility to indicate the individual weight or role of each locus-specific component effect in driving the overall Stroop performance. Thus, this could be considered a limitation of our studies, as assessing a measure of complex and composite nature only grants us insights into the overall picture, leaving us unaware of the specific contributions of the underlying components.

Understanding the distinct contributions of the specific loci is particularly important to gain deeper insights into the neural functioning of proactive and reactive control, as they might operate differently at various levels. For instance, the LWPC-induced proactive control should exert a greater influence on the task and/or stimulus levels, due to its tonic and anticipatory nature, while the ISPC-induced reactive control should exert a more pronounced impact on the stimulus level, even before the detection of a conflict, and, perhaps, on the response one. The investigation of the locus-dependent specific effects of cognitive control processes could also facilitate a more precise exploration of the distinction between the ISPC-induced form of reactive control (which we defined as a "stimulus-attention" association, see Section 1.3) and a later form of reactive control (which is more compatible with the one postulated by the DMC, see Section 1.1 and Figure 1.2), a distinction that we are only introducing here but has consistently surfaced in this study (see Figure 1.6), as the later and more purely reactive form of control is triggered by conflict detection and is expected to primarily affect the response level. Furthermore, this could aid in interpreting the neural mechanisms of proactive and reactive control through the lens of the influential and neuroimaging-based Cascade of Control Model proposed by Banich (2009). This model posits three sequential steps in interference resolution: initially biasing the task-relevant perceptual processes, followed by the relevant representations, and ultimately the relevant response.

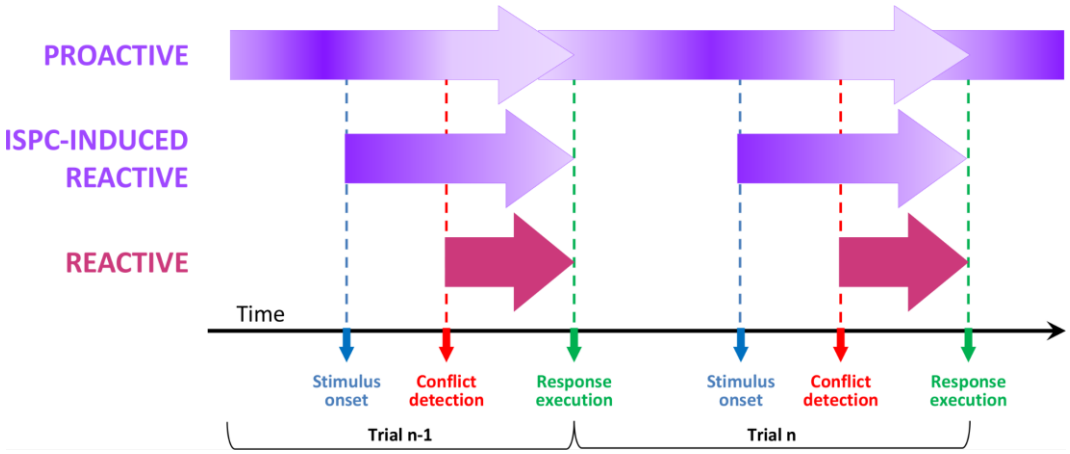

Figure 1.6.
Temporal dynamics of the involvement of proactive and reactive control modes in an exemplar task according to the terminology used in this project. The figure shows two trials of a hypothetical simple conflict task. The relative level of control engagement is reflected by the saturation of the lilac (proactive, intended as operating in anticipation of the conflict; note that ISPC-induced reactive control actually operates proactively in a sense) and fuchsia (reactive, as per the DMC, intended as operating in response to the conflict) colors.

Hence, the potential valuable insights that could arise from knowing the specific weight of the Stroop loci are immeasurable. With this objective in mind, we preregistered and conducted two successive behavioral studies in which we directly decomposed the Stroop effect by separately measuring each component. This decomposition was carried out as systematically as possible in order to overcome the limitations of the rare attempts that have been made previously (e.g., Augustinova et al., 2018), putting forward a number of very specific a-priori hypotheses (and outlining in detail how to test them). The second study represents a development of the first one because, by building upon it, we were able to assess in a fine-grained, parametric way not only the various components (i.e., task, stimulus, and response), thus improving their measurement, but also the additional aspects that could influence interference resolution, such as task asymmetry and the automaticity of the irrelevant task. Furthermore, based on the results of the first study, we refined our hypotheses.

As hypothesized, these studies not only demonstrated a strong consistency with the a priori hypotheses but also yielded highly interesting results, offering valuable insights and laying the foundational step for subsequent investigations.

In this introductory chapter, we have presented a comprehensive overview of the entire thesis project, with the primary aim of elucidating the logical framework that interconnects the various studies and delineating the respective research inquiries that each of them seeks to address. Starting from the next chapter, we will delve into the heart of each study, addressing in greater detail the topics that have been briefly outlined here. This exploration will start with the methodological review of the Stroop task.

1.6. References

Augustinova, M., Silvert, L., Spatola, N., & Ferrand, L. (2018). Further investigation of distinct components of Stroop interference and of their reduction by short response-stimulus intervals. *Acta psychologica*, *189*, 54–62. https://doi.org/10.1016/j.actpsy.2017.03.009

Badre, D., Bhandari, A., Keglovits, H., & Kikumoto, A. (2021). The dimensionality of neural representations for control. *Current Opinion in Behavioral Sciences*, *38*, 20–28. https://doi.org/10.1016/j.cobeha.2020.07.002

Banich, M. T. (2009). Executive function: The search for an integrated account. *Current directions in psychological science*, *18*(2). https://doi.org/10.1111/j.1467-8721.2009.01615.x

Botvinick, M. M., Braver, T. S., Barch, D. M., Carter, C. S., & Cohen, J. D. (2001). Conflict monitoring and cognitive control. *Psychological review*, *108*(3). 10.1037/0033-295x.108.3.624

Braem, S., Bugg, J. M., Schmidt, J. R., Crump, M. J., Weissman, D. H., Notebaert, W., & Egner, T. (2019). Measuring adaptive control in conflict tasks. *Trends in cognitive sciences*. https://doi.org/10.1016/j.tics.2019.07.002

Braver, T. S. (2012). The variable nature of cognitive control: A dual mechanisms framework. *Trends in cognitive sciences*, *16*(2). https://doi.org/10.1016/j.tics.2011.12.010

Braver, T. S., Gray, J. R., & Burgess, G. C. (2007). Explaining the many varieties of working memory variation: Dual mechanisms of cognitive control. *Variation in working memory*, *75*, 106.

Braver, T. S., Kizhner, A., Tang, R., Freund, M. C., & Etzel, J. A. (2021). The Dual Mechanisms of Cognitive Control Project. *Journal of Cognitive Neuroscience*, *33*(9), 1990–2015. https://doi.org/10.1162/jocn_a_01768

Braver, T. S., Paxton, J. L., Locke, H. S., & Barch, D. M. (2009). Flexible neural mechanisms of cognitive control within human prefrontal cortex. *Proceedings of the National Academy of Sciences*, *106*(18), 7351–7356. https://doi.org/10.1073/pnas.0808187106

Bugg, J. M. (2012). Dissociating Levels of Cognitive Control: The Case of Stroop Interference. *Current Directions in Psychological Science*, *21*(5), 302–309. https://doi.org/10.1177/0963721412453586

Bugg, J. M. (2017). Context, conflict, and control. *The Wiley handbook of cognitive control*, 79–96.

Bugg, J. M., & Crump, M. J. C. (2012). In Support of a Distinction between Voluntary and Stimulus-Driven Control: A Review of the Literature on Proportion Congruent Effects. *Frontiers in Psychology*, *3*. https://doi.org/10.3389/fpsyg.2012.00367

Bugg, J. M., & Hutchison, K. A. (2013). Converging evidence for control of color–word Stroop interference at the item level. *Journal of Experimental Psychology: Human Perception and Performance*, *39*(2).

Bugg, J. M., Jacoby, L. L., & Chanani, S. (2011). Why it is too early to lose control in accounts of item-specific proportion congruency effects. *Journal of Experimental Psychology: Human Perception and Performance*, *37*(3). doi: 10.1037/a0019957

Cavanagh, J. F., & Frank, M. J. (2014). Frontal theta as a mechanism for cognitive control. *Trends in cognitive sciences*, *18*(8). https://doi.org/10.1016/j.tics.2014.04.012

Cellier, D., Petersen, I. T., & Hwang, K. (2022). Dynamics of Hierarchical Task Representations. *The Journal of Neuroscience: The Official Journal of the Society for Neuroscience*, *42*(38), 7276–7284. https://doi.org/10.1523/JNEUROSCI.0233-22.2022

Cheng, F. (2021). *Using Single-Trial Representational Similarity Analysis with EEG to track semantic similarity in emotional word processing* (arXiv:2110.03529). arXiv. https://doi.org/10.48550/arXiv.2110.03529

Chiew, K. S., & Braver, T. S. (2017). Context processing and cognitive control: From gating models to dual mechanisms. In *The Wiley handbook of cognitive control* (pp. 143–166). Wiley Blackwell. https://doi.org/10.1002/9781118920497.ch9

Cohen, J. D. (2017). Cognitive control: Core constructs and current considerations. In *The Wiley handbook of cognitive control* (pp. 3–28). Wiley Blackwell. https://doi.org/10.1002/9781118920497.ch1

Cohen, J. D., Dunbar, K., & McClelland, J. L. (1990). On the control of automatic processes: A parallel distributed processing account of the Stroop effect. *Psychological Review*, *97*(3). https://doi.org/10.1037/0033-295x.97.3.332

Davis, T., LaRocque, K. F., Mumford, J. A., Norman, K. A., Wagner, A. D., & Poldrack, R. A. (2014). What do differences between multi-voxel and univariate analysis mean? How subject-, voxel-, and trial-level variance impact fMRI analysis. *NeuroImage*, *97*, 271–283. https://doi.org/10.1016/j.neuroimage.2014.04.037

De Pisapia, N., & Braver, T. S. (2006). A model of dual control mechanisms through anterior cingulate and prefrontal cortex interactions. *Neurocomputing*, *69*(10–12). https://doi.org/10.1016/j.neucom.2005.12.100

D'Esposito, M. (2007). From cognitive to neural models of working memory. *Philosophical Transactions of the Royal Society of London. Series B, Biological Sciences*, *362*(1481), 761–772. https://doi.org/10.1098/rstb.2007.2086

Diamond, A. (2013). Executive functions. *Annual review of psychology*, *64*, 135–168. 10.1146/annurev-psych-113011-143750

Diedrichsen, J., & Kriegeskorte, N. (2017). Representational models: A common framework for understanding encoding, pattern-component, and representational-similarity analysis. *PLoS Computational Biology*, *13*(4), e1005508. https://doi.org/10.1371/journal.pcbi.1005508

Engel, A. K., & Fries, P. (2010). Beta-band oscillations—Signalling the status quo? *Current opinion in neurobiology*, *20*(2). https://doi.org/10.1016/j.conb.2010.02.015

Etzel, J. A., Courtney, Y., Carey, C. E., Gehred, M. Z., Agrawal, A., & Braver, T. S. (2020). Pattern Similarity Analyses of FrontoParietal Task Coding: Individual Variation and Genetic Influences. *Cerebral Cortex*, *30*(5), 3167–3183. https://doi.org/10.1093/cercor/bhz301

Flake, J. K., & Fried, E. I. (2020). Measurement Schmeasurement: Questionable Measurement Practices and How to Avoid Them. *Advances in Methods and Practices in Psychological Science*, *3*(4), 456–465. https://doi.org/10.1177/2515245920952393

Freund, M. C., Etzel, J. A., & Braver, T. S. (2021). Neural Coding of Cognitive Control: The Representational Similarity Analysis Approach. *Trends in Cognitive Sciences*, *25*(7), 622–638. https://doi.org/10.1016/j.tics.2021.03.011

Gluth, S., Rieskamp, J., & Büchel, C. (2012). Deciding When to Decide: Time-Variant Sequential Sampling Models Explain the Emergence of Value-Based Decisions in the Human Brain. *Journal of Neuroscience*, *32*(31), 10686–10698. https://doi.org/10.1523/JNEUROSCI.0727-12.2012

Gonthier, C., Braver, T. S., & Bugg, J. M. (2016). Dissociating proactive and reactive control in the Stroop task. *Memory & Cognition*, *44*(5), Articolo 5.

Gratton, G., Coles, M. G., & Donchin, E. (1992). Optimizing the use of information: Strategic control of activation of responses. *Journal of Experimental Psychology. General*, *121*(4). https://doi.org/10.1037//0096-3445.121.4.480

Gratton, G., Cooper, P., Fabiani, M., Carter, C. S., & Karayanidis, F. (2018). Dynamics of cognitive control: Theoretical bases, paradigms, and a view for the future. *Psychophysiology*, *55*(3). https://doi.org/10.1111/psyp.13016

Gutteling, T. P., Sillekens, L., Lavie, N., & Jensen, O. (2022). Alpha oscillations reflect suppression of distractors with increased perceptual load. *Progress in Neurobiology*, *214*, 102285. https://doi.org/10.1016/j.pneurobio.2022.102285

Hedge, C., Powell, G., & Sumner, P. (2018). The reliability paradox: Why robust cognitive tasks do not produce reliable individual differences. *Behavior Research Methods*, *50*(3). https://doi.org/10.3758/s13428-017-0935-1

Heidlmayr, K., Kihlstedt, M., & Isel, F. (2020). A review on the electroencephalography markers of Stroop executive control processes. *Brain and Cognition*, *146*, 105637. https://doi.org/10.1016/j.bandc.2020.105637

Jacoby, L. L., Lindsay, D. S., & Hessels, S. (2003). Item-specific control of automatic processes: Stroop process dissociations. *Psychonomic Bulletin & Review*, *10*(3), 638–644. https://doi.org/10.3758/BF03196526

Jiang, J., Heller, K., & Egner, T. (2014). Bayesian modeling of flexible cognitive control. *Neuroscience & Biobehavioral Reviews*, *46*, 30–43. https://doi.org/10.1016/j.neubiorev.2014.06.001

Kornblum, S. (1992). *Dimensional overlap and dimensional relevance in stimulus–response and stimulus–stimulus compatibilit*y. In G. E. Stelmach & J. Requin (Eds.), Tutorials in motor behavior, 2 (pp. 743–777).

Kriegeskorte, N., & Diedrichsen, J. (2019). Peeling the Onion of Brain Representations. *Annual Review of Neuroscience*, *42*(1), 407–432. https://doi.org/10.1146/annurev-neuro-080317-061906

Kriegeskorte, N., & Kievit, R. A. (2013). Representational geometry: Integrating cognition, computation, and the brain. *Trends in Cognitive Sciences*, *17*(8), 401–412. https://doi.org/10.1016/j.tics.2013.06.007

Larson, M. J., Clayson, P. E., & Clawson, A. (2014). Making sense of all the conflict: A theoretical review and critique of conflict-related ERPs. *International Journal of Psychophysiology*, *93*(3), 283–297. https://doi.org/10.1016/j.ijpsycho.2014.06.007

Lindsay, D. S., & Jacoby, L. L. (1994). Stroop process dissociations: The relationship between facilitation and interference. Journal of Experimental Psychology: Human Perception and Performance, 20(2). https://doi.org/10.1037/0096-1523.20.2.219

Logan, G. D., & Zbrodoff, N. J. (1979). When it helps to be misled: Facilitative effects of increasing the frequency of conflicting stimuli in a Stroop-like task. Memory & cognition, 7(3). https://doi.org/10.3758/BF03197535

MacLeod, C. M. (1991). Half a century of research on the Stroop effect: An integrative review. *Psychological bulletin*, *109*(2). https://doi.org/10.1037/0033-2909.109.2.163

Miller, E. K., & Cohen, J. D. (2001). An integrative theory of prefrontal cortex function. *Annual review of neuroscience*, *24*(1). 10.1146/annurev.neuro.24.1.167

Nee, D. E., Wager, T. D., & Jonides, J. (2007). Interference resolution: Insights from a meta-analysis of neuroimaging tasks. *Cognitive, Affective, & Behavioral Neuroscience*, *7*(1). https://doi.org/10.3758/CABN.7.1.1

Parris, B. A., Hasshim, N., Wadsley, M., Augustinova, M., & Ferrand, L. (2022a). The loci of Stroop effects: A critical review of methods and evidence for levels of processing contributing to color-word Stroop effects and the implications for the loci of attentional selection. *Psychological Research*, *86*(4). 1029–1053. https://doi.org/10.1007/s00426-021-01554-x

Parris, B. A., Hasshim, N., Wadsley, M., Augustinova, M., & Ferrand, L. (2022b). The loci of Stroop effects: A critical review of methods and evidence for levels of processing contributing to color-word Stroop effects and the implications for the loci of attentional selection. *Psychological Research*, *86*(4). 1029–1053. https://doi.org/10.1007/s00426-021-01554-x

Parsons, S. (2020). *Exploring reliability heterogeneity with multiverse analyses: Data processing decisions unpredictably influence measurement reliability*. PsyArXiv. https://doi.org/10.31234/osf.io/y6tcz

Popal, H., Wang, Y., & Olson, I. R. (2019). A Guide to Representational Similarity Analysis for Social Neuroscience. *Social Cognitive and Affective Neuroscience*, *14*(11), 1243–1253. https://doi.org/10.1093/scan/nsz099

Puccioni, O., & Vallesi, A. (2012a). Conflict resolution and adaptation in normal aging: The role of verbal intelligence and cognitive reserve. *Psychology and Aging*, *27*(4). https://doi.org/10.1037/a0029106

Puccioni, O., & Vallesi, A. (2012b). High cognitive reserve is associated with a reduced age-related deficit in spatial conflict resolution. *Frontiers in human neuroscience*, *6*, 327. 10.3389/fnhum.2012.00327

Puccioni, O., & Vallesi, A. (2012c). Sequential congruency effects: Disentangling priming and conflict adaptation. *Psychological Research*, *76*(5), Articolo 5. https://doi.org/10.1007/s00426-011-0360-5

Schmidt, J. R. (2019). Evidence against conflict monitoring and adaptation: An updated review. *Psychonomic bulletin & revi*ew, 26(3). 10.3758/s13423-018-1520-z

Schmidt, J. R., & Besner, D. (2008). The Stroop effect: Why proportion congruent has nothing to do with congruency and everything to do with contingency. *Journal of Experimental Psychology: Learning, Memory, and Cognition*, *34*(3). https://doi.org/10.1037/0278-7393.34.3.514

Schmidt, J. R., Crump, M. J. C., Cheesman, J., & Besner, D. (2007). Contingency learning without awareness: Evidence for implicit control. *Consciousness and Cognition*, *16*(2), 421–435. https://doi.org/10.1016/j.concog.2006.06.010

Schumacher, E., & Hazeltine, E. (2016). Hierarchical Task Representation: Task Files and Response Selection. *Current Directions in Psychological Science*, *25*, 449–454. https://doi.org/10.1177/0963721416665085

Stroop, J. R. (1935). Studies of interference in serial verbal reactions. *Journal of Experimental Psychology*, *18*(6), 643–662. https://doi.org/10.1037/h0054651

Tafuro, A., Ambrosini, E., Puccioni, O., & Vallesi, A. (2019). Brain oscillations in cognitive control: A cross-sectional study with a spatial stroop task. Neuropsychologia, 133, 107190. https://doi.org/10.1016/j.neuropsychologia.2019.107190

Tafuro, A., Vallesi, A., & Ambrosini, E. (2020). Cognitive brakes in interference resolution: A mouse-tracking and EEG co-registration study. *Cortex*, *133*, 188–200. https://doi.org/10.1016/j.cortex.2020.09.024

Torres-Quesada, M., Funes, M. J., & Lupiáñez, J. (2013). Dissociating proportion congruent and conflict adaptation effects in a Simon–Stroop procedure. *Acta Psychologica*, *142*(2), 203–210. https://doi.org/10.1016/j.actpsy.2012.11.015

CHAPTER 2

The Stroop legacy:
A Cautionary Tale on Methodological Issues

2.1. Introduction

One of the most influential and widely used experimental paradigms in cognitive psychology is the Stroop task (Stroop, 1935). In its most common version, known as the color-word Stroop task, participants are presented with words that denote a color printed in either the same or a different ink color and are required to identify the ink color of the presented word regardless of its meaning. Crucially, the ink color in which the word is displayed and the meaning of the same word can either match (congruent trials, e.g., GREEN displayed in green ink: $GREEN_{green}$) or not (incongruent trials, e.g., GREEN displayed in blue ink: $GREEN_{blue}$). The critical measure is the so-called Stroop effect (SE), which refers to the robust performance decline in incongruent as compared to congruent trials, which is commonly attributed to the interference between reading and color naming (e.g., MacLeod, 1991; Stroop, 1935). Despite being the most classic Stroop task account, this explanation is incomplete and insufficient, as will be discussed profusely throughout this work. Indeed, the need to conduct this review arises precisely from the widespread belief that, in order to obtain a Stroop effect, the only basic requirement is to administer a task with congruent and incongruent stimuli, which is however incorrect or, at least, not sufficient.

Before delving into theoretical and methodological issues, we first provide the reader with definitions of some basic concepts, starting with the Stroop effect, which is commonly computed as the difference in the response time (RT) between incongruent (I) and congruent (C) trials (formally, $SE = RT_{Incongruent} - RT_{Congruent}$). When congruent trials are used as the baseline condition against which to compare RT on incongruent trials, the SE has also been referred to as the Stroop congruency effect (e.g., Egner et al., 2010), Stroop interference effect (e.g., Leung et al., 2000), or total Strop effect (e.g., Brown et al., 1998). Alternatively, neutral trials (e.g., a color-neutral word or a non-word letter string displayed in green ink: CAT_{green} or XXX_{green} respectively), can be used as the baseline condition, allowing one to partition the SE into Stroop interference (SI) and facilitation (SF) effects (but see, e.g., Di Russo & Bianco, 2023, for different nomenclatures). The former, calculated as the difference in RT between incongruent and neutral trials (N) (formally, $SI = RT_{Incongruent} - RT_{Neutral}$), refers to a worse performance for incongruent (I) than neutral words (N); the latter, computed as the difference in RT between neutral and congruent trials (formally, $SF = RT_{Neutral}$

– $RT_{Congruent}$), refers to a better performance for congruent than neutral words. The algebraic sum of SI and SF corresponds to the full SE (formally, SE = SI + SF).

To successfully complete the Stroop task, thus some form of cognitive control, namely the ability to regulate thoughts and actions in accordance with internally maintained behavioral goals (Braver, 2012), needs to be activated (Cohen et al., 1990). Indeed, the Stroop task, quoting Stroop in his original article (1935), is a measure of "interference of color stimuli upon reading words'' [p. 647] and is thus widely used to investigate both interference resolution (e.g., Nee et al., 2007) and selective attention for which it is considered the "gold standard" (MacLeod, 1992). The ability tapped by the Stroop task allows us to selectively attend to specific properties in our environment based on our goals, while reducing the impact of potentially interfering information.

For several decades now, the Stroop task has been serving as a main tool for assessing executive attention disorders and impairments related to the frontal lobe, like anxiety, schizophrenia, dementia, and attention deficit hyperactivity disorder (e.g., Barkley, 1997; Henik & Salo, 2004; Spieler et al., 1996), for neuropsychological practice (e.g., Strauss et al., 2007), and in basic and applied research (e.g., MacLeod, 1992). For all that, many reviews have been conducted in several research fields (e.g., neuropsychology, Scarpina & Tagini, 2017; Periáñez et al., 2021; psychiatry, e.g., Peckham et al., 2010; Joyal et al., 2019; cognitive psychology, e.g., Algom & Chajut, 2019; Parris et al., 2022; Schmidt, 2019). Given this vast amount of studies on the Stroop, including several important reviews, our intention of conducting a further review might not appear so straightforward. For this reason, in the next paragraph, we outline the goal of the present work to elucidate the contribution that we believe this review could give to the Stroop literature.

2.1.1. Goal of the present review

Despite the plethora of studies and reviews on the Stroop task, consensus on many theoretical and methodological aspects is still far from being reached. For example, despite the Stroop effect often being regarded as a proxy for the activation of cognitive control mechanisms, some recent works questioned the validity of control-related and conflict adaptation explanations of it (see Algom & Chajut, 2019; Schmidt, 2019's reviews as examples of two of the most influential ones). In addition to this example, a great variety of theoretical accounts have been put forward to explain the Stroop effect, some of which are in contrast to each other. This notwithstanding, it must be said that discussing such theoretical issues is not the aim of the present review, and we will present only the theoretical accounts useful for our purposes without going into much detail.

Here we instead focus on the validity of the measures obtained with the Stroop task (Flake & Fried, 2020), that is, the extent to which the measures or results obtained using a research task or method actually

represent the intended variable. Measurement validity indeed represents the fundamental requirement for any other form of validity, including the validity of the conclusions drawn from the experimental measures (Flake & Fried, 2020). However, since there are enormous methodological differences among studies employing the Stroop task and its adaptations, the validity of their Stroop measures is challenging to assess. In fact, these differences hinder direct comparisons between studies and, consequently, impede the possibility of drawing firm conclusions, potentially leading to inconsistencies at a theoretical level. For instance, it is emblematic that the Stroop task, along with other well-known experimental paradigms, exhibits the so-called reliability paradox, according to which the Stroop effect, despite being large, lacks reliability (Hedge et al., 2018; see also Viviani et al., 2023, for a more detailed discussion).

The methodological confusion arises from the fact that, since the first study by Stroop, a multitude of Stroop task variants have been devised, often without relying on common guidelines. This is problematic because, as we will discuss in detail later, subsequent studies have highlighted the complex nature of the Stroop effect, demonstrating, for example, that it comprises multiple components (Parris et al., 2022). Therefore, it is crucial that, when we refer to the "Stroop effect", all these components are taken into account. Despite the existence of works (e.g., Kornblum, 1992 discussed in detail later) that have explicitly clarified the necessary characteristics for a task to be considered similar to the classical Stroop and thus be called Stroop, such guidelines are commonly overlooked. Therefore, the message we aim to convey through this review is that methodological consistency among studies is essential whenever the label "Stroop task" is used to ensure a common ground. By claiming this, we mean that since the Stroop task originally proposed by its namesake author ensures a genuine and comprehensive Stroop effect, it represents the model to follow. Therefore, every replication of this task, both in terms of color-word versions and alternative variants, should strive to be methodologically similar to it, as only by using this approach, an accurate comparison of the evidence produced by individual studies is ensured.

The aim of the present work is to overview the tasks that have been denoted as Stroop tasks in the literature from a methodological point of view, to ascertain whether they can rightfully be called Stroop tasks, that is, if they are methodologically similar to the classical color-word version. However, by saying this, we absolutely do not mean that variations altering the classical version should be avoided altogether. On the contrary, if based on sound methodological assumptions, such variations can be useful, for instance, in gaining a better understanding of the nature of the Stroop effect or some of its underlying processes. Nonetheless, it is important that, when such variations do not adhere to the classical Stroop characteristics, they should not be labeled as Stroop tasks. Instead, it is preferable to use labels such as "Stroop-like" task to highlight this distinction and avoid the risk of misleading interpretations.

It should be noted that the methodological discussion in the present paper is not intended as a systematic review[1] of the huge literature on the Stroop task and its alternative versions. Rather, the studies reviewed here must be considered just as examples of the main Stroop task versions serving our purposes of showing the methodological strengths and limitations of the general Stroop category they belong to. For this reason, our work is a narrative review that focuses on the specific methodological aspects we are interested in, to be informative and describe them, thus without specifically focusing on the selected exemplar studies (Uman, 2011). Therefore, we advise readers to consider this work from this perspective while ensuring that we have made every effort to avoid as much as possible any selection bias and to be as clear as possible.

Throughout this work, we will endeavor to demonstrate the reasons for our skepticism regarding the tasks commonly used in the literature, presenting several examples that highlight how the majority of Stroop tasks lack fundamental methodological requirements to be considered as such in all respects. At the same time, our objective is to encourage future studies to pay more attention to methodological aspects and the validity of Stroop effect measures. Nonetheless, our message is not to remain solely attached to the classical version of this task, which may present certain issues, such as the requirement for verbal responses that may not always be feasible, especially in experimental and neuroimaging settings. With a proactive intention, we thus propose an alternative family of Stroop tasks, the spatial variant, to demonstrate an example of an alternative Stroop version that ensures both methodological adequacy and, sometimes, greater flexibility. However, we wish to emphasize that our alternative proposal is not the only possibility, but merely one among many potential methodologically sound versions.

Given that we are not the first to propose a spatial version of the Stroop task and similar tasks have already been employed in the literature, a significant portion of this review will be dedicated to examining whether spatial Stroop tasks in the literature genuinely meet the criteria for being considered methodologically appropriate, that is, similar to the classical Stroop task. Nonetheless, before addressing the methodological requirements of the spatial Stroop task, we will provide an overview of the classical color-word Stroop task and its most popular variations.

Therefore, from a practical standpoint, the review is organized into two main sections. The first section outlines the necessary characteristics for methodologically sound Stroop tasks, followed by an overview of its most popular variations, providing examples to support our skepticism. The second section will focus on

[1] Our intention is not to conduct a systematic review of the literature; hence, we explicitly declare that we avoid doing a detailed and comprehensive search on the literature on the Stroop tasks, which is the requisite of any systematic review (e.g., Uman, 2011). With this, we mean that we do not follow the PRISMA statement (Page et al., 2021), necessary for any systematic review.

the spatial Stroop tasks found in the literature, assessing them and explaining the reasons why we believe they may be a potentially preferable variant over many others.

2.1.2. Object of our methodological inspection

The object of our methodological inspection is the Stroop effect as a whole. In the introduction, we outlined two different approaches for calculating the Stroop effect, one contrasting incongruent and congruent trials, which allows obtaining only a global Stroop effect, and the other using also neutral trials, which allows portioning the Stroop effect into its facilitation and interference components. So far, it is not clear in the literature which of these two procedures is better to use. Indeed, the relative weights of interference and facilitation effects in composing the Stroop effect are currently unknown (MacLeod, 1991; MacLeod & MacDonald, 2000). In addition, whether interference and facilitation arise from a common mechanism (e.g., the congruency relationship between ink color and color name) or not is a further subject of controversy (e.g., Brown, 2011; Di Russo & Bianco, 2023). Given these unresolved controversies, it seems more cautious to us not to distinguish between the two subcomponents. A further reason specifically regards the facilitation effect, whose reliability and stability have been called into question by findings showing that it is considerably smaller than the interference one, as shown by MacLeod & MacDonald's (2000) study, wherein facilitation effects were one fifth the size of interference effects (for further evidence, see Augustinova et al., 2019; Lindsay & Jacoby, 1994). Additionally, Stroop facilitation measures have been shown to be affected by the baseline (i.e., the type of neutral trials) chosen to compute the contrast with congruent trials. Indeed, although colored non-words (e.g., XXX_{green}) and color-neutral words (e.g., $CHAIR_{green}$) are usually used interchangeably, converging evidence suggests that facilitation effects are underestimated when using colored non-words instead of color-neutral words (Augustinova et al., 2019; Brown, 2011). Of note, although it was not tested, the issue of baseline selection may also affect the comparison with incongruent stimuli and thus the calculation of Stroop interference, further supporting our choice not to distinguish between the two subcomponents of the Stroop effect. Finally, the facilitation effect still includes an interference component because a form of conflict occurs even on congruent trials. According to this view, since reading is assumed to be a more dominant and automatic process than identifying the ink color, even congruent trials are affected by a form of conflict, namely task conflict, and thus they cannot be considered as a pure measure of facilitation (Goldfarb & Henik, 2007; MacLeod & MacDonald, 2000; Parris et al., 2022). Indeed, task conflict in congruent trials is particularly evident in some cases (i.e., as a result of specific manipulations), as a phenomenon known as negative facilitation, characterized by longer RTs on congruent trials as compared to neutral ones, due to task conflict in the former but not in the latter (Parris et al., 2023).

Discussing the validity and the best methodological choices for measuring Stroop facilitation and Stroop interference separately goes beyond the scope of the present review, but we highlighted these issues to justify our choice to consider the Stroop effect as a whole, and not portioning it into these components. Moreover, the main reason for this decision is that our aim is to provide a methodological overview of the Stroop task that is as inclusive as possible; therefore, since most of the studies in the literature that used the Stroop task measured the Stroop effect and not its subcomponents, we decided to do the same. It is important to note, however, that most studies use the Stroop task to investigate processes similar to interference resolution, for which we are aware that the Stroop interference effect would be a much better and purer measure.

That being said, to avoid confusion, we will consistently use the generic term "Stroop effect" in the text, even when it would be more accurate to refer specifically to its interference component. We are aware that this may be a limitation, but we believe that it is the only way to ensure the generalization of what we discuss in this review. On the other hand, we believe that a methodical clarification regarding the facilitation-interference relationship would be necessary in the future to bring clarity to the matter.

2.2. The color-word Stroop task: methodological considerations

This section is dedicated to some methodological considerations that we will consider as benchmarks throughout the entire review and, to justify their importance, we will draw on some theoretical accounts, which are required to understand the nature of the Stroop effect.

2.2.1. Stroop effect asymmetry

The basis of the Stroop effect has been classically attributed to the so-called Stroop asymmetry, that is, the fact that task-irrelevant words slow color naming, while task-irrelevant colors interfere with word reading to a lesser extent (e.g., MacLeod, 1991; Melara & Algom, 2003). The prevalent explanation for this asymmetry is the automaticity account, according to which this occurs because the two dimensions imply different amounts of processing effort: naming ink colors requires more attentional resources than reading words, which is automatic and obligatory due to our extensive experience in reading and its consequent storage in procedural memory. Therefore, the more automatized process interferes with the less automatic one, but not vice versa (MacLeod, 1991). Based on these assumptions, the parallel distributed processing account of the Stroop effect (Cohen et al., 1990) is dominant in the literature and postulates that the Stroop asymmetry derives from the unintentional activation of the reading pathway, which is stronger than the weaker color naming one. Automaticity is thus considered on a continuum, relying on the strength of processing which, in turn, depends on the relative strength of the competing processes and can derive from several mechanisms (e.g., the effect of practice).

Alternatively, the commonly observed Stroop asymmetry has been explained by the dimensional discriminability account (Melara & Mounts, 1993), which posits that the relative speed of discrimination between the two dimensions, rather than the strength of processing, underlies such an effect because there is a mismatch in discriminability or salience between colors and words. Dimensional discriminability refers to the perceptual properties of the dimensions and, based on Melara & Algom's (2003) account, words are more discriminable than colors in most of the Stroop studies, explaining why they are processed faster and interfere more. Therefore, by matching the dimensional discriminability (e.g., by reducing the physical size of the words, making the colors more salient than the words, etc.) to render the dimensions equally discriminable, the Stroop effect can be deliberately reduced, eliminated, or even reversed (Algom & Chajut, 2019).

The dimensional discriminability account offers a reasonable explanation for the reverse Stroop effect which, as the name suggests, is produced when the typical Stroop asymmetry is reversed. This effect was first reported by Stroop (1935), who showed that after extensive practice in color naming, reading color words was impaired on incongruent trials. More recent evidence of color interfering with task-relevant word meaning was offered by Blais & Besner's (2007) study, in line with the dimensional discriminability account. In that study, when participants were required to identify a centrally presented colored word by pointing to the response word displayed in one of the four corners of the screen, the response latencies were longer when the target word appeared in an incongruent ink. The automaticity account provides a similar explanation for the reversed direction of interference, that is, it postulates that, if a normally more automatic process associated with one stimulus dimension is altered through radical experimental manipulations, such as those in the dimensional discriminability account, the normally less automatic process can become relatively more automatic, producing interference in the reverse direction (MacLeod, 1991b). In other words, also according to the automaticity account, by changing the difficulty of processing, the interference can affect the process that should be stronger.

Evidence indeed exists in the literature supporting both accounts but, for the purposes of our review, they will not be considered as mutually exclusive. As such, we can speculate that the Stroop effect might be yielded both by differences in automaticity between the two dimensions and by differences in the discriminability of the two dimensions. When the discriminability of the two dimensions is the same, automaticity would be predominant, whereas when their processing automaticity is the same, discriminability would be predominant. With this in mind, researchers using the Stroop task should balance and control for both of them. For example, if automaticity is manipulated expecting that one dimension is more automatic relative to the other, the discriminability of the two dimensions needs to be controlled for. On the other hand, when discriminability is manipulated rendering one dimension more (e.g., perceptually) salient than the other, care must be taken to use equally strong processes. To deliberately avoid favoring

one account over the other, throughout this work, when we need to indicate that one dimension is prevailing over the other, we will use neither the term “more automatic” nor “more salient”, but we will neutrally refer to that dimension as stronger than the other.

2.2.2. Stroop effect characteristics

The complex nature of the Stroop effect is not limited to the coexistence of interference and facilitation effects, but also extends to its composite nature. As such, in this section we provide a brief overview of the Stroop effect characteristics, with the aim of highlighting its fundamental requirements.

Over the years, a wealth of different single-stage theoretical accounts has been proposed to explain the nature of the Stroop effect; they can be divided into two general categories. The so-called late-selection accounts have been predominant in the Stroop literature and attribute the Stroop effect to response conflict, or interference[2], in the response selection phase: in incongruent trials, the irrelevant word meaning elicits a (wrong) response that interferes with the selection of the correct response (Cohen et al., 1990; Posner & Snyder, 1975). In contrast, early-selection accounts attribute the Stroop effect to stimulus conflict, suggesting that, in the stimulus-encoding stage, the irrelevant dimension of the incongruent stimulus interferes with the relevant one. According to some authors, stimulus conflict is perceptual in nature because it arises when colors are implicitly identified (e.g., Hock & Egeth, 1970), whereas others posit its conceptual and/or semantic nature and put forward that interference occurs because the meanings of both the word and color dimensions correspond to colors (e.g., Seymour, 1977). Within this early account framework, it has also been suggested that interference occurs at the task set level due to the conflict between the irrelevant but highly automatized task, that is, word reading, and the relevant task, that is, color naming (e.g., Augustinova et al., 2018; Goldfarb & Henik, 2006, 2007; Parris, 2014).

This distinction notwithstanding, it has been argued that the Stroop effect is better explained in terms of multiple-stage accounts, suggesting that processes at both the stimulus and response levels contribute to it. Stimulus- and response-based processes are not mutually exclusive but simply focus on different aspects of the Stroop task. Accordingly, Zhang and Kornblum (1998a) examined stimulus-stimulus (e.g., between two incongruent stimulus dimensions) and stimulus-response (e.g., between two competing responses) effects both in isolation and in the Stroop task, showing that they interact in contributing to the Stroop effect. Their results suggest that the Stroop effect is due to the combination of stimulus-stimulus and stimulus-response compatibility (De Houwer, 2003; Zhang & Kornblum, 1998).

More recent studies further investigated the specific contribution of different types of conflict in the Stroop task, strengthening the evidence for an even more complex multiple-stage account. Augustinova and

[2] We will use the terms conflict and interference as synonyms for the sake of simplicity.

colleagues (2018) specifically tested the integrative assumption that the overall Stroop interference is composed of task, semantic, and response conflicts. To this aim, they compared response latencies to different stimuli, that is, standard color-incongruent words (e.g., $BLUE_{green}$), associated color-incongruent words (e.g., SKY_{green}), color-neutral words (e.g., DOG_{green}), and color-neutral letter strings (e.g., $XXXX_{green}$), and they then calculated the specific contribution of task (DOG_{green} - $XXXX_{green}$), semantic (SKY_{green} - DOG_{green}), and response ($BLUE_{green}$ - SKY_{green}) conflicts. When vocal responses were used, they clearly identified the behavioral signatures of each of these conflict types. Moreover, in a subsequent study, Augustinova and colleagues (2019) replicated these results and drew special attention to the effect of response modality, showing that the three conflict types contribute to Stroop interference only when vocal responses are used while, when manual ones are used, no task conflict is generated (see Section 1.3.3 for a more detailed discussion on this point).

In a similar vein, Parris and coworkers (2022) conducted a review to specifically investigate the processing levels that contribute to the Stroop effect[3]. They examined the evidence produced by studies in the literature to verify if it is consistent with the hypothesis that the Stroop effect is composed of multiple loci, which can be distinguished into informational and task loci. The former includes stimulus- and response-related conflicts/facilitations corresponding to previous single-stage models (e.g., De Houwer, 2003; Zhang & Kornblum, 1998), whereas the latter coincides with the above-described conflict between task sets. Their conclusions argue in favor of the multiple-stage account, suggesting that the Stroop effect arises at different loci. However, only two independent loci of attentional selection in the Stroop task were clearly differentiated; indeed, while there is evidence that task conflict is distinct from informational conflict, to date, measures distinguishing between stimulus and response conflicts/facilitations are still ambiguous. This notwithstanding, the authors left open the possibility of two distinct loci within the broader informational one, but claimed the importance of developing more adequate models accounting for the multiplicity of Stroop loci. Additionally, neuroimaging evidence seems to point towards the same direction, as shown, for example, by the cascade of control model (Banich, 2009; 2019), which is an influential functional model accounting for Stroop performance in a multiple-stage manner.

Overall, although available findings are somewhat conflicting, evidence that the color-word Stroop effect occurs at different loci is convincing. As such, we can safely claim that, when designing a Stroop task, taking

[3] To note that, as compared to previous works, in Parris et al. (2022), the possible contribution of multiple processing loci has been investigated considering separately Stoop interference and Stroop facilitation. In brief, both imply interference at the task locus, whereas SI also relies on interference at the stimulus and response loci and SF also relies on facilitation at the stimulus and response loci. Therefore, we could say that both SI and SF imply the same processing loci, but with an opposite direction at the stimulus and response loci. Based on that, given our intention to focus on the overall Stroop effect, in the present work, when possible, we will avoid referring to interference and facilitation at these loci. We will instead use more caution, referring in a general manner to the processing loci of the Stroop, except for task conflict which can be safely used.

into account all these possible types (or loci) of the Stroop effect is of considerable importance. Therefore, to yield a Stroop effect involving all the three loci (which, for the sake of simplicity, we will call a complete Stroop effect), color-word Stroop tasks should entail: 1) interference at the task selection level due to conflict between two competing processing streams, naming and reading, with the former being less strong than the latter, 2) interference (and facilitation) at the stimulus processing level due to perceptual and/or semantic overlap between relevant and irrelevant stimulus representations, and 3) interference (and facilitation) at the response selection level due to the overlap between the two vocal responses activated by the ink color and the color name features (De Houwer, 2003; Funes et al., 2010).

As such, in the present review, the presence of three distinct loci will be evaluated in the overviewed studies. It is noteworthy that, while the presence of task conflict depends on the use of two distinct tasks activating competing task sets, the effects at the stimulus and response loci strongly rely on the characteristics of the Stroop stimuli and responses, which, therefore, should be designed carefully. In the next section, we focus on this latter point, discussing a relatively old account that, nonetheless, offers clear guidelines for designing Stroop tasks entailing both stimulus and response conflicts/facilitations.

2.2.3. Stroop stimuli and responses

Both stimulus and response loci are incorporated in the dimensional overlap model put forward by Kornblum (1992) (see also Kornblum et al., 1990, 1999), which outlines the requirements that need to be satisfied to define a task as a Stroop task. This model is based on the concept of dimensional overlap, referred to as the degree of similarity, or correspondence, between two sets of items. Dimensional overlap can also be defined as the extent to which two sets of items have attributes or properties in common. It does not necessarily concern physical similarity, because it is a property of the representation of the sets and not necessarily a physical feature of them. Therefore, dimensional overlap can be perceptual and/or conceptual and can be observed in the stimulus and response sets, in two stimulus sets, or in both. The overlap can be measured on a continuous scale with different levels of similarity, going from totally dissimilar to totally similar. When two sets have dimensional overlap, taking one element from each set, they are either compatible if they match or incompatible if they do not match and interference is produced. Commonly, in the context of the Stroop task, to refer to the same concept, the term congruency, instead of compatibility, is used. Another key concept is the dimensional relevance, which concerns the degree to which the features of the stimulus are informative about the required response, which are defined as irrelevant when they are uninformative. Thus, relevant stimuli to which a participant is instructed to respond are distinguished from irrelevant ones, which should not be attended to but are usually difficult to ignore.

Combining dimensional overlap and dimensional relevance, Kornblum (1992) constructed a taxonomy to classify ensembles (i.e., the types of task) that produce compatibility effects, made of eight types of tasks characterized by increasing levels of dimensional overlap. At the first level, in the type-one ensemble, there is no dimensional overlap. At the opposite extreme, in the type-eight ensemble, there is dimensional overlap between all three task dimensions, namely, the relevant and irrelevant stimuli and the response dimensions. The color-word Stroop task is a typical example of this ensemble type, as there is dimensional overlap between i) the irrelevant stimulus and response dimensions, ii) the relevant stimulus and response dimensions, and iii) the relevant and irrelevant stimulus dimensions.

According to this model, the response modality plays a key role in producing the Stroop effect, since the dimensional overlap between the stimulus and the response depends on this factor. Indeed, to produce interference/facilitation between stimulus and response, the type of response needs to overlap with the stimulus attributes. This implies that, in the color-word Stroop, naming (vocal) responses are needed to elicit interference/facilitation at the response level. Consistent with this, it has been shown that the color-word Stroop effect is considerably reduced with manual as opposed to vocal response modality, confirming the influence of the stimulus-response overlap (e.g., Augustinova et al., 2019; MacLeod, 1991). Nevertheless, the role of response modality remains a frequently ignored methodological issue and, in the literature, color-word Stroop tasks requiring manual (keypress) responses are commonly used (e.g., Ambrosini et al., 2019; Kinoshita et al., 2017; Szűcs & Soltész, 2010; Toth et al., 2019; Vallesi et al., 2017). However, according to Kornblum's taxonomy (Kornblum, 1992), they cannot be considered as type-eight ensembles, or Stroop tasks, due to the lack of dimensional overlap between stimulus and response. Indeed, in Kornblum's taxonomy, verbal Stroop tasks that require manual responses are classified as type-four ensemble and are referred to as Stroop-like tasks.

In the present work, the dimensional overlap model will be used along with the multiple loci account as benchmarks for evaluating the Stroop task methodology. In our opinion, both are useful for our purposes. This is because, while Kornblum's account does not explicitly consider task conflict (but nonetheless all Type-eight ensembles necessarily have task conflict), which is, however, mandatory to yield the Stroop effect, his taxonomy offers a clear framework for assessing in more detail the completeness of Stroop stimuli, especially for what concerns the suitability of the stimuli to produce the effect at the level of response. Indeed, the dimensional overlap model posits that two dimensional overlaps are required to produce a complete effect at the response locus.

2.2.4. Confounding factors

In the previous section, we highlighted the methodological requirements for yielding a complete Stroop effect according to the multiple loci and dimensional overlap accounts, but they are not sufficient to ensure

a methodologically sound Stroop task. Indeed, even when they are all satisfied, other factors might negatively affect the methodological quality of a task and the validity of the obtained measures, that is, confounders not related to the Stroop effect might bias its estimation, and thus they need to be controlled to ensure its validity. Therefore, in a methodological scrutiny, care must be taken to verify whether the task design allows excluding such confounding factors.

Among many possible confounders, one frequently encountered issue in the Stroop task literature regards the so-called priming or sequential effects, which refer to the fact that performance at the current trial (trial n) is influenced by the (partial or total) repetition of the characteristics of the preceding trial (trial n-1). Priming effects are also related to a conflict adaptation phenomenon, also known as the Gratton effect or the congruency sequence effect, which is commonly observed during the execution of the Stroop task. The Gratton effect refers to the fact that the congruency of the preceding trials influences the performance in the current one, with a Stroop effect that is smaller after incongruent trials and larger after congruent ones (Gratton et al., 1992; Kerns et al., 2004). Although it is generally recognized that conflict monitoring processes, mediated by a neural system including the anterior cingulate cortex and the lateral prefrontal cortex, are responsible for this phenomenon (e.g., Botvinick et al., 2001), some theories have provided alternative explanations for it. A detailed discussion of this effect is outside the scope of the present work, so the reader is referred to eminent works on this topic (e.g., Algom & Chajut, 2019; Algom et al., 2022; Schmidt, 2023). However, two main non-strategic explanations have been put forward to account for sequential effects, which both suggest that differences in RT between trial n-1 and trial n are not the result of cognitive control strategies, but exclusively an artifact of repetitions/alternations of either features or responses (Puccioni & Vallesi, 2012a, 2012b, 2012c). The former, known as the priming account, posits that the repetition of one or both stimulus features leads to facilitation effects, whereas the change of both features causes longer RTs (Mayr et al., 2003; Nieuwenhuis et al., 2006). The other explanation relies on the Theory of Event coding, which accounts for binding-type effects in object perception and action planning and proposes the existence of the so-called event files that temporally associate perceptual and action codes. During each Stroop trial, the stimulus and response features are linked in such event files. This gives rise to processing costs if in the next trial only some but not all features of such integrated codes are repeated, due to the need of file updating. Therefore, this theory predicts that performance is hampered if the feature match is only partial, a phenomenon known as the partial-repetition cost (Hommel, 2004; Hommel et al., 2004).

Although these two accounts predict different effects on performance, they both agree on the fact that the number of shared features between two subsequent trials can influence the Stroop and congruency sequence effects, which would thus be biased or confounded by such repetitions. Therefore, to have unbiased estimates of Stroop (and congruency sequence) effects, it is clearly necessary to design priming-

free paradigms with a complete alternation in (at least) first-order trial sequences, that is, in the trial n both the relevant and irrelevant stimulus dimensions should be different as compared to the ones of trial n-1[4]. However, this cannot be achieved by using fewer than four possible irrelevant stimulus features and responses (i.e., the relevant stimulus features). For example, in a classical Stroop task, at least four color words in (the same) four ink colors should be used. Specifically, with three possible stimuli/responses, a repetition of either feature must inevitably occur in first-order trial sequence of two incongruent trials in a row (because each incongruent trial requires using two different features). Even worse, when using only two possible features/responses, only congruent-congruent sequences can be repetition-free, whereas this is unfeasible for any first-order trial sequence including an incongruent trial.

2.2.5. Methodological standards

Throughout the entire work, thus, the tasks used in the studies we reviewed will be evaluated according to whether they are really suitable for measuring the Stroop effect as a whole (complete Stroop effect), as in the classical color-word Stroop task.

To this aim, as necessary standards of methodologically adequate Stroop tasks, we will use:

1) The multiple loci account for the Stroop effect to assess whether the obtained Stroop effect is comprehensive of the effects at the three processing loci detailed above;

2) Kornblum's model to better evaluate the stimulus- and response-related processing levels assumed by multiple loci accounts. Specifically, we assessed whether the stimuli and responses employed ensure both stimulus-stimulus and stimulus-response overlaps.

Additionally, methodologically sound Stroop tasks should also employ experimental designs that allow controlling for confounding effects as much as possible (e.g., avoiding stimulus and response repetitions; see Section 2.4), to ensure measuring the Stroop effect with the necessary validity and reliability.

The importance of setting shared methodological standards arises from the great heterogeneity in the Stroop task literature. Indeed, under this umbrella term, several methodologically different experimental paradigms are included. Therefore, this confusion does not allow correctly interpreting their results, which are often conflicting, probably also due to the fact that the tasks actually measure partially, or even totally, different effects. The goal of the present review is thus to encourage the use of rigorous methodological

[4] It is here important to note that a complete alternation sequence at first-order trials (*n*-1) allows only to reduce binding and priming effects. Indeed, to completely exclude such effects, the repetition sequence of trials earlier than trial *n*-1 should be taken into account to completely exclude possible carryover effects.

criteria to design Stroop tasks, since starting from a common ground would allow having more adequate and valid Stroop effect measures.

The great heterogeneity in the Stroop literature also presented us with the need to use a unique inclusion criterion when selecting the studies, that is, the fact that the authors of the reviewed studies defined the task they used as a Stroop task. This general criterion is fundamental for our purposes of showing that, although all the tasks in the included studies were called "Stroop task" by the authors, many of them did not yield a complete Stroop effect.

2.3. Other Stroop tasks

So far, we have been discussing some methodological aspects relevant to the Stroop task, specifically focusing on the color-word version. However, several alternative adaptations of the color-word Stroop task have been proposed. Thus, we will next present its most known and used variants, discussing them and specifically considering the implications ensuing the methodological aspects we reviewed above.

2.3.1. The picture-word Stroop task

The picture-word Stroop task, also known as picture-word interference task, is an alternative variant of the classical Stroop task. It typically consists of a word (distractor) printed inside a picture (target), which participants are asked to name (e.g., Arieh & Algom, 2002; Lupker, 1979; Rosinski et al., 1975)[5]. As such, conflict between task sets is usually present in this Stroop task category as in the classical Stroop task. Commonly, this Stroop variant is considered similar to the classical color-word Stroop task due to the presence of an asymmetry between words and pictures, that is, the interference is greater from word-to-picture naming than from picture-to-word reading (MacLeod, 1991; Rosinski et al., 1975). However, whether the word-picture interference effect is analogous to the Stroop effect is still a debated issue, as some authors claimed that they are caused by the same mechanisms (e.g., van Maanen et al., 2009), while others argued for their difference, suggesting that the picture-word interference effect occurs only at the level of perceptual encoding (Dell'Acqua et al., 2007). It is probable that these controversial results are due to differences in task design, that is, some experimental manipulations make it conceptually similar to the classical Stroop task, whereas others generate other types of effects. In what follows, we propose a distinction between the major experimental manipulations, proposing some specific labels which, in our

[5] Other sub-variants of this task can also be used, such as those asking for categorization, that is, tasks requiring participants to identify the semantic category of the picture instead of naming it (e.g., Mayor et al., 1988). Picture-word Stroop versions demanding for tasks other than naming are not discussed here because in our view they differ by nature from the classical Stroop tasks since they, for example, necessarily imply lower degrees of overlaps (e.g., considering the entire category and not a single item reduces the overlap between the relevant and irrelevant stimulus dimensions).

view, could help reduce such heterogeneity. We would like to remind the reader that our aim is not to delve into the extensive and intricate literature on the picture-word Stroop task. Rather, our objective is solely to select specific studies as examples of the main manipulation types to examine whether they ensure a complete Stroop effect according to the criteria discussed above.

As outlined by Starreveld and La Heij (2017), semantic relevance, which is inversely related to the number of semantic categories from which the stimuli are selected, is important when comparing classical and picture-word Stroop tasks. Indeed, in the classical Stroop task, there is only one category, namely the color, whereas the number of semantic domains significantly varies across the existent picture-word interference experimental paradigms. This means that, when the picture-word Stroop task includes stimuli from the same semantic category, the produced effects can be equivalent or, at least, closer[6] to the classical Stroop effect. Indeed, in this case, both congruent and incongruent conditions, analogous to the classical Stroop task, are possible: In congruent trials, the picture and the word refer to the same concept (e.g., the picture of a cat with the CAT word superimposed on it; see Figure 2.1A), whereas in incongruent trials, they belong to the same semantic category but refer to different concepts (e.g., the picture of a cat with the BIRD word superimposed on it, which refers to another exemplar of the same semantic category of animals; see Figure 2.1A), producing interference (e.g., Piai et al., 2013; van Maanen et al., 2009). As such, the picture-word Stroop effect, similar to the Stroop effect, can be calculated by comparing incongruent trials with congruent ones. For this reason, this version has been widely used in the literature investigating the Stroop effect. For example, Bugg and colleagues (2011) used a picture-word Stroop task in which words corresponding to one of four animal names were superimposed onto pictures of the same four possible referents. Thus, all stimuli belonged to the same semantic category (for a similar task, see also Gonthier et al., 2016). Moreover, usually in such picture-word Stroop tasks with a single semantic category, all task-irrelevant stimuli are eligible responses in the experiment, which is typical in the classical Stroop tasks. Lastly, according to the dimensional overlap model, picture-word Stroop tasks with one semantic category are classifiable as type-eight ensembles, that is, a Stroop task. Indeed, they ensure not only both stimulus-response overlaps, when using vocal responses, but also the stimulus-stimulus overlap because, although there are two spatially overlapped stimuli, they always have a non-negligible semantic relationship.

For such a similarity, henceforth, we will specifically refer to this version of the task with the label picture-word Stroop task (see Figure 2.1A for an example), with the goal of distinguishing it from a conceptually different version, for which we will use the term picture-word interference task (Figure 2.1B). In the latter case, the task is the same, but the stimuli are taken from different semantic categories, and there are no congruent trials (i.e., trials in which the picture and the word both indicate the same concept),

[6] In fact, it also depends on the size of the stimulus set, which is necessarily limited for the color-word Stroop task, whereas can be potentially unlimited for the picture-word Stroop task.

but only trials with different degrees of picture-word semantic similarity[7]. Therefore, in this case the picture-word interference effect reflects the slowing in picture naming latencies when the picture is displayed with a conceptually related (but different) word –for example, the picture of a cat with the BIRD word superimposed onto it (see Figure 2.1B)– relative to when the word is unrelated –for example, the picture of a table with the CAT word superimposed onto it (see Figure 2.1B) (e.g., van Maanen et al., 2009, Shao et al., 2015).

The resulting picture-word interference effect was for long thought to originate during lexical access (the lexical selection by competition account, Roelofs, 1992; Vigliocco et al., 2004; see also the swinging lexical network account, Abdel Rahman and Melinger, 2009) or during other pre-response stages (i.e., perceptual encoding or activation of conceptual information, Dell'Acqua et al., 2007). So far the evidence is however scanty and contradictory (see Bürki et al., 2020 for a review). The underlying assumption is that when the task-irrelevant word is related to the target, its increased activation level yields competition for the lexical selection of the relevant picture, delaying its name retrieval during a naming task (e.g., Dell'Acqua et al., 2007; Roelofs, 1992). However, according to an alternative view, the response exclusion account, the semantic interference effect arises during the response execution (Mahon et al., 2007) and, thus, after the lexical access.

Therefore, the picture-word interference task produces a semantic interference effect that does not correspond to the one yielded by the classical Stroop task, also due to its semantic nature. Indeed, the semantic effect reflects selective inhibition, which is recruited when several responses are highly coactivated as part of the same response set, but it does not necessarily depend on the presence of an overt distractor stimulus. Therefore, semantic interference could be more similar to a semantic blocking effect, since both reflect selective semantic inhibition, rather than an effect yielded by interference resolution from an irrelevant distractor, such as the Stroop effect (Shao et al., 2015).

In addition to the difference in the underlying mechanism of the experimental effects we just discussed, two other main points have to be considered. First, in the picture-word interference task, the semantic relevance is lower compared to both the classical and the picture-word Stroop task because, to have unrelated trials, at least two semantic categories are typically used (e.g., objects and animals, as in Figure 2.1B). Thus, this important component of the Stroop effect will be small or even absent if many stimuli taken from many different semantic categories are used (Starreveld & La Heij, 2017). The presence of

[7] Nevertheless, in the literature, this distinction is not that clear. Indeed, some tasks can be placed in-between these two distinct forms. For example, Spinelli and colleagues (2019) used a paradigm that here we defined as picture-word Stroop task but, like in picture-word interference tasks, they used more than one semantic category. Therefore, in congruent trials they had proper Stroop stimuli (the word and the picture both refer to the same concept), while in incongruent ones, in which the word was superimposed onto semantically unrelated pictures, the semantic relevance was necessarily lower.

several semantic categories also raises consequent issues related to the semantic gradient between the picture and the word, namely the semantic similarity between the picture and the word categories, which might be a confounding factor.

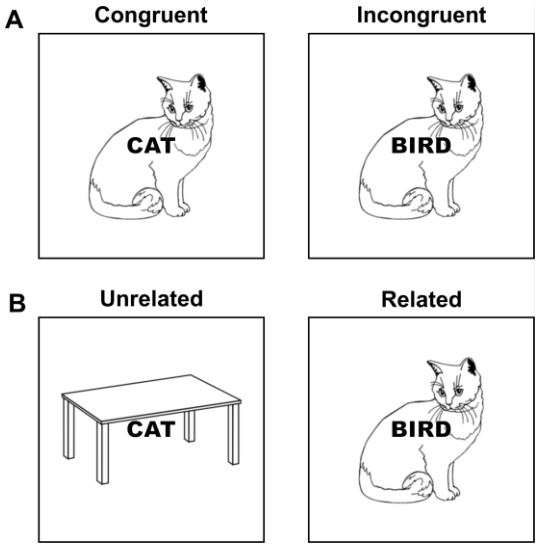

Figure 2.1.
A) Example of the picture-word Stroop stimuli. Participants respond to the picture while ignoring the superimposed word. In the congruent condition, both the task-relevant and task-irrelevant stimuli refer to "cat"), while in the incongruent conditions, the picture (task-relevant) refers to a different item compared to the word (task-irrelevant), but both belong to the same semantic category; **B)** Example of the picture-word interference stimuli. Participants name the picture, ignoring the superimposed word. In the unrelated condition, the task-relevant stimulus is not related to the task-irrelevant one, generating less interference, while in the related condition, the semantic relation between the picture (task-relevant) and the word (task-irrelevant) produces interference.

However, it is still controversial whether higher semantic similarity increases or decreases the experimental effect (Hutson & Damian, 2014), with some studies showing a greater effect for stimuli with greater semantic similarity (Vigliocco et al., 2004) and some others reporting the opposite pattern (Mahon et al., 2007). Therefore, it is not possible to choose semantic categories based on a reliable semantic gradient criterion to control for its confounding effect. A second fundamental difference is that the picture-word interference task involves a lower degree of response-set membership, since usually not all irrelevant words are part of the response set (Starreveld & La Heij, 2017). These methodological differences notwithstanding, the picture-word interference task can be classified as a type-eight ensemble, since there are both the stimulus-response overlaps, if the responses are vocal, and the stimulus-stimulus overlap whose degree, however, depends on the degree of semantic relevance/similarity.

Overall, if the aim is to investigate the Stroop effect, the picture-word Stroop task is preferable to the picture-word interference version, as the picture-word Stroop effect (congruent vs. incongruent) is a total Stroop effect as opposed to the picture-word interference effect (related vs. unrelated). However, although

this experimental paradigm has the advantage of allowing flexibility in the stimulus set selection and in the possible manipulations (e.g., MacLeod, 1991), there are some potential issues to consider, which depend specifically on its linguistic nature. In fact, these issues also regard the classical Stroop task but, since the picture-word Stroop task allows one to select a potentially infinite set of stimuli, the matter is even more relevant for it. First, the same issues described above for the picture-word interference task, related to the degree of semantic similarity between the picture and the word, still apply to the picture-word Stroop task. However, this aspect is usually not explicitly controlled for in existing studies. Moreover, even if the vast majority of picture-word Stroop studies have focused on words belonging to the same category and sharing semantic features, many types of semantic relations affect word processing (e.g., De Deyne et al., 2019; Montefinese & Vinson, 2015), but their impact on picture-word Stroop effects is far from clear. For example, the few picture-word interference studies that have manipulated thematically and associatively related words (i.e., linked by a common situation or thematic context, but belonging to different semantic categories; e.g., the words COW and PASTURE), found no effect or even a naming facilitation (Abdel Rahman & Melinger, 2007; Alario et al., 2000; Costa et al., 2005; de Zubicaray et al., 2013), in contrast to the semantic interference effect robustly observed for categorically related words (e.g., the words COW and RAT), in which semantic similarity is usually derived from a feature production task (McRae et al., 2005; Montefinese et al., 2013).

Moreover, although semantic manipulations have the greatest influence on the Stroop effect, it can also be influenced by phonemic, graphemic, orthographic, and lexical factors. In fact, the orthographic and phonological aspects of the task-irrelevant stimuli and their relation with the task-relevant ones contribute to the Stroop effect (MacLeod, 1991). Therefore, if such linguistic components are not taken into account and balanced or controlled for when designing a picture-word Stroop task (which is a daunting task, due to the very complex interrelations between them), they might influence the magnitude of the Stroop effect. Moreover, the use of linguistic stimuli makes it very hard to adapt these tasks (and all the linguistic variants of the Stroop task) to different languages and, therefore, to generalize conclusions drawn from studies employing them.

2.3.2. The numerical Stroop task

In the numerical Stroop task (see Figure 2.2A), firstly ideated by Henik and Tzelgov (1982), participants are presented with two Arabic digits, both of which are characterized by two dimensions: a physical one, namely font size, and a semantic one, namely numerical magnitude. The typical finding is that participants respond faster to numerically larger numerals appearing in a larger font size and to numerically smaller numerals appearing in a smaller font size (congruent trials) as compared to smaller numerals printed in a larger font size and to larger numerals printed in a smaller font size (incongruent trials), a phenomenon

known as size congruity effect (SCE; Henik & Tzelgov, 1982). Findings regarding the asymmetry direction are mixed, as a congruency effect has been observed for both physical and numerical judgments. Indeed, it is commonly found that physical judgments are affected by task-irrelevant numerical distance, suggesting that numbers have a greater intrusive effect on size judgments than vice versa (Dadon & Henik, 2017). However, also numerical judgments have been shown to be influenced by task-irrelevant physical size (Borgmann et al., 2011). The fact that the SCE can be reversed has been accounted for in some works, which highlighted that the direction of the SCE asymmetry strongly relies on the discriminability of the dimensions and the number of employed values. Therefore, the greater intrusive strength of numbers would occur because commonly a higher amount of number values is presented (e.g., nine values: from 1 to 9), against few options of physical sizes (e.g., two: large vs. small). As mentioned earlier, since it is not our intention to delve into these controversies, we refer the reader to more specific works on this topic (e.g., see Algom et al., 1996; Pansky & Algom, 2002).

Therefore, moving beyond the issue of the asymmetry of the effect and its direction, the numerical Stroop task generally entails conflict between two different tasks, namely physical and semantic judgments. What is less certain is whether the dimensional overlaps at the other processing loci, namely stimulus and response ones, are ensured by numerical Stroop paradigms. According to Kornblum's model, this task enables a dimensional overlap between the relevant and irrelevant stimulus dimensions. However, the stimulus attributes are relative and not absolute values, as they depend on the comparison between two different digit stimuli. Moreover, the so-called symbolic distance effect implies that the judgment speed is influenced by the numerical difference between the two numbers, with faster responses to larger differences (e.g., Tzelgov et al., 1992).

This potential reduction in stimulus-stimulus overlap is overcome by another Stroop adaptation that employs numbers as stimuli, the so-called counting Stroop task (Windes, 1968) (see Figure 2.2B). The counting Stroop task typically consists of presenting numerals (e.g., 1, 2, and 3) in groups of different quantities (e.g., one, two, or three numerals). Participants are required to name the quantity of the numerals, while ignoring their value. The counting Stroop effect arises because, in incongruent trials, where the numeral and quantity do not match (e.g., three 2s are presented, see Figure 2.2B), the response latencies are longer compared to congruent trials, where the numeral and quantity match (e.g., two 2s are presented, see Figure 2.2B). This alternative version ensures not only an asymmetry effect, as naming the quantities of numerals is generally slower than naming the numerals (at least when their perceptual saliency is similar), but also a stimulus-stimulus overlap that more closely resembles the classical Stroop task one.

On the other hand, the presence of a stimulus-response overlap in both the numerical and the counting Stroop tasks deserves some specification. First, only the counting Stroop task is suitable for vocal responses.

When this response modality is used, despite the non-linguistic nature of the task, a stimulus-response overlap is ensured. Indeed, according to the Triple Code Model (TCM) of numerical cognition, numbers have three representational codes, namely Arabic, verbal, and analogical magnitude codes (Dehaene, 1992). Thus, in the counting Stroop task, the verbal code of the response overlaps with the codes of both stimulus attributes, namely, the relevant one referring to the magnitude code and the irrelevant one referring to the Arabic code.

Alternatively, manual responses can be used in both tasks, that is, in the counting Stroop participants can be instructed to use the corresponding keypress responses (e.g., pressing the 1 vs. 2 vs. 3 keyboard buttons to the corresponding numerical quantity), whereas in the numerical Stroop they can provide lateralized manual responses (e.g., left vs. right button press to smaller vs. larger numerical magnitude). Apparently, according to Korblum's view, no stimulus-response overlap can be achieved when using manual responses, as in the counting Stroop there is no relation between the keypress buttons and either the numeral or the quantity, and in the numerical Stroop neither the physical size nor the numerical magnitude ensure such a relation. Nevertheless, in both tasks, the response might overlap with the stimulus if the response is considered to be compatible with the mental representation of magnitudes and numbers, based on the literature pointing out an association between space and numbers. Specifically, according to the Spatial-Numerical Association of Response Codes (SNARC) effect put forward by Dehaene and colleagues (1993), numerals are encoded and converted into magnitude representations and such magnitude information is organized spatially, for example, as a mental number line, with smaller numbers on the left and larger numbers on the right (e.g., Montefinese & Semenza, 2018; Winter et al., 2015). Therefore, there would be a preferential stimulus-response association between smaller magnitudes and left-side responses and larger magnitudes and right-side responses (e.g., Dehaene et al., 1993). Therefore, if the response keys are spatially arranged consistently with the mental number line and/or lateralized to distinguish between smaller and larger magnitudes, the stimulus-response overlap would be warranted. However, such SNARC-related overlap might be weaker than the classical Stroop overlap and not universal, since it may be affected by cultural factors (i.e., the direction of reading and writing; see Dehaene et al., 1993; Zebian, 2005; also see Vallesi et al., 2014, for an analogue phenomenon in the spatio-temporal domain). It is also worth mentioning that a recent registered replication report (Colling et al., 2020) failed to replicate the attentional SNARC effect (Fischer et al., 2003), questioning the strong link between numbers and space.

In general, numerical and counting Stroop tasks could be advantageous for studying cognitive control from a more ecological and flexible point of view (Dadon & Henik, 2017) and to reduce the influence of linguistic factors while still ensuring task conflict. However, they also present some drawbacks, especially the numerical Stroop task. In fact, the counting Stroop task is a type-eight ensemble regardless of the SNARC-related interpretation, whereas the numerical one strongly relies on the SNARC to be considered as

a Stroop task ensuring a stimulus-response overlap. Moreover, the experimental effects elicited by the numerical Stroop task might be affected by non-specific factors, such as the comparison time and the symbolic distance, making its measure less pure and threatening its measurement validity.

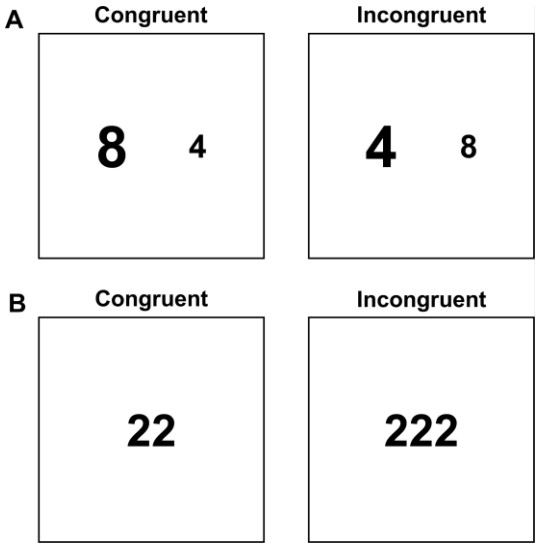

Figure 2.2.
A) Example of the numerical Stroop stimuli. Participants identify the numerically larger digit, while ignoring its physical size. In the congruent condition, the numerically larger digit is also physically bigger, whereas in the incongruent condition, the magnitude (task-relevant) is in contrast with the digit size (task-irrelevant); **B)** Example of the counting Stroop stimuli. Participants indicate how many digits are displayed, ignoring the digit value. In the congruent condition, the digit quantity and the digit value are the same, while in the incongruent condition, the digit quantity (task-relevant) differs from the digit value (task-irrelevant).

In general, numerical and counting Stroop tasks could be advantageous for studying cognitive control from a more ecological and flexible point of view (Dadon & Henik, 2017) and to reduce the influence of linguistic factors while still ensuring task conflict. However, they also present some drawbacks, especially the numerical Stroop task. In fact, the counting Stroop task is a type-eight ensemble regardless of the SNARC-related interpretation, whereas the numerical one strongly relies on the SNARC to be considered as a Stroop task ensuring a stimulus-response overlap. Moreover, the experimental effects elicited by the numerical Stroop task might be affected by non-specific factors, such as the comparison time and the symbolic distance, making its measure less pure and threatening its measurement validity.

2.3.3. The emotional Stroop task

The emotional Stroop task (McKenna, 1986; Williams et al., 1996) (see Figure 2.3) has been developed to examine attentional bias to emotional stimuli (Kappes & Bermeitinger, 2016). It requires participants to name the ink color of words, which can be either emotionally charged (e.g., the word DEATH), usually operationalized in terms of valence (i.e., the degree of pleasantness an individual feels toward a stimulus), or neutral (e.g., the word BOOK). In this task version, the interference effect is computed by subtracting the

RTs to identify the color of neutral words from those to name the color of emotional words, also referred to as the emotional Stroop effect (e.g., Cothran & Larsen, 2008; Larsen et al., 2006). The underlying assumption is that the emotional content of the word interferes with color naming, causing longer RTs in identifying the color of emotional words compared to neutral ones (Wentura et al., 2000). This is again based on the assumption that, when participants are presented with isolated words, they cannot ignore their semantic meaning because they automatically access it (Larsen et al., 2006). Therefore, like in the color-word Stroop task, in the emotional Stroop task there is a task conflict between the stronger word reading and the less strong color naming (Cothran et al., 2012).

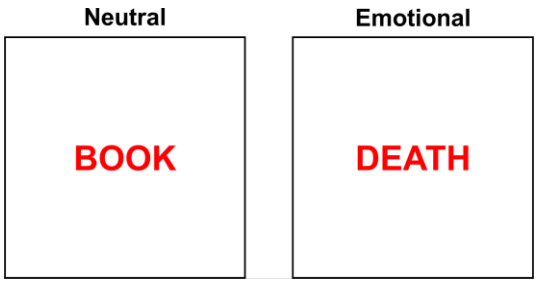

Figure 2.3.
Example of the emotional Stroop stimuli: Participants are requested to name the ink color, while ignoring the word meaning. In the neutral condition, the word has a neutral meaning, while in the emotional condition, the word is emotionally charged but task-irrelevant.

Still, the emotional Stroop task fundamentally differs from the classical Stroop task for several reasons. First, it lacks one of its fundamental properties, that is, the semantic relation between the relevant and irrelevant dimensions. More in detail, in the classic version of the Stroop task, the shared meaning of the compound stimuli allows manipulating the semantic congruency between such dimensions. In contrast, in the emotional Stroop task, there is no semantic or logical relationship between the relevant feature, namely the ink color, and the irrelevant feature, namely the emotional meaning of the word. This prevents generating congruent and incongruent trials and, consequently, the classical Stroop effect cannot be calculated (Algom et al., 2004; Cothran et al., 2012). The lack of semantic relationship between stimulus dimensions also entails no response-set membership because emotional words can never be part of the response set, thus no response conflict/facilitation can be produced.

Another critical aspect of the emotional Stroop task is the absence of lexical equivalence among emotional and neutral words. This represents a crucial difference from the color-word Stroop task, in which each word is presented in both congruent and incongruent conditions, causing an important methodological drawback. As such, Larsen and coworkers (2006) pointed out that the emotional Stroop is a quasi-experimental paradigm, because it does not allow having proper control conditions, as emotional words necessarily differ from control neutral words. Related to this point, there is still another difference from the classical Stroop task. Indeed, while in the classical paradigm the experimental effect can be

calculated at the item level (i.e., for every color word), in the emotional version, it can be measured only at the list-wide level: the absence of congruent and incongruent conditions allows only to compare mean RTs in naming the color of the emotional vs. neutral word lists (Algom et al., 2004; Larsen et al., 2006). Thus, the slowing of responses to emotional stimuli does not reflect a Stroop-like effect, but it could simply reflect a generic slowing to emotional stimuli. Specifically, Algom and colleagues (2004) argued for an automatic vigilance account for such an effect, showing that longer RTs to threat-related stimuli are not specific to the emotional Stroop task requiring ink color naming, but can be observed also in other tasks such as lexical decision tasks, reading speed, and word naming.

Finally, the emotional Stroop task does not allow controlling for possible confounding factors due to the linguistic nature of the stimuli. Indeed, what we highlighted regarding the potential role of confounding linguistic effects in the picture-word Stroop task also applies to the emotional Stroop task. Indeed, the emotional interference effect could also be affected by semantic, lexical, orthographic, or phonological factors, whose effect might be difficult to balance or control for. These aspects are more relevant for this task, compared to the color-word Stroop task, not only because it usually employs a much larger set of stimuli, but especially for the well-known differences that exist between emotional and neutral words, such as the fact that words with affective content generally are longer and have a smaller number of orthographic neighbors than the neutral ones (Larsen et al., 2006; see also Montefinese et al., 2013). Recently, in a multi-experiment study, Crossfield and Damian (2021) addressed this issue by matching neutral and emotionally-valenced words for a number of lexico-semantic variables in an emotional Stroop task. The authors observed that the participants' performance was mostly affected by semantic variables such as the word semantic diversity (i.e., a computationally derived measure of semantic ambiguity based on the variability of the different contexts in which a given word is used; Hoffman et al., 2013) and concreteness (i.e., the extent to which a word is related to sensorial experience), but also the word arousal (i.e., the degree of excitement or activation an individual feels toward a given stimulus, varying from calm to exciting). These results contribute to the longstanding debate on whether valence or arousal alone can produce the emotional Stroop effect. Moreover, they suggest that the valence effect is not powerful enough to generate the emotional Stroop effect by itself once other confounding variables are taken into account.

From Kornblum's model point of view, the lack of conceptual similarity between the relevant and irrelevant dimensions also implies the absence of a stimulus-stimulus overlap. Moreover, this task does not ensure any dimensional overlap between the irrelevant characteristic of the stimulus and the response, as neither vocal nor manual responses can overlap with the emotional meaning of the word. Therefore, the emotional Stroop is not even classifiable as a Stroop-like task.

In addition to the classical emotional Stroop variation, face-word Stroop tasks have been used in the literature as alternative emotional adaptations. Specifically, participants are presented with emotional

words superimposed on faces whose emotional valence can be either congruent or incongruent with the word (e.g., the word HAPPY superimposed onto a face that expresses either happiness or sadness, respectively; Song et al., 2017). Since this experimental paradigm is an emotional form of the picture-word Stroop task, it suffers from the same issues as described above for that task, namely those related to lexical and semantic factors. Moreover, according to the dimensional overlap model, face-word Stroop tasks cannot be classified as type-eight ensembles because, although they ensure a stimulus-stimulus overlap, since the task-relevant and task-irrelevant stimuli have a relationship based on the presence vs. absence of emotion, they can never have a complete stimulus-response overlap, because there is no face-response overlap, regardless of the type of responses used, that is, not even when vocal responses are used (assuming that emotion recognition does not necessarily activate lexical processing).

Overall, both versions of the emotional Stroop task are thus methodologically incomparable with the classical Stroop task. However, if the specific aim is to explore the effect of emotions on Stroop effect resolution, alternative emotional adaptations of the Stroop task may exist, such as the emotional priming Stroop task, in which an emotional vs. non-emotional prime stimulus is presented prior to a classical Stroop target stimulus. Recently, this experimental paradigm has allowed us to investigate how emotional processing affects conflict resolution, comparing neutral vs. sad face stimuli (see Visalli et al., 2022, for further details). This task represents a better alternative as compared to the other emotional Stroop tasks because, while the embedded Stroop task ensures all the required conflict types, including all the dimensional overlaps, it also allows exploring the influence of priming task-irrelevant emotional stimuli on the conflict/facilitation arising immediately after. The emotional priming Stroop task also overcomes another limitation of the emotional Stroop variants, namely lexical and semantic confounds, for example, by using faces or images as emotional priming stimuli, as in our recent study (Visalli et al., 2022).

2.3.4. Other Stroop tasks: conclusions

Taken together, it seems that the majority of the most known Stroop task variations present some theoretical and methodological issues, since they do not fulfill the criteria for yielding a Stroop effect comprehensive of the three required loci-related effects and/or are susceptible to potential confounding issues. Specifically, while it seems that the emotional Stroop and picture-word interference tasks tap on mechanisms that are different from the color-word Stroop task, this is not true for the other Stroop adaptations. In fact, the picture-word Stroop task entails both stimulus- and response-related interference/facilitation, as well as task interference, and has all the required overlaps, but the use of linguistic stimuli that are not only colors increases the possibility that confounding factors, such as the semantic gradient, influence the Stroop effect. This limitation can be overcome by the counting and numerical Stroop tasks, but their Stroop effect, in turn, might be affected by symbolic distance. Moreover,

these tasks, especially the numerical Stroop one, have a SNARC-related stimulus-response overlap. Hence, although these alternative versions have some advantages for specific research topics, using the label "Stroop task" for them is, in some cases, inappropriate from a methodological point of view, as the experimental effects they produce rely on totally or partially different mechanisms. Moreover, even those alternative versions that ensure a complete Stroop effect have some drawbacks that potentially affect it and are difficult to control.

Since our aim is to highlight the importance of methodological rigor when designing Stroop tasks to ensure complete Stroop effects with the required measurement validity, the previously discussed alternative versions seem less adequate. For this reason, here we propose the spatial Stroop task as an alternative Stroop adaptation that potentially meets the required criteria and overcomes the drawbacks of the other versions. In the next section, we discuss this task in more detail, highlighting why it might be preferable compared to the other task versions reviewed above.

2.3.5. The spatial Stroop task

The spatial Stroop task explores the interference/facilitation produced by irrelevant spatial information. Typically, verbal or symbolic stimuli are used to combine a semantic attribute indicating a spatial location with an attribute designating a physical position. As in the classical version, the stimuli can be either congruent or incongruent, depending on whether the physical position corresponds or not with the semantic attribute, producing interference in the second case (see Lu & Proctor, 1995, for an overview). For example, when a location word (i.e., LEFT, the semantic attribute) is presented in an incongruent physical position (i.e., right), RTs are longer compared to congruent conditions (i.e., LEFT presented at the left location) (Pang et al., 2020). From this general definition, it can be noticed that the term spatial Stroop does not necessarily refer to a purely spatial version of the Stroop task, as sometimes verbal stimuli, despite referring to spatial attributes, are employed. However, purely spatial versions of this task can be designed, for example, by replacing location words with non-verbal semantic attributes, such as arrows. Later in this section we will provide some examples of pure spatial Stroop versions, and we will discuss why such pure variants are preferable.

Before that, we will point out why, potentially, the spatial Stroop task can be considered as a methodologically valid alternative version of the Stroop task. To this end, we will use as an example a simple version of a purely spatial paradigm, wherein participants use right-left keypresses to respond to the direction of an arrow (i.e., right- vs. left-pointing) while ignoring the position on the screen where it appears (i.e., in the right or in the left side of the screen). The arrow direction is the relevant information, whereas its position is the irrelevant one. This task works exactly as the classical Stroop task, as it also entails an asymmetric relation between the stimulus dimensions (Lu & Proctor, 1995) and yields a conflict between

two competing task sets. Indeed, it is assumed that the position of a visual stimulus is processed more strongly than its other visual characteristics, such as the pointing direction of an arrow (Viviani et al., 2023). In addition to task conflict, this task entails both stimulus- and response-related conflicts/facilitations and, according to Kornblum's dimensional overlap model, it can be classified as a type-eight ensemble. The three overlaps are indeed all present and, specifically, they can be observed between: (i) the relevant stimulus attribute (direction) and the irrelevant one (position), (ii) the relevant stimulus attribute and the response dimensions, and (iii) the irrelevant stimulus attribute and the response dimensions[8]. The presence of a dimensional overlap between the stimulus dimensions and the response, namely the last two criteria, is strictly related to the response modality, as discussed above. Indeed, to obtain stimulus-response compatibility, responses need to overlap with irrelevant and relevant stimulus attributes. In purely spatial Stroop versions, as in the case of our example, the spatial arrangement of the keypress responses overlaps with each stimulus dimension due to the spatial nature of both the relevant and irrelevant stimulus attributes. By contrast, had the task been designed with vocal responses, or even with non-overlapping manual responses, such overlap would not have been possible.

Overall, the possibility of obtaining a complete Stroop effect with the spatial Stroop task suggests that it represents a valid adaptation of the classical paradigm. Besides being methodologically similar, the spatial Stroop version offers some advantages over the classical vocal Stroop task. The three main advantages are: (i) it does not rely on linguistic processing, as discussed above, (ii) the spatial nature of the stimuli might foster a more domain-general investigation of cognitive control, minimizing the confounding role of linguistic demands, and (iii) it requires manual responses, which are less prone to assessment errors and more suitable for neuroimaging and online studies than verbal responses (for a more detailed discussion, see Viviani et al., 2023).

Taken together, these advantages are related to the fact that the classical Stroop is in general more complex and prone to confounding. Indeed, as discussed above, due to its linguistic nature, the produced interference/facilitation effects might be influenced not only by the semantic relationship between the relevant and irrelevant dimensions, but also by a number of other linguistic variables, which are related to each other in such a complex way that it is very hard to control for them appropriately. Moreover, as we have already mentioned, the use of linguistic materials makes it harder to adapt these variants to other

[8] According to Kornblum's taxonomy, for spatial Stroop tasks employing only spatial stimuli to obtain a type-eight ensemble, responses must be manual (to ensure the overlap between the irrelevant dimension and the response). Therefore, the spatial Stroop effect inevitably includes the Simon effect (representing a type-three ensemble, thus lower in the hierarchy of overlaps), but this does not mean that the Stroop effect is made less pure by the effect of lateralized responses. Rather, lateralized responses are fundamental to ensure the required stimulus-response overlaps and, when responses to spatial stimuli are made vocally, only type-four ensembles and Stroop-like tasks are obtained. It is also important to note that type-eight-ensemble spatial Stroop tasks also inevitably include the Flanker effect (representing a type-four ensemble), which derives from the required stimulus-stimulus overlap.

languages and limits the generalizability of the obtained results and conclusions. For these reasons, the spatial variant represents a valid alternative to bypass these potential drawbacks.

However, it is worthwhile noting that these advantages hold specifically for purely spatial paradigms because they are the only adaptations in which a complete Stroop effect can be elicited. Indeed, in spatial Stroop paradigms comprising both verbal and spatial stimuli, the choice of response modality is more problematic, since there is evidence suggesting that keypress responses to word meaning are affected by irrelevant stimulus position, whereas the interference is much smaller in the opposite direction; moreover, vocal responses to location are influenced by irrelevant word meaning, but not vice versa (Lu & Proctor, 1995). However, notwithstanding the correct response modality being employed, in the mixed versions, the dimensional overlap is necessarily limited to either relevant stimulus and response or irrelevant stimulus and response dimensions, whereas both these overlaps are not simultaneously achievable. Moreover, spatial paradigms with verbal stimuli do not allow a complete reduction of the involvement of linguistic processing, with the consequent limitations outlined above.

In the next section, we shall present an overview of the spatial Stroop tasks that have been used in the literature. Of note, our work does not intend to be a systematic review of the literature on the spatial Stroop task, but has the explicit aim of focusing on the methodology of these paradigms. For this reason, we will not discuss the results of such studies in detail.

2.4. The spatial Stroop task in the literature

Our search for spatial Stroop studies showed that there is a great variety of task versions, as a plethora of stimulus types and manipulations have been used. Hence, to make our discussion more systematic, we will distinguish three categories among which, in our view, only the third one has the potential to yield a complete spatial Stroop effect: position-word, arrow-word, and arrow-position tasks.

2.4.1. Position-word spatial Stroop tasks

In position-word tasks, words designating spatial locations are displayed in congruent or incongruent positions on the screen (see Figure 2.4A). It is noteworthy that in the literature words and positions are usually both considered to be processed in an equally strong way (at least when their perceptual saliency is kept similar). Therefore, when using them together, an asymmetry effect seems less likely as, at least in principle, none of the two tasks appears obviously stronger than the other. The lack of such an asymmetry can be noticed in the studies we will discuss, as some require word reading, while others position naming. Of note, being typically equal the strength of these two tasks, the spatial Stroop effects might also be driven by the effect of discriminability (as discussed above and as predicted by Algom & Chajut, 2019).

Some of the first studies using the spatial Stroop belong to this category, such as the one conducted by White (1969), in which the words NORTH, SOUTH, EAST, and WEST could appear in one of these four positions, and participants had to vocally indicate the position of the word, while ignoring its meaning. Therefore, besides the stimulus-related effects due to the stimulus-stimulus overlap and the task-related conflict, this task has an irrelevant stimulus-response overlap but not a relevant stimulus-response overlap; thus, it still does not produce full response-related effects.

In a more recent study, Luo and Proctor (2013) designed three spatial Stroop paradigms, all of which had in common that both relevant and irrelevant stimulus dimensions referred to “up” or “down” attributes, and participants were instructed to respond using bimanual right-left keypresses to ensure that responses were orthogonal to the relevant stimulus dimension. In Experiment 1, they presented the Chinese characters for UP and DOWN, appearing above or below on the screen. Participants were first asked to respond to the word and, in a second session, to respond to its location. Overall, regardless of their type, the stimuli did not overlap with the response, thus hindering any conflict/facilitation emergence at the level of response. However, both task conflict and stimulus-stimulus overlap were ensured. The other task variations used in that study (Luo & Proctor, 2013) will be discussed in the arrow-word spatial Stroop task section.

In Hilbert and colleagues' study (2014), participants were presented with four squares in the upper, lower, right, or left portions of the screen. The German words for UP, DOWN, RIGHT, and LEFT appeared within one of these four squares and participants were instructed to respond to the square position independently of the word meaning. All participants performed both an analog version of the task, in which they responded verbally, and a digital version, wherein they used four spatially arranged keypresses as the four locations. Therefore, in the analog version, the relevant stimulus did not overlap with the response, whereas in the digital version, the irrelevant stimulus did not overlap with the response. Thus, in neither case, conflict/facilitation effects at the level of response locus could be ensured. Nevertheless, the resultant Stroop effect included conflict at the task level and stimulus-related interference/facilitation.

Pickel and colleagues (2019) presented participants with the same four direction words (UP, DOWN, RIGHT, LEFT), but they could appear only in two possible locations, each obtained from a mix between two physical positions in space (upper right or lower left). Button presses were used for responses to word meaning, thus allowing an overlap only between the irrelevant stimulus and the response. Moreover, this paradigm had a lower degree of overlap between relevant and irrelevant stimulus dimensions, because there were four relevant stimuli but only two irrelevant dimensions, not ensuring full experimental effects at the stimulus level. Thus, in this study, the Stroop effect was driven mainly by the task conflict.

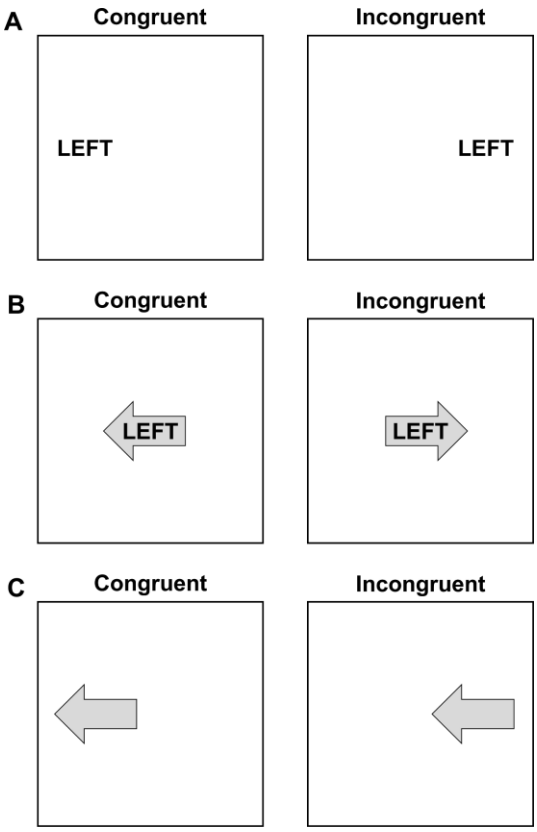

Figure 2.4.
A) Example of the position-word spatial Stroop stimuli. Participants identify the physical position on the screen of a word designating a spatial location (i.e., LEFT word). In the congruent condition, the spatial location word is presented in the same physical position it denotes, whereas in the incongruent condition, the spatial location word (task-relevant) is in contrast with the physical position (task-irrelevant) where it appears. The task can also be reversed, that is, participants name the physical position of the word, ignoring its meaning. In this case, the task-relevant feature is the physical position, whereas the task-irrelevant feature is the spatial location designated by the word. **B)** Example of the arrow-word spatial Stroop stimuli. Participants name the direction of the arrow (i.e., left), ignoring the meaning of the spatial word printed inside. In the congruent condition, the arrow points toward the same spatial position designated by the word, whereas in the incongruent condition, the arrow direction (task-relevant) is in contrast with the spatial location denoted by the word. The task can also be reversed. **C)** Example of the arrow-position spatial Stroop stimuli. Participants identify the direction pointed by the arrow (i.e., left), ignoring the position where the arrow appears. In the congruent condition, the arrow points to the same direction as its physical position, whereas in the incongruent condition, the arrow direction (task-relevant) is in contrast with its physical position (task-irrelevant).

One last example of this category is the study conducted by Schneider (2020), who designed two position-word spatial Stroop tasks. One required participants to respond to the words RIGHT and LEFT, appearing on the right or left of the fixation, while the other required participants to respond to the words UP and DOWN, positioned above or below the fixation. Notably, in both paradigms, responses were bimanual and were made by pressing spatially compatible keys, ensuring also an irrelevant stimulus-response overlap. Thus, the effect of conflict/facilitation was produced at the stimulus locus but not completely at the response locus, missing the relevant stimulus-response overlap. Although task conflict

was also ensured, this paradigm did not produce a complete Stroop effect, besides not being priming-free as only two stimuli were employed (i.e., feature repetitions could not be avoided).

2.4.2. Arrow-word spatial Stroop tasks

Arrow-word tasks entail presenting words referring to directions, embedded in or flanked by arrows (see Figure 2.4B). Differently from position-word arrow Stroop tasks, an asymmetrical relation is possible, as word reading may be conceivably assumed to be stronger than direction identification. Despite that, in the following studies, word reading was not always a task-irrelevant process, and this could be interesting for further investigating the actual existence of such an asymmetry.

One of the first examples is the study conducted by Shor (1970), in which the word names of directions (UP, DOWN, RIGHT, LEFT) were embedded in arrows pointing to these four directions. The task was first to name the arrow direction and then to read the words, guaranteeing in both cases a conflict between task sets. The asymmetry was confirmed, as the naming of arrow directions was slower than the reading of words. Furthermore, this task design ensured the experimental effects at the stimulus locus, thanks to the stimulus-stimulus overlap, but not at the response locus, as the stimulus-response overlap was not complete and depended on the task at hand (i.e., when the task was direction naming, there was an overlap between the irrelevant stimulus and the response, and when the task was word reading, there was an overlap between the relevant stimulus and the response).

Luo and Proctor's (2013) study, which was already introduced in the position-word spatial Stroop task section, included two more experiments, wherein the same direction words (Chinese words for UP and DOWN) were either embedded in an up- or down-pointing arrow (Experiment 2) or flanked by an up- or down-pointing arrow (Experiment 3). Participants again underwent two sessions, responding to the direction word and then to the arrow direction. The major drawback of these two tasks was the same as the position-word one, that is, the total absence of response-related conflict/facilitation, as there was no stimulus-response overlap, due to the orthogonality of the right-left keypress responses.

A very similar study was conducted by Pang and coworkers (2020). To investigate global precedence, they presented participants with Chinese characters (UP, DOWN) embedded in up- or down-pointing arrows and asked them to respond to the character meaning or to the arrow direction by means of right-left keypress responses. In a second experiment, they reversed the stimuli, embedding the arrows in the Chinese characters. Again, according to our view, the Stroop effect was not complete, as by lacking stimulus-response overlap, it did not ensure producing experimental effects at the response locus.

2.4.3. Arrow-position spatial Stroop tasks

In arrow-position tasks, participants are instructed to respond to the direction of an arrow regardless of its position on the screen (e.g., Pires et al., 2018; see Figure 2.4C). In this task, there is an asymmetry between position and direction, as the former task is stronger than the latter.

This variant was used by Funes and coworkers (2007) in a paradigm combining a spatial Stroop task with spatial cueing. The spatial Stroop paradigm consisted of responding to the direction of right-/left-pointing arrows appearing either at the right or at the left of a fixation cross. Among the several experimental manipulations, of interest here is the one regarding response compatibility. More in detail, keypress responses were spatially compatible (e.g., left key for left direction) or incompatible, when the opposite response mapping was used. According to Kornblum's model, only the former case ensures stimulus-response overlap, since the spatial arrangement of the response keys was compatible with the arrow directions and, as a consequence, full response-related effects were generated. In contrast, when the response keys were incompatible, there was no overlap between stimulus and response and no effects at the response locus. In both cases, both task conflict and stimulus-related conflict/facilitation were guaranteed, but priming effects could not be ruled out.

Luo and colleagues (2010) presented up-/down-pointing arrows positioned along the vertical axis and used bimanual right-left keys for responses. Although their aim was to have a pure measure of the Stroop effect, the response key spatial arrangement did not allow for a stimulus-response overlap, and consequently a complete Stroop effect, since it ensured only task conflict and stimulus-related conflict/facilitation.

In Pires and colleagues' (2018) study, participants responded to right-left arrow directions, appearing in one of two lateral boxes (on the right or left of a central box). Responses were made using bimanual right-left button presses. Therefore, according to our methodological criteria, this paradigm produced a Stroop effect comprehensive of all required loci: task conflict, stimulus-related effects due to stimulus-stimulus overlap, and response-related effects due to stimulus-response overlaps. However, the use of only two characteristics makes it vulnerable to priming effects.

In a very recent study, Paap and colleagues (2020) used two versions of the spatial Stroop. The first version was a horizontal arrow Stroop task, with right and left arrows displayed on the right or left of the fixation, whereas the second one was a vertical arrow Stroop task, with up and down arrows presented either above or below the fixation. During both tasks, participants were instructed to respond to the direction of the arrow, using bimanual right-left keypress responses and ignoring position, generating task-related conflict. As highlighted by the authors, the horizontal task ensured both stimulus-stimulus and stimulus-response overlaps, and thus all the three processing loci, while the vertical version generated an

overlap only at stimulus-stimulus level, but not at stimulus-response level, as the response keys were orthogonal to the direction of the arrows, impeding the effects to emerge at the response level.

In the same study discussed previously (see position-word spatial Stroop task section), Schneider (2020) proposed two versions of an arrow-position spatial Stroop task, one with a horizontal alignment and another with a vertical alignment. In the former, participants were instructed to indicate the direction of right-/left-pointing arrows appearing either on the right or the left of the fixation, whereas in the latter they responded to the direction of up-/down-pointing arrows appearing either above or below the fixation. Bimanual responses were made using compatible keypresses, as they were located as a function of the stimulus spatial alignment, thus having the potential to produce in both tasks not only stimulus-stimulus overlap and stimulus-related effects, but also stimulus-response overlaps and complete response-related effects.

Lastly, a very recent study by Spinelli and colleagues (2022) explored conflict adaptation using the color-word task (Experiment 1) and the arrow-position Stroop task (Experiment 2). In the spatial Stroop task, participants responded to one of six possible arrow directions (north-east, east, south-east, south-west, west, north-west), which could appear in one of six circles spatially arranged in the same six locations. Responses were made using keypress buttons whose spatial arrangement was compatible with arrow directions and positions. Hence, this experimental paradigm ensured all the conflicts/facilitations assumed by multiple loci accounts, that is, task conflict, stimulus-related effects due to the stimulus-stimulus overlap, and complete response-related effects due to the stimulus-response overlaps, despite a complex 6x6 stimulus-response mapping.

2.4.4. Methodological considerations

From this methodological review, the first aspect worthy of consideration is that spatial Stroop paradigms involving only effects at the task and stimulus levels, without the involvement of response locus due to totally or partially missing stimulus-response overlaps, seem quite common (see Figure 2.5). Indeed, several authors deliberately declared to use only stimulus-stimulus congruency to have more pure spatial Stroop effects, and explicitly distinguished it from stimulus-response congruency, regarded as a possible confound and/or as typical of just the Simon congruency effect (e.g., Funes et al., 2010; Luo et al., 2010, 2013). However, as highlighted above, both stimulus-stimulus and stimulus-response overlaps are required to obtain a complete spatial Stroop effect. Designing tasks to measure the Stroop effects in a methodologically rigorous way is not an end in itself, but is of fundamental importance to measurement validity (and all the other forms of validity that depend on it) and, in turn, the improvement of Stroop measure validity is essential to enhance our theoretical knowledge about cognitive processes involved in the Stroop task. Indeed, the use of experimental paradigms that only tap on some mechanisms and ignore

others, such as those that measure only task-related and stimulus-related effects, is inconsistent with the goal of obtaining an accurate measure of the Stroop effect because they do not consider the response locus, which is instead involved in Stroop tasks. Of course, if the aim of the study is to explicitly focus on one of the underlying mechanisms, this is warranted, but this has to be clearly stated (and in this case the label Stroop-like task is preferable). Moreover, the use of heterogeneous tasks does not allow us to compare their results across studies, since, if these tasks are inherently different, they inevitably measure different phenomena. Thus, if the Stroop effect includes multiple loci, that is, it involves processing at the level of task, stimulus, and response loci, it is clear that one needs to design tasks encompassing all these loci to obtain a measure as complete as possible.

Secondly, as we previously foreshadowed, position-word and arrow-word spatial Stroop tasks are not ideal versions of this paradigm. Besides not being pure spatial Stroop tasks, some of these mixed variants were not Stroop tasks due to the response modality employed. Since the presence of response effects depends on it, the response modality when the irrelevant stimulus was spatial should have been distinguished from when it was verbal. However, this was not the case, as the majority of studies entailed manual responses, regardless of these theoretical considerations. However, although this assumption was met, the simultaneous presence of a verbal and spatial stimulus would prevent a complete overlap between the stimulus and the response, as the response could overlap only with either the irrelevant or the relevant stimulus, but not with both at the same time, consequently hindering a full conflict at the level of response.

Therefore, in our view, the spatial Stroop tasks that most adhere methodologically to a complete Stroop task definition are the purely spatial ones, such as the arrow-position tasks. Indeed, from a methodological point of view, they are preferable because they potentially guarantee the possibility to produce effects at all the three required loci, ensuring all Kornblum's dimensional overlaps. However, this was not true for a minority of arrow-position tasks which, totally or partially, did not involve the response locus (e.g., Luo et al., 2010). Figure 2.5 summarizes our methodological considerations based on our criteria.

In addition to these considerations, the present literature overview allowed us to notice a further methodological limitation concerning all of the three categories, which should be taken into account when designing a spatial Stroop task. This limitation, specifically, is that the majority of the studies used two-alternative forced-choice tasks, that is, in most of them the relevant/irrelevant dimensions were right vs. left or up vs. down, but rarely more stimuli and responses were used in the same task. The oldest paradigms (Shor, 1970; White, 1969) and few more studies (e.g., Hilbert et al., 2014; Pickel et al., 2019) were exceptions. This is a kind of pitfall, as it poses limitations in the manipulation of the trial list sequence and does not allow controlling for the effect of (partial and total) feature repetition and consequent priming phenomena. Indeed, as outlined above, to provide unequivocal evidence of real congruency and sequential effects, priming-free paradigms with a complete alternation sequence are required at least in first-order

trials. However, as noted in Section 1.3.4, it is impossible to have complete repetition-free sequences by using fewer than four possible responses. Indeed, with three responses, if there are two incongruent trials in a row, one feature must inevitably be repeated in the second trial. The influence of repetition effects appears to be even stronger in the spatial Stroop paradigms we discussed previously, since most of them used two possible alternative responses, in which only congruent-congruent sequences can be repetition-free. To solve this issue, Puccioni and Vallesi (2012a, 2012b, 2012c) designed a four-alternative forced choice spatial Stroop task, which has been shown to properly separate interference resolution from priming effects at least at first-order sequences (priming effects could in principle still be carried out in part from trials earlier than trial n-1).

In the last section of this review, we show that it is possible to design a spatial Stroop task that overcomes the outlined methodological limitations, and provide some examples.

	Study	Task locus	Stimulus locus	Response locus	
			rStim-iStim	rStim-Resp	iStim-Resp
POSITION-WORD	Hilbert et al., 2014 (analog version)	☑	☑	☒	☑
	Hilbert et al., 2014 (digital version)	☑	☑	☑	☒
	Luo & Proctor, 2013 (Exp.1)	☑	☑	☒	☒
	Pickel et al., 2019	☑	▲	☒	☑
	Schneider, 2020 (horizontal)	☑	☑	☒	☑
	Schneider, 2020 (vertical)	☑	☑	☒	☑
	White, 1969	☑	☑	☑	☒
ARROW-WORD	Luo & Proctor, 2013 (Exp. 2)	☑	☑	☒	☒
	Luo & Proctor, 2013 (Exp. 3)	☑	☑	☒	☒
	Pang et al., 2020 (Exp. 1)	☑	☑	☒	☒
	Pang et al., 2020 (Exp. 2)	☑	☑	☒	☒
	Shor, 1970 (Exp. 1)	☑	☑	☒	☑
	Shor, 1970 (Exp. 2)	☑	☑	☑	☒
ARROW-POSITION	Funes et al., 2007 (compatible mapping)	☑	☑	☑	☑
	Funes et al., 2007 (opposite mapping)	☑	☑	☒	☒
	Luo et al., 2010	☑	☑	☒	☒
	Pires et al., 2018	☑	☑	☑	☑
	Paap et al., 2020 (horizontal)	☑	☑	☑	☑
	Paap et al., 2020 (vertical)	☑	☑	☒	☒
	Schneider, 2020 (horizontal)	☑	☑	☑	☑
	Schneider, 2020 (vertical)	☑	☑	☑	☑
	Spinelli et al., 2022	☑	☑	☑	☑

Legend
☑ Satisfied
☒ Not satisfied
▲ Partially satisfied

Figure 2.5.
Summary of the methodological criteria met by each spatial Stroop task, also including Kornblum's overlap levels. rStim, task-relevant stimulus feature; iStim, task-irrelevant stimulus feature; Resp, response.

2.5. Examples of complete spatial Stroop tasks

Puccioni and Vallesi (2012a) designed a spatial Stroop paradigm that satisfies the methodological requirements and overcomes the previously discussed limitations (see Figure 2.6). The task was an arrow-position task consisting of an arrow pointing to four possible directions (upper right, upper left, lower right or lower left) that could appear in one of four positions on the screen (upper right, upper left, lower right or lower left). Participants were instructed to respond to the pointing direction of the arrow by pressing the corresponding key and ignoring the arrow position. Besides being purely spatial, this paradigm ensures a complete Stroop effect, as it encompasses all the required processing loci. Indeed, there is conflict between two different tasks, position and direction identification, with the former being stronger than the latter. Moreover, at the stimulus locus, there is a dimensional overlap between the relevant and irrelevant stimulus dimensions, since the arrows could appear in one of the four corners of the screen and point to one of the same four directions. Lastly, since the spatial arrangement of the response keys is compatible with the direction and position of the stimuli, the dimensional overlap between both stimulus dimensions and the response dimension was also ensured, implying that conflict/facilitation at the response level is complete. Furthermore, the presence of four arrows and four positions allows for a complete alternation of the stimulus feature across first order trial sequences, so that the direction and position of the stimuli in trial n always differ from the direction and position in trial n-1 (Puccioni & Vallesi, 2012b). Notably, in a previous study, we have found that its spatial Stroop effect has a good split-half reliability (0.767) (Capizzi et al., 2017) and that this task is suitable for being implemented with EEG (Ambrosini & Vallesi, 2017; Tafuro et al., 2019), also with mouse responses (Tafuro et al., 2020).

Puccioni and Vallesi's (2012a) paradigm is well suited to variations; indeed, alternative versions of it can be designed that allow satisfying the methodological criteria that we consider fundamental to have a complete Stroop effect. This is what we did in our recent study (Viviani et al., 2023), in which five new alternative spatial Stroop versions were evaluated, considering both the size and internal reliability of their Stroop effects. Specifically, the study aimed at finding an alternative spatial Stroop variant that is more suitable for neuroimaging studies. Indeed, although Puccioni and Vallesi's (2012a) paradigm fulfills all the methodological requirements for yielding a complete spatial Stroop effect, its peripheral spatial arrangement might be problematic during neuroimaging and electrophysiological (e.g., EEG) recordings, as it induces visuospatial attention shifts and a large extent of ocular artifacts.

A detailed description of the tasks is provided by Viviani et al. (2023), while in the present work we just want to highlight that methodologically complete spatial Stroop tasks are feasible. Indeed, all the new versions implied a three-level effect. First, all tasks were designed so that the processing of one dimension was stronger than the processing of the other to ensure a strong task conflict. Regarding this, we need to point out that processing asymmetry was obtained by leveraging the higher processing automaticity of one

dimension relative to the other and/or the higher discriminability/perceptual salience of one dimension as compared to the other (see below for further details). The other two processing loci were also guaranteed to be involved because of the presence of all necessary dimensional overlaps. More in detail, in each of the new versions, the task-relevant feature was the direction of a target arrow, pointing to the upper-left, upper-right, lower-right, or lower-left part of the screen, as in Puccioni and Vallesi (2012a), and participants had to indicate this feature using four keys that were spatially arranged to ensure the dimensional overlap between the stimulus and response dimensions.

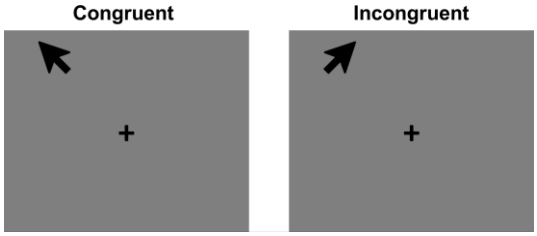

Figure 2.6.
Example stimuli of the arrow-position spatial Stroop task designed by Puccioni and Vallesi (2012a). In the congruent condition (left), the arrow direction and position are both upper-left, while in the incongruent condition (right), the arrow direction is upper-right (task-relevant information), but appears in the upper-left position (task-irrelevant).

In the Perifoveal Stroop, the task-irrelevant information was the position generated by presenting the arrow in one of four small squares around the fixation cross. In the Navon Stroop version, task-relevant small arrows were spatially arranged to form a global arrow, whose direction was the task-irrelevant information, whereas in the Figure-Ground Stroop, the task-relevant small gray arrow was embedded in a large task-irrelevant black arrow. The Flanker Stroop[9] consisted of a central arrow (task-relevant), flanked by eight arrows of the same size, which were task-irrelevant. Lastly, in the Saliency Stroop task, two empty triangles were added to an empty diagonal cross, the smaller indicated the task-relevant direction, whereas the bigger the task-irrelevant one. The reader is referred to Figure 2.7 for examples of congruent and incongruent trials in each of the described tasks.

[9] It might be argued that the Flanker Stroop cannot be considered a Stroop adaptation, since the task-relevant stimulus is not spatially overlapped with the task-irrelevant ones. However, although there is evidence that interference is reduced when task-relevant and task-irrelevant features are spatially separated (Lamers & Roelofs, 2007), our Flanker Stroop task can still be considered a Stroop task. Indeed, according to Kornblum's taxonomy, the overlap is not necessarily perceptual, but it can be conceptual as well. Therefore, as long as the task-relevant and task-irrelevant stimuli can be perceived as an ensemble (as in our case, in which they are minimally distant and perceivable in perifoveal vision), the conceptual overlap is guaranteed. As such our Flanker Stroop is a type-eight ensemble thanks to the presence of task conflict (generated between the processing of the numerous flanking stimuli and the processing of a single feature, see also Viviani et al., 2023), stimulus conflict (due to stimulus-stimulus overlap) and response conflict (due to stimulus-response overlap generated by the compatible spatial arrangement of response keys). Of note, we named it Flanker Stroop based on the presence of flanking task-irrelevant stimuli, but we highlight its fundamental difference from classic Flanker tasks (which are type-four ensembles), that is those formally known as Eriksen Flanker tasks (Eriksen & Eriksen, 1974).

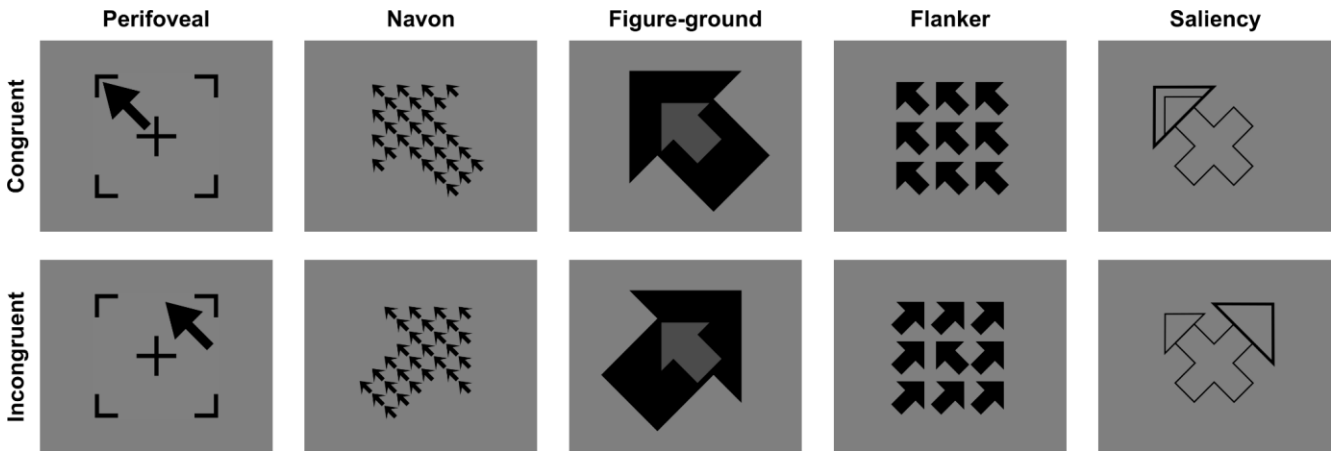

Figure 2.7.
Example of the spatial versions of Stroop tasks proposed by Viviani et al. (2023). In congruent trials, the arrow direction and its position (in the Perifoveal) and the task-relevant arrow direction and the task-irrelevant arrow direction (in the other tasks) are both upper-left, while in incongruent trials, the arrow direction (task-relevant) is upper-left but the arrow position/direction (task-irrelevant) is upper-right.

Therefore, there was always an overlap (perceptual or conceptual) between the relevant and irrelevant stimulus dimensions which, in the case of the Perifoveal Stroop, was between the arrow direction and its position whereas, in the remaining task versions, it was between the task-relevant arrow direction and the task-irrelevant arrow direction. Moreover, in all these variants, the stimulus attributes, both the relevant and irrelevant ones, overlapped with the response as the response keys were selected in order to be spatially compatible with the four directions and also with the positions in the case of the Perifoveal task. Of note, the Peripheral and the Perifoveal Stroop are arrow-position spatial Stroop tasks, whereas the other experimental paradigms do not belong to this category, and they could be better referred to as arrow-arrow spatial Stroop tasks, as the irrelevant dimension is the direction of the task-irrelevant arrow. It might be argued that in these four versions there are not two conflicting task sets, because both task-relevant and task-irrelevant dimensions imply arrow direction processing. However, task conflict is still present, with the only difference that, as claimed above, it was generated not only by leveraging processing automaticity but also by enhancing the perceptual discriminability of the task-irrelevant dimension as compared to the task-relevant one. Hence, in the arrow-arrow variants, two competing task-sets were still necessarily activated by the conceptually or perceptually different characteristics of the two dimensions. For example, in the Navon Stroop, task-related conflict relies on a mix of conceptual and perceptual characteristics, as there is a stronger but task-irrelevant processing stream elaborating the global arrow direction which competes with the less strong but task-relevant processing of local arrow directions. Hence, global vs. local processing is a perceptual characteristic which, however, has also conceptual implications. In contrast, in the Saliency Stroop task, task conflict is driven solely, as the name suggests, by different degrees of saliency between the task-relevant (less salient) and task-irrelevant (more salient) dimensions. This difference notwithstanding

(see Viviani et al., 2023, for a more detailed discussion), the Peripheral and all the novel versions are pure spatial Stroop variants including all the conflict levels.

Lastly, the new versions also satisfied the second methodological point, as they all entailed four relevant and four irrelevant stimulus dimensions, allowing to completely alternate the first-order trial sequences, thus reducing low-level binding and priming effects[10].

2.6. Summary and Conclusion

This study emerged from the need to emphasize the importance of measurement validity in assessing the Stroop effect. While the validity of measurements is undeniably crucial in psychology, it is consistently threatened in the context of the Stroop task literature, mainly due to significant methodological differences across studies. This, in turn, has led to theoretical controversies. The methodological variability comes from the existence of an incredible number of Stroop task variants, often created without adhering to shared guidelines. Therefore, the aim of the present work was to highlight the importance of using rigorous methodological criteria to design Stroop tasks that measure the Stroop effect in a comprehensive and valid way.

In this review, we started with an overview of the classical Stroop effect, highlighting its complex nature, and presenting evidence that demonstrates that it is composed of effects arising at multiple processing levels or loci. Therefore, throughout this work, we stressed that designs generating conflict at the task locus and interference/facilitation at the stimulus and response loci are fundamental to provide complete measures of the Stroop effect, that is, measures that consider such an effect as a whole. We also showed that, in order to meet these requirements to be satisfied, a Stroop task should adhere to the specific characteristics elegantly summarized in Kornblum's works which, although rarely used, provide highly useful practical guidelines in the design of Stroop tasks. Furthermore, we highlighted the role of possible

[10] Four stimulus-response mappings are sufficient to reduce first-order trial repetitions, as outlined above, but it does not have to be intended as the only possible alternative. Indeed, to minimize repetition effects, one needs at least four stimuli and responses, but this represents only a lower bound, since more than four options could also be employed. Indeed, specifically considering the spatial Stroop task, the maximum possible number of stimulus-response overlaps coincides with the maximum number of possible effectors (e.g., the fingers). For example, using more than four stimulus-response mappings could be preferable for controlling for those repetition carryover effects that can be potentially present even if first-order trials are repetition-free. Indeed, as outlined above, to totally control for repetition effects, one should also avoid repetition in the trials earlier than trial n-1, and to do so, the number of stimulus-response mappings has to be increased (of course at the prize of increasing Stimulus-Response mapping complexity). Overall, priming-free Stroop tasks are desirable, at least at first-order trial level, and this can be achieved by using at least four options, while using more than four mappings is a researcher's choice and depends on the experimental question, on the need of controlling for longer carryover effects, and on the feasibility of using complex Stimulus-Response mappings in different experimental contexts (including the type of research participants, e.g., healthy younger adults, neurological patients, older adults, etc.).

confounding factors, such as repetition effects, which should be controlled for (e.g., by using priming-free designs).

After discussing the most popular alternative versions of the Stroop task, we concluded that most of them did not entail the possibility to yield complete Stroop effects. As a result, they cannot be defined as Stroop tasks, as they differ from the classical color-word Stroop task. Indeed, we believe that to ensure validity, each replication of this task should aim to maintain methodological consistency with the classical Stroop task. Only this ensures that meaningful comparisons can be made between evidence produced by different studies.

However, while emphasizing the importance of methodological aspects and the validity of Stroop effect measures in future studies, we did not intend to imply that only classical Stroop tasks should be employed. Instead, we proposed an alternative category of Stroop tasks, namely the spatial variant, as an example of an alternative Stroop version that maintains methodological adequacy, while also offering increased flexibility in specific cases. We thus provided a methodological review of the spatial Stroop tasks in the literature to verify whether they satisfy such criteria. However, we also found that the majority of the spatial Stroop paradigms implemented in the literature lacked response-related effects and, thus, did not ensure a complete Stroop effect.

First, the label spatial Stroop was also referred to non-purely spatial tasks. This is an issue since including verbal stimuli does not allow either to fully leverage the advantages related to the use of exclusively spatial stimuli or to have the required dimensional overlaps to produce response-related effects. Therefore, we suggested that only arrow-position tasks were ideal spatial Stroop paradigms, in the sense that they allowed one to totally exclude linguistic processing. A second fundamental problem was that even among the arrow-position spatial Stroop tasks in the literature, some of them did not ensure a complete spatial Stroop effect, mainly due to the absence of stimulus-response overlaps. Thus, the majority of the discussed paradigms were not classifiable as complete Stroop tasks but fitted better the more cautious definition of Stroop-like paradigms (Kornblum, 1992). A third issue was more general and concerned all the Stroop tasks, that is, the need of using at least four stimulus dimensions in order to control for first-order low-level binding and priming effects.

On the basis of these methodological considerations, we provided some examples of spatial Stroop tasks, which allow one to yield complete spatial Stroop effects and to exclude the influence of trial sequence confounding effects. Nevertheless, this work wants to stress that these paradigms are not the only possible spatial Stroop variations and that, by satisfying the above methodological considerations, several different variations can be conceived and designed. For this reason, our categorization of spatial Stroop tasks is not exhaustive, and arrow-position tasks are not the only purely spatial Stroop paradigms.

For example, we showed that other pure variants can be created, such as some of those presented in Viviani and colleagues' work (2023), which were not arrow-position tasks, but still satisfied the main methodological criteria and yielded large and reliable Stroop effects. Our results indicate that, when using tasks that are methodologically comparable to the classical Stroop task, not only the measure validity but also its reliability was ensured, showing that the Stroop effect can be large and reliable at the same time, in contrast with the issue posed by the reliability paradox.

Overall, although the current literature on spatial Stroop tasks has some methodological limitations, the spatial Stroop represents a valid and promising alternative to the color-word Stroop task and to its several variations. However, careful attention must also be paid when designing spatial Stroop experimental paradigms to satisfy the methodological criteria whose importance was stressed in the present work. In summary, spatial Stroop tasks should (i) be purely spatial and avoid verbal stimuli, (ii) ensure conflict at the level of task, as well as conflict/facilitation at the stimulus and response loci, and (iii) control for repetition effects, at least at first-order trial level, thus using four (or more) stimuli and responses.

However, we want to emphasize that, in proposing the spatial Stroop task as a valid Stroop task variant, we do not intend to imply that it is the only potentially valid alternative. While this review has specifically focused on spatial Stroop due to its ability to exclude certain potentially confounding factors (e.g., the use of linguistic stimuli) and its reliance on universally recognized automatic tasks (e.g., identifying position), other variants may also meet the required methodological criteria. Furthermore, by providing examples of spatial Stroop tasks, our intention was to demonstrate the underlying rationale in a practical manner, with the aim of encouraging other scholars to do the same, while also using different Stroop paradigms.

To conclude, fulfilling these methodological criteria is important because they represent the only means to obtain truly comparable measures of the Stroop effect. As a consequence, if more rigorous task designs are employed, there will be more room for enhancement in the understanding of processes tapped by the Stroop task. Indeed, starting from the same design criteria would ensure that the Stroop effect measures of different studies actually reflect the same phenomenon, and not only a part of it (e.g., the effects at stimulus level), and not confounded by priming effects due to (partial and total) feature repetitions. The take-home message of the present work is in line with other recent works (e.g., Augustinova et al., 2019; Parris et al., 2022), that have highlighted that the nature of the Stroop effect is much more complex than previously expected. Therefore, since there is evidence that the Stroop effect occurs at multiple loci, there is a clear need of designing experimental paradigms capturing all the different types of underlying processes and not just a part of them. To attain a more thorough and comprehensive comprehension of the extensively studied Stroop effect, it is imperative to implement more rigorous methodological practices within the (spatial) Stroop literature. Enhancing measurement validity stands as the sole pathway to achieve this goal.

2.7. References

Abdel Rahman, R., & Melinger, A. (2007). When bees hamper the production of honey: Lexical interference from associates in speech production. *Journal of Experimental Psychology. Learning, Memory, and Cognition*, 33(3), 604–614. https://doi.org/10.1037/0278-7393.33.3.604

Abdel Rahman, R., & Melinger, A. (2009). Semantic context effects in language production: A swinging lexical network proposal and a review. *Language and Cognitive Processes*, 24. https://doi.org/10.1080/01690960802597250

Alario, F. X., Segui, J., & Ferrand, L. (2000). Semantic and associative priming in picture naming. *The Quarterly Journal of Experimental Psychology. A, Human Experimental Psychology*, 53(3), 741–764. https://doi.org/10.1080/713755907

Algom, D., Dekel, A., & Pansky, A. (1996). The perception of number from the separability of the stimulus: The Stroop effect revisited. *Memory & cognition*, *24*, 557-572.

Algom, D., & Chajut, E. (2019). Reclaiming the Stroop Effect Back From Control to Input-Driven Attention and Perception. *Frontiers in Psychology*, 10, 1683. https://doi.org/10.3389/fpsyg.2019.01683

Algom, D., Chajut, E., & Lev, S. (2004). A rational look at the emotional stroop phenomenon: A generic slowdown, not a stroop effect. *Journal of Experimental Psychology. General*, 133(3), 323–338. https://doi.org/10.1037/0096-3445.133.3.323

Algom, D., Fitousi, D., & Chajut, E. (2022). Can the Stroop effect serve as the gold standard of conflict monitoring and control? A conceptual critique. *Memory & Cognition, 50*, 883-897.

Ambrosini, E., & Vallesi, A. (2017). Domain-general Stroop Performance and Hemispheric Asymmetries: A Resting-state EEG Study. *Journal of Cognitive Neuroscience*, 29(5), 769–779. https://doi.org/10.1162/jocn_a_01076

Ambrosini, E., Arbula, S., Rossato, C., Pacella, V., & Vallesi, A. (2019). Neuro-cognitive architecture of executive functions: A latent variable analysis. *Cortex*, *119*, 441-456.

Arieh, Y., & Algom, D. (2002). Processing picture--word stimuli: The contingent nature of picture and of word superiority. *Journal of Experimental Psychology: Learning, Memory, and Cognition*, *28*(1), 221.

Augustinova, M., Parris, B., & Ferrand, L. (2019). The Loci of Stroop Interference and Facilitation Effects With Manual and Vocal Responses. *Frontiers in Psychology*, 10, 1786. https://doi.org/10.3389/fpsyg.2019.01786

Augustinova, M., Silvert, L., Spatola, N., & Ferrand, L. (2018). Further investigation of distinct components of Stroop interference and of their reduction by short response-stimulus intervals. *Acta Psychologica*, 189, 54–62. https://doi.org/10.1016/j.actpsy.2017.03.009

Banich, M. T. (2009). Executive function: The search for an integrated account. *Current Directions in Psychological Science*, *18*(2), Article 2.

Banich, M. T. (2019). The Stroop Effect Occurs at Multiple Points Along a Cascade of Control: Evidence From Cognitive Neuroscience Approaches. *Frontiers in Psychology*, *10*. https://www.frontiersin.org/articles/10.3389/fpsyg.2019.02164

Barkley, R. A. (1997). Behavioral inhibition, sustained attention, and executive functions: Constructing a unifying theory of ADHD. *Psychological Bulletin*, 121(1), 65–94. https://doi.org/10.1037/0033-2909.121.1.65

Blais, C., & Besner, D. (2007). A reverse Stroop effect without translation or reading difficulty. *Psychonomic Bulletin & Review*, 14(3), 466–469. https://doi.org/10.3758/bf03194090

Borgmann, K., Fugelsang, J., Ansari, D., & Besner, D. (2011). Congruency proportion reveals asymmetric processing of irrelevant physical and numerical dimensions in the size congruity paradigm. *Canadian Journal of Experimental Psychology = Revue Canadienne De Psychologie Experimentale*, 65(2), Art. 2. https://doi.org/10.1037/a0021145

Botvinick, M. M., Braver, T. S., Barch, D. M., Carter, C. S., & Cohen, J. D. (2001). Conflict monitoring and cognitive control. *Psychological Review*, 108(3), 624–652. https://doi.org/10.1037/0033-295x.108.3.624

Braver, T. S. (2012). The variable nature of cognitive control: A dual mechanisms framework. *Trends in Cognitive Sciences*, 16(2), 106–113. https://doi.org/10.1016/j.tics.2011.12.010

Brown, T. L. (2011). The relationship between Stroop interference and facilitation effects: Statistical artifacts, baselines, and a reassessment. *Journal of Experimental Psychology. Human Perception and Performance*, 37(1), 85–99. https://doi.org/10.1037/a0019252

Brown, T. L., Gore, C. L., & Pearson, T. (1998). Visual half-field Stroop effects with spatial separation of words and color targets. *Brain and Language*, 63(1), 122–142. https://doi.org/10.1006/brln.1997.1940

Bugg, J. M., Jacoby, L. L., & Chanani, S. (2011). Why it is too early to lose control in accounts of item-specific proportion congruency effects. *Journal of Experimental Psychology. Human Perception and Performance*, 37(3), 844–859. https://doi.org/10.1037/a0019957

Bürki, A., Elbuy, S., Madec, S., & Vasishth, S. (2020). What did we learn from forty years of research on semantic interference? A Bayesian meta-analysis. *Journal of Memory and Language*, 114, 104125. https://doi.org/10.1016/j.jml.2020.104125

Capizzi, M., Ambrosini, E., & Vallesi, A. (2017). Individual Differences in Verbal and Spatial Stroop Tasks: Interactive Role of Handedness and Domain. *Frontiers in Human Neuroscience*, 0. https://doi.org/10.3389/fnhum.2017.00545

Cohen, J. D., Dunbar, K., & McClelland, J. L. (1990). On the control of automatic processes: A parallel distributed processing account of the Stroop effect. *Psychological Review*, 97(3), 332–361. https://doi.org/10.1037/0033-295x.97.3.332

Colling, L. J., Szűcs, D., Marco, D. D., Cipora, K., Ulrich, R., Nuerk, H.-C., Soltanlou, M., Bryce, D., Chen, S.-C., Schroeder, P. A., Henare, D. T., Chrystall, C. K., Corballis, P. M., Ansari, D., Goffin, C., Sokolowski, H. M., Hancock, P. J., Millen, A. E., Langton, S. R., … Ortiz-Tudela, J. (2020). A multilab registered replication of the attentional SNARC effect. *Advances in Methods and Practices in Psychological Science*, 3(2), 143-162..

Costa, A., Alario, F. X., & Caramazza, A. (2005). On the categorical nature of the semantic interference effect in the picture-word interference paradigm. *Psychonomic Bulletin & Review*, 12(1), 125–131. https://doi.org/10.3758/bf03196357

Cothran, D. L., & Larsen, R. (2008). Comparison of Inhibition in Two Timed Reaction Tasks. *The Journal of Psychology*, 142(4), 373–385.

Cothran, D. L., Larsen, R. J., Zelenski, J. M., & Prizmic, Z. (2012). Do Emotion Words Interfere with Processing Emotion Faces? Stroop-Like Interference versus Automatic Vigilance for Negative Information. *Imagination, Cognition and Personality*, 32(1), 59–73. https://doi.org/10.2190/IC.32.1.e

Crossfield, E., & Damian, M. F. (2021). The role of valence in word processing: Evidence from lexical decision and emotional Stroop tasks. *Acta Psychologica*, 218, 103359. https://doi.org/10.1016/j.actpsy.2021.103359

Dadon, G., & Henik, A. (2017). Adjustment of control in the numerical Stroop task. *Memory & Cognition*, 45(6), Art. 6. https://doi.org/10.3758/s13421-017-0703-6

De Houwer, J. (2003). On the role of stimulus-response and stimulus-stimulus compatibility in the Stroop effect. *Memory & Cognition*, 31(3), 353–359. https://doi.org/10.3758/bf03194393

de Zubicaray, G. I., Hansen, S., & McMahon, K. L. (2013). Differential processing of thematic and categorical conceptual relations in spoken word production. *Journal of Experimental Psychology. General*, 142(1), 131–142. https://doi.org/10.1037/a0028717

Dehaene, S. (1992). Varieties of numerical abilities. *Cognition*, 44(1), 1–42. https://doi.org/10.1016/0010-0277(92)90049-N

Dehaene, S., Bossini, S., & Giraux, P. (1993). The mental representation of parity and number magnitude. *Journal of Experimental Psychology: General*, 122(3), 371–396. https://doi.org/10.1037/0096-3445.122.3.371

Dell'Acqua, R., Job, R., Peressotti, F., & Pascali, A. (2007). The picture-word interference effect is not a Stroop effect. *Psychonomic Bulletin & Review*, 14(4), 717–722. https://doi.org/10.3758/BF03196827

Deyne, S., Navarro, D., Perfors, A., Brysbaert, M., & Storms, G. (2019). The "Small World of Words" English word association norms for over 12,000 cue words. *Behavior Research Methods*. https://doi.org/10.3758/s13428-018-1115-7

Di Russo, F., & Bianco, V. (2023). Time Course of Reactive Brain Activities during a Stroop Color-Word Task: Evidence of Specific Facilitation and Interference Effects. Brain Sciences, 13(7), 982.

Egner, T., Ely, S., & Grinband, J. (2010). Going, Going, Gone: Characterizing the Time-Course of Congruency Sequence Effects. *Frontiers in Psychology*, 1. https://www.frontiersin.org/articles/10.3389/fpsyg.2010.00154

Eriksen, B. A., & Eriksen, C. W. (1974). Effects of noise letters upon the identification of a target letter in a nonsearch task. *Perception & psychophysics, 16*(1), 143-149.

Fischer, M. H., Castel, A. D., Dodd, M. D., & Pratt, J. (2003). Perceiving numbers causes spatial shifts of attention. *Nature Neuroscience*, 6(6), 555–556. https://doi.org/10.1038/nn1066

Flake, J. K., & Fried, E. I. (2020). Measurement Schmeasurement: Questionable Measurement Practices and How to Avoid Them. *Advances in Methods and Practices in Psychological Science*, *3*(4), 456–465. https://doi.org/10.1177/2515245920952393

Funes, M. J., Lupiáñez, J., & Humphreys, G. (2010). Sustained vs. transient cognitive control: Evidence of a behavioral dissociation. *Cognition*, *114*(3), Article 3. https://doi.org/10.1016/j.cognition.2009.10.007

Funes, M. J., Lupiáñez, J., & Milliken, B. (2007). Separate mechanisms recruited by exogenous and endogenous spatial cues: Evidence from a spatial Stroop paradigm. *Journal of Experimental Psychology. Human Perception and Performance*, 33(2), 348–362. https://doi.org/10.1037/0096-1523.33.2.348

Goldfarb, L., & Henik, A. (2006). New Data Analysis of the Stroop Matching Task Calls for a Reevaluation of Theory. *Psychological Science*, 17(2), 96–100. https://doi.org/10.1111/j.1467-9280.2006.01670.x

Goldfarb, L., & Henik, A. (2007). Evidence for task conflict in the Stroop effect. *Journal of Experimental Psychology. Human Perception and Performance*, 33(5), 1170–1176. https://doi.org/10.1037/0096-1523.33.5.1170

Gonthier, C., Braver, T. S., & Bugg, J. M. (2016). Dissociating proactive and reactive control in the Stroop task. *Memory & Cognition*, 44(5), 778–788. https://doi.org/10.3758/s13421-016-0591-1

Gratton, G., Coles, M. G., & Donchin, E. (1992). Optimizing the use of information: Strategic control of activation of responses. *Journal of Experimental Psychology. General*, 121(4), 480–506. https://doi.org/10.1037//0096-3445.121.4.480

Hedge, C., Powell, G., & Sumner, P. (2018). The reliability paradox: Why robust cognitive tasks do not produce reliable individual differences. *Behavior Research Methods*, *50*(3), Article 3. https://doi.org/10.3758/s13428-017-0935-1

Henik, A., & Salo, R. (2004). Schizophrenia and the Stroop Effect. *Behavioral and Cognitive Neuroscience Reviews*, 3(1), 42–59. https://doi.org/10.1177/1534582304263252

Henik, A., & Tzelgov, J. (1982). Is three greater than five: The relation between physical and semantic size in comparison tasks. *Memory & Cognition*, 10(4), 389–395. https://doi.org/10.3758/bf03202431

Hilbert, S., Nakagawa, T. T., Bindl, M., & Bühner, M. (2014). The spatial Stroop effect: A comparison of color-word and position-word interference. *Psychonomic Bulletin & Review*, 21(6), 1509–1515. https://doi.org/10.3758/s13423-014-0631-4

Hock, H. S., & Egeth, H. (1970). Verbal interference with encoding in a perceptual classification task. *Journal of Experimental Psychology*, 83(2), 299–303. https://doi.org/10.1037/h0028512

Hoffman, P., Lambon Ralph, M. A., & Rogers, T. T. (2013). Semantic diversity: A measure of semantic ambiguity based on variability in the contextual usage of words. *Behavior Research Methods*, 45(3), 718–730. https://doi.org/10.3758/s13428-012-0278-x

Hommel, B. (2004). Event files: Feature binding in and across perception and action. Trends in Cognitive Sciences, 8(11), 494–500. https://doi.org/10.1016/j.tics.2004.08.007

Hommel, B., Proctor, R. W., & Vu, K.-P. L. (2004). A feature-integration account of sequential effects in the Simon task. *Psychological Research*, 68(1), 1–17. https://doi.org/10.1007/s00426-003-0132-y

Hutson, J., & Damian, M. F. (2014). Semantic gradients in picture-word interference tasks: Is the size of interference effects affected by the degree of semantic overlap? *Frontiers in Psychology*, 5, 872. https://doi.org/10.3389/fpsyg.2014.00872

Joyal, M., Wensing, T., Levasseur-Moreau, J., Leblond, J., T Sack, A., & Fecteau, S. (2019). Characterizing emotional Stroop interference in posttraumatic stress disorder, major depression and anxiety disorders: A systematic review and meta-analysis. *PloS One*, 14(4), e0214998. https://doi.org/10.1371/journal.pone.0214998

Kappes, C., & Bermeitinger, C. (2016). The Emotional Stroop as an Emotion Regulation Task. *Experimental Aging Research*, 42(2), 161–194. https://doi.org/10.1080/0361073X.2016.1132890

Kerns, J. G., Cohen, J. D., MacDonald, A. W., Cho, R. Y., Stenger, V. A., & Carter, C. S. (2004). Anterior cingulate conflict monitoring and adjustments in control. *Science* (New York, N.Y.), 303(5660), 1023–1026. https://doi.org/10.1126/science.1089910

Kinoshita, S., de Wit, B., Aji, M., & Norris, D. (2017). Evidence accumulation in the integrated and primed Stroop tasks. *Memory & Cognition*, 45(5), 824–836. https://doi.org/10.3758/s13421-017-0701-8

Kornblum, S. (1992). Dimensional overlap and dimensional relevance in stimulus-response and stimulus-stimulus compatibility. In G. E. Stelmach & J. Requin (Eds.), *Tutorials in motor behavior*, 2 (pp. 743–777). North-Holland. (Portions of this paper have appeared in "Tutorials in Motor Neuroscience," J. Requin and G. E. Stelmach (Eds.), Kluwer Academic Publishers: Dordrecht, The Netherlands, 1991)

Kornblum, S., Hasbroucq, T., & Osman, A. (1990). Dimensional Overlap: Cognitive Basis for Stimulus-Response Compatibility-A Model and Taxonomy. *Psychological Review*, 97(2), 253–270. Scopus. https://doi.org/10.1037/0033-295X.97.2.253

Kornblum, S., Stevens, G. T., Whipple, A., & Requin, J. (1999). The Effects of Irrelevant Stimuli: 1. The Time Course of Stimulus-Stimulus and Stimulus-Response Consistency Effects With Stroop-Like Stimuli, Simon-Like Tasks, and Their Factorial Combinations. *Journal of Experimental Psychology: Human Perception and Performance*, 25(3), 688–714. Scopus. https://doi.org/10.1037/0096-1523.25.3.688

Lamers, M. J. M., & Roelofs, A. (2007). Role of Gestalt grouping in selective attention: Evidence from the Stroop task. *Perception & Psychophysics*, 69(8), 1305–1314. https://doi.org/10.3758/BF03192947

Larsen, R. J., Mercer, K. A., & Balota, D. A. (2006). Lexical characteristics of words used in emotional Stroop experiments. *Emotion* (Washington, D.C.), 6(1), 62–72. https://doi.org/10.1037/1528-3542.6.1.62

Leung, H.-C., Skudlarski, P., Gatenby, J. C., Peterson, B. S., & Gore, J. C. (2000). An Event-related Functional MRI Study of the Stroop Color Word Interference Task. *Cerebral Cortex*, 10(6), 552–560. https://doi.org/10.1093/cercor/10.6.552

Lindsay, D. S., & Jacoby, L. L. (1994). Stroop process dissociations: The relationship between facilitation and interference. *Journal of Experimental Psychology: Human Perception and Performance*, 20(2), 219–234. https://doi.org/10.1037/0096-1523.20.2.219

Lu, C., & Proctor, R. W. (1995). The influence of irrelevant location information on performance: A review of the Simon and spatial Stroop effects. *Psychonomic Bulletin & Review*, 2(2), 174–207. https://doi.org/10.3758/BF03210959

Luo, C., & Proctor, R. W. (2013). Asymmetry of congruency effects in spatial Stroop tasks can be eliminated. *Acta Psychologica*, 143(1), 7–13. https://doi.org/10.1016/j.actpsy.2013.01.016

Luo, C., Lupiáñez, J., Fu, X., & Weng, X. (2010). Spatial Stroop and spatial orienting: The role of onset versus offset cues. *Psychological Research*, 74(3), 277–290. https://doi.org/10.1007/s00426-009-0253-z

Luo, C., Lupiáñez, J., Funes, M. J., & Fu, X. (2013). Reduction of the Spatial Stroop Effect by Peripheral Cueing as a Function of the Presence/Absence of Placeholders. *PLOS ONE*, 8(7), e69456. https://doi.org/10.1371/journal.pone.0069456

Lupker, S. J. (1979). The semantic nature of response competition in the picture-word interference task. *Memory & Cognition*, 7(6), 485–495. https://doi.org/10.3758/BF03198265

MacLeod, C. M. (1991). Half a century of research on the Stroop effect: An integrative review. Psychological Bulletin, 109(2), 163–203. https://doi.org/10.1037/0033-2909.109.2.163

MacLeod, C. M. (1992). The Stroop task: The "gold standard" of attentional measures. *Journal of Experimental Psychology: General*, 121(1), 12–14. https://doi.org/10.1037/0096-3445.121.1.12

MacLeod, C. M., & MacDonald, P. A. (2000). Interdimensional interference in the Stroop effect: Uncovering the cognitive and neural anatomy of attention. *Trends in Cognitive Sciences*, 4(10), 383–391. https://doi.org/10.1016/S1364-6613(00)01530-8

Mahon, B. Z., Costa, A., Peterson, R., Vargas, K. A., & Caramazza, A. (2007). Lexical selection is not by competition: A reinterpretation of semantic interference and facilitation effects in the picture-word interference paradigm. *Journal of Experimental Psychology. Learning, Memory, and Cognition*, 33(3), 503–535. https://doi.org/10.1037/0278-7393.33.3.503

Mayor, J., Sainz, J., & Gonzalez-Marques, J. (1988). *Stroop and Priming Effects in Naming and Categorizing Tasks Using Words and Pictures*. In M. Denis, J. Engelkamp, & J. T. E. Richardson (A c. Di), Cognitive and Neuropsychological Approaches to Mental Imagery (pp. 69–78). Springer Netherlands. https://doi.org/10.1007/978-94-009-1391-2_6

Mayr, U., Awh, E., & Laurey, P. (2003). Conflict adaptation effects in the absence of executive control. *Nature Neuroscience*, 6(5), 450–452. https://doi.org/10.1038/nn1051

McKenna, F. P. (1986). Effects of unattended emotional stimuli on color-naming performance. *Current Psychological Research & Reviews*, 5(1), 3–9. https://doi.org/10.1007/BF02686591

McRae, K., Cree, G. S., Seidenberg, M. S., & McNorgan, C. (2005). Semantic feature production norms for a large set of living and nonliving things. *Behavior Research Methods*, 37(4), 547–559. https://doi.org/10.3758/bf03192726

Melara, R. D., & Algom, D. (2003). Driven by information: A tectonic theory of Stroop effects. *Psychological Review*, 110(3), 422–471. https://doi.org/10.1037/0033-295x.110.3.422

Melara, R. D., & Mounts, J. R. W. (1993). Selective attention to Stroop dimensions: Effects of baseline discriminability, response mode, and practice. *Memory & Cognition*, 21(5), 627–645. https://doi.org/10.3758/BF03197195

Montefinese, M., & Semenza, C. (2018). Number line estimation and complex mental calculation: Is there a shared cognitive process driving the two tasks? *Cognitive Processing*, 19(4), 495–504. https://doi.org/10.1007/s10339-018-0867-4

Montefinese, M., & Vinson, D. (2015). Can the humped animal's knee conceal its name? Commentary on: "The roles of shared vs. distinctive conceptual features in lexical access." *Frontiers in Psychology*, 6, 418. https://doi.org/10.3389/fpsyg.2015.00418

Montefinese, M., Ambrosini, E., Fairfield, B., & Mammarella, N. (2013). Semantic memory: A feature-based analysis and new norms for Italian. *Behavior Research Methods*, 45(2), 440–461. https://doi.org/10.3758/s13428-012-0263-4

Montefinese, M., Ambrosini, E., Fairfield, B., & Mammarella, N. (2014). The adaptation of the affective norms for English words (ANEW) for Italian. *Behavior research methods, 46*, 887-903.

Nee, D. E., Wager, T. D., & Jonides, J. (2007). Interference resolution: Insights from a meta-analysis of neuroimaging tasks. Cognitive, Affective, & Behavioral Neuroscience, 7(1), 1–17. https://doi.org/10.3758/CABN.7.1.1

Nieuwenhuis, S., Stins, J. F., Posthuma, D., Polderman, T. J. C., Boomsma, D. I., & de Geus, E. J. (2006). Accounting for sequential trial effects in the flanker task: Conflict adaptation or associative priming? *Memory & Cognition*, 34(6), 1260–1272. https://doi.org/10.3758/bf03193270

Paap, K. R., Anders-Jefferson, R., Zimiga, B., Mason, L., & Mikulinsky, R. (2020). Interference scores have inadequate concurrent and convergent validity: Should we stop using the flanker, Simon, and spatial Stroop tasks? *Cognitive Research: Principles and Implications*, 5(1), 7. https://doi.org/10.1186/s41235-020-0207-y

Page, M. J., McKenzie, J. E., Bossuyt, P. M., Boutron, I., Hoffmann, T. C., Mulrow, C. D., Shamseer, L., Tetzlaff, J. M., Akl, E. A., Brennan, S. E., Chou, R., Glanville, J., Grimshaw, J. M., Hróbjartsson, A., Lalu, M. M., Li, T., Loder, E. W., Mayo-Wilson, E., McDonald, S., … Moher, D. (2021). The PRISMA 2020 statement: An updated guideline for reporting systematic reviews. *Systematic Reviews*, *10*(1), 89. https://doi.org/10.1186/s13643-021-01626-4

Pang, C., Qi, M., & Gao, H. (2020). Influence of global precedence on spatial Stroop effect. *Acta Psychologica*, 208, 103116. https://doi.org/10.1016/j.actpsy.2020.103116

Pansky, A., & Algom, D. (2002). Comparative judgment of numerosity and numerical magnitude: attention preempts automaticity. *Journal of Experimental Psychology: Learning, Memory, and Cognition*, *28*(2), 259.

Parris, B. A. (2014). Task conflict in the Stroop task: When Stroop interference decreases as Stroop facilitation increases in a low task conflict context. *Frontiers in Psychology*, 5, 1182. https://doi.org/10.3389/fpsyg.2014.01182

Parris, B. A., Hasshim, N., Wadsley, M., Augustinova, M., & Ferrand, L. (2022). The loci of Stroop effects: A critical review of methods and evidence for levels of processing contributing to color-word Stroop effects and the implications for the loci of attentional selection. *Psychological Research*, 86(4), 1029–1053. https://doi.org/10.1007/s00426-021-01554-x

Parris, B. A., Hasshim, N., Ferrand, L., & Augustinova, M. (2023). Do Task Sets Compete in the Stroop Task and Other Selective Attention Paradigms?. *Journal of cognition, 6*(1), 23. https://doi.org/10.5334/joc.272

Peckham, A. D., McHugh, R. K., & Otto, M. W. (2010). A meta-analysis of the magnitude of biased attention in depression. *Depression and Anxiety*, 27(12), 1135–1142. https://doi.org/10.1002/da.20755

Periáñez, J. A., Lubrini, G., García-Gutiérrez, A., & Ríos-Lago, M. (2021). Construct Validity of the Stroop Color-Word Test: Influence of Speed of Visual Search, Verbal Fluency, Working Memory, Cognitive Flexibility, and Conflict Monitoring. *Archives of Clinical Neuropsychology: The Official Journal of the National Academy of Neuropsychologists*, 36(1), 99–111. https://doi.org/10.1093/arclin/acaa034

Piai, V., Roelofs, A., Acheson, D. J., & Takashima, A. (2013). Attention for speaking: Domain-general control from the anterior cingulate cortex in spoken word production. *Frontiers in Human Neuroscience*, 7, 832. https://doi.org/10.3389/fnhum.2013.00832

Pickel, L., Pratt, J., & Weidler, B. J. (2019). The transfer of location-based control requires location-based conflict. *Attention, Perception & Psychophysics*, 81(8), 2788–2797. https://doi.org/10.3758/s13414-019-01785-6

Pires, L., Leitão, J., Guerrini, C., & Simões, M. R. (2018). Cognitive control during a spatial Stroop task: Comparing conflict monitoring and prediction of response-outcome theories. *Acta Psychologica*, 189, 63–75. https://doi.org/10.1016/j.actpsy.2017.06.009

Posner, M. I., & Snyder, C. R. R. (1975). *Attention and Cognitive Control*. In R. L. Solso (Ed.), Information Processing and Cognition: The Loyola Symposium. Lawrence Erlbaum.

Puccioni, O., & Vallesi, A. (2012a). High cognitive reserve is associated with a reduced age-related deficit in spatial conflict resolution. *Frontiers in Human Neuroscience*, 6. https://doi.org/10.3389/fnhum.2012.00327

Puccioni, O., & Vallesi, A. (2012b). Sequential congruency effects: Disentangling priming and conflict adaptation. *Psychological Research*, 76(5), 591–600. https://doi.org/10.1007/s00426-011-0360-5

Puccioni, O., & Vallesi, A. (2012c). Conflict resolution and adaptation in normal aging: The role of verbal intelligence and cognitive reserve. *Psychology and Aging*, 27(4), 1018–1026. https://doi.org/10.1037/a0029106

Roelofs, A. (1992). A spreading-activation theory of lemma retrieval in speaking. *Cognition*, 42(1–3), 107–142. https://doi.org/10.1016/0010-0277(92)90041-F

Rosinski, R. R., Golinkoff, R. M., & Kukish, K. S. (1975). Automatic Semantic Processing in a Picture-Word Interference Task. *Child Development*, 46(1), 247–253. https://doi.org/10.2307/1128859

Scarpina, F., & Tagini, S. (2017). The Stroop Color and Word Test. *Frontiers in Psychology*, 8, 557. https://doi.org/10.3389/fpsyg.2017.00557

Schmidt, J. R. (2019). Evidence against conflict monitoring and adaptation: An updated review. *Psychonomic Bulletin & Review*, 26(3), 753–771. https://doi.org/10.3758/s13423-018-1520-z

Schmidt, J. R. (2023). Is conflict adaptation adaptive? An introduction to conflict monitoring theory and some of the ecological problems it faces. *Quarterly Journal of Experimental Psychology*, 17470218231161555

Schneider, D. W. (2020). Alertness and cognitive control: Interactions in the spatial Stroop task. *Attention, Perception, & Psychophysics*, 82(5), 2257–2270. https://doi.org/10.3758/s13414-020-01993-5

Seymour, P. H. K. (1977). Conceptual Encoding and Locus of the Stroop Effect. *Quarterly Journal of Experimental Psychology*, 29(2), 245–265. https://doi.org/10.1080/14640747708400601

Shao, Z., Roelofs, A., Martin, R. C., & Meyer, A. S. (2015). Selective inhibition and naming performance in semantic blocking, picture-word interference, and color-word Stroop tasks. *Journal of Experimental Psychology. Learning, Memory, and Cognition*, 41(6), 1806–1820. https://doi.org/10.1037/a0039363

Shor, R. E. (1970). The processing of conceptual information on spatial directions from pictorial and linguistic symbols. *Acta Psychologica*, Amsterdam, 32(4), 346–365. https://doi.org/10.1016/0001-6918(70)90109-5

Song, S., Zilverstand, A., Song, H., d'Oleire Uquillas, F., Wang, Y., Xie, C., ... & Zou, Z. (2017). The influence of emotional interference on cognitive control: A meta-analysis of neuroimaging studies using the emotional Stroop task. *Scientific reports, 7*(1), 2088.

Spieler, D. H., Balota, D. A., & Faust, M. E. (1996). Stroop Performance in Healthy Younger and Older Adults and in Individuals With Dementia of the Alzheimer's Type. *Journal of Experimental Psychology: Human perception and performance*, 22(2), 461

Spinelli, G., Morton, J. B., & Lupker, S. J. (2022). Both task-irrelevant and task-relevant information trigger reactive conflict adaptation in the item-specific proportion-congruent paradigm. *Psychonomic Bulletin & Review*. https://doi.org/10.3758/s13423-022-02138-5

Spinelli, G., Perry, J. R., & Lupker, S. J. (2019). Adaptation to conflict frequency without contingency and temporal learning: Evidence from the picture-word interference task. *Journal of Experimental Psychology. Human Perception and Performance*, 45(8), 995–1014. https://doi.org/10.1037/xhp0000656

Starreveld, P. A., & La Heij, W. (2017). Picture-word interference is a Stroop effect: A theoretical analysis and new empirical findings. *Psychonomic Bulletin & Review*, 24(3), 721–733. https://doi.org/10.3758/s13423-016-1167-6

Strauss, E., Sherman, E. M. S., & Spreen, O. (2007). A Compendium of Neuropsychological Tests: Administration, Norms, and Commentary. *Applied Neuropsychology*, 14(1), 62–63. https://doi.org/10.1080/09084280701280502

Stroop, J. R. (1935). Studies of interference in serial verbal reactions. *Journal of Experimental Psychology*, 18(6), 643–662. https://doi.org/10.1037/h0054651

Szűcs, D., & Soltész, F. (2010). Stimulus and response conflict in the color–word Stroop task: A combined electro-myography and event-related potential study. *Brain Research*, 1325, 63–76. https://doi.org/10.1016/j.brainres.2010.02.011

Tafuro, A., Ambrosini, E., Puccioni, O., & Vallesi, A. (2019). Brain oscillations in cognitive control: A cross-sectional study with a spatial stroop task. *Neuropsychologia*, 133, 107190. https://doi.org/10.1016/j.neuropsychologia.2019.107190

Tafuro, A., Vallesi, A., & Ambrosini, E. (2020). Cognitive brakes in interference resolution: A mouse-tracking and EEG co-registration study. *Cortex; a Journal Devoted to the Study of the Nervous System and Behavior*, 133, 188–200. https://doi.org/10.1016/j.cortex.2020.09.024

Toth, A. J., Kowal, M., & Campbell, M. J. (2019). The Color-Word Stroop Task Does Not Differentiate Cognitive Inhibition Ability Among Esports Gamers of Varying Expertise. *Frontiers in Psychology*, 10, 2852. https://doi.org/10.3389/fpsyg.2019.02852

Tzelgov, J., Meyer, J., & Henik, A. (1992). Automatic and Intentional Processing of Numerical Information. *Journal of Experimental Psychology: Learning, Memory, and Cognition*, 18, 166–179. https://doi.org/10.1037/0278-7393.18.1.166

Uman, L. S. (2011). Systematic Reviews and Meta-Analyses. *Journal of the Canadian Academy of Child and Adolescent Psychiatry*, *20*(1), 57–59.

Vallesi, A., Weisblatt, Y., Semenza, C., Shaki, S. (2014). Cultural modulations of space-time compatibility effects. *Psychon Bull Rev*, 21(3), 666-9. https://doi.org/10.3758/s13423-013-0540-y

Vallesi, A., Mazzonetto, I., Ambrosini, E., Babcock, L., Capizzi, M., Arbula, S., ... & Bertoldo, A. (2017). Structural hemispheric asymmetries underlie verbal Stroop performance. *Behavioural Brain Research*, *335*, 167-173.

van Maanen, L., van Rijn, H., & Borst, J. P. (2009). Stroop and picture-word interference are two sides of the same coin. *Psychonomic Bulletin & Review*, 16(6), 987–999. https://doi.org/10.3758/PBR.16.6.987

Vigliocco, G., Vinson, D. P., Lewis, W., & Garrett, M. F. (2004). Representing the meanings of object and action words: The featural and unitary semantic space hypothesis. *Cognitive Psychology*, 48(4), 422–488. https://doi.org/10.1016/j.cogpsych.2003.09.001

Visalli, A., Ambrosini, E., Viviani, G., Sambataro, F., Tenconi, E., & Vallesi A. (2022). Do irrelevant emotions interfere with proactive and reactive control? Evidence from an emotional priming Stroop task. *PsyArXiv* https://psyarxiv.com/q2j8n/

Viviani, G., Visalli, A., Finos, L., Vallesi, A., & Ambrosini, E. (2023). A comparison between different variants of the spatial Stroop task: The influence of analytic flexibility on Stroop effect estimates and reliability. *Behavior Research Methods*. https://doi.org/10.3758/s13428-023-02091-8

Wentura, D., Rothermund, K., & Bak, P. (2000). Automatic vigilance: The attention-grabbing power of approach- and avoidance-related social information. *Journal of Personality and Social Psychology*, 78(6), 1024–1037. https://doi.org/10.1037//0022-3514.78.6.1024

White, B. W. (1969). Interference in identifying attributes and attribute names. *Perception & Psychophysics*, 6(3), 166–168. https://doi.org/10.3758/BF03210086

Williams, J. M. G., Mathews, A., & MacLeod, C. (1996). The emotional Stroop task and psychopathology. *Psychological Bulletin*, 120(1), 3–24. https://doi.org/10.1037/0033-2909.120.1.3

Windes, J. (1968). Reaction time for numerical coding and naming of numerals. *Journal of Experimental Psychology*. https://doi.org/10.1037/H0026289

Winter, B., Matlock, T., Shaki, S., & Fischer, M. H. (2015). Mental number space in three dimensions. *Neuroscience and Biobehavioral Reviews*, 57, 209–219. https://doi.org/10.1016/j.neubiorev.2015.09.005

Zebian, S. (2005). Linkages between Number Concepts, Spatial Thinking, and Directionality of Writing: The SNARC Effect and the REVERSE SNARC Effect in English and Arabic Monoliterates, Biliterates, and Illiterate Arabic Speakers. *Journal of Cognition and Culture*, 5(1), 165–190. https://doi.org/10.1163/1568537054068660

Zhang, H., & Kornblum, S. (1998). The effects of stimulus–response mapping and irrelevant stimulus–response and stimulus–stimulus overlap in four-choice Stroop tasks with single-carrier stimuli. *Journal of Experimental Psychology: Human Perception and Performance*, 24(1), 3–19. https://doi.org/10.1037/0096-1523.24.1.3

CHAPTER 3

Many Stroops:

The Quest to Improve Stroop Effect Estimates and Reliability.

3.1. Introduction

The Stroop task (Stroop, 1935) is one of the most seminal behavioral paradigms in experimental psychology. It is commonly used to investigate cognitive control (i.e., the ability to regulate thoughts and actions according to behavioral goals; Braver, 2012) and, specifically, interference resolution (Nee et al., 2007). In the original and most widely used version of this task, referred to as the color-word Stroop task, participants are asked to name the ink color of words denoting color names. This task allows researchers to explore the resolution of interference produced on incongruent trials (e.g., MacLeod, 1991; Stroop, 1935): it takes longer (and attracts more errors) to name the ink color of a word that denotes a different color name (incongruent trials) as compared to when the ink color and the word meaning match (congruent trials), the so-called Stroop effect. According to multiple-stage (e.g., De Houwer, 2003; Zhang & Kornblum, 1998) and multiple loci (e.g., Augustinova et al., 2019; Parris et al., 2022) accounts of Stroop interference, the Stroop effect is produced because in incongruent trials participants are required to overcome the interference or conflict at the task, stimulus and response levels. There is indeed an interference between two competing processing streams, reading and color naming, with the former more prevailing than the latter, between relevant and irrelevant stimulus dimensions, and also between the different vocal responses activated by the ink color and the color name (De Houwer, 2003; Freund et al., 2021; Funes et al., 2010).

Despite its widespread and long-standing use, an overlooked and debated methodological aspect of the verbal Stroop task is that it requires vocal responses to fully exert its interference at both the stimulus and the response level (see e.g., MacLeod, 1991). Indeed, the Stroop task is strongly dependent on response modality, as delineated by the dimensional overlap model put forward by Kornblum (1992), which outlines the requirements that need to be satisfied to consider a task as a Stroop task. Indeed, while color-word Stroop tasks requiring vocal responses are categorized as a “type-eight ensemble” (i.e., a Stroop task according to Kornblum’s classification), ensuring dimensional overlap not only between relevant and irrelevant stimulus dimensions but also between them and the response, those requiring manual responses are categorized as a “type-four ensemble” (i.e., a Stroop-like task according to Kornblum’s classification) because they lack the overlap between stimulus and response dimensions. Accordingly, the color-word

Stroop task has been shown to produce larger Stroop effects with vocal as compared to manual responses (e.g., Augustinova et al., 2019).

Several adaptations of the original color-word Stroop task have been proposed in the literature, including spatial versions investigating the interference between relevant and irrelevant spatial information. Among these, we recently designed a spatial Stroop task in which participants are asked to attend to and indicate the direction of an arrow (i.e., the task-relevant feature) while ignoring the location in which it appears (i.e., the task-irrelevant feature) (Puccioni & Vallesi, 2012a, 2012b). Our spatial version of the Stroop task works exactly as the verbal Stroop task and can be considered as one of its purely spatial variants (for a more detailed discussion, see Viviani et al., 2022). Indeed, it ensures a multiple-loci interference at the task, stimulus and response levels. First, it entails an asymmetric relation between the stimulus dimensions because the position of a visual stimulus can be assumed to be processed in a preponderant way as compared to other visual characteristics, such as the pointing direction in the case of an arrow (Lu & Proctor, 1995), thus engendering conflict between two competing tasks. Moreover, it yields conflict both at the stimulus and response levels as it is a "type-eight ensemble" (Kornblum, 1992) because the arrows appear in one of the four corners of the screen and point in one of the same four directions (i.e., upper-left, upper-right, lower-right, and lower-left), thus ensuring the dimensional overlap between the relevant and irrelevant characteristics of the stimulus, and participants provide their responses by using four keys that are spatially arranged to ensure the dimensional overlap between the stimulus and response dimensions. Therefore, our spatial Stroop task assesses the same central interference resolution processes as verbal Stroop tasks. Furthermore, mouse responses can also be employed, thus allowing researchers to investigate the temporal dynamics of the interference resolution processes (Tafuro et al., 2020).

Our spatial Stroop task also presents several methodological advantages over the original, verbal Stroop task. First, it allows to exclude linguistic processing, which might be beneficial, for example, when examining cognitive control in populations with language or reading disorders, as the performance would not be negatively affected by the impaired linguistic abilities. Second, the use of spatial stimuli to investigate cognitive control might promote a more domain-general understanding of cognitive control mechanisms, overcoming the prevalence of linguistic-based accounts and allowing to better investigate hemispheric lateralization by minimizing a potential confound represented by task verbal demands (Ambrosini & Vallesi, 2017; Tafuro et al., 2019). Third, as discussed above, the verbal Stroop task requires vocal responses to fully exert its interference, but they present some methodological issues. Indeed, the current gold standard to assess verbal response times (RTs) is still to mostly rely on human coding, which is extremely tedious, time-consuming, and prone to errors, biases, and other sources of measurement error. Moreover, it is currently not very feasible to reliably record vocal responses in online studies. Finally, vocal responses are problematic for neuroimaging studies, as they introduce movement artifacts related to overt speech that

can contaminate the cognitive control-related signals of interest, also considering that they are temporally non-random, but covary with signal of interest because they are somewhat time-locked to the task timing. By contrast, the spatial Stroop task allows using manual responses, which are easier to record with minimal motion artifacts and low measurement error even in online studies.

Moreover, our spatial Stroop task allows overcoming some methodological issues that are present in most of the spatial versions of the Stroop tasks used in the literature, as we recently discussed in detail (Viviani et al., 2022). Indeed, position-word tasks (with location words displayed in congruent or incongruent positions; e.g., White, 1969) and arrow-word tasks (with location words embedded or flanked by congruent or incongruent arrows; e.g., Shor, 1970) had often been employed, but both do not ensure a complete spatial Stroop effect due to the lack of a full dimensional overlap between stimulus and response dimensions and still rely on verbal processing. Moreover, most studies (including those employing purely spatial Stroop tasks, e.g., Funes et al., 2007; Pires et al., 2018) used two-alternative forced-choice tasks, but this prevents having complete repetition-free trial sequences (for which at least four options are needed), thus making it hard to distinguish conflict resolution/adaptation effects from low-level binding, positive and negative priming effects (for a detailed discussion, see Viviani et al., 2022 and Puccioni & Vallesi, 2012b).

Notwithstanding its advantages, our spatial Stroop task also presents some methodological limitations. Indeed, the arrows appear in peripheral locations on the screen, therefore requiring the deployment of large visuospatial attention shifts and eye movements. This can affect the behavioral measures of the interference resolution processes of interest, especially for extreme visual eccentricities and when mouse movements are required. Moreover, this can also introduce oculomotor artifacts that, albeit not being as problematic as the overt speech and motor artifacts produced by vocal responses, can still contaminate the cognitive control-related signals of interest in neuroimaging studies.

Our aim is to propose novel spatial Stroop tasks that allow overcoming these issues of our original spatial Stroop task, which we will call “Peripheral” due to its spatial arrangement with high stimulus eccentricity. To this aim, we designed five alternative versions allowing for presentation of the experimental stimuli at the center of the screen, while maintaining all the required methodological criteria to yield a complete spatial Stroop interference effect and a complete alternation of the trial sequences. One of these versions, the “Perifoveal” one is a direct adaptation of the Peripheral version in which the arrows appear in perifoveal locations. The other four alternative versions were inspired by the other experimental paradigms generating interference (e.g., the Flanker task) that allowed preserving both the fundamental characteristics of a spatial Stroop task and its methodological advantages over the original verbal Stroop task, as described above. It is noteworthy that these four alternative versions differed from the Peripheral and Perifoveal ones in the manipulation used to engender conflict at the task level. Indeed, to generate asymmetry between the two dimensions, we leveraged not only the higher processing automaticity of one dimension as compared

to the other, but also the higher discriminability/perceptual salience of one dimension relatively to the other, and these two manipulation types were present in different amounts in the newly created tasks. A detailed description of them will be provided in the Method section.

These alternative versions were evaluated in terms of two important features. The first one is their ability to show a large Stroop effect for manual RTs, in line with the dominance assumption (Rouder & Haaf, 2018, 2019): all individuals truly respond slower in incongruent than congruent trials (or, in other words, nobody should show a non-positive Stroop effect). The second one is the internal reliability of their Stroop effects. Indeed, as pointed out by Hedge and coworkers (2018), the reliability of an experimental effect represents a frequently overlooked statistical issue that, if not taken into account properly, might jeopardize the effectiveness of correlational research in cognitive neuroscience and psychology (e.g., Dang et al., 2020; Elliott et al., 2020; Rouder et al., 2019; Wennerhold & Friese, 2020).

Finally, population-level effects and internal reliability were evaluated under different analytical frameworks. The reason is that both cross-subject and cross-trial variability influence estimates of population-level effects and their reliability (Chen et al., 2021). However, the classical test theory analytical approach requires computing participants-by-task scores by averaging participants' performance across trials. This discards any cross-trial variability that may contaminate participants-by-task scores, potentially decreasing not only their accuracy and generalizability, but also their reliability (see also Rouder & Haaf, 2019). Therefore, we used not only a classical analytical approach, but also a multilevel modeling approach that allows assessing the experimental effects of interest while removing intra-subject, trial-by-trial noise and effects of lower-level confounding factors.

3.2. Methods

We report how we determined our sample size, all data exclusions, all inclusion/exclusion criteria, all manipulations, and all measures in the study. All inclusion/exclusion criteria were established prior to data analysis. All data and materials, as well as the code used to run the experimental tasks and generate and analyze the data of the current study, are available from our project repository on the Open Science Framework (OSF) platform at osf.io/5sm9j. No part of the study, including the analyses, was pre-registered.

3.2.1. Procedure and materials

Participants were administered with six versions of a 4-choice spatial Stroop task, all requiring keypress responses to indicate the direction of a target arrow. The experiment was programmed using Psytoolkit (Stoet, 2010, 2017) and administered online (the code and stimuli are available on OSF: osf.io/9hsnw). All the participants were recruited by the experimenters and given a link to perform the task online.

The stimuli were presented in full-screen mode, with a resolution of 800 x 600 pixels, on a gray background (RGB: 128, 128, 128). Each trial started with a fixation stimulus presented at the center of the screen for 500 ms, which participants were instructed to fixate. For all but the Saliency Stroop task, the fixation stimulus consisted in a vertically oriented thin black cross (30 x 30 pixels) enclosed in the partial outline of a black square (94 x 94 pixels), which was then replaced by the experimental stimulus (see Figure 3.1). Moreover, in the Peripheral Stroop task, four white squares (73 x 73 pixels) were also presented during the fixation screen at the four corners of an imaginary square of 600 x 600 pixels centered on the screen. In the Saliency Stroop task, the fixation stimulus consisted in the black outline of a thick diagonal cross (60 x 60 pixels, see Figure 3.1). Then, the experimental stimulus was presented, which was different for each experimental task (see below). The stimulus remained on screen until participant's response or up to a response time-out of 2000 ms. Afterwards, a blank screen constituting the inter-trial interval was presented for 500 ms.

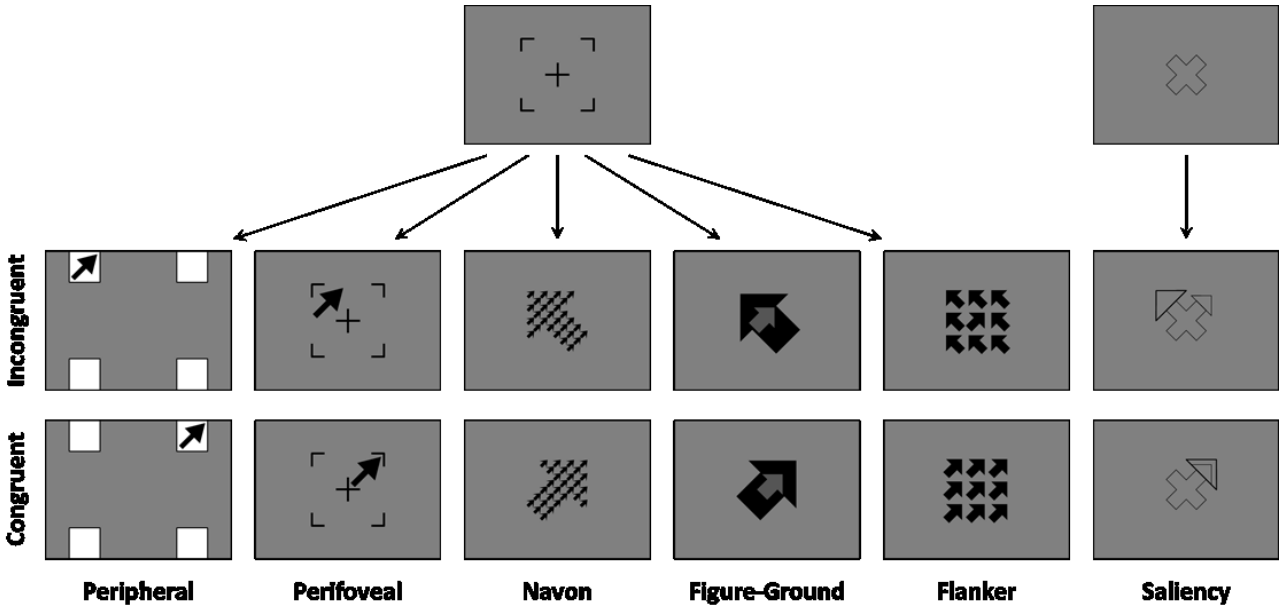

Figure 3.1.
Experimental stimuli for the six spatial Stroop tasks. For each version, an example of incongruent and congruent trials is depicted. The first row shows the fixation stimuli. Note that the stimuli are not to scale for illustrative purposes (see Procedure and Materials for details).

Each of the six spatial Stroop tasks followed the same procedure outlined above but involved different experimental stimuli, as detailed below. However, in all the tasks, participants had to pay attention to a target arrow to indicate its direction, which was thus the task-relevant information, corresponding to the response. The possible directions of the target arrows were always upper-left, upper-right, lower-right, and lower-left and participants were required to provide their responses by using four keys on a computer keyboard, which were spatially arranged to ensure the dimensional overlap between the characteristics of the stimulus and the response. Indeed, the keys E, O, K, and D were associated, in a spatially compatible

fashion, with the upper-left, upper-right, lower-right, and lower-left direction, respectively, and had to be pressed using the left middle, right middle, right index, and left index fingers, respectively. The experimental stimuli also included a task-irrelevant feature that could either match or not with the task-relevant feature, respectively, in congruent and incongruent trials, thus interfering with the participants' decision in incongruent trials (see Figure 3.1):

1) in the *Peripheral Stroop*, the experimental stimulus consisted in an arrow that appeared inside one of those four squares, pointing to one of the same four directions (upper-left, upper-right, lower-right, and lower-left). Participants were instructed to respond to the arrow direction, regardless of the position where it appeared. Trials could thus be either congruent or incongruent, depending on whether the arrow direction (i.e., the task-relevant information) matched or not its position (i.e., the task-irrelevant information);
2) The *Perifoveal Stroop* version was akin to the *Peripheral* one with the difference that the arrow position was manipulated inside the fixation stimulus. Indeed, the partial outline of the square around the fixation cross created the impression of four small squares. Therefore, the arrow was displayed within one of these apparent small squares and, like in the *Peripheral Stroop task*, its pointing direction (i.e., the task-relevant information) could be either congruent or incongruent with its position (i.e., the task-irrelevant information).
3) In the *Navon Stroop* version, the experimental stimulus consisted of 28 small arrows (local level), spatially arranged to form a large arrow (global level). Participants were asked to indicate the direction of the small arrows (i.e., the task-relevant information), regardless of the direction of the large arrow (i.e., the task-irrelevant information). All the small arrows pointed to the same direction which, to manipulate congruency, either matched or not the direction of the large arrow. This task represents a modification of the original Navon task (Navon, 1977) assessing letter identification, whose typical effect relies on the so-called global precedence. In a similar vein, our spatial version using arrows also entailed task-related interference between the more salient and also conceptually stronger processing of the global arrow as compared to the local arrows. Moreover, stimulus conflict was guaranteed by the dimensional overlap between the task-relevant and task-irrelevant arrows, while response conflict was produced by the two dimensional overlaps between response and stimulus information.
4) In the *Figure-Ground Stroop* version, the experimental stimulus consisted of a small grey arrow completely embedded in a large black arrow. The task-relevant information was the direction of the smaller arrow, and the task-irrelevant information was the direction of the outer arrow, and the two arrows again could either match or not. Like the Navon Stroop versions, also this task leverages global precedence, with easier processing of the large arrow compared to the small one, with a consequent global-to-local conflict engendering task-related interference. Moreover, interference was produced at

the stimulus level thanks to the dimensional overlap between the two arrows and at the response level due to the stimulus-response dimensional overlaps.

5) In the *Flanker Stroop,* the experimental stimulus consisted of a black arrow presented in the center of the screen (target), flanked by 8 same-sized black arrows on a 3-by-3 square grid. The task-relevant information was the direction of the central arrow, which could be congruent or not with the flanking arrows. This task represents a modification of the original Flanker task (Eriksen & Eriksen, 1974) assessing letter identification, whose typical interference effect is driven by the higher perceptual numerosity of flanking stimuli as compared to the centrally-presented target. Similarly, our spatial version with arrows leveraged the higher perceptual saliency due to numerosity of the surrounding task-irrelevant arrows as compared to the central task-relevant arrow, producing task conflict. Moreover, interference at the stimulus level was caused by conceptual overlap between the flanking distractors and the central arrow, while interference at the response level was generated by the two dimensional overlaps between the response and the stimulus information.
6) The *Saliency Stroop* version slightly differed from the others, starting with a different fixation cross, which appeared as a thick, empty diagonal cross, which was not replaced by the experimental stimulus. Indeed, the experimental stimulus consisted in two empty triangles, a smaller and thinner one and a larger and thicker one, which appeared at the extremity of one of the four cross arms. In incongruent trials, the two triangles appeared at different extremities, forming an arrow with a large head and one with a small head (target arrow) pointing to different directions; in congruent trials, the two triangles appeared at the same extremity, creating a single arrow with overlapping heads. Participants responded to the direction of the smaller arrow, regardless of the direction of the larger arrow, which was perceptually more salient and, thus, processed more easily. Therefore, in this task, conflict was exclusively driven by this saliency imbalance between the two dimensions. Similarly to the other tasks, stimulus-related conflict occurred due to stimulus-stimulus overlap, while response-related conflict was driven by the two-dimensional overlaps between response and stimulus information.

At the beginning of the experiment, general instructions were provided, informing participants of the procedure, the general task (i.e., indicating the direction of a target arrow), and the response mapping. It was also recommended to execute the experiment in a quiet environment without distractions and to maintain a comfortable posture that allowed them to look straight to the center of the screen and keep the responding fingers in contact with the response keys. Particular care was taken to keep the instructions as simple and clear as possible.

The six tasks were then presented in separate blocks of 72 experimental trials each, preceded by one warm-up trial that was not included in the analyses. The experimental trials were equally divided in congruent and incongruent trials and both the four task-irrelevant and task-relevant characteristics (and

thus the responses) were presented the same number of times. A self-paced break was provided between the blocks, during which a reminder of the response mapping was presented (median duration = 28.9 s, *IQR* = 23.0 s). The experiment lasted less than 23 min in total on average (*M* = 22.7 min, *SD* = 7.1 min).

At the beginning of each block, specific task instructions were presented, illustrating the stimuli and the task to be performed. Participants were also asked to respond as quickly and accurately as possible. The instructions were followed by a sub-block of practice trials, during which participants received feedback on their responses. In case of errors, the task-relevant information and the corresponding response mapping were repeated. Practice trials were presented until participants reached an accuracy of 75% within at least six trials, or for a maximum of 24 trials. In two cases (0.46% of all cases), the accuracy was below 75% within 24 trials, but it was still well above the chance level (62.5 and 70.8%); in four other cases (0.93% of all cases) more than 6 trials were needed to reach the required level of accuracy.

A randomized balanced order of presentation of the six tasks was used, based on a Williams Latin square design (Williams, 1949) to also account for first-order carryover effects. The order of presentation of the trials was pseudo-randomized so that there were at most three consecutive repetitions of congruency, and no repetitions of stimulus characteristics and/or responses, thus avoiding first order priming effects.

3.2.2. Data analysis

The data were analyzed in Jamovi (version 1.6; jamovi.org) and Matlab (version 2019b; The Mathworks, Inc. Natick, MA) to 1) estimate the magnitude of the Stroop effects in the six tasks we used, as well as their across-tasks differences, and 2) estimate their internal consistency reliability based on two analytical approaches. Analyses were performed not only on untransformed RTs, but also on both natural log-transformed RTs (lnRTs) and inverse-transformed RTs (iRTs, computed as -1000/RTs). Indeed, the distribution of RTs was heavily right-skewed and their logarithmic transformation did not eliminate completely the right skewness, so that the lognormal distribution did not provide an adequate fit to our data (see Appendix A, Figure A.1).

We first performed a “standard” general linear model (GLM) analysis, commonly used in cognitive psychology research, to facilitate comparison of our results with existing (and future) findings. This analytical approach requires aggregating participants’ performance across trials to obtain participants-by-task scores, in line with the analytic framework of the classical test theory. However, this discards any trial-by-trial variability that may contaminate participants-by-task scores, potentially decreasing their accuracy and generalizability (see also Rouder & Haaf, 2019).

To avoid this potential problem, we used a multilevel modeling approach (or trial-by-trials hierarchical modeling), which is particularly useful to our aim. Indeed, multilevel modeling allows assessing the

experimental effects of interest (i.e., in our case, the Stroop effects in the different tasks and the differences between them) while partialling out the effects of lower-level confounding factors at the trial level, which can be seen as sources of trial-by-trial noise in the estimation of the Stroop effects at the subject level. This approach would thus provide more accurate and precise estimates of Stroop effects and, consequently, of their reliability as well, by explaining intra-subject/inter-trial sources of variance contributing to measurement error.

Moreover, we assessed the robustness of our results to analytic flexibility (the so-called "researcher degrees of freedom" (Simmons et al., 2011) or "the garden of forking paths" (Gelman & Loken, 2013) by performing a series of robustness checks based on a multiverse analysis approach (Parsons, 2020; Steegen et al., 2016).

Training trials, trials with errors or missed responses (3.97% of trials) and trials with RTs shorter than 150 ms (none of the remaining trials) were excluded from all the analyses. We checked for the presence of participants with low compliance, defined as those having either a mean iRTs more than three standard deviations away from the sample mean or a mean accuracy lower than 75%. Based on these criteria, no participant was excluded from the analyses (see Appendix A, Figure A.2).

3.2.2.1. Assessing the magnitude of the Stroop effects

We first performed a standard GLM analysis using a repeated-measures ANOVA (rmANOVA) with Task (Peripheral, Perifoveal, Navon, Figure-Ground, Flanker, and Saliency) and trial Congruency (Congruent vs. Incongruent) as within-subject factors, and the Huynh-Feldt correction for sphericity violations were applied to the degrees of freedom. Post-hoc comparisons were performed using paired t-tests corrected for multiple comparisons with the Scheffe's method. To better investigate the Task by Congruency interaction of interest (i.e., the across-tasks differences in the Stroop effect), a follow-up rmANOVA was performed on the Stroop effects (i.e., the difference between RTs in Incongruent and Congruent trials) across the six tasks. The statistical significance of the Stroop effect for each task was assessed by means of two-tailed one-sample t tests against 0 and the corresponding effect size estimates were computed as the Cohen's d. These analyses were performed on both RT and accuracy measures (for which we also performed a nonparametric Friedman ANOVA on Stroop effects).

We then performed two multilevel modeling analyses, that is, a linear mixed-effects model analysis (LMM, Baayen et al., 2008) and a random coefficient analysis (RCA, also called random regression or two-step regression, Lorch & Myers, 1990). We also performed RCA because LMMs usually fail to converge when trying to model complex random effects structures, that is, the inter-subject variability in experimental (and confounding) effects, especially when random effects are large and/or there are few observations (Barr et

al., 2013). Consequently, usually a simpler random-effects structure has to be modeled, thus constraining the remaining effects to be the same across participants. This assumption, however, is often untenable, severely limits the generalizability of the results, and prevents assessing the reliability of the effects for which the inter-subject variability is not modeled. By contrast, RCA allows assessing the inter-subject variability in all the modeled effects. Indeed, in RCA, by-subject regressions are first computed, thus allowing all the modeled effects to vary across participants, followed by a one-sample t-test against zero (or equivalent nonparametric tests) to test for their statistical significance.

We included in the LMM several possible confounding predictors that were expected to explain trial-by-trial variability in RTs. Indeed, as explained above, the aim was to obtain more accurate estimates of the Stroop effects, which can indeed be contaminated by these sources of removable noise at the trial level, like longitudinal effects during the task. Specifically, the final model for LMM comprised the following lower-level confounding predictors as fixed effects: i) three continuous predictors for the effect of both the rank-order of the blocks in the experiment (Block) and the rank-order of the trials in each block (Trial), as well as their interaction, to account for potential time-on-task effects like learning/adaptation or fatigue effects (e.g., Möckel et al., 2015); ii) a continuous predictor reflecting the RT of the preceding trial (preRT), to account for the well-known temporal dependency in response times (Baayen & Milin, 2010); iii) a predictor for the fixed effect of error commission in the preceding trial (PostERR), to account for the so-called post-error slowing (Rabbitt, 1966). It is important to note that these fixed effects were modeled not only to improve the model fit and the estimation of the effects of interest, but also to avoid violating the assumption of the independence of observation for linear modeling. We also included two other lower-level confounding predictors as fixed effects, that is, the horizontal and vertical coding of the response (respectively, hResp and vResp), to account for potential differences due to the response hand and finger, respectively. Finally, we modeled the experimental effects of interest and their inter-individual variability by including predictors for the effects of the Stroop version (Task), the trial congruency (Cong), and their interaction, which were included in both the fixed and random part of the model (the inclusion of the effects of interest in the random part is necessary for calculating their reliability). The Wilkinson-notation formula for the final model is:

*RT ~ 1 + Block*Trial + preRT + PostERR + hResp + vResp + Task*Cong + (Task*Cong|Participant)*

The continuous predictors were scaled to facilitate model convergence and the interpretation of the results. We determined the final LMM model by performing a model-building procedure to assess whether the inclusion of the parameters for the above-mentioned effects was justified, using a log-likelihood ratio test to compare progressively more complex models with simpler models (Baayen et al., 2008). After this model-building procedure, we inspected the quantile-quantile plot for the residuals of the final model for evidence of stress in the model fit. We then refitted the final model after removing data points with

absolute standardized residuals exceeding 3. We report the estimated coefficient (*b*), standard error (*SE*), and *t* and *p* value for each fixed effect included in the trimmed final model (note that all the results reported in the present paper refer to the trimmed version of the final models). We calculated the *p* values by using Satterthwaite's approximation of degrees of freedom. An alpha level of .05 was set as the cut-off for statistical significance. Effect sizes for the Task by Congruency interaction of interest were estimated as Cohen's d based on one-sample *t* tests on the random slopes.

As regards the RCA, linear regressions were first run at the subject level using a regression model similar to the final LMM model described above. In this case, the Block predictor was not included in the model because it was confounded with the Task predictor at the subject level. The corresponding formula for the final RCA model is thus:

*RT ~ 1 + Trial + preRT + PostError + hResp + vResp + Task*Congruency*

Again, the model was refitted after exclusion of outliers as described above. Then, the statistical significance and the effect size of the modeled effects was assessed at the group level by performing one-sample *t* tests against 0 on the estimated *b* coefficients for each participant.

We also performed control analyses using multilevel modeling to verify the assumption that this analytical approach provides better estimates of Stroop effects and their reliability by explaining intra-subject/inter-trial sources of variance contributing to measurement error. To this aim, we replicated both LMM and RCA analyses on iRTs without the inclusion of all the trial-level confounds described above and compared their results with those yielded by the full models.

Finally, we examined commonality among spatial Stroop tasks by performing a correlational analysis. Specifically, we computed Pearson's correlations among the participants' Stroop effects for the six tasks, separately for the GLM, LMM, and RCA analyses. The statistical significance of these correlations was corrected for multiple comparisons using the FDR method. We also performed an exploratory factor analysis on the participants' Stroop effects using the maximum likelihood extraction method followed by an Oblimin rotation. The number of factors to be extracted was determined based on parallel analysis.

3.2.2.2. Assessing the internal reliability of the Stroop effects

We first assessed the internal consistency reliability of the GLM-based aggregated Stroop effect in each task by computing split-half correlations corrected with the Spearman-Brown formula (r_{SB}). Specifically, for each task, the observations were randomly split in two subsets and the participants' Stroop effects were computed and correlated between the two subsets.

We then assessed the internal reliability of the Stroop effects estimated using the multilevel modeling approach. Specifically, for each task, the observations were randomly split in two subsets and both LMM and RCA analyses were performed for each subset to model the interindividual variability in the Stroop effect while controlling for the same confounding predictors used in the main analyses described above. Finally, for both the LMM and RCA analyses, the by-subject random slopes for the Cong effects for each task in the two subsets were correlated to obtain the r_{SB} values. We also computed the reliabilities of the Stroop effects yielded by the reduced multilevel models described above, which did not include trial-level confounds.

In all cases, 2000 randomizations were used. We report the median r_{SB} values as well as the corresponding nonparametric 95% confidence intervals ($CI_{95\%}$).

3.2.3. Participants

Seventy-two participants were recruited (42 females and 27 males; mean age = 25.35 years, *SD* = 8.21 years; three participants chose to not indicate gender and age). Participants consisted of a convenience sample recruited using researchers' personal networks and were not compensated for their participation. All procedures performed were in accordance with the ethical standards of the 2013 Declaration of Helsinki for human studies of the World Medical Association. The study was approved by the Ethical Committee for the Psychological Research of the University of Padova (approved protocol reference number: 3725).

Participants' handedness was assessed using the Edinburgh Handedness Inventory (EHI, Oldfield, 1971). The sample comprised six left-handed participants (EHI scores < −50) and nine ambidextrous participants (EHI score between -50 and 50), but the results were substantially the same when excluding either left-handed participants only or together with ambidextrous participants. Two participants reported to suffer from neurological or psychiatric disorders and to be under medication. Again, the exclusion of these participants did not substantially change the reported results, so we decided to not exclude them (see the "LMM - iRT - Control analyses" section of the analysis script available at osf.io/9xfkw).

3.2.3.1. Power analysis

We performed an a-priori power analysis in G* Power (Erdfelder et al., 1996) to compute the minimum sample size required to detect, with a statistical power of .80, the interaction of main interest (i.e., the difference in the Stroop effect across tasks) in a repeated measure ANOVA. We assumed a small-medium Cohen's *d* effect size of .3 (corresponding to η^2_p = .022), a correlation between repeated measures of .70, and a (Huynh-Feldt) non-sphericity correction ε of .5, as estimated conservatively from recent pilot studies with a similar design from our research group. This analysis revealed that at least 48 participants were required. We nonetheless decided to recruit as many participants as possible exceeding the required

sample size, so as to be able to detect even smaller effects (by increasing the statistical power of our analyses) and to increase the precision of the experimental effects estimates.

As regards the power estimation for the LMM analysis, it "is still a largely uncharted terrain containing many open and unresolved issues" (Kumle et al., 2021, p. 3). First, classical analytical approaches to power estimation, like the one used by G*Power, cannot be applied to LMMs because they lack the required flexibility (Kumle et al., 2021). Moreover, to the best of our knowledge, the available analytical solutions proposed to compute power for LMMs are not adequate for our complex model (e.g., the Westfall's approach (Westfall et al., 2014) is only applicable for models with a single two-level fixed effect; see Brysbaert & Stevens, 2018). To solve these issues, the simulation-based approach to power analysis has been proposed for LMMs as a flexible and powerful alternative to analytical approaches (Brysbaert & Stevens, 2018; Green & MacLeod, 2016; Kumle et al., 2021). However, this approach is not suitable in our case, as it requires that an optimal model is selected a-priori, while we adopted a conservative hierarchical model building approach. Moreover, given our aim and the use of novel experimental tasks, no well-powered data are available to allow us to generate accurate artificial data needed to run the simulation, and the complexity of our model and the amount of recorded data made it too computationally intensive to run multiple simulations with varying parameters. Nonetheless, it should be noted that, since we had 36 trials per condition, 45 participants were needed to reach the recommended minimum number of 1600 observations per condition (Brysbaert & Stevens, 2018). It should also be noted that LMMs tend to provide higher power than standard GLM approaches.

3.3. Results

3.3.1. Magnitude of the Stroop effects

Table 3.1 shows the descriptive statistics for the RTs (see Appendix A, Tables A.1-2 and Figure A.3, for the other measures) and the accuracy (percentage of correct trials). Participants' overall accuracy was very high (*M* = 96.0%, range = [86.3% - 99.8%]) and at ceiling in all tasks for congruent trials (> 98.3%; *M* = 98.7%, range = [93.5% - 100%]) but not for incongruent trials (>89.5%; *M* = 93.3%, range = [77.3% - 100%]). Consequently, the participants' Stroop effects on the accuracy heavily depended on their average accuracy (i.e., participants with a very high overall accuracy cannot show a Stroop effect). This severely limits the interpretability of the analyses on accuracy and introduces strong biases in the estimation of the reliability of this measure. For this reason, we do not report here the results of the analyses on the accuracy (but see osf.io/6rzsh for the GLM analysis on accuracy data) and did not assess the internal reliability of this measure.

We report here the results of the analyses performed on iRTs because the distribution of RTs was heavily right-skewed (see Data Analysis section). Moreover, the assumption of normality was violated for the residual of the analyses on both lnRTs and RTs, and the latter also severely violated the homoscedasticity assumption (see Appendix A, Figures A.6, A.8, A15, and A.18). However, the results of the analyses performed on RTs and lnRTs are reported in the supplementary material available from our project repository on the Open Science Framework (see Appendix A, Sections A.4.2-3, A.5.2-3, A.6.2-3).

Table 3.1. Descriptive statistics.

	Peripheral		Perifoveal		Navon		Figure-Ground		Flanker		Saliency	
	M	***SD***	***M***	***SD***	***M***	***SD***	***M***	***SD***	***M***	***SD***	***M***	***SD***
Accuracy												
C	99%	3%	98%	4%	99%	2%	99%	2%	99%	2%	98%	2%
I	90%	9%	90%	11%	96%	6%	94%	8%	95%	7%	96%	6%
Stroop	9%	8%	8%	9%	3%	6%	5%	8%	4%	7%	3%	5%
RT (ms)												
C	586	158	529	169	544	114	500	90	523	124	490	105
I	716	214	658	219	615	140	579	90	586	108	523	108
Stroop	130	87	129	78	71	47	79	29	63	31	32	28

Notes: C, congruent trials; I, incongruent trials.

As regards the GLM-based analysis, the rmANOVA on iRTs revealed the statistical significance of all the investigated effects. The post-hoc comparisons on the main effects of Task [$F(3.44, 244.31) = 33.9$, $p < .0001$, $\eta^2_p = .32$] revealed that participants were significantly slower in performing the Peripheral task as compared to all the other tasks (all *p*s < .003) and significantly faster in performing the Saliency task as compared to all the other tasks (all *p*s < .001). On the other hand, the Perifoveal, the Navon, the Figure-Ground and the Flanker tasks did not significantly differ from each other in terms of iRTs (all *p*s > .109). The effect of Congruency was also significant [$F(1, 71) = 907.2$, $p < .0001$, $\eta^2_p = .93$], with a very high overall Stroop effect ($M = .269$, $SD = .076$). Crucially, the Stroop effects differed across tasks [$F(3.33, 236.55) = 55.7$, $p < .0001$, $\eta^2_p = .44$], albeit they were all significant (all *p*s < .0001) with very high effect sizes (all *d*s > 1.57) and dominance values, that is, the percentage of participants showing a positive Stroop effect (see Figure 3.2 and Table 3.2; see osf.io/cwh73 for the detailed statistics; see also osf.io/49kdh and osf.io/ysmjc for the analyses on lnRTs and RTs, respectively). Indeed, the post-hoc comparisons on the follow-up ANOVA revealed the following pattern of Stroop effects: Perifoveal > Figure-Ground & Peripheral > Flanker > Navon & Saliency.

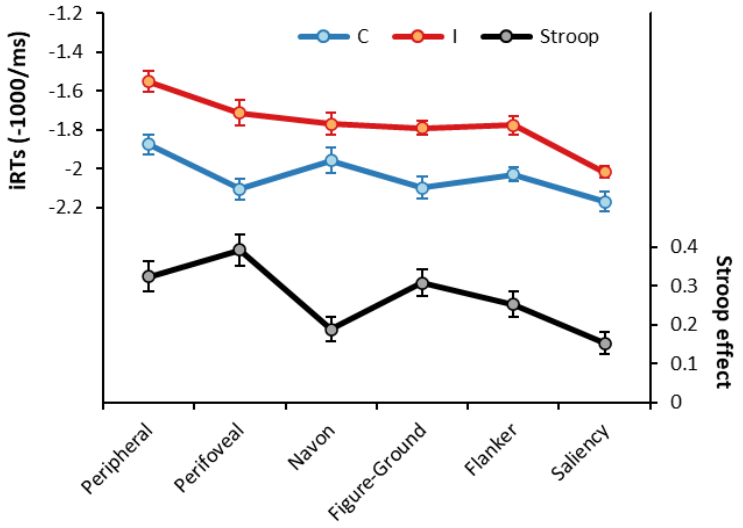

Figure 3.2.
ANOVA results, Congruency*Task interaction. The plot shows the subjects' mean iRTs in Congruent (C, blue line) and Incongruent (I, red line) trials as a function of the Task (x axis). The corresponding Stroop effects are also shown (black line). Error bars represent within-subjects 95% confidence intervals (Morey, 2008).

Table 3.2. Stroop effects for iRTs as a function of the analytical approach.

	GLM					LMM					RCA				
	M	*SD*	*t*	*d*	*Dom*	*M*	*SD*	*t*	*d*	*Dom*	*M*	*SD*	*t*	*d*	*Dom*
Peripheral	0.324	0.137	20.1	2.37	100	0.343	0.113	25.7	3.02	100	0.346	0.145	20.3	2.39	100
Perifoveal	0.391	0.141	23.5	2.77	100	0.415	0.129	27.3	3.21	100	0.408	0.153	22.7	2.67	100
Navon	0.188	0.096	16.7	1.96	95.8	0.197	0.070	24.0	2.83	100	0.197	0.098	17.0	2.00	95.8
FG	0.307	0.120	21.7	2.56	100	0.320	0.100	27.2	3.21	100	0.317	0.121	22.3	2.63	100
Flanker	0.252	0.120	17.7	2.09	98.6	0.262	0.104	21.4	2.53	98.6	0.259	0.119	18.4	2.17	98.6
Saliency	0.152	0.097	13.4	1.58	91.7	0.157	0.064	20.8	2.46	100	0.153	0.099	13.1	1.54	91.7

Notes: iRT, inverse-transformed RTs; GLM, general linear model; LMM, linear mixed-effects model; RCA, random coefficient analysis; Dom, percentage of participants showing a positive Stroop effect; FG, Figure-Ground task (see Data Analysis section for details).

The ANOVA results were replicated by both multilevel modeling analyses. Indeed, the LMM analysis confirmed the statistical significance of the Congruency by Task interaction ($p < .0001$, see Table 3.3), with a similar pattern of the across-tasks differences in Stroop effects described above (see Appendix A, Table A.4). Moreover, albeit the pattern of participants' Stroop effects was accurately recovered by LMM, with high correlations with the Stroop effects observed in the GLM analyses (all $rs > .81$), the corresponding effect sizes were all considerably larger, especially for the Peripheral and Perifoveal tasks, which resulted significantly larger (see Table 3.2; see also Appendix A, Tables A.1-2 and Section A.5.1.4). This was likely due to the partial pooling (also called shrinkage or regularization) used by LMMs to estimate random slopes, which reduced the between-subject variability of the Stroop effects by "shrinking" the participant-specific effects toward the sample average effect based on the assumed normality of their distribution.

Consequently, the LMM consistently underestimated the Stroop effects of participants showing larger Stroop effects and overestimated those of participants showing smaller Stroop effects. Indeed, linear regression analyses revealed that, for all tasks, the slope of the regression line for the Stroop effects yielded by the LMM relative to the GLM approach was significantly lower than 1, while the intercept was significantly larger than 0 (see Appendix A, Section A.5.1.4).

The LMM analysis also revealed that all the confounding predictors significantly modulated participants' iRTs (all *p*s < .0001, see Table 3.3). Specifically, the Trial by Block interaction indicates a learning/adaptation effect (i.e., a reduction of iRTs as the trials within a block went on) that decreased during the experiment (i.e., as the blocks went on). Moreover, there was a significant post-error slowing (i.e., participants' iRTs were significantly higher after an erroneous trial) and a significant temporal dependency in iRTs (i.e., a positive correlation between iRTs at the current and preceding trial). Finally, participants were faster on average in providing a response with the index fingers and with the right hand (note that the participants' EHI score did not significantly modulate this latter effect: $\chi^2(2) = 0.81$, $p = .668$).

The conditional R^2 of the LMM model was .70 and 0.99% of the observations was removed as outliers (>3 absolute standardized residuals) to mitigate the stress of the model fit (i.e., to improve the normality of the residuals, see Appendix A, Figure A.4). The same model was also fitted on both RTs and lnRTs, confirming the results reported above (see Appendix A, Sections A.5.2-3). As anticipated above, however, the assumptions of homoscedasticity and normality of the residuals were violated in the analyses on lnRTs and RTs (see Appendix A, Figures A.6 and A.8), so results obtained on these data should be taken with caution. Moreover, it should be noted that the inclusion of the by-participants random slopes for the Congruency by Task interaction of interest resulted in a singular fit in all cases, likely due to the limited number of observations.

The control LMM analysis performed using the reduced model without confounding predictors confirmed the across-task pattern of Stroop effects, with very high correlations with the Stroop effects observed using the full model (all *r*s > .983). However, participants' Stroop effects obtained using the reduced model were all significantly and consistently smaller than those obtained in the main LMM analysis controlling for the trial-level confounding effects (all *p*s > .0001; see Appendix A, Section A.5.4).

We thus performed the RCA analysis, which replicated the LMM results (see Appendix A, Table A.22). Indeed, the Congruency by Task interaction was significant, with the same pattern of across-tasks differences in Stroop effects revealed by the GLM analysis (see above, see also Appendix A, Table A.23). Notably, both the raw and standardized effect sizes for the Stroop effects were almost identical to those revealed by the GLM analysis (see Table 3.2). Indeed, the pattern of participants' Stroop effects was recovered almost perfectly by RCA, as the correlations with the Stroop effects observed in the GLM analyses

were all very high (all *r*s > .96, see Appendix A, Sections A.3 and A.6.1.4) and higher than those observed for the LMM analysis in all tasks (see Appendix A, Section A.6.1.5).

Table 3.3. LMM results.

Effect	*F*	DF1	DF2	*p*
Block	34.5	1	192.70	< .0001
Trial	729.4	1	28887	< .0001
postERR	437.3	1	29124	< .0001
preRT	799.3	1	28950	< .0001
hResp	111.9	1	28862	< .0001
vResp	375.7	1	28859	< .0001
Trial:Block	23.2	1	28868	< .0001
CONG	437.3	1	72.23	< .0001
TASK	51.6	5	71.21	< .0001
CONG:TASK	58.2	5	88.46	< .0001

Notes: postERR, post-error trials; preRT, iRT at the previous trial; hResp, horizontal coding of the response (i.e., the responding hand: right vs left); vResp, vertical coding of the response (i.e., the responding finger: middle vs index); CONG, Congruency; DF, degrees of freedom. *P* values were computed using the Satterthwaite's approximation

Moreover, all the effects of the confounding predictors on participants' iRTs were confirmed (all *p*s < .001; see Appendix A, Table A.22, for the detailed statistics). The conditional R^2 of the RCA model was .71 and 0.8% of the observations was removed as outliers to mitigate the stress of the model fit (see Appendix A, Figure A.12). Again, the same model was also fitted on both RTs and lnRTs, confirming the results reported above (see Appendix A, Sections A.6.2 and A.6.3), but with violations of the assumptions of homoscedasticity and normality of the residuals (see Appendix A, Figures A.15 and A.18). To further check the robustness of our results, we ran similar RCA analyses after excluding the postERR predictor. Indeed, given the high accuracy, some participants had very few post-error trials, making the estimation of the post-error slowing effect problematic. These analyses confirmed the results reported above.

The control RCA analysis performed using the reduced model without confounding predictors confirmed the across-task pattern of Stroop effects, with very high correlations with the Stroop effects observed using the full model (all *r*s > .976). However, as for the LMM analysis, participants' Stroop effects obtained using the reduced model were all significantly and consistently smaller than those obtained in the main LMM analysis controlling for the trial-level confounding effects (all *p*s > .025; see Appendix A, Section A.6.4).

Finally, the correlational analysis performed to examine commonality across spatial Stroop tasks revealed a specific pattern of intercorrelations among Stroop effects that emerged in all the three analyses we performed (see Appendix A, Sections A.7.1-3). Specifically, there was a significant correlation between

the Stroop effects yielded by the Peripheral and Perifoveal tasks (r = .627, .860, and .594 for the GLM, LMM, and RCA analyses, respectively). Moreover, the Stroop effects for the Saliency task was significantly correlated with those yielded by the Navon (r = .304, .472, and .296), Figure-Ground (r = .491, .860, and .485), and Flanker (r = .443, .802, and .425) tasks. Finally, the Stroop effects yielded by the Figure-Ground and Flanker tasks were significantly correlated (r = .720, .878, and .720). The exploratory factor analysis confirmed this pattern of results. Indeed, it revealed the existence of two latent factors that consistently comprised, respectively, the Peripheral and Perifoveal Stroop effects (all loadings > .73) and the Figure-Ground, Flanker, and Saliency Stroop effects (all loadings > .53). The Navon Stroop effect was inconsistently included in the first factor with small loadings (< .44) and high uniqueness (> .70) (see Appendix A, Table A.54; see also osf.io/zqemg).

3.3.2. Internal reliability of the Stroop effects

Figure 3.3 shows the internal reliability estimates (the median r_{SB} and the corresponding nonparametric $CI_{95\%}$, see also Appendix A, Section A.8) of the Stroop effects for each task as a function of both the analytical approach and the RT transformation.

A first notable result regards the influence of the analytical approach on the internal reliability estimates, which generally tended to be higher and more stable for RCA and LMM approaches as compared to the GLM one. By contrast, the RT transformations differently affected the internal reliability estimates across versions.

Nonetheless, the internal reliability of both the Peripheral and Perifoveal versions was quite high and robust against the choice of the analytical approach and the RT transformation. Indeed, the median r_{SB} values for these versions were consistently higher than .65 (range: from .72 to .88 and from .66 to .85, respectively) with relatively low variability across randomizations, albeit they still tended to be higher and more stable for RCA and LMM approaches as compared to GLM one, and lower for lnRTs and iRTs as compared to untransformed RTs.

By contrast, the internal reliability of the other versions was generally lower and less robust as compared to that of the Peripheral and Perifoveal versions, with higher variability of median r_{sb} values not only across randomizations, but also as a function of both the analytical approach and the RT transformation. Specifically, the internal reliability of the Navon version ranged from .39 to .79, with a similar pattern as the one observed for the Peripheral and Perifoveal versions. Conversely, the internal reliability of both the Figure-Ground and Flanker versions (median r_{sb} values range: from .32 to .93 and from .42 to .95, respectively) tended to be higher and more stable for lnRT and, especially, iRT as compared to RT. Particularly good internal reliability estimates were observed for both versions in the LMM analyses on iRTs.

Finally, the internal reliability of the Saliency version was generally poor (median r_{sb} values range: from .1 to .77), again except for the one observed in the LMM analyses on iRTs.

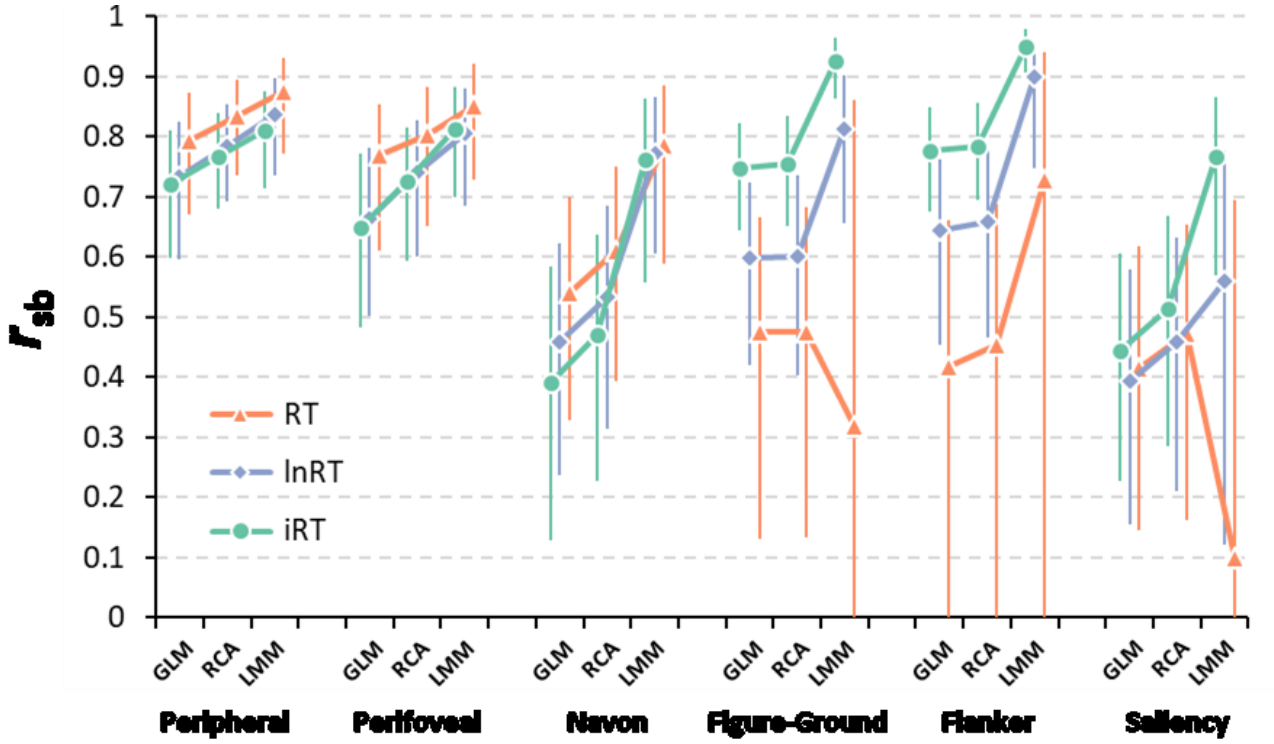

Figure 3.3.
Internal reliability of the Stroop effects. The plot shows the median internal reliability estimates (r_{sb}) of the Stroop effects for each task as a function of both the analytical approach (GLM: general linear model, RCA: random coefficient analysis, LMM: linear mixed-effect model; x axis) and RT transformation (RT: untransformed response times –in orange–, lnRT: natural log-transformed RT –in purple–, iRT: inverse-transformed RT –in green–; see Data analysis section for details). The error bars represent the nonparametric 95% confidence interval.

Interestingly, the internal reliability of the Stroop effects yielded by the control multilevel analyses performed using the reduced models (i.e., without including the trial-level confounding predictors) was lower than that obtained using the full models (see Appendix A, Figure A.26), which also yielded larger Stroop effects.

3.4. Discussion

The spatial Stroop task is an experimental paradigm measuring cognitive control and interference resolution that offers some methodological advantages over the commonly used verbal Stroop task. However, the spatial Stroop tasks used in the literature all have methodological drawbacks that limit their potential of yielding a complete Stroop interference effect that is analogous to that engendered by verbal Stroop tasks. We recently proposed a spatial Stroop task (Puccioni & Vallesi, 2012a) that overcomes these limitations by ensuring conflict at multiple loci, that is, at the task, stimulus and response levels, with

complete alternated trials sequences, thus allowing to measure participants' interference resolution and conflict adaptation abilities effectively. Nonetheless, this task (Peripheral) still has some weaknesses due to the use of peripherally presented visual stimuli. Therefore, we aimed at assessing alternative spatial Stroop versions that maintain the methodological advantages of the Peripheral spatial Stroop task while overcoming its limits. To this aim, we designed five novel versions of the spatial Stroop task (Perifoveal, Navon, Figure-Ground, Flanker, and Saliency) and performed an online study to compare the six spatial Stroop tasks in a within-subjects design. Although we predicted that they all would have produced a spatial Stroop effect, our goal was to identify the task yielding not only the largest and most dominant, but also the most reliable Stroop effect. Moreover, we performed various robustness checks to assess the robustness of our results to analytic flexibility.

3.4.1. Magnitude of the Stroop effects

The analysis assessing the magnitude of the Stroop effects in our tasks revealed that they all yielded very large Stroop effects. Indeed, regardless of the RT transformation of the analytical approach, the d values for all tasks were always well above the value of 0.8 (see Table 3.2), which is commonly considered as the threshold of large effect sizes. This confirms our expectation that all our spatial Stroop paradigms are effective at producing a spatial Stroop effect, in line with the dominance assumption (Rouder & Haaf, 2018, 2019). Our results are thus generally in line with the idea that all individuals have a true positive Stroop effect (i.e., they truly respond more slowly in incongruent compared to congruent trials).

In particular, our original Peripheral Stroop tasks seem to be universal (Parsons, 2020), with all participants showing an estimated positive Stroop effect that was very large and robust to analytic flexibility (median d = 2.09; range: from 1.43 to 3.02; see Appendix A, Section A.3), with the exception of one participant in the RCA analysis on RTs (who nonetheless showed an estimated raw Stroop effect of -1.7 ms, which was indistinguishable from a positive Stroop effect with the resolution of our experimental design). This result confirms our previous findings showing the complete dominance of the Stroop effect yielded by the Peripheral task: all the 287 and 57 participants in the Capizzi and colleagues' (2017) and the Ambrosini and Vallesi (2017) studies, respectively, showed an estimated positive Stroop effect in a GLM-based analysis on lnRTs. Our analyses on the iRTs also revealed that this task yielded a Stroop effect that was consistently larger than those observed in the Navon, Flanker, and Saliency tasks (see Appendix A, Section A.3).

Similar results were obtained for the Perifoveal task, which is a variation of the Peripheral task. Indeed, also in this case all participants showed an estimated positive Stroop effect that was robust and even larger than that yielded by the Peripheral task (median d = 2.47; range: from 1.65 to 3.23; see Appendix A, Section A.3), again except for one participant in the RCA analysis on RTs (who showed a raw Stroop effect of -1.8 ms). Specifically, all the analyses on iRTs revealed that the Perifoveal Stroop effect was significantly larger as

compared to that observed for all the other tasks, including the original Peripheral one (see Appendix A, Tables A.4 and A.23; see also osf.io/cwh73). Since the only difference between these two tasks is the spatial arrangements of the visual stimuli (and the consequently lower eccentricity), these results indicate that large visuospatial attention shifts and/or eye movements were indeed present in the Peripheral task and that they may have led to an underestimation of the corresponding Stroop effect. Some support for the former conclusion comes from the significant main effect of Task, which showed that the Peripheral task had the longest overall RTs, confirming our initial assumption of the methodological limitations of the Peripheral task. Notwithstanding this difference, our results clearly indicated the commonality between the Peripheral and Perifoveal tasks, as their iRTs Stroop effects consistently showed a significant correlation ≥ .60 and loaded on the same latent factor, suggesting that they were related to the same cognitive processes (see Appendix A, Section A.7).

Our analyses also revealed that the universality assumption holds for the Figure-Ground task as well, albeit it presents more radical methodological variations as compared to the two tasks discussed above. In this case, all participants showed an estimated positive Stroop effect that was robust to analytical flexibility and very large (median d = 3.02; range: from 2.56 to 5.52; see Appendix A, Section A.3). Specifically, all the analyses on iRTs revealed that the Figure-Ground Stroop effect was comparable to that observed in the Peripheral task and significantly larger as compared to those observed in the Navon, Flanker, and Saliency tasks (see Appendix A, Tables A.4 and A.23; see also osf.io/cwh73).

Finally, looking at the Flanker task, it showed very large Stroop effects (median d = 2.49; range: from 2.07 to 4.76) but with a lower level of dominance because some participants did not show a positive Stroop effect. By contrast, the Navon and, especially, the Saliency tasks yielded Stroop effects that were smaller and less robust than those observed for the other tasks (see Appendix A, Section A.3).

3.4.2. Internal reliability of the Stroop effects

Despite the dominance and large magnitude of the Stroop effects yielded by the Peripheral and Perifoveal tasks, their internal reliability was quite high and robust against the choice of the analytical approach and the RT transformation, also with a relatively low variability across randomizations (see Figure 3.3 and Appendix A, Section A.8). This is at odds with the reliability paradox (Hedge et al., 2018), and related proposals (Rouder & Haaf, 2019) that if an experimental effect is so large and easily replicable to be called universal (Parsons, 2020), like the ones we obtained here, it would likely tend to have a between-subjects variability that is not large enough to ensure an adequate reliability. Although the reliability of the spatial Stroop effects has hardly ever been reported, our results are in line with Paap and colleagues (2020), who reported a split-half correlation of .81, and with a recent large individual difference study (n = 287, Capizzi et al., 2017) in which we used our Peripheral task to detect a very large spatial Stroop effect on lnRTs

(d = 2.96) with an adequate internal reliability (rSB = .77). It is also important to note here that, given the limited number of trials we used, the internal reliability estimates we obtained here likely represent a lower bound on the actual internal reliability of these tasks. Indeed, as also shown by Hedge and coworkers (2018), there is a clear positive nonlinear relationship between reliability and number of trials. In other words, there is room for improvement for our Peripheral and Perifoveal spatial Stroop task as, by increasing the number of trials, their reliability will inevitably increase.

Concerning the reliability of the Stroop effects yielded by the other tasks, it was quite high for the Figure-Ground task - despite the dominance and large magnitude of the Stroop effects -, at least for the analyses on iRTs. A similar pattern of results was obtained also for the Flanker task, which showed a good internal reliability, despite very large Stroop effects. On the contrary, the Navon and the Saliency tasks, which showed smaller Stroop effects, were also less reliable (see Figure 3.3 and Appendix A, Section A.8).

3.4.3. Impact of the analytical approach

Our results provide support for the idea that multilevel modeling can improve reliability estimates of the experimental effects by separating true experimental effects from measurement error (i.e., the intra-subject, trial-by-trial variability, also called trial noise). Indeed, both the effect size and, especially, the reliability of our iRT Stroop effects were consistently higher for the LMM and RCA analyses as compared to the GLM analysis, which requires aggregating participants' measures across trials, thus ignoring any trial-by-trial variability that may contaminate them and, thus, estimates of experimental effects. More importantly, they were also consistently higher than those estimated using the reduced LMM and RCA models that did not include the confounding predictors accounting for (at least part of) the measurement error. Following the "reliability paradox" study (Hedge et al., 2018), some attempts using multilevel modeling have been made in trying to improve reliability estimates of experimental effects and their correlations (Haines et al., 2020; Rouder & Haaf, 2019), with some promising results, albeit it has been shown that the use of more complex analytical approaches of this type is not sufficient alone to uncover the correlations between experimental effects (Rouder & Haaf, 2019).

Here we made a step further by using the multilevel modeling approach in a more informed way, not only to simply remove trial noise, but also to explain and partial out the effects of lower-level confounding factors at the trial level. Indeed, we claim that part of the intra-subject, trial-by-trial variability is not just noise: at least in part, it represents the effects of well-known longitudinal effects and other confounding effects due to other perceptual, motor, and cognitive processes. These effects can be assumed based on the specific characteristics of the task at hand and the psychological mechanisms that generate behavior. Therefore, they can be included in the analytical model to improve the estimates of the experimental effects of interest and of their reliability as well. Of course, as we detailed in the Introduction, some of these

effects, like the sequential effects due to the trial-by-trial repetitions of the stimulus characteristics, can (and should, whenever possible) be controlled methodologically. We thus advocate the use of such a theoretically informed methodological approach in creating (or selecting) experimental tasks, followed by an informed hierarchical analytical approach to estimate the corresponding experimental effects.

3.4.4. Differences across the task versions

Apart from the evident communality between the Peripheral and Perifoveal tasks that we discussed above, our correlational and exploratory factor analyses were also able to identify the specific methodological differences among our tasks that are important to note here (see Appendix A, Section A.7). First, in the Peripheral and Perifoveal tasks, the irrelevant characteristic of the stimulus is intrinsic to the stimulus itself, while in the Figure-Ground, Flanker, and Saliency tasks it constitutes an extrinsic dimension, that is, it is a physically separate stimulus. The Navon task is peculiar in this aspect because the relevant stimulus (i.e., the large arrow) is created by illusory contour perception given by the spatial arrangement of the irrelevant stimuli (i.e., the small arrows).

Moreover, in the Peripheral and Perifoveal tasks the relevant and irrelevant characteristics (i.e., the position and direction of the arrow, respectively) are different dimensions that are related to different perceptual processes (i.e., the spatial localization of a visual stimulus and the perception of its shape), while in the other tasks the relevant and irrelevant stimulus dimensions not only overlap but are identical and related to the same perceptual process, constituting what Kornblum called a “super-Stroop ensemble” (1992, p. 770). The involvement of a single perceptual process in the Figure-Ground, Navon, Flanker and Saliency tasks might be questionable because it could be interpreted as the absence of task conflict, which, in contrast, has been shown to be required for a complete Stroop effect (Augustinova et al., 2019; Parris et al., 2022). Since we agree with the multiple-loci accounts of the Stroop effect and, recently, we have stressed the importance of methodologically correct spatial Stroop designs (Viviani et al., 2022), we need to clarify why these four tasks can be considered fully-fledged Stroop tasks, ensuring interference not only at the stimulus and response levels but also at the task level. As pointed out in the introduction, they are also characterized by an asymmetrical relation between the two dimensions but, as opposed to the Peripheral and Perifoveal tasks, such asymmetry does not only rely on higher processing automaticity but also on higher perceptual salience of one dimension as compared to the other. Therefore, task conflict is present because our task-relevant stimuli still differ from the task-irrelevant ones from a conceptual and/or perceptual point of view, and, consequently, they activate task-sets that, despite belonging to the more general shape perception processing stream, are distinguishable. This is particularly striking in the Navon version, for which the distinction between local and global processing, together with global precedence, are well-documented. Therefore, it is highly likely that the prevailing but task-irrelevant global processing

interferes with the less habitual but task-relevant local processing. A similar assumption can be extended to the Figure-Ground task, wherein the distinction between global vs local processing streams might be also influenced by perceptual factors. The competing task-sets activated in the Flanker and in the Saliency tasks are instead more likely to be perceptual in nature. In the former, the task-irrelevant processing of surrounding arrows may be stronger because of their higher quantity as compared to the single and less salient central task-relevant arrow, whereas in the second, the task-irrelevant processing of the bigger arrow is stronger than the task-relevant processing of the smaller one for its greater size and saliency.

The pattern of the across-tasks correlations we observed and the results of the exploratory factor analysis could thus reflect these across-tasks methodological differences, which, in turn, could explain our results on the magnitude and reliability of the different Stroop effects. For example, taking the most evident difference concerning task conflict, the fact that the Stroop effect was the most robust and reliable in the Peripheral and Perifoveal tasks might indicate that in these tasks the degree of interference at task level was the highest, probably due to the stronger asymmetry between position and direction processing. When, in contrast, such conflict was involved to a lesser extent due to a more perceptually-based asymmetry, such as in the remaining four tasks, both Stroop effect magnitude and reliability were lower, albeit quite good, especially in the Figure-Ground and Flanker tasks. These findings provide further evidence for the multiplicity of Stroop effect loci, confirming the importance of including all the required interference levels when designing Stroop tasks.

Apart from the above-mentioned methodological differences related to interference resolution, the observed across-task differences in Stroop effect magnitude and reliability could also be explained, at least in part, by differences in non-conflict processes. For example, the across-task pattern of RT Stroop effects derived from the GLM analysis, reported in Table 3.1, seems to be related to the across-task pattern of RTs in Congruent trials: tasks with longer baseline RTs tended to produce larger Stroop effects. This could reflect something similar to what is generally observed, for example, in studies contrasting behavioral performance in older vs. younger adults (Faust et al., 1999). Therefore, across-task differences in general processing demands (or task difficulty) or other non-conflict processes could have modulated the corresponding Stroop effects independently of the underlying differences in produced interference that we discussed above. In line with this interpretation, recent simulations from evidence accumulation models produced larger RT Stroop effects with decreases in mean drift rates (reflecting general processing speed) and increases in boundary separation (reflecting strategic slowing – or more cautious responding) while keeping conflict effects constant (Hedge et al., 2018, 2022). However, the relation between Stroop effect magnitude (and reliability) and baseline performance/task difficulty across our tasks was strongly dependent on the analytical choices. Indeed, it was less evident both in the multilevel analyses on RTs and for RT transformations (see Appendix A); Moreover, it was strongly driven by the results of the Peripheral task,

which showed the slowest baseline performance and very large (and reliable) Stroop effects. More research is thus required to clarify the impact of task general processing requirements and other non-conflict processes on the magnitude and reliability of Stroop effects.

Overall, these results and our methodological considerations highlight the importance for the researchers interested in using the tasks presented here to carefully consider their specific characteristics in light of their research questions, as they may have a non-negligible impact on the ability to identify the behavioral and neurophysiological correlates of Stroop-interference resolution. Moreover, albeit preliminary, our results suggest that our tasks were accurately tailored to adequately assess inter-individual variability in interference resolution and conflict adaptation in different populations and provide further support for the possibility to use these experimental effects in correlational research (e.g., see Ambrosini & Vallesi, 2017).

3.5. Conclusions

Overall, our results suggest that the best alternative to our original Peripheral task is the Perifoveal task. Indeed, they both showed a Stroop effect that was so large and robust to analytical flexibility to be used as a measure of interference resolution and conflict adaptation that satisfies the dominance assumption. Moreover, both the Peripheral and Perifoveal tasks showed an adequate internal reliability, making them viable options for scholars interested in conducting correlational research. The Figure-Ground and the Flanker tasks also showed a good balance between the reliability and the magnitude of the Stroop effect, but they also showed less robustness to analytical flexibility.

3.6. References

Ambrosini, E., & Vallesi, A. (2017). Domain-general Stroop Performance and Hemispheric Asymmetries: A Resting-state EEG Study. Journal of Cognitive Neuroscience, 29(5), 769–779. https://doi.org/10.1162/jocn_a_01076

Augustinova, M., Parris, B., & Ferrand, L. (2019). The Loci of Stroop Interference and Facilitation Effects With Manual and Vocal Responses. Frontiers in Psychology, 10, 1786. https://doi.org/10.3389/fpsyg.2019.01786

Baayen, R. H., Davidson, D. J., & Bates, D. M. (2008). Mixed-effects modeling with crossed random effects for subjects and items. Journal of Memory and Language, 59(4), 390–412. https://doi.org/10.1016/j.jml.2007.12.005

Baayen, R. H., & Milin, P. (2010). Analyzing reaction times. International Journal of Psychological Research, 3(2), 12–28. https://doi.org/10.21500/20112084.807

Barr, D. J., Levy, R., Scheepers, C., & Tily, H. J. (2013). Random effects structure for confirmatory hypothesis testing: Keep it maximal. Journal of Memory and Language, 68(3), 10.1016/j.jml.2012.11.001. https://doi.org/10.1016/j.jml.2012.11.001

Braver, T. S. (2012). The variable nature of cognitive control: A dual mechanisms framework. Trends in Cognitive Sciences, 16(2), 106–113. https://doi.org/10.1016/j.tics.2011.12.010

Brysbaert, M., & Stevens, M. (2018). Power Analysis and Effect Size in Mixed Effects Models: A Tutorial. Journal of Cognition, 1(1), 9. https://doi.org/10.5334/joc.10

Capizzi, M., Ambrosini, E., & Vallesi, A. (2017). Individual Differences in Verbal and Spatial Stroop Tasks: Interactive Role of Handedness and Domain. Frontiers in Human Neuroscience, 0. https://doi.org/10.3389/fnhum.2017.00545

Chen, G., Pine, D. S., Brotman, M. A., Smith, A. R., Cox, R. W., & Haller, S. P. (2021). Trial and error: A hierarchical modeling approach to test-retest reliability. NeuroImage, 245, 118647. https://doi.org/10.1016/j.neuroimage.2021.118647

Dang, J., King, K. M., & Inzlicht, M. (2020). Why Are Self-Report and Behavioral Measures Weakly Correlated? Trends in Cognitive Sciences, 24(4), 267–269. https://doi.org/10.1016/j.tics.2020.01.007

De Houwer, J. (2003). On the role of stimulus-response and stimulus-stimulus compatibility in the Stroop effect. Memory & Cognition, 31(3), 353–359. https://doi.org/10.3758/bf03194393

Elliott, M. L., Knodt, A. R., Ireland, D., Morris, M. L., Poulton, R., Ramrakha, S., Sison, M. L., Moffitt, T. E., Caspi, A., & Hariri, A. R. (2020). What Is the Test-Retest Reliability of Common Task-Functional MRI Measures? New Empirical Evidence and a Meta-Analysis. Psychological Science, 31(7), 792–806. https://doi.org/10.1177/0956797620916786

Erdfelder, E., Faul, F., & Buchner, A. (1996). GPOWER: A general power analysis program. Behavior Research Methods, Instruments, & Computers, 28(1), 1–11. https://doi.org/10.3758/BF03203630

Eriksen, B. A., & Eriksen, C. W. (1974). Effects of noise letters upon the identification of a target letter in a nonsearch task. *Perception & psychophysics*, *16*(1), Art. 1.

Faust, M. E., Balota, D. A., Spieler, D. H., & Ferraro, F. R. (1999). Individual differences in information-processing rate and amount: Implications for group differences in response latency. *Psychological bulletin*, *125*(6), Art. 6.

Freund, M. C., Bugg, J. M., & Braver, T. S. (2021). A Representational Similarity Analysis of Cognitive Control during Color-Word Stroop. Journal of Neuroscience, 41(35), 7388–7402. https://doi.org/10.1523/JNEUROSCI.2956-20.2021

Funes, M. J., Lupiáñez, J., & Humphreys, G. (2010). Sustained vs. transient cognitive control: Evidence of a behavioral dissociation. Cognition, 114(3), 338–347. https://doi.org/10.1016/j.cognition.2009.10.007

Funes, M. J., Lupiáñez, J., & Milliken, B. (2007). Separate mechanisms recruited by exogenous and endogenous spatial cues: Evidence from a spatial Stroop paradigm. Journal of Experimental Psychology. Human Perception and Performance, 33(2), 348–362. https://doi.org/10.1037/0096-1523.33.2.348

Gelman, A., & Loken, E. (2013). The garden of forking paths: Why multiple comparisons can be a problem, even when there is no "fishing expedition" or "p-hacking" and the research hypothesis was posited ahead of time. 17.

Green, P., & MacLeod, C. J. (2016). SIMR: An R package for power analysis of generalized linear mixed models by simulation. Methods in Ecology and Evolution, 7(4), 493–498. https://doi.org/10.1111/2041-210X.12504

Haines, N., Kvam, P. D., Irving, L. H., Smith, C., Beauchaine, T. P., Pitt, M. A., Ahn, W.-Y., & Turner, B. M. (2020). Theoretically Informed Generative Models Can Advance the Psychological and Brain Sciences: Lessons from the Reliability Paradox. PsyArXiv. https://doi.org/10.31234/osf.io/xr7y3

Hedge, C., Powell, G., Bompas, A., & Sumner, P. (2022). Strategy and processing speed eclipse individual differences in control ability in conflict tasks. *Journal of Experimental Psychology. Learning, Memory, and Cognition*, *48*(10), 1448–1469. https://doi.org/10.1037/xlm0001028

Hedge, C., Powell, G., & Sumner, P. (2018). The mapping between transformed reaction time costs and models of processing in aging and cognition. *Psychology and Aging*, *33*(7), 1093–1104. https://doi.org/10.1037/pag0000298

Hedge, C., Powell, G., & Sumner, P. (2018). The reliability paradox: Why robust cognitive tasks do not produce reliable individual differences. Behavior Research Methods, 50(3), 1166–1186. https://doi.org/10.3758/s13428-017-0935-1

Kornblum, S. (1992). Dimensional overlap and dimensional relevance in stimulus–response and stimulus–stimulus compatibility. 2.

Kumle, L., Võ, M. L.-H., & Draschkow, D. (2021). Estimating power in (generalized) linear mixed models: An open introduction and tutorial in R. Behavior Research Methods. https://doi.org/10.3758/s13428-021-01546-0

Lorch, R. F., & Myers, J. L. (1990). Regression analyses of repeated measures data in cognitive research. Journal of Experimental Psychology: Learning, Memory, and Cognition, 16(1), 149–157. https://doi.org/10.1037/0278-7393.16.1.149

Lu, C., & Proctor, R. W. (1995). The influence of irrelevant location information on performance: A review of the Simon and spatial Stroop effects. *Psychonomic Bulletin & Review*, *2*(2), Art. 2. https://doi.org/10.3758/BF03210959

MacLeod, C. M. (1991). Half a century of research on the Stroop effect: An integrative review. Psychological Bulletin, 109(2), 163–203. https://doi.org/10.1037/0033-2909.109.2.163

Möckel, T., Beste, C., & Wascher, E. (2015). The Effects of Time on Task in Response Selection—An ERP Study of Mental Fatigue. Scientific Reports, 5(1), 10113. https://doi.org/10.1038/srep10113

Morey, R. D. (2008). Confidence Intervals from Normalized Data: A correction to Cousineau (2005). Tutorials in Quantitative Methods for Psychology, 4(2), 61–64. https://doi.org/10.20982/tqmp.04.2.p061

Navon, D. (1977). Forest before trees: The precedence of global features in visual perception. *Cognitive Psychology*, *9*(3), 353–383. https://doi.org/10.1016/0010-0285(77)90012-3

Nee, D. E., Wager, T. D., & Jonides, J. (2007). Interference resolution: Insights from a meta-analysis of neuroimaging tasks. Cognitive, Affective, & Behavioral Neuroscience, 7(1), 1–17. https://doi.org/10.3758/CABN.7.1.1

Oldfield, R. C. (1971). The Assessment And Analysis Of Handedness: The Edinburgh Inventory. Neuropsychologia, 9, 97–113. https://doi.org/10.1016/0028-3932(71)90067-4

Paap, K. R., Anders-Jefferson, R., Zimiga, B., Mason, L., & Mikulinsky, R. (2020). Interference scores have inadequate concurrent and convergent validity: Should we stop using the flanker, Simon, and spatial Stroop tasks? Cognitive Research: Principles and Implications, 5(1), 7. https://doi.org/10.1186/s41235-020-0207-y

Parris, B. A., Hasshim, N., Wadsley, M., Augustinova, M., & Ferrand, L. (2022). The loci of Stroop effects: A critical review of methods and evidence for levels of processing contributing to color-word Stroop effects and the implications for the loci of attentional selection. Psychological Research, 86(4), 1029–1053. https://doi.org/10.1007/s00426-021-01554-x

Parsons, S. (2020). Exploring reliability heterogeneity with multiverse analyses: Data processing decisions unpredictably influence measurement reliability. PsyArXiv. https://doi.org/10.31234/osf.io/y6tcz

Pires, L., Leitão, J., Guerrini, C., & Simões, M. R. (2018). Cognitive control during a spatial Stroop task: Comparing conflict monitoring and prediction of response-outcome theories. Acta Psychologica, 189, 63–75. https://doi.org/10.1016/j.actpsy.2017.06.009

Puccioni, O., & Vallesi, A. (2012a). High cognitive reserve is associated with a reduced age-related deficit in spatial conflict resolution. Frontiers in Human Neuroscience, 6. https://doi.org/10.3389/fnhum.2012.00327

Puccioni, O., & Vallesi, A. (2012b). Sequential congruency effects: Disentangling priming and conflict adaptation. Psychological Research, 76(5), 591–600. https://doi.org/10.1007/s00426-011-0360-5

Rabbitt, P. M. (1966). Errors and error correction in choice-response tasks. Journal of Experimental Psychology, 71(2), 264–272. https://doi.org/10.1037/h0022853

Rouder, J., Kumar, A., & Haaf, J. (2019). Why Most Studies of Individual Differences With Inhibition Tasks Are Bound To Fail. https://doi.org/10.31234/osf.io/3cjr5

Rouder, J. N., & Haaf, J. M. (2018). Power, Dominance, and Constraint: A Note on the Appeal of Different Design Traditions. Advances in Methods and Practices in Psychological Science, 1(1), 19–26. https://doi.org/10.1177/2515245917745058

Rouder, J. N., & Haaf, J. M. (2019). A psychometrics of individual differences in experimental tasks. Psychonomic Bulletin & Review, 26(2), 452–467. https://doi.org/10.3758/s13423-018-1558-y

Shor, R. E. (1970). The processing of conceptual information on spatial directions from pictorial and linguistic symbols. Acta Psychologica, Amsterdam, 32(4), 346–365. https://doi.org/10.1016/0001-6918(70)90109-5

Simmons, J. P., Nelson, L. D., & Simonsohn, U. (2011). False-Positive Psychology: Undisclosed Flexibility in Data Collection and Analysis Allows Presenting Anything as Significant. Psychological Science, 22(11), 1359–1366. https://doi.org/10.1177/0956797611417632

Steegen, S., Tuerlinckx, F., Gelman, A., & Vanpaemel, W. (2016). Increasing Transparency Through a Multiverse Analysis. Perspectives on Psychological Science, 11(5), 702–712. https://doi.org/10.1177/1745691616658637

Stoet, G. (2010). PsyToolkit: A software package for programming psychological experiments using Linux. Behavior Research Methods, 42(4), 1096–1104. https://doi.org/10.3758/BRM.42.4.1096

Stoet, G. (2017). PsyToolkit: A Novel Web-Based Method for Running Online Questionnaires and Reaction-Time Experiments. Teaching of Psychology, 44(1), 24–31. https://doi.org/10.1177/0098628316677643

Stroop, J. R. (1935). Studies of interference in serial verbal reactions. Journal of Experimental Psychology, 18(6), 643–662. https://doi.org/10.1037/h0054651

Tafuro, A., Ambrosini, E., Puccioni, O., & Vallesi, A. (2019). Brain oscillations in cognitive control: A cross-sectional study with a spatial stroop task. Neuropsychologia, 133, 107190. https://doi.org/10.1016/j.neuropsychologia.2019.107190

Tafuro, A., Vallesi, A., & Ambrosini, E. (2020). Cognitive brakes in interference resolution: A mouse-tracking and EEG co-registration study. Cortex; a Journal Devoted to the Study of the Nervous System and Behavior, 133, 188–200. https://doi.org/10.1016/j.cortex.2020.09.024

Viviani, G., Visalli, A., Montefinese, M., Vallesi, A., & Ambrosini, E. (2022). *The Stroop legacy: A cautionary tale on methodological issues and a proposed spatial solution*. PsyArXiv. https://doi.org/10.31234/osf.io/qejum

Wennerhold, L., & Friese, M. (2020). Why Self-Report Measures of Self-Control and Inhibition Tasks Do Not Substantially Correlate. Collabra: Psychology, 6(1). https://doi.org/10.1525/collabra.276

Westfall, J., Kenny, D. A., & Judd, C. M. (2014). Statistical power and optimal design in experiments in which samples of participants respond to samples of stimuli. Journal of Experimental Psychology. General, 143(5), 2020–2045. https://doi.org/10.1037/xge0000014

White, B. W. (1969). Interference in identifying attributes and attribute names. Perception & Psychophysics, 6(3), 166–168. https://doi.org/10.3758/BF03210086

Williams, E. (1949). Experimental Designs Balanced for the Estimation of Residual Effects of Treatments. Australian Journal of Chemistry, 2. https://doi.org/10.1071/CH9490149

Zhang, H., & Kornblum, S. (1998). The Effects of Stimulus-Response Mapping and Irrelevant Stimulus-Response and Stimulus-Stimulus Overlap in Four-Choice Stroop Tasks with Single-Carrier Stimuli. Journal of Experimental Psychology. Human Perception and Performance, 24, 3–19. https://doi.org/10.1037//0096-1523.24.1.3

CHAPTER 4

Tango of Control:
The Interplay between Proactive and Reactive Control

4.1. Introduction

In the introductory chapter, we introduced the subject of this thesis, cognitive control, emphasizing that this umbrella term refers to a family of processes required to adaptively regulate, coordinate, and sequence our thoughts and action plans according to the context and internal goals (Braver, 2012; Chiew & Braver, 2017). In addition to emphasizing the significant role of representations (Botvinick et al., 2001; Chiew & Braver, 2017; Cohen, 2017; Duncan, 2010), which will be directly explored in Chapter 6, we have highlighted interference resolution as a central component of cognitive control. Interference resolution refers to the ability to select weaker but task-relevant information when it competes with stronger and more habitual, but task-irrelevant information (Miller & Cohen, 2001; Nee et al., 2007; Tafuro et al., 2019). The need to select task-relevant information among conflicting one is pervasive in everyday life because we are always surrounded by great amount of sensory stimuli and possible actions, but only some of them are appropriate at any given moment (Gratton et al., 2018; Jiang et al., 2014; Nee et al., 2007).

In the last decades, the mechanisms that underlie and adaptively regulate cognitive control have been intensively investigated. However, some methodological and theoretical issues not only undermine an exhaustive understanding of this fundamental process, but also its behavioral signatures are still not clear. What still remains unclear is whether the two mechanisms postulated by the Dual-Mechanisms of Control model (DMC; Braver, 2012; Braver et al., 2007), proactive and reactive control, can be distinguished at the behavioral level. In this chapter, we precisely address this issue by using the Stroop task. To achieve this, we devised a novel methodological approach that incorporates cutting-edge trial-level multilevel modeling techniques, ensuring accurate and reliable estimations of the Stroop effect, while finely manipulating the proxy variables for proactive and reactive control at the trial level. This fine-grained manipulation is crucial for gaining insights into the simultaneous presence and interplay of proactive and reactive control mechanisms while effectively controlling for potential confounding effects arising from low-level processes, such as contingency.

Although in the present work, we explore whether proactive and reactive control are distinct through specific experimental manipulations related to proportion congruency, other approaches to investigate this experimental question could be used. For example, based on the rationale that proactive control is more

resource-demanding (Braver, 2012), it should be specifically affected by behavioral manipulations that overload cognitive resources, through dual tasks or a concurrent working memory task. If the use of this approach left the reactive control mode intact, this would mean that the two control modes are independent. This type of manipulations has been used in the literature but, as we will extensively discuss in this chapter, methodologically adequate manipulations that allow simultaneously distinguishing between proactive and reactive control are still missing. Extending the logic that proactive control is more resource-demanding, some studies have explored this question using healthy aging populations, assuming that proactive control should be affected by a greater decline. Findings are in line with this assumption, revealing a deterioration of proactive control with age, in contrast to intact reactive control (e.g., Braver et al., 2005). In addition to these, lesion-based approaches could be an alternative to behavioral manipulations because they would allow temporarily disrupting not only proactive but also reactive control. However, to accomplish this, it would be necessary for the involved neural areas to be clearly defined and easily stimulable, which is still not the case. The lack of clarity of the implied neural bases is also due to the lack of neuropsychological evidence of a dissociation, as, to the best of our knowledge, there are no studies with patients showing a clear dissociation between proactive and reactive control.

From this brief overview, it is clear that there are multiple possible approaches to dissociate between proactive and reactive control. However, it is also evident that the starting point should be methodological homogeneity, at least in the behavioral paradigms; otherwise, there is a risk of obtaining not robust results. For this reason, to pursue our goal, we have decided to start with a clear paradigm to test specific manipulations, paying attention to methodological rigor. These manipulations, specifically those involving proportion congruency, are widely used in the literature and represent an equally extensive topic. For this reason, in what follows we first describe the classic manipulations commonly employed to engage proactive and reactive control, along with their respective limitations that have been already introduced in Chapter 1. Subsequently, we will discuss how researchers typically address such flaws and highlight the associated costs of proposed solutions. Additionally, we will highlight why the commonly used approaches do not allow truly investigating the separability of the two mechanisms. We will thus propose an alternative approach to solve these issues.

4.1.1. The Stroop task: Proportion Congruency (PC) manipulations and their limitations

In the introductory chapter, we also introduced one of the most commonly used interference paradigms, the Stroop task (MacLeod, 1991; Stroop, 1935; see Section 1.2). In this task, cognitive control is engaged to overcome interference at the task level (i.e., reading vs. color naming), as well as interference occurring at the stimulus and response levels in incongruent trials (Gonthier et al., 2016; see also Chapter 2). Then, in Chapters 2 and 3, we discussed the methodological characteristics of this paradigm, laying the groundwork

for the current chapter. Here, we will delve into the experimental manipulations that are commonly employed to modulate the level of cognitive control engaged and consequently the magnitude of the Stroop effect (Bugg & Crump, 2012).

Cognitive control demand and the consequent magnitude of the Stroop effect can be modulated by manipulating the proportion congruency (PC), that is, the relative frequency/likelihood of congruent trials within the task blocks (Gonthier et al., 2016; Logan & Zbrodoff, 1979). The basic assumption is that information about the PC is used to adjust the cognitive control level and, as the size of the Stroop effect inversely reflects the success of interference resolution, it is postulated that when such effect is relatively small, a greater extent of cognitive control has been recruited (e.g., Braem et al., 2019; Lindsay & Jacoby, 1994). More in detail, in mostly incongruent blocks (low PC), the high probability of encountering incongruent trials and experiencing interference increases cognitive control demands and this yields significantly smaller Stroop effects. In contrast, in mostly congruent blocks (high PC), due to a relatively lower frequency of incongruent trials, cognitive control is laxer and the Stroop effect gets larger (e.g., Lindsay & Jacoby, 1994).

The high flexibility of the PC manipulation makes it suitable for our purpose of differentiating the distinct cognitive control mechanisms (Bugg, 2017; Bugg & Crump, 2012), namely, those postulated by the Dual-Mechanisms of Control model (DMC, Braver, 2012; Braver et al., 2007). As outlined in Chapter 1 (see Section 1.1), the DMC explains the intrinsic variability of cognitive control in terms of different temporal dynamics, postulating that proactive and reactive control are two qualitatively distinct cognitive control modes. The proactive control mode operates actively by maintaining task goals and anticipatorily biasing cognitive processes in a goal-driven manner. Thus, proactive control acts as a preparatory mechanism, engaged in a sustained fashion even before cognitively demanding events, like conflicts, are encountered. When proactive control is exerted, interference is reduced because top-down attentional biases favor the processing of the task-relevant information. By contrast, reactive control is mobilized transiently only as needed on a "just-in-time" basis. As such, reactive control relies upon a "late correction" mechanism reflecting the bottom-up reactivation of task goals to resolve interference.

Previous works using the Stroop task have shown that these two cognitive control modes can be distinguished by manipulating the PC at the list-wide (LWPC) and item-specific (ISPC) levels (Bugg, 2012; Bugg & Crump, 2012)[11]. Indeed, although these PC manipulations produce a similar overall pattern, they favor the use of a cognitive control mode over the other, as the logic behind them is different (Bugg, 2017). The LWPC manipulation is used to stress the adoption of a proactive control mechanism to resolve Stroop

[11] A third type of PC manipulation exists, the context-specific PC. Besides being akin to the ISPC, we will not discuss in detail the context-specific PC as it was not manipulated in the present work, but see Bugg and Crump (2012) and Bugg (2012) for reviews.

interference. It implies varying the PC within experimental blocks, that is, blocks with high LWPC, in which the proportion of congruent trials is higher (e.g., 75% congruent and 25% incongruent), are compared to blocks with low LWPC, wherein the ratio is reversed (e.g., 25% congruent and 75% incongruent). Typically, this manipulation yields the so-called LWPC effect, characterized by smaller Stroop effects in low-LWPC blocks as compared to high-LWPC blocks (e.g., Bugg & Crump, 2012; Lindsay & Jacoby, 1994; Logan & Zbrodoff, 1979). Such an effect would be yielded by a goal-driven modulation of control, which is possible because, after experiencing a number of trials within a block, participants learn the global likelihood of conflict and develop expectancies about the upcoming trials. Low LWPC leads to the implementation of early preparatory strategies operating even before stimulus onset, which entail imposing an attentional bias toward the task-relevant dimension and/or away from the task-irrelevant one. By contrast, when LWPC is high, the more prepotent task-irrelevant dimension is processed preferentially (Braver et al., 2007; Bugg, 2017; Bugg & Chanani, 2011; Bugg & Crump, 2012; Lindsay & Jacoby, 1994; Logan & Zbrodoff, 1979). The highest level of proactive control is observed in low-LWPC blocks, yielding not only shorter RTs on incongruent trials, but also a congruency cost, namely a slowing on congruent trials as compared to congruent trials in high-LWPC blocks, since the attentional biases away from the task-irrelevant dimension, which are imposed anticipatorily and globally, reduce the facilitation on congruent trials (Gonthier et al., 2016).

In contrast, when the ISPC is manipulated, reactive control is dominant. As the name suggests, it is implemented by assigning different PCs to specific sets of items (Jacoby et al., 2003). Essentially, the manipulation targets one feature of an item, which is commonly the task-irrelevant dimension (i.e., the word dimension in the color-word Stroop task). Such stimulus feature signals a specific PC and two conditions can be distinguished within the same block: high ISPC (e.g., 75% probability for the word RED to appear in red ink) and low ISPC (e.g., 25% probability for the word BLUE to occur in blue ink) items. Therefore, low-ISPC items, by signaling a high level of expected interference, are assumed to produce the highest level of reactive control (e.g., Bugg, 2012, 2017; Bugg & Hutchison, 2013) triggered by a fast "stimulus-attention association" (Tafuro et al., 2020).[12] Using this manipulation, previous studies found an ISPC effect, that is, smaller Stroop effects for low- than high-ISPC items (Bugg et al., 2011; Bugg & Hutchison, 2013; Jacoby et al., 2003). The different PC items are randomly intermixed and presented within the same block, and the global probability of congruent and incongruent trials is usually kept equal in that block (LWPC of 50%), so that this manipulation cannot imply a control modulation at the list level. Indeed,

[12] Note that a second, later form of reactive control exists, as discussed in Chapter 1. Indeed, this later reactive control mechanism would come into play to resolve interference when other control processes failed, that is, when proactive control and the faster stimulus-driven reactive control are both low. In this case, indeed, incongruent trials elicit unexpected conflict that has to be resolved by cognitive control mechanisms at a later stage, likely involving the response selection processes. This later form of reactive control thus resembles that of the conflict monitoring account and is more purely reactive (and response-related) in nature (Tafuro et al., 2020). See also figure 1.6.

participants learn the conflict likelihood of the items, but they can use this item-specific information to impose attentional biases only after stimulus onset. The ISPC effect is thus a reactive modulation of control that, by operating on an item-by-item basis, is fast and flexible and is maximal when the item signals a high level of interference (Bugg, 2012, 2017; Bugg et al., 2011; Bugg & Hutchison, 2013).

Overall, PC manipulations are fundamental as they allow scholars to investigate what is referred to as adaptive control, that is, the context-induced and time-varying adjustments intrinsic to cognitive control (Braem et al., 2019). However, several authors have called into question the validity/purity of adaptive control measures, including the PC manipulations discussed so far, claiming that they suffer from methodological issues (see Braem et al., 2019; Schmidt, 2019 for reviews).

First, there is considerable controversy about whether cognitive control per se is necessary to resolve the Stroop interference elicited by PC manipulations or, conversely, whether adaptive control measures are merely the result of much simpler stimulus-stimulus or stimulus-response associative learning processes, as claimed by the contingency hypothesis (Schmidt, 2019; Schmidt et al., 2007; Schmidt & Besner, 2008). This view identifies contingency learning as a more plausible candidate for explaining PC effects, excluding the involvement of any high-level cognitive control modulation. Essentially, it postulates that by learning that responses tend to co-occur with specific stimuli, they can be facilitated. According to this hypothesis, participants' cognitive system implicitly learns the contingencies (or correlations) between the task-irrelevant and the task-relevant stimulus features, namely the responses, and uses the task-irrelevant dimension to predict high-contingency responses. When responses are highly predictable, namely, in high-contingency trials, participants exploit (even implicitly) these learning-based shortcuts and respond faster (Schmidt et al., 2007; Schmidt & Besner, 2008).

The contingency hypothesis challenges especially the ISPC effect, pointing out that such effect is only incidental, since ISPC manipulations are always confounded with contingency (Schmidt, 2019; Schmidt & Besner, 2008). Indeed, to manipulate the PC of the items, the frequency of specific irrelevant-relevant characteristic pairs is necessarily altered as well (Spinelli et al., 2019). In line with this hypothesis, the assessment of contingency learning controlling for PC effect (high- vs. low-contingency items of equal PC) reveals a contingency effect, while the assessment of PC effect controlling for contingency (high- vs. low-ISPC items of equal contingency) yields no residual PC effect (Schmidt, 2013; Schmidt & Besner, 2008; see also Schmidt, 2019, for a detailed review). However, other evidence argues in favor of a more intermediate account that embraces the contribution of both contingency and item-specific control mechanisms. For example, in Bugg and colleagues (2011), the task-relevant dimension signaled the ISPC rather than the task-irrelevant one and this, by equating contingency across conditions, allowed deconfounding ISPC and contingency and finding evidence for a control modulation. When, instead, the task-irrelevant dimension functioned as the ISPC signal, contingency was confounded with ISPC and accounted for its effect, as

predicted by the contingency hypothesis (Schmidt, 2019). Moreover, Bugg and Hutchison (2013, Experiment 3), restoring the traditional ISPC design (the task-irrelevant dimension signaling the ISPC), found an ISPC control modulation when 4-item sets were used, while contingency was dominant when 2-item sets were used, suggesting that bigger set sizes promote reliance on item-specific control, whereas smaller ones favor the use of contingencies. Their findings support the existence of different mechanisms governing the ISCP effect depending upon the set size, with larger sets reducing high-contingency responses and the likelihood of learning contingency associations, especially for responding to incongruent items.

Overall, this issue is still a matter of debate and a detailed discussion goes beyond the scope of the present work (see also Bugg, 2014; Bugg & Hutchison, 2013; Schmidt, 2013, 2019). However, what is clear is the need of methodologically correct/appropriate designs controlling for or removing contingency-related biases from the experimental design to verify whether ISCP effect is, even only partially, due to congruency modulation. To this end, apart from the strategy reported above, another solution is to manipulate contingency learning and ISPC in a partially independent way. When using a color-word Stroop task, this can be done by creating two non-overlapping 2-item-sized sets, so to have: i) the first set with mostly-congruent (MC) words, but mostly-incongruent (MI) colors (viceversa for the second set); ii) MC incongruent words presented only in the other MC colors; iii) MI incongruent words presented only in the other MI colors; iv) for each set, one high-contingency and one low-contingency incongruent word. To measure conflict adaptation effects, low-contingency MC incongruent items are compared to low-contingency MI incongruent items, whereas to measure contingency-related effects, low-contingency MI incongruent items are contrasted to high-contingency MI incongruent items. Of note, for congruent items, this does not dissociate between the two accounts (e.g., Spinelli & Lupker, 2020). Recently, Braem and colleagues (2019) summarized some guidelines on how to design cognitive control tasks avoiding confounds and, for what concerns ISPC manipulations, they suggest creating two sets of overlapping “inducer” items (one for MI and one for MC items) to trigger reactive control and a third set of “diagnostic” items with a PC of 50%, to which the PC-dependent level of cognitive control is assumed to be transferred, to measure the ISPC effect without item-frequency differences. Using the picture-word Stroop task, diagnostic items can be created by choosing a novel set of exemplars of the inducer items which can represent the same inducer item but in a different form (e.g., if among the inducer items there is a picture of a dog, select a different dog picture as a diagnostic item) or by selecting an alternative item belonging to the same category as the inducer item (e.g., if among the inducer items there is a picture of a lion, select a tiger picture as diagnostic item). Alternatively, they propose to use diagnostic items involving new task-irrelevant features, such as diagnostic trials with the same task-relevant features as the MC and MI items paired equally often with incongruent non-inducer task-irrelevant features (e.g., different distractor words in the color-word Stroop task). Faster responses for MI inducer task-relevant features paired with non-inducer incongruent task-irrelevant features than for MC inducer task-relevant features paired with non-inducer incongruent task-irrelevant

features are assumed to reflect a cognitive control-driven ISPC effect without contingency confounds. It is worth mentioning that although these solutions have been proposed in a consensus paper, the same authors admit that they come with cautionary notes. Indeed, they recommend the latter approach but still highlight that it has been rarely tested, and that it is "important to assess its robustness in future studies" [p. 778].

Another potential flaw of adaptive control measures concerns the LWPC manipulation. Some authors indeed pointed out that LWPC effects do not actually depend on list-level information but instead can be explained by a mechanism operating at the item level. Thus, this account excludes any proactive control involvement or, at least, posits that it cannot be elicited by the LWPC manipulation (Blais et al., 2007; Blais & Bunge, 2010; Bugg et al., 2008). Indeed, when low-PC blocks are composed of low-PC items and high-PC blocks are composed of high-PC items, LWPC is confounded with ISPC. To disentangle the two mechanisms, Bugg and Chanani (2011) randomly intermixed, in both high- and low-PC blocks, an additional set of items with an ISPC of 50% (unbiased or diagnostic items) to verify whether an LWPC effect could be observed for such items, which did not provide any item-specific or contingency information. This was the case, suggesting that the LWPC effect was driven by a mechanism using the information at the list-level, and thus it was modulated proactively. This procedure was proposed by Braem and colleagues (2019) too, who agreed on the need to use inducer items that trigger proactive control and diagnostic (or unbiased) items that measure its effect on performance. They also recommended presenting inducer items more frequently than diagnostic ones and using a set of at least three items.

Although there is an emerging consensus on the need to use the approaches described above to design confound-minimized studies (Braem et al., 2019), their implementation comes at a cost. Indeed, both for LWPC and ISPC measures, distinguishing between inducer and diagnostic items is impractical and time-consuming due to the need to measure PC-related effects only on diagnostic items, while excluding inducer ones from the analyses. Moreover, for what concerns ISPC manipulation specifically, the creation of multiple sets of stimuli consisting of a multitude of items is not always feasible as, except for picture-word Stroop tasks, the possible exemplars of items are limited (e.g., for the color-word Stroop task there are just limited colors among which to choose). Lastly, contingency-control manipulations in picture-word Stroop tasks might also be flawed, because when using different diagnostic pictures of the same exemplars of inducer items, response contingencies might still be predictable, while when using diagnostic pictures of the different exemplars but belonging to the same category as inducer items implies the assumption of within-category transfer, which might not always occur. Therefore, in our view, to date there is no methodological approach free from limitations and how to control for PC-related confounders in a feasible and effective way still remains an open question. Here, the solutions proposed by the confound-minimized approaches will be referred to as design-level control, as their purpose is to control for confounders as much as possible at the

level of the experimental design. However, as just described, they imply some costs. As an alternative to this approach, there is the possibility of controlling for confounding effects at the statistical level, for which we will use the label analysis-level control. This statistical approach, which we have adopted here (as described below), offers greater flexibility in the experimental design, thus overcoming the limitations of the approaches controlling for confounders at the design level.

These methodological controversies notwithstanding, the existence of two temporally distinct control modes seems plausible, at least as long as potential confounders are controlled for at the design level. However, the only way of verifying whether proactive and reactive control constitute truly independent mechanisms (Braver et al., 2007), ruling out that they are two poles on a continuum, is by obtaining independent estimates of these effects from the same sample of participants. This was done by Gonthier and colleagues (2016), who tried to dissociate proactive and reactive control by directly contrasting their behavioral signatures in a within-subject design to obtain independent estimates of LWPC and ISPC effects in the same participants. To this end, separate blocks were used: two LWPC blocks (one mostly congruent and one mostly incongruent) along with a set of unbiased items to avoid ISPC-related influence, and one ISPC block including an equal number of mostly congruent and mostly incongruent items, with a LWPC of 50% to exclude LWPC effects. They found not only that LWPC and ISPC manipulations independently reduced the magnitude of the Stroop effect, but also that the two benefit indices were negatively correlated, suggesting that subjects relying more on one mechanism engage less the other one, thus providing evidence that the two effects are elicited by two distinct (i.e., dissociable) control mechanisms.

Although the study by Gonthier and colleagues (2016) provided further and more solid evidence for the separability of LWPC and ISPC effects, thanks to its within-subjects design, and confirmed its suitability for measuring proactive and reactive control, it also suffers from some drawbacks. First, the effect of contingency learning was more strongly controlled for in the LWPC manipulation, for which unbiased diagnostic items were used (see footnote 2), while the influence of contingency on item-specific mechanisms was controlled for by using the task-relevant dimension to signal ISPC, leading to unequal frequencies of unique trial types and irrelevant stimulus characteristics. A second limitation of the study by Gonthier and colleagues (2016) is that, although they use a within-subjects design testing both proactive and reactive control in the same participants, the two control mechanisms were investigated separately, as the LWPC and ISPC manipulations are kept apart and implemented one at a time in different blocks. Indeed, more convincing evidence for their existence as distinct mechanisms would require testing their interaction while both manipulations are implemented. Indeed, this would allow exploring whether and how they covary, informing about the existence of two separate mechanisms.

4.1.2. Aim of the present study and methodological novelties

Motivated by the considerations discussed above, our main aim here is to make a step further, by investigating in a more direct manner whether proactive and reactive control are two separable mechanisms. Essentially, we put forward a new approach that allows manipulating LWPC and ISPC at the same time, while controlling for the effect of stimulus-response associations, such as contingency. Although, to the best of our knowledge, only one attempt has been made to study both of them together using the Stroop task (see Hutchison, 2011), we believe that, to verify the specificity of these two control mechanisms, the most plausible way is to measure participants' performance while both LWPC and ISPC are parametrically varied at the same time. Indeed, by doing so, we can verify whether proactive and reactive control modes have distinct effects on participants' performance. Moreover, if we assume that they are indeed distinct mechanisms, they should also interact as (implicitly) predicted by the DMC model (Braver et al., 2009, 2021; De Pisapia & Braver, 2006). Thus, by measuring both at the same time, we can also test the three-way interaction between the Stroop effect, LWPC and ISPC, which can tell us more about the impact of variable amounts of proactive and reactive control activated by different levels of LWPC and ISPC. Lastly, since previous literature has confirmed the, at least partial, role of contingency on conflict adaptation, we decided not to exclude it but we allowed it to vary orthogonally (as much as possible) with respect to LWPC and ISPC, with the aim to estimate its effect and control for it at the statistical level so to measure the LWPC and ISPC effects regardless of contingency. As a consequence, in our tasks, trials will have at the same time a different level of LWPC, ISPC, and contingency. To do so, we combined this methodological approach with the use of a multilevel trial-level modeling analytical approach to assess the fine-grained effects of our predictors at the subject level, while partialling out the effect of contingency and of other lower-level confounding factors (Viviani et al., 2023 and Chapter 3). As we recently showed, indeed, trial-level confounders represent important sources of trial-by-trial noise that cannot be accounted for by standard general linear models (GLM), which require collapsing trial-level data to obtain participants-by-condition averages. They can instead be effectively estimated and removed by multilevel modeling (see Chapter 3 for a more exhaustive description of the advantages of multilevel modeling over GLM).

Moreover, to pursue our aim, we introduced an important methodological novelty, that is, we manipulated the different PCs at the list-wide and item-specific levels to explore how and to what degree they modulate the Stroop effect dynamically and in a fine-grained way. In other words, we aimed to evaluate the impact of PC on participants' Stroop performance on a trial-by-trial basis, using trial-level LWPC and ISPC estimates computed based on the actual recent history of trial congruency they experienced, rather than on their assumed (future) experience of trial congruency at the block-level.

Indeed, it should be noted that the available literature used the block-level LWPC and ISPC variables, that is, those computed as the number of congruent trials within a block (in total or for each item,

respectively) divided by the total number of trials (in total or for each item, respectively) within the same block. However, these block-level LWPC and ISPC variables correspond for sure to the actual PCs at the end of the block only. This is true even if trial-level PC values are computed based on the trials experienced so far during that block, and especially if they are computed based on the local history of trials (e.g., using a moving window or a forgetting factor). Indeed, due to the commonly used (pseudo)randomization of the trial list, it is not unlikely that the LWPC value at, say, the 20^{th} trial in a block deviates even dramatically from the expected block-level LWPC, being it, for example, as large as 40% and as small as 0% instead of 20%. This is especially important after an unsignalled block transition, especially between blocks with extreme opposite block-level LWPCs (e.g., 20% and 80%). In this case, indeed, the commonly used block-level approach implausibly assumes that, at the very first trial of a new block, participants immediately update their LWPC estimates (from 20% to 80% in this example) and, consequently, their proactive control level. Similarly, commonly used block-level ISPC values neglect the fact that participants first need to experience a sufficient number of trials for each item to estimate its ISPC value, thus unrealistically assuming that the items at the beginning of each block have already been associated to an ISPC value, without previously encountering them. Moreover, the commonly used block-level approach unrealistically assumes that all the trials within a block share the same PC values, not taking into account the fact that the local PCs vary within the block.

Therefore, and since participants are not aware of the probabilistic structure of the task, it is unreasonable to assume that their trial-by-trial performance is modulated by block-level PC values. Instead, it is more plausible to assume, as we do here, that their cognitive system implicitly and continuously estimates trial-level LWPC and ISPC values using some form of statistical learning based on the recent history of overall and item-specific PCs, respectively, implementing a specific level of control accordingly.

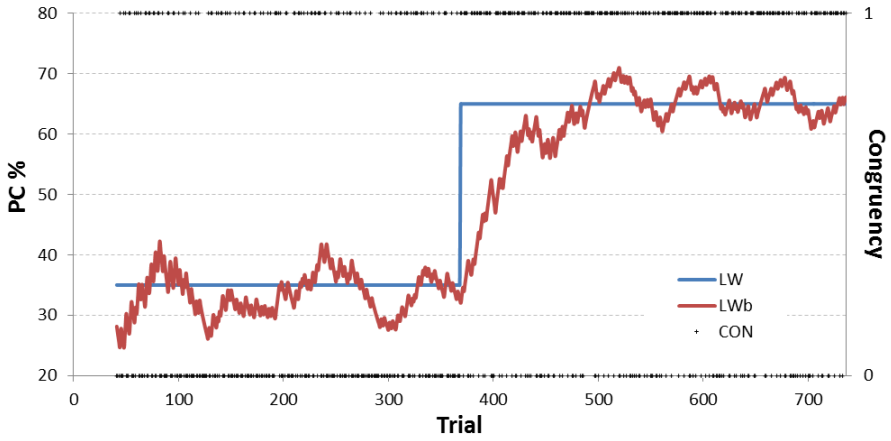

We therefore employed a fine-grained manipulation of LWPC and ISPC, which were estimated trial-by-trial using an ideal Bayesian observer (Mathys et al., 2011). Our approach, thus, allows us to account for and estimate flexible, ongoing adjustments of cognitive control during the task (see Figure 4.1). Trial-by-trial estimates (which we will call continuous variables) were used as predictors in our analyses as they are more realistic than those computed using the block-level occurrences (which we will call discrete variables). Trial-level estimates were also calculated for confounding variables of interest, including contingency, using the same approach.

Figure 4.1.
The plot shows the block-level LWPC (LW, blue line) and its trial-level estimates (LWb, red line) computed using the Hierarchical Gaussian Filter (Mathys et al., 2011) for one of the trial lists used in the experiment. The occurrence of congruent (CON = 1) and incongruent (CON = 0) trials is also depicted as plus signs.

Finally, we addressed the important but frequently overlooked aspect of measure reliability. As highlighted by Gonthier and colleagues (2016), LWPC and ISPC effect indices have unknown psychometric properties, in addition to being effects calculated from difference scores, which, in turn, further reduces their reliability (Thomas & Zumbo, 2012). Despite this awareness, this issue has rarely been addressed in studies using such manipulations, and, as such, our study also aims to explore the reliability of such measures. To this aim, the use of multilevel trial-level modeling of participants' performance is again fundamental, as we recently showed it to ensure estimations of the experimental effects with higher and more stable internal reliability compared to standard GLM approaches (see Chapter 3).

The three points mentioned above were addressed in two Experiments involving four-choice spatial Stroop tasks that require keypress responses to indicate the direction of a target arrow, ignoring its position. Both Experiments used exactly the same experimental procedure and design and differed only in the spatial arrangement of the experimental stimuli (see below), allowing us to assess the robustness of our experimental approach and results. These two spatial Stroop tasks, named Peripheral and Perifoveal spatial Stroop tasks, were chosen as they overcome some limitations intrinsic to the original color-word verbal Stroop task, while also ensuring a complete Stroop effect, that is, an effect including conflict at the task, stimulus, and response levels (see Chapter 2 for more details). In addition to these methodological advantages, in a recent work, we have shown that the Peripheral and Perifoveal spatial Stroop tasks are proper spatial Stroop adaptations, producing Stroop effects that not only have a large magnitude but are also robust to analytical flexibility and have a high and robust internal reliability (Viviani et al., 2023 or Chapter 3).

4.1.3. Hypotheses

As claimed above, we were interested in exploring if and how proactive and reactive control covary and interact to modulate the Stroop effect. To the best of our knowledge, this interaction has rarely been tested before, mainly because LWPC and ISPC have always been manipulated separately (but see Hutchison, 2011). As such, there is no solid evidence of how the Stroop effect is modulated when both proactive and reactive controls are implemented in the same experimental design and neither of whether these two control modes interact. Therefore, we put forward some hypotheses about what we expect to observe, proposing different theoretically plausible alternatives.

All the hypotheses assume that when both LWPC and ISPC are high (lPro-lRea condition), the lowest level of control is applied (i.e., no form of proactive and reactive control is implemented) and thus the Stroop effect should be the largest (equal to 1 in our models). Conversely, when either LWPC or ISPC are low, a high level of proactive and reactive control, respectively, should be implemented (respectively, the hPro-lRea and hRea-lPro conditions), and thus the Stroop effect should be reduced. Finally, when both LWPC and ISPC are low (hPro-hRea condition), the highest level of control should be implemented and thus the smallest Stroop effect should be observed.

The first point that differentiates our hypotheses is the size of the Stroop effect in the hPro-hRea condition. We hypothesized that, if proactive and reactive control do not interact with each other but still separately modulate the Stroop effect, their effects on the Stroop effect will be additive, thus still producing the smallest Stroop effect compared to the other conditions (ADD models; Figure 4.2A). If, in contrast, their interaction is significant, two alternative scenarios are possible: They could interact either in a synergistic (i.e., more than additive) way, producing a reduction of the Stroop effect that is greater than that assumed

by the additive hypothesis (SYN models; Figure 4.2B), or in an antagonistic (i.e., less than additive) way, producing a reduction of the Stroop effect that is smaller than that assumed by the additive hypothesis (ANT models; Figure 4.2C).

The second distinction stems from the possibility that one of the two control modes could have a stronger impact on the Stroop effect than the other. This point differentiates our hypotheses only for what concerns the conditions wherein only proactive control or reactive control is implemented (respectively, hPro-lRea and lPro-hRea), while it should not affect the size of the Stroop effect in the conditions wherein neither or both forms of control are implemented (respectively, lPro-lRea and hPro-hRea). If we assume that proactive and reactive controls have the same strength, the Stroop effect should be the same size in the lPro-lRea and hPro-hRea conditions (Figure 4.2, left plots). Conversely, if we assume that the effect of proactive control is stronger, the Stroop effect should be smaller in the hPro-lRea condition compared to the lPro-hRea condition (Figure 4.2, right plots), while if the effect of reactive control is stronger, the Stroop effect should be smaller in the lPro-hRea condition compared to the hPro-lRea condition (Figure 4.2, middle plots).

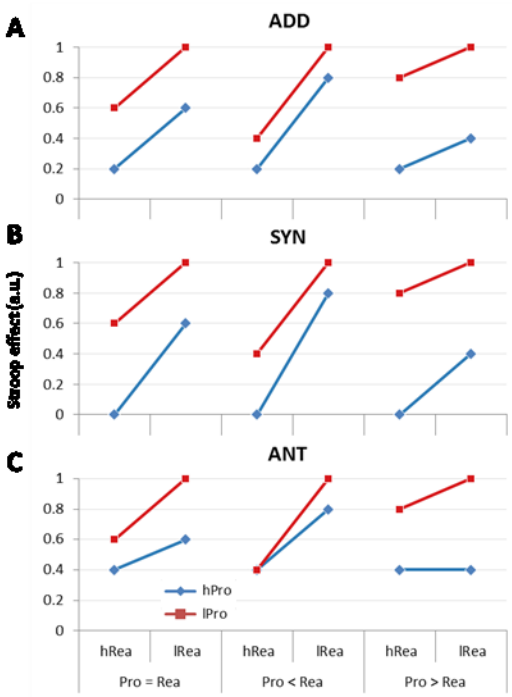

Figure 4.2.
Predicted patterns of Stroop effect modulations by low and high levels (l and h, respectively) of LWPC-related Proactive control (Pro) and ISPC-related Reactive control (Rea) according to our alternative hypotheses. ADD, additive effects of Pro and Rea; SYN, synergistic Pro by Rea interaction; ANT, antagonistic Pro by Rea interaction (see Hypotheses section for more details).

4.2. Experiment 1 - Peripheral

4.2.1. Methods

We report how we determined our sample size, all data exclusions, all inclusion/exclusion criteria, all manipulations, and all measures in the study. All inclusion/exclusion criteria were established prior to data analysis. All data and materials, as well as the code used to run the experimental tasks and generate and analyze the data of the current study, will be made available from our project repository on the Open Science Framework (OSF) platform at osf.io/qmu7g. No part of the study, including the analyses, was pre-registered.

4.2.1.1. Procedure and experimental tasks

The experiment was programmed using Psytoolkit (Stoet, 2010, 2017) and administered online. The stimuli were presented in full-screen mode, with a resolution of 800 x 600 pixels, on a gray background (RGB: 128, 128, 128). Each trial started with a fixation stimulus presented at the center of the screen for 500 ms and participants were instructed to fixate it. Then, the experimental stimulus appeared and remained on the screen until participants responded or up to a response time-out of 2000 ms. Participants had to pay attention to the task-relevant information, which was the pointing direction of a black arrow, and were required to indicate it via button press by using four keys on a computer keyboard, which were E, O, K, and D. These keys were spatially arranged to be compatible with the four possible arrow directions, which could be upper-left, upper-right, lower-right or lower-left, and had to be pressed using the left middle, right middle, right index and left index fingers, respectively. The experimental stimuli were also characterized by task-irrelevant information, which was the position where the arrow appeared. The position of the arrow overlapped with the four task-relevant directions, since the arrow could appear in an upper-left, upper-right, lower-right, or lower-left position. The task-irrelevant position could match or not the task-relevant direction, yielding congruent and incongruent trials, respectively.

In this study, we used a Peripheral spatial Stroop task (Viviani et al., 2023), wherein the target arrow could appear in one of four peripherally-located spatial positions. For this task, the fixation screen consisted of a black cross (36 x 36 pixels) presented at the center of the screen, along with four white squares (73 x 73 pixels) at the four corners of an imaginary square of 600 x 600 pixels centered on the screen. Then, the target arrow was presented inside one of the four peripheral squares, and it could point to one of the same four directions. We used 12 of the 16 possible combinations of arrow positions and directions, as we excluded the four corresponding to the incongruent arrows pointing to the opposite direction (e.g., the arrow appearing at the upper-left corner and pointing toward the bottom-right corner) because they point towards the correct response.

List-wide (LWPC) and item-specific (ISPC) proportions of congruency were simultaneously manipulated to measure both proactive and reactive control, respectively. To this aim, the trial lists were designed by first dividing them into two main blocks made of 320 experimental trials each, with different LWPC values, one with 35% of congruent trials (LW35) and one with 65% of congruent trials (LW65). Then, distinct ISPC levels were used, nested within each LWPC block, so as to have 4 different ISPC values within each block. In the LW35 block, the ISPC ranged from 20% to 50% in steps of 10%, while in the LW65 block, the ISPC ranged from 50% to 80% in steps of 10%. Crucially, by using the same ISPC level (50%) in both LWPC blocks, we were able to assess the pure effect of LWPC (and thus proactive control) on Stroop effects, independently of ISPC (and thus reactive control) and contingency. Moreover, within each block, the occurrence of each position-direction combination was intentionally varied in trying to orthogonalize as much as possible the contingency to LWPC and ISPC, so that the effect of each of these variables could be disambiguated in the statistical analysis. In doing so, we allowed the probability of each of the four directions (and thus the responses) to slightly vary within each sub-block, while keeping the probability of each of the four positions constant. We thus obtained different contingency values , ranging from 5% to 80%, and within each ISPC level, two different contingency values differing by 10% were used for the two possible incongruent trials (see Figure 4.3). In addition to the 640 experimental trials, before each LWPC block, we added sub-blocks of 40 trials to favor the familiarization of participants to the current block LWPC level. Moreover, the 640 experimental trials were divided into 8 sub-blocks with self-paced breaks in between, and at the beginning of each sub-block we added 2 buffer trials. The habituation and buffer trials were then excluded from the analyses. Within each trial-list, the order of presentation of the trials was pseudorandomized using the software Mix (van Casteren & Davis, 2006) to avoid more than four consecutive repetitions of the same congruency and both total and partial repetitions of stimulus characteristics and/or responses in order to control for first-order priming effects.

A second step in trial-list design was to compute trial-wise LWPC, ISCP and contingency for each trial-list version using the Hierarchical Gaussian Filter (HGF, Mathys et al., 2011). HGF is a filter that uses variational Bayes under a mean-field approximation to update the probability of an event on each trial. Specifically, trial-level estimates were computed reflecting trial-by-trial probabilities updated based on: i) the stimulus congruency, for LWPC; ii), the stimulus congruency conditional to a specific position, for ISPC; iii) the target direction (and thus the response) conditional to a specific position, for contingency. The HGF was also used to compute trial-by-trial probabilities of other variables used as confounding predictors in statistical analyses (see below).

Before beginning the task, the participants received general instructions on the procedure, the task, and the response mapping. Considering also that the task was completed online, we took particular care to keep the instructions as simple, detailed, and clear as possible. Participants were asked to respond as

quickly and accurately as possible and recommended performing the task in a quiet environment, maintaining a comfortable posture, and keeping the responding fingers in contact with the response keys. After the instructions, the participants completed a block of 20 practice trials with LWPC and ISPC at 50%, during which they received feedback on their performance, and, in the case of errors or time-out responses, they were also provided with a brief summary of instructions and response mapping. Practice trials were presented until 75% accuracy was reached.

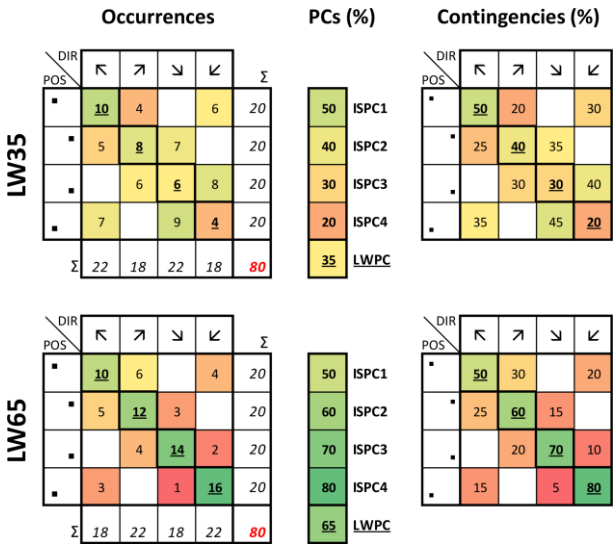

Figure 4.3.
Block-wise structure of the task. Separately for one sub-block of each LWPC block (LW35, top row; LW65, bottom row), the image shows on the left the number of trials (occurrences) with a specific target direction (DIR) and position (POS). For example, in the LW35 sub-block, we had nine trials with the arrow appearing in the lower-left corner, but pointing towards the lower-right corner. The trials in the diagonal are the congruent ones (underscored). For each sub-block, the corresponding contingencies are also shown on the right, while the middle column shows the percentage of congruent trials (LWPC) and of congruent trials specific for each location (ISPC). The color scale indicates the relative probability of each trial type/contingency, as well as the relative level of the LW/ISPCs.

4.2.1.2. Data analysis

Various analyses were conducted to estimate the effect of LWPC and ISPC manipulations on the magnitude of the Stroop effect, while controlling for contingency, and to estimate the internal reliability of our effects. Statistical analyses were conducted using Matlab (version 2017b; The MathWorks, Inc. Natick, MA).

The analyses were performed on inverse-transformed RTs (iRTs, computed as -1000/RTs). This transformation was employed to eliminate the heavy right skewness of the RT distribution, for which the logarithmic transformation was not enough. From the 62720 experimental trials, we excluded trials with incorrect responses (n = 2115, corresponding to 3.37% of the experimental trials), missed responses (n = 235, corresponding to 0.37% of the experimental trials), and RTs shorter than 150 ms (n = 1, corresponding

to <0.01% of the experimental trials), which were all treated as errors, and post-error trials (n = 2103, corresponding to 3.35% of the experimental trials). Control analyses were performed on both untransformed RTs and natural log-transformed RTs (lnRTs) to assess the robustness of the results to analytical flexibility.

We checked for the presence of participants with low compliance, defined as those having either a mean iRTs more than three standard deviations away from the sample mean or a mean accuracy lower than 70% (i.e., the level used in the practice block). Based on these criteria, no participant was excluded from the analyses (see Appendix B, Figure B.2)

Assessing the magnitude of LWPC and ISPC effects

The statistical analyses were performed using a multilevel modeling approach, also called trial-by-trial hierarchical modeling, by performing linear mixed-effects model analyses (LMM, Baayen et al., 2008). This approach is the most suitable for our experimental design and, thus, our aims. Indeed, using multilevel modeling, we were able to assess the distinct impact of LWPC and ISPC, as well as their interaction, in modulating the Stroop effect when they both varied. Moreover, this approach allowed us to do so while partialling out the effect of contingency and other lower-level confounding factors, which represent sources of trial-by-trial noise in the estimation of our effects of interest at the subject level. Finally, this approach allowed us to employ the trial-level estimates of our predictors because, as explained in the Introduction, considering trial-by-trial history is more realistic than using the respective discrete values. Multilevel modeling also allows one to overcome standard general linear model (GLM) drawbacks. Indeed, we recently showed that this approach ensures more accurate and precise estimates of the experimental effects of interest. Moreover, since this approach explains intra-subject/inter-trial sources of variance contributing to measurement error, it also provides better reliability of these estimates (Viviani et al., 2023).

We tested a LMM model defined a priori based on our theoretical assumptions, which we named “continuous full model”. Indeed, this model included the trial-level estimates of our predictors for both experimental manipulations and confounders, indicated by the suffix “b” to the predictor names (because they were estimated using the ideal Bayesian observer). Specifically, in the fixed part of the model, we included several confounding predictors, for the reasons explained above. Each confounder was included based on well-known effects in the literature. Specifically, we included i) a continuous predictor reflecting the iRT of the preceding trial (iRTpre), to account for temporal dependency in RTs (Baayen & Milin, 2010) and thus to avoid violating the assumption of the independence of observations for linear modeling; ii) the continuous predictor for the effect of trial number (trialTOT) to account for potential time-on-task effects, such as the effects of learning/adaptation or fatigue; iii) the horizontal and vertical position of the stimulus on the screen (respectively, hS and vS), to account for potential (e.g., perceptual, attentional) differences

due to the location where the stimulus appeared (left vs right, above vs below, respectively); iv) the horizontal and vertical coding of the response (respectively, hR and vR), to account for potential (e.g., motor) differences due to the response hand and finger, respectively. Lastly, we included predictors for low-level learning effects that have been shown to affect the Stroop interference resolution, threatening the interpretability of the Stroop performance with control-related accounts, that is, v) contingency, which is the conditional probability of the response given the stimulus, P(R|S) (PRSb), and vi) the probability of the response, P(R) (PRb). The experimental effects of interest were modeled by including the predictors for the LWPC and ISCP manipulations (LWb and ISb, respectively) and trial congruency (CON), as well as their interactions. The three-way interaction served to explore whether proactive and reactive control interacted in modulating the Stroop effect, and it was included in both the fixed and random parts of the model, as we assumed that it varied across subjects. The Wilkinson-notation formula for the continuous full model is as follows:

*RT ~ iRTpre + TrialTOT + hS + vS + hR + vR + PRSb + PRb + LWb*ISb*CON + (LWb*ISb*CON|SS)*

The continuous predictors iRTpre, TrialTOT, PRSb, and PRb were centered and scaled at the participant level to facilitate the convergence of the model and the interpretation of the results, while scaling was not necessary for LWb and ISb, since, by calculating their trial-level estimates, they were already on a scale centered at a 50% probability. The predictor for Congruency was coded with the values of 0 and 1 for the Incongruent and Congruent conditions, respectively, with the latter acting as the reference level.

Then, to assess whether there was evidence of stress in the model fit, after fitting the model, we inspected the model residuals and we then re-fitted a trimmed version of the model obtained by excluding data points with absolute standardized residuals exceeding 3.

We report the estimated coefficient (b), standard error (SE), and t and p values for each fixed effect included in the trimmed final model. We calculated the p-values by using Satterthwaite's approximation of degrees of freedom, which was also used to compute the corresponding effect size estimates (d_S) for the experimental effects of interest. The effect sizes for the same effects were also computed as standardized differences based on the participants' estimated condition means based on their random slopes (d_r). An alpha level of .05 was set as the cut-off for statistical significance. We used the participants' random slopes to compute the individual effects of interest (that is, the Stroop effect and its modulation by LWPC, ISPC, and their interaction) and the corresponding dominance values, that is, the percentage of participants showing them.

We also performed some control analyses to verify whether our continuous full model was justified and ensured the best fit to the data. First, the same model was tested also using the block-level estimates of our variables, referred to as discrete variables (discrete full model), to assess the assumed theoretical

advantages of the trial-level estimates (besides favoring comparability with previous literature). To this aim, we compared the Akaike information criterion of the continuous and discrete full models to assess which one better explained our data. Moreover, to verify whether the inclusion of confounders actually increased the model goodness of fit, we compared the continuous full model to a reduced one (continuous reduced model), which included only the variables of theoretical interest but none of the confounding ones, using the log-likelihood ratio test (Baayen et al., 2008). Lastly, in the case in which the triple interaction was not significant, we tested the same continuous full model but after removing the term for the three-way interaction (i.e., leaving the terms for the two 2-way interactions CON_0:LWb and CON_0:ISb), to verify whether its inclusion might have interfered with the estimation of the effects of the two 2-way interactions testing for the distinct effects of proactive and reactive control (continuous full 2-way interaction model).

To assess the robustness of our results to analytical flexibility, control analyses were also performed by replicating LMM results for the continuous full model using another multilevel modeling approach, that is, a random coefficient analysis (RCA, also called random regression or two-step regression; Lorch & Myers, 1990). For the RCA analysis, we first ran linear regressions at the subject level using the same regression model as the final LMM model described above (continuous full model). The Wilkinson-notation formula for the RCA model is:

$$RT \sim iRTpre + TrialTOT + hS + vS + hR + vR + PRSb + PRb + LWb*ISb*CON$$

As for the LMM analysis, the model was refitted after the exclusion of data points with standardized residuals exceeding 3. Then, we assess the statistical significance and effect size of the tested effects at the group level by performing two-tailed one-sample t tests against 0 on the estimated b coefficients for each participant.

We also performed additional analyses to assess the magnitude of the Stroop effect using a general linear model (GLM) approach, which is the standard approach in cognitive psychology and relies on the aggregation of the participants' performance in trials of different conditions to obtain participants-by-condition scores. However, this approach discards any trial-by-trial variability that can contaminate participant-by-condition scores, potentially decreasing their accuracy and generalizability (Rouder & Haaf, 2019). More importantly, GLM analyses are not well-suited for our experimental design because it is incomplete (ISPC is nested in LWPC). This was not an issue for testing the Stroop effect magnitude per se, as we could aggregate congruent and incongruent trials across the LWPC and ISPC levels, but it prevented us from testing the effects of LWPC and ISPC while also controlling for contingency (see Assessing the magnitude of LWPC and ISPC effects). Indeed, due to our manipulation of LWPC, ISPC, and contingency, and since contingency is inevitably confounded with ISPC in congruent trials, we did not have all the required combinations of LWPC, ISPC, and contingency levels, and the trial number for the available combinations

was heavily unbalanced. These limitations notwithstanding, we decided to perform GLM analyses anyway to favor the comparison of our results on the Stroop effect magnitude with the literature.

Assessing the internal reliability of LWPC and ISPC effects

The internal consistency of the experimental effects of interest was assessed for the LMM results by computing split-half Pearson's correlations corrected with the Spearman-Brown formula (r_{SB}). We used 2000 randomizations and calculated both the median r_{SB} values and the corresponding nonparametric 95% confidence intervals ($CI_{95\%}$).

Essentially, observations were randomly split into two subsets and, on each subset, LMM analysis was performed. As highlighted above, this allowed us to model the interindividual variability in the effects of interest (Stroop effect, proactive and reactive control and their interaction), while partialling out the effect of the confounding predictors described above. Then, the by-subject random slopes for the effects of interest in the two subsets were correlated to obtain the r_{SB} values.

4.2.1.3. Participants

For the first experiment, we recruited 98 participants (55 females and 43 males; mean age = 25.89 years, SD = 6.42 years). Participants' handedness was assessed using the Edinburgh Handedness Inventory (EHI, Oldfield, 1971). The sample comprised five left-handed participants (EHI scores < −50) and nine ambidextrous participants (EHI scores between −50 and 50). No participants reported suffering from neurological or psychiatric disorders or being under medication. Participants gave their informed consent to participate in the study, which was conducted in accordance with the ethical standards of the 2013 Declaration of Helsinki for human studies of the World Medical Association. The study was approved by the Ethical Committee for the Psychological Research of the University of Padova.

Participants consisted of a convenience sample recruited using researchers' personal networks and were not compensated for their participation. To determine the sample size for the LMM analysis, the approaches available to date for power analysis are not adequate and/or feasible for our complex statistical model (see Viviani et al., 2023, or Chapter 3, for a detailed discussion), especially because it involves the interaction between continuous predictors. Nonetheless, it should be noted that the RCA and LMM approaches are quite similar and provide similar results (at least regarding the Stroop effects in our experimental paradigm), and the power analysis for RCA is trivial, as it concerns a simple one-sample t-test on the by-subject slopes for the effect of interest. We thus performed an a priori power analysis in G*Power (Erdfelder et al., 1996) to compute the minimum sample size required to detect, with a statistical power of .80, the effect of main interest (i.e., the three-way interaction reflecting the Stroop effect modulation by the interaction between LWPC and ISPC) in a two-tailed one-sample t-test. We

conservatively assumed a small-medium Cohen's d effect size of .35. This analysis revealed that at least 67 participants were required. We nonetheless decided to recruit as many participants as possible, exceeding the required sample size, to be able to detect even smaller effects (by increasing the statistical power of our analyses) and to increase the precision of the experimental effects estimates. It is important here to note that LMMs tend to provide higher power than standard GLM approaches like the one-sample t-test we used here.

4.2.2. Results

4.2.2.1. Magnitude of LWPC and ISPC effects

For all the analyses, we report here only the results for iRTs. Indeed, as mentioned above, the distribution of RTs was heavily right-skewed and the residuals of the analyses on both RTs and lnRTs violated the assumptions of normality and homoscedasticity (see Appendix B, Figures B.1 and B.3-5).

GLM-based analyses were performed using t tests. The overall Stroop effect (i.e., collapsing across LWPC and ISPC values) was significant ($t = 35.50$, $p < .0001$) and with a very large effect size ($d = 3.59$). Our result indicates that all our participants were significantly slower in responding to Incongruent as compared to Congruent trials (dominance = 100%) (see Appendix B, Table B.1).

Regarding the LMM analysis, we first compared the full continuous model to the full discrete model using the AIC model selection and we found that the best-fit model was the full continuous model (AIC = 8352 vs 8436.7 of the full discrete model). Then, we compared our full continuous model with the reduced continuous one by performing the log-likelihood ratio test, which revealed that the full continuous model was justified ($\chi^2(7) = 7530.5$, $p < .0001$), confirming that the inclusion of confounders increased the model fit. As such, here we report the results of the analysis performed on iRTs using the full model with continuous variables.

The conditional R^2 of the LMM model was .69 and 0.84% of the observations was removed as outliers (>3 absolute standardized residuals) to mitigate the stress of the model fit (i.e., to improve the normality of the residuals, see Appendix B, Figure B.3). This analysis revealed that all the confounding predictors were significant in modulating participants' iRTs (all *p*s < .0001, see Table 4.1). Specifically, our results suggest that participants were faster as the trials progressed and when they responded to stimuli appearing on the upper and right sides of the screen using the middle finger and the right hand. Moreover, we found a significant temporal dependency in iRTs (i.e., a positive correlation between iRTs at the current and preceding trial). Lastly, responses were faster when the probability of the response (PRb) was higher.

For what concerns our predictors of interest, we found that the Stroop effect (CON_0) was significant ($p < .0001$), with slower responses to Incongruent trials. The Stroop effect had a very large effect size ($d_r = 3.67$, $d_S = 2.13$) and a dominance value of 100%, that is, all participants showed a positive Stroop effect. The Stroop effect was significantly modulated by LWb ($p < .0001$, $d_r = 1.27$, $d_S = 0.80$, dominance = 92.86%), showing that as LWb increased, the Stroop effect increased, revealing the effect of proactive control. By contrast, the LMM analysis did not reveal a significant modulation of the Stroop effect by ISb ($p = .1121$, $d_r = 0.62$, $d_S = 0.05$, dominance = 70.41%). Moreover, the triple interaction between the Stroop effect, LWb and ISb was not significant ($p = .2461$, $d_r = 0.16$, $d_S = 0.12$, dominance = 57.14%), suggesting that LWb and ISb did not interact in modulating the Stroop effect. Lastly, our analysis revealed a significant effect of Contingency (PRSb, $p = .0005$), indicating that participants responded faster when PRSb was higher.

Table 4.1 – Results of the LMM analysis for Experiment 1 (continuous full model)

Effect	*b*	*SE*	*t*	*df*	*p*
Intercept	-1.9439	0.0350	-55.559	145.60	< .0001
TrialTOT	-0.0923	0.0023	-40.030	1967.43	<.0000
CON_0	0.3521	0.0123	28.620	179.86	<.0000
iRTpre	0.0551	0.0012	47.190	57392.28	<.0000
hS	-0.0104	0.0028	-3.700	12850.75	.0002
vS	-0.0791	0.0027	-29.056	19753.88	<.0000
hR	-0.0351	0.0026	-13.381	34201.64	<.0000
vR	-0.1013	0.0026	-39.379	39671.65	<.0000
LWb	-0.0086	0.0104	-0.825	97.51	.4112
ISb	-0.0135	0.0074	-1.827	435.59	.0684
PRSb	-0.0207	0.0059	-3.497	48890.40	.0005
PRb	-0.1234	0.0133	-9.256	49487.44	<.0000
CON_0:LWb	0.0651	0.0081	8.071	101.81	<.0000
CON_0:ISb	0.0162	0.0102	1.590	939.28	.1121
LWb:ISb	-0.0123	0.0109	-1.132	97.28	.2606
CON_0:LWb:ISb	0.0140	0.0120	1.167	94.08	.2461

Notes: b, coefficient estimates; *SE*, standard error, df, degrees of freedom computed with the Satterthwaite's approximation. See the main text for the spelling out of the acronyms for the effects

To verify whether the effect of the CON_0:ISb interaction was hindered by the triple interaction, we also performed the continuous full 2-way model, excluding the triple interaction and keeping the two double interactions (CON_0:LWb and CON_0:ISb). This analysis confirmed the results reported above, and the interaction between ISb and CON_0 remained non-significant ($p = .0920$, $d_r = 0.50$, $d_S = 0.06$, dominance =

72.45%), confirming that in the Peripheral task, we did not find a significant modulation of the Stroop effect by ISb. Lastly, the effect of PRSb was again significant (p = .0004), showing that participants responded faster when PRSb was higher (see Appendix B, Table B.7).

To confirm these results, RCA analysis was then performed on the iRTs using the continuous full model, namely the model including the triple interaction. All the effects of the confounding predictors on participants' iRTs found in both LMM analyses were confirmed (all *p*s < .004, (see Appendix B, Table B.8)), with the exception of hS. RCA results regarding our predictors of interest partially replicated LMM results. Indeed, we similarly found a significant Stroop effect ($p < .0001$, $d_r = 2.32$, dominance 98.98%), that is, longer iRTs for Incongruent trials, and a significant modulation of the Stroop effect by LWb ($p < .0001$, $d_r = .86$, dominance = 77.55%). Moreover, the interaction between CON and ISb was still not significant ($p = .9344$, $d_r = 0.01$, dominance = 46.94%), replicating previous analysis that failed to reveal the effect of reactive control in modulating the Stroop effect. However, the results of the triple interaction were in contrast with the LMM ones. Indeed, we found that LWb and ISb interacted significantly in modulating the Stroop effect ($p = .0009$, $d_r = 0.35$, dominance = 65.31%). Lastly, the effect of PRSb was significant ($p = .0001$, $d_r = -0.40$), confirming previous results.

Since we found that the effect of PRSb was always significant while the effect of reactive control was never significant, we hypothesized that we did not find it because PRSb might have explained all the variance that could have been explained by the reactive control modulation of the Stroop effect. We thus performed a control analysis, running again the continuous full model after excluding PRSb (continuous full No_PRS model), both using LMM and RCA (see Appendix B, Tables B.9-10). These analyses confirmed the results of the previous ones, except for the fact that, by removing PRSb, the interaction between CON and ISb became significant (both *p*s < .0001, $d_s = 0.84$ and $d_r = 0.83$, respectively). Of note, the inclusion of PRSb in the model was justified and improved the model fit ($\chi^2(1) = 30.1$, $p < .0001$).

4.2.2.2. Internal reliability of LWPC and ISPC effects

We assessed the internal reliability of our effects of interest using LMM to explain intra-subject/inter-trial variance, with the aim of obtaining more precise estimates of it.

As expected, the internal reliability estimate of the Stroop effect was the highest and least variable among our effects of interest, with a median r_{SB} value of .92 and a $CI_{95\%}$ of .89-.94. The internal reliability of the proactive control effect had a median r_{SB} value of .79 and a $CI_{95\%}$ of .67-.87, while the median r_{SB} internal reliability of the reactive control effect was .58 with a $CI_{95\%}$ of .25-.79. Finally, the internal reliability of the triple interaction was similar to that of proactive control, with a median r_{SB} value of .76 and a $CI_{95\%}$ of .65-.83 (see Figure 4.4 and Appendix B, Figure B.9).

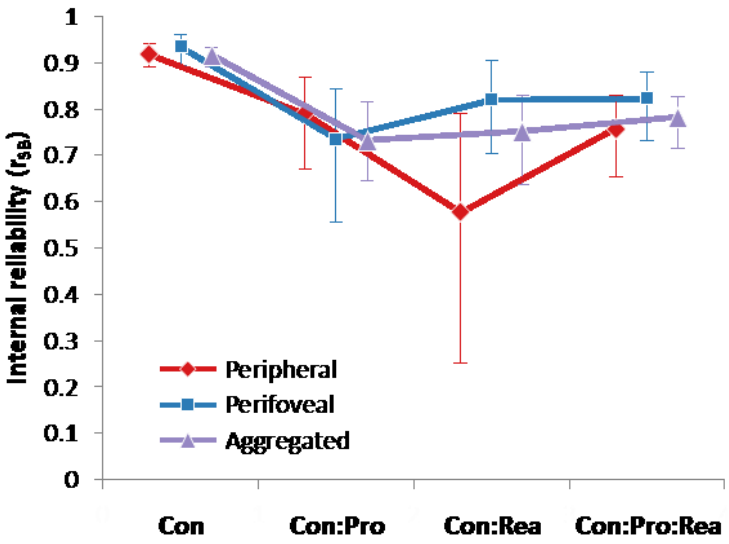

Figure 4.4.
Internal reliability (r_{SB}) of the experimental effects of interest (Con, Stroop effect; Con:Pro, LWb modulation of Stroop effects) in the three analyses (Con:Rea, ISb modulation of Stroop effects; Con:Pro:Rea, interaction between LWb and ISb in modulating the Stroop effects). Error bars represent the non-parametric 95% confidence intervals.

4.2.3. Discussion

The results of our previous study (Viviani et al., 2023) showed that the Peripheral spatial Stroop is an experimental paradigm suitable for yielding a complete Stroop interference effect whose magnitude is also large and robust to analytic flexibility with adequate and robust internal reliability. In contrast to our previous study (Viviani et al., 2023), in which we just assessed the magnitude of the Stroop effect, here we used the same experimental paradigm but with different manipulations with the aim of measuring, simultaneously, the effect of proactive and reactive control in modulating the Stroop effect, as well as their interaction, while controlling for low-level effects, among which contingency.

The analysis assessing the magnitude of such effects revealed different results based on the analytical approach employed. As explained in the methods, the standard GLM-based analysis is largely incompatible with our experimental design and was thus only used to assess overall Stroop effects. The two multilevel analytical approaches, which were instead more adequate for our purposes, showed a partially contrasting scenario. Indeed, both approaches converged on the existence of a proactive control mechanism modulating the Stroop effect, which was shown to be a large and universal effect, and on the absence of a reactive control mechanism that independently modulated the Stroop effect. On the contrary, a significant interaction of proactive and reactive control in modulating the Stroop effect was found only in the RCA-based analysis but not in the LMM-based one, casting shadows on the robustness of such an effect.

A further consistent aspect revealed by our analyses is the relation between reactive control and PRSb. Indeed, they interestingly revealed that when PRSb was statistically controlled for, the ISb-dependent modulation of the Stroop effect was not significant, thus confirming the strong influence of contingency on ISPC-induced reactive control, as suggested by Schmidt (2019) (see also Schmidt & Besner, 2008). Moreover, the fact that the effect of reactive control was unveiled after removing PRSb from the model provides support to our methodological and analytical approaches, which allowed us to control for the impact of contingency at the statistical level, while this is practically impossible to do in a purely methodological way (i.e., with the design-level control). This point will be addressed more in more detail in the general discussion.

Lastly, the internal reliability of the two significant effects of interest was quite high. Specifically, the Stroop effect had a very high internal reliability, characterized also by little variability, whereas the proactive control reliability was more variable but still quite good (see Figure 4.4).

The inconsistencies regarding the interplay between proactive and reactive control observed in the present experiment could be in part explained by the Peripheral spatial Stroop weaknesses assumed also in our previous study (Viviani et al., 2023) and related to the peripheral visual presentation of the stimuli. Specifically, the peripheral arrangement of the stimuli promotes the employment of visuospatial attentional shifts and eye movements to fixate the stimulus and better perceive it, which is a necessary processing step to retrieve the PC specifically associated with the item and then employ reactive control accordingly. However, these processing steps delay the employment of reactive control, as compared to a task using a perifoveal arrangement of the stimuli. This might have hindered the strength of reactive control and, consequently, its interaction with proactive control, thus not allowing us to detect it consistently using different analytical approaches.

Therefore, the use of the Perifoveal task in the second experiment helped us shedding light on the inconsistencies in our results, since we previously found that this experimental paradigm not only overcomes the weaknesses of the Peripheral task, but it is also the best alternative to it among all the task versions considered (Viviani et al., 2023). Indeed, by presenting the stimuli in the perifoveal vision, the Perifoveal spatial Stroop task does not require visuospatial attentional shifts or eye movements, thus it may favor a faster and more efficient reactive control employment.

4.3. Experiment 2 - Perifoveal

4.3.1. Methods

We report how we determined our sample size, all data exclusions, all inclusion/exclusion criteria, all manipulations, and all measures in the study. All inclusion/exclusion criteria were established prior to data analysis. All data and materials, as well as the code used to run the experimental tasks and generate and analyze the data of the current study, will be made available from our project repository on the Open Science Framework (OSF) platform at osf.io/qmu7g. No part of the study, including the analyses, was pre-registered.

4.3.1.1. Procedure and experimental tasks

In this experiment, we used a Perifoveal spatial Stroop task (Viviani et al. 2023), wherein the target arrow could appear in one of four centrally-located spatial positions so that both the task-relevant and task-irrelevant pieces of information could be seen in perifoveal vision. To do so, a different fixation screen was displayed, consisting of a vertically oriented thin black cross (30 x 30 pixels) enclosed in the partial outline of a black square (94 x 94 pixels) presented at the center of the screen. The partial outline of the square around the fixation cross created the impression of four small squares, allowing us to manipulate the position inside the fixation stimulus. Therefore, the target arrow was presented within one of these apparent small squares, and participants were required to indicate its pointing directions regardless of its position. Apart from this aspect, the experimental task and procedures were the same as in Experiment 1.

4.3.1.2. Data Analysis

The analyses were performed as in Experiment 1. As in Experiment 1, we excluded from the analyses training trials, habituation trials, and buffer trials at the beginning of each sub-block. From the resulting 49920 experimental trials, we also excluded trials with incorrect responses (n = 1885, corresponding to 3.78% of the experimental trials), missed responses (n = 57, corresponding to 0.11% of the experimental trials), and RTs shorter than 150 ms (n = 0), which were all treated as errors, and post-error trials (n = 1667, corresponding to 3.34% of the experimental trials).

We checked for the presence of participants with low compliance, defined as those having either a mean iRTs more than three standard deviations away from the sample mean or a mean accuracy lower than 70% (i.e., the level used in the practice block). Based on these criteria, no participant was excluded from the analyses (see Appendix B, Figure B.11)

4.3.1.3. Participants

For this Experiment, we recruited 78 participants (41 females and 37 males; mean age = 24.21 years, SD = 6.43 years). The sample comprised four left-handed participants (EHI scores < −50) and 13 ambidextrous participants (EHI scores between −50 and 50). No participants reported suffering from neurological or psychiatric disorders or being under medication. Participants gave their informed consent to participate in the study, which was conducted in accordance with the ethical standards of the 2013 Declaration of Helsinki for human studies of the World Medical Association. The study was approved by the Ethical Committee for the Psychological Research of the University of Padova.

Participants consisted of a convenience sample recruited using researchers' personal networks and were not compensated for their participation. A power analysis was performed as in Experiment 1; again, we decided to recruit as many participants as possible, exceeding the required sample size, to be able to detect effects even smaller than expected (by increasing the statistical power of our analyses) and to increase the precision of the experimental effects estimates. It is important here to note that LMMs tend to provide higher power than standard GLM approaches like the one-sample t-test we used here.

4.3.2. Results

4.3.2.1. Magnitude of LWPC and ISPC effects

As for the analyses on the Peripheral task, here, we report only the results on iRTs, since the distribution of RTs was heavily right-skewed and the residuals of the analyses on both RTs and lnRTs violated the assumption of normality (see Appendix B, Figures B.10 and B.12-14).

GLM-based analyses using t tests were first used to explore the overall Stroop effect (i.e., aggregating across LWPC and ISPC values). These analyses revealed that participants responded significantly slower to Incongruent as compared to Congruent trials (t = 33.43, p < .0001) with a very large effect size (d = 3.79) and 100% dominance (see Appendix B, Table B.14).

Then, we performed analyses using both the continuous and the discrete full models. We found that the former provided a better fit to the data (AIC = 29422 vs. 29511 of the full discrete model). Then, we compared the continuous full model with the continuous reduced model performing the log-likelihood ratio test, which revealed that the full continuous model was justified ($\chi^2(7) = 2971.6$, p < .0001), suggesting that the inclusion of confounders increased the model fit. As such, here we report the results of the analysis performed on iRTs using the full model with continuous variables.

The conditional R^2 of the LMM model was .63 and 0.84% of the observations was removed as outliers (>3 absolute standardized residuals) to mitigate the stress of the model fit (i.e., to improve the normality of

the residuals, see Appendix B, Figure B.12). All the confounding predictors of our continuous full model significantly modulated participants' iRTs (all *p*s < .04, see Table 4.2). We found that participants were faster as trials went on and when they responded to stimuli appearing in the lower and right halves of the screen using the middle finger and the right hand. Moreover, there was a significant temporal dependency in iRTs (i.e., a positive correlation between iRTs in the current and preceding trial), and the responses were faster when the probability of the response (PRb) was higher.

Table 4.2 – Results of the LMM analysis for Experiment 2 (continuous full model)

Effect	b	SE	t	df	p
Intercept	-2.4845	0.0448	-55.449	128.21	< .0001
TrialTOT	-0.1018	0.0034	-29.687	2686.32	< .0001
CON_0	0.3729	0.0177	21.059	138.27	< .0001
iRTpre	0.0586	0.0017	35.077	45622.01	< .0001
hS	-0.0080	0.0039	-2.072	4301.02	0.0383
vS	0.0110	0.0038	2.888	3793.44	0.0039
hR	-0.0608	0.0038	-16.143	31342.78	< .0001
vR	-0.0723	0.0037	-19.484	29671.40	< .0001
LWb	-0.0002	0.0145	-0.012	78.89	0.9907
ISb	-0.0025	0.0112	-0.223	262.95	0.8238
PRSb	-0.0516	0.0085	-6.062	40688.90	< .0001
PRb	-0.1572	0.0189	-8.300	39539.08	< .0001
CON_0:LWb	0.0668	0.0119	5.606	77.49	< .0001
CON_0:ISb	-0.0066	0.0157	-0.416	422.46	0.6774
LWb:ISb	-0.0311	0.0149	-2.085	78.49	0.0403
CON_0:LWb:ISb	0.0454	0.0204	2.226	78.29	0.0289

Notes: b, coefficient estimates; SE, standard error, df, degrees of freedom computed with the Satterthwaite's approximation. See the main text for the spelling out of the acronyms for the effects.

For what concerns our predictors of interest, the Stroop effect (CON_0) significantly modulated participants' iRTs (*p* < .0001), who showed slower responses to Incongruent trials, with a very large effect size (d_r = 3.01, d_s = 1.79) and a dominance value of 100%, which indicates that all participants showed a positive Stroop effect. As for the Peripheral task, LWPC significantly modulated the Stroop effect (*p* < .0001, d_r = 0.99, d_s = 0.64, dominance = 82.05%), that is, there was an effect of proactive control, with larger Stroop effects as LWb increased. By contrast, the Stroop effect was not significantly modulated by ISb (*p* = .6774, d_r = -0.11, d_s = -0.02, dominance = 42.31%). In contrast to the Peripheral task, here, the three-way interaction was significant (*p* = .0289, d_r = 0.31, d_s = 0.25, dominance = 57.69%), revealing that the LWb and

ISb interacted in modulating the Stroop effect, that is, when both were high (namely, both proactive and reactive control were low), the Stroop effect was larger. Lastly, the effect of Contingency (PRSb) was again significant ($p < .0001$), indicating that participants responded faster when PRSb was higher. As opposed to the analysis on the Peripheral task, here we do not report the continuous full 2-way model, since the triple interaction was significant (but see Appendix B, Table B.16).

We then performed an RCA analysis on the continuous full model, which basically confirmed the results of the LMM analysis. Indeed, all the confounding predictors were in the same direction as the LMM results, and all but hS and vS were significant (all *p*s < .0005). We also found a very large Stroop effect ($p < .0001$, $d_r = 2.09$, dominance 98.72%), as well as its significant modulation by LWb ($p < .0001$, $d_r = 0.60$, dominance = 71.79%). In line with all previous results, the CON_0:ISb interaction was not significant ($p = .7178$, $d_r = -0.04$, dominance = 51.28%), showing no reactive control effect on the Stroop effect. The RCA analysis also confirmed the triple interaction found with the LMM analysis on the Perifoveal task, showing that LWb and ISb significantly interacted in modulating the Stroop effect ($p = .0006$, $d_r = 0.41$, dominance = 65.38%). Also, the effect of PRSb was again significant as in all our analyses ($p = .0001$, $d_r = -0.47$) (see Appendix B, Table B.17).

Lastly, we performed the same control analysis described for the Peripheral Experiment to verify whether the non-significant effect of reactive control was due to the effect of PRSb by rerunning the continuous full model using LMM and RCA but excluding PRSb (continuous full No_PRS model). The results were confirmed but, again, the interaction between CON_0 and ISb became significant after removing PRSb (both *p*s < .0001, $d_s = 0.71$ and $d_r = 0.74$, respectively). Of note, the inclusion of PRSb in the model was justified and improved the model fit ($\chi^2(1) = 18.0$, $p < .0001$) (see Appendix B, Tables B.18-19).

4.3.2.2. Internal reliability of LWPC and ISPC effects

The internal reliability estimate of the Stroop effect was the highest and least variable among our effects of interest, with a median r_{SB} value of .94 and a $CI_{95\%}$ of .89-.96. The internal reliability of proactive control had a median r*SB* value of .74 and a $CI_{95\%}$ of .56-.84, while the median r_{SB} internal reliability of reactive control was .82 with a $CI_{95\%}$ of .70-.91. Finally, the internal reliability of the triple interaction was quite high, with a median r_{SB} value of .82 and a $CI_{95\%}$ of .73-.88 (see Figure 4.4 and Appendix B, Figure B.18).

4.3.3. Discussion

As discussed in our previous study (Chapter 3) and in the Peripheral Experiment discussion, the Perifoveal task has methodological advantages over the Peripheral one, while also showing good statistical properties, as it ensures a large and reliable Stroop effect (Viviani et al., 2023). Although, so far, this experimental paradigm was tested when only Congruency was manipulated (see Viviani et al., 2023), we

expected that its methodological advantages over the Peripheral task could be extended over different experimental manipulations, such as those used in the present study. As such, we predicted that we could have obtained more reliable and robust results by using the Perifoveal Stroop task to simultaneously measure the effect of proactive and reactive control in the modulation of the Stroop effect, as well as their interaction, while also controlling for contingency and other low-level effects.

The results were in line with our predictions and the pattern and magnitude of our effects of interest were consistent across the two multilevel analytical approaches, which showed a significant modulation of the Stroop effect by proactive control alone and by the interaction between proactive and reactive control. Thus, as compared to the Peripheral Experiment, using the Perifoveal task we obtained evidence not only for the effect of proactive control but also for that of the three-way interaction, which was probably favored by the nature of the task that minimized the potential effect of confounders related to the peripheral allocation of attention. Indeed, by allowing a faster identification of the item, the PC associated with it was more effectively activated and reactive control was elicited accordingly. As a consequence, the three-way interaction might have had a larger magnitude, and thus might have been more easily detectable.

Although we found reactive control to interact with proactive control in modulating the Stroop effect, no significant distinct reactive control effect emerged. This finding, obtained using an experimental paradigm that is more likely to favor an ISPC-related reactive control employment, provided further evidence for our hypothesis that, when PRSb was included in the model, there was no residual variance left to be explained by ISb. Indeed, after PRSb was removed from the model, the effect of ISPC-induced reactive control emerged. This control analysis further supported our claim for the need to statistically control for what cannot be controlled for at the design level.

The results for internal reliability were in line with the Peripheral ones. The internal reliability of the Stroop effect was very high and showed little variability. Proactive control still had a good internal reliability, but was somewhat lower and more variable than that of the Stroop effect (see Figure 4.4).

Overall, the methodological premises favoring the Perifoveal spatial Stroop task and the greater consistency of the results across different approaches could indicate that the results obtained using the Perifoveal task were more robust and trustable. However, since they are in contrast with those obtained using the Peripheral task, we performed a between-Experiment analysis to verify whether the patterns of results were actually different between the two experiments.

4.4. Between-Experiments comparisons

4.4.1. Methods

We report how we determined our sample size, all data exclusions, all inclusion/exclusion criteria, all manipulations, and all measures in the study. All inclusion/exclusion criteria were established prior to data analysis. All data and materials, as well as the code used to run the experimental tasks and generate and analyze the data of the current study, will be made available from our project repository on the Open Science Framework (OSF) platform at osf.io/qmu7g. The analyses were not pre-registered.

4.4.1.1. Data analysis

Between-Experiment differences in LWPC and ISPC effects

We run all the previous analyses but now to compare whether the experimental effects differed among the Peripheral and Perifoveal experimental tasks. We again checked for the presence of participants with low compliance, defined as those having either a mean iRTs more than three standard deviations away from the sample mean or a mean accuracy lower than 70% (i.e., the level used in the practice block). Based on these criteria, no participant was excluded from the analyses (see Appendix B, Figure B.20)

First, a GLM analysis was performed to verify whether the Stroop effects obtained in the two experiments differed. Specifically, we compared the overall Stroop effects using a two-sample *t* test and computing Cohen's *d* to obtain the corresponding effect size estimate.

For the LMM analysis, we added to the continuous full model used in the previous analyses the categorical variable Experiment, whose value was set to -.5 for the Peripheral Experiment and .5 for the Perifoveal one. As explained above, based on our theoretical assumptions, we a priori decided to test the model including the trial-level estimates of our predictors and to include all plausible confounders. The Experiment factor was tested in interaction with those predictors that we expected to be modulated by it. As regards low-level predictors, we hypothesized that Experiment, due to the spatial arrangement of the stimuli, interacted with hS and vS (but not with hR and vR since the response effectors were the same), and with PRS since the difference in the stimuli could have affected the contingency effects. Moreover, since we were interested in whether the proactive and reactive control interaction in the Stroop effect modulation differed among the two Experiments, the Experiment factor was also tested in interaction with them in the fixed part, thus including in the model a four-way interaction. The formula for the final model, referred to as the continuous full_btw4 model, is:

RT ~ iRTpre + TrialTOT + hR + vR + PRb +Experiment(hS + vS + PRSb + LWb*ISb*CON) + (LWb*ISb*CON|SS)*

We inspected the results to identify whether the effect of the predictors we tested in interaction with the Experiment factor was significant or not and, in the latter case, we refitted the model without such interactions to exclude the possibility that they could have affected the estimation of the other effects. It is important here to note that the results were essentially the same. Then, we used the random slopes for each participant to obtain the participant's mean for each combination of experimental conditions and compared the experimental effects between the two Experiments using independent-sample *t* tests.

For the RCA analysis, we ran linear regressions at the subject level using the same regression model as the within-subjects analysis (continuous full model), that is, using the following formula:

*RT ~ iRTpre + TrialTOT + hS + vS + hR + vR + PRSb + PRb + LWb*ISb*CON*

After excluding outliers exceeding 3 *SD*, we refitted the model and we compared whether the parameters of interest differed between the two Experiments using independent-sample *t* tests.

These analyses could also help us in case of inconsistencies in the results of the two within-subjects analyses as, by being performed on the two datasets together, it would provide an overall result based on a larger sample.

Assessing the internal reliability of LWPC and ISPC effects

The internal consistency of the experimental effects of interest was assessed for the LMM results in the aggregate sample as described in Experiment 1.

4.4.2. Results

4.4.2.1. Between-Experiments differences in LWPC and ISPC effects

We report here only the results of the analyses performed on iRTs for the same reasons explained above.

The GLM-based analysis using a two-tailed independent-samples *t* test showed that the mean Stroop effects in the two Experiments differed significantly, with the Perifoveal one yielding the larger Stroop effect (M_{diff} = .0832, t = 4.77, p < .0001, d = 0.72).

Regarding LMM analysis, the continuous full_btw4 model revealed that the low-level confounders that we tested in interaction with Experiment were significant, confirming our assumption that the Experiments differed for the horizontal position of the stimulus (*p* = .0172) and for the vertical position of the stimulus (p

< .0001). Moreover, the confounding predictors tested alone were all significant (p < .0001, see Appendix B, Table B.21). Specifically, participants responded faster as trials went on, responded faster to stimuli appearing in the upper and right positions, using the middle finger and the right hand, and when PRb was higher. We also found a significant temporal dependency in iRTs.

For what concerns the predictors of interest tested in interaction with the Experiment factor, the four-way interaction was not significant (p = .1588), revealing that the interaction between LWb and ISb in modulating the Stroop effect was not different between the two Experiments. The Stroop effect and the effects of proactive and reactive control did not differ between the Experiments (p = .4792, p = .6713 and p = .2110, respectively). By contrast, the effect of PRSb was significantly different between the two Experiments (p = .0002), with a greater effect of PRSb in the Perifoveal Experiment as compared to the Peripheral Experiment. Regarding the predictors of interest not tested in interaction with the Experiment, the results confirmed a significant Stroop effect (CON_0), with a very large effect size (p < .0001, d_r = 3.33, d_S = 1.95) and a dominance of 100%, indicating that all participants responded slower to Incongruent trials. Moreover, LWb significantly modulated the Stroop effect (p < .0001, d_r = 1.15, d_s = 0.71, dominance 86.36%), revealing a significant effect of proactive control. Similar to previous analyses, we did not find a significant ISb modulation of the Stroop effect (p = .5849, d_r = 0.12, d_s = 0.02, dominance 55.68%). Interestingly, the three-way interaction between LWb, ISb and CON_0 was significant (p = .0094, d_r = 0.25, d_s = 0.20, dominance 59.09%), suggesting that LWb and ISb interacted in modulating the Stroop effect. This result was in line with the Perifoveal task results but not with the Peripheral ones, and provided additional evidence for the interaction of proactive and reactive control in the modulation of the Stroop effect. Lastly, the effect of PRSb was again significant (p < .0001), indicating that participants responded faster when PRS was higher (see Appendix B, Table B.21).

As explained in the methods section, we performed the same model but after excluding the interactions between Experiment and the predictors that resulted non-significant in the previous analysis, which essentially consisted in removing the interactions between Experiment and the experimental effects of interest (i.e., the effect of proactive and reactive control, as well as their interaction, in modulating the Stroop effect). This model (continuous full_btw model), is basically identical to the ones performed on the two Experiments separately, but here it was run on the two datasets aggregated together. As such, since the separate within-subjects analyses on the two Experiments revealed contrasting results, this analysis also helped us to resolve the inconsistencies between them, by verifying whether, by removing Experiment, the three-way interaction survived.

This analysis confirmed the results reported above for the continuous full_btw4 model. The conditional R^2 of the model was .72 and 0.95% of the observations was removed as outliers (>3 absolute standardized residuals) to mitigate the stress of the model fit (i.e., to improve the normality of the residuals, see

Appendix B, Figure B.22). The effects of low-level confounders, as well as their interaction with the Experiment factor, remained significant and in the same direction as in the previous analysis (see Table 4.3). Regarding the predictors of interest, the Stroop effect was again significant with a large effect size (p < .0001, d_r = 3.28, d_S = 1.95) and complete dominance. LWb still significantly modulated the Stroop effect (p < .0001, d_r = 1.16, d_s = 0.72, dominance = 87.5%), confirming the effect of proactive control. Similarly to the previous analysis, the ISb modulation of the Stroop effect was not significant (p = .4792, d_r = 0.15, d_s = .02, dominance = 56.82%). Lastly, the three-way interaction between LWb, ISb and CON_0 was again significant (p = .0150, d_r = 0.24, d_s = 0.19, dominance = 55.68%), indicating that LWb and ISb interacted in modulating the Stroop effect, and when they were both high, participants showed larger Stroop effects. Thus, these results confirmed both those from the Perifoveal Experiment and those reported above for the between-Experiments continuous full_btw4 model results.

Table 4.3 – Results of the LMM analysis for the btw-studies analysis (continuous full_btw model)

Effect	b	SE	t	df	p
Intercept	-2.2029	0.0278	-79.225	273.92	< .0001
TrialTOT	-0.0967	0.0020	-48.649	5466.32	< .0001
CON_0	0.3612	0.0105	34.470	311.05	< .0001
iRTpre	0.0568	0.0010	58.150	102923.55	< .0001
hS	-0.0103	0.0023	-4.394	17358.21	< .0001
vS	-0.0330	0.0023	-14.442	20631.10	< .0001
hR	-0.0463	0.0022	-21.001	72402.04	< .0001
vR	-0.0899	0.0022	-41.542	74362.37	< .0001
LWb	-0.0057	0.0087	-0.653	175.99	0.5144
ISb	-0.0083	0.0064	-1.291	656.11	0.1972
PRSb	-0.0356	0.0050	-7.152	91065.10	< .0001
PRb	-0.1335	0.0111	-11.977	92613.89	< .0001
CON_0:LWb	0.0658	0.0069	9.590	177.58	< .0001
CON_0:ISb	0.0063	0.0089	0.708	1198.54	0.4792
LWb:ISb	-0.0214	0.0090	-2.389	175.94	0.0180
CON_0:LWb:ISb	0.0279	0.0113	2.458	174.02	0.0150
Exp	-0.4712	0.0448	-10.523	182.63	< .0001
hS:Exp	-0.0098	0.0041	-2.376	17548.36	0.0175
vS:Exp	0.1047	0.0041	25.703	22145.14	< .0001
PRSb:Exp	-0.0229	0.0053	-4.357	336.10	< .0001

Notes: b, coefficient estimates; SE, standard error, df, degrees of freedom computed with the Satterthwaite's approximation. See the main text for the spelling out of the acronyms for the effects

RCA analysis was then performed to confirm between-Experiments LMM results and this was the case. Indeed, all the predictors of interest were not significantly different in the two Experiments (all *p*s > .14, see Appendix B, Table B.23). Therefore, this analysis confirmed the robustness of the results obtained with RCA.

Confounding predictors were all significant (all *p*s < .04, see Appendix B, Table B.22) and in the same direction as the previous results, except for vS, for which we obtained contrasting results in the two Experiments. Here, we found that participants were faster in responding to stimuli appearing in the upper part of the screen, as for the Peripheral Experiment. In line with previous results, we found a very large Stroop effect (p < .0001, d_r = 2.18, dominance = 98.86%), which was significantly modulated by LWb (p < .0001, d_r = 0.71, dominance = 75%) but not by ISb (p = .8147, d_r = -0.02, dominance = 48.86%). Moreover, LWb and ISb interacted significantly in modulating the Stroop effect (*p* < .0001, d_r = 0.37, dominance = 65.34%), which is consistent with the RCA results from both Experiments. The effect of PRSb was also significant (*p* < .0001, d_r = -0.43) (see Appendix B, Table B.22).

Given that between-Experiments results also showed that PRSb was significant but the CON_0 by ISb interaction was not, we further tested our hypothesis that we did not find it because PRSb explained all the variance that could have been explained by the reactive control modulation of the Stroop effect. For both the LMM and the RCA analyses, the continuous full_btw No_PRS model showed the same pattern of results, both for confounders and predictors of interest, with the only exception that, after removing PRSb from the model, the interaction between CON_0 and ISb became significant (*p*s < .0001) and with large effect sizes (d_r = 0.72 and 0.76, respectively; see Appendix B, Tables B.24-25). Of note, the inclusion of PRSb in the model was justified and improved the model fit ($\chi^2(2) = 138.4$, *p* < .0001).

4.4.2.2. Comparison with the hypothesized models

Lastly, we compared our results to the models we put forward in the Introduction to verify which one better explained the patterns we obtained. We decided to compute such a comparison directly on the data aggregated over the two Experiments, that is, those used in the between-Experiments analysis with the continuous full model. Specifically, we correlated the overall observed pattern of Stroop effects predicted by the LMM analysis (Figure 4.5A) with those predicted by each of our a priori models to identify which had the highest correlation. We found that the observed Stroop effects were correlated the most with the model assuming an antagonistic interaction with a higher effect of proactive compared to reactive control (r = .97) (see Figure 4.5B for all correlations).

4.4.2.3. Internal reliability of LWPC and ISPC effects in the aggregated sample

As expected, the internal reliability estimate of the Stroop effect was the highest among our effects of interest, with a median r_{SB} value of .92 and a $CI_{95\%}$ of .89-93. The internal reliability of proactive control had a median r_{SB} value of .73 and a $CI_{95\%}$ of .64-.82, while the median r_{SB} of reactive control was .75, with a $CI_{95\%}$ of .64-.83. Finally, the internal reliability of the triple interaction was similar, with a median r_{SB} value of .78 and a $CI_{95\%}$ of. .71-.83 (see Figure 4.4).

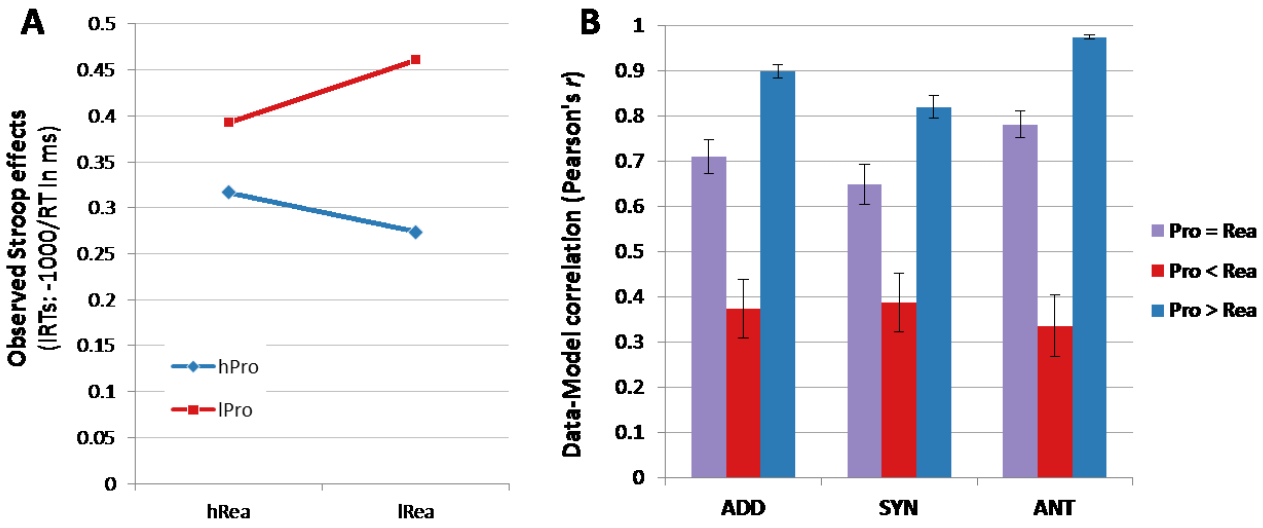

Figure 4.5.
A) The plot shows the observed pattern of Stroop effects, as estimated by the LMM continuous full_btw model, as a function of the level of proactive control (hPro, blue line, corresponding to low-LWb conditions; lPro, blue line, corresponding to high-LWb conditions) and reactive control (hRea, corresponding to low-ISb conditions; lRea, corresponding to high-ISb conditions). **B)** Correlations between the observed pattern of Stroop effects and the hypothesized models (see the Hypotheses section). Error bars represent the standard error of the correlation. ADD, additive effects models; SYN, synergistic effects models; ANT, antagonistic effects models; Pro, Proactive control effect; Rea, Reactive control effect.

4.5. General discussion

According to the Dual-Mechanism of control model (DMC, Braver, 2012; Braver et al., 2007), cognitive control operates via two distinct mechanisms, proactive and reactive control, which are qualitatively different in terms of their temporal dynamics. Although this model could account for the great variability intrinsic to this ability, the evidence currently available for it is not compelling. In the laboratory, the DMC has been frequently assessed with the Stroop task, which allows varying the Proportion of Congruency (PC) at the list-wide (LWPC) and/or at the item-specific (ISPC) levels to specifically target proactive and reactive control, respectively. However, these manipulations have been called into question, especially by the contingency hypothesis, which claims that they elicit low-level processes instead of control-driven ones (Schmidt, 2019; Schmidt et al., 2007; Schmidt & Besner, 2008). Although several confound-minimized manipulations have been proposed to solve this issue, in our view, they still suffer from some limitations and are impractical. Moreover, the two control mechanisms have always been explored separately by implementing each PC manipulation one at a time, which prevents from assessing their specific effects when both are manipulated and, especially, the interplay between the two control mode mechanisms.

Therefore, to date, there is no compelling evidence clearly supporting the existence of two distinct mechanisms, while also controlling for the potential influence of low-level confounders. Our aim here was

indeed to tackle this issue by combining multilevel modeling, the state-of-the-art trial-level analytical approach to estimate the Stroop effect effectively and reliably (see Viviani et al., 2023) and its control-related modulations with a novel methodological approach allowing to manipulate both LWPC and ISPC in a fine-grained way at the trial-by-trial level.

In brief, our main results consistently indicate that proactive control induced by trial-level LWPC manipulations modulated the Stroop effect, whereas ISPC-induced reactive control did not, probably due to the confounding effect of contingency. However, both control modes interacted in modulating the Stroop effect.

4.5.1. Advantages of our methodological and analytical approach

Before elaborating on the findings, it is worthy to discuss the methodological and analytical novelties of the present study, to fully understand their advantages compared to classical approaches primarily implying design-level control only. To make a step further, we used an analysis-level control, leveraging trial-level multilevel modeling to put forward a new approach in which LWPC and ISPC were manipulated simultaneously. This is indeed a more effective way to i) directly explore whether proactive and reactive control can coexist, that is, whether each mechanism can be active while also the other is activated; ii) investigate whether proactive and reactive control interact, since if we assume that they are distinct mechanisms, it is also plausible that they interact as (implicitly) postulated by the DMC. Moreover, to control for contingency-related effects, we did not balance stimulus-response combinations so as to make the contingency orthogonal to LWPC and ISPC as much as possible, and then we controlled for its effect at the statistical level.

Overall, our approach introduces some main novelties, which our data suggested to be advantageous as compared to the traditional approaches used in the literature.

The first original aspect of our approach consisted of calculating the trial-wise probabilities of our variables of interest. These provided more realistic estimates of our variables at each trial, because they were based on the updating of the trial-by-trial probability based on the trial history. Our expectation of a better model fit when using continuous as compared to discrete values was indeed confirmed by the model comparisons that we performed. Notably, these findings offer indirect support for frameworks that started conceptualizing cognitive control in terms of Bayesian inference (Jiang et al., 2014; Parr et al., 2023), suggesting a potential alignment between the observed results and the principles of the predictive brain (Clark, 2013).

The second novel aspect of our study concerns the analytical approach, as we used multilevel modeling, which was particularly suitable for our aims. First, it allowed us to assess all our experimental effects of

interest at the same time, that is, the Stroop effect, proactive control, reactive control and their interaction in modulating the Stroop effect, which was our main aim and was not feasible using classical GLM-based approaches. As detailed in the Methods sections, GLM analyses were used just to assess the overall Stroop effect (and thus allowing its comparison with the existing studies) but they were not suitable for our experimental design and aim. Indeed, the second important advantage of multilevel modeling was that it ensured that the estimates of our effects were partialled out from the effect of lower-level confounders at the trial level, which represent sources of trial-by-trial noise that can affect the estimation of the effects at the subject level. This advantage, in line with the results of our previous study (Viviani et al., 2023), was confirmed by the comparisons of the full model with the reduced one, which showed that, in all our analyses, the former better explained our data. These results suggest that including in the model low-level predictors based on the characteristics of the task at hand ensured that the estimates of our effects of interest were more accurate and precise since intra-subject/inter-trial sources of variance, that contribute to measurement error, were explained. Moreover, using this approach, we successfully cleaned our effects of interest from the effect of contingency which represents a great issue when using PC manipulations as, in our view (see Section 4.1.1), they can hardly be properly controlled at the design level only. Indeed, it should be noted that it is practically impossible to de-confound ISPC and contingency measures for congruent trials, as they are both computed in the same way (i.e., the ratio between the occurrence of congruent trials and the total number of trials for that item within a block). Our results indeed indicate that controlling for the effects of contingency at the analysis level, that is, by including it in the model, represents a valid alternative to controlling for it at the design level. We indeed found that ISPC-related results changed dramatically when contingency was removed from the statistical model as compared to when it was included. This indicates that not controlling for contingency-related effects severely affected the results, leading to misleading conclusions about spurious effects of reactive control.

4.5.2. LWPC and ISPC effects and between-Experiments differences

The Peripheral and the Perifoveal Experiments yielded contrasting results for what concerns the three-way interaction (namely, between the Stroop effect, LWPC and ISPC), with the former not finding any interaction between proactive and reactive control in Stroop effect modulation and the latter showing it instead. To shed light on this discrepancy, a between-Experiments analysis was performed, by running a model that compared the effects of interest as well as the low-level ones that were assumed to be different (i.e., stimulus position and contingency) to assess whether they differed between the two Experiments. Low-level results confirmed our assumption that the two Experiments implied different effects of stimulus position, which was quite predictable as the Perifoveal task had been intentionally designed to reduce visuospatial attention shifts and/or eye movements. Moreover, the difference in contingency might also be explained in terms of different spatial arrangements, as the greater effect of contingency in the Perifoveal

task might have been explained by the lower eccentricity of the stimuli. The keypresses used to provide responses were indeed spatially arranged more similarly to the Perifoveal stimuli, as they also had a low eccentricity. This might have led to a greater stimulus-response overlap in the Perifoveal task[13] which, in turn, might have favored the learning of stronger stimulus-response associations. No Experiment-dependent difference was instead observed for the effects of interest.

Given that between-Experiments results revealed that the two Experiments were not different for what concerns the effects of interest, we aggregated the two samples to assess the results on both Experiments together, as this could tell us more about which pattern of results was more consistent, that is, whether the emerging results on the aggregated samples were more compatible with the Peripheral or the Perifoveal within-subjects results. Importantly, the analysis on the aggregated sample, as compared to the within-subjects ones, was expected to yield more robust evidence by ensuring more power and more precise estimates. Interestingly, the results of the aggregated analysis reflected those obtained in the Perifoveal Experiment, although that was the Experiment with the smaller sample size. Essentially, we found again that proactive control, but not reactive control, modulated the Stroop effect, and that both control modes interacted in modulating the Stroop effect.

Therefore, for what concerns the three-way interaction, these results could seem in contradiction with the between-Experiments results that did not reveal its significance as, after aggregating the two samples, they showed results in line with one Experiment but not with the other. To try to explain this inconsistency, we put forward a possible explanation based on the results of our previous study (Viviani et al., 2023, Chapter 3), wherein we found that the greater visuospatial attention shifts characterizing the Peripheral task led to an underestimation of the Stroop effect magnitude whereas, when they were reduced, such as in the Perifoveal task, the Stroop effect was more robust and larger. As such, these attentional shifts might have reduced the magnitude of the three-way interaction in the Peripheral task, making it not detectable with the within-subjects analysis, probably because the Peripheral Experiment was too underpowered to detect it, but revealing such interaction in the aggregated samples analysis, thanks to the greater power. Of note, the direction of the three-way interaction in the Peripheral task tested alone, despite being not significant, was consistent with the direction of the three-way interaction in the Perifoveal and in the aggregated sample, supporting our hypothesis that the difference among the two Experiments was not qualitative but just quantitative due to the effect of visuospatial attention shifts. This notwithstanding, the difference in the magnitude of the two three-way interactions in the two Experiments was not large enough to be significant and thus could not be detected by the between-Experiments analysis. Therefore, this interpretation would reconcile our apparently contrasting results, supporting both the presence of distinct

[13] According to Kornblum (e.g., 1992), stimulus-response overlap is fundamental to yield a complete Stroop effect (see also Chapter 2), thus the stronger such overlap, the greater the Stroop effect.

patterns, as shown by the within-subjects results, and the absence of evidence for a difference among the Experiments, as found in the between-Experiments results, allowing us to more safely rely on the aggregated sample results to draw our conclusions.

The robustness of the pattern of results provided by the aggregated sample analysis appears to be well substantiated also by the RCA analyses which served us to confirm LMM results. Indeed, the RCA analyses did not show contradictory results and always revealed that the Stroop effect was modulated by proactive control alone and by the interaction between proactive and reactive control. Therefore, this further supported our interpretation that the lack of a significant three-way interaction in the Peripheral Experiment alone using LMM analysis was the consequence of the underestimation of such effect due to the factors discussed above. Still, the fact that this effect emerged only under certain conditions and depending on the analytical approach leads us to suggest taking it with some caution and indicates that further investigations are needed before drawing definitive conclusions about it.

A result that was instead always consistent was the absence of the main effect for the reactive control modulation of the Stroop effect. Indeed, none of our analyses showed a significant interaction between item-specific proportion congruency and the Stroop effect (ISb and CON_0). The absence of such interaction was observed also in one of the control analyses performed on the Peripheral Experiment using the LMM approach, in which we removed from the model the three-way interaction, as it was not significant, to assess whether it interfered with the estimation of reactive control effects. Even after excluding the three-way interaction, the effect of reactive control by itself did not emerge, suggesting that it was not masked by the three-way interaction.

Therefore, to provide a possible explanation for why ISPC-induced reactive control alone never modulated the Stroop effect, we performed control analyses on both single and aggregated samples by excluding from the model the contingency predictor. This was done because there is extensive literature showing that reactive control is specifically confused with contingency when ISPC is manipulated (e.g., Schmidt, 2019; Schmidt & Besner, 2008). Moreover, as explained above, it is very difficult to totally decorrelate contingency and ISPC at the design level while also keeping this manipulation item-specific. As a consequence, we assumed that the effect of ISb and CON_0 interaction might have been non-significant since Contingency (PRSb) included in the model explained all its variance. This was exactly the case: in all the control analyses, the removal of PRSb produced the same pattern of results, except for the interaction between ISb and CON_0, which became significant after this change. Thus, these consistent results confirmed our assumption that PRSb alone can explain all the variance of reactive control modulation and have several implications, as detailed in the following paragraph.

First, ISPC-induced reactive control and contingency are intrinsically related since the manipulation used to induce such a mechanism is inevitably confused with contingency, especially for congruent items. Second, as confound-minimized designs that have been proposed in the literature are, in our view, unpractical and partially flawed (see Section 4.1.1), the more adequate approach to control for contingency is the analysis-level one, as it effectively estimated the contingency-related confounding effect, allowing us to suggest that our estimation of reactive control effects was not biased by contingency. As discussed above, the model comparisons provided further evidence in favor of analysis-level control, which showed that the observed data were better explained when confounding predictors, among which contingency, were included in the statistical model. The third implication regards the fact that, although ISPC-induced reactive control alone was not significant, its interaction with proactive control to modulate the Stroop effect was significant even when contingency was in the model, suggesting that our experimental design was effective at yielding a reactive control effect partialled out from contingency, albeit an indirect one. This claim was further supported by another follow-up control analysis testing a model wherein PRSb and ISb were switched, so that, instead of ISb, PRSb was included in the three-way interaction to assess whether PRSb interacted with LWb in modulating the Stroop effect, that is, to exclude that the PRSb effect was masked by the inclusion of ISb. This, however, did not occur as the three-way interaction did not result significant, providing further evidence for the significant role of ISb in the three-way interaction and also indicating that it was successfully partialed out from the effect of contingency (see Appendix B).

A further result robust to analytical flexibility, and thus consistent across all our analyses, was the Stroop effect modulation by proactive control, which is in line with previous findings (e.g., Bugg & Chanani, 2011; Hutchison, 2011). Indeed, the interaction between LWb and CON_0 was not only always significant in our main LMM and RCA analyses, but it was also accompanied by d values that were greater than .5, which is considered the threshold of medium effect sizes. In the aggregated sample results, proactive control had a medium-to-large effect size (d = .71) and a dominance of almost 87%, indicating that our paradigms were effective in producing a proactive control effect in the expected direction in most of the participants (i.e., larger Stroop effects when LWb was higher).

It has to be noted also that this evidence for a proactive control modulation of the Stroop effect was obtained while controlling for possible confounding factors that might influence it. Indeed, whether LWPC manipulation is effective in inducing a control mechanism operating at the list-level and not just at the item level has been challenged. Essentially, some authors argued that LWPC is inevitably confused with ISPC since low-PC blocks are composed of low-PC items and high-PC blocks are composed of high-PC items (e.g., Blais et al., 2007; Blais & Bunge, 2010; Bugg et al., 2008). This is an inevitable consequence of LWPC manipulation. Indeed, although we tried to orthogonalize LWPC and ISPC as much as possible, our predictors were still correlated. However, by using multilevel modeling and including both predictors in the

model, we were able to control for that confound. Therefore, since the LWPC by Congruency interaction consistently emerged, as opposed to the ISPC by Congruency interaction, which was never significant, we can reasonably claim that the observed variance was explained by the proactive (but not by the reactive) control manipulation. These results further highlighted the advantages of analysis-level control, which can overcome issues that cannot easily be addressed by the design-level control.

The last important result concerns the magnitude of the Stroop effect. Although in this work we were not specifically interested in the Stroop effect per se, it was essential that our paradigms yielded an effect that was robust, and this was the case. The Stroop effect was indeed observed in all our analyses and was characterized by very large effect sizes. Specifically, in the aggregated analysis, it had a d value of 1.95 and all individuals showed a true positive Stroop effect, that is, they all responded more slowly in incongruent compared to congruent trials, as indicated by a dominance of 100%. These results are in line with those from our previous study, in which we found that both the Peripheral and the Perifoveal tasks were effective in producing large Stroop effects. However, the present results did not confirm the larger Stroop effects we found for the Perifoveal as compared to the Peripheral task in our previous study (Viviani et al., 2023, Chapter 3). Indeed, albeit in the same direction, this between-task difference was not significant in the present study.

Overall, this complex pattern of results allows us to start to answer one of our research questions, that is, whether proactive control exists per se also while reactive control is present and vice versa, and whether they interact as well. For the reasons explained above, such a question will be addressed considering the results produced by the aggregated sample analysis because its higher statistical power ensured more precise estimates of the effects of interest, which, inter alia, did not differ among the two Experiments.

Interestingly, our results suggest that proactive control independently operated by modulating the magnitude of the Stroop effect, even when reactive control was manipulated, whereas ISPC-induced reactive control did not affect the Stroop effect by itself, but it only interacted with the proactive control in modulating the Stroop effect. As such, this might indicate that, overall, proactive control is stronger than reactive control, but this claim will be better discussed in the testing of a priori formal model section.

However, care must be taken in interpreting this pattern of results. Indeed, there is no clear evidence against reactive control that exists independently of proactive control because of the limitations of the ISPC manipulation that have been pointed out in the literature and confirmed in our work. Indeed, what clearly stood out from our work, and especially from the comparison between the main results and the control ones, was that the effect of reactive control was masked by that of contingency to such an extent that, when both were included in the statistical model, contingency alone explained all the variance. As already pointed out, this is very likely to be the consequence of the imperfect orthogonalization due to the

inevitable overlap of contingency and ISPC for congruent trials. However, although the correlation between our ISb and PRSb predictors was not that high (17% of shared variance), contingency still preferentially emerged as a significant modulator of participants' performance, suggesting its stronger influence. This claim seems to be in line with previous works showing that the ISPC effect was only incidental and exclusively due to contingency learning (e.g., Schmidt, 2019; Schmidt & Besner, 2008). It is worth noting that the conclusions drawn by the contingency learning account have been quite radical, pointing towards a mere low-level associative learning, rather than conflict-related resolution of the interference in the Stroop task. However, our data do not seem to support such an extreme view either, revealing that a more intermediate and balanced position might better fit the available data.

Essentially, on the one hand, our results are consistent with the contingency learning account for what concerns the inevitable influence of contingency learning on performance. Contingency prevailed especially over ISPC-induced reactive control which, when considered by itself, did not survive the presence of such low-level learning effect. Therefore, we agree on the need to control for contingency learning and that considerable attention must be paid in interpreting reactive control effects. However, our results also revealed that the impact of reactive control still remained significant even after partialling out the effect of contingency, that is, when reactive control interacted with proactive control in modulating the Stroop effect. Therefore, it might be that contingency is stronger than reactive control per se, but this does not necessarily exclude a strategic implementation of control, which can also operate in a reactive way but only when moderated by proactive control levels. Such modulation was, in fact, specifically driven by reactive control as shown by one of our control analyses, as discussed above (also see Appendix B), which allowed us to exclude the role of contingency learning in such a higher-level modulation. More importantly, the pattern of the significant interaction between proactive and reactive control in modulating the Stroop effect offers another alternative explanation for the fact that the reactive control modulation of the Stroop effect did not reach the significance level per se. Indeed, as we discuss in detail below, our results indicate that the effect of reactive control emerges only when the level of proactive control is low. However, in our models the effect of the interaction between congruency and the trial-level ISPC estimate is conditional to an intermediate level of the trial-level LWPC estimate and, consequently, an intermediate level of proactive control, which thus could have been high enough to prevent the need for reactive control.

Hence, our work contributed to provide consistent evidence for the specificity of the proactive control mechanism, by showing that it operates independently from the concurrent activation of reactive control and/or contingency learning. Moreover, we have provided initial evidence that cognitive control can also operate through a reactive control mechanism. The latter, however, emerges only in interaction with proactive control as, when assessed by itself, it can be explained mainly by contingency. This pattern thus

suggests that proactive control is mainly engaged to solve Stroop interference, with a greater impact on participants' performance, as compared to ISPC-induced reactive control.

4.5.3. Testing of a-priori formal models

The pattern of results discussed above suggested that, although proactive and reactive control interacted, the former had a stronger effect than the latter, as it also operated by itself. At first glance, this claim matches one alternative of our a priori hypotheses, that is, the one predicting a dominant role of proactive over reactive control. However, we tested all of our hypotheses to verify whether our data actually correlated the most with that alternative or whether another model better fitted the pattern of results we found.

The model that was more highly correlated to our data, and thus that best explained the obtained pattern of results, was the one predicting the dominance of proactive over reactive control and an antagonistic interaction between them. This result thus confirmed the asymmetrical pattern we observed in our results. Moreover, it further supported our claim that proactive control had a stronger effect than reactive control. This is in line with the fact that, in all our analyses, reactive control did not survive by itself and thus it would have been odd if our data were better explained by the model implying an equal strength of proactive and reactive control or, even more, by the model predicting the dominance of reactive control.

What is even more noteworthy here, as it emerged less straightforwardly from our results, was the direction of the three-way interaction. The fact that the best model was the one predicting an antagonistic interaction provides a better insight into how proactive and reactive control interacted to modulate the Stroop effect. This suggests that proactive and reactive control interacted in an antagonistic manner and, when both were high, they yielded a Stroop effect reduction that was smaller than that predicted by their additive effects. This means that one of the two mechanisms produced a mitigation of the strength of the effect of the other. As the stronger control mode was the proactive one, it can be assumed that it exerted such moderator effect on reactive control, probably because this latter mechanism was not useful or effective; in other words, the possibility of relying on the trial-level LWPC estimates to exert proactive control, the stronger and more effective mode, made the implementation of reactive control unnecessary. Figure 4.5A clearly displays this, as can be seen from the pattern of observed results, when proactive control was high (blue line, hPro-hRea and hPro-lRea conditions), the Stroop effect did not decrease (and was even numerically larger) when both control strategies were available (hPro-hRea) as compared to when just proactive control strategies were implemented (hPro-lRea). By contrast, when proactive control was low (red line, lPro-hRea and lPro-lRea conditions), the Stroop effect was lower when reactive control was implemented (lPro-hRea), even if still higher than that observed under proactive control, as compared to when no control mode was available (lPro-lRea).

Importantly, the observed pattern of the interaction between proactive and reactive control in modulating the Stroop effects is well in line with the DMC proposal (De Pisapia & Braver, 2006), which assumes that reactive control preferentially operates when proactive control is not possible or advantageous. However, to the best of our knowledge, this interplay between proactive and reactive control has never been tested directly, by actually manipulating the corresponding experimental variables, like LWPC and ISPC, respectively. Indeed, DMC-inspired studies investigating or interpreting the behavioral and neurophysiological correlates of proactive and reactive control usually only varied LWPC (or LWPC-like) experimental variables and then assumed that reactive control operated for lower levels of proactive control. Our results thus represent a substantial contribution to the field by showing, for the first time, the actual fine-grained pattern of the proactive-reactive control interplay in modulating Stroop performance. More importantly, our results also raise severe concerns about the assumptions made by the existing studies mentioned above, namely, that when there is no or low proactive control, then reactive control must necessarily be active. Indeed, our results clearly showed that, when LWb was high (and thus proactive control was low), the Stroop effect decreased only when ISb was low (and thus reactive control was high), whereas it was very large when ISb was also high (and thus reactive control was low). In other words, high levels of LWPC would be a necessary but not sufficient condition for the activation of reactive control, as it can actually be implemented only when there are low levels of ISPC. It is important here to note that this argument is valid only for the "faster" or "associative" form of reactive control, that is, the one signaled by ISPC (or other forms of stimulus-related information) that, in turn, activates a sort of stimulus-attention association to apply attentional biases to stimulus-related processing in a reactive way (Tafuro et al., 2020; Bugg, 2017; Bugg & Crump, 2012).

Overall, the model testing confirmed in a more straightforward way what we obtained from our analyses. Therefore, it did not add more information to the result parameters we present in Table 4.3. However, we believe that it could add two main strengths to the present work: i) the graphical representation displaying the model better showing the results provides a clearer and more easily interpretable overview of the pattern of results; ii) it encourages comparability with other works testing both similar and distinct hypotheses.

4.5.4. Internal reliability

The internal reliability of our effects of interest was overall quite high for all of our analyses. In the results from the aggregated sample, the internal reliability of the effects was always higher than .73. The Stroop effect showed the highest internal reliability with an r_{SB} value of .92, and this value was even higher than those obtained in our previous study (Viviani et al., 2023), probably due to the higher number of trials used in the present study. Indeed, we previously found that the Peripheral task had an internal reliability of

.80, whereas here it reached an r_{SB} value of .92, and the Perifoveal task had an internal reliability of .80, whereas here it reached an r_{SB} value of .94. Moreover, all of these values had low variability across randomizations.

The internal reliability of the proactive control effect was slightly lower, but still remained quite high (r_{SB} value of .73 in the aggregated sample) and was similar not only to that of the reactive control effect (r_{SB} value of .75 in the aggregated sample), but also to that of the three-way interaction (r_{SB} value of .78). This latter result is surprising, since the reliability of differential effects is generally lower.

Overall, these results confirmed our previous findings (Viviani et al., 2023), as they are still at odds with the reliability paradox (Hedge et al., 2018) and related proposals (Rouder & Haaf, 2019) according to which, if an experimental effect is large and universal, its internal reliability can hardly be large enough. As such, this further supports our choice of using multilevel modeling which, by allowing explaining intra-subject/inter-trial variance, has been shown to effectively provide more precise estimates of the effects of interest.

4.6. Conclusions

In two behavioral Experiments, we aimed to investigate the dual-mechanisms of control model (DMC) and its application to the Stroop task by developing a novel methodological approach and combining it with the state-of-the-art trial-level multilevel modeling that ensures accurate and reliable estimates of the Stroop effect. This approach allowed us not only to manipulate LWPC and ISPC simultaneously, but also in a fine-grained way at the trial level, which is crucial for understanding the coexistence and interaction of proactive and reactive control, while also controlling for the confounding effects of low-level processes, including contingency.

Our results provided consistent evidence for the existence of LWPC-dependent proactive control mechanisms modulating Stroop performance regardless of confounders and also ISPC-dependent reactive control levels. Moreover, albeit we did not find evidence for the existence of specific ISPC-dependent reactive control effects, they still interacted with proactive control in modulating Stroop performance, with the characteristic pattern assumed by the DMC.

Although further research is needed to validate these findings and understand the nature of the three-way interaction between congruency and proactive and reactive control, thanks to our novel approach, our study provided new insights into the DMC model and the cognitive mechanisms underpinning the modulation of the Stroop effect. These insights specifically concern three points; first, our results reveal that using trial-level estimates of the PC provides a better account of adaptive control employment, thus

encouraging future studies to do the same to reach a more realistic understanding of adaptive control modulations. Second, thanks to the simultaneous and fine-grained manipulation of LWPC and ISPC, we provided evidence for the interplay between proactive and reactive control in modulating the Stroop effect, which set the bases for further studies that deepen the understanding of the two control modes postulated by the DMC. Third, thanks to our analysis-level control approach used to control for (and estimate) the effect of contingency, we unveiled the interplay between ISPC-induced reactive control and contingency, shedding light on the related still unresolved diatribe between pure associative learning and adaptive control accounts of the Stroop performance, promoting a more moderate view. Overall, our results valuably contribute to the ongoing research on cognitive control mechanisms and their implications for understanding human cognition.

4.7. References

Baayen, R. H., Davidson, D. J., & Bates, D. M. (2008). Mixed-effects modeling with crossed random effects for subjects and items. Journal of memory and language, 59(4).

Baayen, R., & Milin, P. (2010). Analyzing reaction times. International Journal of Psychological Research, 3(2). https://doi.org/10.21500/20112084.807

Blais, C., & Bunge, S. (2010). Behavioral and neural evidence for item-specific performance monitoring. Journal of Cognitive Neuroscience, 22(12).

Blais, C., Robidoux, S., Risko, E. F., & Besner, D. (2007). Item-Specific Adaptation and the Conflict-Monitoring Hypothesis: A Computational Model. Psychological Review, 114(4), 1076–1086. https://doi.org/10.1037/0033-295X.114.4.1076

Botvinick, M. M., Braver, T. S., Barch, D. M., Carter, C. S., & Cohen, J. D. (2001). Conflict monitoring and cognitive control. Psychological Review, 108(3), 624–652. https://doi.org/10.1037/0033-295x.108.3.624

Braem, S., Bugg, J. M., Schmidt, J. R., Crump, M. J., Weissman, D. H., Notebaert, W., & Egner, T. (2019). Measuring adaptive control in conflict tasks. Trends in cognitive sciences. https://doi.org/10.1016/j.tics.2019.07.002

Braver, T. S. (2012). The variable nature of cognitive control: A dual mechanisms framework. Trends in cognitive sciences, 16(2). https://doi.org/10.1016/j.tics.2011.12.010

Braver, T. S., Gray, J. R., & Burgess, G. C. (2007). Explaining the many varieties of working memory variation: Dual mechanisms of cognitive control. Variation in working memory, 75, 106.

Braver, T. S., Satpute, A. B., Rush, B. K., Racine, C. A., & Barch, D. M. (2005). Context Processing and Context Maintenance in Healthy Aging and Early Stage Dementia of the Alzheimer's Type. Psychology and Aging, 20(1), 33–46. https://doi.org/10.1037/0882-7974.20.1.33

Braver, T. S., Kizhner, A., Tang, R., Freund, M. C., & Etzel, J. A. (2021). The Dual Mechanisms of Cognitive Control Project. Journal of Cognitive Neuroscience, 33(9), 1990–2015. https://doi.org/10.1162/jocn_a_01768

Braver, T. S., Paxton, J. L., Locke, H. S., & Barch, D. M. (2009). Flexible neural mechanisms of cognitive control within human prefrontal cortex. Proceedings of the National Academy of Sciences, 106(18). 7351–7356. https://doi.org/10.1073/pnas.0808187106

Bugg, J. M. (2012). Dissociating Levels of Cognitive Control: The Case of Stroop Interference. Current Directions in Psychological Science, 21(5), 302–309. https://doi.org/10.1177/0963721412453586

Bugg, J. M. (2014). Conflict-triggered top-down control: Default mode, last resort, or no such thing? Journal of Experimental Psychology: Learning, Memory, and Cognition, 40, 567–587. https://doi.org/10.1037/a0035032

Bugg, J. M. (2017). Context, conflict, and control. The Wiley handbook of cognitive control, 79–96.

Bugg, J. M., & Chanani, S. (2011). List-wide control is not entirely elusive: Evidence from picture–word Stroop. Psychonomic Bulletin & Review, 18(5), 930–936. https://doi.org/10.3758/s13423-011-0112-y

Bugg, J. M., & Crump, M. J. (2012). In support of a distinction between voluntary and stimulus-driven control: A review of the literature on proportion congruent effects. Frontiers in psychology, 3, 367. https://doi.org/10.3389/fpsyg.2012.00367

Bugg, J. M., & Hutchison, K. A. (2013). Converging evidence for control of color–word Stroop interference at the item level. Journal of Experimental Psychology: Human Perception and Performance, 39(2).

Bugg, J. M., Jacoby, L. L., & Chanani, S. (2011). Why it is too early to lose control in accounts of item-specific proportion congruency effects. Journal of Experimental Psychology: Human Perception and Performance, 37(3). doi: 10.1037/a0019957

Bugg, J. M., Jacoby, L. L., & Toth, J. P. (2008). Multiple levels of control in the Stroop task. Memory & cognition, 36(8).

Chiew, K. S., & Braver, T. S. (2017). Context processing and cognitive control: From gating models to dual mechanisms. In The Wiley handbook of cognitive control (pp. 143–166). Wiley Blackwell. https://doi.org/10.1002/9781118920497.ch9

Clark, A. (2013). Whatever next? Predictive brains, situated agents, and the future of cognitive science. The Behavioral and Brain Sciences, 36(3). https://doi.org/10.1017/S0140525X12000477

Cohen, J. D. (2017). Cognitive control: Core constructs and current considerations. In The Wiley handbook of cognitive control (pp. 3–28). Wiley Blackwell. https://doi.org/10.1002/9781118920497.ch1

De Pisapia, N., & Braver, T. S. (2006). A model of dual control mechanisms through anterior cingulate and prefrontal cortex interactions. Neurocomputing, 69(10–12). https://doi.org/10.1016/j.neucom.2005.12.100

Diamond, A. (2013). Executive Functions. Annual Review of Psychology, 64(1), 135–168. https://doi.org/10.1146/annurev-psych-113011-143750

Duncan, J. (2010). The multiple-demand (MD) system of the primate brain: Mental programs for intelligent behaviour. Trends in Cognitive Sciences, 14(4).

Gonthier, C., Braver, T. S., & Bugg, J. M. (2016). Dissociating proactive and reactive control in the Stroop task. Memory & Cognition, 44(5).

Gratton, G., Cooper, P., Fabiani, M., Carter, C. S., & Karayanidis, F. (2018). Dynamics of cognitive control: Theoretical bases, paradigms, and a view for the future. Psychophysiology, 55(3). https://doi.org/10.1111/psyp.13016

Hedge, C., Powell, G., & Sumner, P. (2018). The reliability paradox: Why robust cognitive tasks do not produce reliable individual differences. Behavior Research Methods, 50(3). https://doi.org/10.3758/s13428-017-0935-1

Hutchison, K. A. (2011). The interactive effects of listwide control, item-based control, and working memory capacity on Stroop performance. Journal of Experimental Psychology: Learning, Memory, and Cognition, 37(4).

Jacoby, L. L., Lindsay, D. S., & Hessels, S. (2003). Item-specific control of automatic processes: Stroop process dissociations. Psychonomic Bulletin & Review, 10(3).

Jiang, J., Heller, K., & Egner, T. (2014). Bayesian modeling of flexible cognitive control. Neuroscience & Biobehavioral Reviews, 46, 30–43. https://doi.org/10.1016/j.neubiorev.2014.06.001

Kornblum, S. (1992). Dimensional overlap and dimensional relevance in stimulus–response and stimulus–stimulus compatibility. In G. E. Stelmach & J. Requin (Eds.), Tutorials in motor behavior, 2 (pp. 743–777).

Lindsay, D. S., & Jacoby, L. L. (1994). Stroop process dissociations: The relationship between facilitation and interference. Journal of Experimental Psychology: Human Perception and Performance, 20(2). https://doi.org/10.1037/0096-1523.20.2.219

Logan, G. D., & Zbrodoff, N. J. (1979). When it helps to be misled: Facilitative effects of increasing the frequency of conflicting stimuli in a Stroop-like task. Memory & cognition, 7(3). https://doi.org/10.3758/BF03197535

Lorch, R. F., & Myers, J. L. (1990). Regression analyses of repeated measures data in cognitive research. Journal of Experimental Psychology: Learning, Memory, and Cognition, 16(1). https://doi.org/10.1037/0278-7393.16.1.149

MacLeod, C. M. (1991). Half a century of research on the Stroop effect: An integrative review. Psychological bulletin, 109(2). https://doi.org/10.1037/0033-2909.109.2.163

Mathys, C., Daunizeau, J., Friston, K. J., & Stephan, K. E. (2011). A bayesian foundation for individual learning under uncertainty. Frontiers in Human Neuroscience, 5, 39. https://doi.org/10.3389/fnhum.2011.00039

Miller, E. K., & Cohen, J. D. (2001). An integrative theory of prefrontal cortex function. Annual review of neuroscience, 24(1). 10.1146/annurev.neuro.24.1.167

Nee, D. E., Wager, T. D., & Jonides, J. (2007). Interference resolution: Insights from a meta-analysis of neuroimaging tasks. Cognitive, Affective, & Behavioral Neuroscience, 7(1). https://doi.org/10.3758/CABN.7.1.1

Parr, T., Holmes, E., Friston, K. J., & Pezzulo, G. (2023). Cognitive effort and active inference. Neuropsychologia, 184, 108562. https://doi.org/10.1016/j.neuropsychologia.2023.108562

Rouder, J. N., & Haaf, J. M. (2019). A psychometrics of individual differences in experimental tasks. Psychonomic Bulletin & Review, 26(2). https://doi.org/10.3758/s13423-018-1558-y

Schmidt, J. R. (2013). Questioning conflict adaptation: Proportion congruent and Gratton effects reconsidered. Psychonomic Bulletin & Review, 20(4), 615–630. https://doi.org/10.3758/s13423-012-0373-0

Schmidt, J. R. (2019). Evidence against conflict monitoring and adaptation: An updated review. Psychonomic bulletin & review, 26(3). 10.3758/s13423-018-1520-z

Schmidt, J. R., & Besner, D. (2008). The Stroop effect: Why proportion congruent has nothing to do with congruency and everything to do with contingency. Journal of Experimental Psychology: Learning, Memory, and Cognition, 34(3). https://doi.org/10.1037/0278-7393.34.3.514

Schmidt, J. R., Crump, M. J. C., Cheesman, J., & Besner, D. (2007). Contingency learning without awareness: Evidence for implicit control. Consciousness and Cognition, 16(2), 421–435. https://doi.org/10.1016/j.concog.2006.06.010

Spinelli, G., & Lupker, S. J. (2020). Item-specific control of attention in the Stroop task: Contingency learning is not the whole story in the item-specific proportion-congruent effect. Memory & Cognition, 48, 426–435.

Spinelli, G., Perry, J. R., & Lupker, S. J. (2019). Adaptation to conflict frequency without contingency and temporal learning: Evidence from the picture–word interference task. Journal of Experimental Psychology: Human Perception and Performance, 45, 995–1014. https://doi.org/10.1037/xhp0000656

Stoet, G. (2010). PsyToolkit: A software package for programming psychological experiments using Linux. Behavior Research Methods, 42(4). https://doi.org/10.3758/BRM.42.4.1096

Stoet, G. (2017). PsyToolkit: A Novel Web-Based Method for Running Online Questionnaires and Reaction-Time Experiments. Teaching of Psychology, 44(1). https://doi.org/10.1177/0098628316677643

Stroop, J. R. (1935). Studies of interference in serial verbal reactions. Journal of experimental psychology, 18(6), Articolo 6, 643–662. https://doi.org/10.1037/h0054651

Tafuro, A., Ambrosini, E., Puccioni, O., & Vallesi, A. (2019). Brain oscillations in cognitive control: A cross-sectional study with a spatial Stroop task. Neuropsychologia, 133, 107190. https://doi.org/10.1016/j.neuropsychologia.2019.107190

Tafuro, A., Vallesi, A., & Ambrosini, E. (2020). Cognitive brakes in interference resolution: A mouse-tracking and EEG co-registration study. Cortex, 133, 188–200. https://doi.org/10.1016/j.cortex.2020.09.024

Thomas, D. R., & Zumbo, B. D. (2012). Difference Scores From the Point of View of Reliability and Repeated-Measures ANOVA: In Defense of Difference Scores for Data Analysis. Educational and Psychological Measurement, 72(1), 37–43. https://doi.org/10.1177/0013164411409929

van Casteren, M., & Davis, M. H. (2006). Mix, a program for pseudorandomization. Behavior Research Methods, 38(4), 584–589. https://doi.org/10.3758/BF03193889

Viviani, G., Visalli, A., Finos, L., Vallesi, A., & Ambrosini, E. (2023). A comparison between different variants of the spatial Stroop task: The influence of analytic flexibility on Stroop effect estimates and reliability. Behavior Research Methods. https://doi.org/10.3758/s13428-023-02091-8

CHAPTER 5

Following the waves:
A Univariate Exploration of Control Processes

5.1. Introduction

In the previous Chapter, we highlighted that whether proactive and reactive control are distinguishable at the behavioral level is still far from being clear, providing some initial evidence for that. However, this matter is even more unresolved at the electrophysiological level. Indeed, how cognitive control functions in our brain has been investigated extensively over the past decades but, this effort notwithstanding, many questions regarding its underlying neural mechanisms remain unanswered.

Just as in behavioral studies, researchers have sought to uncover the electrophysiological signatures of cognitive control and interference resolution by examining performance on the Stroop task alongside electrophysiological measures. Event-Related Potentials (ERPs) have been extensively used to study control processes and the N2, N450, and LP components have been commonly reported (for reviews see for example Heidlmayr et al., 2020; Larson et al., 2014). These ERP components have been generally interpreted based on the conflict monitoring account (Botvinick et al., 2001). For example, the unified model by Heidlmayr and colleagues (2020) proposes the following time course in the Stroop ERP correlates: a fronto-central N2 component reflecting conflict monitoring generated by the anterior cingulate cortex (ACC), a centro-posterior N450 reflecting interference suppression generated by ACC and prefrontal cortex (PFC), and a late positive component (LPC) reflecting conflict resolution. It should be noted that the centro-posterior N450, consisting in a less prominent P3-like positivity for incongruent stimuli (and thus a negative deflection in the incongruent - congruent difference wave), has been labeled inconsistently in the literature (e.g., P3 by West, 2000, Ninc by Appelbaum, and MPN by West 2000; see also Di Russo & Bianco, 2023); here we will use the label P3-like.

More recently, there has been a growing interest in exploring oscillatory signals, which subserve important functions in the brain. As such, investigating process-dependent changes of spectral power across different frequency bands through event-related spectral perturbations (ERSPs) can provide additional information, as compared to ERPs, and thus valuable insights into cognitive control processes (Engel & Fries, 2010; Heidlmayr et al., 2020). The frequency bands most commonly associated with cognitive control are theta (4-7 Hz), alpha (8-12 Hz), and beta (13-30 Hz). Such frequency band functional meaning has been

interpreted based on existing theoretical frameworks, but in a less direct manner as compared to the above-described ERPs. For example, it has been proposed that theta frequency signals the need of cognitive control during conflicting situations, especially over mid-frontal scalp regions (e.g., Cavanagh & Frank, 2014; Hanslmayr et al., 2008; Mückschel et al., 2016), alpha frequency is a marker of inhibition involved in the suppression of the processing of irrelevant items (e.g., Gutteling et al., 2022; Jensen & Mazaheri, 2010), and beta frequency is implied in the maintenance of the cognitive set favoring endogenous top-down biases and in the modulation of response conflict (Engel & Fries, 2010; Wang et al., 2014).

All these ERP and ERSP signatures emerged quite consistently across studies (although not always in the same direction or with the same characteristics), but the functional meanings attributed to them highly depend on the adopted theoretical framework, and the landscape of cognitive control theories is heterogeneous. As we already mentioned in Chapter 1 (see Section 1.1), we chose to adopt the Dual-Mechanisms of control model (DMC) proposed by Braver and colleagues (Braver, 2012; Braver et al., 2007) instead of the conflict monitoring model (Botvinick et al., 2001). This was based on the fact that, the DMC, by expanding the single mechanism postulated by the conflict monitoring model, accounts for different time scales of control effects and, thus, allows explaining commonly observed forms of cognitive control adjustments (i.e., conflict adaptation (CA) and proportion congruency (PC) effects). The DMC proposal of the existence of two qualitatively and temporally distinct control mechanisms, proactive and reactive modes, is supported by available evidence showing the need for multiple control mechanisms to account for commonly observed effects (Torres-Quesada et al., 2013).

In the present study, we will thus adopt the DMC as our theoretical framework to investigate cognitive control more comprehensively, considering the different temporal dynamics of the two control mechanisms, with a particular emphasis on proactive control, which has been less investigated. Besides being a clear framework, the DMC has the advantage to have inspired extensive literature that has used specific manipulations to distinguish between the two control modes by targeting the PC at the list-wide (LWPC) and item-specific (ISPC) levels, especially when using the Stroop task (Bugg, 2012; Bugg & Crump, 2012). Please refer to Chapter 4 for a detailed description of the LWPC and ISPC manipulations.

As is evident from the overview of the electrophysiological evidence presented above, the electrophysiological correlates of cognitive control have been less frequently studied from the DMC perspective. Only a few studies have indeed tried to dissociate proactive and reactive control signatures. For what concerns ERPs measured during the Stroop task, to date, findings are not conclusive. For example, Tillman and Wiens (2011) found greater N450 amplitude in incongruent compared to congruent trials when LWPC was high, as compared to low-LWPC blocks, interpreting this component as a marker of greater interference. In contrast, West and Bailey (2012) revealed greater N450 (also called medial frontal negativity, MFN) amplitude in incongruent trials in low LWPC blocks, interpreting this ERP component as the

correlate of proactive control. Moreover, by finding greater medial posterior negativity (MPN) amplitude in high LWPC blocks, they proposed that this component was a marker of reactive control[14]. In another study, Appelbaum and colleagues (2014) found that the frontocentral negative-polarity incongruency wave (Ninc) was sensitive to the overall level of conflict, whereas the late positive component (LPC) was increased in high LWPC blocks, thus when proactive control was reduced. Regarding ERSPs, findings are even more scarce, and to the best of our knowledge, still no study has investigated the spectral dynamics of proactive and reactive control using the Stroop task in the DMC framework. In contrast, using the AX-Continuous Performance Task, Eisma and colleagues (2021) found that reactive control was associated with higher theta power than proactive control.

Overall, to date it is difficult to draw firm conclusions about ERP and ERSP correlates of proactive and reactive control due to the heterogeneity among the experimental paradigms and the manipulations used. Indeed, EEG studies investigating control from a DMC perspective have rarely employed the PC manipulations, especially those for reactive control (i.e., ISPC). Although the validity of such PC manipulations in tapping control-related mechanisms have been called into questions (i.e., by the contingency hypothesis, for a review see Schmidt, 2019; see also Chapter 4), there is evidence that the PC approach has the potential to answer quantitative questions about control-based adjustments (e.g., Braem et al., 2019; Bugg & Crump, 2012). Therefore, taking advantage of shared manipulations and experimental rigor should be the first step towards the understanding of the electrophysiological processes underlying proactive and reactive control. Moreover, no compelling evidence exists either for whether the two control mechanisms are independent and separable at the electrophysiological level, as postulated by the DMC. Indeed, to date such dissociation has been explored mainly using the fMRI technique, which has provided evidence for anatomical and functional distinctions (e.g., Braver, 2012 see also Braver et al., 2021). However, given that the main DMC fundamental tenet is that the two mechanisms have distinct temporal dynamics, the higher temporal resolution of the EEG technique might provide even more valuable insights by directly testing the DMC explicit predictions regarding such temporal dynamics. Indeed, EEG technique has the potential to provide a more fine-grained distinction between sustained proactive processes and transient reactive ones.

Here, we capitalize on our previous behavioral study, wherein we directly addressed this issue by putting forward a new approach to simultaneously manipulate LWPC and ISPC, while controlling for the effect of contingency (see Chapter 4). As such, the aim of the present study is to investigate the ERP and ERSP correlates of proactive and reactive control, assessing whether they are distinguishable at the neural level.

[14] This interpretation is consistent with the DMC and is based on the assumption that when proactive control is low, reactive control is high. Indeed, according to De Pisapia and Braver (2006), when LWPC is high, cognitive control is likely to be engaged reactively.

Since, to do so, both control mechanisms need to be activated at the same time (Jiang et al., 2014), we will measure participants' EEG activity while both LWPC and ISPC are manipulated using a spatial Stroop task. Indeed, if we assume that proactive and reactive control co-exist, each mechanism should modulate Stroop performance also while the other is activated. We will thus verify this assumption by simultaneously testing both the interaction between LWPC and the Stroop effect, reflecting proactive control, and the interaction between ISPC and the Stroop effect, reflecting reactive control. Manipulating both LWPC and ISPC will also allow us to explore for the first time the interplay between proactive and reactive control in modulating Stroop effect neural markers (i.e., by testing the three-way interaction between Stroop effect, LWPC and ISPC). Moreover, we will allow contingency to vary to accurately estimate its impact on Stroop performance and ER(S)P correlates and to partial out its effect in the statistical analyses (i.e., to measure LWPC and ISPC effects regardless of contingency).

Our study was aimed to assess the effects of the simultaneous LWPC and ISPC manipulations which, to the best of our knowledge, has never been done before within the same experimental paradigm. Another additional aim was to explore how the PC manipulation at each level modulates cognitive control adjustments on a trial-by-trial basis. This is motivated by the assumption that, since participants are not informed about the block-level probabilistic structure of the task (which is the basis for the computation of LWPC and ISPC in all existing studies), they cannot be aware of it. It is instead more likely that they implicitly and progressively infer it from the trial-by-trial variations of the PC. As such, at each given trial, participants would implement a specific level of control because they estimate the PC at the current trial based on the history of previous trials. This scenario is more plausible than assuming that participants exert the same level of control for every trial within a block regardless of the local temporal variations of PC, as assumed by all existing studies using traditional block-wise approaches, which therefore do not account for the flexible adjustments of cognitive control. Indeed, the classical LWPC manipulation relies on the implausible assumption that all the trials within each block have the same PC value and that, at each block transition, the PC is immediately updated. Similarly, traditional ISPC estimates neglect that participants first need to experience each item for a while to attribute to each of them an ISPC value, thus unrealistically assuming that the items at the beginning of the experiment have already been associated to a PC value, without previously encountering them.

To account for trial-by-trial variations, we will leverage a fine-grained manipulation of LWPC and ISPC, which will be estimated trial-by-trial using an ideal Bayesian observer. Trial-by-trial estimates (which we will call continuous variables) will be used as predictors in our analyses, as they are more realistic than those computed using the block-level occurrences (which we will call discrete variables). Note that we will compute trial-level estimates also for confounding variables of interest, such as contingency. A further advantage of using these continuous variables is that it allows us to better orthogonalize LWPC, ISPC, and

contingency predictors. Indeed, our discrete LWPC and ISPC predictors inevitably shared a large portion of variance with each other (≈46%) and shared, respectively, ≈7% and ≈13% of variance with contingency; by contrast, the portion of variance shared between our continuous LWPC and ISPC predictors dropped dramatically (≈3%), as did that shared between them and contingency (≈2% and ≈5%, respectively).

As mentioned above, we will use a spatial Stroop paradigm requiring four-choice keypress responses to indicate the direction of a target arrow appearing in a congruent or incongruent spatial position. The spatial Stroop version is preferable over the original color-word verbal one, as it ensures a complete Stroop effect including conflict at the task, stimulus and response levels even while using manual responses, which are less problematic (i.e., easier to record and less prone to artifactual movements) than vocal ones, especially for neuroimaging studies (Viviani et al., 2023). Specifically, we will adopt the perifoveal version of it, which we have shown to produce a Stroop effect that is large, robust to analytical flexibility, with a high internal reliability and, for the spatial arrangement of the stimuli, is assumed to produce fewer physiological artifacts (i.e., ocular movements) during EEG recordings (Viviani et al., 2023).

5.2. Methods

5.2.1. Experimental task and stimuli

We administered a perifoveal spatial Stroop task as the one used in Chapter 4. The task was implemented in Psychtoolbox and also response times (RTs) and accuracy were recorded. Participants were seated at about 57 cm from the monitor. Stimuli were presented in full-screen mode on a 19-inch monitor, with a resolution of 1920 x 1080 pixels, and they appeared on a gray background (RGB: 128, 128, 128). Participants were instructed to pay attention to the task-relevant information, which was the pointing direction of the arrow, and were required to indicate it regardless of the task-irrelevant information, which was the position where it appeared. Each trial started with a fixation stimulus presented at the center of the screen for 1700 ms, consisting in a vertically oriented thin black cross (39 x 39 pixels) enclosed in the partial outline of a black square (117 x 117 pixels), and participants were instructed to fixate it. The partial outline of the fixation stimulus created the impression of four small squares, each of which denoted a position, which could be upper-left, upper-right, lower-right or lower-left. Then, the experimental stimulus appeared and remained on the screen until participants responded or up to a response time-out of 1500 ms. The experimental stimulus was a small black arrow, presented within one of the four apparent small squares/positions and it could indicate one of four possible directions, which were upper-left, upper-right, lower-right or lower-left. To respond, they pressed one of four possible keys on a computer keyboard (E, O, K and D) using the left middle, right middle, right index and left index fingers. The keys were spatially arranged to be compatible with the four possible arrow directions (and also with the four possible

positions). The task-relevant arrows could either match or not the task-irrelevant position, yielding congruent and incongruent trials, respectively. We used 12 out of the 16 possible combinations of arrow directions and positions, since we excluded the four incongruent arrows pointing to the opposite direction as they pointed to the response and thus were less incongruent than the other incongruent off-diagonal stimuli (e.g., the arrow appearing in the upper-left position and pointing towards the lower-right direction).

List-wide (LWPC) and item-specific (ISPC) proportions of congruency were simultaneously manipulated to measure proactive and reactive control, respectively. Moreover, since we were interested in measuring the trial-by-trial PC variations, we varied both LWPC and ISPC as much as possible. To this aim, we designed a trial list composed of 17 small blocks, including 40 experimental trials each. The blocks could have three different LWPC values: 30% of incongruent trials (LW30), 50% of incongruent trials (LW50) and 70% of incongruent trials (LW70). The blocks with different LWPC values were intermixed in order not to have two consequent blocks with the same LWPC and to counterbalance all the possible LWPC transitions. Then, distinct ISPC levels were nested within each LWPC block, so as to have a minimum of 2 different ISPC values within each block. In the LW70 blocks, the ISPC could be 40% or 80%, in the LW50 blocks, the ISPC could be 20%, 40%, 50%, 60% or 80%, and in the LW30 blocks ISPC could be 20% or 60%. Moreover, within each block, the occurrence of each position-direction combination was intentionally varied with the aim of orthogonalizing as much as possible contingency to LWPC and ISPC, so that the effect of these three variables could be disambiguated in the statistical analysis. To do so, we slightly varied within each block the probability of each of the four directions (and thus the response; from 15% to 37.5%), while keeping the probability of each of the four positions constant. We thus obtained that the majority of the trials had distinct levels of LWPC, ISPC and Contingency, with this latter ranging from 10% to 80%, in steps of 10%. In addition to the 680 experimental trials, we added 16 training trials at the beginning of the task, with LWPC and ISPC both at 50%. Thirty-second breaks were placed every 90 trials and they did not correspond to the transitions between experimental blocks (which were not signaled to participants). The order of blocks was decided a priori, as described above and, within each block, the order of presentation of the trials was pseudorandomized using the software Mix (van Casteren & Davis, 2006) to avoid more than four consecutive repetitions of the same congruency and both total and partial repetitions of stimulus characteristics and/or response to control for first-order priming effects.

With this procedure, we obtained a trial list composed of discrete variables, that is, computed on the block-level occurrences. However, as discussed in the introduction, our aim was to use the trial-level estimates as predictors in our analyses. Therefore, in a second step, we computed trial-by-trial probabilities of our variables of interest, namely LWPC and ISPC, but also of Contingency and other variables used as confounding predictors in the statistical analyses (see below). To do so, we used the Hierarchical Gaussian Filter (Mathys et al., 2011), which uses variational Bayes under a mean-field approximation to update the

probability of an event on each trial. As such, trial-level estimates were calculated based on the update of trial-by-trial probabilities of i) the stimulus congruency, for LWPC; ii) the stimulus congruency conditional to a specific position, for ISPC; iii) the response (corresponding to the target direction) conditional to a specific position, for Contingency; iv) the response.

General instructions regarding the procedure, the task and the response mapping were provided to participants before the beginning of the task. They were instructed to respond as quickly and accurately as possible and were encouraged to maintain a comfortable posture, while keeping the responding fingers in contact with the response keys, and to avoid movements as much as possible. During the 16 practice trials, they received feedback on their performance accuracy and, in case of errors or time-out responses, were provided with a brief summary of instructions and response mapping. Blocks of practice trials were presented until 75% accuracy was reached.

5.2.2. EEG recording and pre-processing

The data were recorded at 500 Hz using BrainAmp amplifiers (Brain Products, Munich, Germany) from 64 Ag/AgCl electrodes mounted on an elastic cap (EASYCAP GmbH, Germany), according to the 10-10 system. We also recorded electrooculographic activity with an electrode placed under the left eye. The channel impedances were measured and adjusted until they were kept below 10 kΩ before testing. All electrodes were referenced online to FCz during the recording and an electrode positioned at AFz was used as ground.

Offline signal preprocessing was performed with MATLAB (Version 2017b; The MathWorks, Inc. Natick, MA) using scripts created ad hoc based on the functions from the EEGLAB toolbox (version 14.1.2; Delorme & Makeig, 2004). All criteria were established prior to data analysis.

Channels F1 and F2 were removed in all participants due to technical issues during the recording. Then, continuous raw data were filtered offline using zero-phase Hamming-windowed sinc FIR high-pass and low-pass filters (cut-off frequencies: 0.1 and 45 Hz, transition bandwidth: 0.2 and 10 Hz. respectively). Moreover, to facilitate the identification and removal of artifacts, we created a temporary cleaner dataset to be submitted to the independent component analysis (ICA) algorithm (Winkler et al., 2015). Specifically, we performed the following temporary pre-processing steps: 1) we applied a stronger high pass filter (cut-off frequency: 1 Hz, transition bandwidth: 2 Hz); 2) we detected and removed bad channels by means of the *clean_rawdata* function, using a maximum flatline duration of 5 s and a correlation threshold of .8 (these criteria led to the exclusion of 1.34 channels of average, SD = 1.89, range = [0 – 8]). ICA was then performed on this temporary dataset, using the fastICA algorithm with a symmetric approach, followed by equivalent dipole fitting performed using *dipfit*. To identify non-brain components (e.g., eye movements, blinks, and muscular activity), we first used an automatic selection procedure based on an IClabel classification

probability of being brain IC lower than 50% and a residual variance higher than .2 according to the *dipfit* model. Then, we visually inspected all the components to confirm or modify the automatically flagged ones based on their scalp topography, dipole location, evoked time course and power spectrum.

The ICA solution was applied to the original dataset (after excluding bad channels in it too, so to have the same number of channels in the two datasets) and the previously identified artifactual ICs were rejected, obtaining EEG data cleaned from artifacts detected by ICA.

Subsequently, removed channels (including F1 and F2) were interpolated by using a spherical spline method (Perrin et al., 1989) and data were re-referenced to a common average reference. To detect and remove bad epochs, we used a two-step procedure. We first segmented data into epochs (from -1700 ms to 1500 ms, corresponding to the duration of the experimental trials) with respect to the stimulus onset and we used an automatic procedure to detect artifactual epochs based on extreme values (threshold: +/- 125 μV) and improbability and kurtosis criteria (for both, SD > 6 for the single-channel and SD > 4 for the global threshold). We then segmented data into longer epochs (from -1900 ms to 2200) and used the Trial by Trial (TBT) plugin of EEGLAB, which allowed rejecting and interpolating channels on a trial-by-trial basis. Specifically, epochs with more than 6 bad channels were removed whereas, if this criterion was not met, the channels were interpolated. The three criteria together led to the exclusion, on average, of 6.68 epochs (SD = 4.08, range = [0 – 17]). After these steps, we removed the ocular electrode and re-referenced all channels to a common average reference. Lastly, we saved two distinct clean datasets: one dataset without baseline correction, since in some analyses we were interested in the entire pre-stimulus time window, and one dataset on which we applied a baseline correction from -200 to 0 ms. An additional clean dataset was then created by locking the baseline-corrected data to the response time for that trial and epoching them using a temporal window ranging from -2000 to 700 ms.

5.2.3. Data analyses

The statistical analyses were performed using the same statistical approach for the behavioral and EEG data (i.e., the dependent variables, DV). We used a multilevel modeling approach by performing a random coefficient analysis[15] (RCA, also called random regression or two-step regression; (Lorch & Myers, 1990). This approach allowed us to assess the specific impact of LWPC and ISPC, as well as their interaction, in modulating the Stroop effect when they both varied. Moreover, by using multilevel modeling, we were able to employ the trial-level estimates of our predictors while partialling out the effect of contingency and of other lower-level confounding factors, which represent sources of trial-by-trial noise in the estimation of

[15] We decided to use RCA instead of linear mixed-effects model analysis (Baayen et al., 2008) because the latter is computationally less efficient and does not allow controlling for the effect of many confounders at the participant level (since including such effects in the random part the model causes convergence issues).

our effects of interest at the subject level (see Viviani et al., 2023 for a more exhaustive description of the advantages of multilevel modeling over standard general linear model). In brief, this approach consists in first running multiple linear regressions at the participant level and then assessing statistical significance of the tested effects at the group level.

We defined a-priori the statistical model to test, based on our theoretical assumptions and our previous behavioral results (see Chapter 4), using the trial-level estimates of predictors for the effects of both the experimental manipulations and confounders, indicated by the suffix "b" added to the predictor name. The confounding predictors, which were included to fit well-known effects in the literature, were i) the continuous predictor for the effect of trial number within each block (TrialBlock) interacting with the continuous predictor for the effect of block number (Block) to account for potential time-on-task effects, such as the effects of learning/adaptation or fatigue; ii) a continuous predictor reflecting the inverse-transformed RTs (iRTs, computed as -1000/RTs) of the preceding trial (iRTpre), to account for temporal dependency in response times (Baayen & Milin, 2010) and thus to avoid violating the assumption of the independence of observations for linear modeling; iii) the horizontal and vertical position of the stimulus on the screen (respectively, hS and vS), to account for potential differences due to the location where the stimulus appeared (left vs right, above vs below, respectively); iv) the horizontal and vertical coding of the manual response (respectively, hR and vR), to account for potential differences due to the response hand and finger, respectively. Moreover, we modeled the effects that have been shown to affect the Stroop effect resolution through low-level learning mechanisms, by including the trial-level predictors for the effects of v) the contingency, namely the conditional probability of the response given the stimulus (i.e., P(R|S), PRSb), and vi) the probability of response (P(R), PRb). The experimental effects of interest were modeled by including the predictors for LWPC and ISPC (LWb and ISb, respectively) and trial congruency (CON), as well as their interactions. In particular, the three-way interaction between our effects of interest was included to explore whether proactive and reactive control interacted in modulating the Stroop effect. The Wilkinson-notation formula for the continuous full model is:

$$DV \sim TrialBlock*Block + hS + vS + hR + vR + iRTpre + PRSb + PRb + CON*LWb*ISb$$

The continuous predictors iRTpre, TrialBlock and Block were centered and scaled at the participant level to facilitate the model convergence and the interpretation of results. The confounding variables for the horizontal/vertical stimulus position and manual response were coded as .5 and -.5, with .5 indicating stimuli appearing in the right and the upper quadrant for hS and vS, respectively, and responses given using the right hand and middle finger for hR and vR, respectively. The predictor for Congruency was coded with the value of -.5 and .5 for the congruent and incongruent conditions, respectively. Lastly, PRSb, PRb, LWb and ISb did not require any transformation since they were already estimated on a scale centered at a 50% probability. After fitting the model, we assessed whether there was evidence of stress in the model fit, by

inspecting the model residuals and then refitting a trimmed version of the model, wherein we excluded data points with absolute standardized residuals exceeding 3.

After running the regressions at the participant level, we assessed statistical significance of each predictor at the group level by performing two-tailed one-sample *t* tests against 0 on the estimated b coefficients for each participant, whereas for variables for which we had a clear directional hypothesis, one-tailed one-sample *t* tests were performed. Specifically, for the behavioral analysis, we expect to find the Stroop effect (i.e., longer RTs for Incongruent compared to Congruent trials) and, for what concerns the interactions, we predicted that as either LWb or ISb increased, the Stroop effect increased. In contrast, we expected that higher values of PRSb and PRs were related to shorter RTs.

We reported the mean of the estimated coefficients (b) for each participant, the standard deviation (SD), and *t* and *p* values for each effect included in the trimmed final model. Moreover, for the experimental effects, we computed the effect sizes as Cohen's d and dominance values as the percentage of participants showing each effect. An alpha level of .05 was set as the cut-off for statistical significance.

In the case in which the three-way interaction was not significant, we tested the same continuous full model but after removing it, to verify whether its inclusion might have interfered with the estimation of the effects of the two 2-way interactions which separately tested the specific effects of proactive and reactive control (continuous 2-way interaction model).

A control analysis was also performed to verify whether the inclusion of continuous variables in the model was justified and ensured the best fit to the data, assessing the assumed theoretical advantage of the trial-level estimates. To do so, the same regression models were fitted using the block-level estimates of our variables, referred to as discrete variables (discrete full model), and then the r^2 of the continuous and discrete full models were compared to assess which one better explained our data. This control analysis was performed only on the behavioral data, and in the case in which the continuous model resulted in a better model fit, it was the only model run in the subsequent EEG analyses.

5.2.3.1. Behavioral analysis

Behavioral analyses were performed on inverse-transformed RTs (iRTs, computed as -1000/RTs) as this transformation eliminates the heavy right-skewness of RTs distribution more effectively than the logarithmic transformation. We excluded from the analyses the training trials (no participant needed more than one training cycle of 16 trials). From the resulting 27200 trials, we also excluded trials rejected in the EEG pre-processing (n = 304, corresponding to 1.12% of the experimental trials), as well as the first trial of each block, error trials (which comprise incorrect and missed responses), and post-error trials (n = 1643, corresponding to 6.11% of the remaining trials).

As explained above, behavioral analyses were run on control models as well, to verify which model better explained our data so to choose which one to use in the EEG analyses. Therefore, we ran both the full and 2-way interaction models and both the continuous and discrete models.

5.2.3.2. ERP analysis

Event-related potentials (ERPs) were extracted to obtain pre-stimulus, stimulus- and response-locked ERP datasets. Pre-stimulus ERPs were extracted from the stimulus-locked non-baseline-corrected data in a temporal window ranging from -1000 to 0 ms, whereas stimulus-locked ERPs were extracted from the stimulus-locked baseline-corrected data from 0 to 1000 ms. Lastly, baseline-corrected response-locked data were used to extract response ERPs in a temporal window ranging from -500 to 500 ms around the RT.

Three separate analyses were then run on the three ERP datasets, using the same exclusion criteria described in the behavioral analysis section so as to have the same set of trials. Specifically, we ran multiple linear regressions as detailed above for each channel, time point, and participant. Then, at the group level, we performed two-tailed one-sample *t* tests against 0 on the participants' estimated regression coefficients. Of note, on stimulus-locked and response-locked ERPs, we ran the same model reported above (continuous full model), whereas on the pre-stimulus ERPs we ran a model including only the predictors that were meaningful in the pre-stimulus phase, excluding Congruency, the related interactions and the confounders related to the stimulus and response (i.e., hS, hR, etc.). In contrast, we kept in the model the time-on-task confounders and all the predictors related to the trial-level probabilities, both the congruency- and the (stimulus-)response-related ones, as we were interested in exploring how such probabilities were computed, maintained, and updated before stimulus appearance. The resulting pre-stimulus model formula was:

pre-Stim ERPs ~ *TrialBlock*Block + iRTpre + PRSb + PRb + LWb + ISb*

Statistical significance for the effects of interest was then tested using the threshold-free cluster-enhancement (TFCE) method, which optimized the detection of both diffuse, low-amplitude effects and localized, high-amplitude ones, while correcting for multiple comparisons with non-parametric permutation tests (Smith & Nichols, 2009). TFCE was applied on all the channels and time points, using 5000 permutations.

Our aim was to assess whether the ERP Stroop effect was modulated by the interaction of LWPC and ISPC manipulations and, if it was not the case, we excluded the three-way interaction from the model to separately explore LWPC and ISPC modulations (2-way interaction model, see above). Moreover, since behavioral results revealed that the data were better explained by the continuous model as compared to the discrete one (see Results), ERP analyses were performed only on continuous models.

We then ran mass-brain-behavior correlations, correcting them using the TFCE method. Specifically, we ran multiple linear regressions at the participant level using iRTs as the DV and included in the model the ERPs (for each channel, time point, and trial). As above, we performed three separate analyses on the three ERP datasets with the same model used for both the behavioral and the post-stimulus ERP analyses. Subsequently, we used the ERP results to mask the obtained significant correlations so to report only the correlation results that were related to significant ERP effects. In the case in which ERP results for the continuous full model were the same as those for the 2-way interaction model, correlations were run only on the former.

5.2.3.3. ERP latency analysis

The Residue Iteration Decomposition (RIDE) method (Ouyang et al., 2015) was used to extract trial-wise latencies of ERP cognitive components. The RIDE approach assumes that the ERP waveform consists of distinct overlapping components: the sensory S component, time-locked to stimulus onset, the response-related R component, time-locked to RT, and central cognitive C components that exhibit variable latencies from trial to trial. RIDE follows an iterative process: (1) estimation of single trial latencies for the C components, (2) decomposition of S, C, and R components based on stimulus onsets, estimated C latencies, and RTs, (3) use of the decomposed C in (2) as a template to re-estimate C latencies, and (4) repetition of steps 2 and 3 until convergence is achieved. Using RIDE, hence, it is possible to obtain trial-wise latencies of the C component. Given that the latency of the central cognitive component (C) is determined based on its spatiotemporal pattern, the RIDE algorithm returns a single latency value for the whole scalp for each trial. The RIDE analysis was run on each participant's EEG stimulus-locked baseline-corrected dataset. Epochs ranged from -100 to 1300 ms to allow a good estimation of S and R components. Since the RIDE analysis requires all epochs to include RT, epochs from trials with RT >= 1000ms were excluded from the analysis. Finally, the time windows for component extraction were [0, 500] ms for S component, [100, 900] ms for C component, [−300, 300] ms around RTs for the R components. Statistical analyses on the C latencies were performed as described in the Data Analysis section.

5.2.3.4. Source analysis

We estimated the neuronal sources of our scalp-based ERP data at the trial level using the Brainstorm toolbox (Tadel et al., 2011). In particular, we estimated the current strength dynamics of the EEG cortical sources using the depth-weighted minimum norm estimation approach (Baillet et al., 2001) and a boundary element methods (BEM) conductive head model generated with OpenMEEG (Gramfort et al., 2010; Kybic et al., 2005) using the adaptive integration method. The solution space was constrained to the estimated cerebral cortex, modeled as a three-dimensional grid of 15002 vertices representing elementary current dipoles based on the FreeSurfer brain template (FSAverage; see Fischl et al., 1999). The obtained solution of

the inverse problem was used to compute the current strength time courses at the trial level for each of the three datasets we used for the analyses, that is, the pre-stimulus, stimulus and response ERP datasets. Then, the source-level stimulus-locked ERP dataset was z-scored with respect to the 200-ms time window before stimulus appearance, while both the pre-stimulus and the response-locked ones were z-scored with respect to the entire epoch (respectively, from -1500 to 0 ms and from -500 to 500 ms). Again, we used the same exclusion criteria described in the behavioral analysis section so to have the same set of trials. All the source-level ERP data were finally averaged across the vertices composing each of the 210 parcels of the Brainnetome atlas (Fan et al., 2016) to reduce spatial dimensionality for the subsequent mass-univariate analyses, and converted into absolute values. The statistical analyses were conducted for each time point and parcel as described for the scalp-level ERP data and results were corrected for multiple comparisons using the TFCE procedure.

5.2.3.5. ERSP analysis

ERSPs were extracted from both stimulus- and response-locked non-baseline-corrected data. Time-frequency decomposition was performed via modified complex Morlet wavelet convolution in the frequency range from 4 and 30 Hz (linearly spaced, 1 Hz resolution) using wavelets with a temporal window ranging from 750 to 533 ms, which corresponds to a linearly increasing number of cycles (from 3 to 12 cycles, linearly spaced, for the 4 and 30 Hz frequencies, respectively). The baseline correction was applied trial by trial using the average power in the time window used in the analysis (i.e., from -1500 to 1500 ms for stimulus-locked data and from -500 to 300 ms for response-locked data).

Three separate analyses were then run on pre-stimulus, stimulus-, and response-locked ERSPs, using the same exclusion criteria described in the behavioral analysis section so as to have the same set of trials. Specifically, we ran multiple linear regressions for each channel, frequency, time point, and participant and then, at the group level, we performed two-tailed one-sample *t* tests against 0. Statistical significance was then tested using the TFCE method as described above (Smith & Nichols, 2009).

Our aim was to assess whether the ERSP Stroop effect was modulated by the interaction of LWPC and ISPC manipulations, and since ERP analysis revealed that the 2-way interaction model confirmed the full model (see Results), we ran only this latter for computational reasons. Of note, as for the ERP analyses, a different model was tested for pre-stimulus ERSPs.

5.2.4. Participants

We recruited 41 participants (28 females and 13 males; mean age = 24.71 years, SD = 3.76 years), but one was excluded due to technical problems during the EEG recording. No participants reported having suffered from neurological or psychiatric disorders and to be under medication.

Participants consisted of a convenience sample recruited using researchers' personal networks and were compensated for their participation (25 €). We performed an a priori power analysis in G*Power (Erdfelder et al., 1996) to compute the minimum sample size required to detect, with a statistical power of .80, the interactions of main theoretical interest (that is, those between Congruency and either LWPC and ISPC, assessing respectively proactive and reactive control modulation of Stroop effects) in a two-tailed one-sample *t* test on the by-subjects slopes. We assumed a medium Cohen's d effect size of at least 0.5 based on the results of our previous studies (Tafuro et al., 2020; see Chapter 4). This analysis revealed that at least 34 participants were required. We nonetheless decided to recruit as many participants as possible exceeding the required sample size, so as to be able to detect even smaller effects (by increasing the statistical power of our analyses) and to increase the precision of the experimental effect estimates. Note that the final sample size of 40 participants ensured us to be able to find effects as small as d = 0.45.

5.3. Results

5.3.1. Behavioral results

As described in the method section, we first assessed whether our trial-level estimates better explained the data by comparing the R^2 of the continuous full model and the discrete full model and we found that the best-fit model was the continuous full one (one-tailed $t(39) = 2.20$, $p = .0167$, $d = 0.349$).

As such, only the results of the analysis on iRTs using the model with continuous variables are reported. We found that all the lower-level confounding predictors but the hS were significant in modulating participants' iRT (all *p*s <.001, see Table 5.1), indicating that participants were slower as trials went on and when they responded to stimuli appearing in the upper quadrant of the screen, while they were faster when they responded using the right hand and the middle finger. Moreover, we found a significant temporal dependency in iRTs (i.e., positive correlation between iRTs at the current and preceding trial). Lastly, the effect of our confounding predictors of interest, namely PRb and PRSb, was also significant as participants responded faster when PRb ($p < .0001$, d = -1.28) and PRSb ($p < .0001$, d = -1.36) were higher.

Regarding our predictors of interest, we found that the Stroop effect (CON) was significant ($p < .0001$) and with a very high effect size (d = 3.59), with slower responses to Incongruent trials. Moreover, all participants showed a positive Stroop effect, as indicated by a dominance value of 100%. In addition, the Stroop effect was significantly modulated by LWb (CON x LWb, $p < .0001$, d = 1.21, dominance = 95%) and the interaction effect was in the predicted direction, that is, longer iRTs as LWb increased. By contrast, the ISb modulation of the Stroop effect was not significant (CON x ISb, $p = .982$, $d = -.34$, dominance = 65%). Lastly, the three-way interaction between Stroop effect, LWb and ISb was not significant ($p = .21$, $d = .2$, dominance = 45%), indicating that LWb and ISb did not interact in modulating the Stroop effect.

Table 5.1 – Results of the RCA analysis on the behavioral data

Effect	M	SD	t(39)	p	d	Dom
Intercept	-2.151	0.347	-39.24	< .0001	-6.205	100
iRTpre	0.066	0.033	12.58	< .0001	1.989	100
Block	-0.080	0.062	-8.18	< .0001	-1.293	95
TrialBlock	0.001	0.014	0.56	.5813	0.088	47.5
CON	0.324	0.090	22.71	< .0001	3.590	100
LWb	0.021	0.034	3.81	.0005	0.602	77.5
ISb	0.013	0.025	3.25	.0024	0.514	75
PRSb	-0.048	0.035	-8.63	< .0001	-1.365	90
PRb	-0.091	0.072	-8.07	< .0001	-1.276	82.5
hS	-0.015	0.051	-1.92	.0628	-0.303	60
vS	0.029	0.051	3.55	.0010	0.561	75
hR	-0.074	0.107	-4.38	.0001	-0.692	72.5
vR	-0.133	0.117	-7.20	< .0001	-1.139	87.5
Block:TrialBlock	0.013	0.014	5.88	< .0001	0.929	77.5
CON:LWb	0.063	0.052	7.65	< .0001	1.210	95
CON:ISb	-0.027	0.079	-2.16	.9816	-0.342	65
LWb:ISb	0.011	0.033	2.12	.0408	0.335	70
CON:LWb:ISb	0.013	0.062	1.29	.2062	0.203	45

Notes: M, mean of the coefficient estimates; *SE*, standard error; Dom, percentage of participants showing that effect. See the main text for the spelling out of the acronyms for the effects

Since the three-way interaction was not significant, we tested the same model but after removing it (continuous 2-way interaction model; see methods), to assess whether it interfered with the estimation of the effects of the two 2-way interactions separately testing the effect of proactive and reactive control. We found that this was not the case, as the pattern of results remained unchanged, suggesting that including the three-way interaction did not interfere with the estimation of the other effects. For this reason, we decided to continue testing the continuous full model also in the subsequent EEG analyses.

5.3.2. ERP and brain-behavior correlation results

5.3.2.1. Stimulus-locked ERPs

RCA analysis on stimulus-locked ERPs performed using the continuous full model revealed that ERPs were significantly modulated by Congruency, proactive control (Congruency x LWb interaction), and Contingency (PRSb) (see Figure 5.1).

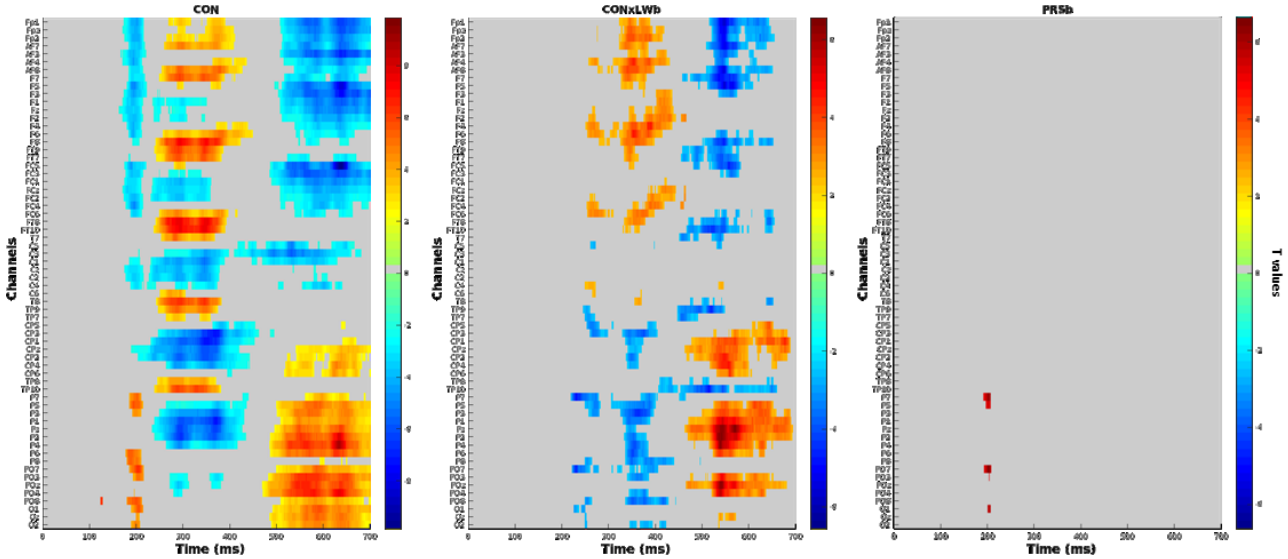

Figure 5.1.
Results of the RCA analysis on stimulus-locked ERPs. The raster diagrams show channels/timepoints significantly modulated by the effect indicated in the corresponding title. Significant effects are reported as t values that are color mapped to indicate positive and negative differences (warm and cold colors, respectively).

The effect of Congruency was observed in a first temporal cluster in an early time-window (from 176 to 216 ms) peaking at around 200 ms and distributed bilaterally over posterior electrodes, characterized by a greater negativity for Congruent as compared to Incongruent trials and resembling the well-known N170 or posterior N2 component. This posterior spatial cluster was coupled with a frontal spatial cluster, which was slightly left-lateralized, with a greater P2 positivity for Congruent than Incongruent trials (see Figure 5.2).

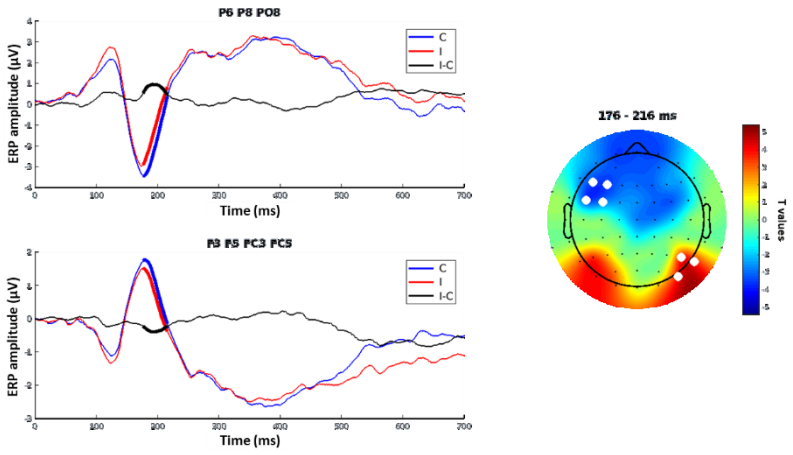

Figure 5.2.
The figure shows the Congruency effect in the first cluster revealed by the RCA analysis on stimulus-locked ERPs. The trace plots on the left show the ERPs for Congruent (C, in blue) and Incongruent (I, in red) trials, as well as the corresponding difference wave reflecting the ERP Stroop effect (in black), averaged over the channels indicated by white markers in the topoplot on the right and reported in the title of the trace plots. The time window of the significant effect is indicated by the thicker portion of the plots. The topoplot on the right shows the t values averaged over the significant time window (which is also indicated in the title).

Subsequently, Congruency modulated a spatio-temporal cluster peaking at around 300 ms (236 – 432 ms), characterized by an enhanced P3-like positive deflection for Congruent trials at centro-parietal electrodes. An additional cluster was found in a similar time-window (240 – 420 ms, peak at around 290 ms), distributed bilaterally over frontal scalp regions, resembling a so-called LFN (lateral frontal negativity) and showing a greater negative deflection for Congruent trials (see Figure 5.3).

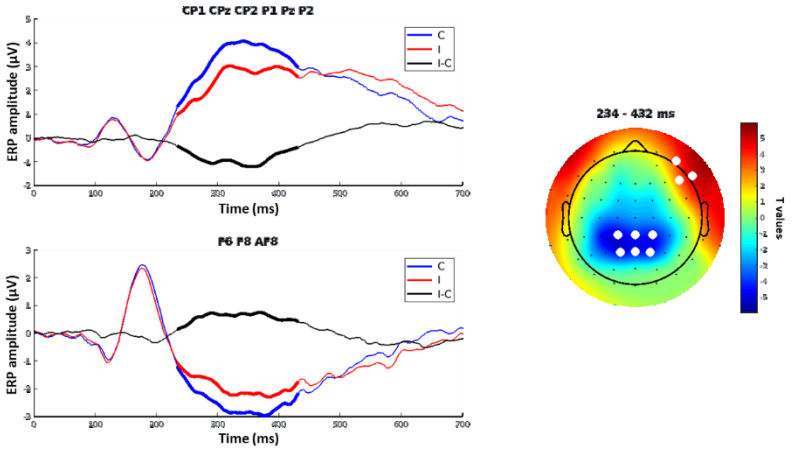

Figure 5.3.
The figure shows the Congruency effect in the second cluster revealed by the RCA analysis on stimulus-locked ERPs. See Figure 5.2 for conventions.

Significant Congruency-related ERP modulations were observed also in later time-windows with two spatio-temporal clusters akin to late potential (LP) components. In a temporal cluster ranging from 488 to 750 ms, Incongruent trials elicited a more sustained negativity at left frontal electrodes and a more sustained positivity at parietal electrodes, bilaterally but more right-lateralized (see Figure 5.4).

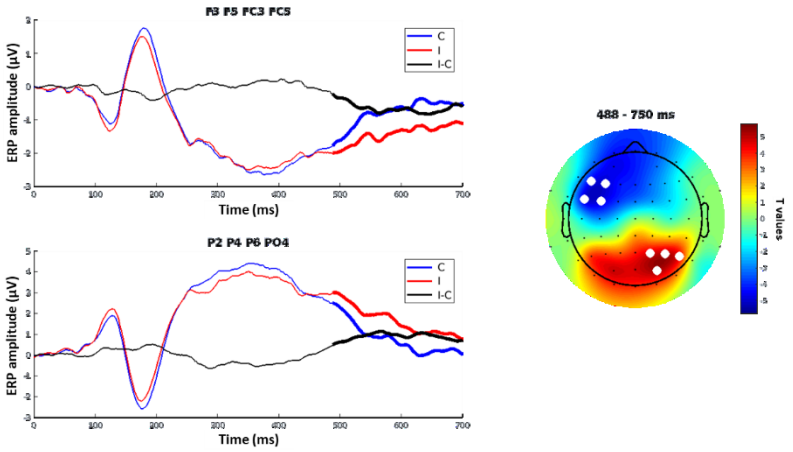

Figure 5.4.
The figure shows the Congruency effect in the third cluster revealed by the RCA analysis on stimulus-locked ERPs. See Figure 5.2 for conventions.

Lastly, we found two post-response components (from 800 to 1000 ms), that is, a centro-frontal cluster characterized by a more negative ERP for Incongruent trials and a bilateral temporal cluster characterized by a more positive ERP to Incongruent trials.

The effect of proactive control revealed by the interaction between Congruency and LWb (see Figure 5.1) was significant in a first temporal cluster (254 - 278 ms) peaking at 270 ms and reflecting the initial part of the LFN, revealing larger ERP Stroop effects (i.e., larger difference between Incongruent and Congruent trials) for higher LWb levels, with a greater negative deflection for Congruent trials. In the same time-window, we found a second spatial cluster over posterior scalp regions, bilateral but more strongly left-lateralized, and reflecting the initial part of a P3-like component characterized by larger Stroop effects for higher LWb levels, with a greater positive deflection for Congruent trials (see Figure 5.5).

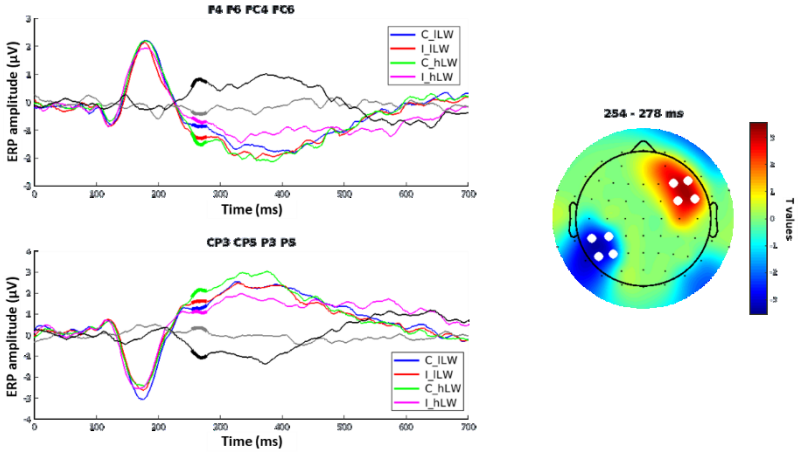

Figure 5.5.
The figure shows the Congruency by LWb effect in the first cluster revealed by the RCA analysis on stimulus-locked ERPs. The trace plots show the ERPs for low-LWb Congruent (C_lLW, in blue) and Incongruent (I_lLWb, in red) trials, for high-LWb Congruent (C_hLW, in green) and Incongruent (I_hLW) trials, and for the corresponding difference wave reflecting the ERP Stroop effect in low- and high-LWb conditions (in gray and black, respectively), averaged over the channels indicated by white markers in the topoplot on the right and reported in the title of the trace plots. See Figure 5.2 for other conventions.

The same pattern of ERP modulations was observed slightly later. In a time window from 330 to 430 ms and peaking at around 350 ms, we observed larger ERP Stroop effects for high-LWb trials, with a negative deflection for Congruent trials. This frontal spatial cluster was coupled with a left parietal cluster, in which we observed a P3-like component, with larger Stroop effects for higher LWb and greater positive deflection for Congruent trials (see Figure 5.6). A third cluster, emerging slightly later (340 - 440 ms) over right temporo-parietal electrodes, was different from the other two: while for high LWb we found a more positive deflection for Congruent trials, for low LWb we found a more positive deflection for Incongruent trials.

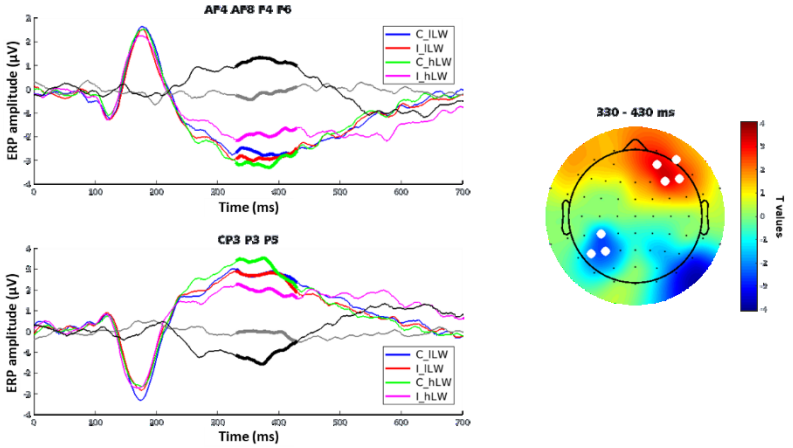

Figure 5.6.
The figure shows the Congruency by LWb effect in the second cluster revealed by the RCA analysis on stimulus-locked ERPs. See Figure 5.5 for conventions.

Finally, we found a proactive control modulation of the ERP Stroop effect in two later spatio-temporal clusters. One cluster ranged from 470 to 680 ms, reflecting the parietal LP (the descending part of the P3), as suggested by the centro-parietal scalp distribution and the larger Stroop effect for higher LWb, but with a more sustained positivity for Incongruent trials. In a similar time-window, we observed the reverse amplitude pattern at frontal electrodes, bilaterally, related to the frontal LP (see Figure 5.7).

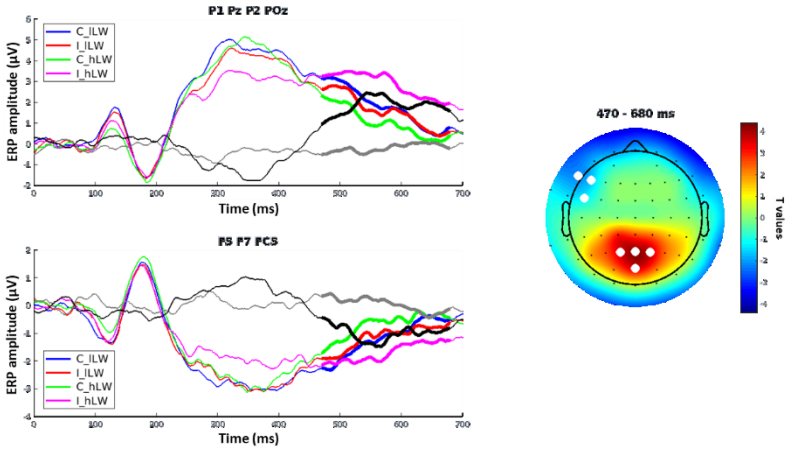

Figure 5.7.
The figure shows the Congruency by LWb effect in the third cluster revealed by the RCA analysis on stimulus-locked ERPs. See Figure 5.5 for conventions.

Lastly, we found that Contingency significantly modulated the ascending part of the early N170 ERP component (from 192 to 208), with greater negativity at left parieto-occipital electrodes for low-PRS trials (see Figures 5.1 and 5.8).

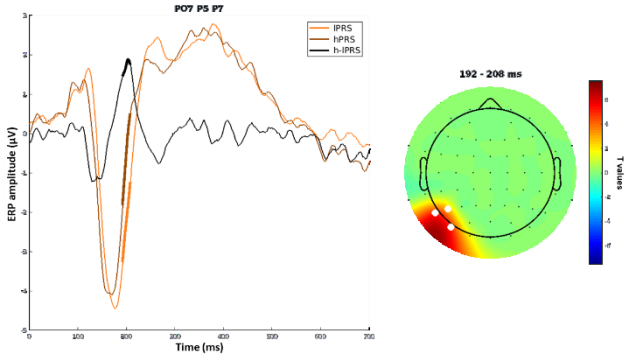

Figure 5.8.
The figure shows the PRSb effect revealed by the RCA analysis on stimulus-locked ERPs. The trace plots on the left show the ERPs for low-PRSb (lPRS, in orange) and high-PRSb (hPRS, in brown) trials, as well as the corresponding difference wave (in black), averaged over the channels indicated by white markers in the topoplot on the right and reported in the title of the trace plots. The time window of the significant effect is indicated by the thicker portion of the plots. See Figure 5.2 for other conventions.

Brain-behavior correlations using stimulus-locked ERPs revealed that the identified components generally explained the behavioral performance. In particular, we found that the frontal P2 over both fronto-polar and frontal electrodes modulated the behavioral performance, with the amplitude of the former related to better performance and that of the latter inversely related to the performance. Additionally, we observed a significant effect of both the parietal P3-like component and its frontal counterpart, as revealed by more prominent ERPs related to a better performance. Lastly, behavioral performance was explained by both frontal and parietal LP components, with greater LP amplitude related to worse performance (see Figure 5.9).

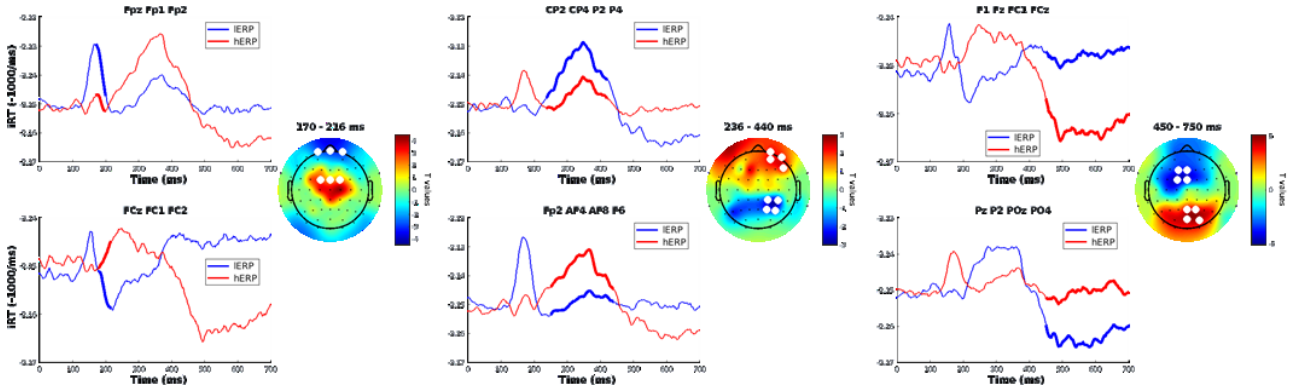

Figure 5.9.
The figure shows the significant brain-behavior correlations for stimulus-locked ERPs. The trace plots on the left of each panel show the predicted iRTs (-1000/ms; lower values indicate better performance) for ERPs 2 SDs lower (lERP, in blue) and higher (hERP, in red) than the average, averaged over the channels indicated by white markers in the topoplot on the right and reported in the title of the trace plots. See Figure 5.2 for other conventions.

Of note, our control analysis using a model in which the contingency predictor was removed replicated the results reported above, confirming that they were not biased by low-level stimulus-response associations and indeed reflect specific control-related modulations. Moreover, they revealed two significant ISPC-dependent modulations of ERP Stroop effect, an early and very phasic one at around 240 ms over left parieto-occipital channels, with a larger positivity for high-ISPC Incongruent trials and low-ISPC Congruent trials (that is, those with the highest probability of occurrence), and a later one from 420 to 520 ms over left central channels, with a larger positivity for high-ISPC Congruent trials (that is, those with the least amount of reactive control need). However, these results cannot be interpreted safely as they are confounded with the effect of contingency, which was not controlled for in this control analysis, so they will not be discussed.

5.3.2.2. Response-locked ERPs

Response-locked ERP analysis using the continuous full model found a significant effect of Congruency only and revealed three distinct temporal clusters (see Figure 5.10).

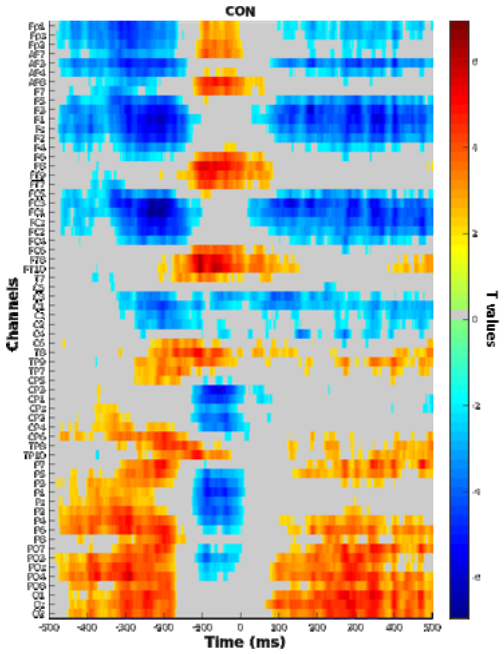

Figure 5.10.
Results of the RCA analysis on response-locked ERPs. See Figure 5.1 for conventions.

The first one peaked at about -200 ms before response (from -450 to -140) and corresponded to the pre-response time-window. Within this temporal cluster, we found a posterior spatial cluster, characterized by a more sustained positivity for Incongruent trials, and a left frontal spatial cluster, characterized by a more sustained PRN (pre-response negativity) for Incongruent trials (see Figure 5.11).

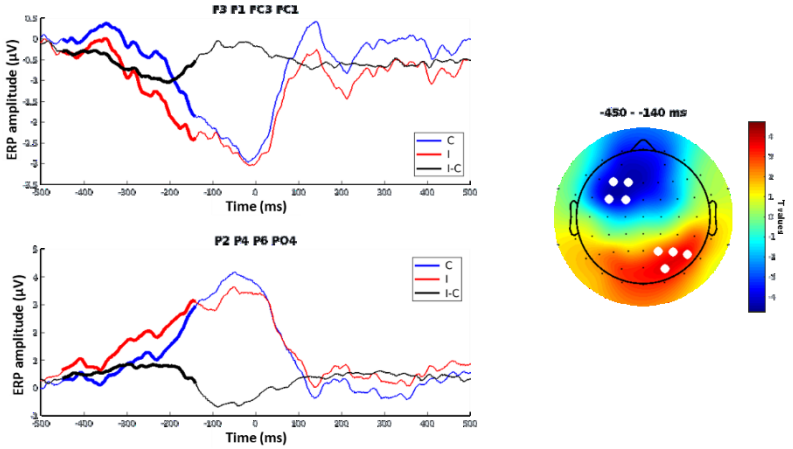

Figure 5.11.
The figure shows the Congruency effect in the first cluster revealed by the RCA analysis on response-locked ERPs. See Figure 5.2 for conventions.

In the peri-response time-window (approximately from -120 to 0 ms), a parietal cluster peaking at about -30 ms was observed, characterized by greater positivity for Congruent trials, coupled with a bilateral frontal cluster peaking at about -100 ms, with greater negativity for Congruent trials (see Figure 5.12).

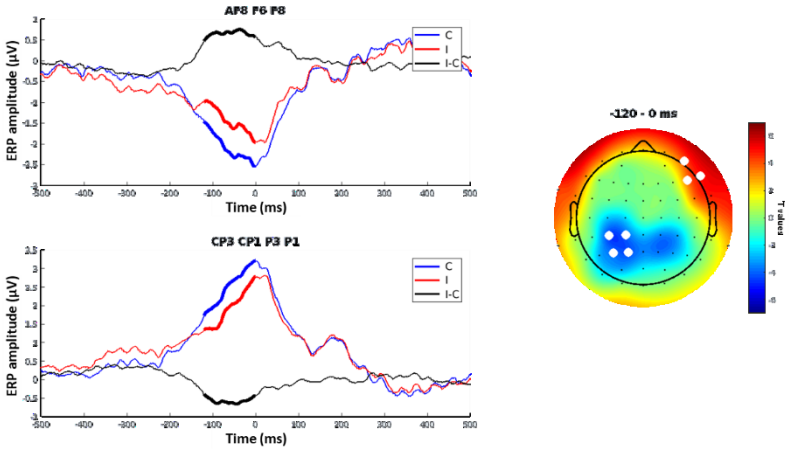

Figure 5.12.
The figure shows the Congruency effect in the second cluster revealed by the RCA analysis on response-locked ERPs. See Figure 5.2 for conventions.

Lastly, in the post-response phase (from 90 to 500 ms), we distinguished two additional components: a negative deflection more prominent for Incongruent trials, distributed over left frontal scalp regions, resembling a CRN (correct-response negativity), and a positive deflection more prominent for Congruent trials, distributed over occipital scalp regions (see Figure 5.13).

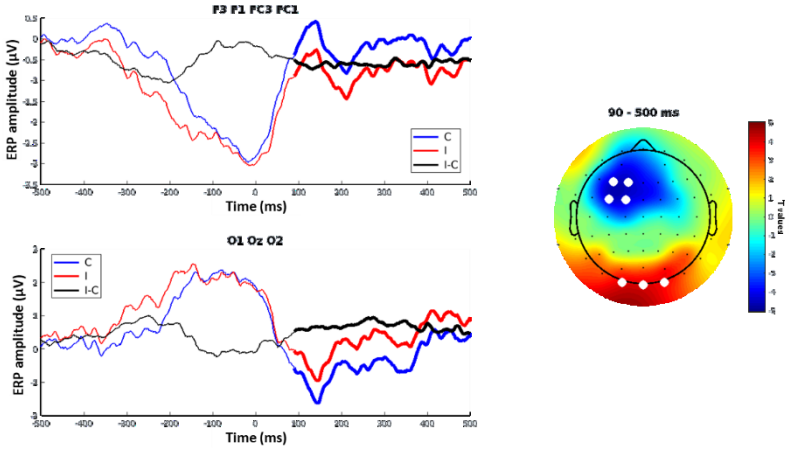

Figure 5.13.
The figure shows the Congruency effect in the third cluster revealed by the RCA analysis on response-locked ERPs. See Figure 5.2 for conventions.

Two of the identified ERP components correlated with behavioral performance as well. Specifically, the pre-response cluster over both parietal and left frontal electrodes explained behavior with greater amplitudes related to longer RTs. Additionally, behavior was modulated by the peri-response parietal and frontal clusters, as revealed by greater amplitudes related to a better performance (see Figure 5.14).

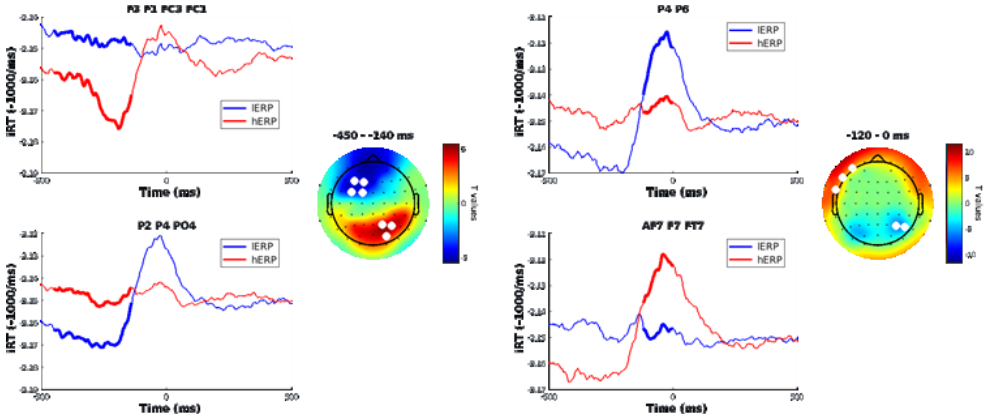

Figure 5.14.
The figure shows the significant brain-behavior correlations for response-locked ERPs. See Figure 5.9 for conventions.

As explained in the method section, control analyses using the continuous 2-way interaction models were also performed to assess whether the inclusion of the three-way interactions interfered with the two 2-way interactions, but again no reactive control modulation was found and the general pattern of results was confirmed, both for stimulus- and response-locked ERPs.

5.3.2.3. Pre-Stimulus ERPs

Lastly, we found that Contingency (PRSb) and the Response Probability (PRb) significantly modulated pre-stimulus ERPs.

For what concerns Contingency, we found an extended temporal cluster ranging from -1000 ms to stimulus appearance, characterized by a more sustained positivity for high-PRSb trials, distributed over mid-frontal scalp regions. Moreover, we observed a more temporally limited cluster (from -720 to -110) at occipital electrodes, characterized by a more sustained negativity for high PRSb trials. In the same time-window, we also found a right-lateralized temporal negativity, more prominent for high PRSb trials (see Figure 5.15).

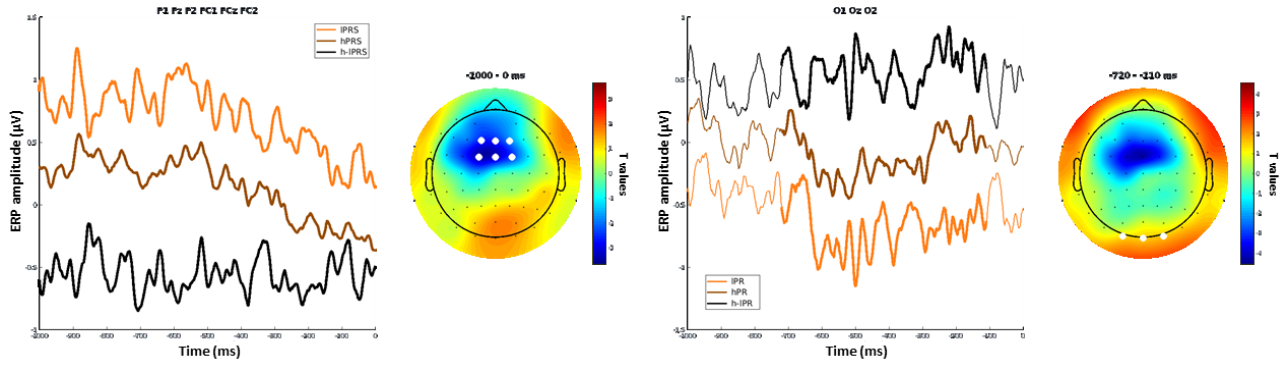

Figure 5.15.
The figure shows the effect of PRSb revealed by the RCA analysis on pre-stimulus ERPs. The trace plots on the left of the left and right panels show,respectively, the ERPs for low-PRSb and low-PRb (lPRS and lPR, in orange) and high-PRSb and high-PRb (hPRS and hPR, in brown) trials, as well as the corresponding difference wave (in black), averaged over the channels indicated by white markers in the topoplot on the right and reported in the title of the trace plots. See Figure 5.8 for other conventions.

The effect of Response Probability revealed two spatio-temporal clusters. The former ranged from -620 to -520 ms and was characterized by a greater positive deflection for high-PRb trials at mid-frontal electrodes, followed by a second cluster ranging from -400 to -200 and characterized by a greater positive deflection for high PRb trials at central electrodes.

Behavioral performance was modulated by both the mid-frontal and the occipital ERP components, with a negative relationship between amplitude and performance.

5.3.2.4. Stimulus-locked ERP latency

Results are reported in Table 5.2. Concerning our variables of interest, the only significant effects were found for CON ($p < .001$, $d = 0.56$) and CON x LWb ($p < .001$, $d = 0.61$). In particular, C latencies were longer for Incongruent than Congruent trials, and this difference increased with increasing LWb.

Table 5.1 – Results of the RCA analysis on the behavioral data

Effects	t(39)	p	d
(Intercept)	0.44	.664	0.07
iRTpre	2.48	.018	0.39
Block	-0.33	.740	-0.05
TrialBlock	1.40	.169	0.22
CON	3.79	<.001	0.60
LWb	1.09	.281	0.17
ISb	-0.34	.739	-0.05
PRSb	-1.50	.142	-0.24
PRb	0.04	.972	0.01
hS	-0.60	.555	-0.09
vS	3.18	.003	0.50
hR	-1.16	.254	-0.18
vR	-0.64	.524	-0.10
Block:TrialBlock	1.19	.240	0.19
CON:LWb	3.83	<.001	0.61
CON:ISb	-0.21	.834	-0.03
LWb:ISb	1.02	.312	0.16
CON:LWb:ISb	0.69	.493	0.11

Notes: See the main text for the spelling out of the acronyms for the effects

5.3.3. Source analysis results

Source analyses were performed to investigate the effects of our experimental manipulations on the cortical electrophysiological activity using a massive approach.

5.3.3.1. Stimulus-locked ERPs

In the stimulus-locked data, after correction, only Congruency and Response Probability clusters survived.

The analyses revealed that the cortical sources of Congruency effects can be divided into three main temporal clusters. First, from about 260 ms, we found a positive cluster distributed over right medial parietal regions, accompanied by a negative cluster distributed over right ventral and lateral occipito-temporal areas, both peaking at 282 ms. Subsequently, at about 320 ms, the positive cluster disappeared, and only the ventral and lateral occipito-temporal one remained significant till 380 ms.

Subsequently, from approximately 360 to 1000 ms, a widespread and sustained positive cluster emerged. This cluster was observed mainly over medial frontal regions, including the bilateral paracentral lobule and the supplementary motor area (SMA), and peaking at about 460 ms. In addition to these medial frontal regions, from about 460 to 600 ms, bilateral lateral (pre-)frontal and anterior temporal regions were observed, peaking at 500 ms. Then, after 690 ms, only a dorsal ACC pattern remained significant.

A last small temporal cluster was then observed from 800 ms over insula and left opercoli.

For what concerns Response Probability, we found a first early cluster (from about 250 to 344 ms), distributed over left posterior parietal cortex and then, after 290 ms and till 540 ms, the cluster expanded over left insula, anterior superior temporal regions and occipital areas. Finally, a small later cluster (from about 500 to 540 ms) was observed over left sensorimotor areas.

5.3.3.2. Response-locked ERPs

Response-locked analyses revealed the cortical sources of both Congruency and Contingency, which survived after correction.

Specifically, two clusters were observed for Congruency: a pre- and peri-response (from about -166 to 60 ms) negative left cluster distributed over ventrolateral and opercular prefrontal areas, and a post-response (from about 62 to 174 ms) positive right cluster, distributed over occipito-temporal areas and TPJ. This latter cluster was characterized also by sustained effect over a posterior superior temporal sulcus (STS) region, which remained significant till 370 ms.

The cortical source of Contingency was found in a negative right-lateralized cluster, spanning from -440 to -140, and distributed over medial frontal and posterior cingulate areas, including also the SMA.

5.3.3.3. Pre-stimulus ERPs

Source analysis of pre-stimulus data revealed that the cortical sources of LWb and ISb survived after correction. Specifically, for LWb, we found a positive right cluster spanning from about -920 to -820 ms, distributed over medial frontal areas, including SMA. The effect of ISb was instead revealed by a positive right cluster from about -440 to stimulus appearance, distributed over dorsolateral PFC cortex, inferior frontal sulcus (IFS), insula and anterior ventro-lateral temporal regions.

5.3.4. ERSP results

5.3.4.1. Stimulus-locked ERSPs

RCA analysis on stimulus-locked ERSPs performed using the continuous full model revealed that Congruency, proactive control (Congruency x LWb) and Contingency (PRSb) significantly modulated the spectral power across different frequencies.

For Congruency (see Figure 5.16), we found an early cluster in Theta (approximately from 20 to 360 ms) mainly distributed over both frontopolar scalp regions and right parieto-occipital, characterized by a greater power increase for Congruent trials compared to Incongruent trials (see Figure 5.17). The same scalp regions also showed a greater steady relative decrease in power for Congruent trials in a later cluster from about 850 to 1200 ms. We also found a Theta clusters from about 420 to 750 ms over both mid-fronto-central and right temporal channels, showing a steeper power reduction for Congruent trials (see Figure 5.17). In the Theta-Alpha frequency bands we also found a late cluster, from about 1000 ms till the end of the window over bilateral central channels, showing a steeper power increase for Congruent trials.

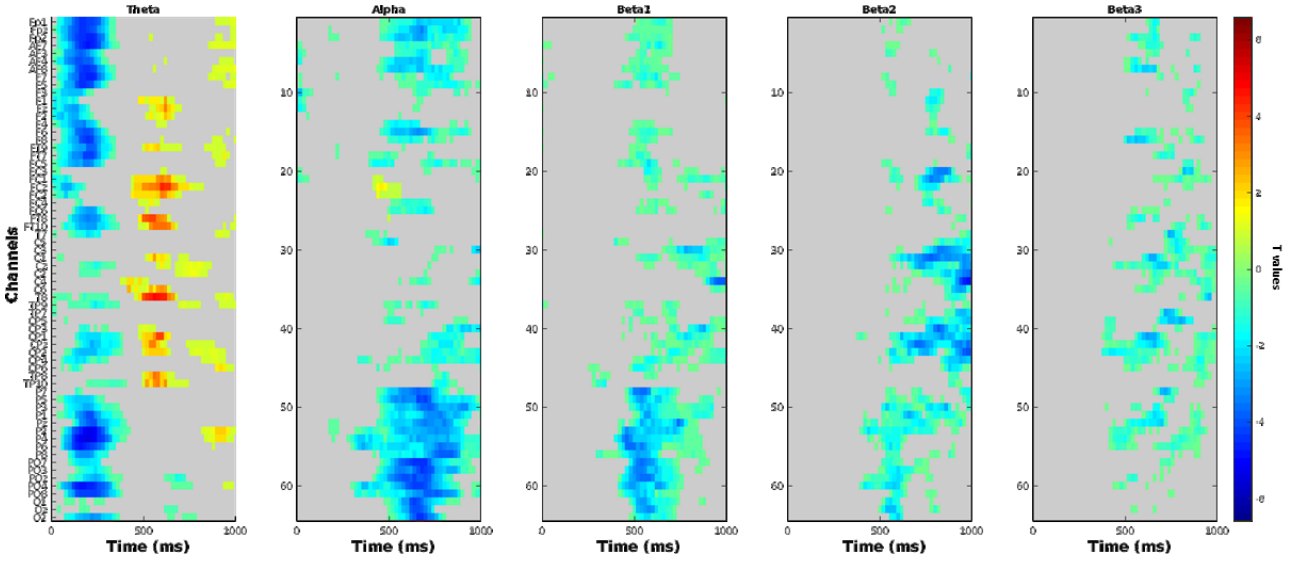

Figure 5.16.
Results of the RCA analysis on stimulus-locked ERSPs. The raster diagrams show channels/timepoints significantly modulated by the Congruency effect, averaged over the frequencies for the different bands. See Figure 5.1 for conventions.

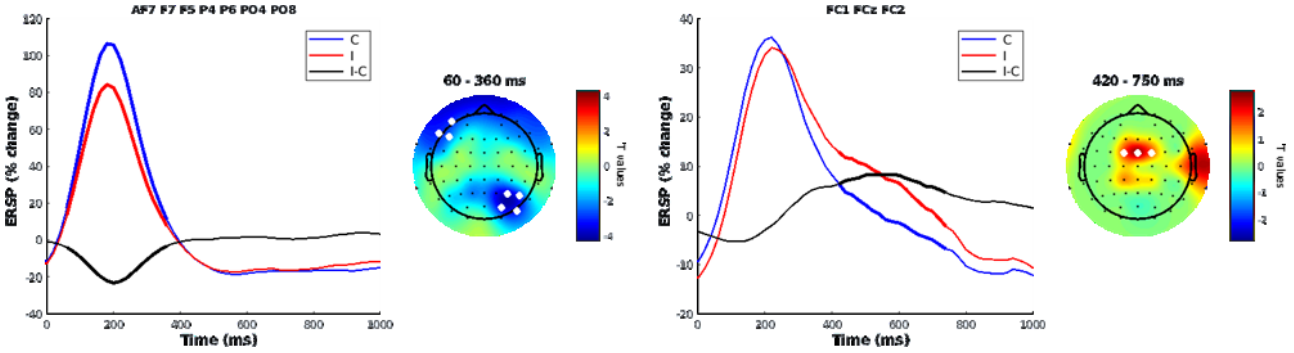

Figure 5.17.
The figure shows the Congruency effect in the first (left panel) and second (right panel) Theta clusters revealed by the RCA analysis on stimulus-locked ERSPs. The trace plots on the left show the ERSPs for Congruent (C, in blue) and Incongruent (I, in red) trials, expressed as % change from the baseline, as well as the corresponding difference wave reflecting the ERSP Stroop effect (in black), averaged over the channels indicated by white markers in the topoplot on the right and reported in the title of the trace plots. See Figure 5.2 for other conventions.

As regards the Alpha frequency band, we found an earlier (from approximately 300 to 850 ms) greater and more sustained power suppression for Incongruent trials over bilateral parieto-occipital and right prefrontal scalp regions (see Figure 5.18). A similar pattern of power reduction for Incongruent trials was also found for the entire Beta band, which was however observed over more medial posterior regions (see Figure 5.18).

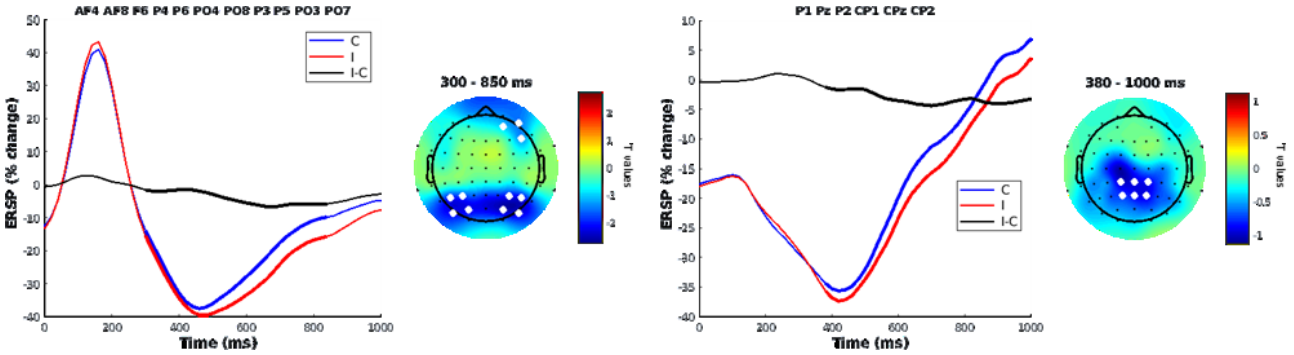

Figure 5.18.
The figure shows the Congruency effect in the Alpha (left panel) and Beta (right panel) clusters revealed by the RCA analysis on stimulus-locked ERSPs. See Figure 5.17 for conventions.

The analysis also showed the effect of proactive control on ERSPs, revealed by the interaction between Congruency and LWb (see Figure 5.19).

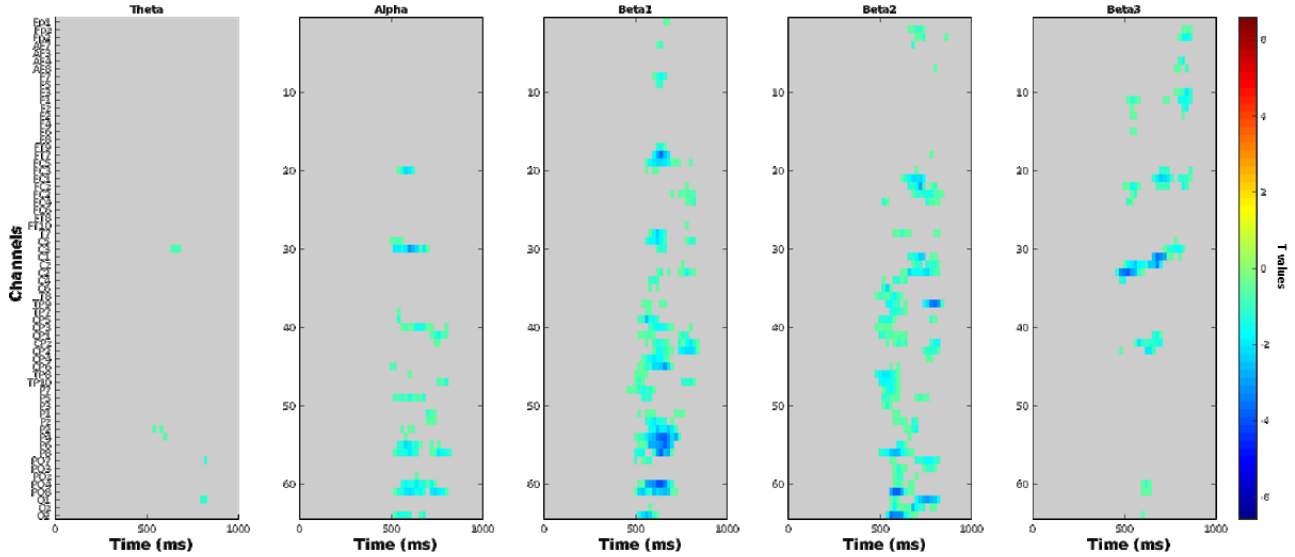

Figure 5.19.
Congruency by LWb interaction on stimulus-locked ERSPs. See Figure 5.16 for conventions.

This effect was found in a cluster involving Alpha and Beta1 over right parieto-occipital and left central channels, and in a cluster mainly involving higher frequencies (Beta2 and Beta3) over medial fronto-central and bilateral posterior channels. For all frequencies, the effect was found in a consistent time-window approximately ranging from 460 to 860 ms and showed the same pattern. Specifically, we found a greater ERSP Stroop effect, with a more sustained power reduction for Incongruent trials in the high-LWb condition as compared to high-LWb Congruent trials and to all the other conditions (see Figure 5.20).

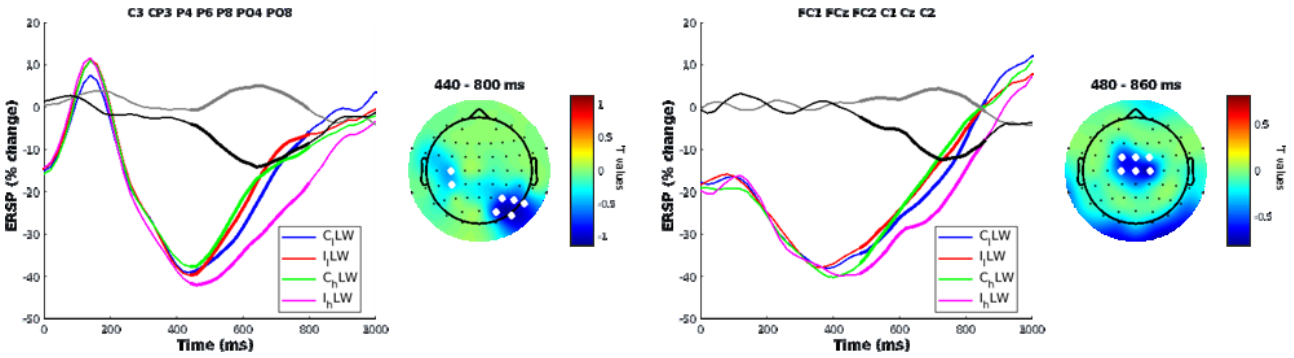

Figure 5.20.
The figure shows the Congruency by LWb effect on stimulus-locked ERSPs in the Alpha-Beta1 (left panel) and Beta2-3 (right panel) frequency bands. See Figures 5.5 and 5.17 for conventions.

Lastly, Contingency modulated significantly a first small medial occipito-parietal cluster involving Alpha-Beta2 frequency bands from 440 to 700 ms, with a greater and more sustained power reduction for low-PRSb trials. Later, and till 1120 ms, two significant clusters were observed in Beta1-2 frequency bands, at bilateral central electrodes, revealing a greater relative power increase for high-PRSb trials.

5.3.4.2. Response-locked ERSPs

The response-locked analysis found significant Congruency (Figure 5.21) and Contingency ERSPs. The results pertaining to the post-response temporal window are not reported here for the sake of conciseness.

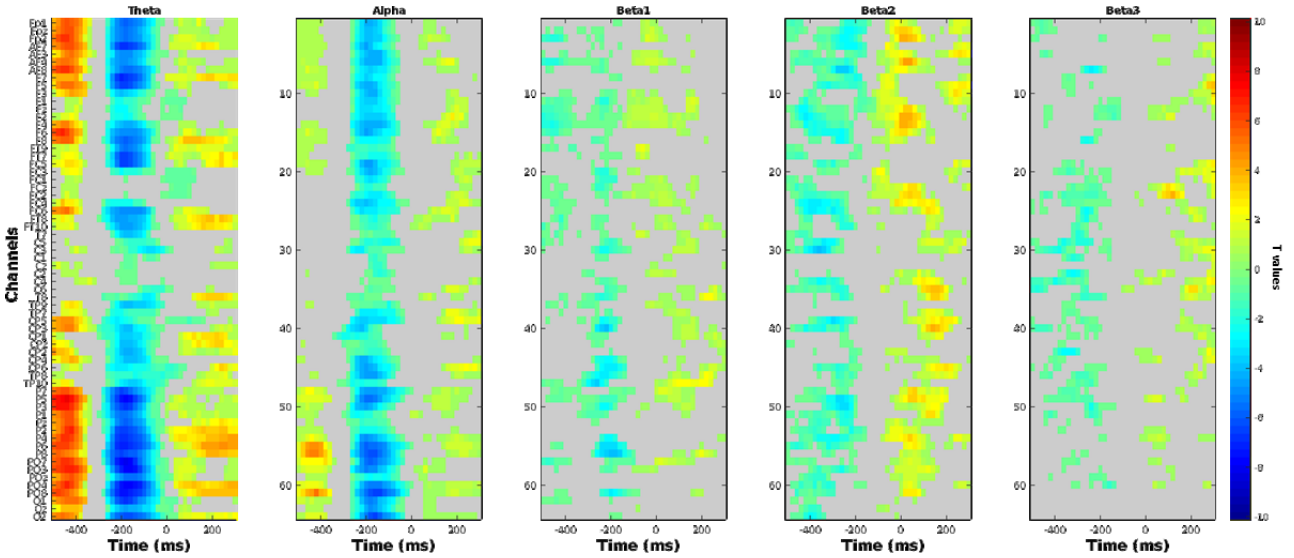

Figure 5.21.
Congruency effect on response-locked ERSPs. See Figure 5.16 for conventions.

Regarding Congruency effect, bilateral fronto-parietal electrodes showed a greater Theta and Alpha power increase for Incongruent trials in the early pre-response time-window (-500 to -340), followed by an inverted pattern in a later pre-response window (-300 to 0 ms) (see Figure 5.22).

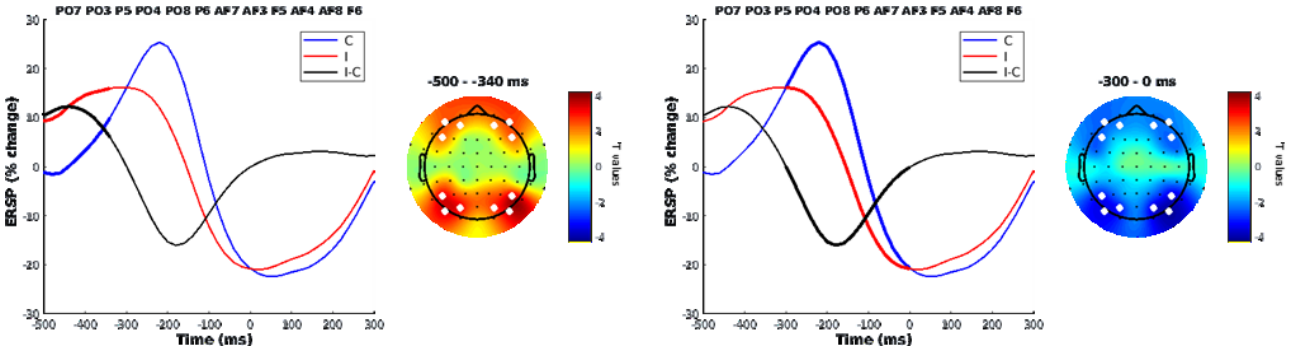

Figure 5.22.
The figure shows the Congruency effect in the Theta-Alpha frequency bands revealed by the RCA analysis on response-locked ERSPs. See Figure 5.17 for conventions.

Additionally, we found a widespread cluster peaking over bilateral central channels, which showed a more pronounced power decrease for Incongruent trial for Beta2-3 frequencies in an earlier pre-response phase (from -500 to -160) and for Beta1 frequencies in a later pre-response window (from -280 to -140 ms) over more posterior channels (see Figure 5.23).

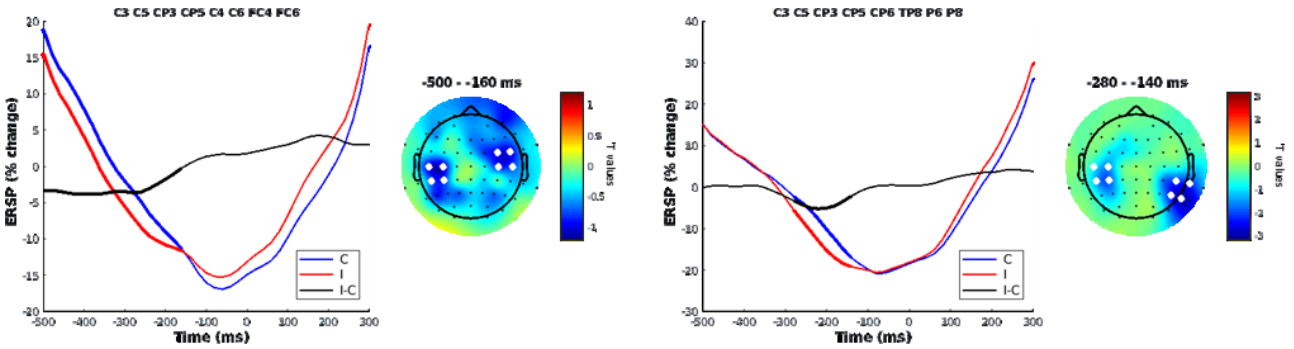

Figure 5.23.
The figure shows the Congruency effect in the Beta2-3 (left panel) and Beta1 (right panel) frequency bands revealed by the RCA analysis on response-locked ERSPs. See Figure 5.17 for conventions.

This was followed by a widespread cluster in the peri-response phase (from -120 to 100 ms), mainly distributed over right frontal channels, wherein the pattern of Beta power was reversed, with a greater and more sustained Beta2 power decrease for Congruent trials (see Figure 5.24).

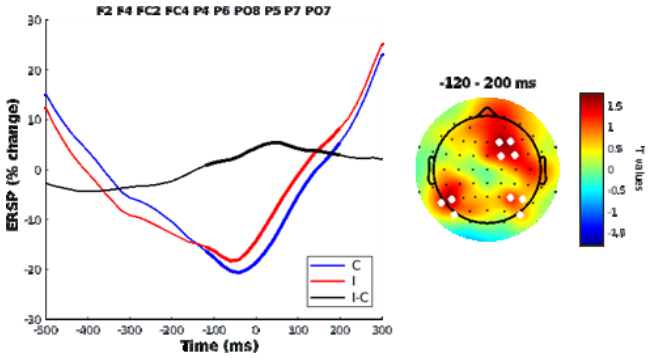

Figure 5.24.
The figure shows the peri-response Congruency effect in the Beta2 frequency band revealed by the RCA analysis on response-locked ERSPs. See Figure 5.24 for conventions.

The effect of Contingency on response-locked ERSPs involved only the Theta frequency band, with a right parieto-occipital cluster in the early pre-response phase (from -500 to -400 ms), characterized by a more pronounced power increase for low-PRSb trials.

5.3.4.3. Pre-stimulus ERSPs

Lastly, pre-stimulus ERSPs were modulated by LWPC, Contingency and Response Probability. Specifically, LWb modulated early pre-stimulus high-Alpha ERSPs (from about -1260 to -1110 ms) mainly over mid-right fronto-central electrodes, showing a power increase for high-LWb trials and a power decrease for low-LWb trials.

Contingency modulation involved all frequency bands in an early pre-stimulus time window, ranging approximately from -1260 to -1000 ms, with a widespread cluster mainly distributed over frontopolar and parietal channels, characterized by a power increase for low-PRSb trials. In the same scalp regions, we found a more pronounced and more sustained Alpha-Beta1 power decrease for high-PRSb trials both in an earlier (from -1500 to -1300 ms) and in a later (from -700 ms till stimulus onset) pre-stimulus window. In the same time window, for all Beta frequencies, the high-PRSb trial power decrease was still observed but became steeper and was mainly distributed over bilateral central scalp regions. Lastly, from about -360 to -60 ms before stimulus, we found a small parietal cluster involving Theta, characterized by a greater relative power increase for low-PRSb trials.

The effect of Response Probability was then found in the modulation of aAlpha frequency band from about -520 to -200, with a left centro-parietal and a slightly right-lateralized prefrontal cluster showing a power increase for high-PRb trials compared to a power decrease for low-PRb trials.

5.4. Discussion

In the present study, we aimed to investigate the electrophysiological correlates of cognitive control by adopting the Dual-Mechanisms of Control (DMC) framework. Our main goal was to differentiate between proactive and reactive control and determine if each mechanism operates independently when the other is assumed to be activated as well.

While researchers have made efforts to uncover the neural signatures of cognitive control and interference resolution, there are still many inquiries lacking definitive answers. Moreover, most studies have predominantly focused on reactive forms of cognitive control from a conflict monitoring perspective, largely neglecting proactive and anticipatory mechanisms. To date, our understanding of proactive and reactive control primarily stems from fMRI studies and thus primarily regards its anatomical and functional organization. However, fMRI lacks the temporal resolution required to directly test the central tenet of the DMC, which emphasizes the distinct temporal dynamics characterizing proactive and reactive control. Techniques with high temporal resolution, such as EEG, are better suited for exploring these dynamics. Although a few EEG studies have attempted to dissociate proactive and reactive control by mainly focusing on ERPs, their findings remain inconclusive due to methodological heterogeneity. For instance, the direct manipulation of both mechanisms was not performed in studies like West and Bailey's (2012), where only proactive control was manipulated, and the ERP correlates for reactive control were inferred from the absence of proactive control.

To address these gaps, we explored ERP correlates of Stroop resolution. To overcome previous limitations, our experimental paradigm was carefully designed, incorporating methodological rigor to

effectively dissociate the correlates of proactive and reactive control. We employed a spatial Stroop task with perifoveal stimuli, manipulating the proportion of congruent trials (PC) at both the list-wide level (LWPC) and the item-specific level (ISPC). Indeed, previous literature suggests that manipulating LWPC reveals proactive control, while manipulating ISPC highlights reactive control. In contrast to prior studies, our approach introduced three key novelties. Firstly, we simultaneously manipulated LWPC and ISPC to examine their specific effects on Stroop effect resolution and explore their interplay. Secondly, we controlled for the well-known effect of contingency, manipulating it to be as orthogonal as possible to LWPC and ISPC, and included it as a predictor in our statistical model. Lastly, all analyses were conducted on the trial-level estimates of our variables, enabling a more realistic and fine-grained assessment of LWPC, ISPC, and confounding effects.

5.4.1. Advantages of our experimental manipulations and statistical approach

The behavioral results provided evidence for the advantages of our experimental paradigm and manipulations (in line also with Chapter 4 results). Indeed, given their innovative nature, we first tested them on the behavioral data to verify their assumed advantages and to make reasonable decisions about the subsequent EEG analyses. Of note, similar manipulations were also employed in our previous behavioral study. Thus, the present behavioral results, which were generally consistent with our previous results, contributed to strengthen our previous findings and were in turn based on more solid evidence.

In particular, we found that trial-level estimates of our variables were indeed more adequate than the block-level ones in reflecting temporal dynamics of cognitive control (and confounding) effects as, when we compared the continuous and discrete models, we found that the former better explained the data. These results confirmed our assumption that trial-level variables for LWPC and ISPC better account for cognitive control flexibility. Indeed, by taking into account the history of previous trials, our trial-level variables were dynamically updated trial-by-trial and created probabilistic expectations for PC of the upcoming trials, that, in turn, flexibly adjusted the control level to implement. In contrast, as explained in more details in the introduction, these flexible adjustments are instead not accounted for by traditional block-wise approaches. Moreover, trial-by-trial updating is also well-suited for variables such as contingency, which also relies on the trial history and needs to be updated continuously. Based on that, and to fully leverage our fine-grained manipulations, we decided to perform the subsequent EEG analyses testing only the continuous model.

An additional fundamental aspect of our design was that we simultaneously manipulated both proactive and reactive control, which allowed us to explore whether the two control mechanisms may co-exist. To leverage our experimental design, we used a multilevel modeling approach, which allowed us to test our

two experimental effects of interest at the same time[16]. As such, our finding that proactive control was significant, even when reactive control was present, suggests the existence of a distinguishable form of control implemented proactively to modulate the behavioral performance. On the other hand, we did not find the behavioral markers for reactive control, in line with our prior study results (see Chapter 4) highlighting that, in contrast to the strong Stroop effect modulation exerted by proactive control alone, reactive control effect on the Stroop effect was only indirect, that is, it exerted its effect by modulating the impact of proactive control on the Stroop effect. However, when testing in the present study the three-way interaction to explore the potential interplay between proactive and reactive control, its effect was not significant, in contrast to our previous study (Chapter 4). This apparent inconsistency might be explained by the difference in the sample sizes between the two studies (N =175 vs N = 40), along with the fact that the three-way interaction we found in the previous study was not so large and, especially, not so robust.

To get a better insight into reactive control, we ran two control analyses, starting with testing the same model but after the removal of the three-way interaction, to verify whether it interfered with reactive control, by masking it. Not only this was not the case, as again reactive control did not emerge, but we also found that the model including the three-way interaction did not interfere with the estimation of any of the other effects, reason for which we decided to keep using the full model in the subsequent EEG analyses. The second control analysis was instead performed by removing from the model the predictor for contingency, since there is evidence in the literature suggesting that the ISPC manipulation is more commonly confused with contingency; thus, the assumed reactive interference resolution might be nothing but the effect of learning stimulus-response associations (e.g., Schmidt, 2007; Schmidt, 2019). As predicted, we found that, without controlling for contingency, the effect of reactive control was significant, indicating that, in the full model, contingency explained all the variance of reactive control. This result suggests that, when interference must be resolved in a reactive manner, no cognitive control but low-level learning is implemented. However, as highlighted in our previous behavioral study (Chapter 4), this appears to be a too extreme view, whereas a more moderate alternative interpretation could be plausible. We proposed that the effect of contingency is stronger than that of reactive control per se, but still reactive control can be strategically implemented, especially when proactive control is not engaged. Of note, given the present results, this remains a tentative interpretation due to the absence of a significant three-way interaction. This possibility could be however explored by comparing the resulting performance patterns predicted by the alternative models, since the effect of contingency should be opposite to that of reactive control, and this was the case. When contingency was in the model, the modeled behavioral pattern was in line with

[16] The use of multilevel modeling was not just the only way to simultaneously test proactive and reactive control, but it also allowed us to improve their estimates at the subject-level. Indeed, by including in the model also lower-level confounders, the estimates of proactive and reactive control were partialed out from their effects at the trial level, since intra-subject/inter-trial sources of variance that contribute to measurement error were explained (see also Chapter 3 for a more detailed discussion).

what predicted by the contingency hypothesis, that is, a better performance for high-PRS trials, regardless of congruency (i.e., no Stroop effect differences). In contrast, with the no-contingency model, the significant effect of reactive control was accompanied by a modeled pattern consistent with a control-induced Stroop effect resolution, opposite to the other, that is, a larger Stroop effect when ISPC was higher. To summarize, our results thus confirm the idea that overlooking the effect of contingency unavoidably poses the risk that results are misleadingly attributed to cognitive control, while in fact were driven by contingency. However, this notwithstanding, we leave open the possibility that Stroop interference is resolved also via a reactive control mechanism.

This leads to the third advantage of our study, which specifically regards the statistical approach. Indeed, given the fundamental effect of contingency, as shown also by its large effect size (d = -1.36), by varying contingency and including it in the statistical model, we effectively partialled its effect out, ensuring that proactive and reactive control results did not reflect the effect of contingency. Therefore, we confirmed what was found in our previous studies (Viviani et al., 2023; Chapter 4), that is, the advantage of using multilevel modeling approach to control for the effect of possible confounders. The latter, in our case, were not only contingency but also response probability and lower-level ones.

5.4.2. Control-related stimulus ERPs

Our results regarding the ERPs locked to the stimulus revealed some control-related effects, each composed of distinct ERP components appearing at different times in the post-stimulus time window.

Starting with congruency, in the early time-window, we found two components associated with visuo-spatial attentional processes. First, we found a negative deflection over bilateral posterior electrodes, greater for Congruent trials, whose pattern resembles that of the N170 (also called visual N2, N2p or N2pb) found for example by Soltész et al. (2011) and Zurrón et al. (2013). This finding suggests an enhanced processing of visual characteristics of the target when it is made of two compatible features, such as in the Congruent condition. Additionally, we found a frontal positive deflection greater for Congruent stimuli and also reflecting heightened processing of congruent stimuli, a finding aligning with previous studies labeling this pattern as P2 component (Szűcs & Soltész, 2010). Moreover, we found that the amplitude of the P2 component explained the behavioral performance, with higher amplitude correlating with shorter RTs.

Compared to Stroop ERP literature, we did not find any early conflict-related component such as the fronto-central N2, which is characterized by greater negative amplitude for Incongruent stimuli (Folstein & Van Petten, 2008; Larson et al., 2014). This notwithstanding, we found that the behavioral performance was modulated by a frontal negative component and, when its amplitude was higher, RTs increased. This

significant correlation might reflect the effect of the conflict-related frontal N2, based on their spatio-temporal patterns, whose significant effect might have been masked by the stronger effect of P2.

Two other components modulated by Congruency and with a more clear conflict-related pattern were then observed in a later time window (from about 250 to 430 ms) that actually included two clusters related to the same ERPs. In particular, we found a positive centro-parietal P3-like component whose amplitude was attenuated in Incongruent relatively to Congruent trials. This pattern aligns with ERP literature on interference processes and strictly resembles the medial parietal negativity (MPN) found by West & Bailey (2012), the P3 found by West & Alain (2000), Zurrón et al. (2013) and Vurdah et al. (2023), the N450 found by Tillman & Wiens (2011) and Lansbergen & Kenemans, (2008; see also Di Russo & Bianco, 2023) and the Ninc of Appelbaum et al. (2014). Although with different labels, this component, which we will call P3-like, seems to be related to conflict processing in a peculiar way. Indeed, when participants do not experience interference, such as in Congruent trials, no P3 amplitude attenuation was observed, whereas the occurrence of interference, such as in Incongruent trials, induced a "negative deflection of the P3 wave" (West & Alain, 2000). This more difficult processing of the stimulus due to the experienced conflict calls for the intervention of cognitive control (e.g., Vurdah et al., 2023); this attenuation would thus reflect conflict processing (e.g., Zurrón et al., 2013) and possibly the activation of processes involved in response conflict (e.g., Tillman & Wiens, 2011). The P3 amplitude attenuation observed in Incongruent trials could also be explained in light of the results of the RIDE analyses performed on the latency of the cognitive component of the ERP, which likely correspond to our P3-like ERP component. Indeed, the later latencies we found for incongruent compared to congruent trials, which would reflect a delayed engagement of P3-related cognitive processes due to conflict processing in Incongruent trials, might have caused the P3 attenuation observed in those trials.

Moreover, the neural generators of the P3-like component were found to be located in a large cluster of medial parietal and frontal regions, including also the ACC, confirming the role of this latter region in conflict evaluation and processing (e.g., Lansbergen & Kenemans, 2008). Specifically, we found that this cluster of regions was more active during incongruent trials, suggesting its role in detecting conflict and subsequently modulating other regions, whose activity was reflected in the attenuation of the P3-like component. Our interpretation is further supported by our correlation results showing that the amplitude of the P3-like component was positively related to the behavioral performance. This suggests that participants' performance was unaltered when the P3-like amplitude was the largest, but it dramatically worsened as a function of the P3-like amplitude attenuation, which thus would reflect conflict processing. This finding seems in line with Zurrón et al. (2013), who showed that the P3 amplitude correlated negatively with task difficulty.

Along with the P3-like component, we found a lateral frontal negativity (LFN) resembling the pattern of the P3-like component but with a reversed polarity. Indeed, its amplitude was again reduced for Incongruent trials, which showed less negativity. A component with a similar scalp distribution and with the same pattern was identified by West & Alain (2000), who classified it as the reversed polarity of the N450 and by Lansbergen & Kenemans (2008) who, by computing the difference wave, labeled it as P450. Similarly to the P3-like, the positive deflection observed in the LFN seems to reflect the engagement of conflict evaluation processes reflected in medial parietal and frontal activity. Again, also the amplitude of this component was positively related to performance with the same pattern as that observed for the P3-like component.

Two later LP components were also found to be modulated by Congruency from approximately 480 to 750 ms. These two waves appear to be the descending/ascending part following the P3-like and LFN components, respectively, as suggested by the temporal contiguity, but, as opposed to the previous ones, they showed the reversed pattern for Congruent vs Incongruent trials. Indeed, the later parietal component revealed a more sustained positivity for Incongruent trials, whereas the frontal one showed a more sustained negativity for Incongruent trials. Moreover, their amplitude was negatively related to performance, further suggesting that the enhanced sustained positivity/negativity during Incongruent trials induced slower responses. Both these LP components are consistent with previous findings. For instance, Appelbaum et al. (2014) found a similar positive potential deflection over parietal areas, labeled as late positive component (LPC), whereas Lansbergen & Kenemans (2008) identified both a parietal and a frontal component, referred to as sustained potential (SP), negative-SP and positive-SP, respectively. These LPs have been interpreted as signaling the need for increased recruitment of cognitive control and conflict resolution (Appelbaum et al., 2014; Larsen et al., 2006; West & Bailey, 2012). Moreover, they might reflect interference resolution as suggested also by the cortical localization of their sources which was found in the dorsal ACC and dorso-medial PFC. Our results are consistent with what was found by Lansbergen & Kenemans (2008), that is, a similar cortical localization in the ACC. Based on that, they proposed that the earlier P3-like and the later LP have a common origin, as they are elicited in the same brain regions but by slightly different neural populations. In line with these findings, our P3-like and LP results seem to reflect different stages of Stroop interference resolution, with the former involved in early conflict processing/monitoring and the latter in subsequent and more complex conflict resolution processes.

After 800 ms, the LP component pattern continued but shifted to different scalp areas, with the sustained positivity for Incongruent trials becoming more temporal and the sustained negativity becoming more fronto-medial. These components were found to be elicited by insular regions and might reflect later task-related cognitive control level assessment and readjustment (Appelbaum et al., 2014; Larsen et al., 2006), which could imply the computation of the current PC level and its updating.

Proactive control modulation of the ERPs partially overlaps that by Congruency, as indicated by the fact that most of the ERP components of Congruency were also modulated by proactive control. This is in line with the prediction that Congruency ERPs are modulated differently depending on the specific amount of exerted proactive control.

Specifically, proactive control modulated the two same conflict-related components found for Congruency, namely the P3-like and the LFN, in the same time-window. As compared to the P3-like and LFN Congruency modulation, we found a slight difference in the scalp distribution of their proactive control modulations, with more lateral clusters. Additionally, the P3-like component was left-lateralized, whereas the LFN was more right-lateralized. Of note, the association between a frontal component and proactive control has been found also by previous studies, such as West & Bailey (2012) (i.e., MFN) and Appelbaum et al. (2014) (Ninc), but their components were observed more medially.

More in detail, we found that the P3-like pattern was consistent with our predictions, as Stroop effects were larger when proactive control was low, due to a greater positive deflection for Congruent trials and a more attenuated positivity for Incongruent trials for high-LWb trials. This indicates that, when a low level of proactive control was implemented, the P3-like component was emphasized during congruent trials. By contrast, its greater negative deflection during incongruent trials may signal the processing of the unexpected conflict and the sudden need of a greater amount of control, which could be implemented only in a reactive manner. A similar interpretation could account for the proactive control modulation of the LFN, as the attenuated negativity for Incongruent trials during low proactive control conditions might reflect unexpected conflict processing. On the other hand, for both components, when proactive control was high, no dramatic amplitude attenuation was observed, as the higher conflict probability made participants readier to face interference. In line with the DMC, when the probability of conflicting trials is higher, participants can establish in advance a task context on which they rely on, filtering out the irrelevant information. In contrast, when conflicting trials are less probable, it is more beneficial to rely on the conceptual information, as it is frequently equivalent between task-relevant and task-irrelevant information (see also West & Alain, 2000). As such, in high conflicting conditions, as participants engage in proactive control and do not require a late correction, no amplitude attenuation is needed. When instead they face unexpected conflict, the need for further conflict resolution processes is subserved by the amplitude attenuation. This proposed functional role of the P3/LFN amplitude attenuation reflecting (unexpected) conflict processing is also perfectly in line with the observed brain-behavior correlations we discussed above, as in high-LWb conditions the Congruent trials, showing the largest P3/LFN amplitudes, are those with the best performance, whereas the Incongruent trials, showing the most marked P3/LFN amplitude attenuation, are those with the worst performance.

However, no effect of proactive control was found for earlier visual-attentional processes (i.e., neither on N170 or P2 modulation), which is quite unexpected due to the nature of this control mode that, by definition, should affect early perceptual and attentional processes. However, we hypothesized that the processes of proactive control are evident later in time because, to be implemented, they require a representation of the global conflict likelihood. However, univariate approaches like those employed here are not sensitive to representations, which, by being encoded at the brain level through distributed multivariate activity patterns, require analytical approaches suitable for that, such as multivariate pattern analysis (Freund et al., 2021). This issue will be further introduced in the conclusions and addressed in Chapter 6.

In a slightly later time-window (from about 340 to 440 ms), proactive control modulated a right temporo-parietal component which revealed a different pattern as compared to the previous waves. Specifically, when proactive control was low, Congruent trials elicited a more positive deflection, whereas when it was high, Incongruent trials elicited a positive deflection. This finding might be related to the relative probability associated with the two different LWPC conditions, so that the higher amplitude was associated with the Congruency conditions that was more probable in each LWPC conditions. Therefore, this component does not seem to be specifically related to conflict processing. Instead it reflects the higher readiness to the stimuli that are more probable in each condition (i.e., congruent when LWPC is high, incongruent when LWPC is low).

As for Congruency, we found a proactive control modulation for two later conflict-induced LP waves, which again reflected the descending and ascending parts of the P3-like and LFN, respectively. The parietal and the frontal LPs were characterized by larger Stroop effects when proactive control was low and by a more sustained positivity/negativity during Incongruent trials in the low proactive control condition. Additionally, they negatively correlated with the behavioral performance, with higher amplitudes associated with longer RTs. This pattern is similar to the one found for Congruency and can thus be interpreted in terms of interference resolution. This notwithstanding, the presence or absence of a proactive control modulation induced a different need of interference suppression. Indeed, when proactive control is high and conflict is expected, less conflict resolution is required since interference is resolved in a more anticipatory manner. On the other hand, when proactive control is lacking, Incongruent trials require a greater amount of cognitive control to resolve the unexpected interference, and this might be subserved by the higher amplitudes of the LPs observed here. Such results are in line for example with those by Appelbaum et al. (2014), who also found that low proactive control induced an increase of the parietal LP component (called LPC), corroborating our assumption that the enhanced LP amplitude signals the need of greater conflict processing due to the reduced level of preparatory proactive control.

5.4.3. Control-related response ERPs

Our response-locked ERP results revealed three congruency-dependent modulations of ERP components appearing at distinct time windows.

First, in a pre-response time-window, we found a parietal positivity paralleled by a mid-frontal negativity, which were both more marked for Incongruent trials. In particular, the latter ERP component would correspond to the so-called mid-frontal pre-response negativity (PRN) or N-40, which has been observed only when a choice between alternative responses has to be made (Vidal et al., 2011), reflecting response conflict. This ERP component was thus proposed to reflect response selection (Carbonnell et al., 2013; Vidal et al., 2003), especially when it is more challenging, that is, when there is response conflict due to concurrent activation of incorrect responses (Burle et al., 2016). We thus interpret the more marked PRN we observed in Incongruent trials as a marker of the detection of the conflict at the response level. This interpretation is further supported by our correlation results showing that the amplitude of the PRN component was negatively related to the behavioral performance, indicating that participants' performance was unaltered when the PRN amplitude was the largest, but it dramatically improved as a function of the PRN amplitude attenuation. This is in line with the finding that no (or, at least, a strongly attenuated) PRN is observed when there is no response conflict and thus no response selection is required (Vidal et al., 2011), like in Congruent trials in our study, leading to faster responses.

We also found a congruency-dependent modulation of ERPs just before the response, with a bilateral parietal positivity coupled with a polar and bilateral frontal negativity that were more marked for congruent trials. These ERPs also correlated with participants' behavioral performance, with participants showing slower responses when the neural signatures reflected by the ERPs were weaker. We also found the cortical sources of these Stroop ERPs to be distributed over ventrolateral and opercular prefrontal areas, which are known to mediate response selection and inhibition. These results thus indicate that the observed ERPs components are likely associated with the efficiency and accuracy of response execution, and suggest that they could also reflect final stages of Stroop interference resolution related to response-response competition (e.g., see Chen et al., 2011).

Finally, we found a congruency-dependent modulation of post-response ERPs, with a posterior positivity coupled with a mid-frontal negativity, both more marked for Incongruent trials. In particular, the latter ERP component would correspond to the so-called correct-related negativity (CRN, Grützmann et al., 2014; Vidal et al., 2000), an ERP component proposed to reflect response evaluation processes, in particular those related to post-response conflict monitoring and uncertainty about response correctness (Vastano et al., 2020), which are more relevant in Incongruent trials.

However, our results also showed that the Stroop effects we found for the response-locked ERPs were not significantly modulated by our PC manipulations. At first sight, these negative results, especially that related to the PRN, are in contrast with a recent mouse-tracking-EEG coregistration study from our lab (Tafuro et al., 2020), in which we found larger PRN Stroop effects for low-PC trials. That finding indeed suggested that PRN may reflect a "reactive control brake" to suppress an incorrect motor plan (i.e., a mouse movement in that case) and thus counteract the interference at the response level to provide the correct response, in line with the proposed role of the PRN as a marker of reactive control engagement (e.g., Czernochowski et al., 2010). However, it should be noted that our previous finding was specifically related to the suppression of an ongoing motor act (i.e., the peak deceleration of a mouse movement), while here we analyzed ERPs locked at participants' RTs, which constitute the final outcome of the Stroop interference resolution and reflect a response output (i.e., a key press) that cannot (easily) be corrected. Therefore, the lack of ISPC-dependent modulations of the PRN Stroop effect could also indicate that our manipulations assessing the cognitive control modulation of Stroop interference in our study mostly targeted stimulus–stimulus competition at the stimulus processing stage (i.e., the stimulus locus, Parris et al., 2022; see also De Houwer, 2003; Zhang & Kornblum, 1998), rather than response-response competition at the response selection stage (i.e., the response locus), which instead likely was the primary target of cognitive control in our previous mouse-tracking-EEG study. It is important here to note that our ISPC modulation specifically targeted the type of reactive control mechanism mediated by the fast stimulus-attention association, which is assumed to act before the response selection stage (Tafuro et al., 2020; Bugg, 2012, 2017; Bugg & Hutchison, 2013). This point will be addressed more in detail in the conclusions.

5.4.4. Control-related stimulus ERSPs

Our results regarding the ERSPs locked to the stimulus revealed two main control-related effects, that is, Congruency and proactive control.

Congruency-dependent ERPS modulations were also quite in line with what was found for ERPs. In discussing our ERPS results, we will thus try to link them not only to the available ERSP literature, but also to the ERP components we identified.

Starting with Theta frequency, the early cluster found over bilateral frontal and right parietal scalp regions, revealing a greater power increase for Congruent trials, probably reflects the Theta involvement in both visuo-spatial attentional processing of the target and performance enhancement.

Firstly, the enhanced power increase for Congruent trials can be related to the N170 component that we found in similar scalp regions (i.e., posterior electrodes), which we explained as enhanced visual processing in case of two compatible features, such as Congruent trials (Soltész et al., 2011; Zurrón et al., 2013). The

relation between this Theta congruency modulation and the N170 component is also supported by a previous work by Freunberger and colleagues (2011), showing that Theta modulated the N170 component in parieto-occipital regions (they called it visual P2). Moreover, our finding is also in line with ERPS literature, that has provided evidence for the functional role of Theta band in enhancing target processing, as shown by works revealing the involvement of this frequency in conscious target perception and procedural resource allocation during visual perception (Slagter et al., 2009; van Vugt, 2014).

Secondly, the greater Theta power increase for Congruent trials is consistent with our frontal P2 component, whose greater amplitude correlated with better performance, probably suggesting a Theta modulation of the P2 component as well. This interpretation is also in line with the acknowledged functional role of phasic Theta in working memory and performance enhancement (Klimesch, 1999).

Moreover, for its spatio-temporal pattern, the same result, namely the greater decrease in Theta power for Incongruent trials, can be linked to our P3 component as well, which also showed an amplitude attenuation for Incongruent trials. This interpretation is in line with the proposed role of Theta activity in mediating the P3 component (e.g., Başar et al., 2001; Demiralp et al., 2001). As such, we speculate that the Theta modulation we found could also reflect the processing of unexpected conflict, in line with our interpretation of the P3 functional role.

In the later cluster that we found over similar scalp regions, Theta frequency modulation of Congruency showed instead a greater steady relative decrease in power for Congruent trials. This finding, which could be related to the frontal and parietal LP ERP components, is likely to reflect the later functional role of Theta frequency in increasing the recruitment of cognitive control and conflict resolution.

Theta frequency was involved in signaling the need for control recruitment also in an earlier cluster, observed at around the response, over mid-fronto-central and right temporal clusters, as suggested by the greater power increase for Incongruent trials. This results, which is in line with classical findings of mid-frontal Theta increase for Incongruent trials, might also reflect the oscillatory activity underlying the frontal N2 that we found to modulate behavioral performance, which, by showing greater negative amplitude for Incongruent trials, was also associated to conflict-related processing.

The other analyzed frequencies modulated Congruency as well, revealing greater Alpha and Beta power reduction for Incongruent trials, starting from approximately 300 ms and sustained in time (till 850 ms). This power suppression was observed over right prefrontal scalp regions and over bilateral parieto-occipital scalp regions, with a more medial distribution for Beta bands. This finding is partially consistent with that found by Tafuro and colleagues (2019), who suggested the functional role of especially Beta2 and Beta3 frequencies in selecting the task-relevant information during interference resolution. Moreover, the congruency-dependent Alpha modulation we found in lateral parieto-occipital scalp regions is in line with

the functional role of this frequency band in the integration of stimulus perceptual information to activate the relevant task-set (S-R rule) and response (Nurislamova et al., 2019), and in goal-directed suppression of the irrelevant spatial information (Cohen & Ridderinkhof, 2013).

Proactive-dependent ERPS modulations were also consistent with our ERP results, revealing that proactive control modulation affected similar conflict-related ERSPs found for Congruency. Specifically, the greater Alpha and Beta1 power reduction found for Incongruent trials in the high-LWb condition over right parieto-occipital scalp regions partially overlapped at the spatial level with the congruency-dependent Alpha suppression for Incongruent trials discussed above, which however showed a more bilateral pattern. This more pronounced power suppression for Incongruent trials when proactive control was low might have the functional role of signaling the need of a greater amount of cognitive control to resolve the interference, required because conflict was unexpected. In contrast, when proactive control was high, such power suppression was not required as participants, by expecting a higher conflict probability, were readier to resolve interference of Incongruent trials. The same pattern was also found for Beta2 and Beta3 suppression but over more mid-central scalp regions, revealing the functional role of Beta2 and Beta3 frequency bands as well in signaling the need of a greater control recruitment in case of unexpected conflict. Moreover, this modulation implied the same scalp regions observed for congruency-related Beta2 and Beta3 ERSPs. Overall, these proactive control-related modulations of ERPSs can be related to the corresponding modulation we found for the P3-like component. Indeed, the greater P3-like attenuated positivity for Incongruent high-LWb trials might rely on the greater power suppression of Alpha and Beta frequencies found for the same condition, as suggested also by their similar distribution over centro-posterior scalp regions. This interpretation is further supported by findings showing the role of Alpha suppression in generating the P3 component (Bernat et al., 2007).

These ERSP results, complementing and validating the modulation pattern found for ERPs, offer valuable insights into the functioning of proactive control. In fact, both analyses revealed that this modulation directly affected congruency correlates, as demonstrated by the involvement of similar correlates in both congruency-related and proactive control-related ER(S)Ps. Notably, while the modulation for ERPs shares temporal characteristics, the proactive control modulation in ERSPs seems to occur slightly later in time.

5.4.5. Control-related response ERSPs

Our results regarding the ERSPs locked to the response revealed only the control-related effect of Congruency, with a peculiar pattern. We found a Theta and Alpha greater power increase for Incongruent trials in an early pre-response time window over bilateral parieto-occipital and prefrontal scalp regions, followed by an inversion of the power pattern over the same regions till the response. These results may indicate the involvement of these low-frequency EEG oscillations in mediating conflict processing to guide

behavior. This interpretation is in line with the role of lower frequencies, and especially Theta, in mediating the integration and prioritization of information to enable goal-directed control processes, like the selection of the relevant task set (Capizzi et al., 2020; Cooper et al., 2015), by promoting parieto-frontal information transfer and integration (e.g., Sauseng et al., 2010) in an earlier phase of conflict processing. Our interpretation is also supported by the fact that the congruency-dependent Alpha modulation we found just before the response was consistent with the corresponding effect we found in the stimulus-locked analysis, also reflecting the integration of perceptual information to select the relevant task set and response (see above).

We also found a congruency-dependent effect for higher frequencies, with a greater suppression of Beta power in an early pre-response time window also involving bilateral parieto-frontal scalp regions. This result further supports our interpretation of the role of Beta EEG oscillations in selecting the task-relevant information to resolve Stroop interference.

5.5. Summary and conclusions

To sum up, our complex pattern of results provides interesting insights into control-related Stroop effect modulations while both control modes were explicitly manipulated.

The first key finding regards proactive control, for which we identified the specific ER(S)P correlates. Indeed, in line with DMC predictions, we found that proactive control exerted a modulatory influence on the same ER(S)P components found for Congruency. When low-LWPC elicited higher proactive control, thanks to anticipatory attentional allocation, the Stroop effect was reduced; when instead the high-LWPC did not induce a proactive control modulation, such anticipatory strategies were not implemented. To be noted that proactive control correlates were observed after partialling out the effect of all the other predictors, including ISPC and contingency, thus more genuinely reflecting the specific effect of proactive control only. What instead is not so consistent with the DMC predictions, is the temporal/functional dynamic of the proactive control ER(S)P we found. Indeed, given the early and anticipatory nature of this control mode, we expected to find earlier LWPC-dependent modulations of processes preceding conflict detection and reflecting the assumed proactive mechanisms, even before stimulus appearance (see e.g., Bianco et al., 2021, showing control-related modulations of different pre-stimulus ERPs; see also Perri et al., 2021). These effects should occur in addition to what we observed, that is, the ER(S)P correlates engaged when proactive control was low and interference could not be anticipated. Our interpretation for the absence of such a finding is that interference anticipation more strongly relies on the representation of the global likelihood of conflict, which however cannot be explored using the analytical techniques employed in this study (see below).

Second, it is worth discussing more in depth what we found for reactive control. Although we observed that the effect of contingency manipulation overshadowed the impact of reactive control, this was not true for reactive control in general. Specifically, we believe that a distinction should be made between ISPC-induced reactive control and reactive control as a late correction mechanism per se. When reactive control results from the ISPC manipulation, it reflects stimulus-attention associations, with each item inducing a specific attentional modulation based on its PC (Tafuro et al., 2020; Bugg, 2012, 2017; Bugg & Hutchison, 2013). Thus, by knowing that conflict is more probable for items with low-PC, participants can implement attentional strategies that are reactive in nature, as first the stimulus must be seen, but they can potentially start being executed even before conflict detection since they only require stimulus identity as input. Therefore, the fact that ISPC and contingency effects are hard to disentangle can be due to their similarity, also in terms of temporal characteristics. Indeed, also the effect of contingency, by implying that each stimulus elicits more or less strongly a response based on previous stimulus-response associations, can start immediately after stimulus appearance. As such, after seeing each stimulus, both these two alternative strategies could be activated, but probably the early reactive control modulation induced by ISPC is not so strong to survive while controlling for the other. This notwithstanding, we were able to observe ER(S)P correlates of a second form of reactive control (i.e., a greater P3-like attenuation, a greater and more sustained Alpha/Beta1 right posterior suppression, and a greater and more sustained Beta2-3 central suppression for high-LWPC incongruent stimuli). Indeed, we found that a later reactive control mechanism came into play when other control processes failed, that is, when proactive control was low, incongruent trials elicited unexpected conflict, consequently activating cognitive control mechanisms at a later stage to resolve such interference. This second reactive control type thus resembles that of the conflict monitoring and DMC accounts and is more purely reactive in nature.

Moreover, ISPC-induced control, by prompting attentional strategies immediately after stimulus presentation, is likely to act on the stimulus locus of the Stroop task. Therefore, it should not be observed at the response level either, in line with our results. Since our experimental design did not allow us to clearly disentangle the effects of ISPC on stimulus versus response loci (Parris et al., 2022), we were unable to observe a significant ISPC-related effect, probably because its small effect was masked by the effect of contingency. Further studies are warranted to explore this issue more comprehensively.

Alternatively, the absence of observable ISPC-related reactive control may be that due to the fact that it operates at a representation level, which the univariate analyses performed here cannot detect. Specifically, classical univariate approaches, by abstracting a limited number of experimental factors, can only shed light on what occurs at the process level, that is, whether the process is present or absent (alternatively, more or less engaged), neglecting dynamic modulations induced by representations, which instead are the core of most cognitive control theories, including the DMC. Indeed, PC-dependent modulations in general are likely

to rely on representations, which are distributed and high-dimensional patterns in the brain containing the required information for dynamically modulating the control level to execute (Freund et al., 2021). In the present study, we made a step in that direction, by manipulating our variables trial-by-trial, thus obtaining more dynamic estimates to be used in the analysis. This however is not enough, and more sophisticated multivariate techniques are needed to explore it effectively. This approach, in addition to providing insights into ISPC-induced reactive control, could also shed light on the early representations required for proactive control to anticipate interference, as highlighted above. Based on that, future studies using multivariate analytical methods should be conducted to directly explore cognitive control representations, and this is exactly the topic of Chapter 6.

One last point regards the consistent absence of a three-way interaction between proactive and reactive control in the modulation of the Stroop effect. Although we found it in our prior behavioral study (see Chapter 4), such finding appears to be elusive and not robust enough to draw conclusions on it. Moreover, our interpretation of results regarding reactive control leaves open the possibility that such three-way interaction exists but, by testing such interaction including only the ISPC-dependent reactive control and not the later reactive control form, we could not observe it here. As such, this hypothesis should be tested in future studies using either reactive control manipulations specifically targeting the response locus or measures assessing the conflict at the response selection stage.

To conclude, our study provides valuable insights into the ER(S)P correlates of proactive and reactive cognitive control during Stroop interference resolution. It highlights the significant influence of proactive control on interference resolution and sheds initial light on the distinction between ISPC-related and late correction reactive control mechanisms. The absence of observable ISPC-related effects could be attributed to the confounding effect of the contingency manipulation, the potential stimulus locus of ISPC-related control, or the reliance on representations that may not be readily detected by univariate analyses. Further investigations employing more refined multivariate techniques are warranted to elucidate these mechanisms more comprehensively and enhance our understanding of cognitive control processes.

5.6. References

Appelbaum, L. G., Boehler, C. N., Davis, L. A., Won, R. J., & Woldorff, M. G. (2014). The dynamics of proactive and reactive cognitive control processes in the human brain. Journal of cognitive neuroscience, 26(5).

Baayen, R. H., Davidson, D. J., & Bates, D. M. (2008). Mixed-effects modeling with crossed random effects for subjects and items. Journal of memory and language, 59(4).

Baayen, R., & Milin, P. (2010). Analyzing reaction times. International Journal of Psychological Research, 3(2). https://doi.org/10.21500/20112084.807

Baillet, S., Riera, J., Marin, G., Mangin, J., Aubert, J., & Garnero, L. (2001). Evaluation of inverse methods and head models for EEG source localization using a human skull phantom. Physics in medicine & biology, 46(1).

Başar, E., Başar-Eroglu, C., Karakaş, S., & Schürmann, M. (2001). Gamma, alpha, delta, and theta oscillations govern cognitive processes. International Journal of Psychophysiology, 39(2), 241–248. https://doi.org/10.1016/S0167-8760(00)00145-8

Bernat, E. M., Malone, S. M., Williams, W. J., Patrick, C. J., & Iacono, W. G. (2007). Decomposing delta, theta, and alpha time–frequency ERP activity from a visual oddball task using PCA. International Journal of Psychophysiology, 64(1), 62–74. https://doi.org/10.1016/j.ijpsycho.2006.07.015

Bianco, V., Berchicci, M., Mussini, E., Perri, L. V., Quinzi, F., and Di Russo, F.. "Electrophysiological evidence of anticipatory cognitive control in the stroop task." Brain Sciences 11, no. 6 (2021): 783.

Botvinick, M. M., Braver, T. S., Barch, D. M., Carter, C. S., & Cohen, J. D. (2001). Conflict monitoring and cognitive control. Psychological review, 108(3).

Braem, S., Bugg, J. M., Schmidt, J. R., Crump, M. J., Weissman, D. H., Notebaert, W., & Egner, T. (2019). Measuring adaptive control in conflict tasks. Trends in cognitive sciences. https://doi.org/10.1016/j.tics.2019.07.002

Braver, T. S. (2012). The variable nature of cognitive control: A dual mechanisms framework. Trends in cognitive sciences, 16(2).

Braver, T. S., Gray, J. R., & Burgess, G. C. (2007). Explaining the many varieties of working memory variation: Dual mechanisms of cognitive control. Variation in working memory, 75, 106.

Braver, T. S., Kizhner, A., Tang, R., Freund, M. C., & Etzel, J. A. (2021). The Dual Mechanisms of Cognitive Control Project. Journal of Cognitive Neuroscience, 33(9), 1990–2015. https://doi.org/10.1162/jocn_a_01768

Bugg, J. M. (2012). Dissociating Levels of Cognitive Control: The Case of Stroop Interference. Current Directions in Psychological Science, 21(5), 302–309. https://doi.org/10.1177/0963721412453586

Bugg, J. M. (2017). Context, conflict, and control. The Wiley handbook of cognitive control, 79–96.

Bugg, J. M., & Crump, M. J. (2012). In support of a distinction between voluntary and stimulus-driven control: A review of the literature on proportion congruent effects. Frontiers in psychology, 3, 367. https://doi.org/10.3389/fpsyg.2012.00367

Bugg, J. M., & Hutchison, K. A. (2013). Converging evidence for control of color–word Stroop interference at the item level. Journal of Experimental Psychology: Human Perception and Performance, 39(2).

Burle, B., van den Wildenberg, W. P. M., Spieser, L., & Ridderinkhof, K. R. (2016). Preventing (impulsive) errors: Electrophysiological evidence for online inhibitory control over incorrect responses. Psychophysiology, 53(7), 1008–1019. https://doi.org/10.1111/psyp.12647

Capizzi, M., Ambrosini, E., Arbula, S., & Vallesi, A. (2020). Brain oscillatory activity associated with switch and mixing costs during reactive control. Psychophysiology, 57(11), e13642. https://doi.org/10.1111/psyp.13642

Carbonnell, L., Ramdani, C., Meckler, C., Burle, B., Hasbroucq, T., & Vidal, F. (2013). The N-40: An electrophysiological marker of response selection. Biological Psychology, 93(1), 231–236. https://doi.org/10.1016/j.biopsycho.2013.02.011

Cavanagh, J. F., & Frank, M. J. (2014). Frontal theta as a mechanism for cognitive control. Trends in cognitive sciences, 18(8).

Chen, A., Bailey, K., Tiernan, B. N., & West, R. (2011). Neural correlates of stimulus and response interference in a 2-1 mapping stroop task. International Journal of Psychophysiology: Official Journal of the International Organization of Psychophysiology, 80(2), 129–138. https://doi.org/10.1016/j.ijpsycho.2011.02.012

Cohen, M. X., & Ridderinkhof, K. R. (2013). EEG source reconstruction reveals frontal-parietal dynamics of spatial conflict processing. PloS One, 8(2), e57293. https://doi.org/10.1371/journal.pone.0057293

Cooper, P. S., Wong, A. S., Fulham, W. R., Thienel, R., Mansfield, E., Michie, P. T., & Karayanidis, F. (2015). Theta frontoparietal connectivity associated with proactive and reactive cognitive control processes. Neuroimage, 108, 354–363.

Czernochowski, D., Nessler, D., & Friedman, D. (2010). On why not to rush older adults—Relying on reactive cognitive control can effectively reduce errors at the expense of slowed responses. Psychophysiology, 47(4), 637–646. https://doi.org/10.1111/j.1469-8986.2009.00973.x

Delorme, A., & Makeig, S. (2004). EEGLAB: an open source toolbox for analysis of single-trial EEG dynamics including independent component analysis. Journal of neuroscience methods, 134(1).

De Houwer, J. (2003). On the role of stimulus-response and stimulus-stimulus compatibility in the Stroop effect. Memory & Cognition, 31(3).

Demiralp, T., Ademoglu, A., Comerchero, M., & Polich, J. (2001). Wavelet analysis of P3a and P3b. Brain Topography, 13(4), 251–267. https://doi.org/10.1023/a:1011102628306

De Pisapia, N., & Braver, T. S. (2006). A model of dual control mechanisms through anterior cingulate and prefrontal cortex interactions. Neurocomputing, 69(10–12).

Di Russo, F., & Bianco, V. (2023). Time Course of Reactive Brain Activities during a Stroop Color-Word Task: Evidence of Specific Facilitation and Interference Effects. Brain Sciences, 13(7), 982.

Eisma, J., Rawls, E., Long, S., Mach, R., & Lamm, C. (2021). Frontal midline theta differentiates separate cognitive control strategies while still generalizing the need for cognitive control. Scientific Reports, 11(1). https://doi.org/10.1038/s41598-021-94162-z

Engel, A. K., & Fries, P. (2010). Beta-band oscillations—Signalling the status quo? Current opinion in neurobiology, 20(2).

Erdfelder, E., Faul, F., & Buchner, A. (1996). GPOWER: A general power analysis program. Behavior Research Methods, Instruments, & Computers, 28(1). https://doi.org/10.3758/BF03203630

Fan, L., Li, H., Zhuo, J., Zhang, Y., Wang, J., Chen, L., Yang, Z., Chu, C., Xie, S., Laird, A. R., Fox, P. T., Eickhoff, S. B., Yu, C., & Jiang, T. (2016). The Human Brainnetome Atlas: A New Brain Atlas Based on Connectional Architecture. Cerebral Cortex, 26(8), 3508–3526. https://doi.org/10.1093/cercor/bhw157

Fischl, B., Sereno, M. I., Tootell, R. B., & Dale, A. M. (1999). High-resolution intersubject averaging and a coordinate system for the cortical surface. Human brain mapping, 8(4).

Folstein, J. R., & Van Petten, C. (2008). Influence of cognitive control and mismatch on the N2 component of the ERP: A review. Psychophysiology, 45(1), 152–170. https://doi.org/10.1111/j.1469-8986.2007.00602.x

Freunberger, R., Werkle-Bergner, M., Griesmayr, B., Lindenberger, U., & Klimesch, W. (2011). Brain oscillatory correlates of working memory constraints. Brain Research, 1375, 93–102. https://doi.org/10.1016/j.brainres.2010.12.048

Freund, M. C., Etzel, J. A., & Braver, T. S. (2021). Neural Coding of Cognitive Control: The Representational Similarity Analysis Approach. Trends in Cognitive Sciences, 25(7), 622–638. https://doi.org/10.1016/j.tics.2021.03.011

Gramfort, A., Papadopoulo, T., Olivi, E., & Clerc, M. (2010). OpenMEEG: opensource software for quasistatic bioelectromagnetics. Biomedical engineering online, 9(1).

Grützmann, R., Riesel, A., Klawohn, J., Kathmann, N., & Endrass, T. (2014). Complementary modulation of N2 and CRN by conflict frequency. Psychophysiology, 51(8), 761–772. https://doi.org/10.1111/psyp.12222

Gutteling, T. P., Sillekens, L., Lavie, N., & Jensen, O. (2022). Alpha oscillations reflect suppression of distractors with increased perceptual load. Progress in Neurobiology, 214, 102285. https://doi.org/10.1016/j.pneurobio.2022.102285

Hanslmayr, S., Pastötter, B., Bäuml, K.-H., Gruber, S., Wimber, M., & Klimesch, W. (2008). The electrophysiological dynamics of interference during the Stroop task. Journal of Cognitive Neuroscience, 20(2).

Heidlmayr, K., Kihlstedt, M., & Isel, F. (2020). A review on the electroencephalography markers of Stroop executive control processes. Brain and Cognition, 146, 105637. https://doi.org/10.1016/j.bandc.2020.105637

Jensen, O., & Mazaheri, A. (2010). Shaping Functional Architecture by Oscillatory Alpha Activity: Gating by Inhibition. Frontiers in Human Neuroscience, 4. https://www.frontiersin.org/articles/10.3389/fnhum.2010.00186

Jiang, J., Heller, K., & Egner, T. (2014). Bayesian modeling of flexible cognitive control. Neuroscience & Biobehavioral Reviews, 46, 30–43. https://doi.org/10.1016/j.neubiorev.2014.06.001

Johnston, P., Robinson, J., Kokkinakis, A., Ridgeway, S., Simpson, M., Johnson, S., Kaufman, J., & Young, A. W. (2017). Temporal and spatial localization of prediction-error signals in the visual brain. Biological Psychology, 125, 45–57. https://doi.org/10.1016/j.biopsycho.2017.02.004

Klimesch, W. (1999). EEG alpha and theta oscillations reflect cognitive and memory performance: A review and analysis. Brain Research. Brain Research Reviews, 29(2). https://doi.org/10.1016/s0165-0173(98)00056-3

Kybic, J., Clerc, M., Abboud, T., Faugeras, O., Keriven, R., & Papadopoulo, T. (2005). A common formalism for the integral formulations of the forward EEG problem. IEEE transactions on medical imaging, 24(1).

Lansbergen, M. M., & Kenemans, J. L. (2008). Stroop interference and the timing of selective response activation. Clinical Neurophysiology: Official Journal of the International Federation of Clinical Neurophysiology, 119(10), 2247–2254. https://doi.org/10.1016/j.clinph.2008.07.218

Larsen, R. J., Mercer, K. A., & Balota, D. A. (2006). Lexical characteristics of words used in emotional Stroop experiments. Emotion (Washington, D.C.), 6(1), Articolo 1. https://doi.org/10.1037/1528-3542.6.1.62

Larson, M. J., Clayson, P. E., & Clawson, A. (2014). Making sense of all the conflict: A theoretical review and critique of conflict-related ERPs. International Journal of Psychophysiology, 93(3), 283–297. https://doi.org/10.1016/j.ijpsycho.2014.06.007

Lorch, R. F., & Myers, J. L. (1990). Regression analyses of repeated measures data in cognitive research. Journal of Experimental Psychology: Learning, Memory, and Cognition, 16(1). https://doi.org/10.1037/0278-7393.16.1.149

Mathys, C., Daunizeau, J., Friston, K. J., & Stephan, K. E. (2011). A bayesian foundation for individual learning under uncertainty. Frontiers in Human Neuroscience, 5, 39. https://doi.org/10.3389/fnhum.2011.00039

Mückschel, M., Stock, A.-K., Dippel, G., Chmielewski, W., & Beste, C. (2016). Interacting sources of interference during sensorimotor integration processes. NeuroImage, 125, 342–349. https://doi.org/10.1016/j.neuroimage.2015.09.075

Nurislamova, Y. M., Novikov, N. A., Zhozhikashvili, N. A., & Chernyshev, B. V. (2019). Enhanced Theta-Band Coherence Between Midfrontal and Posterior Parietal Areas Reflects Post-feedback Adjustments in the State of Outcome Uncertainty. Frontiers in Integrative Neuroscience, 13, 14. https://doi.org/10.3389/fnint.2019.00014

Ouyang, G., Sommer, W., & Zhou, C. (2015). A toolbox for residue iteration decomposition (RIDE)—A method for the decomposition, reconstruction, and single trial analysis of event related potentials. Journal of Neuroscience Methods, 250, 7–21. https://doi.org/10.1016/j.jneumeth.2014.10.009

Parris, B. A., Hasshim, N., Wadsley, M., Augustinova, M., & Ferrand, L. (2022). The loci of Stroop effects: A critical review of methods and evidence for levels of processing contributing to color-word Stroop effects and the implications for the loci of attentional selection. Psychological Research, 86(4), 1029–1053. https://doi.org/10.1007/s00426-021-01554-x

Perri, R. L., Bianco, V., Facco, E., & Di Russo, F. (2021). Now you see one letter, now you see meaningless symbols: Perceptual and semantic hypnotic suggestions reduce Stroop errors through different neurocognitive mechanisms. Frontiers in neuroscience, 14, 600083

Perrin, F., Pernier, J., Bertrand, O., & Echallier, J. (1989). Spherical splines for scalp potential and current density mapping. Electroencephalography and clinical neurophysiology, 72(2).

Sauseng, P., Griesmayr, B., Freunberger, R., & Klimesch, W. (2010). Control mechanisms in working memory: A possible function of EEG theta oscillations. Neuroscience & Biobehavioral Reviews, 34(7).

Schmidt, J. R. (2019). Evidence against conflict monitoring and adaptation: An updated review. Psychonomic bulletin & review, 26(3). 10.3758/s13423-018-1520-z

Schmidt, J. R., Crump, M. J. C., Cheesman, J., & Besner, D. (2007). Contingency learning without awareness: Evidence for implicit control. Consciousness and Cognition, 16(2), 421–435. https://doi.org/10.1016/j.concog.2006.06.010

Slagter, H. A., Lutz, A., Greischar, L. L., Nieuwenhuis, S., & Davidson, R. J. (2009). Theta Phase Synchrony and Conscious Target Perception: Impact of Intensive Mental Training. Journal of Cognitive Neuroscience, 21(8), 1536–1549. https://doi.org/10.1162/jocn.2009.21125

Smith, S. M., & Nichols, T. E. (2009). Threshold-free cluster enhancement: Addressing problems of smoothing, threshold dependence and localisation in cluster inference. Neuroimage, 44(1).

Soltész, F., Goswami, U., White, S., & Szűcs, D. (2011). Executive function effects and numerical development in children: Behavioural and ERP evidence from a numerical Stroop paradigm. Learning and Individual Differences, 21(6), 662–671. https://doi.org/10.1016/j.lindif.2010.10.004

Szűcs, D., & Soltész, F. (2010). Stimulus and response conflict in the color–word Stroop task: A combined electro-myography and event-related potential study. Brain Research, 1325, 63–76. https://doi.org/10.1016/j.brainres.2010.02.011

Tadel, F., Baillet, S., Mosher, J. C., Pantazis, D., & Leahy, R. M. (2011). Brainstorm: A user-friendly application for MEG/EEG analysis. Computational intelligence and neuroscience, 2011, 8.

Tafuro, A., Ambrosini, E., Puccioni, O., & Vallesi, A. (2019). Brain oscillations in cognitive control: A cross-sectional study with a spatial stroop task. Neuropsychologia, 133, 107190.

Tafuro, A., Vallesi, A., & Ambrosini, E. (2020). Cognitive brakes in interference resolution: A mouse-tracking and EEG co-registration study. Cortex; a Journal Devoted to the Study of the Nervous System and Behavior, 133, 188–200. https://doi.org/10.1016/j.cortex.2020.09.024

Tillman, C. M., & Wiens, S. (2011). Behavioral and ERP indices of response conflict in Stroop and flanker tasks. Psychophysiology, 48(10), 1405–1411. https://doi.org/10.1111/j.1469-8986.2011.01203.x

Torres-Quesada, M., Funes, M. J., & Lupiáñez, J. (2013). Dissociating proportion congruent and conflict adaptation effects in a Simon–Stroop procedure. Acta Psychologica, 142(2), 203–210. https://doi.org/10.1016/j.actpsy.2012.11.015

van Casteren, M., & Davis, M. H. (2006). Mix, a program for pseudorandomization. Behavior Research Methods, 38(4), 584–589. https://doi.org/10.3758/BF03193889

van Vugt, M. K. (2014). Cognitive architectures as a tool for investigating the role of oscillatory power and coherence in cognition. NeuroImage, 85, 685–693. https://doi.org/10.1016/j.neuroimage.2013.09.076

Vastano, R., Ambrosini, E., Ulloa, J. L., & Brass, M. (2020). Action selection conflict and intentional binding: An ERP study. Cortex; a Journal Devoted to the Study of the Nervous System and Behavior, 126, 182–199. https://doi.org/10.1016/j.cortex.2020.01.013

Vidal, F., Burle, B., Grapperon, J., & Hasbroucq, T. (2011). An ERP study of cognitive architecture and the insertion of mental processes: Donders revisited. Psychophysiology, 48(9), 1242–1251. https://doi.org/10.1111/j.1469-8986.2011.01186.x

Vidal, F., Grapperon, J., Bonnet, M., & Hasbroucq, T. (2003). The nature of unilateral motor commands in between-hand choice tasks as revealed by surface Laplacian estimation. Psychophysiology, 40(5), 796–805. https://doi.org/10.1111/1469-8986.00080

Vidal, F., Hasbroucq, T., Grapperon, J., & Bonnet, M. (2000). Is the «error negativity» specific to errors? Biological Psychology, 51(2–3), 109–128. https://doi.org/10.1016/s0301-0511(99)00032-0

Viviani, G., Visalli, A., Finos, L., Vallesi, A., & Ambrosini, E. (2023). A comparison between different variants of the spatial Stroop task: The influence of analytic flexibility on Stroop effect estimates and reliability. Behavior Research Methods. https://doi.org/10.3758/s13428-023-02091-8

Vurdah, N., Vidal, J., & Viarouge, A. (2023). Event-Related Potentials Reveal the Impact of Conflict Strength in a Numerical Stroop Paradigm. Brain Sciences, 13(4). https://doi.org/10.3390/brainsci13040586

Wang, K., Li, Q., Zheng, Y., Wang, H., & Liu, X. (2014). Temporal and spectral profiles of stimulus–stimulus and stimulus–response conflict processing. Neuroimage, 89, 280–288.

West, R., & Alain, C. (2000). Effects of task context and fluctuations of attention on neural activity supporting performance of the stroop task. Brain Research, 873(1), 102–111. https://doi.org/10.1016/s0006-8993(00)02530-0

West, R., & Bailey, K. (2012). ERP correlates of dual mechanisms of control in the counting Stroop task. Psychophysiology, 49(10), 1309–1318. https://doi.org/10.1111/j.1469-8986.2012.01464.x

Winkler, I., Debener, S., Müller, K.-R., & Tangermann, M. (2015). On the influence of high-pass filtering on ICA-based artifact reduction in EEG-ERP. 4101–4105.

Zhang, H., & Kornblum, S. (1998). The Effects of Stimulus-Response Mapping and Irrelevant Stimulus-Response and Stimulus-Stimulus Overlap in Four-Choice Stroop Tasks with Single-Carrier Stimuli. Journal of experimental psychology. Human perception and performance, 24, 3–19. https://doi.org/10.1037//0096-1523.24.1.3

Zurrón, M., Ramos-Goicoa, M., & Díaz, F. (2013). Semantic Conflict Processing in the Color-Word Stroop and the Emotional Stroop. Journal of Psychophysiology, 27(4), 149–164. https://doi.org/10.1027/0269-8803/a000100

CHAPTER 6

Cracking the DMC Code:
A Multivariate Exploration of Control Representations

6.1. Introduction

The importance of representations for cognitive control has been emphasized from the beginning of this thesis (see Chapter 1), but it has become evident from the results and conclusions of the previous chapter. We have indeed highlighted that by focusing only on processes and remaining blind to representational patterns, we may not have fully captured the neural dynamics of cognitive control. This applies to both LWPC-induced proactive control, for which we did not find correlates preceding conflict detection, and ISPC-induced reactive control, for which we did not find observable ER(S)Ps. These (null) empirical findings and the conclusions drawn on them are quite in line with how cognitive control functioning is commonly described: a mechanism that, to flexibly regulate behavior, operates by maintaining and updating internal representations of the information necessary for executing the processes involved in task performance (Cohen, 2017; Sakai, 2008). Such representations encode multiple information, such as the goals and the relevant stimulus/response features, to influence and coordinate individuals' perceptual, motor and cognitive processes. By doing so, they enable individuals to act in the most appropriate way for the given goal and context, effectively completing demanding tasks (Cellier et al., 2022; D'Esposito, 2007; Kriegeskorte & Diedrichsen, 2019; Schumacher & Hazeltine, 2016).

Before delving into why representations have a pivotal role in cognitive control, it is essential to elucidate the concept of representation within the context of neuroscience. Broadly speaking, a representation can be defined as the neural symbolic counterpart of specific aspects/features of the external world. It is thus endowed with content to carry information, which in turn has the function of producing an effect on cognitive processes and behavior (deCharms and Zador, 2000). However, while patterns of neural activity are commonly referred to as representations in neuroscience, it is crucial to acknowledge the absence of a universally shared definition and consensus on their precise meaning and function. This lack of a precise definition in turns implies heterogeneity in the exploration of representations in neuroscience (Baker et al., 2021). With the aim of systematizing the role of representations in neuroscience, Baker and colleagues (2021) outlined three essential criteria for defining a neural representation. First, to consider a representation as the neural counterpart of an external world feature, it has to correlate with it, that is, they should match. This aspect, which is the most commonly

considered, is not enough to classify a neural pattern as a representation. The second important criterium regards the function of representations, highlighting that the neural pattern representing a feature should also have an effect on the behavior. Establishing whether a representation explains behavior allows disentangling between neural pattern that correlate with the feature and do have an effect on behavior and those that correlate but do not have such effect. In addition to this, something further is needed, as representations should serve some aim. This teleological aspect can be investigated having clear hypotheses about whether and how the neural representation is implied in reaching a specific aim. Based on these criteria, it is thus clear that a biunivocal relation between neural patterns and external features is meaningless if not integrated into a causal and teleological view.

Returning to cognitive control, representations form the foundation of numerous cognitive control theories (Badre et al., 2021; Braver, 2012; Cellier et al., 2022; Cohen et al., 1990). Indeed, in specifying cognitive control in terms of representations, theories describe the information encoded by the activity of neural units, such as neuron ensembles or areas (Freund, Etzel, et al., 2021; Kriegeskorte & Diedrichsen, 2019). Furthermore, the concept of representation offers a powerful/robust explanation of cognitive control brain functioning by bridging cognition and brain activity. Indeed, it has been posited that neuronal activity serves the specific function of representing and transforming contents by encoding them as activity patterns which downstream neurons use to produce successful behavior (Diedrichsen & Kriegeskorte, 2017; Kriegeskorte & Diedrichsen, 2019; Kriegeskorte & Kievit, 2013). Hence, the linkage between cognition and brain activity through representation would provide valuable insights into understanding cognitive control dynamics at the neural level. Moreover, this assumption that representations are involved in cognitive control would meet the criteria proposed by Baker and colleagues (2021) for defining a representation as such, as it implies also causal and teleological aspects.

Despite the undeniable significance of representations in understanding cognitive control, they have not been the primary focus of investigation. Our poor understanding of control representations is thus likely to be one of the reasons why, after more than half a century, we still lack a comprehensive description of how cognitive control operates (Freund, Etzel, et al., 2021). Cognitive control representations have been neglected because of the analytical methods employed by most neuroimaging studies which, so far, have mainly described brain activity using mass-univariate approaches (Freund, Etzel, et al., 2021; Kriegeskorte & Diedrichsen, 2019). In particular, this term refers to the most classical neuroimaging analyses, in which a small number of abstract factor levels (i.e., the experimental conditions, like congruent and incongruent ones) are defined, and according to which experimental stimuli are aggregated. Then, the signal for each abstract condition is extracted, often after averaging across trials (and/or across voxels or recording channels for fMRI and M/EEG, respectively, and/or across samples for M/EEG), and statistics are computed

to contrast the obtained functional measures across the different conditions (Cheng, 2021; Etzel et al., 2020; Freund, Etzel, et al., 2021).

This univariate analytical approach offers insights into the overall level of activation and changes in activity elicited by experimental manipulations, for example by revealing which condition elicits a higher control demand, and this is taken as the hallmark of the underlying process (Cheng, 2021). However, it completely discards the rich information reflected in the multidimensional nature of neural signals (Gluth et al., 2012; Popal et al., 2019) and consequently cannot effectively identify representational content (Freund, Etzel, et al., 2021). Therefore, despite univariate analyses being powerful for revealing activation differences (Friston et al., 1994), they provide only process-level measures which are indirect proxies of control representations (Freund, Etzel, et al., 2021). Indeed, unveiling control processes provides us with insights into the function of a neural unit (e.g., a brain region) abstracted over the encoded information, but it does not allow us to reveal how such information is represented, that is, how it is encoded by that neural unit (Diedrichsen & Kriegeskorte, 2017; Freund, Etzel, et al., 2021). As such, the contribution of studies using the classical approach is necessary but incomplete (Freund, Etzel, et al., 2021).

It is very likely that cognitive control processes rely on representations, as noted above, and that these representations are encoded in a complex manner through distributed patterns of activity (e.g., Etzel et al., 2020). Thus, there is a clear need to use methods sensitive to the multidimensional coding underlying such representations to better understand the content of the neural code used by representations (Badre et al., 2021). Therefore, to overcome the limitations of univariate approaches, using multivariate approaches is fundamental to measure such multivariate distributed patterns of information, by assessing whether and how information is encoded in a distributed manner and by testing its specific contribution to reveal the representational content (Davis et al., 2014; Popal et al., 2019).

To address the gaps in cognitive control literature, researchers have started employing multivariate approaches, also known as multivariate pattern analysis (MVPA), confirming the hypothesized advantages. For example, Qiao and colleagues (2017) revealed how task set dynamic changes are represented at the neural level; Kikumoto and Mayr (2020) showed that integrated representations encompassing relevant rules, stimuli and responses were involved in successful action selection; Etzel and colleagues (2020) found evidence that multivariate approaches were effective at revealing working memory-related content even when univariate activity levels did not change; Freund, Bugg and coworkers (2021) demonstrated theory-based functional dissociations during the completion of the Stroop task; and Cellier and colleagues (2022) characterized the properties of task representations (see also Badre et al., 2021, for a brief review of dimensionality of control representations).

Although MVPA was initially developed to be used with fMRI for investigating spatially distributed multivariate patterns, this approach has also garnered recognition and adoption in EEG (and MEG) research (Fahrenfort et al., 2018). The use of MVPA with EEG not only enables harnessing the aforementioned advantages of the multivariate approach but also enhances EEG analysis sensitivity by identifying differences between conditions that are more challenging to detect through univariate analyses (Fahrenfort et al., 2017). Furthermore, MVPA EEG analyses have the potential to provide valuable insights into neural representations that may be less accessible using fMRI, due to the advantage of a higher temporal resolution. Specifically, by examining the temporal dynamics of neural activation patterns, MVPA with EEG can capture the inherent dynamic nature of representations more effectively and hold the promise of potentially detecting interactions between representations (Badre et al., 2021; Cellier et al., 2022).

Based on the foregoing, the aim of this study is to further advance the understanding of cognitive control by employing a multivariate approach to explore the Dual-Mechanisms of Control model (DMC; Braver, 2012; Braver et al., 2007). Specifically, our investigation focuses on the representational perspective of the two postulated control modes, namely proactive and reactive control. More precisely, the present study builds upon our previous study (see Chapter 5), in which we examined the correlates of proactive and reactive control using univariate analyses (ERPs and ERSPs). As exploring cognitive control processes (i.e., using univariate techniques) is necessary but not sufficient to achieve a comprehensive understanding of cognitive control (Freund, Etzel, et al., 2021), here we focus on how proactive and reactive control are encoded at the neural level. Hence, by doing so, we may obtain a more comprehensive view beyond the univariate results, which only indicate the specific cognitive processes involved, shedding light on the representational content encoded within these processes. Consequently, we could also gain valuable insights into the interplay between cognitive processes and their associated neural representations, as these aspects are inherently interconnected (Cheng, 2021).

From a practical standpoint, we will leverage the high temporal resolution provided by the EEG technique, as discussed earlier. Moreover, we will adopt a multimethod approach, utilizing the two most common multivariate techniques, to explore both the encoding and decoding of cognitive control representations. The following paragraph will offer a more comprehensive description of these two techniques, emphasizing their respective advantages, limitations, and their interrelationship.

6.1.1. MVPA methods: encoding and decoding models

In neuroimaging studies, multivariate analyses use two predominant methods, decoding and encoding[17]. The former takes neural activity patterns as input to predict condition/stimulus information, thereby investigating the causal process through which it could be interpreted. The latter entails utilizing the description of information about experimental conditions/stimuli as input to predict brain patterns, thereby attempting to capture the causal process that generates a representation (e.g., Kriegeskorte & Diedrichsen, 2019; Kriegeskorte & Douglas, 2019; Wu et al., 2006). It is important to note that a decoder does not serve as the inverse of an encoder (Kriegeskorte & Diedrichsen, 2019), but still can be considered complementary as they operate in opposite directions (Kriegeskorte & Douglas, 2019; Naselaris et al., 2011).

A decoding model serves as a tool to uncover the content of the neural code by assessing whether the brain pattern contains a specific type of information (Kriegeskorte & Douglas, 2019). In the literature, decoding models are usually denoted as classification-based decoders or classifiers (Freund, Etzel, et al., 2021). In general terms, classification involves the determination of a decision function, which takes various features in an exemplar data and predicts the corresponding class of that particular example (Mahmoudi et al., 2012). The most commonly employed decoder is the linear classifier which takes the activity pattern as input and returns as output class labels to which stimuli belong to (Duda et al., 2001). Hence, linear decoding has been employed to reveal the explicit information present in the neural pattern, that is, whether such pattern contains a specific category-related representation and whether it allows discriminating between classes (Kriegeskorte & Kievit, 2013). The underlying assumption is that successful classification indicates discriminability between classes and, in turn, the presence of information about the decoded variable(s) in that activity pattern (Diedrichsen & Kriegeskorte, 2017; Kriegeskorte & Douglas, 2019; Kriegeskorte & Kievit, 2013; Nili et al., 2014; Popal et al., 2019).

In the field of cognitive control, there has been a noticeable increase in the use of classification-based decoding methods in recent years (Cole et al., 2016; Freund, Etzel, et al., 2021; for a review see Woolgar et al., 2011). However, since this type of classifiers can only address binary questions, they remain strongly tied to univariate approaches, limiting the full exploitation of the potential offered by multivariate analyses (Freund, Etzel, et al., 2021). Additionally, linear classifiers might fail in classifying if the information is encoded in a complex format (Kriegeskorte & Douglas, 2019).

[17]In the current study, we will use the term Multivariate Pattern Analysis (MVPA) to refer to the broader category of multivariate analyses, encompassing both decoding and encoding models. However, it should be noted that in the literature, MVPA is often used interchangeably with decoding, and thus, in this case, MVPA is exclusively employed to refer to classification questions addressed by decoding models. Additionally, the acronym MVPA can also refer to Multivoxel Pattern Analysis (Mahmoudi et al., 2012) and thus specifically employed in fMRI studies, where the objective is to classify spatial patterns based on experimental conditions.

The limits posed by linear classifiers (i.e., they can only decode categorical variables, that is, predict class labels) can be overcome by using regression-based decoding, which allows a more fine-grained decoding of the neural activity pattern. Indeed, regression-based decoding uses the multivariate pattern of brain activity in each trial to predict continuous experimental or performance variables (Bode et al., 2021; Cohen et al., 2011; Popal et al., 2019). An example of regression-based decoding approach is the ridge regression, a method to estimate the coefficients of multiple-regression model (i.e., the strength with which each feature of the multivariate brain activity pattern contributes to the decoding performance) when the independent variables (i.e., the features constituting the multivariate brain activity pattern) are very numerous and/or have a high degree of multicollinearity. This is particularly important in EEG decoding, because the multivariate patterns used in regression-based decoding are usually composed by numerous features (e.g., the scalp distribution of voltage values at a given time or the time points of an ERP trace at a given channel) that are also highly correlated due to the high spatial and temporal autocorrelation in EEG signals.

However, regardless of which decoding model is used, whether it is a classifier or a regression, decoding cannot explore the entire representational space (Diedrichsen & Kriegeskorte, 2017). Indeed, the principal constraint of decoding models is their insensitivity to how information is encoded within the neural pattern (Popal et al., 2019). As such, their limited power in disentangling the format of the information does not allow fully characterizing how it is represented at the neural level, that is, which specific features are encoded and the strength of each of them (Diedrichsen & Kriegeskorte, 2017; Nili et al., 2014). What is even more crucial is that when we use a decoder we cannot be aware of the precise information exploited by it, making impossible any type of inference on whether the information used for decoding is the same as that actually employed by the brain for representation. As such, successful decoding does not warrant that what has been decoded reflects that there is a represented information (see Ritchie et al., 2019 for a detailed discussion on implausibility of the so-called decoder's dictum). Given these drawbacks, decoders do not appropriately allow the modeling of brain information processing, as they oversimplify excessively, thus overlooking the complexity of the underlying computations (Kriegeskorte & Diedrichsen, 2019; Kriegeskorte & Douglas, 2019) and are potentially biologically and psychologically implausible (Ritchie et al., 2019). Indeed, at the neural level, a representation can be conceptualized as a multidimensional space, characterized by a specific representational geometry constituted by a neural population code representing a specific content and the format in which it is encoded. The neural activity pattern can take the form of many combinations giving rise to a rich representational space, which decoders are insensitive to (Kriegeskorte & Diedrichsen, 2019; Kriegeskorte & Kievit, 2013).

To go beyond decoder limitations, encoding models can be used as they offer the advantage of testing complex predictions concerning the rich representational space (Diedrichsen & Kriegeskorte, 2017),

thereby ideally providing a more comprehensive explanation of the activity pattern (Kriegeskorte & Douglas, 2019). Indeed, by predicting the brain activity pattern from the properties of the experimental conditions, encoding models can serve as brain-computational models (Kriegeskorte & Douglas, 2019). In the neuroimaging literature, this is commonly performed using Representational Similarity Analysis (RSA), a type of encoding model that serves for exploring the higher-order representational space to get the whole picture of it (Diedrichsen & Kriegeskorte, 2017; Kriegeskorte et al., 2008). It works by making predictions about the rich representational geometry and by testing different computational models, to evaluate the representational strength of each of them (Cellier et al., 2022; Kriegeskorte et al., 2008; Kriegeskorte & Diedrichsen, 2019). As such, by employing RSA, it becomes possible to thoroughly describe the representational geometry, encompassing all represented features, their relative strength and the interrelationships among the activity patterns associated with different features (Diedrichsen & Kriegeskorte, 2017).

One of the main advantages of RSA in the study of cognitive functions is its flexibility in comparing different types of representational spaces. This flexibility stems from its focus on the (dis)similarity structure of neural activity patterns rather than the activity patterns themselves (Kriegeskorte et al., 2008). Additionally, RSA explicitly models the representational structure, allowing for inference in a forward manner, namely, from the representational model to the brain pattern, as opposed to decoding models, which operate in the opposite direction and, as a result, are agnostic in characterizing the content of the representations (Freund, Etzel, et al., 2021; Popal et al., 2019). As such, through RSA, it is possible to test competing representational models, as well as their interactions and while controlling for confounders, in order to assess the extent to which they can explain the similarity observed in brain activity patterns. This thus allows probing existing theories (e.g., Freund, Etzel, et al., 2021). In practical terms, this is done by quantifying the degree of similarity, quantified in terms of distance, between brain activation patterns and the pattern predicted by theory-based models through the use of representational dissimilarity matrices (RDMs), which contain the information content and reflect its organization (e.g., Diedrichsen & Kriegeskorte, 2017; Etzel et al., 2020; Kriegeskorte et al., 2008; Kriegeskorte & Kievit, 2013). Lastly, leveraging MVPA using RSA methods overcomes the limited biological and psychological plausibility of decoding methods by directly linking the space of the activation patterns and the structure of behavior (Ritchie et al., 2019).

The flexibility and the capability to directly test the representations theorized by models of cognitive control make RSA particularly well-suited for exploration in this area. To explore cognitive control, the adoption of the RSA framework is still relatively uncommon (Freund, Etzel, et al., 2021). However, in cases where it has been utilized, it has confirmed its advantages and suitability (e.g., Cellier et al., 2022; Etzel et al., 2020; Freund, Bugg, et al., 2021; Kikumoto & Mayr, 2020).

Given the remarkable advantages of RSA in providing a full characterization of representations compared to decoding models, it is essential to elaborate on our objective of employing a multimethod approach, encompassing both RSA and decoding, to explain why both methods can be beneficial in investigating proactive and reactive control from a representational perspective. In the present study, decoding will be used following RSA, based on the rationale that, if information is encoded, it should also be available to be read by downstream neurons for it to be used (Kriegeskorte & Diedrichsen, 2019). By doing so, we will first seek to finely characterize the representational geometry of proactive and reactive control using RSA. Subsequently, a decoding model will be employed to determine whether such information patterns are truly available for use, that is, whether its successful decoding is possible. Of note, we adopted a regression-based approach because the content of such representations is likely to be complex and linear classifiers might be too simplistic and thus not suitable for decoding it. Specifically, we used ridge regression, which not only allows decoding the neural activity pattern in a fine-grained manner, but can also be used with continuous variables as those used in the present study (see below).

6.1.2. Aim of the present study

As stated above, our aim is to test one of the most influential models of cognitive control, the DMC, proposed by Braver and colleagues (Braver et al., 2007; Braver, 2012). Previous neuroimaging studies have investigated the DMC, but, as for cognitive control in general, the understanding of how the two control mechanisms operate at the neural level is still elusive. In our prior ER(S)P study (see Chapter 5), we observed evidence for proactive control ER(S)P correlates but found no such evidence for ISPC-induced reactive control. This may be attributed to the univariate approach utilized, which neglected that the dynamic modulations of the PC might act upon representations rather than processes. In the present study, our aim is to advance this line of research by delving into the investigation of cognitive control-related multivariate activity patterns.

Although previous studies have applied MVPA to study cognitive control in the context of the Stroop task (Freund, Bugg, et al., 2021), to the best of our knowledge, no existing work has utilized the LWPC and ISPC manipulations to specifically target proactive and reactive control, respectively. Here, we will manipulate both of them simultaneously to explore whether the two mechanisms co-exist while also the other is activated (see Chapters 4 and 5). Furthermore, to better account for the dynamic and flexible nature of cognitive control, we will manipulate PC-induced control adjustments on a trial-by-trial basis to better account for the flexibility in cognitive control dynamics (see Chapters 4 and 5 for advantages). These trial-level manipulations are extremely suitable for being used with RSA, as by avoiding collapsing trials into a small number of abstract conditions, they generate a condition-rich design which allows to

comprehensively characterize the representational space, thus fully leveraging RSA advantages (Diedrichsen & Kriegeskorte, 2017).

6.2. Methods

6.2.1. Procedure and experimental task

The present study is a re-analysis of the EEG data collected for the study presented in Chapter 5. Therefore, the procedure, experimental task, and stimuli are described there.

6.2.2. EEG recording and pre-processing

The EEG recording and preprocessing are described in Chapter 5.

6.2.3. Data analysis

We conducted two multivariate analyses, RSA and Decoding, the details of which will be provided in the subsequent sections. Despite each of them involving different computations, the variables used in the analyses were the same. Here we describe how we computed them for both analyses.

Given that the experimental task was still the perifoveal spatial Stroop, each experimental stimulus was characterized by a relevant feature, the arrow direction, and an irrelevant feature, the arrow position. We thus had two categorical variables: i) direction (DIR), corresponding to the correct response with four possible values (the four directions: upper-left, upper-right, lower-right, lower-left), and ii) position (POS), corresponding to the stimulus position with four possible values (the four position: upper-left, upper-right, lower-right, lower-left). From these two categorical variables, we were able to calculate the binary variables that we used in the analyses. These are:

1. congruency (CON), which takes the value of -.5 when DIR is equal to POS (Congruent, Con), or .5 when DIR is different from POS (Incongruent, Inc);
2. horizontal position of the stimulus on the screen (hS), which takes the values of -.5 for left POS or .5 for right POS;
3. vertical position of the stimulus on the screen (vS), which takes the values of -.5 for lower POS or .5 for upper POS;
4. the horizontal coding of the manual response (hR), which takes the values of -.5 for left DIR or .5 for right DIR;
5. the vertical coding of the manual response (vR), which takes the values of -.5 for lower DIR or .5 for upper DIR.

For what concerns the other variables, based on the reasons extensively described throughout the thesis (see Chapters 1, 4, 5), analyses were performed on trial-level estimates. To compute these trial-level variables, we started from the block-level ones, corresponding to the ones described in the experimental task and stimuli section. We then used the Hierarchical Gaussian Filter (Mathys et al., 2011), which uses variational Bayes under a mean-field approximation to update the probability of an event on each trial. As such, all the trial-level variables were computed as probability based on the update of trial-by-trial probabilities and using all the trials, including the practice ones, as follows:

1. List-wide Proportion Congruency (LWb) is the trial-by-trial probability of the stimulus CON, so to compute it, HGF uses the CON binary variable.
2. Item-specific Proportion Congruency (ISb) is the trial-by-trial probability of the stimulus CON conditional to a specific POS, so HGF calculated it using the binary variable of CON for each POS. By doing so, we obtained a trial-level PC for each POS. Therefore, for each trial, we had 4 estimates, one for the PC of the POS of the stimulus at that trial, and three for the PC for the POS that are not observed at that trial. We will thus refer to the distribution of the 4 Item-specific PCs as total ISPC (ISbt). From this, we selected the ISPC of the POS of each trial, referring to it as ISb. Lastly, we computed a measure taking into account both ISb and ISbt, by comparing the probability of ISb to the average of the ISbt probabilities, using the Kullback-Leibler divergence (DKL). This variable, called weighted ISPC (ISbw), provides a better estimate of ISb at each trial, as it also takes into account its weight relative to the PC values associated with the other POS at the same trial.
3. Contingency (Response probability given the stimulus, PRS), is the trial-by-trial probability of the target DIR (corresponding to the response) conditional to a specific POS. To calculate it, HGF used the categorical variable of DIR conditional to each POS, thus obtaining 4x4 estimates (namely, 4 PR estimates for each POS), so we will refer to it as total PRS (PRSbt). From these estimates, we then extracted the correct one, that is, the one corresponding to both DIR and POS observed at each trial. Lastly, weighted PRS was computed (PRSbw) using DKL as described for ISbw.
4. Lastly, we also computed the trial-level estimates for the low-level variables described above (hS, vS, hR, vR), referring to them as PhS, PvS, PhR, and PvR, respectively. These variables reflect the trial-by-trial probability to encounter a specific horizontal/vertical position and to respond using a specific response hand/finger. To compute it, HGF used each low-level binary variable.

We excluded from the analyses the training trials. From the resulting 27200 trials, we also excluded trials rejected in the EEG pre-processing (n = 304, corresponding to 1.12% of the experimental trials), as well as the first trial of each block, error trials (which comprise incorrect and missed responses), and post-error trials (n = 1643, corresponding to 6.11% of the remaining trials).

6.2.4. Representational similarity analysis (RSA)

RSA works by computing the so-called representational dissimilarity matrices (RDMs), which encapsulate the information content and how it is organized. RDMs are built comparing the distance (which reflects the dissimilarity) between each pair of conditions/trials for the theory-based information (model RDMs) and for the multivariate brain activation pattern (brain RDMs). Then, the representational geometry of the experimental variables based on theoretically specified models, namely the model RDMs, are fitted to the representational geometry observed in the neural activation patterns, namely the brain RDMs. The obtained representational similarities indicate which model better explains the observed neural activation pattern (Diedrichsen & Kriegeskorte, 2017; Etzel et al., 2020; Freund, Etzel, et al., 2021; Kriegeskorte et al., 2008; Kriegeskorte & Kievit, 2013).

The analytical approach classically (and most often) used in the EEG encoding (but also decoding) literature is the so-called time-resolved approach. In this approach, the brain RDMs are computed for each time point using the whole multivariate spatial patterns of EEG activity (i.e., the scalp distribution of the ERP voltages at a given time). By contrast, in the space-resolved approach, the brain RDMs are computed for each channel using the whole multivariate temporal patterns of EEG activity (i.e., the time course of the ERP voltage at a given channel). Both approaches suffer from one main drawback. Indeed, the use of all the information in one dimension (i.e., either time or space) yields results that are blind to such dimension. So, with the unidimensional time- and space-resolved approaches, it is not possible to get insights into (and thus draw inference about) which time points and channels, respectively, most contributed to encode the representations based on the experimental variables. Therefore, even if both unidimensional analyses are performed, the interpretability of the results is considerably limited as the two sets of results cannot be interpreted in an integrated manner.

To overcome this issue, the so-called searchlight approach can be used (e.g., Popal et al., 2019). In this approach, brain RDMs are computed for each time point and channel using a limited portion of the multivariate spatio-temporal (i.e., multidimensional) pattern of EEG activity (i.e., the ERP voltages in a time window around the tested time point for a spatial window around the tested channel). This spatio-temporal approach ensures a better understanding of the multivariate patterns, as it allows using both spatial and temporal information simultaneously while allowing for both spatial and temporal inferences. However, this approach still remains blind to spectral information, which might be rich in representational meaning. Indeed, evoked changes in spectral power in different frequency bands are known to play an important functional role in encoding (and communicating) different types of information. Therefore, a natural development of using both spatial and temporal patterns is to also use spectral patterns to get a more complex multidimensional, multivariate picture of how the brain encodes theory-based representations.

Therefore, we employed such spatio-temporo-spectral analyses to fully leverage the complex nature of the EEG signal. To do so, we used a searchlight approach by computing brain RDMs for each time point, channel, and frequency using a limited portion of the multidimensional spatio-temporo-spectral pattern of EEG spectral activity (i.e.., the event-related spectral perturbation (ERSP) values in a time window around the tested time point, for a spatial window around the tested channel, and a spectral window around the tested frequency; see below and Figure 6.1).

6.2.4.1. Theoretical RDM computation

To explicitly test whether the observed multivariate EEG patterns encoded our experimental variables, we modeled them as trial-by-trial representational dissimilarity matrices (RDM) as detailed in what follows:

1. for hS, vS, hR, vR, CON, we calculated the trial-by-trial pairwise Euclidean distances. Therefore, since these variables are binary, in the obtained RDMs, there is trial-to-trial similarity when both trials have the same value (e.g., for CON, both trials are congruent or both are incongruent), and dissimilarity when one trials have a different value (e.g., for CON, one trial is congruent and the other is incongruent.
2. In order to obtain an RDM that specifically reflected the presence of conflict, in line with Freund, Bugg, et al., (2021), we computed logical divergences based on the CON RDM. Specifically, in the resulting conflict RDM there is trial-to-trial similarity when both trials are incongruent, thus involving conflict (vs. dissimilarity when one trial or both are congruent, this not involving conflict). Thus, this RDM reflects CON in the incongruent trials (CON_I). We also computed a complementary RDM (CON_C), reflecting the absence of Conflict, with trial-to-trial similarity when both trials are congruent. We choose to not compute an RDM reflecting the congruency similarity and directly computed based on the binary CON variable (which corresponds to the logical union of the CON_C and CON_I RDMs) because, in that case, the obtained theoretical model would have additionally assumed that the similarities between pairs of congruent trials and pairs of incongruent trials would have been the same.
3. To explore the representations of the task-related features, that is, both the task-relevant one (direction, corresponding to the required response) and the task-irrelevant one (position), as in Freund, Bugg, et al., (2021), we computed an RDM reflecting trial-to-trial similarity when the two trials have the same target feature (i.e., same arrow direction), referred to as Target RDM, and a RDM reflecting trial-to-trial similarity when the two trials have the same distracting feature (i.e., same arrow position), referred to as Distractor RDM. To do so, we computed logical divergences using the DIR and POS categorical variables, respectively.
4. LWb RDM was computed to be symmetric by using the pairwise Jensen-Shannon divergences; these were computed based on the two DKL values obtained by comparing the LWb probability of each trial of the pair to the mean LWb probability of the two trials.
5. PhS, PvS, PhR, and PvR RDMs were computed using the same approach described for LWb.

6. for ISb, we first computed an RDM based on the ISb probability for the item (POS) presented in each trial, weighted for the average of the 4 possible ISb probabilities by using DKL. The trial-by-trial pairwise dissimilarities were then computed as Euclidean distances. We also computed a total ISb RDM (ISb_t) based on the four ISb values and computed using the pairwise symmetric Chi-squared (Taneja, 2005).
7. PRSb RDMs were computed as ISb ones. We first computed an RDM based on the PRSb probability of the actual response for the POS presented in each trial, weighted for the average of the 16 possible PRSb probabilities (resulting from the combination of the four responses conditional to each POS) by using DKL. The trial-by-trial pairwise dissimilarities were then computed as Euclidean distances. We also computed a total PRSb RDM (PRSb_t) based on the multinomial probability distributions and computed using the pairwise Symmetric Chi-squared (Taneja, 2005).

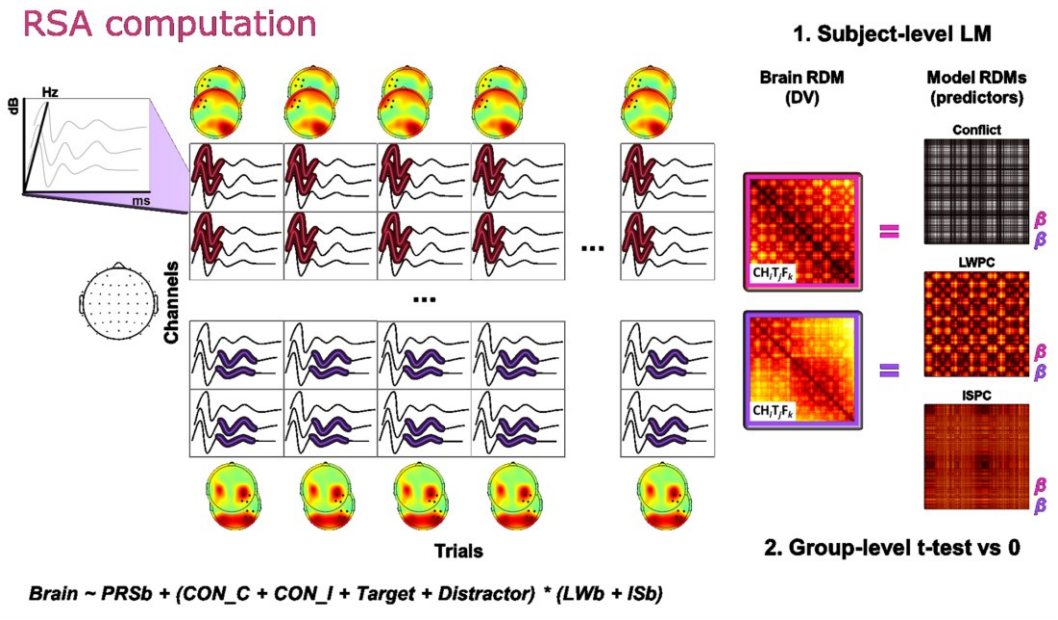

Figure 6.1.
Schematic representation of searchlight RSA computation. From right to left: Competing representational accounts (modeled as Representational Dissimilarity Matrices (RDMs); here are shown some examples of model RDMs that we used, namely that for Conflict, LWPC and ISPC) are used to predict EEG RDMs (here are shown two examples of brain RDMs. On the left: An example of two EEG RDM computations is shown. The fuchsia EEG RDM is computed by correlating the ERSP for one channel and its neighbors (black dots on the upper topoplots), for the central timepoint of the time window highlighted in fuchsia, and for a frequency band and its neighbors (for simplicity, here we represent only three frequency bands, and, in this case, only two of them are selected). This is performed across trials, thus correlating the same channels, time points, and frequencies from the first to the last trial. The lilac EEG RDM is computed in the same way, but now correlating different channels, time points and frequencies. This is done for each channel and its neighbors, each time point with a temporal window of 80 ms, and each frequency with a 7-Hz spectral window, across trials. From up to bottom: Trial-level two-step multiple regression analysis. First, multiple linear regressions are performed for each participant using the formula shown below, resulting in beta values (slopes), reflecting the representational strength of each brain RDM in explaining the observed brain activation pattern. Then, one-sample t tests are performed on the obtained beta values to assess group-level effects.

6.2.4.2. Brain RDM computation

As mentioned above, we employed a spatio-temporo-spectral RSA approach to fully leverage the complex nature of the EEG signal. To this aim, we first performed a time-frequency decomposition using modified complex Morlet wavelet convolution in the frequency range from 4 and 30 Hz (i.e., from Theta to Beta3 frequencies, linearly spaced, with a 1-Hz resolution) to obtain ERSP values with a 20-ms temporal resolution. The employed wavelets had temporal windows ranging from 750 to 533 ms, which corresponds to a linearly increasing number of cycles (from 3 to 12 cycles, linearly spaced, for the 4 and 30 Hz frequencies, respectively). The baseline correction was applied trial by trial using the average power in the entire time window (i.e., from -1500 to 1500 ms for stimulus-locked data and from -500 to 300 ms for response-locked data).

For each participant, the trial-by-trial spatio-temporo-spectral RDMs were then computed using the obtained ERSP data by correlating the ERSPs values for each channel, time point, and frequency using a searchlight approach based on each channel neighbors (defined using an Euclidean distance < 50 mm), an 80-ms time windows (corresponding to five time points), and a 7-Hz spectral window (see also Figure 6.1).

A common practice in the literature involves employing classification accuracy as dissimilarity measure. Nevertheless, we opted not to adopt this measure as it, by converting continuous dissimilarity measures into binary outcomes (correct vs. incorrect), is less informative and less sensitive than directly using the continuous RDMs (Walther et al., 2016).

RSA was performed in three distinct time windows. For stimulus-locked data, we distinguished between pre-stimulus (from -1000 to 0 ms) and post-stimulus (from 0 to 1000 ms) windows, with 0 referring to stimulus onset. For response-locked data, we used a peri-response time window ranging from -500 to 300 ms, with 0 referring to the response time.

6.2.4.3. RSA computation

The theory-based model RDMs (see above) were used to predict the EEG RDMs using a condition-rich RSA approach based on trial-level multilevel modeling. Specifically, we used trial-level two-step multiple regressions at the whole-brain level: multiple linear regressions were first performed for each participant to predict the observed brain RDMs using as predictors the model RDMs as detailed below; then, group-level one-sample t-tests were performed on the obtained b values (slopes) reflecting the corresponding representational strengths (see also Figure 6.1).

For the post-stimulus analyses, this analytical approach is similar to the full factorial RSA used by Freund, Bugg, et al. (2021), as we included the same four theory-based models, that is, the two conflict-related

models CON_C and CON_I and the two task-related models Target and Distractor. However, we also controlled for the effect of contingency (PRSb) to exclude that the observed results could be explained by this lower-level variable (as per the contingency hypothesis, see Schmidt, 2019, for a review). More importantly, as our experimental question specifically regards the effect of LWPC/ISPC on interference resolution, our regression model also included the interactions between both Conflict-related and Task-related RDMs and both LWPC and ISPC RDMs. Indeed, we were interested in exploring how the latter PC representations are encoded in the brain depending on the representations of both the presence/absence of conflict and both the task-relevant/irrelevant features.

Therefore, for both the post-stimulus and the response-locked RSA analyses, the model formula was:

*Brain ~ PRSb + (CON_C + CON_I + Target + Distractor) * (LWb + ISb)*

As regards the pre-stimulus analysis, both the Conflict-related and Task-related models could not be used, as they reflect representations of features that are unknown before stimulus appearance. Moreover, in this analysis, for ISb and PRSb we used the representational models based on the multinomial probability distributions, instead of those based on the weighted univariate probabilities (see Section 6.2.4.2), because the latter are also based on features that are unknown before stimulus appearance, while the former allowed us to investigate whether the brain encode the multivariate representations of these experimental variables. For the same reason, we also tested the representational models reflecting the expectations about the low-level features of the stimulus position and the response. The LWb RDM was also included in the model:

Brain ~ PhS+PvS+PhR+PvR+PRSb_t+ISb_t+LWb

Before fitting the multiple linear regressions (using ordinary least squares), the upper triangles of the model RDMs were unwrapped into vectors and z-scored to be assembled into the RSA design matrix.

Then, we assessed the statistical significance and effect size of the tested effects at the group level by performing one-sample t-tests against 0 on the estimated b coefficients for each participant. One-tailed and two-tailed tests were performed, respectively, for the encoding strength of the single model RDMs and for the interaction terms.

For each predictor included in the statistical model, we thus obtained a spatio-temporo-spectral statistical parametric map of observed t values with 1-channel, 20-ms, and 1-Hz resolution, which correspond to 88128 tests for both the stimulus-locked analyses (i.e., 64 channels x 51 time points x 27 frequencies) and 70848 tests for the response-locked analysis (i.e., 64 channels x 51 time points x 27 frequencies). These statistical parametric maps were corrected for multiple comparisons by using a cluster-

based permutation approach based on the *tmass* statistics, using 2000 permutations to estimate the null distribution.

To further limit the risk of type-I errors and to aid the identification of the most consistent results, the corrected statistical parametric maps were further masked using both an alpha threshold of .005 and a cluster size threshold of 40 connected samples.

6.2.5. Ridge-based decoding

Ridge regression decoding is a regularized version of ordinary least square multiple linear regression that uses the multivariate pattern of neural activity in each trial to predict continuous dependent variables like participants' performance measures or, more commonly, experimental variables. In doing so, ridge regression allows mitigating the multicollinearity issue that affects EEG data by using a regularization method.

The ridge-regression decoding analysis was performed using a searchlight approach similar to that used for RSA. Indeed, we computed the spatio-temporo-spectral multivariate pattern of ERSP activity, which in this approach serves as the design matrix to predict the experimental variables, by using the same spatio-temporo-spectral searchlight, but in this case, data were smoothed in time (using a 5-samples moving average) and downsampled (every 2 time points) to reduce measurement noise. Moreover, since this analysis is more computationally intensive as compared to RSA, we limited the resolution of the analytical space. Specifically, the spatial dimension was downsampled by testing the 31 channels corresponding to the extended 10-20 system (i.e., Fp1/2, F7/3/z/4/8, FT9/10, FC5/1/2/6, T7/8, C3/z/4, TP9/10, CP5/1/2/6, P7/3/z/4/8, O1/2), the temporal dimension was downsampled by a factor of 2, thus obtaining a final 40-ms resolution, and the spectral dimension was downsampled by keeping five frequency bands: Theta (4-7 Hz), Alpha (8-12 Hz), Beta1 (13-18 Hz), Beta2 (19-24 Hz), Beta3 (25-30 Hz).

We tested different models for the post- and pre-stimulus analyses for the reasons explained above (see Section 6.2.4.3) but the predicted variables corresponded to the trial-level experimental variables and Bayesian estimates detailed above (see Section 6.2.3). Indeed, differently from RSA, the ridge-regression analysis aims to decode the trial-level experimental variables, rather than the corresponding theoretical trial-by-trial RDMs, so it was not possible to try decoding the pairwise dissimilarity variables such as CON_C, CON_I, Target, and Distractor. The predicted variables for the post-stimulus analyses were the low-level binary variables hS, vS, hR, and vR; the low-level continuous estimate of contingency, PRSb; the binary variable of interest CON; the continuous estimates of LWPC and ISPC (LWb and ISb, respectively), as well as their interaction with CON. For the pre-stimulus analysis, the predicted variables were the low-level continuous estimates PhS, PvS, PhR, and PvR, and the continuous estimate of LWPC, LWb.

A five-fold stratified cross-validation loop with three repetitions was implemented and classification was performed using the LDA algorithm. After a preliminary optimization, we set the lambda hyperparameter (which set the magnitude of the applied regularization) to .1. The performance parameter was the mean squared error of the decoding prediction.

Statistical significance of the results was calculated using a non-parametric approach as in Linde-Domingo et al. (2019). Specifically, we computed 150 permutations at the participant level and we compared results to null distribution using permutation tests for significance (10000 permutations). Lastly, the obtained statistical non-parametric maps were corrected for multiple comparisons using a similar cluster-based permutations approach as that used in the RSA analyses.

Finally, we performed an intersection analysis to identify the spatio-temporo-spectral samples for which there was both a significant (corrected) encoding of a given theoretical representational model and a significant (corrected) decoding of the corresponding experimental variable (e.g., the spatio-temporo-spectral mask of significant results of the encoding of either the CON_C and CON_I RDMs was intersected with the spatio-temporo-spectral mask of significant ridge-regression decoding of the CON variable). To note that the intersection analysis could not be performed for the Target and Distractor RDMs, as they did not have a corresponding trial-level experimental variable, as explained above.

6.3. Results

6.3.1. Representational similarity analysis

We performed spatio-temporo-frequency RSA to explore the representational structure of proactive and reactive control, assessing whether the observed multivariate spatio-temporo-spectral brain activity patterns were explained by the theory-based representations postulated by the DMC. As explained above, the model also included predictors for confounders, but their effect will not be reported here, for the sake of conciseness. Moreover, for stimulus-locked analyses, we will present only results found within 600 ms, whereas for response-locked ones, we will report only pre- and peri-response results.

6.3.1.1. Stimulus-locked data

RSA on stimulus-locked data showed that the absence of conflict (CON_C), Target, Distractor, and LWPC were significantly represented. Additionally, we found the representations of LWPC interacting with the absence of Conflict (LWPC*CON_C), Conflict (LWPC*CON_I), Target (LWPC*Target), and of ISPC interacting with the absence of Conflict (ISPC*CON_C) and Distractor (ISPC*Distractor).

In particular, CON_C was significantly encoded by the spatio-temporo-spectral brain patterns in two clusters: an earlier one from 240 to 400 ms over left fronto-central electrodes and mainly involving the Beta2 band (see Figure 6.2), followed by a cluster (from about 420 to 540 ms) over right temporo-parietal regions in the same band.

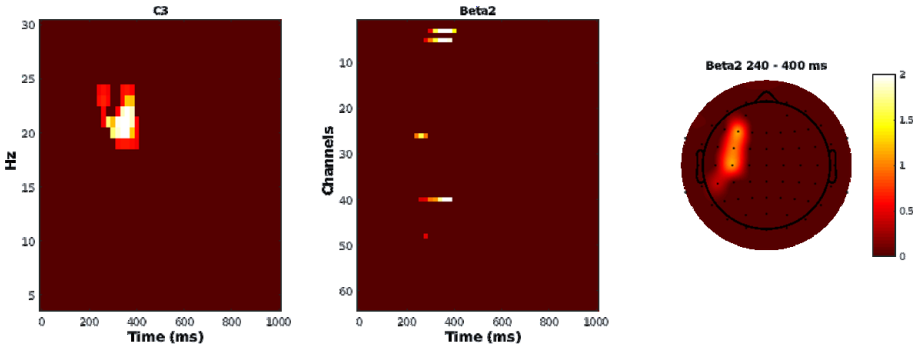

Figure 6.2.
RSA effect of CON_C on stimulus-locked data. The raster diagram on the left shows timepoints/frequencies significantly modulated by the effect for the channel indicated in the title; the one in the middle shows timepoints/channels significantly modulated by the effect for the frequencies in the band indicated in the title. The topoplot shows the scalp distribution of the effects for the same frequencies in the time window indicated in the title. Significant effects are reported as t values, using the colormap corresponding to the colorbar near the topoplot.

The Target was significantly represented by the multivariate activity pattern in an early cluster till 340 ms distributed over central electrodes, slightly right lateralized and involving Beta1 and low Beta2 frequencies, followed by a right mid-frontal cluster till 500 ms in the Beta3 band.

The Distractor was instead significantly encoded by three clusters of multivariate activity; a Beta3 cluster spanning from about 200 to 320 ms with a central scalp distribution and a Beta1 cluster from about 260 to 380 ms over left centro-parietal electrodes. From about 480 to 660 ms, there was a Beta2 cluster distributed over right prefrontal and central electrodes.

The multivariate activity representing LWPC was found in an early Theta cluster from 120 to 300 ms over left parietal scalp regions (see Figure 6.3).

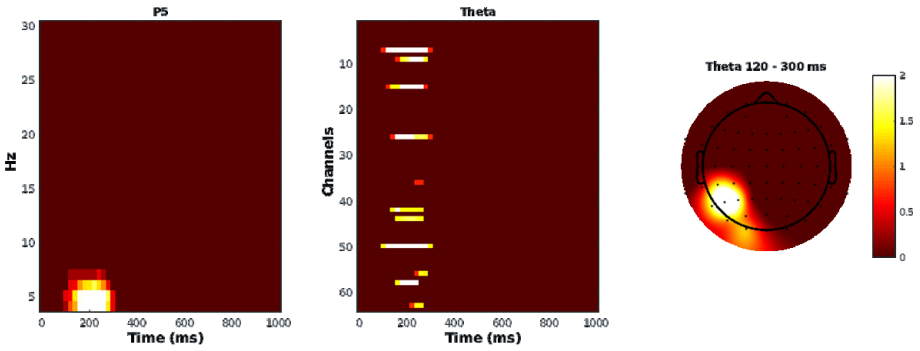

Figure 6.3.
RSA effect of LWPC on stimulus-locked data. See Figure 6.2 for conventions.

The multivariate activity pattern significantly represented the interaction between LWPC and the absence of Conflict (LWPC*CON_C) in a right centro-parietal cluster from 380 to 560 ms, involving high Alpha frequencies.

The interaction between LWPC and Conflict (LWPC*CON_I) was significantly encoded by multivariate activity patterns in four clusters. We found two early clusters (from about 240 to 380 ms), a Beta2 one over right temporo-parietal electrodes, and a Theta one over mid-frontal scalp regions, slightly right-lateralized and including also low Alpha frequency. From about 360 ms, we found a Beta1 cluster over right fronto-central electrodes and a Beta3 cluster over left fronto-central electrodes.

The significant multivariate activity patterns representing the interaction between LWPC and Target were identified in three early clusters and four later ones. At stimulus appearance, there was a Beta1 cluster lasting till 160 ms over left parietal electrodes, followed by an Alpha cluster over right prefrontal electrodes (see Figure 6.4) and a Beta1 cluster mainly over left fronto-temporal electrodes, both lasting till about 300 ms. From 400 till about 600 ms, we found a Beta3 cluster, first over left temporal scalp regions and then over right posterior scalp regions. Lastly, from about 520 to 700 ms, there were a Beta3 cluster over right midfrontal electrodes and an Alpha cluster over left centro-parietal electrodes.

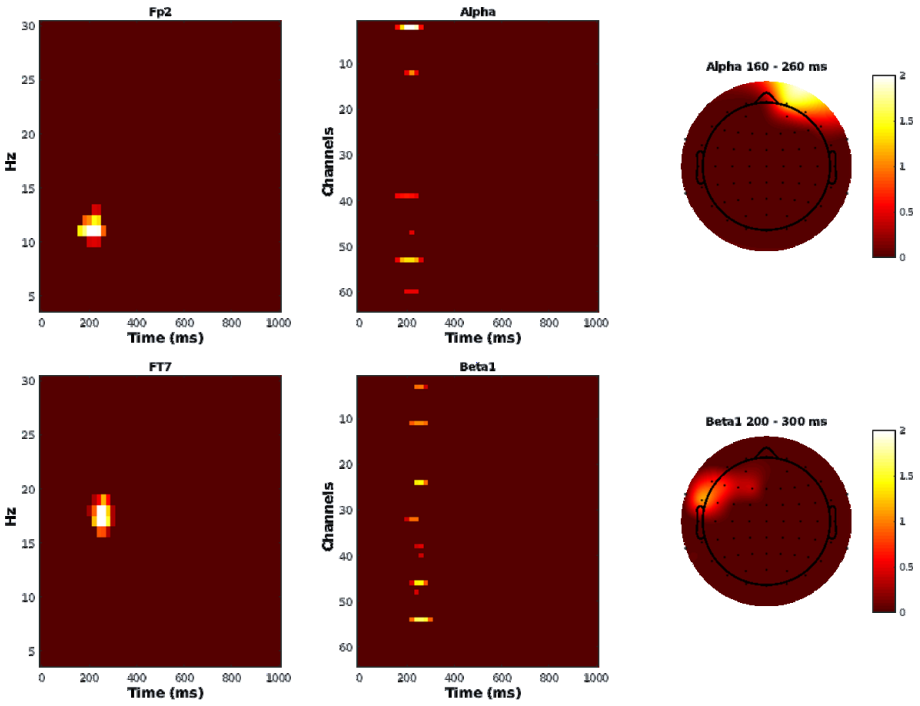

Figure 6.4.
RSA effect of the LWPC*Target interaction on stimulus-locked data. The upper and lower panels show, respectively, the results for the Alpha and Beta1 cluster. See Figure 6.2 for conventions.

The multivariate activity pattern significantly represented the interaction between ISPC and the absence of Conflict in a first early and widespread Alpha cluster (from 160 to 340 ms) mainly over right parieto-occipital scalp regions (see Figure 6.5) and then in a Beta2 cluster (from 300 to 420 ms) distributed over left fronto-central electrodes.

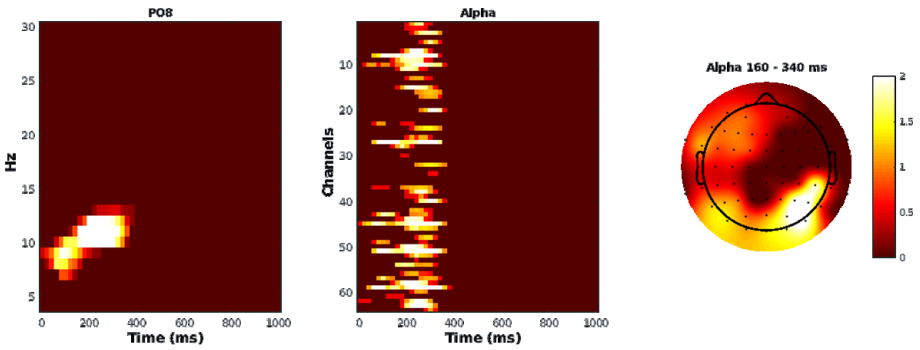

Figure 6.5.
RSA effect of the ISPC*CON_C interaction on stimulus-locked data. See Figure 6.2 for conventions.

Lastly, the multivariate activity representing the ISPC by Distractor interaction was observed in three clusters: two early ones immediately after stimulus, one involving Beta1/2 frequencies over left frontal electrodes till 140 ms, and one involving Theta over left centro-parietal electrodes till 380 ms. From 240 to 420 ms, we found a right centro-parietal cluster involving the Beta2 and Beta3 bands (see Figure 6.6).

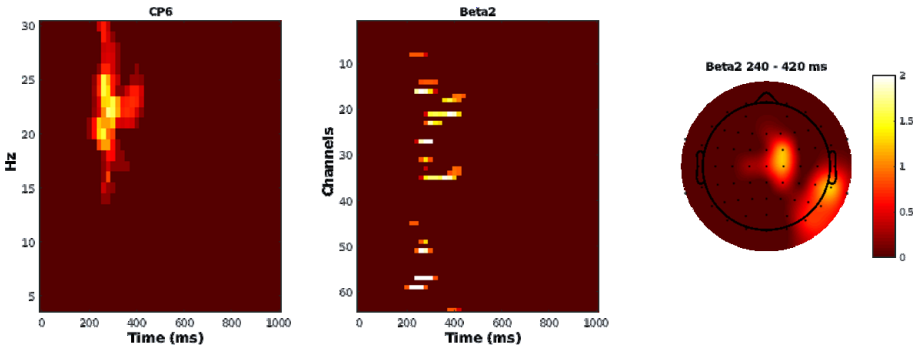

Figure 6.6.
RSA effect of the ISPC*Distractor interaction on stimulus-locked data. See Figure 6.2 for conventions.

6.3.1.2. Response-locked data

RSA on response-locked data revealed that Conflict (CON_I), Distractor, LWPC and ISPC were significantly represented. Moreover, we found the representations of LWPC interacting with the absence of conflict (LWPC*CON_C), Conflict (LWPC*CON_I), and Distractor (LWPC*Distractor), and of ISPC interacting with the absence of conflict (ISPC*CON_C), Conflict (ISPC*CON_I), Target (ISPC*Target) and Distractor (ISPC*Distractor).

Specifically, the presence of Conflict (CON_I) was significantly represented by the multivariate activity pattern in a left-lateralized fronto-central cluster, found in the peri-response time window (from -40 to 40 ms) and involving Beta1 and Beta2 frequencies (see Figure 6.7).

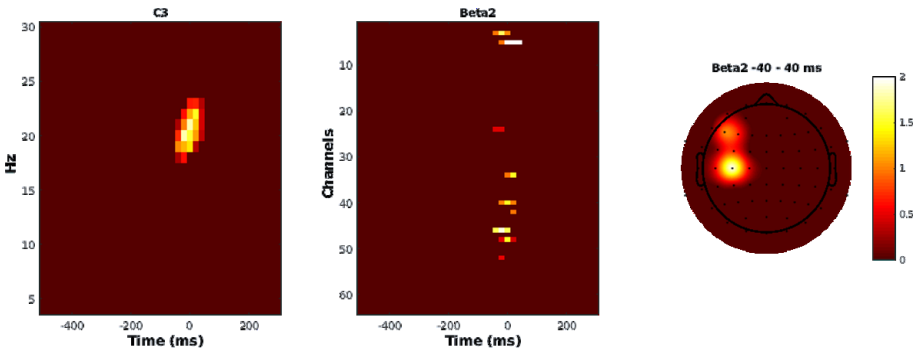

Figure 6.7.
RSA effect of CON_I on response-locked data. See Figure 6.2 for conventions.

The Distractor representation was found in the multivariate activity of two pre-response clusters: one earlier (from -300 ms) Alpha and Beta1 cluster over right parietal electrodes, and a later (from -120 to -40 ms) Theta and Alpha cluster over left fronto-central scalp regions.

LWPC was significantly encoded by the multivariate pattern in three clusters. In the pre-response, from -300 to -160 ms, we found a Theta and Alpha cluster mainly distributed over left centro-posterior scalp

regions. Moreover, there was a Beta1 right parietal cluster (from -240 to -120 ms), followed by a Beta3 left fronto-temporal cluster lasting till response (see Figure 6.8).

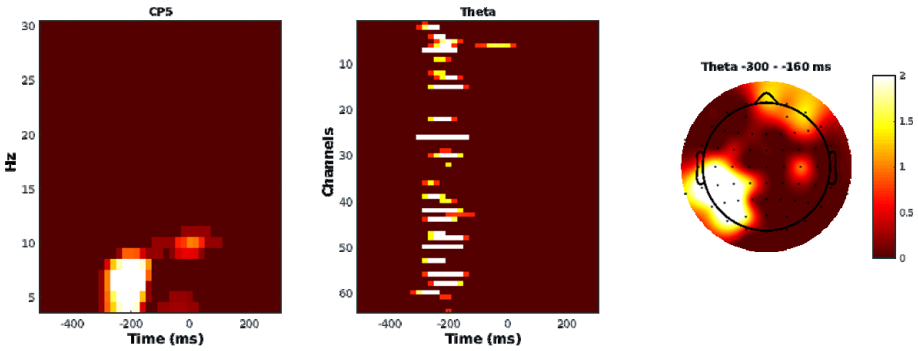

Figure 6.8.
RSA effect of LWPC on response-locked data. See Figure 6.2 for conventions.

The representation of ISPC was instead significantly encoded in the pre-response time window from -280 to -180 ms by the multivariate activity pattern of a Beta2 cluster distributed over left fronto-centro-parietal scalp regions (see Figure 6.9).

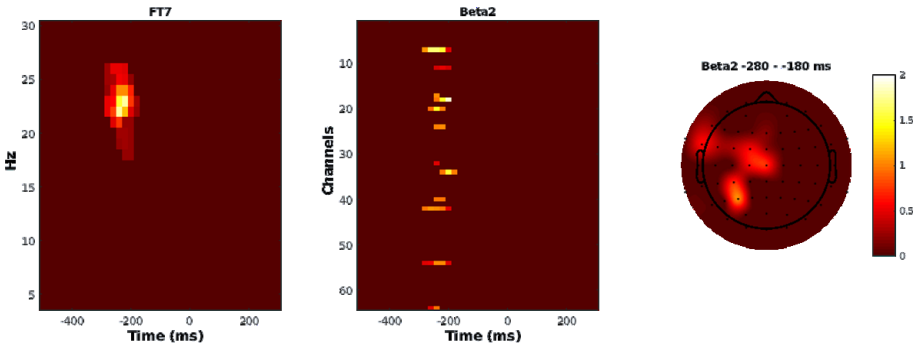

Figure 6.9.
RSA effect of ISPC on response-locked data. See Figure 6.2 for conventions.

The interaction between LWPC and the absence of Conflict was significantly encoded by multivariate activity patterns in five clusters: two pre-response clusters from about -480 to 360 ms, involving Theta frequency over mid-frontal electrodes and Beta1 band cluster over left frontal electrodes. Moreover, from -380 to -200 ms, we found a Beta3 cluster over left posterior electrodes, followed by a cluster involving Theta over left centro-parietal scalp regions and lasting almost till response (see Figure 6.10). In the peri-response time window, there was a Theta cluster over right fronto-central electrodes.

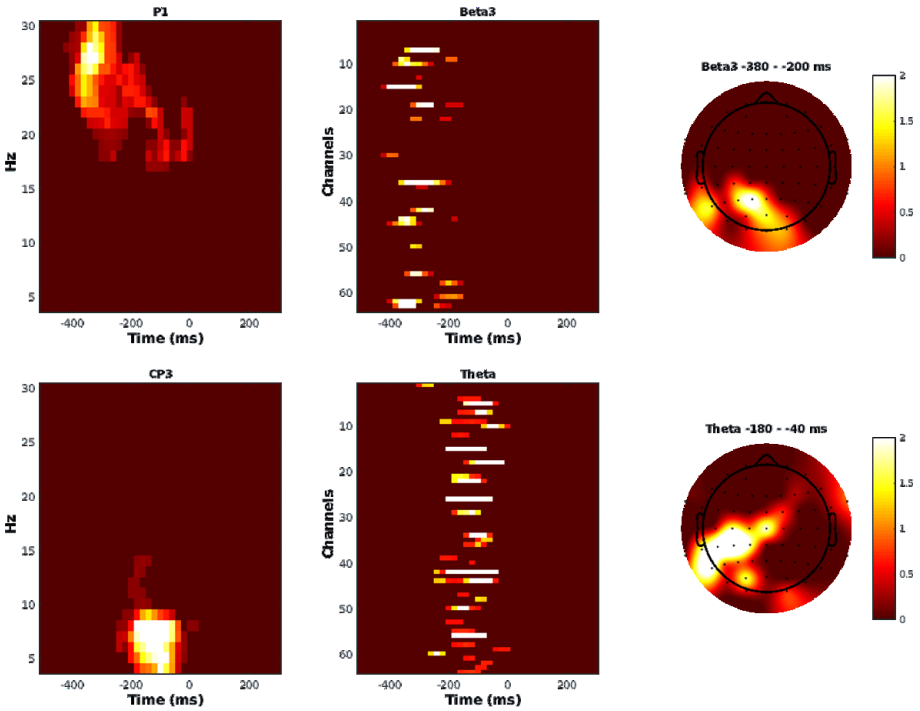

Figure 6.10.
RSA effect of the LWPC*CON_C interaction on response-locked data. The upper and lower panels show, respectively, the results for the Beta and Theta bands. See Figure 6.2 for conventions.

LWPC interacted with Conflict as well, and this was significantly encoded by the multivariate activity pattern in three clusters. An earlier and a later cluster (from -500 to -420 ms and from -220 to -100 ms), mainly distributed over parietal electrodes, slightly left-lateralized, and involving Theta band (see Figure 6.11). Two additional small clusters were found in the late pre-response time window (from about -80 to -20 ms), one over left temporal electrodes, involving Alpha frequency, and a occipital one involving Beta1 band.

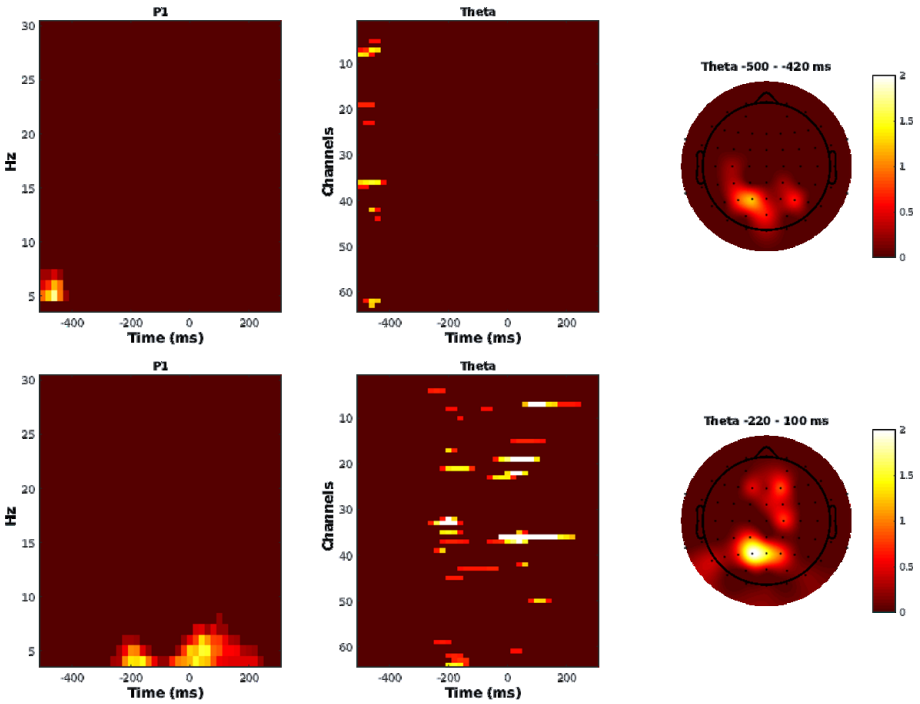

Figure 6.11.
RSA effect of the LWPC*CON_I interaction on response-locked data. The upper and lower panels show, respectively, the results for the earlier and later Theta cluster. See Figure 6.2 for conventions.

The multivariate activity representing the LWPC*Distractor interaction was observed in two clusters: one before the response (from -440 ms), distributed over right pre-frontal electrodes and involving Beta2 band (see Figure 6.12), and one around the response, over right parietal electrodes and involving Beta1 frequency.

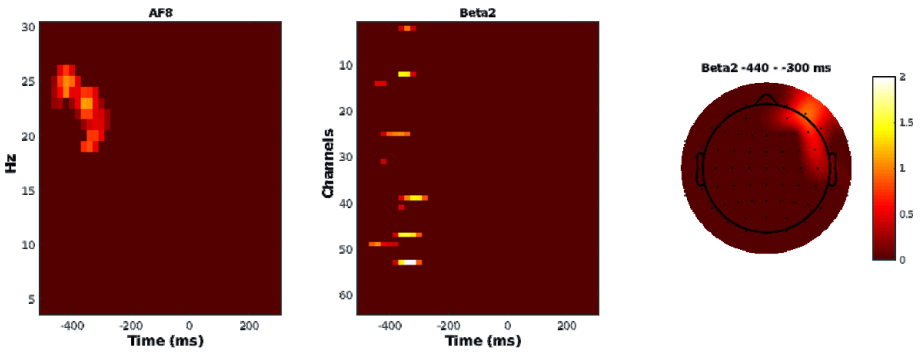

Figure 6.12.
RSA effect of the LWPC by Distractor interaction on response-locked data. See Figure 6.2 for conventions.

The representation of the interaction between ISPC and the absence of conflict (CON_C) was significantly encoded by the multivariate pattern in four clusters. Three were in the pre-response time-window: a Beta1/2 cluster over right parietal electrodes from -220 to -20 ms, a Theta widespread cluster distributed mainly over right fronto-temporo-posterior electrodes from -140 to 0 ms (see Figure 6.13), and

a Beta2/3 cluster over parietal electrodes from -60 to 0 ms. Around the response, we found a left central cluster involving Theta band.

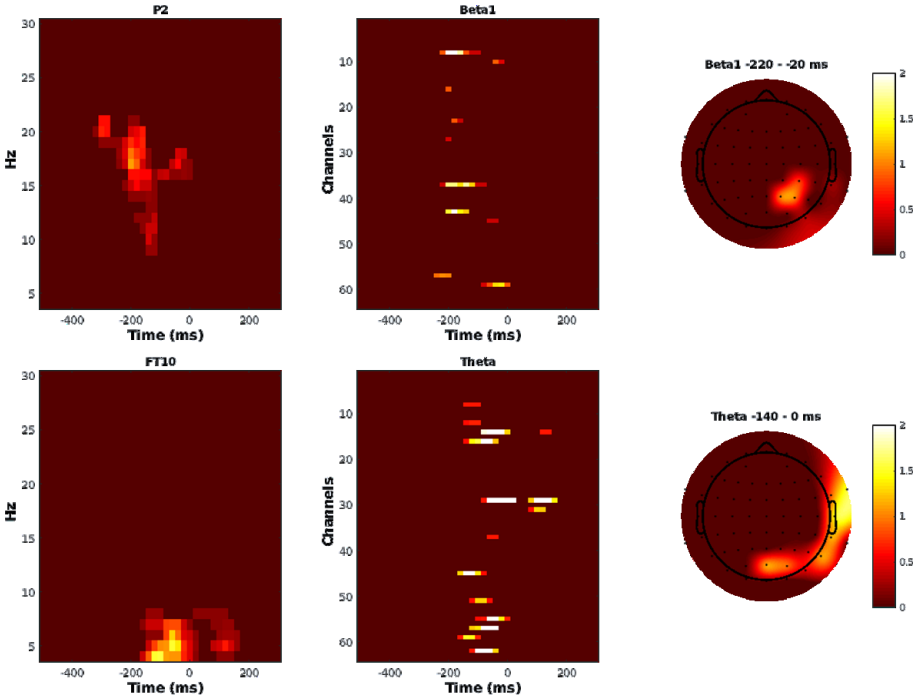

Figure 6.13.
RSA effect of the ISPC*CON_C interaction on response-locked data. The upper and lower panels show, respectively, the results for the Beta1 and Theta cluster. See Figure 6.2 for conventions.

We also found the representation for the interaction between ISPC and Conflict (CON_I), in four pre-response clusters. From -500 to -460 ms, there was a cluster involving Theta over left frontal scalp regions, followed by three clusters from about -240 to -100 ms, one over right fronto-central electrodes involving Beta2 frequency, one over right posterior electrodes involving Alpha frequency (see Figure 6.14), and a widespread one mainly distributed over left fronto-polar regions involving Theta band.

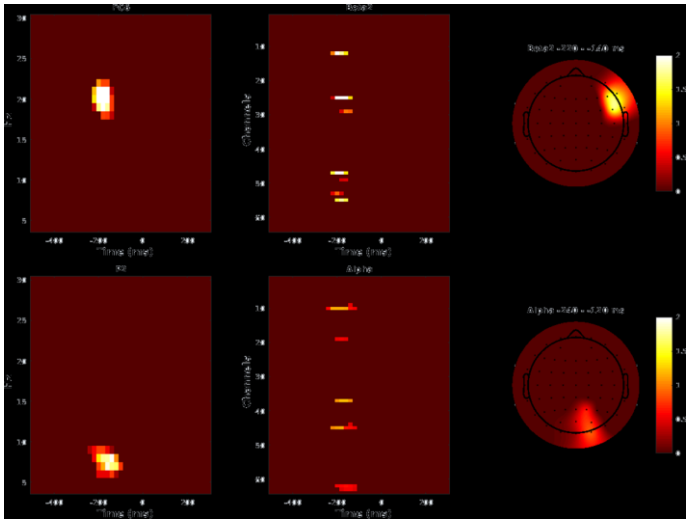

Figure 6.14.
RSA effect of the ISPC*CON_I interaction on response-locked data. The upper and lower panels show, respectively, the results for the Beta2 and Alpha cluster. See Figure 6.2 for conventions.

The multivariate activity pattern significantly encoded the ISPC*Target interaction in five clusters. In the early pre-response (from about -500 to -400 ms), there was a widespread Beta2 cluster mainly over left fronto-temporal electrodes and a Beta1 cluster over right parietal electrodes, followed by a small posterior cluster involving Beta1 over left posterior electrodes (see Figure 6.15). Around the response, we found an Alpha fronto-polar cluster and a Beta2 centro-parietal cluster (see Figure 6.15).

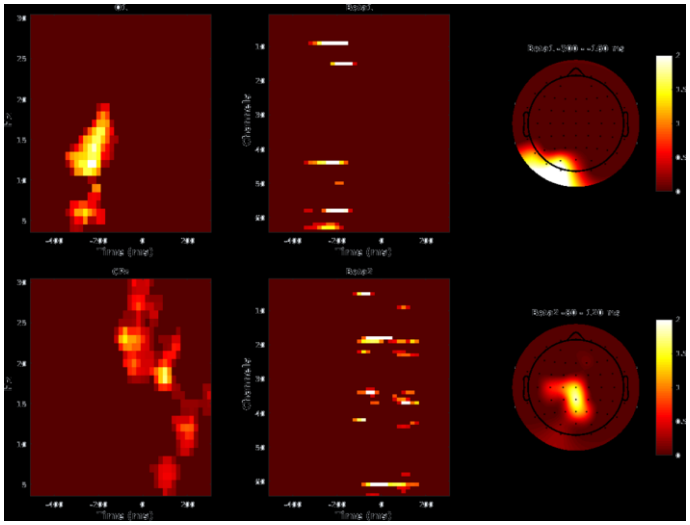

Figure 6.15.
RSA effect of the ISPC*Target interaction on response-locked data. The upper and lower panels show, respectively, the results for the Beta1 and Beta2 cluster. See Figure 6.2 for conventions.

Lastly, the interaction between ISPC and Distractor was significantly encoded by the multivariate pattern in two clusters. In the pre-response time window (from -500 to -40 ms), we found a sustained and

widespread fronto-posterior cluster involving Theta, Alpha, and Beta1 frequencies, followed, in the peri-response, by a Beta3 cluster distributed over posterior scalp regions (see Figure 6.16).

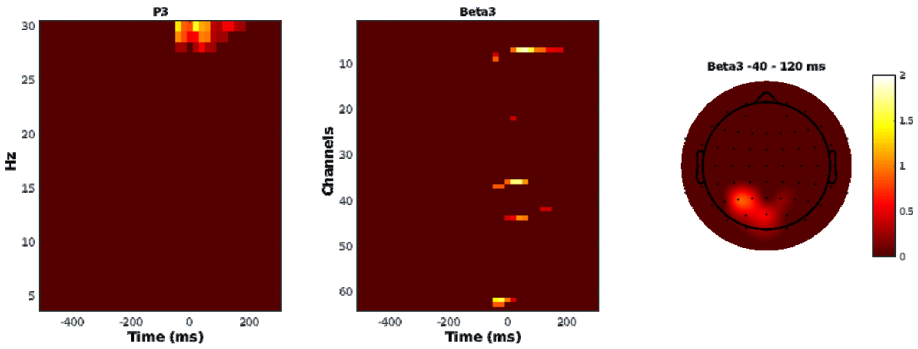

Figure 6.16.
RSA effect of the ISPC*Distractor interaction on response-locked data. See Figure 6.2 for conventions.

6.3.1.3. Pre-stimulus data

RSA on pre-stimulus data did not find any significant representation for our variables of interest, but only for low-level ones (i.e., PhS, PvS, PhR, and PvR, not reported here).

6.3.2. Ridge-based decoding

We performed ridge-based decoding to explore whether the spatio-temporo-spectral multivariate activity pattern predicted the continuous variables we manipulated to test proactive and reactive control. As for RSA results, we will report only the significant results for the effects of interest and, for stimulus-locked analyses, the results found within 600 ms, whereas for response-locked ones, the pre- and peri-response results.

6.3.2.1. Stimulus-locked data

Ridge regression on stimulus-locked data revealed that Congruency (CON), LWPC, ISPC and the interaction between ISPC and Congruency (ISPC*CON) were successfully decoded.

In particular, the spatio-temporo-spectral multivariate pattern successfully predicted Congruency in two clusters. The first cluster ranged from 240 to 440 ms mainly over posterior scalp regions and involved Alpha frequency, followed by a Theta cluster from about 320 to 520 ms distributed bilaterally over centro-parietal electrodes.

LWPC was significantly predicted by the multivariate activity pattern of a first early cluster involving Alpha frequency over mid-frontal, left centro-parietal and right temporal scalp regions. Subsequently, from

about 320 ms, we found a Theta fronto-centro-parietal cluster and a Beta1 cluster over bilateral frontal, mid-central and parietal electrodes.

The multivariate activity pattern predicted ISPC early in time in four clusters: A left frontal and bilateral parietal cluster ranging from 120 to 200 ms and involving Alpha band, followed by three clusters ranging from about 200 to 300 ms, one involving Theta frequency over centro-parietal electrodes, one involving Beta1 over left centro-frontal and right posterior electrodes and one involving Beta2/3 frequencies over left frontal electrodes.

Successful decoding of the interaction between ISPC and CON relied on the multivariate activity pattern in two clusters. A first early Beta2 cluster was expressed over right parietal and left fronto-central scalp regions which, from 200 ms, involved Beta1 frequency. An additional early cluster was found (from 120 to 280 ms), involving Theta and Alpha frequencies over occipito-parietal electrodes.

6.3.2.2. Response-locked data

Ridge regression on response-locked data successfully decoded Congruency (CON), LWPC, ISPC, and the interaction between ISPC and Congruency (ISPC*CON).

The multivariate activity pattern successfully predicted Congruency in an early and sustained cluster in the pre-response time window (from -500 to -20 ms), distributed bilaterally over posterior regions and involving Theta, Alpha, and Beta1 frequencies.

LWPC was successfully predicted by the multivariate activity pattern of a pre-response left parieto-temporal and right parietal and frontal cluster involving Theta and Alpha bands.

The multivariate activity pattern predicted ISPC in three pre-response clusters. The earlier (from -380 to -220 ms) involved Alpha frequency and was distributed over left prefrontal and bilateral posterior scalp regions, while the second (from about -240 to -60 ms) involved Theta frequency and was distributed over fronto-polar and right fronto-parietal electrodes. A third cluster was found at around -220 ms before response, involving Beta1 and Beta2 frequencies over left frontal, midfrontal and right posterior scalp regions.

Contingency was predicted by the multivariate activity pattern of an early and sustained pre-response cluster (from about -500 to -60 ms), distributed over right prefrontal and bilateral posterior electrodes, involving Theta, Alpha and Beta2 frequencies.

Lastly, the interaction between ISPC and Congruency was successfully decoded from the multivariate activity pattern from -300 ms, in a Beta1 cluster over right posterior scalp regions. Moreover, in the late

pre-response time window and around the response (from about -140 to 100 ms), we found a Theta and Alpha cluster distributed over centro-posterior electrodes.

6.3.2.3. Pre-stimulus data

Ridge-decoding on pre-stimulus data did not successfully predict any of our variables of interest, but only low-level ones (i.e., PvS and PvR, not reported here). Of note, the pre-stimulus multivariate activity patterns successfully predicted RTs in a Theta and Alpha cluster at about -60 ms, with a widespread distribution.

6.3.3. RSA-Ridge intersection

RSA and ridge decoding results were then compared to test whether, to decode our variables, ridge regression used the same multivariate activity patterns that we had previously identified encoding the same variables. Indeed, exploring commonalities allowed us to verify whether the information patterns of the representations were available for successful decoding and in turn, to provide stronger evidence for the representations we found.

It is important to note that one-to-one comparisons were not always feasible, since some variables that were meaningful to be modeled as RDMs in the RSA analysis could not be used in the ridge analysis. For example, CON_I and CON_C used in the RSA correspond to CON in the ridge analysis, which included both of them. As such, we compared results for both CON_C and CON_I to those for CON, and the same was done for the interactions. In contrast, LWPC and ISPC were directly comparable, whereas Target and Distractor could not be compared as they could not be included in the ridge statistical model.

This notwithstanding, we tried to perform comparisons as meaningful as possible. In what follows, we will report the results for the comparisons that have shown multivariate activity patterns in common between RSA and ridge regression.

6.3.3.1. Stimulus-locked data

Analyses on stimulus-locked data showed multivariate activity patterns in common between CON_C and CON, between LWPC, and between the ISPC*CON_C and ISPC*CON interactions.

Specifically, the multivariate activity patterns in common between CON_C and CON were found in two clusters: a first cluster early in time (from about 120 to 200 ms), involving Beta3 frequency and distributed over central scalp regions, left lateralized, followed by a cluster distributed over the same electrodes but involving the entire Beta band (see Figure 6.17).

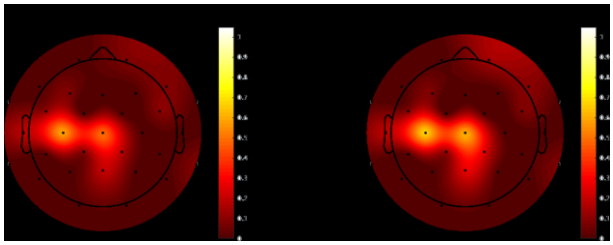

Figure 6.17.
RSA-Ridge intersection effect of CON_C/CON on stimulus-locked data. See Figure 6.2 for conventions.

The multivariate activity patterns found by both analyses for LWPC were found in an early Theta and Alpha cluster (from about 80 to 360 ms) distributed over parietal electrodes and more left lateralized (see Figure 6.18).

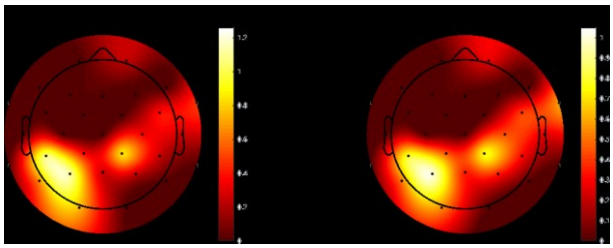

Figure 6.18.
RSA-Ridge intersection effect of LWPC on stimulus-locked data. See Figure 6.2 for conventions.

Lastly, the interactions ISPC*CON_C and ISPC*CON shared common multivariate activity patterns in an early cluster from 0 to 360 ms, involving Alpha frequency and distributed over right posterior scalp regions.

6.3.3.2. Response-locked data

Response-locked analyses revealed similar multivariate activity patterns for CON_I and CON, LWPC, and ISPC. Additionally, ISPC*CON_C and ISPC*CON interactions and ISPC*CON_I and ISPC*CON interactions shared multivariate activity patterns.

In particular, we found that CON_I and CON shared the multivariate activity patterns in the early pre-response time window (from about -500 to -220 ms), in a Theta and Beta1 cluster over left posterior electrodes and in the peri-response time window (from -140 to 20 ms), in a cluster involving the same frequencies but distributed over left fronto-central and right parietal scalp regions (see Figure 6.19).

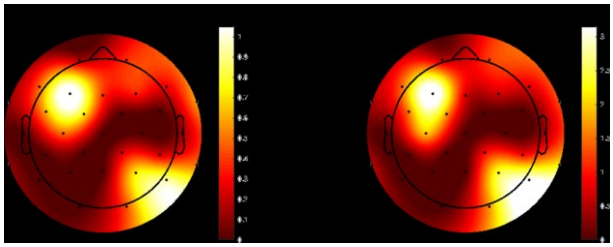

Figure 6.19.
RSA-Ridge intersection effect of CON_I/CON on response-locked data. See Figure 6.2 for conventions.

The shared multivariate activity patterns for LWPC were found in a pre-response cluster from about -420 to -60 ms involving Theta and Alpha frequencies and distributed over left temporo-parietal electrodes (see Figure 6.20).

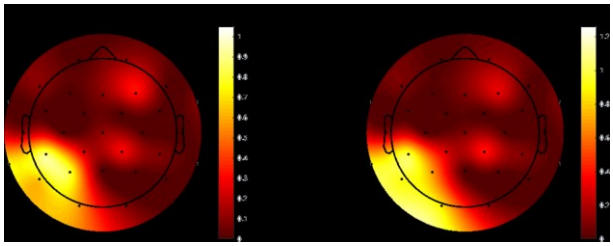

Figure 6.20.
RSA-Ridge intersection effect of LWPC on response-locked data. See Figure 6.2 for conventions.

The multivariate activity patterns found by both analyses for ISPC involved Beta2 frequencies at about 220 ms before response and over left fronto-central electrodes (see Figure 6.21).

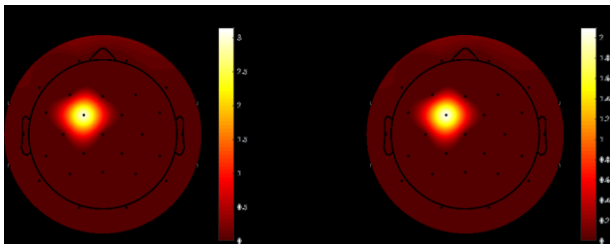

Figure 6.21.
RSA-Ridge intersection effect of ISPC on response-locked data. See Figure 6.2 for conventions.

The ISPC*CON_C and ISPC*CON interactions shared common multivariate activity patterns in two pre-response clusters: an earlier (from -260 to -20 ms) cluster over right parietal electrodes involving Beta2 frequency, and a later (from -140 to 140 ms) cluster over left centro-parietal and right parietal electrodes, involving Theta and Alpha frequencies (see Figure 6.22).

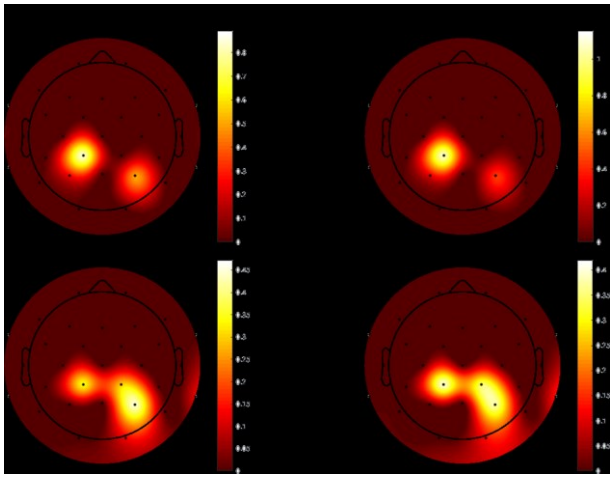

Figure 6.22.
RSA-Ridge intersection effect of the ISPC*CON_C/CON interaction on response-locked data. See Figure 6.2 for conventions.

Lastly, we also identified common multivariate activity patterns for the interactions ISPC*CON_I and ISPC*CON in two pre-response clusters: a widespread one involving Alpha band from -220 to -20 ms mainly distributed over left frontal and medial parietal scalp regions, and a smaller one involving Beta2 frequency from -180 to -140 ms over left centro-parietal electrodes.

6.3.3.3. Pre-stimulus data

In the pre-stimulus time window, no multivariate activity pattern in common survived.

6.4. Discussion

Cognitive control works through the retention and updating of internal representations containing the information required for task execution (Cohen, 2017; Sakai 2008). Given their pivotal role, representations stand at the core of numerous theories of cognitive control (Badre et al., 2021; Braver, 2012; Cellier et al., 2022; Cohen et al., 1990). However, our understanding of these representations remains limited, which accounts for the lack of a comprehensive understanding of cognitive control dynamics at the neural level (Freund, Etzel, et al., 2021).

In the present study, our aim was to advance in this direction by investigating one of the most influential models of cognitive control, the Dual-Mechanisms of Control (DMC; Braver, 2012; Braver et al., 2007). Specifically, our goal was to explore whether and how proactive and reactive control are encoded at the neural level. To pursue our aim, in an EEG study, we manipulated LWPC and ISPC at the trial level to induce proactive and reactive control, respectively, and then we employed Multivariate Pattern Analysis (MVPA) approaches which, despite having been employed previously to study cognitive control, have not yet been

utilized to investigate these two control modes. In particular, we employed the two most predominant multivariate techniques to investigate both the encoding and decoding of proactive and reactive control representations. RSA was first used to directly test the representations theorized by the DMC and to characterize the representational geometry of proactive and reactive control representations. Then, assuming that, if the representational content is encoded, then it should also be available for downstream neurons to use it, ridge regression decoding was used to verify whether successful decoding was possible, that is, whether such informational patterns were available. For both MVPA techniques, we adopted a spatio-temporo-spectral approach to fully exploit the information carried by the EEG signal, and we were then able to intersect RSA and ridge regression results to identify converging evidence for such representations.

Before delving into the discussion of our results, it is necessary to provide a preamble to underscore the difficulty (and limitations) inherent in our aim to explore representations of cognitive control. Indeed, investigating representations in neuroscience poses challenges, not only methodologically (as evident in the issues related to MVPA and especially decoding methods, as outlined in the introduction) but also in terms of the very meaning of representations. This issue is first of all relevant from a philosophical point of view as mapping world features onto neural functioning in an intuitive manner, presupposing that the brain functions just as we perceive the world and truly relies on the verbal definitions we use to describe it, is already a significant problem in itself. Without being certain that the verbal categories commonly employed when studying the brain, such as functions and mechanisms, are not merely indefinable essences but rather entities genuinely existing and utilized/present in the brain, there is a possibility that we are overlooking the true essence of how the brain operates (Brick et al., 2022; Duncan, 2010). However, addressing this huge issue, which also concerns neural representations, goes beyond the scope of the present work and would require more than one PhD thesis (but see Brick et al., 2022 for a deep discussion on this topic). The second challenge has been outlined in the introduction of this Chapter, that is the lack of a precise definition of representation. Therefore, given our aim of exploring cognitive control representations, in discussing our results we will try to stuck as much as possible to the criteria provided by Baker and colleagues (2021), which are clear and systematic. This will be of particular importance because cognitive control is already a complex construct in itself, making it even more challenging to understand the implied representations, and it is probably not the first construct from which one should start to comprehend the meaning and functioning of neural representations. This notwithstanding, most of the fundamental aspects provided by Baker and colleagues (2021) to define a representation as such are generally ensured by our approach. First, by using RSA we directly measure the correlation between world features, modelled as RDMs, and neural activation patterns, thus being able to explore whether they match or not. Second, by having hypotheses about how cognitive control functions, we can quite safely ensure that the identified representations have a teleological side, that is, are used with specific purposes. What instead cannot be

ensured by our approach is the causal effect of these representations on behavior, which would require to perform further analyses, such as RSA-behavior correlations, which were not included in the present work because they would have required a much larger sample size than that we used here. Therefore, they will be performed in future ad-hoc studies.

6.4.1. Conflict representations

Before delving into proactive and reactive control representations, we will discuss whether and how the presence (or absence) of Conflict was represented. Conflict-related representations were fundamental to explore as both proactive and reactive control modes, according to the DMC, are postulated to depend on the presence or absence of Conflict. Therefore, it is reasonable to assume that, at the representational level, the encoding of the presence or absence of conflict can influence the encoding of LWPC and ISPC representations, which are necessary to implement the required amount of proactive and reactive control, respectively. Thus, to modulate LWPC and, especially, ISPC encoding, a Conflict representation should also be encoded per se. To explore this hypothesis using RSA, we modeled two distinct RDMs, one representing the absence (CON_C) and one representing the presence (CON_I) of Conflict.

Our analysis revealed that, at the stimulus level, only the absence of Conflict was encoded, while at the response level, only the presence of Conflict was represented around the time of the response.

The fact that the presence of Conflict was more strongly represented around the time of the response, but not early in time after stimulus appearance, could suggest that this representational encoding could be related to conflict resolution at the response level. Nonetheless, it is important to acknowledge that our study did not specifically manipulate response conflict and that this type of conflict constitutes just one of the conflict components included in the Stroop effect (i.e., there are also stimulus and task conflicts, see Viviani et al., 2023; see also Chapters 2 and 7). Therefore, this leaves open the possibility for the effect of other forms of Conflict-related representations in modulating PC representations. This notwithstanding, the stronger Conflict representation emerging late in time might also reflect a form of conflict that cannot be resolved by the proactive and reactive control modes manipulated in this study, as discussed in Chapter 5. Indeed, our ISPC manipulation induces an early form of reactive control relying on stimulus-attention associations (Tafuro et al., 2020; Bugg, 2012, 2017; Bugg & Hutchison, 2013), which could act to resolve the conflict at the stimulus level. However, a later form of conflict can arise at the response level when proactive and ISPC-dependent reactive control mechanisms fail in resolving the earlier form of conflict at the stimulus level, and thus a more response-related and late-in-time form of control needs to be implemented. This later form of reactive control, more akin to the late correction mechanism postulated by the DMC and the later stages of control resolution postulated by the Cascade of Control model (Banich, 2009), could thus have contributed here to strengthen Conflict representation encoding at the response

level (in line with our ER(S)P results, see Chapter 5; see also Tafuro et al., 2020). Moreover, this interpretation is in line with the adaptive control models assuming that conflict detection occurs in the response module (i.e., conflict is detected when two incompatible responses are activated), thus explaining why Conflict representation is encoded only when response conflict occurs (Botvinick et al., 2001).

However, we also speculate that early conflict detection is more likely to be more easily detected by a standard process-based analysis than by a representation-based one like our RSA analysis. What we found here is thus more likely to be the consequence of conflict detection processes that contributed to create a representation of the current presence of Conflict, which then could have been used to resolve it in response-related control stages, and to update the PC-related estimates to control performance in following trials. Moreover, the absence of Conflict was also encoded, quite after stimulus appearance and at the stimulus level, probably indicating a complex relation between conflict detection processes and the encoding of Conflict-related representations.

Moreover, the fact that both the presence and absence of Conflict were, at least partially, spatially and spectrally overlapped, suggests that they might be complementary aspects of the same complex representation. Indeed, they were both encoded mainly through left fronto-central Beta2 activity. This points to the functional role of Beta frequency band in encoding conflict-related representations, in line with findings suggesting its involvement in inhibiting competing task sets and selecting relevant task sets and information to support task performance (Cellier et al., 2021, Riddle et al., 2020, Buschman et al., 2012; Antzoulatos & Miller, 2016; Spitzer & Haegens, 2017; see also Tafuro et al., 2019).

The multivariate activity pattern encoding for Conflict was also effectively used by ridge regression to decode our Congruency variable. Indeed, although with ridge regression we had to test the presence and absence of Conflict altogether, by including in the model Congruency which comprises both (see Section 6.2.5), we found multivariate activity patterns in common between RSA and ridge results. In particular, both revealed, late after stimulus appearance, a left central cluster involving Beta frequencies and, around the response, a left fronto-central cluster involving Beta1 frequency. The fact that multivariate activity patterns similar to those found by RSA significantly predicted Congruency provides stronger evidence for the Conflict representation. Additionally, in ridge-based analysis, finding a similar pattern at the stimulus and response level by testing the entire Conflict representation further supports our interpretation above, that is, although Conflict is more strongly represented during response-related processes, it relies on a complex representational pattern that starts to be encoded after stimulus and strongly relies on conflict at the response level.

6.4.2. Proactive control-related representations

To induce proactive control, we manipulated LWPC and, assuming that it is dynamically updated based on trial history, we estimated it at the trial-level obtaining its continuous values. At the neural level, we expected to find a representation of LWPC which would serve as the basis for implementing proactive control. The underlying assumption is that, if such representation can be identified, it means that it is available to be used by downstream processes of proactive control. Testing the similarity between model-based LWPC RDM and the observed brain patterns thus provided a means to investigate the presence of proactive control from a representational perspective.

LWPC representation should be available relatively early and before response to enable the implementation of the required level of proactive control. Our findings support this assumption, as we found the representation of LWPC at both the stimulus and response levels early in time. Specifically, at the stimulus level, the representation of LWPC was encoded in a left occipito-parietal cluster as early as 120 ms after the stimulus onset (till 300 ms), and its encoding involved Theta frequency. Therefore, its early nature could enable it to be accessed and utilized proactively. The decoding results further supported the RSA-based finding, showing that the same multivariate activity pattern was used by ridge regression to predict LWPC. Indeed, the intersection analysis indicated the involvement of a Theta cluster over left parietal scalp regions during a similar time window (from 80 to 360 ms), thus revealing strong converging evidence for how LWPC is encoded at the stimulus level.

Response-based results were consistent with stimulus-based findings. RSA revealed a left centro-parietal Theta cluster before response. Although this cluster was significant still quite early in the pre-response time window (from -300 ms before response), it emerged slightly later than the stimulus-locked cluster, probably due to a motor involvement, as also suggested by the concomitant presence of a Beta1 cluster over right parietal scalp regions. The intersection between RSA and ridge results showed that the multivariate activity pattern used to predict LWPC at the response level involved the same Theta left parietal cluster identified by RSA, which was also observed in a similar time window before response. As such, this provides converging evidence for the role of the LWPC representation in modulating not only stimulus-locked, but also response-locked neural activity.

The fact that LWPC representation was encoded by lateralized posterior Theta activity is consistent with the available evidence for the importance of this frequency band for the encoding of new information (Klimesch, 1999), as well as the formation of complex memory representations and the transfer of information into and out of long-term memory (Lisman, 2010; Sans-Dublanc et al., 2017; Backus et al., 2016; Lega et al., 2012). Indeed, in order to represent the trial-by-trial dynamics of our manipulated LWPC, the experienced Congruency has to be integrated with the memory of the recent history of Congruency,

and the obtained updated LWPC representation has to be retrieved to adapt proactive control engagement.

The specific LWPC representation, revealed by both our analyses, thus suggests that such a representational pattern was robust and had a strong cognitive nature, as it was similar at both the stimulus and response levels, and not specifically locked to either purely perceptual- or response-dependent encoding. Given its proactive and early nature, one might speculate that the representation of LWPC could be observed even before the stimulus onset. However, we did not find evidence for a significant pre-stimulus encoding, likely because it is cognitively demanding to sustain an active representation constantly, and it is more efficient to activate it early as soon as the stimulus appears. As such, we could speculate that it was encoded even before stimulus appearance but that the strength of such encoding was not enough to be revealed. Future studies should adopt more sensitive experimental and analytical approaches to unveil whether this is the case (see Section 8.5.2).

Our statistical model tested also the interactions between LWPC and the presence/absence of Conflict, which were central to our aim of exploring proactive control representations. Indeed, these interactions could show how the representational content necessary to implement proactive control was dynamically used based on Conflict presence/absence and the multivariate activity patterns encoding for that. Such dynamics may act directly on the LWPC encoding, modifying it, but also the involvement of additional multivariate activity patterns could be plausible.

The interaction between the absence of Conflict and LWPC was significant both at the stimulus and the response levels, but the more consistent results were the response-locked ones, as they more strongly reflected a modification of the representation of LWPC by the representation of the absence of Conflict. Indeed, we found that the interaction was encoded as a multivariate activity pattern observed over left-parietal scalp regions, as for LWPC, and in a similar time window (from -380 ms before response), and involving Beta3 frequency, but also Theta band, as for LWPC. Although these findings were not supported by ridge regression results, they plausibly reflect a direct modulation of the LWPC representation by the absence of Conflict. Moreover, identifying such direct modulation at the response but not at the stimulus level, might be due to the greater strength of the complex representational pattern of Conflict at the response level, as suggested above. Indeed, it probably took time for the absence of Conflict to be represented, and consequently to use the LWPC representation accordingly.

The interaction between Conflict and LWPC was again more robust at the response level. Indeed, it was encoded by a multivariate activity pattern very similar to LWPC, with an early pre-response and sustained Theta cluster over parietal scalp regions, slightly left lateralized. As such, as it overlapped with LWPC representation, it is likely that the presence of Conflict directly modulated the LWPC encoding pattern. The

finding of such modulation at the response but not at the stimulus level is in line with our interpretation above, that is, Conflict was more strongly represented at the response level and thus it took some time for it to be encoded and then, in turn, for its effect to modulate the LWPC representation.

Overall, our RSA results provided evidence that LWPC was modulated by Conflict representations and that the strength of this modulation was greater at the response level than at the stimulus level. Indeed, both response-related Conflict representations (CON_C and CON_I) showed clear evidence for it, by directly modulating the LWPC multivariate activity pattern. However, also stimulus-locked Conflict representations modulated LWPC encoding, and relatively early in time, suggesting a role for these effects in subserving proactive control processes, even though more indirectly, namely through distinct multivariate activity patterns. Therefore, it is plausible that a complex interplay between the presence and the absence of Conflict modulated the LWPC encoding, and this modulation started to be encoded at the stimulus level, but became stronger at the response level as proactive control representations might be used to proactively control responses. It has to be noted that these findings were obtained only with RSA analyses, thus were not confirmed in the opposite decoding direction, probably because the complexity of such multivariate activity patterns was too high and not so strong to be clearly decoded.

The two additional interactions we tested for LWPC contributed instead to explore how proactive control might work, that is, whether it enhances strength of representations related to the goal (LWPC*Target) or reduces the strength of those related to the distracting task/features (LWPC*Distractor). Of note, they could be explored only using RSA and thus we did not have bidirectional evidence for them.

The interaction between LWPC and Target was encoded by early multivariate activity patterns at the stimulus level, but not at the response level. This result is in line with a proactive control modulation of the goal that should occur in advance, being more related to the task set compared to the response level. Indeed, the LWPC representation should contain the information regarding the level of proactive control that needs to be implemented immediately after stimulus onset so as to enhance Target representation accordingly. For example, when proactive control is higher (i.e., when Conflict is more probable), the representation of Target should be stronger. Such interaction was encoded by an Alpha right prefrontal cluster and a Beta1 left lateral cluster from about 160 to 300 ms, while Target was represented by a central cluster in the same time window involving Beta1 band. Therefore, it seems that proactive control modulated in a complex manner the Target representation. The fact that the encoding of Target representation, as well its modulation by LWPC, involved the Alpha/Beta1 frequencies activity is in line with the role of these frequency bands in representing task-relevant, stimulus-specific information and in encoding the content of working memory (Michelmann et al., 2022; Kikumoto & Mayr, 2018; Kikumoto et al., 2022).

The interaction between LWPC and Distractor was found only at the response level. Specifically, it was encoded quite early (from -440 ms) by a multivariate activity pattern involving Beta2 frequency over right prefrontal scalp regions. Therefore, this might reflect the proactive control modulation of the Distractor representation held in working memory (e.g., Estefan et al., 2023), which could work by reducing the strength of its encoding at the motor level. This modulation did not overlap with the multivariate activity pattern found to encode Distractor representation per se at the response level, as it was observed later, over more posterior right scalp regions and involving Beta1 band, suggesting again a complex modulatory pattern.

Overall, these findings contribute valuable insights to the existing literature, offering quite robust and converging evidence for the specific representation of proactive control. Indeed, these representations are likely utilized by the proactive control processes previously identified through studies employing univariate approaches (for example, those found in our ER(S)P study, see Chapter 5). Moreover, we provided initial insights into how Conflict-related representations modulated proactive control. Testing such complex modulation was possible thanks to our continuous LWPC manipulation that allowed us to use a model RDM for LWPC reflecting in a fine-grained manner proactive control, which was thus more suitable for revealing its dynamic modulations. Lastly, our findings suggest that proactive control might work by enhancing the strength of goal representation at the stimulus level, but also by reducing the strength of the distracting representation at the response level.

6.4.3. Reactive control-related representations

Reactive control was induced by manipulating ISPC, which, similarly to LWPC, is likely to be dynamically updated based on trial history. However, unlike LWPC, which involves a single binomial distribution, the manipulation of ISPC induces the trial-by-trial updating of four binomial distributions (the PC of each possible position), with only one of them being the one observed by participants (the PC of the observed stimulus position). Therefore, for the analyses we used trial-level estimates of the ISPC weighting it relatively to the ISPC values of the other positions at the same trial. This allowed us to test the ISPC representation with a high degree of precision.

To explore reactive control from a representational standpoint, we assessed the similarity between the model-based ISPC RDM and the observed brain patterns. Indeed, discovering that ISPC is encoded at the neural level would imply that it is accessible for downstream processes that execute reactive control. Before delving into its neural encoding, a clarification is necessary. As noted in Chapters 1 and 5, the manipulation of ISPC induces a form of reactive control which is early in nature as it relies on stimulus-attention associations (Tafuro et al., 2020; Bugg, 2012, 2017; Bugg & Hutchison, 2013). This is because participants, upon seeing the stimulus (and thus its position), can activate the PC associated with that item

and engage a specific amount of reactive control accordingly. Therefore, despite the reactive nature of the control mechanism induced by ISPC, the encoding of its representation may not necessarily be observed exclusively around the response, and it may also be encoded early in time. Our RSA results were only partially consistent with this assumption, revealing that ISPC was not encoded at the stimulus level, but its encoding was significant early in time at the response level.

While our expectation was to observe also a stimulus-locked ISPC representation, the strength of its encoding at the stimulus level might not have been sufficient to be detected by RSA due to the time required for its activation. Indeed, since it cannot be activated proactively, that is, before seeing the stimulus, it likely requires a variable amount of time to be stably encoded. However, ridge regression decoding on stimulus-locked data successfully predicted ISPC through early multivariate activity patterns occurring within 300 ms after stimulus, and involving Theta, Alpha and Beta2 frequencies mainly over left fronto-centro-parietal scalp regions.

Conversely, RSA showed that ISPC was prominently encoded at the response level, indicating its direct impact at the response level. To be noted that, as hypothesized above, it was significantly represented quite early before response, from about -280 ms (till -180 ms), in a left fronto-centro-parietal cluster involving Beta2 frequency. This multivariate activity pattern also overlapped with the one used by ridge regression to predict response-locked ISPC, providing converging evidence for the involvement of left fronto-central Beta2 frequency at about -220 ms. The early encoding of ISPC at the level of response might reflect that stimulus-attention associations were activated early in time but were specifically linked to response. As such, this representation could have subsequently enabled the implementation of reactive processes operating at the level of the response.

Therefore, we identified the ISPC representation necessary for the execution of reactive control processes. The stable encoding of this representation at the response level and mainly involving left Beta2 frequency may suggest a strong involvement of response-related representations in the implementation of reactive control, in line with the functional role of this frequency band in encoding task-relevant representations to guide downstream action selection mechanisms (Buschman et al., 2012; Sherfey et al., 2020; see also Cannon et al., 2014). Nevertheless, the early encoding of response-locked ISPC, coupled with ridge regression successfully predicting ISPC using a similar stimulus-locked multivariate activity pattern, hints that ISPC encoding might initiate almost immediately following stimulus onset, albeit with a somewhat lesser strength.

The representation of ISPC was explored also in the pre-stimulus time window, but using a different RDM that reflected the similarity between all four possible positions, as it is not possible to know which one will appear before seeing the stimulus. Although this representation should be active before the stimulus

onset, to allow the selection of the PC associated with the observed position, we did not find evidence for its encoding before stimulus appearance. It is likely that, just like pre-stimulus LWPC, sustaining an anticipatory representation throughout the entire pre-stimulus period is cognitively demanding and, for this reason, probably its encoding was not strong enough to be detected (see also Section 8.5.2).

Similarly to proactive control-related representations, we also explored how Conflict-related representations modulated the encoding of ISPC representation, by testing it in interaction with the presence/absence of Conflict.

The interaction between the absence of Conflict and ISPC was encoded both at the stimulus and at the response levels. Specifically, the stimulus-locked ISPC representation was modulated by the absence of Conflict early, from 160 ms onwards, mainly over right parieto-occipital scalp regions and involving Alpha frequency. This multivariate activity pattern was also used to decode the ISPC*CON interaction by ridge regression, as shown by the intersection results. Therefore, these findings support our prior interpretation that ISPC starts to be encoded at the stimulus level but it takes time for it to be stably encoded. Indeed, the absence of Conflict, by showing a role in modulating the stimulus-locked encoding of ISPC immediately after stimulus onset, probably reflects the necessary time for it to be stably encoded, suggesting that, as it emerged, the absence of Conflict modulated its encoding strength. This is also consistent with the fact that, later in time, from 300 ms, RSA revealed an additional significant representation for such interaction, involving Beta2 over left fronto-central scalp regions. This encoding pattern overlapped with that for ISPC alone, which may reflect the result of the direct modulatory effect of the absence of Conflict on the ISPC encoding.

The response-locked interaction between CON_C and ISPC was encoded in the pre-response time window, first in a Beta1/2 cluster over right parietal scalp regions, and then in a Theta cluster over right temporo-parietal scalp regions. Ridge regression-RSA result intersection was found for both clusters, showing that they implied the same multivariate activity patterns used to decode the response-locked ISPC*CON interaction. Such converging evidence for an earlier right parietal Beta1/2 cluster and a later parietal Theta cluster provides further evidence for the previously identified strong encoding of ISPC at the response level and further suggests that the strength of the ISPC encoding was modified through a complex modulation by the absence of Conflict. Indeed, the ISPC informational content, mainly represented over left fronto-central scalp regions through Beta2 frequency, was modulated by response-locked representations encoded through the same frequency but more posteriorly.

The interaction between ISPC and Conflict was encoded only at the response level, specifically from -240 ms before response, mainly represented over right posterior scalp regions involving Alpha frequency and over right fronto-central scalp regions involving Beta2 frequency. The intersection between the RSA and

ridge regression results provided converging evidence for the involvement of these clusters, showing that their multivariate activity patterns were also employed in decoding the response-locked ISPC*CON interaction. At the temporal level, the encoding of the interaction representation had a timing similar to the encoding of ISPC and the previous interaction (ISPC*CON_C). As such, this suggests that not only ISPC representation was encoded quite early before response, but also that in the same temporal window its strength was modulated by Conflict-related representations. Moreover, this modulation occurred in a direct manner, as suggested by the Beta2 involvement in both the encoding of ISPC and in the modulation of its strength through Conflict representation. This finding suggests a relevant role of Beta2 in dynamically marking the reactive control-related representation.

Overall, we found evidence that ISPC was modulated by Conflict-related representations and that this modulation was stronger at the response level. Both the presence and absence of Conflict, through a complex interplay, were involved in modulating ISPC representation strength after seeing the stimulus and retrieving its PC, for response-related processes. Furthermore, our results show that ISPC was encoded and modulated within a specific time window, although it started to be encoded early after stimulus onset.

Finally, the other two interactions contributed to exploring how reactive control operates. In particular, the interaction between ISPC and Target was encoded at the response level only. This is in line with a reactive control modulation of the goal, whose strength, upon seeing the stimulus and retrieving its PC, plausibly requires time to be modulated by the ISPC representational content. Furthermore, it suggests that even though the representation of ISPC is cognitive in nature, it may operate by modulating early in time the response aspects of goal representation, as suggested by its encoding in a left posterior cluster from -300 ms involving Beta1 frequency. Additionally, the cluster found around the response time and involving centro-parietal Beta2 frequency could reflect a direct modulatory effect as it partially overlapped with the one of ISPC representation.

Lastly, we found that the interaction between ISPC and Distractor was encoded both at the stimulus and response levels. In particular, the stimulus-locked representation of this interaction emerged from 240 ms over right centro-parietal scalp regions, in Beta2/3 frequencies, while the response-locked representation relied on a sustained pre-response fronto-posterior and spectrally widespread cluster and on a peri-response posterior cluster involving Beta3 frequency. It is therefore reasonable to suggest that ISPC modulated the Distractor representation in two phases: first, after stimulus onset, reducing its strength at the perceptual level, and then diminishing the representational strength of the Distractor representation by acting at the response level.

Overall, aided by the use of a finely detailed model RDM reflecting the ISPC dynamics, our findings extend beyond prior literature. Indeed, we found initial but converging evidence for the specific

representation of ISPC-induced reactive control, revealing that it was characterized by an encoding pattern distinct from that of proactive control. To the best of our knowledge, such distinction has never been revealed at the neural level before. This could likely be attributed to the fact that prior studies primarily employed univariate approaches, which lack sensitivity in detecting reactive control signatures, as this type of control is more likely rooted in representation rather than process. In our preceding study (see Chapter 5), utilizing univariate analyses on the same dataset, we indeed did not find any evidence for ER(S)P correlates of ISPC-induced reactive control processes. This absence of evidence might have been attributable to the overshadowing effects of contingency mechanisms at the process level. However, the fact that in the present study, while still controlling for contingency, we were able to uncover ISPC-related reactive control encoding patterns, might suggest that the employed multivariate approaches are indeed more suitable for exploring the multivariate nature of reactive control representations.

Furthermore, our analyses provided insights into how conflict-related representations modulated the ISPC representation, thereby revealing a complex picture of such dynamics. Finally, our results unveiled how reactive control might function, that is, by strengthening goal representation at the response level, and diminishing distracting representation strength at both perceptual and motor levels.

6.5. Conclusions

In the pursuit of our aim of ascertaining whether and how proactive and reactive control representations are encoded at the neural level, we provided evidence for distinct encoding patterns for each of these two control modes, revealing that proactive and reactive control can be differentiated at the neural level.
Indeed, in doing so, we were also able to characterize proactive and reactive encoding patterns, showing that proactive control representation acts at both stimulus and response levels, and that reactive control representation starts to be activated after the stimulus onset but it is more specifically linked to response. This evidence was robust and converging as it derived from the intersection of RSA and ridge regression results.

While these findings expand the existing literature on proactive control by offering evidence for the representations underlying its previously identified processes, they hold even greater significance for reactive control. In the case of reactive control, indeed, our results are particularly revealing, as they provide initial but substantial evidence for the actual existence of an ISPC-induced reactive control mechanism at the neural level and confirm that reactive control has a complex multivariate nature, that can thus be uncovered effectively by multivariate approaches.

Furthermore, our results provided further insights on proactive and reactive control dynamics. First, we found that conflict-related representations exerted distinct modulatory effects on proactive and reactive control representations, showing a plausible scenario of dynamic utilization of LWPC and ISPC representations contingent on the presence or absence of conflict. Second, our results suggest that LWPC and ISPC representations might be then used to enhance the strength of the goal information and diminishing the strength of the distracting information in different manners, thus providing further evidence for their functional dissociation.

6.6. References

Antzoulatos, E. G., & Miller, E. K. (2016). Synchronous beta rhythms of frontoparietal networks support only behaviorally relevant representations. *eLife*, *5*, e17822. https://doi.org/10.7554/eLife.17822

Backus, A. R., Schoffelen, J.-M., Szebényi, S., Hanslmayr, S., & Doeller, C. F. (2016). Hippocampal-Prefrontal Theta Oscillations Support Memory Integration. *Current Biology*, *26*(4), 450–457. https://doi.org/10.1016/j.cub.2015.12.048

Badre, D., Bhandari, A., Keglovits, H., & Kikumoto, A. (2021). The dimensionality of neural representations for control. *Current Opinion in Behavioral Sciences*, *38*, 20–28. https://doi.org/10.1016/j.cobeha.2020.07.002

Baker, K. S., Pegna, A. J., Yamamoto, N., & Johnston, P. (2021). Attention and prediction modulations in expected and unexpected visuospatial trajectories. PLoS ONE, 16(10 October). Scopus. https://doi.org/10.1371/journal.pone.0242753

Banich, M. T. (2009). Executive function: The search for an integrated account. *Current directions in psychological science*, *18*(2). https://doi.org/10.1111/j.1467-8721.2009.01615.x

Bode, S., Feuerriegel, D., Schubert, E., & Hogendoorn, H. (2021). *Decoding continuous variables from EEG data using linear support vector regression (SVR) analysis with the Decision Decoding Toolbox (DDTBOX)* (p. 2021.05.31.446502). bioRxiv. https://doi.org/10.1101/2021.05.31.446502

Botvinick, M. M., Braver, T. S., Barch, D. M., Carter, C. S., & Cohen, J. D. (2001). Conflict monitoring and cognitive control. *Psychological review*, *108*(3). 10.1037/0033-295x.108.3.624

Braver, T. S. (2012). The variable nature of cognitive control: A dual mechanisms framework. *Trends in Cognitive Sciences*, *16*(2), Article 2.

Braver, T. S., Gray, J. R., & Burgess, G. C. (2007). Explaining the many varieties of working memory variation: Dual mechanisms of cognitive control. *Variation in Working Memory*, *75*, 106.

Brick, C., Hood, B., Ekroll, V., & de-Wit, L. (2022). Illusory Essences: A Bias Holding Back Theorizing in Psychological Science. Perspectives on Psychological Science, 17(2), 491–506. https://doi.org/10.1177/1745691621991838

Bugg, J. M. (2012). Dissociating Levels of Cognitive Control: The Case of Stroop Interference. *Current Directions in Psychological Science*, *21*(5), 302–309. https://doi.org/10.1177/0963721412453586

Bugg, J. M. (2017). Context, conflict, and control. *The Wiley handbook of cognitive control*, 79–96.

Bugg, J. M., & Hutchison, K. A. (2013). Converging evidence for control of color–word Stroop interference at the item level. *Journal of Experimental Psychology: Human Perception and Performance*, *39*(2).

Buschman, T. J., Denovellis, E. L., Diogo, C., Bullock, D., & Miller, E. K. (2012). Synchronous Oscillatory Neural Ensembles for Rules in the Prefrontal Cortex. *Neuron*, *76*(4), 838–846. https://doi.org/10.1016/j.neuron.2012.09.029

Cannon, R. L., Baldwin, D. R., Diloreto, D. J., Phillips, S. T., Shaw, T. L., & Levy, J. J. (2014). LORETA Neurofeedback in the Precuneus: Operant Conditioning in Basic Mechanisms of Self-Regulation. *Clinical EEG and neuroscience*, *45*(4). https://doi.org/10.1177/1550059413512796

Cellier, D., Petersen, I. T., & Hwang, K. (2022). Dynamics of Hierarchical Task Representations. *The Journal of Neuroscience: The Official Journal of the Society for Neuroscience*, *42*(38), 7276–7284. https://doi.org/10.1523/JNEUROSCI.0233-22.2022

Cheng, F. (2021). *Using Single-Trial Representational Similarity Analysis with EEG to track semantic similarity in emotional word processing* (arXiv:2110.03529). arXiv. https://doi.org/10.48550/arXiv.2110.03529

Cohen, J., Asarnow, R., Sabb, F., Bilder, R., Bookheimer, S., Knowlton, B., & Poldrack, R. (2011). Decoding Continuous Variables from Neuroimaging Data: Basic and Clinical Applications. *Frontiers in Neuroscience*, *5*. https://www.frontiersin.org/articles/10.3389/fnins.2011.00075

Cohen, J. D. (2017). Cognitive control: Core constructs and current considerations. In *The Wiley handbook of cognitive control* (pp. 3–28). Wiley Blackwell. https://doi.org/10.1002/9781118920497.ch1

Cohen, J. D., Dunbar, K., & McClelland, J. L. (1990). On the control of automatic processes: A parallel distributed processing account of the Stroop effect. *Psychological Review*, *97*(3). https://doi.org/10.1037/0033-295x.97.3.332

Cole, M. W., Ito, T., & Braver, T. S. (2016). The Behavioral Relevance of Task Information in Human Prefrontal Cortex. *Cerebral Cortex*, *26*(6), 2497–2505. https://doi.org/10.1093/cercor/bhv072

Davis, T., LaRocque, K. F., Mumford, J. A., Norman, K. A., Wagner, A. D., & Poldrack, R. A. (2014). What do differences between multi-voxel and univariate analysis mean? How subject-, voxel-, and trial-level variance impact fMRI analysis. *NeuroImage*, *97*, 271–283. https://doi.org/10.1016/j.neuroimage.2014.04.037

deCharms, R. C., & Zador, A. (2000). Neural representation and the cortical code. Annual Review of Neuroscience, 23, 613–647. https://doi.org/10.1146/annurev.neuro.23.1.613

D'Esposito, M. (2007). From cognitive to neural models of working memory. *Philosophical Transactions of the Royal Society of London. Series B, Biological Sciences*, *362*(1481), 761–772. https://doi.org/10.1098/rstb.2007.2086

Diedrichsen, J., & Kriegeskorte, N. (2017). Representational models: A common framework for understanding encoding, pattern-component, and representational-similarity analysis. *PLoS Computational Biology*, *13*(4), e1005508. https://doi.org/10.1371/journal.pcbi.1005508

Duda, R., Hart, P., & G.Stork, D. (2001). Pattern Classification. In *Wiley Interscience* (Vol. xx).

Duncan, J. (2010). How Intelligence Happens. Yale University Press.

Estefan, D. P., Fellner, M. C., Kunz, L., Zhang, H., Reinacher, P., Roy, C., Brandt, A., Schulze-Bonhage, A., Yang, L., Wang, S., Liu, J., Xue, G., & Axmacher, N. (2023). *Maintenance and transformation of representational formats during working memory prioritization* (p. 2023.02.08.527513). bioRxiv. https://doi.org/10.1101/2023.02.08.527513

Etzel, J. A., Courtney, Y., Carey, C. E., Gehred, M. Z., Agrawal, A., & Braver, T. S. (2020). Pattern Similarity Analyses of FrontoParietal Task Coding: Individual Variation and Genetic Influences. *Cerebral Cortex*, *30*(5), 3167–3183. https://doi.org/10.1093/cercor/bhz301

Fahrenfort, J. J., van Driel, J., van Gaal, S., & Olivers, C. N. L. (2018). From ERPs to MVPA Using the Amsterdam Decoding and Modeling Toolbox (ADAM). *Frontiers in Neuroscience*, *12*. https://www.frontiersin.org/articles/10.3389/fnins.2018.00368

Fahrenfort, J. J., van Leeuwen, J., Olivers, C. N. L., & Hogendoorn, H. (2017). Perceptual integration without conscious access. *Proceedings of the National Academy of Sciences*, *114*(14), 3744–3749. https://doi.org/10.1073/pnas.1617268114

Freund, M. C., Bugg, J. M., & Braver, T. S. (2021). A Representational Similarity Analysis of Cognitive Control during Color-Word Stroop. *Journal of Neuroscience*, *41*(35). https://doi.org/10.1523/JNEUROSCI.2956-20.2021

Freund, M. C., Etzel, J. A., & Braver, T. S. (2021). Neural Coding of Cognitive Control: The Representational Similarity Analysis Approach. *Trends in Cognitive Sciences*, *25*(7), 622–638. https://doi.org/10.1016/j.tics.2021.03.011

Friston, K. J., Holmes, A. P., Worsley, K. J., Poline, J.-P., Frith, C. D., & Frackowiak, R. S. J. (1994). Statistical parametric maps in functional imaging: A general linear approach. *Human Brain Mapping*, *2*(4), 189–210. https://doi.org/10.1002/hbm.460020402

Gluth, S., Rieskamp, J., & Büchel, C. (2012). Deciding When to Decide: Time-Variant Sequential Sampling Models Explain the Emergence of Value-Based Decisions in the Human Brain. *Journal of Neuroscience*, *32*(31), 10686–10698. https://doi.org/10.1523/JNEUROSCI.0727-12.2012

Kikumoto, A., & Mayr, U. (2018). Decoding hierarchical control of sequential behavior in oscillatory EEG activity. *eLife*, *7*, e38550. https://doi.org/10.7554/eLife.38550

Kikumoto, A., & Mayr, U. (2020). Conjunctive representations that integrate stimuli, responses, and rules are critical for action selection. *Proceedings of the National Academy of Sciences*, *117*(19), 10603–10608. https://doi.org/10.1073/pnas.1922166117

Kikumoto, A., Mayr, U., & Badre, D. (2022). The role of conjunctive representations in prioritizing and selecting planned actions. *eLife*, *11*, e80153. https://doi.org/10.7554/eLife.80153

Klimesch, W. (1999). EEG alpha and theta oscillations reflect cognitive and memory performance: A review and analysis. *Brain Research. Brain Research Reviews*, *29*(2). https://doi.org/10.1016/s0165-0173(98)00056-3

Kriegeskorte, N., & Diedrichsen, J. (2019). Peeling the Onion of Brain Representations. *Annual Review of Neuroscience*, *42*(1), 407–432. https://doi.org/10.1146/annurev-neuro-080317-061906

Kriegeskorte, N., & Douglas, P. K. (2019). Interpreting encoding and decoding models. *Current Opinion in Neurobiology*, *55*, 167–179. https://doi.org/10.1016/j.conb.2019.04.002

Kriegeskorte, N., & Kievit, R. A. (2013). Representational geometry: Integrating cognition, computation, and the brain. *Trends in Cognitive Sciences*, *17*(8), 401–412. https://doi.org/10.1016/j.tics.2013.06.007

Kriegeskorte, N., Mur, M., & Bandettini, P. (2008). Representational similarity analysis—Connecting the branches of systems neuroscience. *Frontiers in Systems Neuroscience*, *2*. https://www.frontiersin.org/articles/10.3389/neuro.06.004.2008

Lega, B. C., Jacobs, J., & Kahana, M. (2012). Human hippocampal theta oscillations and the formation of episodic memories. *Hippocampus*, *22*(4), 748–761. https://doi.org/10.1002/hipo.20937

Linde-Domingo, J., Treder, M. S., Kerrén, C., & Wimber, M. (2019). Evidence that neural information flow is reversed between object perception and object reconstruction from memory. *Nature Communications*, *10*(1). https://doi.org/10.1038/s41467-018-08080-2

Lisman, J. (2010). Working Memory: The Importance of Theta and Gamma Oscillations. *Current Biology*, *20*(11), R490–R492. https://doi.org/10.1016/j.cub.2010.04.011

Mahmoudi, A., Takerkart, S., Regragui, F., Boussaoud, D., & Brovelli, A. (2012). Multivoxel pattern analysis for FMRI data: A review. *Computational and Mathematical Methods in Medicine*, *2012*, 961257. https://doi.org/10.1155/2012/961257

Mathys, C., Daunizeau, J., Friston, K. J., & Stephan, K. E. (2011). A bayesian foundation for individual learning under uncertainty. *Frontiers in Human Neuroscience*, *5*, 39. https://doi.org/10.3389/fnhum.2011.00039

Naselaris, T., Kay, K. N., Nishimoto, S., & Gallant, J. L. (2011). Encoding and decoding in fMRI. *NeuroImage*, *56*(2), 400–410. https://doi.org/10.1016/j.neuroimage.2010.07.073

Nili, H., Wingfield, C., Walther, A., Su, L., Marslen-Wilson, W., & Kriegeskorte, N. (2014). A Toolbox for Representational Similarity Analysis. *PLOS Computational Biology*, *10*(4), e1003553. https://doi.org/10.1371/journal.pcbi.1003553

Popal, H., Wang, Y., & Olson, I. R. (2019). A Guide to Representational Similarity Analysis for Social Neuroscience. *Social Cognitive and Affective Neuroscience*, *14*(11), 1243–1253. https://doi.org/10.1093/scan/nsz099

Qiao, L., Zhang, L., Chen, A., & Egner, T. (2017). Dynamic Trial-by-Trial Recoding of Task-Set Representations in the Frontoparietal Cortex Mediates Behavioral Flexibility. *The Journal of Neuroscience: The Official*

Journal of the Society for Neuroscience, *37*(45), 11037–11050. https://doi.org/10.1523/JNEUROSCI.0935-17.2017

Riddle, J., Vogelsang, D. A., Hwang, K., Cellier, D., & D'Esposito, M. (2020). Distinct oscillatory dynamics underlie different components of hierarchical cognitive control. *Journal of Neuroscience*. https://doi.org/10.1523/JNEUROSCI.0617-20.2020

Ritchie, J. B., Kaplan, D. M., & Klein, C. (2019). Decoding the Brain: Neural Representation and the Limits of Multivariate Pattern Analysis in Cognitive Neuroscience. The British Journal for the Philosophy of Science, 70(2), 581–607. https://doi.org/10.1093/bjps/axx023

Sakai, K. (2008). Task set and prefrontal cortex. *Annual Review of Neuroscience*, *31*, 219–245. https://doi.org/10.1146/annurev.neuro.31.060407.125642

Sans-Dublanc, A., Mas-Herrero, E., Marco-Pallarés, J., & Fuentemilla, L. (2017). Distinct Neurophysiological Mechanisms Support the Online Formation of Individual and Across-Episode Memory Representations. *Cerebral Cortex*, *27*(9), 4314–4325. https://doi.org/10.1093/cercor/bhw231

Schmidt, J. R. (2019). Evidence against conflict monitoring and adaptation: An updated review. Psychonomic bulletin & review, 26(3). 10.3758/s13423-018-1520-z

Schumacher, E., & Hazeltine, E. (2016). Hierarchical Task Representation: Task Files and Response Selection. *Current Directions in Psychological Science*, *25*, 449–454. https://doi.org/10.1177/0963721416665085

Sherfey, J., Ardid, S., Miller, E. K., Hasselmo, M. E., & Kopell, N. J. (2020). Prefrontal oscillations modulate the propagation of neuronal activity required for working memory. *Neurobiology of Learning and Memory*, *173*, 107228. https://doi.org/10.1016/j.nlm.2020.107228

Spitzer, B., & Haegens, S. (2017). Beyond the status quo: A role for beta oscillations in endogenous content (re) activation. *Eneuro*, *4*(4).

Tafuro, A., Ambrosini, E., Puccioni, O., & Vallesi, A. (2019). Brain oscillations in cognitive control: A cross-sectional study with a spatial stroop task. *Neuropsychologia*, *133*, 107190.

Tafuro, A., Vallesi, A., & Ambrosini, E. (2020). Cognitive brakes in interference resolution: A mouse-tracking and EEG co-registration study. *Cortex*, *133*, 188–200. https://doi.org/10.1016/j.cortex.2020.09.024

Taneja, I. J. (2005). *Bounds On Triangular Discrimination, Harmonic Mean and Symmetric Chi-square Divergences* (arXiv:math/0505238). arXiv. https://doi.org/10.48550/arXiv.math/0505238

Viviani, G., Visalli, A., Montefinese, M., Vallesi, A., & Ambrosini, E. (2023). The Stroop legacy: A cautionary tale on methodological issues and a proposed spatial solution. *Behavior Research Methods*. https://doi.org/10.3758/s13428-023-02215-0

Walther, A., Nili, H., Ejaz, N., Alink, A., Kriegeskorte, N., & Diedrichsen, J. (2016). Reliability of dissimilarity measures for multi-voxel pattern analysis. *NeuroImage*, *137*, 188–200. https://doi.org/10.1016/j.neuroimage.2015.12.012

Woolgar, A., Thompson, R., Bor, D., & Duncan, J. (2011). Multi-voxel coding of stimuli, rules, and responses in human frontoparietal cortex. *NeuroImage*, *56*(2), 744–752. https://doi.org/10.1016/j.neuroimage.2010.04.035

Wu, M. C.-K., David, S. V., & Gallant, J. L. (2006). Complete functional characterization of sensory neurons by system identification. *Annual Review of Neuroscience*, *29*, 477–505. https://doi.org/10.1146/annurev.neuro.29.051605.113024

CHAPTER 7

Back to the Origin:
Decomposing the Stroop effect

7.1. Introduction

In this chapter, we will address a topic introduced at the outset of this thesis, namely, the composite nature of the Stroop effect. However, our approach in this chapter extends beyond a review of the hypotheses put forth in the literature. Instead, we will directly investigate whether there is empirical evidence that the Stroop effect indeed arises from the effect of multiple components.

To understand the objective of this chapter, we need to jump back to Chapter 2 (Section 2.2.2), where we briefly summarized the theoretical accounts that have evolved over the years to explain the characteristics of the Stroop effect. The initial efforts to explain it as a single-stage effect, attributing it to response-based processes (also known as late-selection accounts; e.g., Posner & Snyder, 1975) or stimulus-based processes (called early-selection accounts; e.g., Hock & Egeth, 1970; Seymour, 1977), were subsequently supplanted by multiple-stage accounts that posited that it could be the result of both of them (De Houwer, 2003; Zhang & Kornblum, 1998) or even of more than two processes, suggesting a more complex nature than initially thought (e.g., Risko et al., 2006).

A recent review by Parris and colleagues (2022) explored whether there is evidence in the literature that the Stroop effect is composed of multiple loci, that is, whether different processing levels contribute to it. They distinguished between stimulus- and response-related loci (together referred to as informational loci), and task locus, with the former two implied in generating both interference and facilitation effects, and the latter involved in interference only. Specifically, stimulus-related effects arise due to the overlap between the irrelevant and the relevant stimulus features, while the response-related effects arise from the overlap between the stimulus and the response. Task conflict, instead, arises when two task sets compete for resources. They overall found support for the multiple-loci account, suggesting that evidence in the literature indicates that the Stroop effect arises at different loci, but that stimulus and response loci are still hardly disambiguated by the (limitations of the) existing measures. This notwithstanding, they claim that models of Stroop task performance should more effectively account for such multiple loci nature.

We have based all the studies included in this thesis on Parris and colleagues' (2022) conclusions, always taking particular care to ensure that the designed Stroop tasks guarantee stimulus, response, and task loci.

However, the existence of these three separate loci has been taken for granted as, to the best of our knowledge, there are no previous studies that have empirically investigated the existence of these loci in spatial Stroop tasks. With the aim of directly exploring the existence of multiple loci in the Stroop task, in this study, we decompose the Stroop effect by separately measuring each of these sub-components to verify their existence in our spatial Stroop task.

Previous attempts of decomposing the Stroop effect have been made, but specifically targeting verbal versions of the Stroop task (mainly color-word and semantic Stroop tasks). Specifically, Augustinova and colleagues (2018), focusing on Stroop interference only, explored whether it was composed of semantic (or stimulus), response, and task conflicts. They found evidence of these conflict types, but only when vocal responses were used (see Chapter 2 for more details). However, their findings cannot be extended to the spatial Stroop task used here. This is because Stroop tasks involving verbal stimuli are inherently different from spatial Stroop tasks, and these differences, additionally, bring along some methodological issues.

When trying to isolate stimulus conflict using verbal Stroop tasks, more than one verbal processing layer has to be taken into account, such as lexical, semantic, and phonological ones. However, as suggested by Parris and colleagues (2022), the measures used for this purpose are themselves problematic. This was plausibly the reason for which, in Parris and colleagues' (2022) review, no clear evidence was found for the existence of separate mechanisms for stimulus and response conflicts. Conversely, by using spatial versions of the Stroop task we could overcome this issue, specifically focusing on purer stimulus-related processing, excluding the complexity related to the use of verbal stimuli. The fact that verbal stimuli imply several processing layers leads to the second difference, that is, in verbal Stroop tasks each of these layers might activate a different sub-task. For this reason, different neutral stimuli can be used, implying, in turn, that different possible measures of conflict can be computed, both at the stimulus and task levels. However, Augustinova and colleagues (2018) only considered one of these linguistic layers, namely the semantic one, neglecting the possible effect of lexical and phonological processes. This work thus cannot be entirely extended to verbal Stroop tasks either. Moreover, it overall reinforces the suggestion we extensively put forward in the entire thesis: to circumvent such complexity, the use of spatial Stroop tasks seems to be advantageous, not only for the reasons outlined in the previous chapters, but also when trying to decompose the Stroop effect, as we will do in the work reported in this chapter. This complexity also emerges from other works that have decomposed the Stroop effect using verbal Stroop tasks (Quetard et al., 2023) because, in trying to address such complexity, the task locus was neglected, thus still not providing clear evidence either for the assumed multiple-loci nature or for the weight of each locus. Aware of such complexity, the same authors proposing the multiple-loci account, which also included the task locus, in a subsequent review pointed out that there is still not a clear measure for task interference, and even questioned the role of task interference in Stroop performance, providing alternative accounts for the

most commonly used measure of task interference, that is, reverse facilitation (for a review see Parris et al., 2023).

Therefore, the advantageous use of the spatial Stroop task may allow us to more clearly distinguish stimulus, response, and task loci, overcoming the previously highlighted issues, including those related to the task locus measure, as explained later. Moreover, in the present study, we addressed a further open question, that regarding the facilitation effect. As explained in the Introduction of Chapter 2, it is widely known that the Stroop effect is composed of both an Interference Effect (IE) and a Facilitation Effect (FE), which can be disentangled only by using appropriate neutral conditions. However, Stroop facilitation has generally received much less attention than the global Stroop effect and the IE, probably because its magnitude has often been observed to be smaller and less consistent. In addition to whether it is truly smaller, which is probably mainly due to the fact that its measure strongly relies on the type of neutral baseline used to calculate it, knowledge is even more scarce regarding the processing levels contributing to it (Brown, 2011) and their separability from interference-related ones (Di Russo & Bianco, 2023). Therefore, with the aim of decomposing the Stroop effect as comprehensively as possible, we will distinguish IE and FE, thus exploring not only the processing levels contributing to the global Stroop effect, but also those specifically contributing to the facilitation and interference effects. Therefore, to separately assess interference and facilitation at the stimulus and response loci, we will also use neutral stimuli, which will be contrasted to incongruent and congruent ones. By contrast, the task locus necessarily entails only interference caused by the simultaneous presence of two tasks (i.e, the activation of a secondary task cannot facilitate the execution of the primary task).

To pursue our aims, we started by pre-registering and performing a pilot study. This is not included in the present Chapter but its pre-registration form can be found at osf.io/zhckv. In brief, we designed different experimental tasks requiring button-press responses and characterized by specific types of interference (and facilitation), except for the Stroop task, which comprises all interference and facilitation levels. For what concerns the first two interference and facilitation types, we used the dimensional overlap model and the relative taxonomy proposed by Kornblum (1992) as a reference guide.

Based on that, we designed i) a Stroop-like (Flanker) task to investigate the stimulus locus, due to the overlap between relevant and irrelevant stimulus features, ii) a Simon task to explore the response locus, due to the overlap between the irrelevant stimulus feature and the response. Moreover, we designed a simple identification task requiring participants to indicate the position of a visual stimulus (POS, a stimulus-response compatibility task) that, by having the overlap between the relevant stimulus feature and the response, but no irrelevant stimulus features, was used as a baseline task due to the absence of both interference and facilitation effects. Lastly, to isolate the effect of task conflict, we used a task-switching paradigm, wherein participants were required to switch between the Simon and the POS tasks.

The assumption here was that embedding the POS task within a mixed block in which the Simon task was also present, the latter task set (i.e., process and respond to the stimulus color) was tonically activated also when participants performed the POS task (i.e., process and respond to the stimulus position), even during repeat neutral POS trials, in which no task switching was required and no irrelevant stimulus color was present, thus causing task-level interference.

In that pilot study we aimed to directly decompose the Stroop effect by separately measuring each of its sub-components assumed by the multiple loci hypothesis (i.e., stimulus- and response-based conflict/facilitation and task conflict, Parris et al., 2021), while also distinguishing between interference and facilitation at the stimulus and response levels. We then pre-registered (osf.io/etbrp) and conducted a subsequent study, which is the object of the present Chapter, based on the results obtained from the pilot study. The aim of the second study was to make a further step in the same direction, by more directly addressing our experimental questions.

As in our pilot study, we designed different experimental tasks characterized by stimulus and response interference (and facilitation), except for the Stroop task, which comprises all interference and facilitation levels, and we did this by using Kornblum's (1992) taxonomy as reference guide. To explore the response locus, we used the same paradigm of our previous study, namely the Simon task (Sim, irrelevant stimulus – response overlap), whereas we used a Stroop-like task in place of the Flanker task to assess the stimulus locus. The latter task, indeed, presents some methodological characteristics, like entailing the same process (i.e., color identification) as both the relevant and irrelevant tasks and using physically separate stimuli to signal the task-relevant and task-irrelevant stimulus dimensions, which require the assumption that color identification has different levels of automaticity based on its task-relevance. By contrast, the Stroop-like task entails two distinct tasks which, in this study, were color identification and reading (we called this task verbal Stroop, VS). Moreover, the Stroop-like task implies the overlap between relevant and irrelevant stimulus features, but since responses to verbal stimuli were given manually, no stimulus-response overlap was present, distinguishing this task from the Stroop task.

Compared to our previous study, here we measured task interference more directly, proposing a task interference measure that could overcome the issue inherent to the previously employed measures, as discussed above, thus more effectively filling the gap highlighted by previous works (Parris et al., 2023). Indeed, in the pilot study, we used a task-switching paradigm with participants required to switch between the Simon and the POS tasks. We then analyzed neutral POS trials, in which no task switching was required and no irrelevant stimulus color was present, to isolate task-level interference, assuming that they were affected by the concurrent activation of the other task set (as extensively shown by the literature on task switching). However, by isolating task interference in this way, we used a task that differed greatly from the Stroop task (that we wanted to decompose) and required the use of the task-

switching paradigm (for which we collected many trials, but we used less than half). Here we still used the same assumption, but we directly manipulated the task interference by comparing paradigms involving a single identification task to paradigms involving the same task along with another conflicting task that is exogenously activated. We assumed that task interference could be isolated by comparing neutral trials (thus free from other types of facilitation/interference) in paradigms involving two conflicting tasks to trials involving the same primary task and stimuli (which are necessarily neutral), but presented within a single task paradigm. Indeed, the neutral trials in conflict tasks involving two task-sets imply the same task and stimuli as the trials presented in a identification task, but since they appear intermixed with congruent and incongruent trials, which activate also the alternative conflicting task (Parris et al., 2023), they should also elicit the conflicting task and are thus likely to be affected by task interference, yielding a worse performance than single task identification neutral trials (free from all types of facilitation and interference). In practical terms, for each paradigm involving task conflict for the presence of two tasks, we included in the study a paradigm implying just the relevant of the two tasks (and the same of very similar stimuli) so to have one identification block for each task, namely a block implying a single task. As such, we had four identification tasks: Position task (POS, corresponding to the POS task used in the pilot study), Direction task (DIR), Word task (WRD), and Color task (COL, corresponding to the COL mapping task used in the pilot study). These single tasks were needed as the task interference paradigms were the Simon task (Sim, COL vs POS), two verbal Stroop-like tasks, requiring participants to indicate either the stimulus ink color, like in the original color-word Stroop (VSc, COL vs WRD), or the color indicated by the word, like in the reverse word-color Stroop (VSw, WRD vs COL), respectively, and two spatial Stroop tasks, requiring participants to indicate either the stimulus direction, like in our original spatial Stroop task (SSd, DIR vs POS), or its position (SSp, POS vs DIR), respectively.

To provide a more comprehensive understanding of Stroop performance, beyond exploring the existence and weight of the three assumed loci, here we directed our attention to additional factors that might have a substantial impact on the final performance. These factors include the task automaticity and the asymmetry between the tasks, which are typically taken for granted and, to the best of our knowledge, have rarely been quantified. Their influence was initially explored in the pilot study, but here we made even greater efforts to better investigate them.

Task automaticity was indeed worthy of greater attention, as we predicted that it plays a significant role in modulating the performance in the paradigms involving task conflict. Specifically, we defined automaticity as the strength/easiness of processing of a stimulus feature. In the pilot study, we just focused on the automaticity of the relevant task (i.e., the automaticity of processing the relevant stimulus features). In contrast, here, by separately measuring the performance in each single

identification task, we were able to estimate the precise weight of automaticity of each task, regardless of whether it is relevant or irrelevant. Moreover, as in the pilot study, we assumed that automaticity also reflects how prepotent the responses elicited by the tasks are (that is, how automatic the S-R mapping is). It is also important to note that, by estimating task automaticity based on the identification task performance, our measure also takes into account the dimension discriminability/saliency of the employed stimuli (Melara & Algom, 2003).

By also using the automaticity of the irrelevant task, we refined our hypotheses about the facilitation, interference, and congruency effects at the stimulus and response levels. In particular, here we assumed that the degree of stimulus/response facilitation/interference exerted by the irrelevant task directly depends on its automaticity: if the processing of the irrelevant information and its S-R mapping are more automatic, we assumed that they should exert a greater facilitation/interference in processing and responding to the relevant information, with greater facilitation/interference at both the stimulus and response levels.

Task asymmetry was instead defined as the difference in the automaticity of the two tasks involved in conflict tasks. In our pilot study, we (arbitrarily) assigned an asymmetry score to each conflict paradigm, whereas here, we could make a step further. By obtaining the precise estimates of automaticity for each task, we were able to directly compute task asymmetry by calculating the relative automaticity of the two tasks (i.e., the irrelevant task automaticity divided by the relevant task automaticity). We indeed expected that task interference would be greater when the irrelevant task is more automatic than the relevant one. Therefore, task interference effects were then weighted using the corresponding task asymmetry estimates.

Finally, based on the results of our pilot study, to further refine our hypotheses about the facilitation, interference, and congruency effects, we considered the relative weight of task interference and both stimulus and response loci of facilitation/interference in contributing to the overall performance in conflict tasks.

7.2. Methods

We report how we determined our sample size, all data exclusions, all inclusion/exclusion criteria, all manipulations, and all measures in the study. All inclusion/exclusion criteria were established prior to data analysis. We will make all data and materials available from our project repository on the Open Science Framework (OSF) platform at osf.io/j9w7p. As already mentioned, the study was pre-registered on OSF (osf.io/etbrp).

This was a cross-sectional observational study. Participants were not randomly assigned to different conditions and performed the same experimental tasks, with the only difference that the tasks were presented in two different orders (see below). No blinding was involved and participants were not informed about the experimental manipulations before the experiment.

7.2.1. Experimental tasks and procedure

The experiment was programmed using Psytoolkit (Stoet, 2010, 2017) and administered online. All the participants were recruited by the experimenters and given a link to perform the task online. The stimuli were presented in full-screen mode, with a resolution of 800 x 600 pixels, on a gray background (RGB: 166, 166, 166). Each trial started with a fixation stimulus presented at the center of the screen for 700 ms and participants were instructed to fixate it. For all the tasks, the fixation stimulus consisted in a vertically oriented thin black cross (24 x 24 pixels) enclosed in the partial outline of a black square (110 x 110 pixels), which was then replaced by the experimental stimulus (see Figures 7.1-2). Next, the experimental stimulus was presented until participant's response or up to a response time-out of 2000 ms, whatever came first. Each of the tasks involved different experimental stimuli, as detailed below, based on their task-relevant and (potential) task-irrelevant features (see Figure 7.1-2):

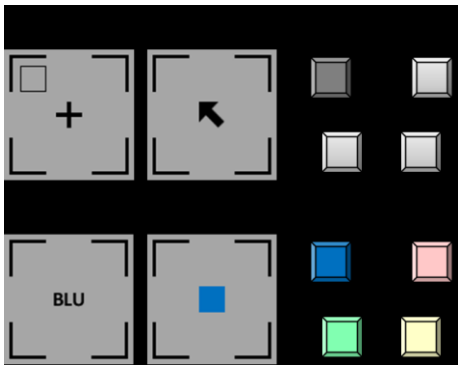

Figure 7.1.
S-R mapping in the identification tasks. The top row shows the two identification tasks involving an automatic, spatial S-R mapping between the relevant feature of the stimulus (POS, stimulus position; DIR, arrow direction) and the response keys, which were arranged spatially to have a strong dimensional overlap with the four possible relevant spatial features of the stimuli. The bottom row shows the two identification tasks involving an arbitrary, non-spatial, color-coded S-R mapping between the relevant feature of the stimulus (WRD, meaning of the color word; COL, stimulus color) and the response keys (here colored according to the four possible relevant features of the stimuli for illustrative purpose). In all cases, the required response was that corresponding to the upper-left key (displayed with higher saturation).

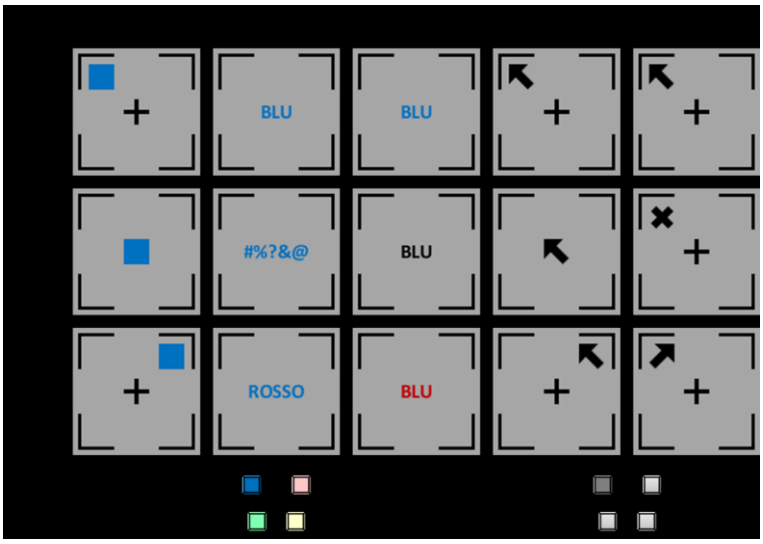

Figure 7.2.
Exemplar Congruent (C, top row), Neutral (N, middle row), and Incongruent (I, bottom row) stimuli in the conflict tasks. In all examples shown here, the response to be provided is that corresponding to the upper-left key (which also mapped the BLU word/color). In all the Incongruent trials shown here, the incorrect response evoked by the irrelevant stimulus feature is that corresponding to the upper-right key (which also mapped the READ word/color). The irrelevant stimulus feature has a neutral/null value in the Neutral stimuli, so it does not evoke a response. Task abbreviations: Simon (Sim), Verbal Stroop responding to color (VSc), Verbal Stroop responding to word (VSw), Spatial Stroop responding to direction (SSd), Spatial Stroop responding to position (SSp). See Section 7.2.1 for details.

1. Position identification task (POS). This is a classical S-R compatibility (SRC) task, a Type-2 ensemble. The stimulus was a small square (24 x 24 pixels) that was presented at one of four possible positions inside the fixation stimulus (i.e., upper-left, upper-right, lower-right, or lower-left), corresponding to the task-relevant feature, and it was empty (i.e., not colored) and with a black outline, so there was no task-irrelevant feature.
2. Direction identification task (DIR). This is a classical S-R compatibility (SRC) task, a Type-2 ensemble. The stimulus was a small arrow (24 x 24 pixels) that pointed towards one of four possible directions (i.e., upper-left, upper-right, lower-right, or lower-left), corresponding to the task-relevant feature, and was presented at the center of the fixation stimulus and colored in black, so there was no task-irrelevant feature.
3. Word identification task (WRD). This is a classical simple choice reaction time task, a Type-1 ensemble. The stimulus was the Italian word for one of four possible colors (i.e., blue, red, yellow, or green, corresponding to the Italian words BLU, ROSSO, GIALLO, and VERDE), corresponding to the task-relevant feature, which was presented in uppercase, bold Calibri font at the center of the fixation stimulus (maximum dimensions: 55 x 14 pixels), and was printed in black, so there was no task-irrelevant feature.
4. Color identification task (COL). This is a classical simple choice reaction time task, a Type-1 ensemble. The stimulus was a small square (24 x 24 pixels) that was colored in one of the same four possible colors

used in the WRD task (i.e., blue, red, yellow, or green, corresponding to the RGB codes [68, 114, 196], [255, 0, 0], [255, 255, 255], and [0, 128, 50]), corresponding to the task-relevant feature, and was presented at the center of the fixation stimulus, so there was no task-irrelevant feature.

5. Simon task (Sim). This is an adaptation of the classical Simon task, a Type-3 ensemble. The stimulus was a small square (24 x 24 pixels) that was colored in one of the same four possible colors used in the COL task, corresponding to the task-relevant feature, and was presented in one of five possible positions inside the fixation stimulus, that is, the same four possible positions used in the POS task, which were used as the task-irrelevant feature in the Congruent and Incongruent conditions, or the central position for the Neutral condition.
6. Color-word Verbal Stroop task (VSc). This is the classical color-word Stroop task with manual responses, a Type-4 (or Stroop-like) ensemble. The stimulus was one of the same four possible color words used in the WRD task or a non-pronounceable character string (#%?&@), which were printed in one of the same four possible colors used in the COL task, corresponding to the task-relevant feature. The meaning of the color words was the task-irrelevant feature used in the Congruent and Incongruent conditions; the non-pronounceable character string was instead used for the Neutral condition.
7. Word-color Verbal Stroop task (VSw). This is the standard reverse Stroop task with manual responses, a Type-4 (or Stroop-like) ensemble. The stimulus was one of the same four possible color words used in the WRD task, whose meaning was the task-relevant feature, which were printed in either one of the same four possible colors used in the COL task, corresponding to the task-irrelevant feature used in the Congruent and Incongruent conditions, or in black for the Neutral condition.
8. Direction-position Spatial Stroop task (SSd). This is the Perifoveal spatial Stroop task we used in all the studies of the present thesis, a Type-8 ensemble. The stimulus was the same arrow used in the DIR task, which pointed towards one of the same four possible directions (i.e., upper-left, upper-right, lower-right, or lower-left), corresponding to the task-relevant feature, and was presented in one of the same five possible positions used in the Sim task, that is, the same four possible positions used in the POS task, which were used as the task-irrelevant feature in the Congruent and Incongruent conditions, or the central position for the Neutral condition.
9. Position-direction Spatial Stroop task (SSp), a Type-8 ensemble. This is the reverse variant of the SSd task. The stimulus was either the same arrow used in the DIR task or a thick black diagonal cross (22 x 22 pixels), which was created based on the arrow stimuli (i.e., the arms of the cross corresponded to the tail of the arrow). The stimulus was presented in one of the same four possible positions used in the POS task, corresponding to the task-relevant feature. The arrow stimulus pointed towards one of the same four possible directions (i.e., upper-left, upper-right, lower-right, or lower-left) used in the DIR task, corresponding to the task-irrelevant feature used in the Congruent and Incongruent conditions. The cross stimulus was instead used for the Neutral condition.

In all the tasks, participants had to pay attention to and indicate the task-relevant feature of the stimulus, corresponding to the response. Participants were required to indicate their response by selecting one out of four keys on a computer keyboard, which were E, O, K, and D, by using the left middle, right middle, right index and left index fingers, respectively. These keys were spatially arranged to be compatible with the possible spatial features of the non-neutral stimuli, that is, either the position or the direction, which could be upper-left, upper-right, lower-right, or lower-left (see above). Therefore, this S-R mapping ensured the dimensional overlap between the response and the spatial features of the stimuli in the tasks involving at least one of these spatial features (i.e., POS, DIR, Sim, SSd, and SSp; see table 7.1). By contrast, there was no S-R dimensional overlap for the non-spatial feature of the stimuli, that is, either the color or the meaning of the word, as well as for the neutral task-irrelevant spatial feature of the stimuli, that is, the central position for the Sim and SSd tasks (see table 7.1).

Based on the task-relevant and the task-irrelevant stimulus features, we manipulated congruency in the conflict tasks so as to have Congruent, Neutral and Incongruent stimuli. More in detail, Congruent and Incongruent stimuli were those wherein the relevant and irrelevant features matched and did not match, respectively, whereas Neutral stimuli were those wherein the irrelevant feature was either missing or neutral (e.g., a non-pronounceable character string). The first four tasks (i.e., POS, DIR, WRD, and COL) were thus simple identification tasks that did not involve a task-irrelevant feature, so they only involved Neutral trials (see Figure 7.1). Conversely, the remaining tasks also involved Congruent and Incongruent trials based on the irrelevant stimulus feature, and thus can be considered as conflict tasks (see Figure 7.2).

Table 7.1. Classification of the experimental tasks and conditions and parameters for the hypotheses

Task_ Congruency	Ensemble type	S Type		Dimensional Overlap			LOCI - dummy			LOCI - weighted			AUT/ASY		
		S_{REL}	S_{IRR}	S-S	S_{REL}-R	S_{IRR}-R	S	R	T	S	R	T	S_{REL} AUT	S_{IRR} AUT	ASY
POS	2	POS	-	-	1	-	-	-	0	-	-	0	2.5	-	2.5
DIR	2	DIR	-	-	1	-	-	-	0	-	-	0	2.25	-	2.25
WRD	1	WRD	-	-	0	-	-	-	0	-	-	0	1.75	-	1.75
COL	1	COL	-	-	0	-	-	-	0	-	-	0	1.6	-	1.6
Sim_C	3	COL	POS	0	0	1	0	1		0	0.1675	-0.2578	1.6	2.5	1.5625
Sim_N				0	0	0	0	0	-1	0	0	-0.2578			
Sim_I				0	0	1	0	-1		0	-0.1675	-0.2578			
VSc_C	4	COL	WRD	1	0	1	1	0		0.11725	0	-0.1805	1.6	1.75	1.09375
VSc_N				0	0	0	0	0	-1	0	0	-0.1805			
VSc_I				1	0	1	-1	0		-0.1173	0	-0.1805			
VSw_C	4	WRD	COL	1	0	1	1	0		0.1072	0	-0.1509	1.75	1.6	0.91429
VSw_N				0	0	0	0	0	-1	0	0	-0.1509			
VSw_I				1	0	1	-1	0		-0.1072	0	-0.1509			
SSd_C	8	DIR	POS	1	1	1	1	1		0.1675	0.1675	-0.1833	2.25	2.5	1.11111
SSd_N				0	1	0	0	0	-1	0	0	-0.1833			
SSd_I				1	1	1	-1	-1		-0.1675	-0.1675	-0.1833			
SSp_C	8	POS	DIR	1	1	1	1	1		0.15075	0.15075	-0.1485	2.5	2.25	0.9
SSp_N				0	1	0	0	0	-1	0	0	-0.1485			
SSp_I				1	1	1	-1	-1		-0.1508	-0.1508	-0.1485			

Notes. S Type, the task evoked by the relevant and irrelevant stimulus features (S_{REL} and S_{IRR}, respectively); S, stimulus; R, response; T, task; AUT, automaticity; ASY, asymmetry. See the description of the tasks (Section 7.2.1) for the corresponding abbreviations.

The experimental trials were 36 for both the POS and DIR tasks and 108 for the WRD and COL task, which were balanced across the four relevant features and were all Neutral as explained above. The experimental trials were 108 for all the conflict tasks, balanced across the relevant and irrelevant features and the three congruency conditions. The trials for the different tasks were presented in the same block, at the beginning of which there was a buffer trial. Self-paced breaks were provided at the end of each task block.

Before each task block, the participants completed a practice block of either 12 (for the identification tasks) or up to 28 trials (for the conflict tasks), during which they received feedback on their performance and, in the case of errors or time-out responses, they were also provided with a brief recap of the instructions and the response mapping. For the conflict tasks, practice trials were presented until 70% accuracy was reached (but no less than 12 trials were presented). Within each task block, the order of presentation of the trials was pseudorandomized using the software Mix (van Casteren & Davis, 2006) to avoid more than four consecutive repetitions of the same congruency and both total and partial repetitions of stimulus characteristics and/or responses in order to control for first-order (positive and negative) priming effects.

At the beginning of the experiment, general instructions were provided, informing participants of the procedure and the general task (i.e., indicating the relevant feature of a visual stimulus by pressing a keyboard key). Participants were also recommended to execute the experiment in a quiet environment without distractions and to maintain a comfortable posture that allowed them to look straight to the center of the screen and keep the responding fingers in contact with the response keys. Particular care was taken to keep the instructions as simple and clear as possible. Before executing each task (i.e., before each practice block), specific task instructions were presented, illustrating the stimuli, the task to be performed, and the stimulus-response mapping. Participants were also asked to respond as quickly and accurately as possible.

We used two block orders to control for the confounding time-on-task effect by including the block order in the multilevel models used in the analyses. The two block orders were decided a-priori based on theoretical and practical reasons. Specifically, in each order, each identification task was presented before the conflicting task requiring to respond to the same relevant feature and having the same S-R mapping (e.g., WRD before VSw). This was especially important for the tasks requiring to respond to words (WRD and VSw) and colors (Simon, COL, VSc), for which the S-R mapping is arbitrary and, thus, has to be learnt by participants. Moreover, these tasks were presented in the same half of the experimental session. Moreover, to be sure that participants had learnt the color and word keys before executing the experimental tasks, single task blocks for COL and WRD were longer than the other single task blocks (108 vs 36 trials) so that the first 72 trials served as mapping (not included in the analyses), whereas only the last

36 ones were analyzed. The two block orders were: i) DIR, SSd, POS, SSp, COL, VSc, WRD, VSw, Sim; ii) COL, VSc, WRD, VSw, Sim, DIR, SSd, POS, SSp.

7.2.2. Measures and Hypotheses

Our experimental design corresponds to a within-subject (repeated-measures) design, as all participants completed all the experimental tasks and conditions, which can be described as a 2-factor (9 (Task: POS, DIR, COL, WRD, Sim, VSc, VSw, SSd, SSp) x 3 (Congruency: Congruent, C; Neutral, N; Incongruent, I)) incomplete design. The design is incomplete because in the four identification tasks, Congruent and Incongruent trials are not feasible (only Neutral ones can be used) (see Table 7.1).

In Table 7.1, all the tasks, as well as the experimental conditions deriving from the combination of Task and Congruency, are classified based on the methodological criteria that guided our hypotheses. Specifically, the tasks are first classified as the ensemble types as per the Kornblum's (1992) taxonomy (see above), based on the type of stimulus features they involved (i.e., POS, DIR, WRD, and COL, which are coded in the same way as for the four simple identification tasks requiring to respond to them). Then, based on both the ensemble type and the type of relevant and (potential) irrelevant stimulus feature, we coded the experimental conditions based on the presence (1) or absence (0) of the dimensional overlaps between the relevant and irrelevant stimulus features (S_{REL} and S_{IRR}, respectively) and between them and the response (R). It is important here to note that no dimensional overlaps were assumed when the irrelevant stimulus feature was Neutral; moreover, no S_{REL}-S_{IRR} or S_{IRR}-R dimensional overlap was possible for the simple identification tasks because they did not involve an irrelevant stimulus feature.

Moreover, to directly test our hypotheses regarding the experimental effects at the three loci, as per the multiple loci account (Parris et al., 2022), we operationalized them by using three categorical predictors for the stimulus, response, and task loci (S, R, and T, respectively). Based on the involved dimensional overlaps for both the S and R loci, we coded the Congruent and Incongruent conditions as +1 and -1, respectively, to operationalize an improvement (facilitation effect) and a decline (interference effect) in performance as compared to the Neutral conditions due to the S_{IRR} effect; the Neutral conditions were thus coded as 0 to act as the reference level. In this way, the facilitation/interference effect in the conflict tasks were assumed to specifically operate at the locus where there was a dimensional overlap involving S_{IRR}. Consequently, no facilitation/interference effects were possible for the simple identification tasks due to the lack of S_{IRR}.

For the task locus, we operationalized the task interference (T_IE) using a code of 0 for the simple identification tasks, for which there was no secondary task, and -1 for all the conflict tasks, for which a secondary task set was assumed to be automatically activated by the irrelevant stimulus feature (Parris et

al., 2023). Task interference is indeed assumed to emerge from the concomitant (automatic) activation of a secondary task while performing the relevant task (see Figure 7.3).

Based on the Congruency conditions, we computed participants' Congruency effects (CE) in the conflict tasks as the difference between RT in incongruent (I) and congruent (C) trials (formally, CE = RT_I - RT_C). CE can also be obtained by summing interference effect (IE) and facilitation effect (FE) (CE = IE + FE). In turn, participants' IE were computed as the difference between I and Neutral trials (N) (formally, IE = RT_I - RT_N), whereas FE were computed as the difference between N and C trials (formally, FE = RT_N - RT_C) (see Figure 7.3).

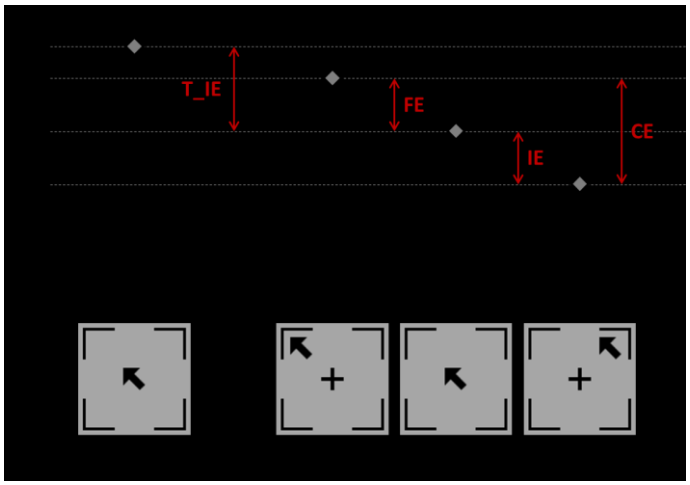

Figure 7.3.
Assumed pattern of performance in a simple identification task (DIR) and the corresponding conflict task having the same relevant stimulus, namely Spatial Stroop direction, and the corresponding experimental effects. Note that the two conditions used to assess the task interference effect (T_IE) are here matched for both the stimulus and the task/S_{REL} (relevant stimulus feature).

It is important here to note that the FE and IE for our verbal Stroop-like tasks are equivalent to the pure facilitation and interference effects at the S locus. Indeed, these tasks are Type-4 ensembles, which only involve the S_{REL}-S_{IRR} dimensional overlap (i.e., between the ink color and the meaning of the color word), but do not involve the S_{IRR}-R dimensional overlap due to the arbitrary S-R mapping. Moreover, the FE and IE for the Simon task are equivalent to the pure facilitation and interference effects at the R locus. Indeed, this task is a Type-3 ensemble, which only involves the S_{IRR}-R dimensional overlap (i.e., between the stimulus position and the response) due to the automatic spatial S-R mapping we employed, but does not involve the S_{REL}-S_{IRR} dimensional overlap. By contrast, the FE and IE for our Stroop tasks originate from both S and R loci, as assumed by the multiple loci account (Parris et al., 2022).

The IE at the task level (T_IE) was computed contrasting each identification task to the Neutral condition of the corresponding conflict task involving the same relevant stimulus feature. Indeed, due to the absence of a task-irrelevant feature, the four identification tasks could not activate a secondary task set, which was instead

automatically activated in the corresponding conflict tasks by the irrelevant stimulus feature (Parris et al., 2023). We chose to use the N condition to compute the T_IE in order to avoid confounding its estimate with the concomitant FE/IE that occurred at the S and R level for C and I trials, respectively. More importantly, the trials in each identification task and those in the N condition of the corresponding conflict task both required participants to perform the same task (e.g., identify the arrow direction for the DIR and SSd task) and use the very same (or very similar) stimuli (e.g., the same arrow presented centrally and pointing toward the upper-left direction) and the same S-R mapping. In other words, the only relevant difference between each identification task and the N trials of the corresponding conflict tasks is the block context, that is, the fact that the latter were embedded in a block in which C and I trials were also included, which were constituted by stimuli also entailing an irrelevant feature that is (automatically) processed, as evidenced by the FE and IE.

Our experiment design thus allowed us to test the following hypotheses:

1) A set of auxiliary hypotheses for the basic effects reported in the literature for all the conflict tasks we used. Specifically, for all these tasks, we predicted to observe both an FE, that is, a better performance to C as compared to N trials, and an IE, that is, a better performance to N as compared to I trials (see above). These hypotheses needed to be satisfied first, in order to proceed with verifying our background assumptions. Note that for both the S-locus (i.e., the Stroop-like task) and the Stroop effects, two possible contrasts were possible (for VSc and VSw, and for SSd and SSp, respectively):

H1.1a (VSc_FE, or S_FE1): (VSc_C - VSc_N) > 0;
H1.1b (VSw _FE, or S_FE2): (VSw_C -VSw_N) > 0;
H1.2a (VSc_IE, or S_IE1): (VSc_N - VSc_I) > 0;
H1.2b (VSw _IE, or S_IE2): (VSw_N - VSw_I) > 0;
H1.3 (Sim_FE, or R_FE): (Sim_C - Sim_N) > 0;
H1.4 (Sim_IE, or R_IE): (Sim_N - Sim_I) > 0;
H1.5a (SSd_FE, or Str_FE1): (SSd_C - SSd_N) > 0;
H1.5b (SSp_FE, or Str_FE2): (SSp_C - SSp_N) > 0;
H1.6a (SSd_IE, or Str_IE1): (SSd_N - SSd_I) > 0;
H1.6b (SSp_IE, or Str_IE2): (SSp_N - SSp_I) > 0;

Moreover, as detailed above, by having both simple identification tasks and conflict tasks with Neutral conditions, we were also able to measure the pure effect of task interference, obtaining five T_IE measures:

H1.7a (POS_IE or T_IE1): (POS - SSp_N) > 0;
H1.7b (DIR_IE or T_IE2): (DIR - SSd_N) > 0;
H1.7c (WRD_IE or T_IE3): (WRD - VSw_N) > 0;
H1.7d (COL_IEa or T_IE4): (COL - VSc_N) > 0;
H1.7e (COL_IEb or T_IE5): (COL - Sim_N) > 0;

2) A set of hypotheses on the CE effects in our conflict tasks, which were related to and directly dependent on H1s (note that if the hypotheses about a specific pair of FE and IE held true, the hypothesis about the corresponding CE held also necessarily true). We predicted to find the verbal Stroop and Simon

CEs, which indicate a better performance on C than I trials, reflecting the sum of pure FE/IE effects at the S and the R locus, respectively:

H2.1 (VSc_CE, or S_CE1): (VSc_C - VSc_I) > 0, or (S_FE1 + S_IE1) > 0;
H2.2 (VSw_CE, or S_CE2): (VSw_C - VSw_I) > 0, or (S_FE2 + S_IE2) > 0;
H2.3 (Sim_CE, or R_CE): (Sim_C - Sim_I) > 0, or (R_FE + R_IE) > 0;

We also predicted to find the Stroop CE:

H2.4 (SSd_CE, or Str_CE1): (SSd_C - SSd_I) > 0, or (SSd_FE1 + SSd_IE1) > 0;
H2.5 (SSp_CE, or Str_CE2): (SSp_C - SSp_I) > 0, or (SSp_FE2 + SSp_IE2) > 0;

3) A set of hypotheses that allowed us to answer our main experimental question about the interplay between effects at the different loci, that is, whether and to what degree the Stroop task implies interference (and facilitation) at multiple loci (ML: the S, R and T levels). Based on the multiple loci account, we expected the Stroop CE (and also the Stroop IE and FE) to be greater than the corresponding single effects in both the Stroop-like and the Simon task. Indeed, the Stroop task should entail CEs at both the S and R loci, while the CEs for the Stroop-like and Simon tasks were expected to entail only one of them, respectively (it is important here to note that all the three tasks entail task interference in all conditions). It is also important to note that, for simplicity, at this stage we were making some assumptions: 1) all the effects does not depend on the type of irrelevant task/feature (but see below for predictions taking this aspect into account); 2) the S and R effects do not interact with each other (but see below for predictions taking this aspect into account); 3) the S and R effects have the same magnitude; 4) all the effects does not depend on the general performance in the task yielding them. We made 18 directional hypotheses as follows :

H3.1a-f (FE_MLa-f): (Str_FE1 & Str_FE2) - (S_FE1 & S_FE2 & R_FE) > 0;
H3.2a-f (IE_MLa-f): (Str_IE1 & Str_IE2) - (S_IE1 & S_IE2 & R_IE) > 0;
H3.3a-f (CE_MLa-f): (Str_CE1 & Str_CE2) - (S_CE1 & S_CE2 & R_CE) > 0;

4) A set of hypotheses to test for the possible interaction between the effects at the three loci. Indeed, one of the following three possible alternatives may be observed:

i) the Stroop effects are given by the sum of the effects at the multiple loci (additive hypothesis, ADD);
ii) the Stroop effects are the result of the synergic interaction of the single effects at the multiple loci, implying that it is greater than their simple sum (synergic interaction, SYN);
iii) the Stroop effects result from the antagonist interaction between the single effects, implying that they are smaller than their simple sum (antagonist interaction, ANT).

We arbitrarily assumed a 40% increase/decrease of the effect of multiple FEs/IEs, respectively, for the SYN and ANT hypotheses. These alternative hypotheses were tested with two-tailed t-tests, but we predicted that the Stroop effects are not the result of the simple sum of the pure effects at the S and R loci,

since there is no available strong evidence for their independence. Rather, we predicted that the Stroop effects are smaller than their sum (ANT), because of the likely non-complete separability of the S and R loci.

H4.1a-d (Str_FEs_ADD): Str_FEs - (S_FEs + R_FE) = 0;
H4.1e-h (Str_FEs_SYN): Str_FEs - (S_FEs + R_FE) > 0;
H4.1i-n (Str_FEs_ANT): Str_FEs - (S_FEs + R_FE) < 0;
H4.2a-d (Str_IEs_ADD): Str_IEs - (S_IEs + R_IE) = 0;
H4.2e-h (Str_IEs_SYN): Str_IEs - (S_IEs + R_IE) > 0;
H4.2i-n (Str_IEs_ANT): Str_IEs - (S_IEs + R_IE) < 0;
H4.3a-d (Str_CEs_ADD): Str_CEs - (S_CEs + R_CE) = 0;
H4.3e-h (Str_CEs_SYN): Str_CEs - (S_CEs + R_CE) > 0;
H4.3i-n (Str_CEs_ANT): Str_CEs - (S_CEs + R_CE) < 0;

5) All the hypotheses detailed above, derived from the multiple loci and dimensional overlap accounts, are specifically related to the pattern of experimental effects (i.e., FE, IE, and CE) that can be observed in conflict tasks. As such, and for the sake of simplicity, they were assumed to be independent from the general performance in the specific tasks. Therefore, we also developed a set of hypotheses for the general pattern of results. To do so, we assessed the impact of other effects known in the literature to modulate the performance in the Stroop task (and in any conflict task, more generally).

In particular, we assessed whether the performance in our tasks was modulated by the automaticity (or strength) of both the processing of the stimulus features used in our tasks (i.e., POS, DIR, WRD, and COL) and their mapping onto the responses elicited by them (i.e., how automatic their S-R mapping was). We also assessed whether the performance in our tasks was modulated by the so-called task asymmetry.

In order to initially define our hypotheses, we assigned an overall automaticity score (AUT) to the different tasks, taking into account both processing and S-R mapping automaticity, which we derived from our pilot study and adapted based on the literature findings and our expectations. These AUT scores were then used to specify the scores to assess the impact of task asymmetry (ASY), which we directly defined as the ratio in the AUT score of the two tasks involved in conflict tasks (i.e., irrelevant task AUT / relevant task AUT).

However, these parameters were also estimated more accurately based on the participants' performance we observed in the simple identification tasks in the present study, so as to have more precise hypotheses about the general pattern of performance in the conflict tasks (see below):

Specifically, for the AUT parameters:

i) the POS task required responding to the stimulus position, which we assumed had the most automatic processing and the strongest S-R mapping. We thus gave POS the highest AUT score. In our pilot study, the mean iRT in the POS task was around 2.5, so we gave an AUT score of 2.5 to the POS task;

ii) the DIR task required responding to the pointing direction of an arrow, which we assumed having a rather automatic processing and a strong S-R mapping, so overall it should take a slightly lower AUT score (10%, arbitrarily decided) as compared to the POS task. We thus gave an AUT score of 2.25 to the DIR task, that is, 10% lower than that of the POS task;

iii) the COL task required responding to the stimulus color, whose processing was assumed to be not so automatic and which, especially, had an arbitrary S-R mapping (so there is no SREL-R dimensional overlap), thus it should take the lowest AUT score. In our pilot study, the mean iRT in the last 36 trials of the COL task was around 1.6, so we gave an AUT score of 1.6 to the COL task;

iv) the WRD task required responding to the meaning of color words, which was assumed to be a strongly automatic process but also had an arbitrary S-R mapping, since responses were provided manually (so there is no SREL-R dimensional overlap), so overall it should take a slightly higher AUT score as compared to the COL task. We thus gave an AUT score of 1.75 to the WRD task, that is, about 10% higher than that of the COL task.

For the ASY parameters:

i) the single tasks only entailed a relevant task, so we gave it an ASY score of 0;

ii) the Simon task entailed the relevant COL task (AUT = 1.6) and the irrelevant POS task (AUT = 2.5), thus taking an ASY score of 2.5/1.6 ≈ 1.56;

iii) the VSc task entailed the relevant COL task (AUT = 1.6) and the irrelevant WRD task (AUT = 1.75), thus taking an ASY score of 1.75/1.6 ≈ 1.09;

iv) the VSw task entailed the relevant WRD task (AUT = 1.75) and the irrelevant COL task (AUT = 1.6), thus taking an ASY score of 1.6/1.75 ≈ 0.91;

v) the SSd task entailed the relevant DIR task (AUT = 2.25) and the irrelevant POS task (AUT = 2.5), thus taking an ASY score of 2.5/2.25 ≈ 1.11;

vi) the SSp task entailed the relevant POS task (AUT = 2.5) and the irrelevant DIR task (AUT = 2.25), thus taking an ASY score of 2.25/2.5 = 0.9

Based on the considerations about task automaticity, we thus had the following hypotheses for the differences in general performance across our identification tasks:

H5.1: POS - DIR > 0;
H5.2: DIR - WRD > 0;
H5.3: WRD - COL > 0;

Based on the considerations about both task automaticity and asymmetry, we expected to observe the following pattern of general performance (i.e., net of FE/IE) across our conflict tasks, considering conflict Neutral trials only (that are free of FE/IE at the S and R loci), which correspond to 4 additional sequential directional hypotheses:

H5.4: SSp_N - SSd_N > 0;

H5.5: SSd_N - VSw_N > 0;
H5.6: VSw_N - VSc_N > 0;
H5.7: VSc_N - Sim_N > 0;

Moreover, as we mentioned in the Introduction, we also took into account the estimated AUT parameter of the irrelevant task to refine our estimations about FE/IE/CE at both the S and R loci. Indeed, we assumed that if the processing of the irrelevant stimulus feature and its S-R mapping are more automatic, then they should exert a greater facilitation/interference in processing and responding to the relevant stimulus feature, with greater facilitation/interference at both the S and R levels. Therefore, we used the irrelevant task AUT to weight the corresponding FE/IE at the S and R loci. For example, using the parameters detailed above, we assigned to the stimulus facilitation effect in the VSw task a parameter of 1.6 (corresponding to the estimated AUT parameter for the irrelevant COL task), while we assigned to the stimulus facilitation effect in the VSc task a parameter of 1.75 (corresponding to the estimated AUT parameter for the irrelevant WRD task).

We also took into account the estimated ASY parameters to refine our estimations about the task interference effects, as we expected to find a greater task interference when the irrelevant task is more automatic than the relevant one (e.g., for the SSd task) as compared to when the relevant task is more automatic than the irrelevant one (e.g., for the SSp task). Therefore, task interference effects were weighted using the corresponding ASY estimates.

Based on these considerations, we defined a further set of hypotheses about FE/IE/CE:

H6.1a-c: The S-related effects will be larger in the VSc compared to the VSw task
H6.2a-c: The Stroop effects will be larger in the SSd compared to the SSp task
H6.3a-d: The following pattern of task interference effects will be observed: Sim > SSd > VSc > VSw > SSp

Finally, as we also mentioned above, we further refined our hypotheses about the FE/IE/CE in conflict tasks based on the results of our pilot study. Specifically, we assigned different weights to task interference and to facilitation/interference effects at both stimulus and response loci. Specifically, in our previous study we found a Stroop CE of about 0.44, which corresponds to about 26.8% of the performance in the Stroop Neutral condition (about 1.66), free of CE/IE at the S and R loci. Therefore, since we assumed for simplicity that the Stroop CE should correspond to the sum of both FE and IE at both the S and R loci (under the ADD model, see above), we assigned to these four constituting effects (i.e., S_FE, S_IE, R_FE, and R_IE) a weight of 6.7% (i.e., one fourth of 26.8%).

Similarly, in our pilot study we found a task interference effect of about 0.42, which corresponds to about 16.5% of the performance in the corresponding identification task (about 2.46), free of task interference. Therefore, we used for task interference predictions, which were based on the

corresponding ASY parameters, a weight 16.5% (because we dummy coded task interference contrasts as 0 vs -1).

To sum up, taking together all the sources of performance modulations detailed above, we expected that the pattern of our results in the different experimental conditions is modulated by both the task automaticity (AUT) and asymmetry (ASY) scores, which would add to the multiple loci (ML) effects detailed above, giving the hypothesized patterns of results shown in Figure 7.4.

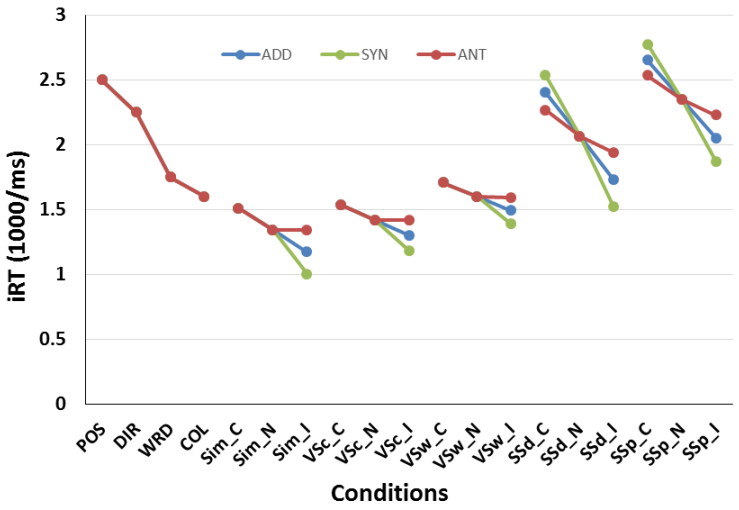

Figure 7.4.
Predicted performance (iRT: 1000/RT in ms) in all the experimental conditions under the assumption of no interaction between the effects at the different loci (ADD, blue line), or either a synergistic (SYN, green line), or an antagonistic (ANT, red line) interaction. See the description of the tasks (Section 7.2.1) for the abbreviations.

As we wrote above, after having tested H5.1-3, we estimated the AUT scores of each identification task based on the participants' actual performance, so to replace the estimates based on our pilot study with these more precise estimates.

7.2.3. Data analysis

We were specifically interested in measuring RTs. Accuracy was measured but not analyzed as we predicted it would be too high. Raw RTs were transformed into inverse-transformed RTs (iRTs, computed as 1000/RTs to directly map participants' performance: higher iRTs values reflect better performance). We decided a priori that our outcome variable were iRTs, as previously we repeatedly found that it is distributed more normally as compared to untransformed RTs and log-transformed ones (see for example Viviani et al., 2023).

We first checked for participants' compliance, excluding those with overall iRTs longer than -3 SDs from the entire sample, as well as those that did not complete all the tasks or with an overall accuracy lower than 70% (i.e., the accuracy level targeted in the practice blocks). Moreover, we excluded from the iRT analyses the trials with incorrect or missed responses, or with RTs lower than 150 ms, which were all treated as errors, as well as the first trial of each block. The first 72 trials of the COL and WRD identification tasks (i.e., the Type-1 ensemble tasks) were not analyzed because they served to let participants familiarize themselves with the arbitrary S-R mapping for the tasks that required them to respond either to colors or to word meaning.

A first set of analyses was performed to directly test our directional hypotheses about interference, facilitation, and congruency effects (i.e., IE, FE, and CE, respectively) across tasks (see Section 7.2.2). To do so, we performed the corresponding planned pairwise comparisons using one-tailed one-sample t-tests, while two-tailed one-sample t-tests were used to test H4s. The TOST analysis (Lakens, 2017) was used to test for equivalence in case of non-significant results. For the TOST, the smallest effect size of interest (SESOI) was set as Cohen's d = .35 (corresponding to the minimum effect size that a one-tailed one-sample t-test can detect with a statistical power of .80 and the planned sample size of 52, see below).

We also tested our hypotheses regarding FE and IE at the different loci and the general pattern of the results in the experimental conditions by correlating participants' performance in the different Task by Congruency conditions to the different hypothesized patterns detailed above. This analysis also allowed us to further test for the alternative hypotheses of either additive effects at the three loci or their synergic or antagonist interactions.

We assessed the internal consistency (reliability) of the effects in each task by computing split-half correlations corrected with the Spearman-Brown formula (r_{SB}). Specifically, for each task, the observations were randomly split in two subsets (2000 randomizations were used) and the participants' effects were computed and correlated between the two subsets. We reported the median r_{SB} values as well as the corresponding nonparametric 95% confidence intervals ($CI_{95\%}$).

A standard $p < .05$ criterion was used for significance testing for all the analyses. Effect sizes were computed as Cohen's d. We pre-registered additional multilevel modeling analyses that are still ongoing and thus are not reported here.

7.2.4. Participants

We recruited 126 participants (98 females and 18 males; mean age = 21.91 years, *SD* = 4.51 years). Participants' handedness was assessed using the Edinburgh Handedness Inventory (EHI, Oldfield, 1971).

The sample comprised ten left-handed participants (EHI scores < −50) and ten ambidextrous participants (EHI scores between −50 and 50). No participants reported suffering from neurological or psychiatric disorders or being under medication. Participants gave their informed consent to participate in the study, which was conducted in accordance with the ethical standards of the 2013 Declaration of Helsinki for human studies of the World Medical Association. The study was approved by the Ethical Committee for the Psychological Research of the University of Padova.

Participants consisted of a convenience sample recruited from the available university students and social pools and the link to the online experiment was spread among as many potential participants as possible using researchers' professional and social networks.

We used G*Power to conduct the power analysis on one- and two-tailed one-sample t tests, which were used to perform the planned pairwise comparisons to test our hypotheses (see Section 7.2.2). Our goal was to obtain a .8 power to detect a small-to-medium effect size of d = .35 at the standard .05 alpha error probability. This analysis revealed that 52 and 67 participants were needed, respectively for one- and two-tailed one-sample t tests. We also used the TOSTER worksheet (Equivalence_Tests_TOSTER.xlsx; Lakens, 2016) to compute the sample size required to perform the planned TOST analyses assuming a smallest effect size of interest of d = .35 with an alpha of .05 and a power of .80. This analysis revealed that 70 participants are needed.

Our target sample size was thus of 70 participants, but we tried to recruit as many participants as possible in a one-month period, exceeding the required sample size, to improve statistical power and the precision of our estimates, also because we expected that some participants could not complete all the tasks and/or could be excluded from the analyses due to poor performance.

7.3. Results and Discussion

Three participants were excluded from the analyses based on our exclusion criteria, because their overall accuracy (64.6%, 10.8%, and 7.9%) indicated poor performance. Figure 7.5 shows the participants' performance, in terms of iRT, in all the experimental conditions.

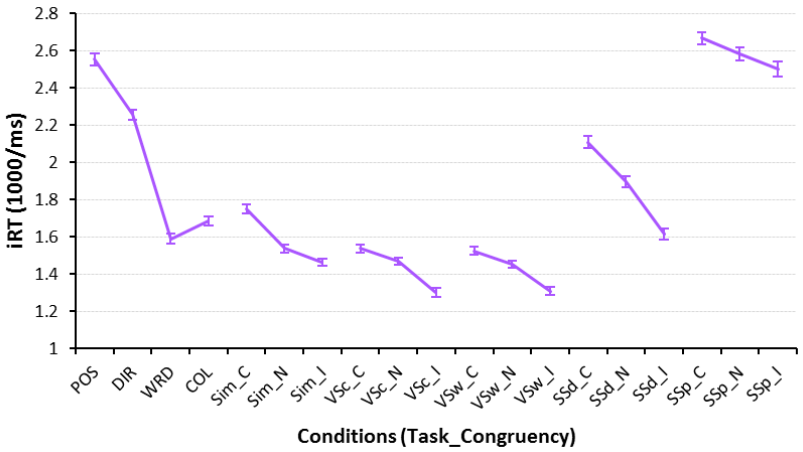

Figure 7.5.
Observed performance (iRT: 1000/RT in ms) in all the experimental conditions (Task by Congruency combinations). The error bars indicate the SE. See the description of the tasks (Section 7.2.1) for the abbreviations.

Table 7.2 shows the outcomes of the first set of our hypotheses, which regards the FE and IE in the five conflict tasks, and Figure 7.6 shows the corresponding observed effects.

Table 7.2. Results of the first set of (auxiliary) hypotheses regarding facilitation and interference effects

H	Loci_Eff	Task	M	SD	t(122)	p	d	DOM (%)	TOST
H1.3	R_FE	Sim	0.212	0.130	18.09	< .0001	1.632	96.7	
H1.1a	S_FE1	VSc	0.068	0.101	7.47	< .0001	0.674	73.2	
H1.1b	S_FE2	VSw	0.072	0.103	7.77	< .0001	0.701	74.0	
H1.5a	Str_FE1	SSd	0.213	0.119	19.92	< .0001	1.796	96.7	
H1.5b	Str_FE2	SSp	0.083	0.138	6.71	< .0001	0.605	74.8	
H1.4	R_IE	Sim	0.072	0.090	8.85	< .0001	0.798	74.8	
H1.2a	S_IE1	VSc	0.169	0.132	14.28	< .0001	1.287	90.2	
H1.2b	S_IE2	VSw	0.144	0.121	13.21	< .0001	1.191	89.4	
H1.6a	Str_IE1	SSd	0.280	0.115	27.13	< .0001	2.446	99.2	
H1.6b	Str_IE2	SSp	0.081	0.171	5.24	< .0001	0.473	70.7	
H1.7e	T_IE5	Sim	0.149	0.169	9.79	< .0001	0.883	82.1	
H1.7d	T_IE4	VSc	0.218	0.159	15.19	< .0001	1.370	91.1	
H1.7c	T_IE3	VSw	0.138	0.276	5.53	< .0001	0.499	82.1	
H1.7b	T_IE2	SSd	0.361	0.233	17.16	< .0001	1.547	95.1	
H1.7a	T_IE1	SSp	-0.030	0.200	-1.67	.9516	-0.151	35.0	*

Notes. H, hypothesis (see Section 7.2.2); R, effect at the response locus; S, effect at the stimulus locus; Str, Stroop effect (i.e., effect at both S and R loci); T, effect at the task locus; FE, facilitation effect; IE, interference effect; DOM%, effect dominance, corresponding to the percentage of participants showing the effect. The asterisk in the TOST column indicates effects that are significantly smaller than the SESOI. See the description of the tasks (Section 7.2.1) for the corresponding abbreviations.

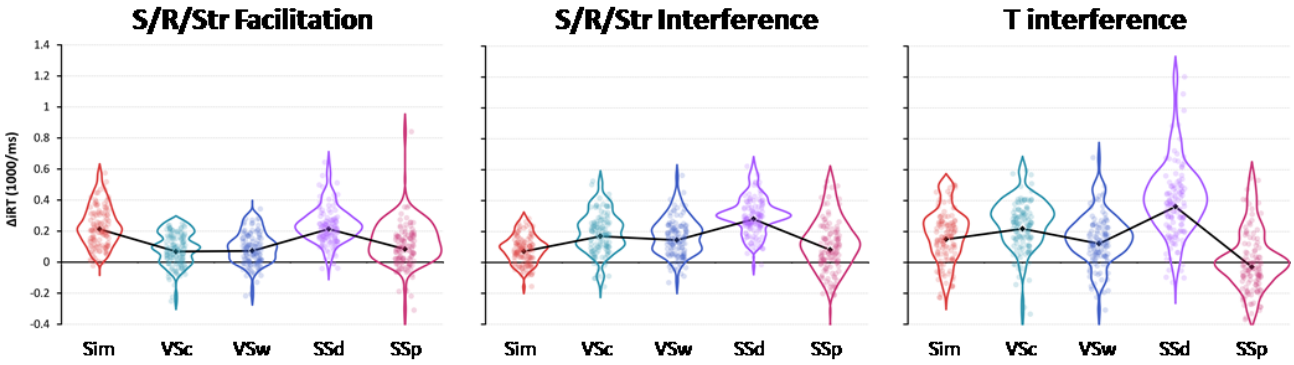

Figure 7.6.
Results of the first set of hypotheses. Experimental facilitation/interference effects (expressed as iRT differences) observed in the conflict tasks involving the different loci (S, stimulus; R, Response; T, Task; Str, Stroop, corresponding to both S and R loci). The violin plots illustrate the distribution of the participants' effects (each dot is the effect of one participant). The superimposed black line plot indicates the sample average.

The analyses confirmed all but one of our 15 auxiliary directional hypotheses. Specifically, all the facilitation effects (reflecting the better performance in C compared to N trials) were significant, with effect sizes ranging from medium (0.605) to very high (1.796) and dominance (i.e., percentage of participants showing the effect) ranging from 73.2 to 96.7%. Similarly, all the interference effects at the S/R loci (reflecting the better performance in N compared to I trials) were significant, with effect sizes ranging from medium (0.473) to very high (2.446) and dominance ranging from 70.7 to 99.2%. The task interference effects (T_IE), reflecting the better performance in simple identification tasks (requiring to respond to a single, task-relevant stimulus feature) compared to that in N trials in the corresponding conflict tasks (also entailing a task-irrelevant stimulus feature in both C and I trials), were significant in all but the SSp task, with effect sizes ranging from medium (0.499) to very high (1.547) and dominance ranging from 82.1 to 95.1%. By contrast, the T_IE was not significant and in the opposite direction compared to our hypothesis, but the TOST revealed that it was significantly smaller than the SESOI ($t(122) = 2.21$, $p = .0144$).

As regards the internal consistency of the FE/IE effects at the stimulus and response loci, it was generally low for the facilitation effects (see Figure 7.7), especially for the SSp task (median $r_{SB} = .174$) and the Stroop-like VSc and VSw tasks (median $r_{SB} = .201$ and .300); the SSd task showed the highest reliability (median $r_{SB} = .593$), followed by the Sim task (median $r_{SB} = .478$). The reliability of the interference effects was generally higher, except for the Sim task, for which it was very poor (median $r_{SB} < .001$). Again, the SSd task showed the highest internal consistency (median $r_{SB} = .683$). As regards the internal consistency of the task interference effect, it was consistently higher than that of FE/IE effects (see Figure 7.7), especially for the SSd and VSw tasks (median $r_{SB} = .924$ and .910, respectively).

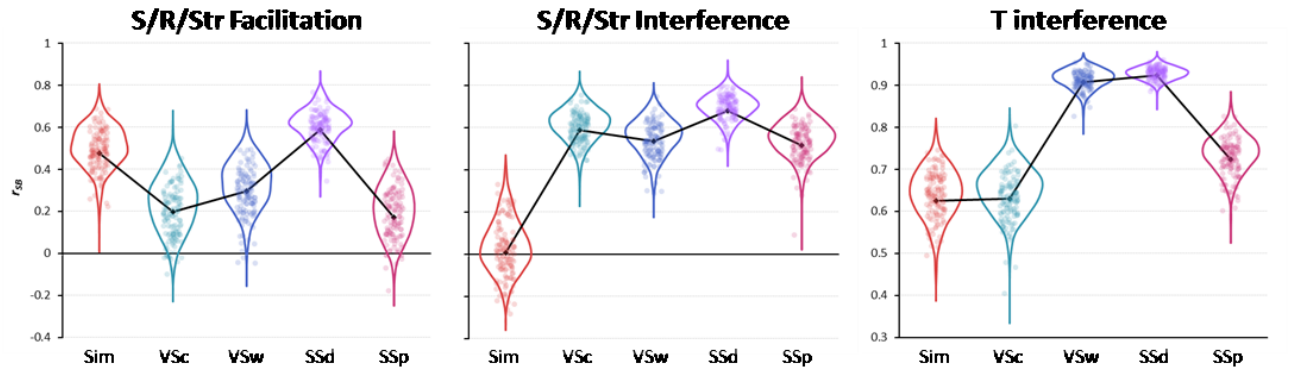

Figure 7.7.
Internal consistency reliability of the experimental facilitation/interference effects observed in the conflict tasks involving the different loci (S, stimulus; R, Response; T, Task; Str, Stroop, corresponding to both S and R loci). The violin plots illustrate the distribution of r_{SB} values (each dot is the r_{SB} obtained in one of the 2000 random splits). The superimposed black line plot indicates the average.

Overall, the results of the first set of our hypotheses confirmed our predictions and established the necessary prerequisites for the subsequent sets of hypotheses.

First, we found that all our conflict tasks produced both facilitation and interference effects, which was fundamental to our subsequent aim of exploring whether such effects arise from multiple loci. Moreover, it is interesting to note that facilitation effects were observed quite consistently and, in some cases, with effect sizes and dominance values comparable to those of interference effects, suggesting that this often neglected component of the Stroop effect may instead play a prominent role in contributing to it. Therefore, as highlighted in the introduction, the fact that the facilitation effect has been commonly found to be smaller (and less consistently) than the interference effect, may probably be attributed to the inadequacy of the neutral baselines commonly used to calculate it, which is a thorny issue especially when using verbal Stroop tasks (Brown, 2011). It should also be noted, however, that the internal consistency of the interference effects was generally higher than that of facilitation effects, which was generally poor (except for the Simon task, for which the pattern was reversed). The low reliability of facilitation effects may thus be a contributing cause for the observation that the facilitation effect is typically smaller and less stable compared to the interference effect in the existing studies.

One interesting finding is that the facilitation and interference effects yielded by the SSd task (i.e., the task used in the studies presented in the present thesis) were not only the largest and most dominant ones, but also the ones with the highest reliability, confirming it as a methodologically valid task to investigate Stroop performance. By contrast, the effects yielded by its reversed version, the SSp task, appeared to be consistently smaller, less dominant, and less reliable (see the results for our fifth set of hypotheses below, for the corresponding statistical test).

Overall, thus, our results about facilitation and interference effects thus suggest the importance of using neutral conditions, revealing also that facilitation and interference effects can be disentangled. Moreover, they provide further evidence for the advantages of using spatial versions of the Stroop task, especially the SSd, namely the one we used in the present thesis.

The second relevant finding regards task interference. Specifically, our results provide initial evidence for our hypothesis that when neutral trials are presented intermixed with congruent and incongruent trials, namely in conflict task blocks, also the alternative conflicting task set is inevitably activated, thus producing task interference. Indeed, the fact that RTs to respond to these neutral trials were longer as compared to RTs responding to neutral trials in pure identification blocks, which involved identical (or very similar) stimuli activating the same task set, suggest that this was very likely due to the interference between two conflicting task sets. Therefore, our findings not only reveal that task interference may indeed be present, likely affecting Stroop performance, in contrast with Parris and colleagues' (2023) latest review, but also provide a possible effective way to measure its effect, even with very high reliability for the SSd and VSw tasks, overcoming limitations of the previously employed measures. Of note, the only result not in line with our predictions, that is, the absence of task interference in the SSp task, does not jeopardize the effectiveness of our task interference measure. Indeed, this negative finding is likely attributed to the inherent asymmetry characteristics of the SSp task. Specifically, the task set associated with POS, which was the relevant task in the SSp task, may be too strong and automatic to be influenced by the task set linked to DIR, thus consequently resulting in a lack of interference from the irrelevant DIR task set, despite its high automaticity.

Table 7.3 shows the outcomes of the second set of our hypotheses, which regarded the CE in the five conflict tasks, and Figure 7.8 shows the corresponding observed effects.

Table 7.3. Results of the second set of hypotheses regarding congruency effects

H	Loci_Eff	Task	M	SD	t(122)	p	d	DOM (%)	TOST
H2.3	R_CE	Sim	0.284	0.138	22.73	< .0001	2.050	99.2	
H2.1	S_CE1	VSc	0.238	0.131	20.12	< .0001	1.814	98.4	
H2.2	S_CE2	VSw	0.216	0.121	19.81	< .0001	1.787	97.6	
H2.4	Str_CE1	SSd	0.493	0.161	33.97	< .0001	3.063	100.0	
H2.5	Str_CE2	SSp	0.164	0.198	9.22	< .0001	0.831	80.5	

Notes. See Table 7.2 for conventions

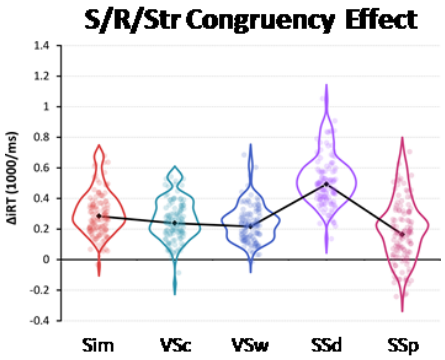

Figure 7.8.
Results of the second set of hypotheses. Experimental congruency effects (expressed as iRT differences) observed in the conflict tasks involving the different loci (S, stimulus; R, Response; T, Task; Str, Stroop, corresponding to both S and R loci). The violin plots illustrate the distribution of the participants' effects (each dot is the effect of one participant). The superimposed black line plot indicates the sample average.

The analyses confirmed all of our 5 directional hypotheses (but given the results reported above for H1s, this was necessarily true for all the conflict tasks, as all the pair of hypotheses about S/R FE and IE were both confirmed, and CE are equivalent to the sum of FE and IE). Specifically, all the congruency effects (reflecting the better performance in C compared to I trials) were significant, with effect sizes ranging from high (0.831) to very high (3.063) and dominance ranging from 80.5 to 100%.

As regards the internal consistency of the congruency effects, it was good for the Sim and SSp task (median r_{SB} = .637 and .687, respectively) and, especially, the SSd task (median r_{SB} = .837) (see Figure 7.9). The internal consistency of the Stroop-like task was instead lower (median r_{SB} = .559 and .550).

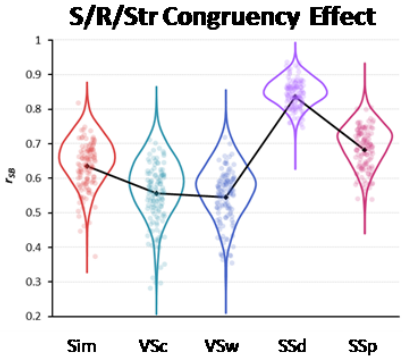

Figure 7.9.
Internal consistency reliability of the experimental congruency effects observed in the conflict tasks involving the different loci (S, stimulus; R, Response; T, Task; Str, Stroop, corresponding to both S and R loci). The violin plots illustrate the distribution of r_{SB} values (each dot is the r_{SB} obtained in one of the 2000 random splits). The superimposed black line plot indicates the average.

Although this second set of hypotheses was directly dependent on the first one, the finding that all our tasks showed CE furnishes additional evidence for the suitability of our conflict tasks and further strengthens the foundation upon which we tested the hypotheses of interest to address our research questions. Indeed, these findings revealed that even when contrasting congruent to incongruent conditions, the resulting effects were very large and characterized by high dominance values, reaching the 100%. Specifically, the task yielding the largest effect size, a 100% dominance to be called universal, and the highest internal consistency was the SSd task. This result, in line with the findings of our previous study (Viviani et al., 2023, and Chapter 3), further confirms the goodness of this experimental paradigm and substantiates our choice to use it in the present thesis. It is also worth noting that these results emerged in this study even without the use of a multilevel modeling approach, unlike the Chapter 3 study, suggesting that even when trial noise was not excluded, this paradigm yielded large and reliable Stroop effect measures.

Table 7.4 shows the results of the third set of our hypotheses, regarding the difference between the Stroop effects, involving both the S and R loci, and the Stroop-like and Simon effects, involving either the S or R loci, respectively. We thus compared the FE/IE/CE at each of the two Stroop tasks with those at the Stroop-like and at the Simon tasks. Figure 7.10 shows the corresponding observed differential effects.

Table 7.4. Results of the third set of hypotheses on the difference between Stroop and S/R effects

H	Loci_Eff	Str Task	S/R Task	M	SD	t(122)	p	d	DOM (%)	TOST
H3.1c	FE_ML3	SSd	Sim	0.001	0.173	0.08	.4684	0.007	51.2	*
H3.1a	FE_ML1	SSd	VSc	0.145	0.147	10.95	< .0001	0.988	88.6	
H3.1b	FE_ML2	SSd	VSw	0.141	0.155	10.04	< .0001	0.906	78.9	
H3.1f	FE_ML6	SSp	Sim	-0.128	0.173	-8.26	> .9999	-0.745	18.7	ns
H3.1d	FE_ML4	SSp	VSc	0.015	0.165	1.02	.1550	0.092	46.3	*
H3.1e	FE_ML5	SSp	VSw	0.011	0.163	0.75	.2269	0.068	49.6	*
H3.2c	IE_ML3	SSd	Sim	0.208	0.147	15.69	< .0001	1.415	92.7	
H3.2a	IE_ML1	SSd	VSc	0.111	0.168	7.32	< .0001	0.660	75.6	
H3.2b	IE_ML2	SSd	VSw	0.136	0.157	9.62	< .0001	0.867	83.7	
H3.2f	IE_ML6	SSp	Sim	0.009	0.194	0.54	.2966	0.048	48.8	*
H3.2d	IE_ML4	SSp	VSc	-0.088	0.211	-4.63	1.0000	-0.418	29.3	ns
H3.2e	IE_ML5	SSp	VSw	-0.063	0.194	-3.60	.9998	-0.325	39.8	ns
H3.3c	CE_ML3	SSd	Sim	0.210	0.187	12.44	< .0001	1.122	85.4	
H3.3a	CE_ML1	SSd	VSc	0.256	0.209	13.60	< .0001	1.226	87.0	
H3.3b	CE_ML2	SSd	VSw	0.277	0.187	16.39	< .0001	1.478	95.9	
H3.3f	CE_ML6	SSp	Sim	-0.119	0.227	-5.82	1.0000	-0.525	26.0	ns
H3.3d	CE_ML4	SSp	VSc	-0.073	0.232	-3.50	.9997	-0.316	33.3	ns
H3.3e	CE_ML5	SSp	VSw	-0.052	0.213	-2.71	.9961	-0.244	36.6	ns

Notes. Ns, non-significant. See Table 7.2 for other conventions.

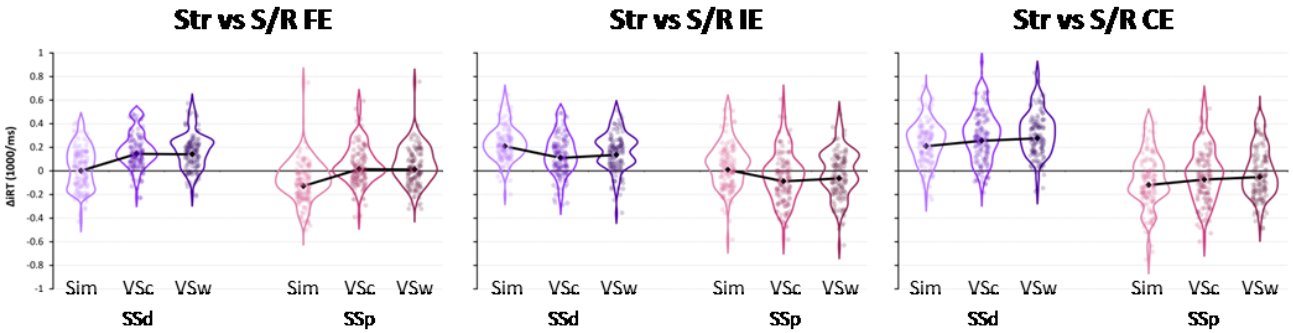

Figure 7.10.
Results of the third set of hypotheses. Difference between the FE/IE/CE effects (expressed as iRT differences) observed in each of the two Stroop tasks (involving both the S and R loci) and those observed in the Simon and the two Stroop-like tasks (involving either the S or R loci, respectively). The violin plots illustrate the distribution of the participants' effect difference (each dot is the effect of one participant). The superimposed black line plot indicates the sample average.

The analyses confirmed all but one of our 9 directional hypotheses regarding the Stroop effect in the SSd task. Specifically, the SSd FE was larger than both the VSc and VSw ones originating at the S locus, with large effect sizes (0.988 and 0.906, respectively) and high dominance (78.9 and 88.6%, respectively), but were basically indistinguishable from the Sim FE (TOST: $t(122) = -3.80$, $p = .0001$). The IE and CE yielded by the SSd task were all larger than those yielded by the Sim, VSc, and VSw tasks, with effect sizes ranging from medium (0.660) to very high (1.478) and dominance ranging from 75.6 to 95.9%. By contrast, and contrary to our hypotheses, none of the effects yielded by the SSp task was larger than those yielded by the non-Stroop conflict tasks. Specifically, the SSp FE were only numerically larger than both the VSc and VSw ones originating at the S locus, but with an effect size significantly smaller than the SESOI (TOST: $t(122) = -2.86$ and -3.13, $p = .0011$ and $.0024$, respectively), and the same was true for the SSp IE as compared to the Sim one (TOST: $t(122) = -3.35$, $p = .0005$). However, in all other cases the effects yielded by the SSp task were even smaller than those yielded by the non-Stroop conflict tasks (and they would have been significantly smaller at a two-tailed test).

The results from this third set of analyses showed that the SSd task, which demonstrated to be the most effective among the conflict tasks, produced a Stroop effect that confirmed (almost all of) our predictions and provided initial evidence for the presence of the assumed loci. In contrast, the SSp task did not confirm our predictions, exhibiting a pattern opposite to what was expected.

Starting with the SSd task, our results suggested that the Stroop Congruency Effect (CE) was larger than the respective single effects observed in both the Stroop-like and the Simon tasks. Thus, this difference may be attributed to the multiple-locus nature of the SSd task, including both S and R loci, in comparison to the other tasks involving only one of these two loci. If we had tested our experimental question solely on the CE, we would have suggested that it is likely to be composed of both S and R loci, but we would have

missed a significant portion of the entire pattern that instead emerged thanks to the differentiation between FE and IE.

The findings regarding the IE are in line with predictions, showing that the IE in the SSd was always greater than IE in all the other tasks, thus suggesting that the IE produced by this Stroop task was bigger probably because it arose from two loci, S and R, instead of one locus, as the other tasks.

The findings regarding the FE are not totally in line with our predictions, but still very interesting. The fact that the FE in the SSd task was not significantly different from the FE in the Simon task suggests, although indirectly by analogy, that facilitation in the Stroop task may be essentially equivalent to the facilitation in the Simon task. Thus, this likely suggests that in the Stroop task, the FE may be primarily driven by response facilitation. Furthermore, the larger FE observed in the Stroop task compared to the two Stroop-like tasks may suggest that response facilitation in the Stroop task might be more pronounced than any facilitation at the stimulus level (if such stimulus-level facilitation exists). It is worth noting that in this third set of hypotheses, we had not yet considered the AUT of the irrelevant task, as we did in the sixth set of hypotheses. In the latter, we indeed refined our predictions regarding FE and IE based on the level of automaticity of the irrelevant task. Given that both facilitation and interference effects were expected to be greater as the automaticity of the irrelevant task increased, more specific hypotheses that took this into account were likely to provide more valuable insights. This was particularly relevant, for example, in the comparison between the FE in the SSd task and the FE in the Simon task, both of which involve the same irrelevant task, namely POS, which is also the most automatic.

Moving on to the results regarding the SSp task, the fact that the obtained pattern was entirely opposite to what was predicted could be attributed, as in the previous results, to the idea that the POS task is even more strong and automatic than what we expected and estimated. Indeed, the results reported so far suggest that the relevant POS task may not only be completely immune to the interference from the irrelevant but exogenously activated DIR task (see above), but may also be partially resistant to both interference and facilitation at the stimulus and response loci exerted by the irrelevant DIR task, as also suggested by the apparent relatively lower magnitude of these effects, compared to the SSd task (see above). Based on our assumptions, these findings are quite surprising because the irrelevant DIR task should still exert pronounced effects, as it is the second most automatic task. However, they are partially in line with the idea that the irrelevant task has to be more automatic than the relevant one to exert facilitation/interference effects, an idea that is evident in the common definition of the cognitive processes assessed with the Stroop tasks. Therefore, refining the effect of the loci using the automaticity of the irrelevant task, as we did with our sixth set of hypotheses, may be helpful in gaining a better understanding of these results.

Table 7.5 shows the outcomes of the fourth set of our hypotheses, which explored whether and how the individual S and R effects interacted in composing the Stroop effects. Specifically, these hypotheses directly tested whether the Stroop effects, thought to originate at both the S and R loci, could be explained as the sum of the two effects originating at each of these loci, as predicted by a simple additive model, or if they were smaller or larger than this sum. We thus compared the FE/IE/CE at each of the two Stroop tasks with the sum of those yielded by the Sim task and those yielded by either of the two Stroop-like tasks. Figure 7.11 shows the corresponding observed differential effects.

It is crucial to emphasize that these hypotheses were built on the ones in the third set, which had to be confirmed first. In other words, if the Stroop effects were not greater in magnitude than both the S and R ones individually, it became unjustifiable to investigate whether they were greater (or even equal) to the cumulative effects of both the S and R components. However, for the sake of completeness, we report the results for all the pre-registered tests.

Table 7.5. Results of the fourth set of hypotheses on the additive vs. interactive nature of S/R effects in composing Stroop effects

H	Loci_Eff	Str Task	S+R Task	M	SD	t(122)[a]	p	d	TOST
H4.1a[b]	Str_FE_ADD1	SSd	Sim+VSc	-0.067	0.191	-3.89	.0002	-0.351	
H4.1b[b]	Str_FE_ADD2	SSd	Sim+VSw	-0.071	0.209	-3.77	.0003	-0.340	
H4.1c[b]	Str_FE_ADD3	SSp	Sim+VSc	-0.197	0.192	-11.35	< .0001	-1.024	
H4.1d[b]	Str_FE_ADD4	SSp	Sim+VSw	-0.201	0.203	-11.00	< .0001	-0.992	
H4.2a	Str_IE_ADD1	SSd	Sim+VSc	0.039	0.188	2.31	.0227	0.208	
H4.2b	Str_IE_ADD2	SSd	Sim+VSw	0.064	0.188	3.80	.0002	0.343	
H4.2c[b]	Str_IE_ADD3	SSp	Sim+VSc	-0.160	0.227	-7.81	< .0001	-0.705	
H4.2d[b]	Str_IE_ADD4	SSp	Sim+VSw	-0.135	0.219	-6.81	< .0001	-0.614	
H4.3a	Str_CE_ADD1	SSd	Sim+VSc	-0.028	0.231	-1.34	.1814	-0.121	*
H4.3b	Str_CE_ADD2	SSd	Sim+VSw	-0.007	0.233	-0.32	.7515	-0.029	*
H4.3c[b]	Str_CE_ADD3	SSp	Sim+VSc	-0.357	0.258	-15.33	< .0001	-1.382	
H4.3d[b]	Str_CE_ADD4	SSp	Sim+VSw	-0.335	0.261	-14.28	< .0001	-1.288	

Notes. [a] Two-tailed paired-sample t-test. [c] These hypotheses are not justified given the results of H3s hypotheses. See Table 7.2 for conventions.

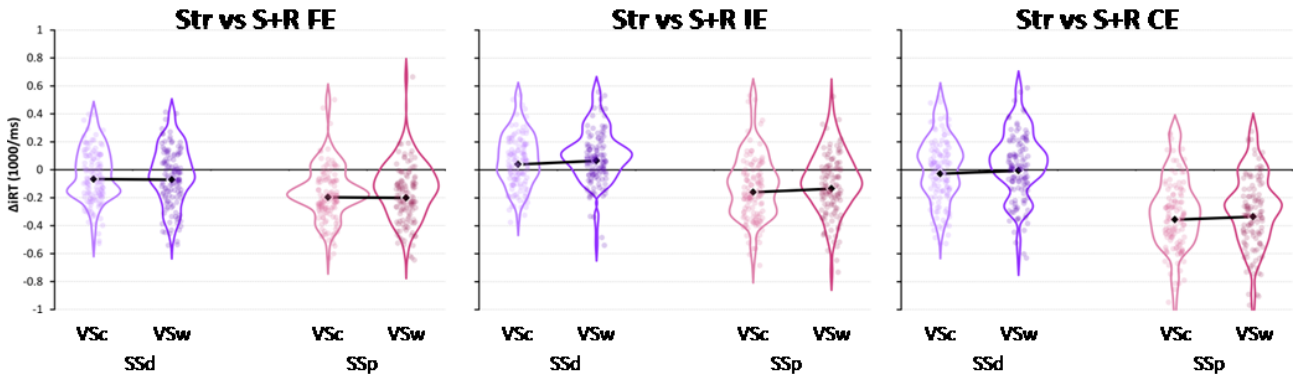

Figure 7.11.
Results of the fourth set of hypotheses. Difference between the FE/IE/CE effects (expressed as iRT differences) observed in each of the two Stroop tasks (involving both the S and R loci) and the sum of those observed in the Simon and each of the two Stroop-like tasks (involving either the S or R loci, respectively). The violin plots illustrate the distribution of the participants' effect difference (each dot is the effect of one participant). The superimposed black line plot indicates the sample average.

Eight of the 12 hypotheses (namely, all the 6 involving the SSp effects and the 2 involving the SSd FE) were not justified based on the results regarding the third set of hypotheses, as noted above. All of these pairwise comparisons showed that the Stroop effect was significantly smaller than the sum of the S and R effects. As regards the remaining hypotheses, the SSd IE was significantly larger than the sum of the S and R IE, but with effect sizes that were small (0.208 and 0.343) and even numerically smaller than our SESOI. The SSd CE was instead not significantly different from the sum of the S and R CE, as also indicated by the significant results of the TOST analysis ($t(122) = 2.54$ and 3.56, $p = .0062$ and .0003).

Overall, the results from the fourth set of hypotheses appeared to support our predictions, namely that the loci in the Stroop CE were likely to interact in an antagonistic way, thus producing effects smaller than their sum.

However, most of these hypotheses were not justified based on the results of the third set of hypotheses, as explained above. Therefore, these results should be taken with caution. Moreover, this set of hypotheses was limited to exploring the interplay of only the S and R loci, without yet considering the role of task interference in overall Stroop performance. Subsequent tests instead provided much more informative insights into the interplay between all the loci.

Table 7.6 shows the outcomes of the fifth set of our hypotheses, which examined differences in overall performance across our tasks. As detailed in Section 7.2.2, these hypotheses were initially formulated based on the AUT and ASY scores we estimated from the performance in the POS and COL tasks, as observed in our pilot study. Additionally, they were based on the assumptions we made for the DIR and WRD tasks, respectively, which were themselves based on those earlier estimations.

Table 7.6. Results of the fifth set of hypotheses about the pattern of across-tasks differences in overall performance

H	Task1	Task2	M	SD	t(122)	p	d	TOST
H5.1	POS	DIR	0.296	0.201	16.35	< .0001	1.474	
H5.2	DIR	WRD	0.667	0.364	20.34	< .0001	1.834	
H5.3	WRD	COL	-0.096	0.289	-3.69	.9998	-0.332	ns
H5.4	SSp	SSd	0.687	0.332	22.95	< .0001	2.069	
H5.5	SSd	VSw	0.444	0.307	16.04	< .0001	1.446	
H5.6	VSw	VSc	-0.016	0.166	-1.09	.8602	-0.098	*
H5.7	VSc	Sim	-0.068	0.149	-5.05	> .9999	-0.455	ns

Notes. All the hypotheses predicted a better performance in Task1 compared to Task2. Note that only neutral trials were used for these tests. See Table 7.2 for conventions.

As regards the hypotheses about the simple identification tasks, the results confirmed that the performance was better in the POS compared to the DIR task, which in turn had a better performance compared to the WRD (and COL, not shown) task. However, contrary to our expectations, the performance in the WRD task was worse, rather than better, than that in the COL task. As regards the hypotheses about the conflict tasks, the results confirmed that the performance was better in the SSp compared to the SSd task, which in turn had a better performance compared to the VSw (and VSc and Sim, not shown) task. However, contrary to our expectations, the performance in the VSw task was statistically indistinguishable (TOST: $t(122) = 2.80$, $p = .0030$) and numerically worse, rather than better, than that in the VSc task. Moreover, and again contrary to our expectations, the performance in the VSc task was worse, rather than better, than that in the Sim task.

As we noted above, these hypotheses were based on our assumptions about the overall performance in the DIR and WRD identification tasks, which were in turn built upon the performance in the POS and COL identification tasks observed in our pilot study. The predicted pattern was confirmed for what concerns POS and DIR, with the former representing the most automatic task, and both of them being more automatic than the other tasks. Therefore, these results suggest that the use of POS as the irrelevant task in spatial Stroop tasks seems the optimal choice, as it is effective in eliciting strong facilitation and interference effects.

However, as clearly shown by the results we just reported, we were wrong in assuming that word reading, even if responding by button presses was required, is more automatic and easier than responding to colors. This finding is unexpected as our assumption of WRD more automatic than color was based on the literature which, although less attention has been devoted to reverse Stroop tasks (reading color words, ignoring their ink color), has quite consistently shown that print colors typically interfere with (or facilitate) color reading with a less extent (e.g., Blais & Besner, 2007; MacLeod, 1991; Stroop, 1935). However, our results regarding the performance in the Stroop-like tasks seem to be consistent with prior

findings revealing a reverse Stroop effect when participants performing reverse Stroop tasks were required to point to matching colors (Blais & Besner, 2007; Durgin, 2000). As such, it is plausible that the use of manual responses, as required in our task, has made color identification more automatic than word reading, with the latter losing its assumed greater automaticity when, after reading the word, responses had to be provided using keypress responses. This reversed asymmetry between color identification and word reading may thus have been the result of less strong S-R mapping when the reading output had to be transcoded as a manual response, an issue worth being investigated further in the future.

Although our predictions based on the pilot revealed to be wrong, as per our pre-registration, we then refined our hypotheses about the pattern of performance differences across our conflict tasks based on the participants' performance we observed in the identification tasks in this study. The revised AUT estimates were as follows (our initial estimates are reported in brackets): POS = 2.5522 (2.5); DIR = 2.2565 (2.25); COL = 1.6856 (1.6); WRD = 1.5894 (1.75). Accordingly, the revised ASY estimates were as follows (our initial estimates are reported in brackets): SSp = 0.8861 (0.9); VSc = 0.9365 (1.0938); VSw = 1.0678 (0.9143); SSd = 1.1285 (1.1111); Sim = 1.5243 (1.5625). It is important here to emphasize that the revised ASY estimates assume a reversed pattern of task asymmetry between VSw and VSc tasks, given that the COL task had a better performance than the WRD one. As a result, the revised hypotheses about the pattern of overall performance in the conflict tasks were SSp > SSd > VSc > Sim > VSw. The revised hypotheses correctly predicted a better performance in VSc as compared to VSw. However, they still erroneously predicted a better performance in VSc as compared to Sim, which showed a surprisingly good performance in spite of its predicted very high ASY score. This totally unexpected result could be speculatively explained by the fact that the two tasks involved in the Simon, although very asymmetric, rely on totally different neural/cognitive codes, so that when participants responded to colors, ignoring the position was easier than ignoring the word meaning, because the latter shared the same code as identifying colors, also due to the fact that in the VSc colors and words implied in our task the same response mapping.

Overall, by testing these hypotheses we added an additional layer of complexity, exploring not only the existence and interplay between the loci, but also the influence of well-established effects on the modulation of the overall performance in conflict tasks, namely task automaticity and task asymmetry, finding initial evidence that they both strongly depended on the response modality.

Table 7.7 shows the outcomes of the sixth set of our hypotheses, which examined the across-tasks difference in the effects at the S and R loci after weighting them by the AUT score of the irrelevant stimulus feature (which causes the S/R facilitation/interference effects), as well as the across-tasks difference in the task interference effects after weighting them by the ASY estimates.

Table 7.7. Results of the sixth set of hypotheses about the effects weighted for AUT/ASY

H	Effect	Task1	Task2	M	SD	t(122)	p	d	TOST
H6.1a	FE	VSc	VSw	-0.004	0.137	-0.33	0.6292	-0.030	*
H6.1b	IE	VSc	VSw	0.025	0.189	1.49	0.0693	0.134	*
H6.1c	CE	VSc	VSw	0.021	0.174	1.36	0.0889	0.122	*
H6.2a	FE	SSd	SSp	0.130	0.177	8.14	< .0001	0.734	
H6.2b	IE	SSd	SSp	0.199	0.206	10.74	< .0001	0.968	
H6.2c	CE	SSd	SSp	0.329	0.232	15.73	< .0001	1.418	
H6.3a	TIE	Sim	SSd	-0.212	0.274	-8.55	> .9999	-0.771	ns
H6.3b	TIE	SSd	VSc	0.144	0.262	6.07	< .0001	0.547	
H6.3c	TIE	VSc	VSw	0.080	0.314	2.82	0.0028	0.255	
H6.3d	TIE	VSw	SSp	0.168	0.338	5.51	< .0001	0.497	

Notes. All the hypotheses predicted a larger effect in Task1 compared to Task2. See Table 7.2 for conventions.

The hypotheses about the difference in magnitude for the effects in the VSc vs. VSw tasks were not confirmed. The TOST revealed that the differences in the effects were significantly smaller than the SESOI (all $|t|s(122) > 2.39$, all $ps < .0091$). However, this also entails that the same hypotheses based on the AUT score estimated based on the performance in the identification tasks in the present study were also not confirmed.

As discussed above, these results for the two Stroop-like tasks may have strongly relied on the response modality, which showed a stronger influence than we expected. However, as we here considered AUT as an ensemble of both processing strength and S-R mapping, we could not disentangle the effect of each of them. Future studies are thus required to provide evidence for our interpretation that the unexpected observed pattern was due to the use of manual responses. For example, this could be done by comparing tasks with the same processing strength but with different response mappings (e.g., responding to COL with manual vs verbal responses).

Although we could precisely quantify the extent to which manual responses contributed to yielding similar effects in the two Stroop-like tasks, these findings suggest that the use of manual responses may pose challenges when employing verbal Stroop(-like) tasks. This issue holds relevance for the Stroop literature, where it is common to encounter tasks labeled as Stroop but employing manual responses. This would pose a validity issue not only because, as extensively discussed in Chapter 2, these tasks should instead be categorized as Stroop-like tasks, but also because the use of this response modality may impact task asymmetry to an extent that is not yet fully understood, leading to unexpected effects. This observation is in line with the findings of Augustinova and colleagues (2019), who reported that, when using verbal Stroop tasks, the manual response modality does not engender task conflict.

Conversely, the hypotheses about the difference in magnitude for the effects in the SSd vs. SSp tasks were all confirmed with large effect sizes. These findings seem to be the consequence of what was found above, that is, that the POS task set was the strongest and most automatic one. Moreover, finding that CE, FE, and IE were greater when POS was the irrelevant task than when DIR was the irrelevant task may suggest that by using such an automatic irrelevant task, such effects are observed in the expected direction. Therefore, as argued above, designing spatial Stroop tasks using DIR as the relevant and POS as the irrelevant task appears to be effective in order to obtain CE, FE and IE with large effect sizes. Moreover, the fact that the DIR task set, despite being very automatic, did not yield similar effects when used as the irrelevant task further suggests that using spatial versions of the Stroop task, by relying upon a clear task asymmetry, is advantageous. This becomes evident when we compare these results with those obtained from the comparison between VSc and VSw, whose involved tasks, as discussed earlier, did not show a clear asymmetry, as the asymmetry seemed to be strongly contingent on the response modality. Indeed, the use of manual responses in the VSc and VSw may be problematic, not only because it renders them not genuine Stroop tasks but Stroop-like tasks, but also because even when intentionally employed as such, the impact of task asymmetry when manual responses are used remains unclear. However, as discussed in Chapter 2, the utilization of manual responses versus verbal responses can have advantages, and since manual responses are adequate (and necessary) in spatial Stroop tasks, we overall reinforce our argument that spatial Stroop tasks surpass verbal ones in various respects.

Finally, the hypotheses about the difference in magnitude for the task interference effects across our conflict tasks were all confirmed with small-medium effect sizes, apart from the one predicting a larger T_IE in Sim as compared to SSd, which instead showed the opposite pattern. Overall, these results provided initial evidence for our assumption that the asymmetry between the tasks may affect the amount of task interference, so when the asymmetry is greater, the task interference should be larger. However, this was not true for the Simon task. Indeed, as shown from the comparison between task interference in the Simon and in the SSd, a counterintuitive pattern emerged. These two tasks implied the same irrelevant task set, POS, but different relevant task sets, namely COL for Simon and DIR for SSd. Following the logic underlying task interference, given that COL was assumed to be the least automatic, in the Simon we should have observed greater task interference than the SSd. However, we speculated that this may not have been the case because POS and COL, as suggested above, may imply more distinct neural/cognitive codes as compared to POS and DIR in the SSd, in which there might have been greater task interference due to the fact that these two tasks conceivably rely on much more similar neural/cognitive codes and have the same strong (and not arbitrary) response mapping as well.

If we consider this finding concerning less task interference in the Simon task compared to the SSd task, along with the previously discussed finding of better performance in the Simon task compared to the VSc

task, we could make a consideration: task interference may not depend solely on the asymmetry between the tasks, even though this seems to be necessary, as suggested by the other results that aligned with our predictions. In addition to this, a sort of dimensional overlap between the two tasks might be required. Indeed, our results suggest that if such an asymmetry is at its maximum but the two tasks do not share the same neural codes, or the response mapping used to respond to the relevant task does not overlap or is not strongly interconnected with the response mapping activated by the irrelevant task, as in the Simon task, task interference is probably reduced. The dynamics are again more complex than expected, suggesting the need for future studies to further elucidate this matter. For instance, future research could consider predicting task interference not only in terms of the asymmetry between the tasks but also by weighing its effect based on a form of dimensional overlap between the tasks.

We finally tested our hypotheses regarding the experimental effects at the different loci, also considering the overall pattern of the results in the experimental conditions, modulated not only by the S_{REL} and S_{IRR} AUT, but also by the task ASY scores, which we used to weight the multiple loci (ML) effects, as detailed above. The observed data were better fitted by the ANT model, assuming an antagonistic interaction between the effects at the S, R, and T loci, with a very high correlation of r = .9425 (see Figure 7.12).

The finding that the ANT model was the one better explaining the performance in our conflicting tasks provides further evidence in line with the results obtained from the fourth set hypothesis. As highlighted previously, indeed, these latter results could shed light on the antagonistic interplay between the S and R loci only. Now, we could instead move beyond that, because this last set of results took into account also the task locus. The fact that the loci interacted in an antagonistic manner, thus producing an effect that was smaller than their sum, was not so unexpected, and was indeed predicted. This is based on the assumption that the S and R loci are plausibly strongly interconnected. Our findings align with Parris and colleagues' (2022) conclusions, which claimed that there is evidence for an informational locus, but that the S and R loci included in it are difficult to disentangle. Their conclusion, however, was only partially true. Indeed, with our experimental design, we showed initial evidence that these two loci can be disentangled, obtaining pure measures of both the S and the R loci, as suggested by our findings in the third set of hypotheses. Specifically, the finding that the IE was larger than both IE in the Stroop-like tasks and the IE in the Simon task may suggest that we had successfully distinguished between the effects of the S and R loci. In contrast to the conclusions of Parris and colleagues (2022), we argue that it might be not so much the measures of the S and R loci that are problematic, as it seems that they can be disentangled. Rather, their antagonistic interaction probably lies in the fact that when generating performance in the Stroop task, these loci might be interconnected, given their anatomical and functional similarities at the brain level.

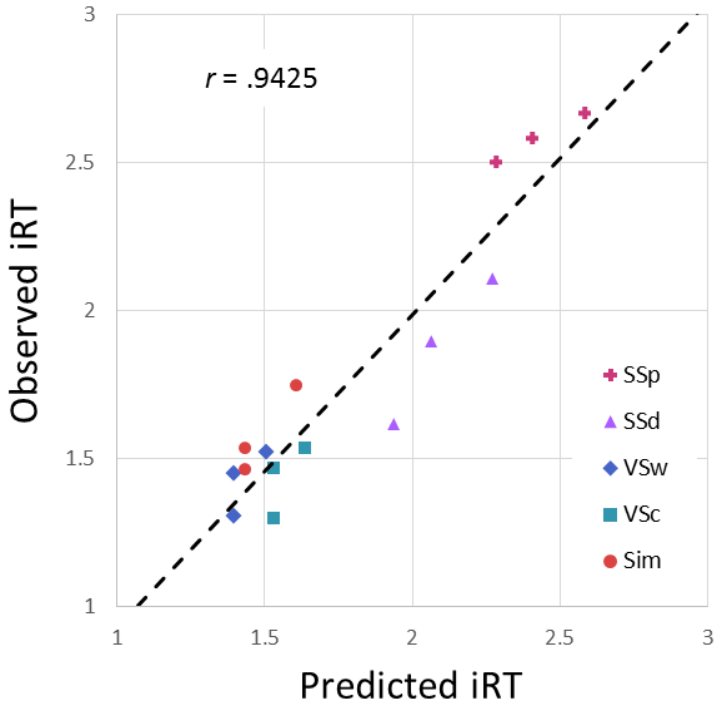

Figure 7.12.
Correlation between the predicted (x axis) and observed (y axis) pattern of performance in the experimental conditions under the assumption of an antagonistic interaction between the effects at the three loci.

Overall, with this final study we provided initial but valuable insights into how the Stroop performance might be generated, not only showing the effect of each specific locus, but also revealing that they are likely to interact in an antagonistic manner. However, one of the issues that remain to be addressed is whether this antagonistic interplay occurs only between the S and R loci which, as previously mentioned, would make sense given their strong interconnectedness, while the task locus has an additive effect. Alternatively, it is possible that the antagonistic interplay also involves the task locus. Although we predict that the first option is more plausible, as highlighted by Parris and colleagues (2022), who found initial evidence that the task locus can be distinguished from the first two loci, and therefore, it is expected to have more of an additive effect, the analyses presented so far cannot test this hypothesis. While this aspect is not covered in the current chapter, our pre-registration outlines how to test this hypothesis. Due to time constraints, we have not yet conducted the remaining planned analyses, but these will be conducted shortly to provide more detailed insights into the dynamics of Stroop performance.

7.4. Summary and Conclusion

In this chapter, we directly explored the composite nature of the Stroop effect, which throughout the entire thesis was used as a methodological benchmark to design valid spatial Stroop tasks. Given that the multiple-loci hypothesis for the Stroop performance relies on evidence that is not completely compelling, as highlighted in the introduction, and it derives mainly from studies using verbal versions of the Stroop task, it was necessary to explore its empirical foundation using spatial versions of the Stroop task, which are more suitable for this purpose, as they exclude the confounding effects that are inherent to verbal Stroop tasks (i.e., the involvement of distinct linguistic layers).

Therefore, our aim here was to distinguish the stimulus, response and task loci in the spatial Stroop task to directly assess their influence on both the Stroop facilitation and interference effects and, ultimately, on the Stroop performance. Based on a prior pilot pre-registered study, we could refine our measures for the explored loci and put forward and test very specific a priori hypotheses, considering not only the effect of each locus, but also the weight of task automaticity and of the asymmetry between the tasks.

Overall, our study revealed that the Stroop performance may indeed have originated from the three hypothesized loci, which interacted in an antagonist manner. However, thanks to our distinction between facilitation and interference, we found evidence that it was mainly the interference effect that originated from the interplay between all the three loci; the facilitation effect, instead, was mostly due to the effect at the response locus, suggesting that Stroop facilitation might essentially be response facilitation. Our study has not only set the first step, showing these initial but interesting findings, which require additional analyses to elucidate the nature of such interplay, as already delineated in the pre-registration form, but it has also brought forth many other intriguing insights. For example, the task set influence might also differentially affect facilitation and interference effects (see Di Russo & Bianco, 2023), an open question that merits further investigation.

One key aspect of the present study is that we provided an effective alternative to measure task interference, overcoming the limitations of previously used measures, showing that it likely affects Stroop performance, in contrast with Parris and colleagues (2023). Indeed, the comparison between neutral trials presented in conflict tasks, thus intermixed with congruent and incongruent trials, and neutral trials presented in simple identification tasks, revealed longer RTs, which might thus be attributed to the concomitant activation of two conflicting task sets. However, our results also led us to suggest that, contrary to our expectations, this might not occur when the relevant task is too strong and automatic, such as the POS task used here, which was not influenced by the interfering effect of the irrelevant task set of DIR.

Our basic results, namely those regarding the facilitation and interference effects observed in all our conflict tasks, are informative for the Stroop literature in general, as they showed that, in contrast with previous findings, facilitation was consistently observed, even if with poor internal consistency. It was also relevant that the SSd, which is the task used in all the studies included in the present thesis, showed the largest, most dominant, and most reliable facilitation and interference effects, not only providing further evidence for its methodological validity, but also overcoming one of the main limitations of the present thesis, namely the use of only congruent and incongruent trials, which allowed us to compute only the global measure of Stroop effect. Our future studies will thus capitalize on the present study, and also neutral conditions will be included to disentangle facilitation and interference effects, which is significant also for our purpose of exploring proactive and reactive control.

Lastly, an aspect worthy of consideration is the role of task automaticity and task asymmetry, which often goes unnoticed when decomposing the Stroop performance but, as highlighted by our results, likely has an impact that should not be overlooked. For what concerns the automaticity of the task sets involved in conflict tasks, which we considered as an ensemble of both processing strength and S-R mapping, our results suggested that weighting the facilitation and interference effects for it is important to more precisely predict the performance, in all conflict tasks and not only in the Stroop task. However, one limitation of this study was that we could not disentangle the effect of the two components involved in automaticity, which however will be necessary in future studies, as highlighted by our results, some of which were in contrast with our predictions probably for this precise reason. Indeed, when estimating the automaticity of the tasks, specific attention should be paid to the response modality employed, whose importance was for example suggested by the fact that using manual responses made the COL task-set, which is always assumed to be not so automatic, more automatic than WORD reading, which instead is commonly predicted to be quite automatic. The task automaticity was predicted and also shown to be directly involved in task asymmetry (computed as the difference between the automaticity of the two tasks), which in turn affected task interference. But again, some of our predictions were not satisfied, probably because task interference is not so simply affected by task asymmetry, but the effect of asymmetry strongly relies also on whether the two tasks share or not neural/cognitive codes. As such, even though asymmetry is the greatest, if the two conflicting tasks do not share such neural/cognitive codes (i.e., in the Simon task), the task interference might be reduced. Overall, our results thus provided initial and potentially useful insights into task asymmetry, leading us to propose that a sort of dimensional overlap between the two tasks is required for task asymmetry to fully exert its effect.

Overall, this study addressed and started to answer some important open questions, while at the same time uncovering further inquiries that require more thorough investigation due to their complexity. This thus paves the way for many future studies on this interesting and complex matter.

7.5. References

Augustinova, M., Parris, B., & Ferrand, L. (2019). The Loci of Stroop Interference and Facilitation Effects With Manual and Vocal Responses. Frontiers in Psychology, 10, 1786. https://doi.org/10.3389/fpsyg.2019.01786

Augustinova, M., Silvert, L., Spatola, N., & Ferrand, L. (2018). Further investigation of distinct components of Stroop interference and of their reduction by short response-stimulus intervals. Acta Psychologica, 189, 54–62. https://doi.org/10.1016/j.actpsy.2017.03.009

Blais, C., & Besner, D. (2007). A reverse Stroop effect without translation or reading difficulty. Psychonomic Bulletin & Review, 14(3), 466–469. https://doi.org/10.3758/bf03194090

Brown, T. L. (2011). The relationship between Stroop interference and facilitation effects: Statistical artifacts, baselines, and a reassessment. Journal of Experimental Psychology. Human Perception and Performance, 37(1), 85–99. https://doi.org/10.1037/a0019252

De Houwer, J. (2003). On the role of stimulus-response and stimulus-stimulus compatibility in the Stroop effect. Memory & Cognition, 31(3), 353–359. https://doi.org/10.3758/bf03194393

Di Russo, F., & Bianco, V. (2023). Time Course of Reactive Brain Activities during a Stroop Color-Word Task: Evidence of Specific Facilitation and Interference Effects. Brain Sciences, 13(7), 982.

Durgin, F. H. (2000). The reverse Stroop effect. Psychonomic Bulletin & Review, 7(1), 121–125. https://doi.org/10.3758/bf03210730

Hock, H. S., & Egeth, H. (1970). Verbal interference with encoding in a perceptual classification task. Journal of Experimental Psychology, 83(2), 299–303. https://doi.org/10.1037/h0028512

Kornblum, S. (1992). Dimensional overlap and dimensional relevance in stimulus–response and stimulus–stimulus compatibility. 2.

Lakens, D. (2017). Equivalence Tests. Social Psychological and Personality Science, 8(4), 355–362. https://doi.org/10.1177/1948550617697177

MacLeod, C. M. (1991). Half a century of research on the Stroop effect: An integrative review. Psychological Bulletin, 109(2), 163–203. https://doi.org/10.1037/0033-2909.109.2.163

Melara, R. D., & Algom, D. (2003). Driven by information: A tectonic theory of Stroop effects. Psychological Review, 110(3), 422–471. https://doi.org/10.1037/0033-295x.110.3.422

Parris, B. A., Hasshim, N., Ferrand, L., & Augustinova, M. (n.d.). Do Task Sets Compete in the Stroop Task and Other Selective Attention Paradigms? Journal of Cognition, 6(1), 23. https://doi.org/10.5334/joc.272

Parris, B. A., Hasshim, N., Wadsley, M., Augustinova, M., & Ferrand, L. (2022). The loci of Stroop effects: A critical review of methods and evidence for levels of processing contributing to color-word Stroop effects and the implications for the loci of attentional selection. Psychological Research, 86(4), 1029–1053. https://doi.org/10.1007/s00426-021-01554-x

Posner, M. I., & Snyder, C. R. R. (1975). Attention and Cognitive Control. In R. L. Solso (Ed.), Information Processing and Cognition: The Loyola Symposium. Lawrence Erlbaum.

Risko, E. F., Schmidt, J. R., & Besner, D. (2006). Filling a gap in the semantic gradient: Color associates and response set effects in the Stroop task. Psychonomic Bulletin & Review, 13(2), 310–315. https://doi.org/10.3758/BF03193849

Seymour, P. H. K. (1977). Conceptual Encoding and Locus of the Stroop Effect. Quarterly Journal of Experimental Psychology, 29(2), 245–265. https://doi.org/10.1080/14640747708400601

Stroop, J. R. (1935). Studies of interference in serial verbal reactions. Journal of Experimental Psychology, 18(6), 643–662. https://doi.org/10.1037/h0054651

van Casteren, M., & Davis, M. H. (2006). Mix, a program for pseudorandomization. Behavior Research Methods, 38(4), 584–589. https://doi.org/10.3758/BF03193889

Viviani, G., Visalli, A., Finos, L., Vallesi, A., & Ambrosini, E. (2023). A comparison between different variants of the spatial Stroop task: The influence of analytic flexibility on Stroop effect estimates and reliability. Behavior Research Methods. ttps://doi.org/10.3758/s13428-023-02091-8

Zhang, H., & Kornblum, S. (1998). The Effects of Stimulus-Response Mapping and Irrelevant Stimulus-Response and Stimulus-Stimulus Overlap in Four-Choice Stroop Tasks with Single-Carrier Stimuli. Journal of Experimental Psychology. Human Perception and Performance, 24, 3–19. https://doi.org/10.1037//0096-1523.24.1.3

Equivalence_Tests_TOSTER.xlsx. (2016). https://osf.io/https://osf.io/qzjaj

CHAPTER 8

General Discussion

8.1. From where we started: overview of background and aims

The present doctoral thesis aimed to shed light on a complex and still open issue: the comprehensive understanding of cognitive control. Cognitive control is among the cognitive abilities that most distinctly characterize human beings, as it enables us to flexibly regulate our behavior in order to achieve our goals (Chiew & Braver, 2017; Cohen, 2017). By replacing automatic responses with adaptive behaviors, cognitive control frees ourselves to act appropriately within a given context and in accordance with our objectives (Miller & Cohen, 2001).

The undeniable significance of cognitive control has led to numerous efforts over the past decades dedicated to unraveling its functioning and neural underpinnings. However, despite these endeavors, our knowledge in this domain remains limited. Various theories have been proposed, exhibiting considerable heterogeneity among them. While some of these theories are supported by robust evidence, others are less so. Yet, this diversity has contributed to rendering the landscape of our understanding even more intricate and obscure. It is evident that achieving a true comprehensive understanding of cognitive control within the scope of a thesis is not feasible. Nonetheless, our endeavor has been to make our contribution as significant as possible by rigorously addressing this intricate aspect of human cognition, both at the theoretical and methodological levels.

In particular, two theoretical assumptions have served as the guiding thread for this thesis, with the first being the selection of the theoretical framework to be adopted. Given the multitude of existing theories, it is indeed crucial to opt for and consistently employ a single theoretical framework in order to better systematize the results. This facilitates the coherent interpretation of both the behavioral signatures and the functional significance of neural correlates. Specifically, we have embraced the dual mechanism of control model (DMC; Braver, 2012; Braver et al., 2007) for this purpose. As extensively expounded throughout this work, this model represents an advancement compared to classical models like the conflict monitoring one (Botvinick et al., 2001). The DMC model has the advantage of comprehensively elucidating commonly observed phenomena, such as the proportion of congruency effects, and accommodating the intrinsic variability inherent to cognitive control. Therefore, the rationale behind our adoption of the DMC model stems from its capacity to address the complexity of cognitive control, a facet which renders it unrealistic to attribute to a single mechanism (Braver, 2012, 2012; Torres-Quesada et al., 2013).

Consequently, our utilization of this model has steered our exploration of cognitive control towards presupposing the existence of two distinct control modes, proactive and reactive control, and we aimed to ascertain the potential separability between these modes, evaluating whether they are genuinely distinct.

The second critical theoretical premise, which we have underscored from the outset but that has become notably pronounced during our exploration of neural correlates (see Chapters 5 and 6), centers on the significance of representations. While our understanding of cognitive control remains limited, representations stand out as its core components. In fact, the behavioral flexibility ensured by cognitive control is assumed to heavily rely on the maintenance and continual adjustment of goal representations (Chiew & Braver, 2017; Cohen, 2017; Diamond, 2013; Miller & Cohen, 2001). It is through these representations encoded at the neural level that downstream neurons can enact the neural processes essential for executing goal-relevant actions. The notion of representations, encompassing the neural basis capable of encoding all requisite goal-related information, thus assumes a fundamental role in fully understanding the dynamics of cognitive control (Cellier et al., 2022; D'Esposito, 2007; Diedrichsen & Kriegeskorte, 2017; Kriegeskorte & Diedrichsen, 2019; Schumacher & Hazeltine, 2016).

The potential of the representational perspective on cognitive control is also recognized by the theories delineating cognitive control in terms of representations (e.g., Badre et al., 2021; Braver, 2012; Cohen et al., 1990; Freund et al., 2021; Kriegeskorte & Diedrichsen, 2019). This conceptualization can be extended to encompass the predictions of the DMC. At the foundation of the two control modes, one can posit the existence of representations that encode information relevant to achieving the goal, expecting these representations to exhibit distinctions based on whether the goal is pursued in a proactive or reactive manner. Therefore, to gain a deeper understanding of cognitive control, it becomes evident that considering representations is essential, and this involves directly testing theories regarding cognitive control. Our current limited comprehension of cognitive control may indeed stem from the significant oversight of representations, with instead the primary focus often centered on processes that serve merely as indirect proxies for them (Freund et al., 2021). Therefore, investigating these representations and their relationship with processes would enable a more comprehensive understanding of cognitive control.

These considerations thus elucidate the overarching objective of this doctoral thesis: to delve into both the neural processes of cognitive control and the neural representations upon which these processes depend. Given our adoption of the DMC as the theoretical framework, we have undertaken a specific examination of the neural processes and representations associated with both proactive and reactive control. The aim has been to ascertain whether these control modes exhibited distinct characteristics at the neural level. However, given the absence of robust evidence for this separability even at the behavioral level, we found it necessary to take a step back and first verify the distinctness of the behavioral signatures of proactive and reactive control as well.

8.2. Tracing Our Path: Methodological and statistical considerations

The objective of this thesis was multifaceted, and to achieve it effectively, besides establishing theoretical foundations, we had to accord significant importance to methodological rigor. Consequently, while addressing our research questions, we have both highlighted and addressed various methodological and statistical issues. These challenges assumed substantial significance within this project, serving as the foundational bedrock and essential means for attaining our goals. However, these methodological and statistical aspects were not solely the path through which we navigated to achieve our objectives; they also formed an integral and pivotal component of this work. Hence, they warrant thorough discussion and can be summarized into the following three key points.

8.2.1. Methodological and statistical properties of the Stroop effect

The first relevant aspect we addressed pertained to the methodological and statistical properties of the measure to employ, which is intertwined with the primary methodological decision we needed to make – namely, the selection of the experimental paradigm.

We commenced with the premise that, within cognitive psychology, the experimental paradigm is pivotal, given that it is the sole tool at our disposal for gauging cognitive processes. Measurement in psychology is particularly intricate, as cognitive phenomena are often explored through latent constructs that remain unobservable directly. Consequently, when there is no strong evidence regarding the measure validity, we encounter a deficiency in the essential information required to assess each type of validity and, consequently, the validity of the study conclusions (Flake & Fried, 2020).

For all the studies envisaged in this project, we opted to employ the Stroop task (Stroop, 1935), a highly influential and widely used interference task. Its extensive history spanning nearly a century in evaluating interference resolution has yielded an extensive body of literature underscoring the generation of a universal effect by this paradigm (Parsons, 2020). Furthermore, our selection was influenced by the task suitability for experimental manipulations that differentiate between proactive and reactive modes, aligning precisely with our aim. However, despite the undeniable advantages of the Stroop task as a paradigm, selecting the most suitable version for our purposes was not straightforward, as such benefits cannot be automatically extended to all the variants that have been proposed. Indeed, these variants exhibit a high degree of heterogeneity among themselves to the extent that some might not warrant the label of Stroop task. Labeling them as such could potentially jeopardize measurement validity, as the measure attainable through these variants might not truly reflect what is intended to be measured. Therefore, in selecting the most appropriate Stroop version for our studies, we aimed to prioritize measurement validity. As such, we assessed various Stroop variants to determine which ones yielded a

Stroop effect that closely resembled the original effect in all respects. However, this preliminary work, originally conceived solely for the purpose of selecting a methodologically valid Stroop version, has shed light on the profound methodological confusion that plagues the extensive literature on the Stroop task. The pressing need for systematization compelled us to undertake a significantly larger effort—a methodological review of the Stroop task, outlined in Chapter 2. This endeavor was undertaken not only to benefit the current thesis project but also to contribute to the literature on this subject.

Among the primary merits of this review is the provision of a structured approach to designing methodologically robust Stroop tasks, underscoring the crucial point that, in order to obtain valid measures of Stroop effects, these tasks must account for its multifaceted nature. Our main message in brief was that, considering that the Stroop effect arises from multiple loci, experimental designs that generate conflict at the task locus while inducing interference/facilitation at the stimulus and response loci are essential for producing comprehensive measurements of the Stroop effect and in turn upholding measurement validity.

The second strength of the review lies in the fact that, having determined that a significant portion of the most known alternative adaptations of the Stroop task lacked the capacity to yield valid Stroop effect measures, we proposed a solution. This involves employing spatial Stroop tasks that tap spatial interference by presenting stimuli with semantic attributes indicating a spatial location while simultaneously displayed in a physical position. A methodologically sound example of this task is the one used in our previous studies and proposed by Puccioni and Vallesi (2012a,b,c). The strength of this Stroop adaptation, although only when realized in purely spatial versions, is twofold. It not only generates a comprehensive Stroop effect involving interference between two competing task sets and stimulus- and response-related conflicts/facilitations, but it also addresses certain drawbacks associated with the classical Stroop version, such as reducing linguistic confounding and requiring manual responses.

Overall, the review constituted a preliminary effort that enabled us to clarify the methodological principles for designing methodologically valid Stroop tasks. This clarification is important for two reasons: firstly, these principles consistently emerged throughout the entire project, proving relevant not only for our work but also for the broader Stroop literature; secondly, the review aided us in selecting a valid measure of the Stroop effect.

In psychology, as in any scientific discipline, the utilization of valid measures is undoubtedly crucial; however, this alone is insufficient. Therefore, having established the required methodological characteristics for the measure we intended to employ, in Chapter 3, we investigated its statistical properties, with a specific focus on reliability. Indeed, although often overlooked, reliability is fundamental for examining interindividual differences through correlational research in cognitive neuroscience and psychology (e.g., Dang et al., 2020; Elliott et al., 2020; Rouder et al., 2019; Wennerhold & Friese, 2020).

Moreover, assessing the reliability of our measure was particularly crucial considering the reliability paradox (Hedge et al., 2018) and related proposals (Rouder & Haaf, 2019), according to which experimental effects that are large and consistently replicable to the extent of being deemed universal (Parsons, 2020), much like the Stroop effect, are likely to lack sufficient reliability. Therefore, to ensure that the chosen Stroop measure was not only valid and capable of eliciting a large Stroop effect, but also reliable, we conducted a subsequent study, preliminary to the entire project. We seized this opportunity to examine alternative spatial Stroop versions to the one proposed by Puccioni and Vallesi, termed Peripheral spatial Stroop. Indeed, while this spatial Stroop version is methodologically sound and adheres to the established criteria, it does have some potential weaknesses stemming from its use of peripherally presented stimuli. As a result, five alternative spatial Stroop task versions were devised, retaining the methodological benefits of the Peripheral spatial Stroop while addressing its limitations.

One of the strengths of this study was our utilization of an innovative approach to assess reliability, which provided evidence contrary to the reliability paradox and offered a solution to overcome it. Specifically, we demonstrated that multilevel modeling approaches effectively improved the precision of the estimates of our experimental effects by disentangling true experimental effects from measurement error, represented by trial-by-trial variability (also known as trial noise) within subjects. This in turn enhanced the reliability of our experimental effects. Demonstrating that this approach enhances the reliability of measurements was significant not only for reliability itself, but also to emphasize the general utility of employing multilevel modeling approaches to estimate experimental effects with precision, which is of utmost importance in (psychological) research. This conclusion also relies on another strength of this study, in which we assessed the robustness of results to analytical flexibility by directly comparing different analytical approaches (as well as different measure transformations). We thus can safely claim that multilevel modeling approaches, by providing more precise and reliable estimates of the experimental effects, are preferable as compared to GLM. For these reasons, multilevel modeling analyses were then used in the entire project.

Overall, this study has not only offered valuable insights into relevant statistical issues, such as reliability and analytical flexibility, but it has also provided a significant statistical groundwork for the current project. This foundation enabled us to identify the most suitable spatial Stroop task as the one yielding a Stroop effect that was the largest, the most robust to analytical flexibility, and the most reliable. These statistical properties, besides the methodological ones, were mainly satisfied by the spatial Stroop task called Perifoveal. It works exactly as the Peripheral one, while overcoming its limitations. Indeed, it mitigates possible biases due to eye movements and (re)orienting of visuospatial attention. Therefore, the Perifoveal spatial Stroop task, being suitable for neuroimaging and electrophysiological studies, was then used in all the subsequent studies, both behavioral and EEG ones.

8.2.2. Validity of proactive and reactive control measures and how to test them

After identifying a Stroop effect measure that was methodologically valid and with adequate statistical properties, these same facets were again investigated, albeit with a shift in focus toward measures of proactive and reactive control. Chapter 4, which presents the behavioral study, precisely tackled this subject. In striving to identify the behavioral signatures of the two control modes, it also served to test and validate a novel approach for accomplishing this goal, also for subsequent studies.

The necessity to devise a means of obtaining valid measures for proactive and reactive control arose from the fact that approaches commonly employed in the literature suffer from limitations that jeopardize the validity of the resultant measures. Our critique is not so much directed at the manipulations employed to elicit proactive and reactive control, namely, the List-Wide Proportion Congruency (LWPC) and the Item-Specific Proportion Congruency (ISCP), respectively, but rather at the approaches with which these manipulations are commonly employed. In particular, these approaches have primarily emerged in response to a significant critique directed toward the manipulations of the PC, which is referred to as the contingency hypothesis (Schmidt, 2019; Schmidt & Besner, 2008). If this hypothesis were to entirely account for the effects of PC manipulations, the implication would be a complete lack of validity in the obtained measures of proactive and reactive control. This would stem from the fact that what is being measured does not align with the intended construct – the proactive and reactive modulation of the Stroop effect – but rather reflects the mere effect of something else at a considerably lower level, namely, stimulus-response associative learning processes. We completely agree with the necessity to control and exclude the possibility that the effect of PC manipulations is biased by the contingency effect. However, what we do not align with is the commonly employed approach that we have termed the design-level control, which has been conceived for this purpose. Briefly, this family of approaches, also recommended in a consensus paper (Braem et al., 2019) and described more extensively in Chapter 4, involves meticulously controlling the experimental design (i.e., by using inducer and diagnostic items) to prevent any contingency effect.

While it might seem beneficial to methodically eliminate every potential low-level effect at the level of the experimental design, in our view, these approaches are not only excessively impractical and time-consuming but also not always feasible. Furthermore, some of them are founded on assumptions that might not always be assured. What holds even greater significance is that, in their efforts to control for confounding variables at the design level, these approaches substantially compromise the measurement validity of the DMC assumption. In fact, they are all purposely limited to manipulating only one control mode at a time (in order to control for the effect of the other one), inherently excluding the possibility of simultaneously manipulating both the LWPC and ISPC. As a consequence, by measuring only one control mode at a time, it becomes impossible to discern the impact of the other control mode, even though, in

accordance with the DMC, it is inevitably evoked given the assumed dual-mechanism nature of control. To eliminate the influence of the unmeasured control mode, its PC should ideally be set at 100. However, this manipulation is not possible. Commonly, to nullify the unmeasured control mode, the PC is set at 50, implying that this control mode, though unmeasured, is elicited at an average level, but its effect is then neglected.

A direct consequence of the infeasibility of design-level control approaches to simultaneously manipulate both LWPC and ISPC is the inability to test the interaction between proactive and reactive control. However, their interplay is indeed implicitly assumed by the DMC, given that reactive control should prevail when proactive control is unfeasible or less advantageous (e.g., Braver, et al., 2009; 2021; De Pisapia & Braver, 2006). The solution we proposed to ensure the validity of measures for proactive and reactive control was to test them when both are manipulated, that is, by simultaneously varying both the LWPC and the ISPC. This approach enables a direct examination of the DMC assumption positing the coexistence of proactive and reactive control, by revealing whether each mechanism is activated while the other is also in operation. Furthermore, by having precise knowledge of the PC at both the list-wide and item-specific levels, we can effectively track the impact of each control mode on performance. And lastly, we can also explore the interplay between proactive and reactive control by testing the interaction between LWPC and ISPC.

The advantages elucidated above, and particularly the accurate tracking of each control mode effect, were further augmented by our utilization of trial-by-trial estimates of LWPC and ISPC. Indeed, the conventional manipulations of LWPC and ISPC, even when implemented simultaneously, are insufficient to provide an accurate estimation of the impact of each control mode at each trial. This limitation arises from the fact that these manipulations are traditionally computed at the block level. Specifically, LWPC and ISPC are derived by calculating the number of congruent trials (either overall or for each item, respectively) within a block, divided by the total number of trials (either overall or for each item, respectively) within the same block. However, these block-level LWPC and ISPC variables unequivocally correspond to the actual PCs solely at the conclusion of the block. Instead, the PCs in the middle, and especially at the beginning of the blocks, do not genuinely reflect the PC estimated by participants, given that participants are not typically aware of the probabilistic structure of the task. Participants are thus likely to continuously, trial-by-trial, implicitly estimate the LWPC and ISPC values using some form of statistical learning based on the history of previous trials, and then implement a specific level of control accordingly. Consequently, when LWPC and ISPC are calculated at the block level, the resulting measures of proactive and reactive control are inherently not fully valid. The design-level control approach works by operationalizing LWPC and ISPC as block-level measures, given that the PC from an individual trial can be meaningfully interpreted only when aggregated across all trials, lacking meaningful significance when taken in isolation. However, as elucidated

earlier, this approach is not realistic, and it does not accurately reflect adaptive control, which is inherently dynamic and more likely to operate at the trial level. What we have done, therefore, is to vary both LWPC and ISPC at the design level and then, starting from these block-level measures, we estimated trial-by-trial LWPC and ISPC utilizing an ideal Bayesian observer. These estimates were then employed as predictors in our analyses. By doing so, we obtained more fine-grained and realistic measures, thus enhancing the measurement validity of proactive and reactive control. The comparisons between models including block-level vs trial-level predictors indeed revealed that the latter models better explained the data, so trial-level predictors were then used for all our analyses (see Chapter 4, but also Chapter 5).

Both these novelties were implemented, overcoming the limitations of conventional design-level approaches. However, to maximize the efficiency and flexibility of our approach, and to control for confounding factors that are typically addressed at the design level, we introduced another innovation: analysis-level control. For instance, even though LWPC and ISPC were manipulated to be as orthogonal as possible with respect to contingency, our design could not entirely exclude the influence of low-level learning effects. Hence, we employed multilevel modeling approaches and, by including contingency as a predictor in the model, we could control for its effect. The findings that ISPC-related effects, which are very likely to be confounded with contingency, consistently emerged when contingency was removed from the statistical model suggest that the inclusion of contingency in the model is necessary to control for that (see Chapter 4). Another advantage of our statistical approach (see Chapter 3) is that the utilization of multilevel modeling analyses enhanced the precision of our experimental effect estimates, as noted above. By incorporating predictors not only for confounders like contingency but also for low-level variables reflecting trial-by-trial variability into the model, we were thus able to disentangle effects due to trial noise from the true experimental effects. Model comparisons, conducted before the analyses of interest, indeed showed that including all the confounders in the model increased the model fit (see Chapter 4). Furthermore, these statistical models were the only ones that enabled us to leverage our simultaneous manipulation of proactive and reactive control, which was not easily achievable through classical GLM-based approaches (see Chapter 4). Indeed, by employing multilevel modeling, we could concurrently estimate the effects of proactive and reactive control, along with their interaction, in modulating the Stroop effect.

Overall, with our approach and its relative advantages, we were able to achieve our objective of obtaining proactive and reactive control measures that were not only more valid but also more reliable.

8.2.3. MVPA potential and methodological choices

The same novel approach, validated in the behavioral study, was subsequently used in the EEG study. The findings presented in Chapter 5 provided additional empirical evidence for the advantages delineated

in the behavioral study. This evidence was not solely rooted in the behavioral analyses conducted within the EEG study, but extended to the ERP and ERSP analyses as well.

The advantages of our approach transcended behavioral measurements alone, extending to EEG measures because they allowed us to achieve more precise estimations of the dynamics of proactive and reactive control at the neural level. Particularly noteworthy was our capability to examine the neural correlates of each mechanism even when the other was concurrently activated, in addition to unveiling the neural underpinnings of their potential interplay. Moreover, the neural evidence we obtained was founded on more precise estimations of the effects. This was possible thanks to the multilevel modeling analyses using trial-by-trial predictors for proactive and reactive control, which take full advantage of EEG high temporal resolution.

One aspect that our approach alone could not achieve was the unveiling of proactive and reactive control representations. As extensively emphasized throughout the entire thesis, representations are fundamental for comprehending cognitive control and therefore deserve the same level of attention dedicated to the study of processes. This consequently leads us to another novel aspect of the present project: the analysis of our electrophysiological data using multivariate analytical approaches, in addition to univariate ones, with the aim of exploring not only processes but also representations. The results of the univariate analyses further underscored the necessity of incorporating multivariate approaches: The ER(S)P results suggested that solely exploring proactive and reactive control processes was insufficient, and that investigating the representations underlying these processes was also imperative to achieve a more comprehensive understanding of proactive and reactive control.

The fundamental significance assumed by the multivariate analyses employed in the current project to delineate the neural correlates of proactive and reactive control more precisely is particularly evident from the results. This aspect will be elucidated in the forthcoming section, where we will provide a comprehensive overview of our findings and endeavor to establish connections between univariate and multivariate results. Within this current paragraph, we briefly discuss the most relevant methodological advantages of the multivariate approaches we used.

A first general strength lies in our utilization of MVPA on EEG data which, due to the superior temporal resolution of EEG compared to fMRI, has the potential to more effectively capture the intrinsic dynamic nature of representations (Badre et al., 2021; Cellier et al., 2022). This aspect held particular importance in light of our aim to explore proactive and reactive control, whose representations are likely to be extremely dynamic. Additionally, considering that one of the main assumptions of the DMC is their temporal distinctiveness, investigating whether proactive and reactive control representations rely on temporally distinct neural encoding patterns using high temporal resolution seems to be advantageous.

The second strength lies in the fact that our MVPA was not limited to decoding, which does not enable the exploration of the entire representational space due to its insensitivity to rich representational spaces (Diedrichsen & Kriegeskorte, 2017; Kriegeskorte & Diedrichsen, 2019; Kriegeskorte & Kievit, 2013). To overcome this notable limitation of decoding models, we chose to primarily use Representational Similarity Analysis (RSA). This approach offers the advantage of testing complex predictions and thereby characterizing the representational space in a more fine-grained manner, encompassing all represented features and their interrelationships (Diedrichsen & Kriegeskorte, 2017). By using RSA, we also maximally leveraged our trial-level multilevel modeling approach. Indeed, RSA is extremely flexible as the models to be tested are specified through Representational Dissimilarity Matrices (RDMs). Therefore, by utilizing dissimilarity measures based on comparisons between (distributions of) probabilities, we maximized the probabilistic nature of our trial-level variables. Lastly, the specific RSA approach we employed to compute brain RMDs played a substantial role in characterizing the representational space in a complex manner. Unlike more traditional time-resolved and space-resolved approaches, our utilization of a searchlight approach concurrently incorporating portions of spatial, temporal, and spectral EEG information, enabled us to fully harness the intricate nature of the EEG signal. Given that our ERSP results provided additional relevant information beyond ERPs, we recognized the importance of incorporating spectral information in our MVPA analyses as well. Overall, this searchlight approach enabled us to obtain more comprehensive multidimensional, multivariate pictures of how proactive and reactive control were encoded at the neural level. Simultaneously, it increased the interpretability of our outcomes, as we were not entirely blind to any specific piece of information by utilizing only a part of each information at a time.

The third strength of our MVPA analyses is that, even though we believe that RSA offers significant advantages over decoding, we chose not to exclude decoding, as we recognized its potential in providing a more comprehensive picture. In fact, by employing decoding following RSA, we intentionally aimed to explore a fundamental assumption concerning the functional role of representations. It has been proposed that the functional role of cognitive control representations is to encode the required information (i.e., goal-related information) at the neural level so that downstream neurons enacting neural processes can utilize such information to execute goal-relevant actions (Cellier et al., 2022; D'Esposito, 2007; Diedrichsen & Kriegeskorte, 2017; Kriegeskorte & Diedrichsen, 2019; Schumacher & Hazeltine, 2016). Thus, one way to explore this assumption is to investigate whether such encoded information is truly available for use, and decoding can serve such a purpose. The successful decoding could indeed indicate the availability of such information. Moreover, by employing both approaches, we were able to intersect their results. The overlaps that revealed similar neural activation patterns allowed us to suggest that, if both approaches consistently identified the same neural activation pattern, the evidence in favor of it was stronger.

One final point warrants a brief discussion, that is, the decoding technique we employed. Indeed, by using ridge-based decoding, we overcame the limitations of more conventional decoding techniques, namely classification-based ones. Although classification-based methods are widely used (Cole et al., 2016; Freund et al., 2021; Woolgar et al., 2011), they can only address binary questions and thus remain closely tied to univariate approaches, limiting the full potential offered by multivariate analyses (Freund et al., 2021). Therefore, ridge-based decoding allowed us to avoid constraining the decoding of representations to binary questions, as classification-based methods do. Indeed, the latter are overly simplistic, whereas ridge-based decoding enabled us to decode our trial-level variables in a more fine-grained manner, capturing neural activity patterns with greater precision and ultimately enhancing comparability with our RSA results (Bode et al., 2021; Cohen et al., 2011; Popal et al., 2019).

Before concluding the discussion on the advantages of our MVPA approach, we must make a specification. As mentioned earlier, our study was designed to accommodate both univariate and multivariate analyses. Therefore, it represents just an initial attempt to lay the groundwork for future studies. If future studies are purposefully designed to exclusively employ multivariate approaches, they will be able to provide further support for (and potentially refine) the preliminary conclusions drawn here.

8.3. The road so far: Key Findings for Proactive and Reactive Control

Based on our overarching goal of studying cognitive control in the context of the DMC framework, which posits the existence of two distinct control modes – proactive and reactive – we initiated our investigation with a behavioral study. Exploring the neural underpinnings of proactive and reactive control would have been premature without first identifying the behavioral signatures that reflect the effects of these control modes on performance. Neural dynamics gain indeed meaning only when observable in behavior. Despite the numerous behavioral studies that have examined the effects of proactive and reactive control, as opposed to the relatively fewer neuroimaging and electrophysiological studies, so far, there is still no clear behavioral evidence supporting the separability of proactive and reactive control. This primarily stems from the prevalent use of design-level control approaches and, consequently, robust empirical support for the existence of two distinct mechanisms, while also controlling for the potential influence of low-level confounders, is still lacking.

As of today, the primary evidence supporting the separability of proactive and reactive control stems from a study conducted by Gonthier and colleagues (2016), who examined proactive and reactive control separately in the same participants, manipulating each mechanism at a time. This, however, resulted only in providing partial evidence due to the inherent limitations of single-mechanism manipulations in ensuring measurement validity, as outlined above (see Section 8.2.2). Therefore, by leveraging the advantages of our

innovative approach to rigorously examine the behavioral effects of these control modes, we aimed to provide a more solid empirical basis for the proactive and reactive control distinct existence at the behavioral level.

While our behavioral findings provided compelling evidence for only one of the control mechanisms, namely proactive control, their contribution is significant due to the complex and intriguing pattern they revealed. Further complexity has also been suggested by our EEG findings which, in line with the behavioral results, have more clearly highlighted the existence of specific correlates for proactive control only but have also provided valuable insights into reactive control mechanism(s). Indeed, thanks to the use of a multimethod EEG approach, involving both univariate and multivariate analyses, the emerging picture is far from simple, indicating initial evidence that what is postulated by the DMC may be true, but in reality, things may not be so straightforward.

In what follows, we aim to summarize our key findings by linking behavioral and EEG results to provide a comprehensive overview of proactive and reactive control. This will first be done separately for each control mode and then, in the final section, we will compare them to draw conclusions.

8.3.1. Behavioral and Neural correlates of interference

The Stroop effect has been the critical measure that we have consistently employed throughout the entire project. It reflects the cost in performance due the Stroop interference that was experienced, and thus, the behavioral Stroop effect is the outcome of the cognitive processes that have been implemented to execute the task. As such, we have used it as the key measure to assess the effect of the investigated control mechanisms, as the proactive and reactive control mechanism engagement could be observed only as their effects on Stroop effect magnitude. Therefore, before delving into our comprehensive discussion on our proactive and reactive control results, we first have to discuss the findings on the Stroop effect. Based on these premises, at the behavioral level it was a fundamental prerequisite to observe a Stroop effect that was large, robust to analytical flexibility, and reliable, and this was the case. Whether we consider the Peripheral or the Perifoveal paradigms in the behavioral study, as well as the behavioral results derived from the EEG study using the Perifoveal spatial Stroop task, a common thread emerged. In all these cases, we consistently observed a Stroop effect characterized by very large effect sizes and high values of reliability. Moreover, such results were consistent and robust, regardless of the employed analytical approach, with the Stroop effect showing a 100% of dominance, meaning that it was observed in the expected direction in all our participants. Finding a consistent Stroop effect signature provided a solid foundation for our aim, since observing a substantial Stroop effect served as a crucial backdrop against which we could examine the effect of proactive and reactive control.

However, response times are only the final output of the cognitive processes required to perform the Stroop task, and thus the behavioral investigation of the Stroop effect does not allow making inferences on how the interference-related processes operate and unfold over time. The EEG is thus vital to solve this issue and unveil the temporal dynamics and real-time evolution of the neural activity reflecting these cognitive processes that are finally translated into the behavioral Stroop effect. In turn, assessing interference-related neural processes was essential as it provided a foundational context for then examining how proactive and reactive control mechanisms modulated them. Therefore, by first establishing the neural underpinnings of Stroop interference, we were better equipped to investigate whether and how proactive and reactive control modes influence and interact with these neural processes.

In our investigation of interference-related processes using univariate analyses, we identified a consistent pattern that unfolded in three main steps across both ERPs and ERSPs. This pattern likely represents the temporal sequence of neural processes involved in detecting and handling interference.

In the initial stage, interference affected visuo-spatial perceptual and attentional processes. This was evident from the bilateral posterior N170 and frontal P2 ERP components, which play key roles in processing the target stimuli. These components are particularly enhanced when the target consists of two compatible features, as seen in the case of Congruent stimuli, in line with prior research (Soltész et al., 2011; Szűcs & Soltész, 2010; Zurrón et al., 2013). Therefore, during this early stage, when interference was present due to the incompatibility of stimulus features, the amplitude of these components was reduced, likely reflecting the initial phase of interference processing. The P2 functional role was further supported by its correlation with behavioral performance. Specifically, the attenuation of the P2 component led to worse performance (longer RTs), further indicating a more challenging target processing during Incongruent trials. We proposed that both of these ERP components were modulated by Theta frequency activity over bilateral frontal and right parietal scalp regions, aligning with prior research that has established a relation between Theta frequency and the N170 component (Freunberger et al., 2011). Moreover, there is evidence supporting a similar functional role of Theta in visuo-spatial attentional processing and performance enhancement (Klimesch, 1999), specifically by enhancing target processing (Slagter et al., 2009; van Vugt, 2014).

Following the initial early visuo-attentional phase, there was a subsequent involvement of conflict-related processes, signaling the necessity for recruiting control mechanisms. While we did not clearly observe an increase in fronto-central negativity (N2 component) for Incongruent stimuli, as is typically reported in the literature (Folstein & Van Petten, 2008; Larson et al., 2014), this absence might be attributed to the stronger effect of the P2 component. However, brain-behavior correlations unveiled that a greater negativity of a frontal component modulated performance with longer RTs, indicative of heightened conflict-related processing demands. This interpretation was further substantiated by our ERSP

results, which revealed the presence of classical mid-frontal Theta activity characterized by a greater power increase during conflict trials (e.g., Cavanagh & Frank, 2014; Hanslmayr et al., 2008).

Conflict-related processing entered a third stage, revealing a complex pattern of interference resolution. In this phase, conflict was first reflected by a notable attenuation in the amplitude of the centro-parietal P3-like component and the lateral frontal negativity (LFN). This pattern aligns with findings from studies such as Vurdah et al., (2023), West & Alain (2000), and Zurrón et al., (2013) for the former, and Lansbergen & Kenemans (2008), and West & Alain (2000) for the latter. Both of these components exhibited a peculiar pattern: in the absence of conflict, no amplitude attenuation was observed; however, such attenuation became evident when conflict was experienced. Our findings are also supported by the positive correlation between the amplitude of these components and task performance. Moreover, since their neural generators were located across a broad cluster of medial parietal and frontal regions, including the ACC, these components may reflect conflict processing. From about 480 ms the voltage pattern of these components reversed, showing two later LP components over similar scalp regions (in line with Appelbaum et al., 2014; Lansbergen & Kenemans, 2008), whose cortical sources were found in the dorsal ACC and dorso-medial PFC.

Overall, these results suggest that this third stage involves interference resolution which unfolds in a complex manner, with the earlier components serving the functional role of conflict processing and the later ones conflict resolution, in line with Lansbergen and Kenemans' (2008) findings. Moreover, such dynamics were characterized by distinct latencies, as shown by our RIDE analysis, revealing that during Incongruent trials the engagement of these components was delayed by conflict processing (e.g., Lansbergen & Kenemans, 2008). These components were probably modulated by the power suppression observed for Alpha and Beta frequencies in a similar time window, suggesting the functional role of these frequencies in conflict processing. Specifically, the suppression of Beta2 and Beta3 frequencies was probably implied in the selection of task-relevant information (Tafuro et al., 2019), while Alpha suppression is likely reflective of the necessary activation of the relevant task set and response to overcome interference (Nurislamova et al., 2019) and may also reflect the goal-directed suppression of irrelevant spatial information (Cohen & Ridderinkhof, 2013).

Response-locked analyses offered a deeper understanding of response conflict occurring at this stage, revealing two successive ERPs within a similar time window as the P3-like component. During conflict trials, we observed an early increase in frontal negativity (PRN) coupled with an enhanced parietal positivity. This was followed by a voltage pattern inversion, with all these components also influencing behavioral performance. The functional role of these components relates to response competition, which occurs when alternative conflicting responses are pre-activated. These response-locked components thus likely reflect response selection and inhibition of irrelevant responses, aligning with findings from prior studies (e.g.,

Burle et al., 2016; Carbonnell et al., 2013; Chen et al., 2011; Vidal et al., 2003). Our ERSP results also provided evidence regarding the involvement of Theta and Alpha/Beta frequencies during this response-related stage. These findings complemented our understanding of the functional role of the identified ERPs in response conflict. Specifically, Theta activity may be implied in the selection of the relevant task set (Capizzi et al., 2020; Cooper et al., 2015; Sauseng et al., 2010), and this probably occurs by prioritizing the stimulus information through Alpha/Beta frequencies involvement (Nurislamova et al., 2019). These neural processes likely represent the response-related counterparts of the stimulus-locked Alpha/Beta activity.

Although the pattern revealed by univariate analyses is inherently complex, a deeper understanding was attained through multivariate analysis findings. These findings not only elucidated the intricacies of conflict processes but also provided evidence for the representations that underlie them. Although no previous literature provided us with a firm foundation for interpretations, we attempted to establish connections between univariate and multivariate findings and offer tentative explanations.

Specifically, we postulated that the visuo-spatial attentional processes observed in the initial stage of interference resolution (N170 and P2), which were more pronounced during Congruent trials (indicating an absence of conflict), might have played a role in creating a representation of the absence of Conflict. This representation could thus be subsequently encoded by a left-lateralized Beta2 neural activity pattern. Then, the absence of Conflict representation could have influenced the LFN and P3-related processes, contributing to the observed greater amplitude during Congruent trials. Conversely, when this representation, specific to the absence of Conflict, remained inactive due to the presence of Conflict, it led to an amplitude attenuation in the P3/LFN components.

The situation was different at the response level, where a very early PRN component signaling conflict may have contributed to form a representation for the presence of Conflict, which was encoded at the response level by Beta2 activity over left motor regions. Then, this Conflict representation could have been used to modulate later conflict resolution processes, potentially influencing response selection processes, as indicated by the similar spectral involvement of the Beta2 frequency found in response-locked ERSP analyses. Therefore, the delayed identification of Conflict representation in our multivariate analyses might be attributed to the necessity of conflict to be initially detected by processes mainly relying on response competition.

8.3.2. Behavioral and Neural correlates of proactive control

One of the key findings of the present thesis is that both behavioral and EEG analyses converged on indicating the existence of a proactive control mechanism modulating the Stroop effect, revealing also its neural dynamics.

Briefly, proactive control is postulated to modulate interference in an anticipatory manner, and thus the main prediction was that when proactive control level is high, the interference, by being anticipated, can be reduced. This pattern should thus be observed both at the behavioral level, with reduced Stroop effects, and at the neural level, with a modulation of the conflict-related correlates. Of note, at the neural level this premise holds for the univariate analyses only, and from a representational perspective, we expected to find, early in time, a representation of LWPC that, by encoding the global likelihood of conflict, would serve as the basis for implementing proactive control processes.

The behavioral signatures we obtained for proactive control are robust and compelling, as the behavioral results for both the behavioral and the EEG studies showed the hypothesized proactive modulation of the Stroop effect, with smaller Stroop effects when the LWPC was lower, thus when proactive control was higher. This effect was not only robust across all our analyses (both LMM and RCA) and highly reliable, but it also exhibited consistently medium to large effect sizes (greater than .5). Furthermore, this proactive control effect was observed in the vast majority of our participants, with a dominance value of nearly 87%.

Our novel approach, involving the simultaneous manipulation of LWPC and ISPC and the analysis-level control strategy, allows us to confidently assert that the observed proactive control effect was estimated net of the effect of reactive control (as well as of contingency). This revealed that proactive control operated independently from the concurrent activation of reactive control (and/or contingency). Therefore, this finding provides robust and compelling evidence for the existence of a proactive control mechanism, substantiating that it can operate by itself. Moreover, thanks to our approach, we were able to reveal the dominance of proactive control as the stronger control mode. This conclusion is not only supported by the lack of strong evidence for a standalone reactive control mechanism but also by our interpretation of the three-way interaction results based on our a-priori hypothesis testing. Indeed, the model that best fitted our data predicted the dominance of proactive over reactive control. Additionally, our results revealed an antagonistic interplay between proactive and reactive control. This sheds light on the role of proactive control, demonstrating that it serves as a moderator for the effect of reactive control, thereby further emphasizing its dominance.

As for interference, the assessment of proactive control at the behavioral level provides valuable insights into the modulation of RTs (in terms of Stroop effect reduction). However, this behavioral measure only captures the final output of proactive control processes. To gain a deeper understanding of these processes, investigating their neural correlates and temporal dynamics, using the EEG was again crucial. This is particularly relevant because the DMC posits specific assumptions about the temporal characteristics of proactive control.

Our investigation of proactive control-related processes through univariate analyses revealed that proactive control primarily influenced the conflict-related ER(S)Ps discussed earlier, suggesting that proactive control played a direct role in modulating conflict detection and resolution. However, it is worth noting that this modulation did not involve cognitive processes preceding conflict detection, which may seem contrary to expectations and DMC postulates, since proactive control is assumed to act by imposing an attentional bias to relevant stimuli/processes even before conflict occurrence. However, we will provide a plausible (but speculative) explanation for this observation shortly.

Proactive control initially modulated the P3-like and LFN components over similar but more lateralized scalp regions compared to those identified for interference and, subsequently, it also modulated the LP components identified earlier. These findings align with previous research (Appelbaum et al., 2014; West & Bailey, 2012). Therefore, they suggest that these modulations influenced both the earlier conflict detection and the later interference resolution components. Specifically, when proactive control was high, participants were better prepared to experience conflict, resulting in a reduced need for these processes. This may be because they anticipated interference and, as a result, did not need to resolve it when encountered. Hence, in conditions of high proactive control, there was no significant attenuation in P3/LFN amplitude followed by an increase of LP amplitude when participants encountered conflict trials. Conversely, the greater amplitude attenuation followed by the greater increase in amplitude that we observed during unexpected conflict trials, that is, when Incongruent trials were encountered during low proactive control conditions, suggests that participants needed to make a late correction to manage unexpected conflict. This has to be done using a form of reactive mechanism, which implies engaging in a just-in-time manner in greater conflict processing, both in terms of conflict detection and interference resolution.

Furthermore, we posited that this late conflict processing, necessary when proactive control was low, was modulated in a manner akin to the conflict-related processes discussed earlier. Specifically, this modulation involved Alpha and Beta power reduction, serving the functional role of signaling the need for a greater amount of control, necessary as conflict arose unexpectedly. In contrast, when proactive control was high, such power reductions were unnecessary because participants could anticipate and pre-engage the required control level. These spectral modulations likely influenced mainly the earlier ERP components, given their similar pattern, with more substantial evidence pointing to the role of Alpha suppression in the generation of the P3 component (Bernat et al., 2007).

If we were to base our conclusions solely on the results discussed so far, we would claim that, at the neural level, the effect of proactive control is strong and evident. However, the processes underlying this effect are counterintuitive. This is because the effects of proactive control that we found on ER(S)Ps predominantly reflected the differences in neural processes when proactive control was absent/low, that

is, enhanced conflict processing required when unexpected conflict was encountered. In other words, the ER(S)P Stroop effects were only observed when LWPC was high, with more pronounced ER(S)P for Incongruent than Congruent trials. We interpreted these findings as the correlate of the enhanced conflict processing required when unexpected conflict was encountered. This, in turn, triggered a late form of "just in time" reactive control, which, as we will discuss below, is inherently distinct from the ISPC-induced reactive control. Therefore, in a sense, our ER(P)S results seem to shed light on the neural dynamics of when proactive control was not engaged, leading us to assume that, since such no ER(S)P Stroop effect reflecting conflict processing was observed when proactive control was high, something must have occurred earlier to prevent it from being necessary. However, this is only an indirect assumption that is not supported by evidence regarding what these early mechanisms might be. A further crucial point is the fact that the ER(S)P correlates of proactive control we found are related to conflict processing, in contrast to the assumptions of the DMC. Indeed, according to DMC, proactive control is a tonic mechanism with neural correlates that should be evident even before conflict processing, possibly modulating perceptual processes to reflect the effect of the attentional bias. Despite expecting to find some early processes related to proactive control, our ER(S)P results overall support one of the fundamental assumptions of this thesis: that investigating univariate correlates allows us to identify only the processes, but a crucial role in understanding the neural dynamics of cognitive control is played by representations, which can only be investigated using multivariate techniques. Representations are particularly important for the proactive control mode because we can assume that, to implement proactive processes of interference anticipation, our brain must rely on a representation that encodes, in a distributed and complex manner, the global likelihood of conflict. Therefore, relying on such a representation that specifies when conflict is highly predictable is probably the best explanation for why, during conditions of conflict but with high proactive control, the late reactive conflict-related processes, as we have seen from our univariate analyses, were not found to be engaged. This interpretation, to be supported, needs to verify whether LWPC is encoded in the brain, and that is exactly what we did, providing positive evidence for it and for how it was modulated.

As done previously, in discussing the results of the representations, we will try to link them to the univariate findings to provide more comprehensive interpretations, which, however, are speculative and require future studies.

The identification of the LWPC representation, evident early in time both at the stimulus and response levels, aligned seamlessly with the assumptions of the DMC regarding the proactive control temporal dynamics and also underscored the pronounced cognitive nature of this representation. Furthermore, the consistent finding that it was encoded through a left centro-parietal activation pattern, involving Theta frequency, as revealed by both RSA and ridge regression analyses, enhanced the robustness of this result. Previous studies showing the functional role of Theta frequency in the encoding and formation of complex

memory representations (e.g., Lisman, 2010; Sans-Dublanc et al., 2017; Backus et al., 2016) are aligned with our result, suggesting that LWPC can be considered a sort of complex memory representation containing the global likelihood of Conflict, that has formed based on previous trial congruency. Therefore, if the brain encodes the global likelihood of conflict, we may assume that this representation subsequently informs downstream cognitive processes. Although this marks an initial stride towards elucidating the neural multivariate correlates of proactive control, it does not provide a complete account of the proactive control underlying neural dynamics at work. The fact that we have identified an LWPC representation, without ascertaining the presence of an early process (and, if present, its corresponding ER(S)P correlates) that utilized this representation to anticipate interference, represents a limitation of the current study. As such, it necessitates further investigation in future research endeavors.

Our multivariate investigations have also provided deeper insights into how the LWPC representation was dynamically utilized in response to the presence or absence of Conflict. Our findings overall indicate that the LWPC representation was encoded early in time, but its use, or strength, was shaped by the contextual presence or absence of Conflict.

Regarding the Conflict absence, the preliminary formation of the CON_C representation might have been a prerequisite. As elucidated earlier, this representation likely emerged subsequent to visuo-spatial attentional processes relying on the N170 and P2 components. The absence of Conflict representation might have then influenced the LWPC representation by directly modulating its encoding pattern, considering their spatial and temporal overlap. This modulation was further reflected in the involvement of the Beta2 frequency, characterizing the CON_C representation, as well as the Theta frequency characterizing the standalone LWPC representation. This integrative perspective is likely to reflect the potential mechanism by which the strength of the LWPC representation was adjusted to be subsequently used.

Similarly, distinct stages were also assumed to modulate the LWPC representation in response to the presence of Conflict. First, the representation of Conflict was encoded, initiated by processes signaling Conflict via the early PRN component (see above). Then, the representation of Conflict appears to have modulated the LWPC representation quite directly, as suggested by the spatial and spectral overlap observed in the interaction pattern, suggesting a direct influence of the Conflict representation on the LWPC representation.

To conclude this section, we provide an alternative explanation for the absence of specific proactive control-related processes. We suggest that it could be that proactive control per se operates not through a specific process but rather has effects on processes directly involved in successful task execution. It is plausible that the LWPC representation is not used by a process itself, but rather, after being modulated by

the presence/absence of Conflict, the information it encodes is used to modulate the strength of the Target and Distractor representations. It could then be the strength of these representations, in turn, that would produce the predicted behavioral effects. For instance, when the LWPC representation is enhanced by the presence of Conflict, as described earlier, it could lead to an enhanced Target representation (and/or a weakening of the Distractor representation). Subsequently, given that a strong Target representation is crucial for task success, it is possible that interference is experienced to a lesser extent when the Target representation is strong, and thus it is anticipated. Consequently, there may be no need for late reactive mechanisms to resolve interference. This scenario would perfectly reflect a high level of engagement of proactive control.

Interpreting proactive control from this purely representational perspective suggests that it may not require a distinct process per se to be implemented. This may explain why the interaction we found between LWPC and interference in our univariate analyses actually reflected only the absence of proactive control. Furthermore, it suggests that proactive control may exist at the level of processes, but it relies more on the specific processes directly involved in target prioritization (and/or distractor inhibition), which thus should be explored. Our multivariate results regarding the interaction between LWPC and Target/Distractor provided support for this explanation.

The interaction between LWPC and Target, encoded by an Alpha right prefrontal cluster and a Beta1 left lateral cluster early in time, could thus reflect that LWPC modulated the strength of the Target representations so that this could then be used by downstream processes accordingly, based on the level of proactive control (i.e., enhancing the Target strength when proactive control was higher). The involvement of Alpha and Beta frequencies further supports these interpretations, as previous evidence has shown the functional role of these frequencies in the selection of the task-relevant stimulus-specific information and in working memory encoding (Michelmann et al., 2022; Kikumoto & Mayr, 2018; Kikumoto et al., 2022), which are essential to pursue the goal encoded in the Target representation.

Concurrently, the LWPC representation was also implicated in modulating the representation of the Distractor. In this case, it likely weakened the Distractor representation when proactive control was higher. The interaction, encoded by an early right prefrontal cluster involving Beta2, is consistent with previous findings suggesting a functional role of Beta frequency in modulating the processing of dominant information (Engel & Fries, 2010).

Therefore, in summary, it is plausible that proactive control relies on a representation containing information about the global likelihood of conflict. The strength of this representation seems to be modulated by the presence or absence of conflict and, in turn, the proactive control representation may modulate the strength of representations of task goal and distractor. These latter representations are

indeed assumed to contain information about the required level of prioritization of task-relevant information and of inhibition of distractors. Consequently, these pieces of information may then be used to implement the necessary processes, ultimately producing the proactive control effect.

8.3.3. Behavioral and Neural correlates of reactive control

Our investigation of reactive control has not yielded results as clear as those regarding the presence of proactive control. When it comes to reactive control, the picture is considerably more complex. Nevertheless, thanks to our approach, which allowed us to test the three-way interaction and statistically control for the effect of contingency, and through multivariate analyses, the pattern of results we obtained has provided us with valuable insights, which appear to indicate a complex yet intriguing pattern.

Before discussing our findings, however, we must make a preliminary remark. According to the most common description of the DMC, reactive control in the Stroop task represents a late correction mechanism activated just in time, especially when conflict is detected. Investigating such a late reactive correction would require inducing participants to implement reactive mechanisms after conflict detection, as needed. However, this is challenging to manipulate directly. The manipulation typically employed to tax reactive control, which we also used, involves varying the PC at the item level. This variation prompts participants to engage reactive mechanisms based on the conflict likelihood indicated by the item, and not on the conflict actual occurrence. It thus induces stimulus-attention associations (Tafuro et al., 2020; Bugg, 2012, 2017; Bugg & Hutchison, 2013), which are reactive in the sense that they require knowledge of the item to determine the associated likelihood of conflict, subsequently enabling the application of appropriate reactive mechanisms. However, this occurs immediately after viewing the stimulus, and it is not contingent on conflict detection. Therefore, the ISPC manipulation, which provides a more controllable means of inducing reactivity, instigates a reactive control mechanism that differs from the later purely reactive one postulated by the DMC, involving a sort of proactive component (see Figure 1.6).

Based on these considerations, the primary prediction is that when an item triggers a high level of reactive control, interference can be reduced even before encountering the actual conflict. Therefore, although it is a reactive mechanism as it follows the stimulus, interference is, in a sense, (proactively) anticipated (see Figure 1.6). This pattern should manifest both at the behavioral level, with reduced Stroop effects, and at the neural level, with a modulation of conflict-related correlates. The neural modulation theoretically might occur in a manner similar to proactive control but with a longer latency, as prior identification of the stimulus is required to activate stimulus-attention associations. However, as we observed, the nature of proactive control processes was not as early; thus, based on those results alone, it could be anticipated that this assumption might not be supported in our findings of reactive control as well. From a representational perspective, similar to LWPC, we expected to identify an ISPC representation

relatively early in time since it relies on the stimulus. This representation, by encoding the likelihood of conflict associated with each of the four items, would serve as the foundation for implementing reactive control processes that could utilize the informational content associated with each observed stimulus.

The behavioral results for ISPC-induced reactive control are robust and consistent, but in a negative sense: all our behavioral analyses, both from the behavioral study and the EEG study, demonstrated no significant modulation of the Stroop effect by reactive control. However, this is not the sole result we observed, and indeed, discussing the other effects is even more interesting.

The first crucial point is that this result was obtained net of the effect of contingency. Therefore, controlling for contingency by including it in the model allowed us to disentangle its effect from that of ISPC. This was further confirmed by the fact that, when we removed contingency from the model, it indeed emerged that reactive control was modulating the Stroop effect. Hence, we could confidently assert that when assessed independently, reactive control did not operate separately from the concurrent activation of contingency (and/or proactive control). In fact, reactive control effects can be predominantly explained by contingency. However, our results do not exclude the possibility of an ISPC-induced reactive mechanism either, which leads to the second crucial point. This was only made possible by testing the three-way interaction between proactive, reactive, and Stroop effect, the significant effect of which suggested the existence of a reactive mechanism that, albeit indirectly, modulated the Stroop effect. Indeed, reactive control interacted with proactive control in modulating the Stroop effect, even when the contingency effect was statistically controlled for. The effect of this interaction, however, was not robust as it did not emerge in all our behavioral analyses. Indeed, it was observed in the behavioral study using the Perifoveal paradigm and in the aggregated sample, but not in the behavioral study using the Peripheral paradigm and in the EEG study using the Perifoveal paradigm. Despite these inconsistencies, the possible reasons for which are discussed in Chapter 4, our results provide initial evidence for the fact that a strategic control implementation can also operate reactively but is contingent on the level of proactive control. Specifically, the fact that the effect of ISPC-induced reactive control emerged only when the level of proactive control was low indicated that the implementation of reactive control was not the preferred control mode for participants, who resorted to it only when the proactive control mechanism was not available.

Our univariate EEG results were consistent with the observation that we did not find a substantial behavioral effect of ISPC-induced reactive control, as they did not reveal a significant influence of ISPC-induced reactive control on the univariate correlates. As the behavioral study, our EEG study also employed an analysis-level control approach to account for the effect of contingency, and as observed in the behavioral study, when contingency was included in the model, it better explained the data. Consequently, our univariate results revealed the correlates for contingency but not those for ISPC-induced reactive control. However, the univariate analyses did not either reveal the three-way interaction that emerged in

the behavioral study. This discrepancy may be due to the less robust nature of this effect, as discussed earlier, and the possibility that the EEG study was underpowered to detect it. Therefore, based on these results, we cannot draw insights that explain the interaction between proactive and reactive control found in the behavioral study, nor can we confidently assert the existence of a mechanism, albeit not dominant, of ISPC-induced reactive control, as we did not find the ER(S)P correlates for it.

Nevertheless, our results seem to support the existence of a different form of reactive control, late in nature, which more closely resembles the "late correction" reactive control model postulated by the DMC, that is, the mechanism engaged to resolve conflict when other forms of conflict failed (or were not activated). As mentioned earlier, if we examine the results of the proactive control modulation of the ER(S)P from another perspective, namely when proactive control was low, they indeed seem to indicate a late reactive mechanism. In fact, when participants were not proactively prepared, they had to make a late correction to handle unexpected conflict trials, as highlighted by the greater P3/LFN amplitude attenuation followed by the later LP amplitude increase, modulated by the Alpha and Beta power reduction. In addition to the correlates found when proactive control was low, we also identified some response-locked interference-related ER(S)Ps that were not modulated by proactive control and may reflect a late form of reactive control as well, which seems to be inherently linked to response-locked conflict processing. Indeed, we hypothesized that such late reactive mechanism, for which we did not have a specific manipulation, was first reflected in the early mid-frontal pre-response negativity (PRN), which has been shown to signal conflict at the level of response when alternative conflicting responses are pre-activated (Burle et al., 2016; Carbonnell et al., 2013; Vidal et al., 2003). Theta and Alpha frequency power increase and Beta2 power suppression, which probably mediated such negativity increase, instead likely reveal that such response-locked conflict was managed by processes subserving the integration and prioritization of task-relevant information (Capizzi, et al., 2020; Cooper et al., 2015). Moreover, we assumed that the subsequent attenuated polar and bilateral frontal negativity, reflecting the final stages of response conflict resolution (Chen et al., 2011), might also reflect the final stages of the late reactive control mechanism. Therefore, these results suggest that conflict at the response level may play a significant role in late reactive control.

Overall, such findings, by showing the processes occurring when proactive control was low and when there was high response conflict, plausibly reflect the ER(S)P correlates of a late form of reactive control, which works by signaling the need for a greater amount of control at the response level to resolve unexpected interference. Moreover, these results, and especially those related to the absence of proactive control, are in line with the assumption of the DMC, according to which when proactive control is low, control is engaged reactively (Braver et al., 2009, 2021; De Pisapia & Braver, 2006).

The results discussed so far seem to support the existence of a late reactive control mechanism, engaged upon conflict detection, rather than an ISPC-induced reactive mechanism relying on the conflict likelihood. However, these two forms of reactive control do not necessarily exclude each other. Indeed, it could be that both forms of reactive control exist, and the relatively weaker effect of ISPC-induced reactive control at the behavioral level might have made it less detectable in neural processes. This probably occurred also because stimulus-response associations (i.e., contingency learning), on which participants more likely rely, might have overshadowed the ISPC-induced reactive control effect. However, this does not necessarily exclude the possibility that the brain encodes ISPC, thus having an ISPC-induced reactive control representation, as our results indeed indicate. Of note, it might seem pointless to represent ISPC if it is not subsequently used to implement ISPC-induced reactive control processes. However, as we discussed for proactive control, it is more likely that representations of PC do not serve to implement specific control processes but instead serve to modulate the representations of the Target and/or Distractor. The information contained in the PC representations could indeed be used to implement target prioritization and/or distractor inhibition processes. This likely holds true for ISPC-induced reactive control as well. In line with that, we observed that ISPC representation was indeed encoded at the neural level. This encoding, involving a Beta2 left fronto-centro-parietal cluster, was response-locked and quite early before response. The discovery of this early pre-response encoding, not contingent on conflict detection, further reinforced the notion that ISPC induces a form of reactive control that relies on stimulus-attention associations, influenced by the likelihood of conflict rather than the actual occurrence of conflict. Moreover, our results suggest that by encoding the information about the conflict likelihood of the specific items prominently through Beta2 frequency, such representation probably served the encoding of task-relevant information to guide downstream action selection (Buschman et al., 2012; Sherfey et al., 2020; see also Cannon et al., 2014). This consequently implies that the brain likely utilizes this information in some way.

However, as said above, the encoded ISPC-related information may not be primarily utilized by downstream processes of reactive control, in line with our univariate results. Instead, it might be employed to directly modify the strength of the encoding of Target and Distractor representations. Insights into this assumption were provided by the results concerning the interactions between ISPC and Target/Distractor, which likely indicate how ISPC-induced reactive control operated at the representational level. These interactions were indeed encoded at the neural level: the Target representation was modulated at the response level only in a left posterior cluster from -300 ms involving Beta1 frequency; the Distractor representation was modulated at both the stimulus and response levels, involving a Beta2/3 right centro-parietal cluster and Beta3 fronto-posterior clusters, respectively. Our MVPA results thus may suggest that ISPC informational content was used to reactively (i.e., upon seeing the stimulus and retrieving its ISPC) modulate the Target encoding, whose representational strength could have then guided task-relevant information prioritization accordingly, by means of task-relevant stimulus-specific information selection

and working memory-related processes, as suggested by Beta1 frequency involvement (Michelmann et al., 2022; Kikumoto & Mayr, 2018; Kikumoto et al., 2022). Moreover, ISPC reactively modulated the Distractor encoding, which, when reactive control was higher, might have reduced the strength of the distracting feature/task, first at the perceptual level and then at the response level. The encoding of this interaction through Beta2/3 frequencies suggests that this might have occurred by modulating the processing of the dominant information (Engel & Fries, 2010).

Overall, our reactive control findings suggest a complex scenario: MVPA results indicate that a strategic implementation of reactive control based on ISPC is plausible, but this seems to operate only at the representational level. Furthermore, it appears to coexist with a more purely reactive mechanism occurring after encountering conflict, which is likely to be more evident at the process level. However, we cannot exclude that even the late form of reactive control could operate at the representational level, but further studies are needed to support this idea. This could be investigated, for example, by testing the representation of conflict at the response level since the late reactive mechanism is more predominant at this level. Furthermore, to support the existence of both reactive mechanisms, future studies should manipulate both of them to gain further insights into their distinctions or commonalities.

8.3.4. Conclusions: What can we say about proactive and reactive control?

Drawing firm conclusions about proactive and reactive control from our results is not a straightforward task, but we can certainly assert that the pattern we have uncovered is extremely intricate. Our objective of investigating whether the control modes postulated by the Dual-Mechanisms of Control (DMC) model exhibit specific behavioral and EEG signatures has been partially achieved, as we provided initial evidence for that. Nonetheless, it is even clearer that overly simplistic characterizations are not possible. At the outset of our investigation, we were aware of the inherent complexity of the subject matter, so we endeavored to address as much as possible the issues highlighted by prior literature. Ultimately, however, we have unveiled a reality that is even more complex than initially expected.

Our behavioral results indicated that proactive control exerted a distinct and stronger influence on participants' performance by modulating the magnitude of the Stroop effect. On the other hand, the reactive control induced by ISPC did not exhibit by itself a direct impact on the Stroop effect. Interestingly, participants' performance was better explained by the contingency manipulation rather than by the ISPC one, implying that participants relied more on learning associations between stimuli and responses, rather than (estimating and) using the item-specific PC information to control their behavior. Nonetheless, our analysis revealed an additional layer of complexity, which was possible only thanks to the inclusion of the three-way interaction between LWPC, ISPC and the Stroop effect. We found that ISPC-induced reactive control did indeed modulate the Stroop effect, but this modulation depended upon the level of proactive

control, suggesting that ISPC-induced reactive control can modulate the Stroop effect only when proactive control is low. This revealed that the strategic deployment of control mechanisms can operate in a reactive manner as well, but still proactive control is the prevailing control mechanism influencing the behavioral performance.

This behavioral exploration allowed us to ensure that any neural findings we subsequently uncovered could be properly contextualized within the framework of behaviorally observed control mechanisms. In sum, our EEG analyses employing multiple approaches have demonstrated that proactive control engaged both process-level and representational mechanisms, whereas reactive control predominantly hinged on representations. Delving into further detail, proactive control exhibited a direct influence on conflict detection and resolution through the modulation of conflict-related ER(S)Ps. While this revealed specific univariate correlates related to proactive control, implying its engagement at the level of processes, it primarily reflected neural dynamics associated with the absence of proactive control rather than a specific proactive process operating earlier to anticipate interference. Conversely, we did not find any impact of reactive control on ER(S)P correlates. Nevertheless, our univariate analyses seem to point to the existence of a late reactive mechanism, likely triggered when both LWPC-induced and ISPC-induced reactive control modes were absent and/or ineffective. This mechanism appeared to exert a more prominent effect at the response level. Consequently, this form of reactive control might predominantly reflect the detection and resolution of response conflict.

Relying solely on these univariate results, we can thus conclude that they partially align with the assumptions posited by the DMC as we found two distinct control modes characterized by specific ER(S)P correlates. The former corresponds to a proactive control mode induced by LWPC, for which however we did not find a specific correlate for the process underlying interference anticipation; rather, we did identify specific correlates for when interference anticipation failed (i.e., as in the case of high LWPC). Evidence for proactive control ER(S)Ps, based solely on when it was engaged to a lower extent, thus offers incomplete support for the mechanism postulated by the DMC, as its neural dynamics can only be indirectly inferred. The same holds true for the second mechanism, the reactive one, for which we also found indirect evidence. Indeed, it did not correspond to the one we manipulated, namely the ISPC-induced reactive control, but rather it represented a late mechanism resulting from the absence of proactive control when interference occurred unexpectedly and when there was high response conflict. Therefore, this leads to two considerations. First, the reactive control postulated by the DMC at the level of processes appears to be more related to response conflict and, in line with DMC assumptions, this is the mechanism engaged when proactive control is not activated (Braver et al., 2009, 2021; De Pisapia & Braver, 2006). The second consideration is that, even though ISPC is the manipulation predominantly used in the literature to measure

reactive control in light of the DMC, it may not be entirely suitable for this purpose, as it does not fully capture the late correction characteristic of the reactive control postulated by the DMC.

The multivariate results have enriched these findings, albeit with further increase in complexity. They have indeed shown that proactive and reactive control strongly relied on representations, suggesting that they probably operate at the representational level. Not only have we found that the brain encoded both LWPC and ISPC and that the strength of this encoding was modulated by the presence/absence of Conflict, but also that such informational content was used to modulate the strength of Target and Distractor representations. This latter finding thus provides a plausible way of how LWPC-induced proactive and ISPC-induced reactive mechanisms might operate. The effects of these manipulations, besides being better captured by analyses considering neural patterns that are multivariate and distributed, are in line with what is postulated for proactive control by the DMC, given the early nature of the LWPC representation, and plausibly explain what we were did not identify with univariate analyses, namely the early mechanisms of interference anticipation. Regarding ISPC-induced reactive control, it cannot be entirely in line with the DMC since, as explained earlier, the most commonly postulated reactive mechanism is more akin to a late correction. However, discovering that ISPC is represented suggests that reactive control can also rely on a strategic allocation of attention, which allows for interference anticipation, albeit in a reactive manner, namely after seeing the stimulus.

It is noteworthy that the modulation of the Target and Distractor representations occurred in a similar manner by both LWPC and ISPC representations. Specifically, LWPC and ISPC representations involved Beta1 frequency for the modulation of the Target, whereas Beta2/3 frequencies were involved in the modulation of the Distractor. However, this modulation occurred at distinct levels: proactive control influenced the Target at the stimulus level and at an earlier stage, compared to reactive control, which influenced it at the response level and at a later stage, as it would be expected. The Distractor, on the other hand, was influenced at the stimulus level and earlier by LWPC, while it was influenced at both the stimulus and response levels and at a later stage by ISPC. In addition to revealing that both proactive and reactive control modes are likely to operate at the representational level, this pattern of similarities and differences suggests that LWPC- and ISPC-induced control modes are qualitatively similar in certain aspects but distinct in terms of timing and level of action.

Therefore, what we can infer from our overall results is that proactive and reactive control are not merely two fingerprints of the same mechanism. In contrast, cognitive control likely operates through multiple mechanisms. These include the LWPC-induced and ISPC-induced mechanisms, which are qualitatively similar in that they both involve a strategic deployment of control which, in both cases, allows for the anticipation of interference, albeit through different means and timings. These two control modes would primarily (and exclusively for what concerns ISPC-induced reactive control) operate at the level of

representations. In other words, the informational content encoded by the LWPC and ISPC representations is not used to implement specific proactive and reactive processes, but rather to modulate the representation of the goal and the distractor, according to the current level of proactive and reactive control. This informational content, in turn, is used to modulate the processes that enable the execution of goal-directed behavior. Conversely, when such strategic control modes are not sufficiently engaged or cannot be implemented, a third form of control must come into play to resolve interference at the last moment.

Overall, yes, our results seem to suggest that cognitive control operates via two distinct control modes, proactive and reactive. However, it is interesting to note that they appear to suggest a scenario composed of three mechanisms, rather than two, with the most robust evidence, based on our data, supporting the existence of a proactive mechanism. However, since our goal is to understand how cognitive control works rather than proposing further fragmentation, aware that it would increase inconsistencies even more, we limit ourselves to suggesting that, in light of our results, further studies are urgently needed, especially to clarify the differences observed between the two reactive control mechanisms.

8.4. Where we are going: Future developments

The complexity of the object of study has been further heightened by our utilization of a (methodologically valid) Stroop task. Indeed, the paradigm we employed was designed to induce a Stroop effect encompassing task, stimulus, and response effects (Parris et al., 2022; see also Chapter 2). While this was pivotal in ensuring measurement validity, there is a flip side: the effect we obtained, upon which we measured the proactive and reactive control effects, constitutes a global composite outcome of effects operating at multiple levels. However, if the Stroop effect is indeed composed of multiple loci, proactive and reactive control mechanisms are very likely to distinctly influence each of the implied layers. Therefore, just as it is true that focusing only on RTs provides only the output of cognitive processes but leaves us blind to the unfolding neural dynamics, to gain a better understanding of how proactive and reactive control operate, it is necessary to assess whether they act differently at different loci, and if so, how. However, apart from some earlier attempts (Augustinova et al., 2018; 2019), there are not many studies that have quantitatively decomposed the Stroop effect, to assess whether multiple loci are actually implied and, if so, to estimate the contribution of each locus at the empirical level.

Driven by the goals of assessing whether the Stroop effect resulting from methodologically valid paradigms is actually composed of distinct/independent loci and, if it is true, of estimating their weights, we conducted the study outlined in Chapter 7. This study served a dual function of better understanding the Stroop effect itself and how it is affected by proactive and reactive control. It included two experiments

(the first of which served as a pilot for the second one), beginning anew from the behavioral measures necessary to establish a solid foundation. This study not only allowed us to estimate the contribution of the assumed loci, confirming their existence, but also to take into account other aspects such as distinguishing between facilitation and interference effects, which was not considered in our previous studies, and addressing crucial factors in interference tasks, such as the role of automaticity of the two tasks involved and the asymmetry between them.

In brief, in the study outlined in Chapter 7, we designed distinct interference tasks, all implying interference at the task locus. These tasks were different as they also implied effects at distinct loci, according to the Kornblum's taxonomy: the stimulus locus only (for this we had two Stroop-like tasks), the response locus only (for this we had one Simon task), and the stimulus and response loci (for this we had two spatial Stroop tasks, one of which was very akin to the perifoveal spatial Stroop task employed in all our studies). As stated above, for each task, we also included neutral conditions to calculate not only the global effect (called Congruency effect, which corresponds to the global Stroop effect in the Stroop task), but also its constituents, namely the interference effect (IE) and the facilitation effect (FE). This thus allowed us not only to explore the existence of each locus, but also to better assess the involvement of each locus in generating the facilitation and interference effects, separately. It is indeed possible that, although the Stroop effect is assumed to involve all the three loci, its constituent effects imply just one (or a different mixture) of them.

The first key finding of our study was that all our interference tasks yielded both facilitation and interference effects, confirming all our a priori hypotheses, with one exception that is discussed more in detail in Chapter 7 and not relevant to the present discussion. Moreover, by testing the set of hypotheses regarding the composite measure including both FE and IE, namely the Congruency Effect (CE), we provided evidence that the perifoveal spatial Stroop task employed in this thesis was the most suitable interference paradigm, as it yielded the largest CE, characterized by a 100% dominance, and with the highest reliability (which further supports the results presented in Chapter 3). These results did not provide a direct answer to our question, but they still represented the necessary condition that had to be satisfied before proceeding testing our core hypotheses, namely those related to the loci. Moreover, they suggest that the measure of task interference that we used, which to the best of our knowledge was novel as compared to previously employed ones, was valid, thus effectively measuring the pure effect of interference at the task level. This was significant, because it allows filling a gap in the literature, considering that, as highlighted by Parris et al. (2023), there is still no clear and effective measure of task interference.

The second set of results, on the other hand, delves deeper into our aim of exploring whether the Stroop task implies more than one processing locus, and specifically whether it involves both stimulus and response loci (the task locus for this set of hypothesis was taken for granted as we directly compared all our

interference tasks which thus, by assumption, should involve task interference, as also shown by the results discussed above). Specifically, we tested directional hypotheses assuming that the CE in the Stroop task (and also the IE and FE), which should imply both the stimulus and response loci, should be bigger than the CE (and IE and FE) in the other conflict tasks. Results were generally in line with this prediction for the perifoveal spatial Stroop task requiring to respond to the direction, thus the one employed in this thesis (see Chapter 7 for a better explanation for why the perifoveal spatial Stroop requiring to respond to the position yielded the opposite pattern of results, in contrast with our predictions). Specifically, this spatial Stroop task produced a CE (but also IE and FE) always bigger than the ones produced by the tasks assumed to imply just one locus (stimulus or response locus), namely the Stroop-like tasks and the Simon task. This result suggests that when the task taps only one locus, the resulting effect is smaller than when two loci are involved, thus supporting the multiple-loci nature of the Stroop task. However, we found a relevant exception to this: the FE produced by the Stroop task was equal to that produced by the Simon task, suggesting (although indirectly) that the FE of our spatial Stroop task actually primarily implied facilitation at the response level or, in other words, the FE of our spatial Stroop task was mostly composed of response facilitation. Overall, this suggests that it is the interference component of the CE of the Stroop task that implies multiple loci, while the facilitation component is probably entirely originating from the response locus.

The last set of results that we will discuss here added further complexity to the overall picture. Specifically, we tested other hypotheses regarding the overall pattern of performance when task interference was also considered. Moreover, in these analyses, we also took into account the level of automaticity of the relevant task, as better explained in Chapter 7. Our findings were not only in line with our expectations of a multiple loci nature of the Stroop task, but they also provided additional insights into the relationship between the distinct loci. Indeed, we found that Stroop performance depended on the performance at the baseline task, which reflects the cost of identification and, more importantly, on the effects at the stimulus, response and task loci, which interacted with each other. Therefore, adding to the results we have just discussed, this study indicates that the interference effect originates from the interplay of all loci, whereas the facilitation effect probably originates from the response locus only. Therefore, the fact that, in our spatial Stroop task, the IE and the FE seem to comprise a different number of loci, as we initially hypothesized but with no more specific a priori predictions, is extremely relevant as it further supports the importance of using tasks involving a neutral condition to distinguish between IE and FE. Indeed, distinguishing between these two components of the CE is not an end in itself, but is fundamental to better account for their distinct nature which, in turn, could be differently affected by mechanisms such as the control modes we investigated in this thesis. As discussed previously, the absence of a neutral condition represented a limitation of the present thesis, but thanks to this final study, we validated a potential solution to overcome this limitation. Overall, these findings add a further layer of complexity,

which however can be leveraged in future explorations of proactive and reactive control by our group and others.

The natural progression of this study is thus to investigate whether proactive and reactive control indeed affect the Stroop loci differently. Building upon the contribution of each locus to the Stroop performance provided by the study in Chapter 7, we will be in a position to empirically test some a priori hypotheses regarding the distinct impact of each control mode on the three loci. These hypotheses are grounded not only in the postulated nature of the two mechanisms, but also in our empirical findings. For example, our EEG results consistently showed that the effect of proactive control was mainly exerted at the stimulus level, probably suggesting its direct impact on the stimulus locus, but we can also hypothesize that proactive control should affect the task locus, given its anticipatory nature (as also suggested by the early LWPC encoding we found). Conversely, regarding reactive control, both the ISPC-induced and (especially) the late reactive mechanisms are more likely to affect the response locus, given their strong response-locked nature emerged from our results. Moreover, understanding the specific effect on each locus could be useful in disentangling these two forms of reactive control. Specifically, ISPC-induced reactive control can also be assumed to affect the stimulus locus because it relies on stimulus-attention associations, although we did not find evidence for that.

Moreover, capitalizing on the results of this behavioral study, we will design studies that allow overcoming a significant limitation of the majority of the studies included in the current thesis. As noted above, this regards the fact that we measured the effect of proactive and reactive control on the Stroop effect intended as Congruency effect, thus including in unknown amounts IE and FE. While this approach has provided valuable insights into the overall picture, it has left us unaware of the specific contributions of the multiple underlying constituents of the overall Stroop effect. Therefore, the behavioral study reported in Chapter 7 provided a solid foundation that has allowed us to validate a paradigm identical to the one used previously, but now incorporating a neutral condition. This enhancement ensures that, in future studies, we will be capable of evaluating the distinct influence of proactive and reactive control on both the interference and facilitation effects. In our previous studies, assessing the overall Stroop effect could only determine, for instance, whether there was a reduction in the Stroop effect under low-PC conditions. However, this reduction derives from both shorter RTs to incongruent stimuli and longer RTs to congruent stimuli (but in variable and unknown amounts). Therefore, by incorporating separate measures for interference and facilitation effects, we will be able to ascertain whether low PC conditions result in a reduction in both the interference and facilitation effects.

Additionally, separately measuring interference and facilitation is particularly relevant in light of our results that have shown a substantial difference in terms of the involved loci between the overall Stroop effect and its components. Being aware that the Stroop facilitation seems to involve mainly the response

locus, while the Stroop interference also implies the stimulus and task loci, is particularly relevant for testing the hypotheses outlined earlier in a more fine-grained manner. As such, discerning the specific loci implicated in interference and facilitation facilitates a more targeted investigation, for which we propose the following predictions. Given that we previously predicted that proactive control should affect more the stimulus locus, and that the stimulus locus is implied only in the interference effect, in future studies we will specifically test the impact of proactive control on the interference effect, thus focusing on the contrast between incongruent and neutral stimuli. Conversely, to explore how proactive control affects the task locus, we will compare its effect on neutral trials of the Stroop task with trials in a simple discrimination task, in which no task interference should occur, thus isolating the measure of task interference we validated. For what concerns ISPC-induced reactive control, its effect on the stimulus locus can be explored as explained for proactive control, thus on the interference effect. By contrast, whether it affects the response locus could be explored using both the facilitation and interference effects, as the response locus seems to be involved in both. In turn, finding that ISPC-induced reactive control truly affects both the stimulus and response loci will offer the possibility of disentangling it from the late reactive control. Indeed, based on the logic that the effect is bigger when it involves more loci, given that the late reactive control can theoretically imply only the response locus, its effect should be in principle smaller than the effect of ISPC-induced reactive control, if this latter implies both stimulus and response loci, thus potentially distinguishing the two reactive mechanisms.

In our forthcoming studies, we will begin with a behavioral study aimed at elucidating the behavioral signatures of proactive and reactive control in consideration of the locus weights determined in Chapter 7. Subsequently, we will conduct an EEG study employing the same logic, with the specific goal of elucidating how each control mode influences each Stroop locus and the specific underlying unfolding. This investigation will also provide an opportunity to establish connections with influential models like the Cascade of Control Model (Banich, 2009). By uncovering the precise neural correlates that underlie the impact of control modes on each locus, we can evaluate whether our findings align with the postulations of this model, which is based on the Stroop task in general. This alignment may potentially facilitate the extension of that model principles to the neural dynamics of proactive and reactive control. In pursuing this objective, we will not solely rely on univariate analyses but will also incorporate multivariate analyses, given the potential they have demonstrated in the present thesis.

8.5. Other directions to explore: Open questions

The present thesis work has provided additional insights into the behavioral signatures and neural dynamics of proactive and reactive control. However, as emphasized earlier, this endeavor has revealed that the landscape is even more complex than initially expected. Therefore, while we have addressed some

crucial research questions, such as identifying the existence of ISPC-induced reactive control and its reliance on representations, we have also unveiled numerous further research questions that demand exploration.

One of these open questions has been delineated in the previous section, in which we explained how we have laid the groundwork for the first step, along with our planned approach to address it in the future. Besides this one, there are other open questions that we have not yet had the opportunity to begin addressing, but their relevance has become clear throughout the entire thesis. Below, we present the primary ones.

8.5.1. The dynamic duo of reactive control

The first of these open questions has already been mentioned in the discussion of our results and concerns the fact that our findings suggest the existence of two reactive control modes. In our discussion, we attempted to offer a plausible explanation for the existence of both a strategic ISPC-induced reactive control and a late form of reactive mechanism. However, it is important to note that our interpretation was necessarily tentative because we manipulated only one of these two reactive control mechanisms. Therefore, the evidence for the late reactive mechanism was indirect, as it emerged as the mechanism that remained after accounting for the two we manipulated. To directly test whether two reactive control modes exist, it would be necessary to manipulate both of them simultaneously. This is based on the same logic that we have employed in this thesis: if we want to directly ascertain whether two mechanisms are distinct entities, we need to manipulate both of them at the same time to understand if one exists even when the other is engaged. This goal could be achieved, for instance, by manipulating the ISPC to induce a strategic reactive control mode and manipulating the response conflict to isolate the remaining reactive control when the strategic reactive control has been accounted for. Our proposal to use response conflict as a proxy for the late form of reactive control is grounded in two key reasons, as detailed below.

First, the findings from this thesis indicate that the late form reactive control, which emerged when the effects of the two manipulated controls were accounted for, exhibited a predominantly post-conflict, response-locked nature. This is supported by our finding that the early response-locked PRN component played a significant role in signaling the presence of conflict between competing responses, implying that conflict detection primarily occurred at the response level. Furthermore, our MVPA results align with this interpretation, demonstrating that the representation of conflict required time to be encoded, likely relying on conflict signals from the PRN component. Thus, it became stably encoded only at the response level, probably because it was a consequence of response competition. Of note, this does not imply that conflict resolution affects only the response. As we emphasized earlier, considering the involvement of Beta2 frequency in its encoding, conflict may contribute to conflict resolution through both response selection

processes and stimulus prioritization. However, this implies that the conflict at the response level plays a key role, leading us to suggest that the most effective way to manipulate it is by varying the frequency of response-level conflict.

The second reason relies instead on the findings of a previous unpublished behavioral study not reported here, that we conducted to specifically manipulate response conflict, before fully developing the idea of the dual nature of reactive control that we are proposing here. We did so by parametrically varying the probability of the four possible responses, so as to have some responses that were pre-activated more strongly than others in incongruent trials. The idea is that it is harder to overcome the conflict between an erroneous but strongly pre-activated response and the correct but weekly pre-activated response, as compared to the opposite situation. This study indeed revealed that this was the case, suggesting that the measure of response conflict we proposed can be used to manipulate the level of control needed to resolve the Stroop interference at the response locus.

To better understand the existence and potential relationship between the two reactive mechanisms, it would be preferable to manipulate them while keeping the level of proactive control stable, in order to obtain a specific result for reactive control only. However, to verify if we can indeed talk about three control mechanisms, a subsequent study would be necessary to determine if, by manipulating all of them together, they still remain separate entities.

8.5.2. The phantom anticipator: what happens before the stimulus onset?

The second pressing open question pertains to the neural dynamics occurring within the pre-stimulus time window. We intentionally did not mention the negative findings we found for the pre-stimulus time-window previously in this concluding discussion, as we believe it deserves separate consideration. The absence of univariate and multivariate correlates in the pre-stimulus phase represents one of the major limitations of the results reported in this thesis, which therefore needs to be investigated more thoroughly in future research.

All our EEG analyses, both multivariate and univariate ones, were performed also in the pre-stimulus time window because, given the strategic nature of the control mechanisms triggered by PC manipulations, it was plausible to assume (and we hypothesized) that such probabilities were computed, maintained, and updated prior to the stimulus presentation. Naturally, within the statistical model utilized for the pre-stimulus analyses, predictors for low-level confounders and Congruency (or Conflict for RSA) were excluded. This exclusion was justified by their dependency on the subsequently presented stimulus, rendering them meaningless before stimulus onset.

Besides the probabilistic nature of PC manipulations, it was conceivable to identify some neural dynamics before stimulus onset, given the characteristics of the control modes induced by such manipulations. This is particularly evident for proactive control which, by definition, is an anticipatory and sustained control mechanism, suggesting its tonic activation even before stimulus presentation. Concerning ISPC-induced reactive control, the situation is less clear, especially when considering the definition provided by the DMC. As mentioned earlier, the predominant DMC definition aligns better with the late reactive mechanism rather than that induced by ISPC. This is why we previously suggested that the ISPC manipulation might not be the most suitable for probing reactive control, if it is intended as a late correction mechanism. However, despite this controversy, since ISPC-induced reactive control relies on stimulus-attention associations, it is likely that the EEG multivariate correlates of the encoding of these associations should be detectable even before stimulus onset. Indeed, if so, these associations can then be activated and selected when the stimulus is revealed. Consequently, although it may appear counterintuitive for ISPC, both PC manipulations were included in the pre-stimulus model.

As for the univariate analyses, in the pre-stimulus time window, we predominantly found the electrophysiological correlates, both ERPs and ERSPs, related to probabilities of the lower-level effects, namely those considered confounding factors for PC manipulations. Among these, the contingency effect emerged as the most prominent, suggesting that such stimulus-response associations are strong enough to be identifiable even in the pre-stimulus phase. This finding aligns with, for example, the interpretation we provided regarding the absence of ISPC-induced reactive control, in which we hypothesized that it was overshadowed by the stronger and more consistent effect of contingency. The correlates of these confounding factors have intentionally not been discussed, as this goes beyond the scope of this thesis. However, what is certain is that future studies are necessary to delve deeper into them, especially at the neural level, given their prominent role found here. Moreover, the ERSPs results revealed a significant effect of LWPC in the early pre-stimulus time window which, however, exhibited a pattern that was not so clear and strong. Thus, we preferred to cautiously avoid making inferences on this pattern. Nevertheless, despite the difficult interpretability of this result, it might suggest that indeed some neural dynamics might occur in such a time window, providing further motivation for investigating it more thoroughly in the future.

The fact that the univariate results did not show specific PC correlates in the pre-stimulus period actually was not such an unexpected finding, as it could be anticipated that, in this time window, there were no actual processes occurring but rather representations being encoded. For this reason, with the multivariate analyses, we expected to find such representations, but this was not the case. Indeed, just as the univariate results, our multivariate results showed that low-level confounders were quite consistently encoded, but the PC was not. This finding surprised us and is challenging to interpret.

The more plausible tentative explanation, based on the data we currently have, is that, for both LWPC and ISPC, actively sustaining an anticipatory representation throughout the entire pre-stimulus period is too demanding, and for this reason, their encoding probably could not be detected. Therefore, from a functional point of view, it might be more convenient to maintain these representations at a sub-threshold level and reactivate them as soon as the stimulus appears. This aligns with the fact that both LWPC and ISPC encodings, in the post-stimulus period, were quite early, suggesting that it is unreasonable to assume that these representations were created from scratch just after the stimulus.

To test this assumption, in future studies, we will try to stress the encoding of PC in the pre-stimulus phase, inducing participants to keep these representations more active and, therefore, with a stronger encoding pattern. One way to do this, for example, is to vary the inter-trial-interval (ITI). In the present thesis, we always used a fixed and relatively long ITI (1500 ms), which might have led participants to try timing themselves with the stimulus appearance without requiring to keep the PC representations strongly active for so long. Therefore, by becoming accustomed to this, they might have implicitly reduced the strength of encoding of PC representations since they were sure they would not need them within that 1500 ms. Conversely, if participants do not know when the stimulus will appear, they might keep these representations more strongly encoded so that they can use them at any moment when the stimulus appears. An alternative manner would be maintaining long and variable ITIs but clearly signaling stimulus onset (e.g., with a 500-ms pre-stimulus screen) to induce participants activating PC representations just-in-time for when they are needed.

8.6. Conclusions

As we conclude this phase of our research journey, it is evident that cognitive control is not a singular, unitary entity but a complex mechanism that can operate through multiple modes. What emerges also clearly is that it can operate through processes, but when control is modulated by contextual requests (i.e., PC-induced cognitive control), its implementation strongly relies on informational patterns that are encoded in the brain as representations. These representations would contain the information regarding the conflict likelihood that can then be used by control processes, but they could also serve to modulate the representations involved in goal-directed behaviors, whose encoded information might then be used by lower-level processes.

Our work has made initial but significant strides in advancing the understanding of cognitive control. By elucidating the qualitative differences in control mechanisms within the DMC framework and employing a range of innovative methodologies, we have provided interesting evidence that represents another small

step toward the comprehension of this intricate cognitive phenomenon. Moreover, looking forward, our research opens the door to numerous exciting avenues for further exploration.

8.7. References

Appelbaum, L. G., Boehler, C. N., Davis, L. A., Won, R. J., & Woldorff, M. G. (2014). The dynamics of proactive and reactive cognitive control processes in the human brain. Journal of cognitive neuroscience, 26(5).

Augustinova, M., Parris, B., & Ferrand, L. (2019). The Loci of Stroop Interference and Facilitation Effects With Manual and Vocal Responses. Frontiers in Psychology, 10, 1786. https://doi.org/10.3389/fpsyg.2019.01786

Augustinova, M., Silvert, L., Spatola, N., & Ferrand, L. (2018). Further investigation of distinct components of Stroop interference and of their reduction by short response-stimulus intervals. Acta Psychologica, 189, 54–62. https://doi.org/10.1016/j.actpsy.2017.03.009

Backus, A. R., Schoffelen, J.-M., Szebényi, S., Hanslmayr, S., & Doeller, C. F. (2016). Hippocampal-Prefrontal Theta Oscillations Support Memory Integration. Current Biology, 26(4), 450–457. https://doi.org/10.1016/j.cub.2015.12.048

Badre, D., Bhandari, A., Keglovits, H., & Kikumoto, A. (2021). The dimensionality of neural representations for control. Current Opinion in Behavioral Sciences, 38, 20–28. https://doi.org/10.1016/j.cobeha.2020.07.002

Banich, M. T. (2009). Executive function: The search for an integrated account. Current directions in psychological science, 18(2).

Bernat, E. M., Malone, S. M., Williams, W. J., Patrick, C. J., & Iacono, W. G. (2007). Decomposing delta, theta, and alpha time–frequency ERP activity from a visual oddball task using PCA. International Journal of Psychophysiology, 64(1), 62–74. https://doi.org/10.1016/j.ijpsycho.2006.07.015

Bode, S., Feuerriegel, D., Schubert, E., & Hogendoorn, H. (2021). Decoding continuous variables from EEG data using linear support vector regression (SVR) analysis with the Decision Decoding Toolbox (DDTBOX) (p. 2021.05.31.446502). bioRxiv. https://doi.org/10.1101/2021.05.31.446502

Botvinick, M. M., Braver, T. S., Barch, D. M., Carter, C. S., & Cohen, J. D. (2001). Conflict monitoring and cognitive control. Psychological review, 108(3).

Braem, S., Bugg, J. M., Schmidt, J. R., Crump, M. J., Weissman, D. H., Notebaert, W., & Egner, T. (2019). Measuring adaptive control in conflict tasks. Trends in cognitive sciences.

Braver, T. S. (2012). The variable nature of cognitive control: A dual mechanisms framework. Trends in cognitive sciences, 16(2).

Braver, T. S., Gray, J. R., & Burgess, G. C. (2007). Explaining the many varieties of working memory variation: Dual mechanisms of cognitive control. In Variation in working memory (pp. 76–106). Oxford University Press.

Braver, T. S., Kizhner, A., Tang, R., Freund, M. C., & Etzel, J. A. (2021). The Dual Mechanisms of Cognitive Control Project. Journal of Cognitive Neuroscience, 33(9), 1990–2015. https://doi.org/10.1162/jocn_a_01768

Braver, T. S., Paxton, J. L., Locke, H. S., & Barch, D. M. (2009). Flexible neural mechanisms of cognitive control within human prefrontal cortex. Proceedings of the National Academy of Sciences, 106(18).

Bugg, J. M. (2012). Dissociating Levels of Cognitive Control: The Case of Stroop Interference. Current Directions in Psychological Science, 21(5), 302–309. https://doi.org/10.1177/0963721412453586

Bugg, J. M. (2017). Context, conflict, and control. The Wiley handbook of cognitive control, 79–96.

Bugg, J. M., & Hutchison, K. A. (2013). Converging evidence for control of color–word Stroop interference at the item level. Journal of Experimental Psychology: Human Perception and Performance, 39(2).

Burle, B., van den Wildenberg, W. P. M., Spieser, L., & Ridderinkhof, K. R. (2016). Preventing (impulsive) errors: Electrophysiological evidence for online inhibitory control over incorrect responses. Psychophysiology, 53(7), 1008–1019. https://doi.org/10.1111/psyp.12647

Buschman, T. J., Denovellis, E. L., Diogo, C., Bullock, D., & Miller, E. K. (2012). Synchronous Oscillatory Neural Ensembles for Rules in the Prefrontal Cortex. Neuron, 76(4), 838–846. https://doi.org/10.1016/j.neuron.2012.09.029

Capizzi, M., Ambrosini, E., Arbula, S., & Vallesi, A. (2020). Brain oscillatory activity associated with switch and mixing costs during reactive control. Psychophysiology, 57(11), e13642. https://doi.org/10.1111/psyp.13642

Carbonnell, L., Ramdani, C., Meckler, C., Burle, B., Hasbroucq, T., & Vidal, F. (2013). The N-40: An electrophysiological marker of response selection. Biological Psychology, 93(1), 231–236. https://doi.org/10.1016/j.biopsycho.2013.02.011

Cavanagh, J. F., & Frank, M. J. (2014). Frontal theta as a mechanism for cognitive control. Trends in cognitive sciences, 18(8).

Cellier, D., Petersen, I. T., & Hwang, K. (2022). Dynamics of Hierarchical Task Representations. The Journal of Neuroscience: The Official Journal of the Society for Neuroscience, 42(38), 7276–7284. https://doi.org/10.1523/JNEUROSCI.0233-22.2022

Chen, A., Bailey, K., Tiernan, B. N., & West, R. (2011). Neural correlates of stimulus and response interference in a 2-1 mapping stroop task. International Journal of Psychophysiology: Official Journal of the International Organization of Psychophysiology, 80(2), 129–138. https://doi.org/10.1016/j.ijpsycho.2011.02.012

Chiew, K. S., & Braver, T. S. (2017). Context processing and cognitive control: From gating models to dual mechanisms. In The Wiley handbook of cognitive control (pp. 143–166). Wiley Blackwell. https://doi.org/10.1002/9781118920497.ch9

Cohen, J., Asarnow, R., Sabb, F., Bilder, R., Bookheimer, S., Knowlton, B., & Poldrack, R. (2011). Decoding Continuous Variables from Neuroimaging Data: Basic and Clinical Applications. Frontiers in Neuroscience, 5. https://www.frontiersin.org/articles/10.3389/fnins.2011.00075

Cohen, J. D. (2017). Cognitive control: Core constructs and current considerations. In The Wiley handbook of cognitive control (pp. 3–28). Wiley Blackwell. https://doi.org/10.1002/9781118920497.ch1

Cohen, J. D., Dunbar, K., & McClelland, J. L. (1990). On the control of automatic processes: A parallel distributed processing account of the Stroop effect. Psychological Review, 97(3), Articolo 3. https://doi.org/10.1037/0033-295x.97.3.332

Cohen, M. X., & Ridderinkhof, K. R. (2013). EEG source reconstruction reveals frontal-parietal dynamics of spatial conflict processing. PloS One, 8(2), e57293. https://doi.org/10.1371/journal.pone.0057293

Cole, M. W., Ito, T., & Braver, T. S. (2016). The Behavioral Relevance of Task Information in Human Prefrontal Cortex. Cerebral Cortex (New York, NY), 26(6), 2497–2505. https://doi.org/10.1093/cercor/bhv072

Cooper, P. S., Wong, A. S., Fulham, W. R., Thienel, R., Mansfield, E., Michie, P. T., & Karayanidis, F. (2015). Theta frontoparietal connectivity associated with proactive and reactive cognitive control processes. Neuroimage, 108, 354–363.

Dang, J., King, K. M., & Inzlicht, M. (2020). Why Are Self-Report and Behavioral Measures Weakly Correlated? Trends in Cognitive Sciences, 24(4). https://doi.org/10.1016/j.tics.2020.01.007

De Pisapia, N., & Braver, T. S. (2006). A model of dual control mechanisms through anterior cingulate and prefrontal cortex interactions. Neurocomputing, 69(10–12).

D'Esposito, M. (2007). From cognitive to neural models of working memory. Philosophical Transactions of the Royal Society of London. Series B, Biological Sciences, 362(1481), 761–772. https://doi.org/10.1098/rstb.2007.2086

Diamond, A. (2013). Executive functions. Annual review of psychology, 64, 135–168.

Diedrichsen, J., & Kriegeskorte, N. (2017). Representational models: A common framework for understanding encoding, pattern-component, and representational-similarity analysis. PLoS Computational Biology, 13(4), e1005508. https://doi.org/10.1371/journal.pcbi.1005508

Elliott, M. L., Knodt, A. R., Ireland, D., Morris, M. L., Poulton, R., Ramrakha, S., Sison, M. L., Moffitt, T. E., Caspi, A., & Hariri, A. R. (2020). What Is the Test-Retest Reliability of Common Task-Functional MRI Measures? New Empirical Evidence and a Meta-Analysis. Psychological Science, 31(7). https://doi.org/10.1177/0956797620916786

Engel, A. K., & Fries, P. (2010). Beta-band oscillations—Signalling the status quo? Current opinion in neurobiology, 20(2).

Flake, J. K., & Fried, E. I. (2020). Measurement Schmeasurement: Questionable Measurement Practices and How to Avoid Them. Advances in Methods and Practices in Psychological Science, 3(4), 456–465. https://doi.org/10.1177/2515245920952393

Folstein, J. R., & Van Petten, C. (2008). Influence of cognitive control and mismatch on the N2 component of the ERP: A review. Psychophysiology, 45(1), 152–170. https://doi.org/10.1111/j.1469-8986.2007.00602.x

Freunberger, R., Werkle-Bergner, M., Griesmayr, B., Lindenberger, U., & Klimesch, W. (2011). Brain oscillatory correlates of working memory constraints. Brain Research, 1375, 93–102. https://doi.org/10.1016/j.brainres.2010.12.048

Freund, M. C., Etzel, J. A., & Braver, T. S. (2021). Neural Coding of Cognitive Control: The Representational Similarity Analysis Approach. Trends in Cognitive Sciences, 25(7), 622–638. https://doi.org/10.1016/j.tics.2021.03.011

Gonthier, C., Braver, T. S., & Bugg, J. M. (2016). Dissociating proactive and reactive control in the Stroop task. Memory & Cognition, 44(5).

Hanslmayr, S., Pastötter, B., Bäuml, K.-H., Gruber, S., Wimber, M., & Klimesch, W. (2008). The electrophysiological dynamics of interference during the Stroop task. Journal of Cognitive Neuroscience, 20(2).

Hedge, C., Powell, G., & Sumner, P. (2018). The reliability paradox: Why robust cognitive tasks do not produce reliable individual differences. Behavior Research Methods, 50(3). https://doi.org/10.3758/s13428-017-0935-1

Kikumoto, A., & Mayr, U. (2018). Decoding hierarchical control of sequential behavior in oscillatory EEG activity. eLife, 7, e38550. https://doi.org/10.7554/eLife.38550

Kikumoto, A., Mayr, U., & Badre, D. (2022). The role of conjunctive representations in prioritizing and selecting planned actions. eLife, 11, e80153. https://doi.org/10.7554/eLife.80153

Klimesch, W. (1999). EEG alpha and theta oscillations reflect cognitive and memory performance: A review and analysis. Brain Research. Brain Research Reviews, 29(2), Articolo 2. https://doi.org/10.1016/s0165-0173(98)00056-3

Kriegeskorte, N., & Diedrichsen, J. (2019). Peeling the Onion of Brain Representations. Annual Review of Neuroscience, 42(1), 407–432. https://doi.org/10.1146/annurev-neuro-080317-061906

Kriegeskorte, N., & Kievit, R. A. (2013). Representational geometry: Integrating cognition, computation, and the brain. Trends in Cognitive Sciences, 17(8), 401–412. https://doi.org/10.1016/j.tics.2013.06.007

Lansbergen, M. M., & Kenemans, J. L. (2008). Stroop interference and the timing of selective response activation. Clinical Neurophysiology: Official Journal of the International Federation of Clinical Neurophysiology, 119(10), 2247–2254. https://doi.org/10.1016/j.clinph.2008.07.218

Larson, M. J., Clayson, P. E., & Clawson, A. (2014). Making sense of all the conflict: A theoretical review and critique of conflict-related ERPs. International Journal of Psychophysiology, 93(3), 283–297. https://doi.org/10.1016/j.ijpsycho.2014.06.007

Lisman, J. (2010). Working Memory: The Importance of Theta and Gamma Oscillations. Current Biology, 20(11), R490–R492. https://doi.org/10.1016/j.cub.2010.04.011

Miller, E. K., & Cohen, J. D. (2001). An integrative theory of prefrontal cortex function. Annual review of neuroscience, 24(1).

Nurislamova, Y. M., Novikov, N. A., Zhozhikashvili, N. A., & Chernyshev, B. V. (2019). Enhanced Theta-Band Coherence Between Midfrontal and Posterior Parietal Areas Reflects Post-feedback Adjustments in the State of Outcome Uncertainty. Frontiers in Integrative Neuroscience, 13, 14. https://doi.org/10.3389/fnint.2019.00014

Parris, B. A., Hasshim, N., Ferrand, L., & Augustinova, M. (2023). Do Task Sets Compete in the Stroop Task and Other Selective Attention Paradigms? Journal of Cognition, 6(1), 23. https://doi.org/10.5334/joc.272

Parris, B. A., Hasshim, N., Wadsley, M., Augustinova, M., & Ferrand, L. (2022). The loci of Stroop effects: A critical review of methods and evidence for levels of processing contributing to color-word Stroop effects and the implications for the loci of attentional selection. Psychological Research, 86(4), 1029–1053. https://doi.org/10.1007/s00426-021-01554-x

Parsons, S. (2020). Exploring reliability heterogeneity with multiverse analyses: Data processing decisions unpredictably influence measurement reliability. PsyArXiv. https://doi.org/10.31234/osf.io/y6tcz

Popal, H., Wang, Y., & Olson, I. R. (2019). A Guide to Representational Similarity Analysis for Social Neuroscience. Social Cognitive and Affective Neuroscience, 14(11), 1243–1253. https://doi.org/10.1093/scan/nsz099

Puccioni, O., & Vallesi, A. (2012a). Conflict resolution and adaptation in normal aging: The role of verbal intelligence and cognitive reserve. Psychology and Aging, 27(4), Articolo 4. https://doi.org/10.1037/a0029106

Puccioni, O., & Vallesi, A. (2012b). High cognitive reserve is associated with a reduced age-related deficit in spatial conflict resolution. Frontiers in human neuroscience, 6, 327.

Puccioni, O., & Vallesi, A. (2012c). Sequential congruency effects: Disentangling priming and conflict adaptation. Psychological Research, 76(5), Articolo 5. https://doi.org/10.1007/s00426-011-0360-5

Rouder, J., Kumar, A., & Haaf, J. (2019). Why Most Studies of Individual Differences With Inhibition Tasks Are Bound To Fail. https://doi.org/10.31234/osf.io/3cjr5

Rouder, J. N., & Haaf, J. M. (2019). A psychometrics of individual differences in experimental tasks. Psychonomic Bulletin & Review, 26(2). https://doi.org/10.3758/s13423-018-1558-y

Sans-Dublanc, A., Mas-Herrero, E., Marco-Pallarés, J., & Fuentemilla, L. (2017). Distinct Neurophysiological Mechanisms Support the Online Formation of Individual and Across-Episode Memory Representations. Cerebral Cortex, 27(9), 4314–4325. https://doi.org/10.1093/cercor/bhw231

Sauseng, P., Griesmayr, B., Freunberger, R., & Klimesch, W. (2010). Control mechanisms in working memory: A possible function of EEG theta oscillations. Neuroscience & Biobehavioral Reviews, 34(7).

Sherfey, J., Ardid, S., Miller, E. K., Hasselmo, M. E., & Kopell, N. J. (2020). Prefrontal oscillations modulate the propagation of neuronal activity required for working memory. Neurobiology of Learning and Memory, 173, 107228. https://doi.org/10.1016/j.nlm.2020.107228

Schmidt, J. R. (2019). Evidence against conflict monitoring and adaptation: An updated review. Psychonomic bulletin & review, 26(3).

Schmidt, J. R., & Besner, D. (2008). The Stroop effect: Why proportion congruent has nothing to do with congruency and everything to do with contingency. Journal of Experimental Psychology: Learning, Memory, and Cognition, 34(3).

Schumacher, E., & Hazeltine, E. (2016). Hierarchical Task Representation: Task Files and Response Selection. Current Directions in Psychological Science, 25, 449–454. https://doi.org/10.1177/0963721416665085

Slagter, H. A., Lutz, A., Greischar, L. L., Nieuwenhuis, S., & Davidson, R. J. (2009). Theta Phase Synchrony and Conscious Target Perception: Impact of Intensive Mental Training. Journal of Cognitive Neuroscience, 21(8), 1536–1549. https://doi.org/10.1162/jocn.2009.21125

Soltész, F., Goswami, U., White, S., & Szűcs, D. (2011). Executive function effects and numerical development in children: Behavioural and ERP evidence from a numerical Stroop paradigm. Learning and Individual Differences, 21(6), 662–671. https://doi.org/10.1016/j.lindif.2010.10.004

Stroop, J. R. (1935). Studies of interference in serial verbal reactions. Journal of experimental psychology, 18(6).

Szűcs, D., & Soltész, F. (2010). Stimulus and response conflict in the color–word Stroop task: A combined electro-myography and event-related potential study. Brain Research, 1325, 63–76. https://doi.org/10.1016/j.brainres.2010.02.011

Tafuro, A., Ambrosini, E., Puccioni, O., & Vallesi, A. (2019). Brain oscillations in cognitive control: A cross-sectional study with a spatial stroop task. Neuropsychologia, 133, 107190.

Tafuro, A., Vallesi, A., & Ambrosini, E. (2020). Cognitive brakes in interference resolution: A mouse-tracking and EEG co-registration study. Cortex, 133, 188–200. https://doi.org/10.1016/j.cortex.2020.09.024

Torres-Quesada, M., Funes, M. J., & Lupiáñez, J. (2013). Dissociating proportion congruent and conflict adaptation effects in a Simon–Stroop procedure. Acta Psychologica, 142(2), 203–210. https://doi.org/10.1016/j.actpsy.2012.11.015

van Vugt, M. K. (2014). Cognitive architectures as a tool for investigating the role of oscillatory power and coherence in cognition. NeuroImage, 85, 685–693. https://doi.org/10.1016/j.neuroimage.2013.09.076

Vidal, F., Grapperon, J., Bonnet, M., & Hasbroucq, T. (2003). The nature of unilateral motor commands in between-hand choice tasks as revealed by surface Laplacian estimation. Psychophysiology, 40(5), 796–805. https://doi.org/10.1111/1469-8986.00080

Vurdah, N., Vidal, J., & Viarouge, A. (2023). Event-Related Potentials Reveal the Impact of Conflict Strength in a Numerical Stroop Paradigm. Brain Sciences, 13(4), Articolo 4. https://doi.org/10.3390/brainsci13040586

Wennerhold, L., & Friese, M. (2020). Why Self-Report Measures of Self-Control and Inhibition Tasks Do Not Substantially Correlate. Collabra: Psychology, 6(1). https://doi.org/10.1525/collabra.276

West, R., & Alain, C. (2000). Effects of task context and fluctuations of attention on neural activity supporting performance of the stroop task. Brain Research, 873(1), 102–111. https://doi.org/10.1016/s0006-8993(00)02530-0

West, R., & Bailey, K. (2012). ERP correlates of dual mechanisms of control in the counting Stroop task. Psychophysiology, 49(10), 1309–1318. https://doi.org/10.1111/j.1469-8986.2012.01464.x

Woolgar, A., Thompson, R., Bor, D., & Duncan, J. (2011). Multi-voxel coding of stimuli, rules, and responses in human frontoparietal cortex. NeuroImage, 56(2), 744–752. https://doi.org/10.1016/j.neuroimage.2010.04.035

Zurrón, M., Ramos-Goicoa, M., & Díaz, F. (2013). Semantic Conflict Processing in the Color-Word Stroop and the Emotional Stroop. Journal of Psychophysiology, 27(4), 149–164. https://doi.org/10.1027/0269-8803/a000100

APPENDIX A:

Supplementary Materials for Chapter 3

A.1. Distributional analysis

See the "Distributional analysis" section in the ManyStroopScript.m file

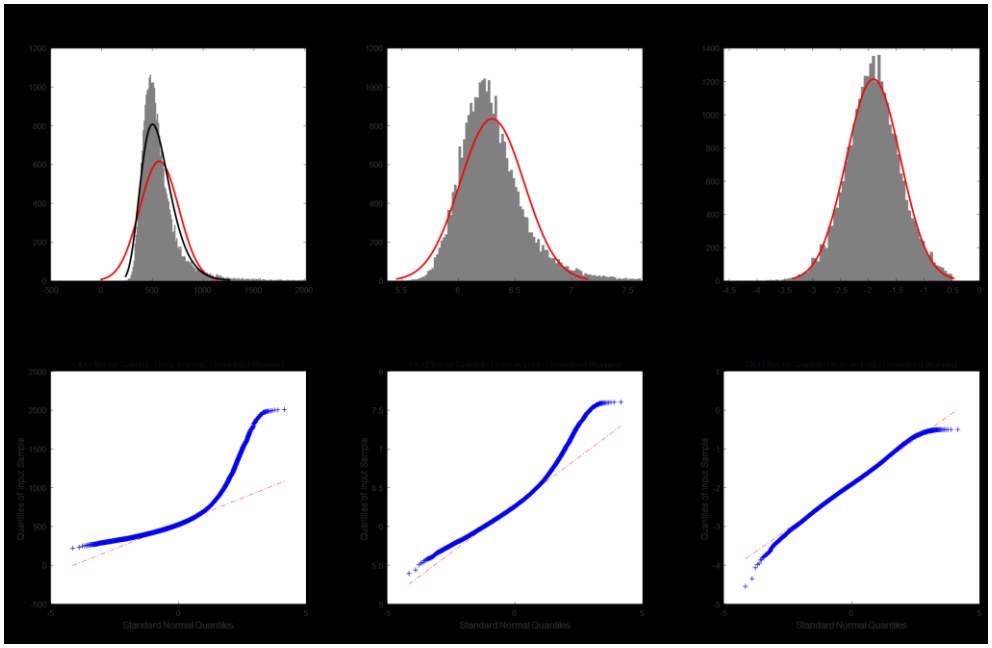

Figure A.1. Distributional analysis of participants' response times.
The top row shows the histograms of untransformed RT values (left panel), natural log-transformed RTs (lnRT, middle panel), and inverse-transformed RTs (iRT, right panel), computed as -1000/RT. The superimposed red curves represent the normal density function fitted to the data. The black curve for the RT distribution represents the lognormal density function fitted to the data. The number of bins was determined using the Freedman-Diaconis rule as implemented in the Matlab *histcounts* function. The bottom row shows the corresponding Q-Q plots.

A.2. Compliance checking

See the "Check for SS compliance" section in the ManyStroopScript.m file

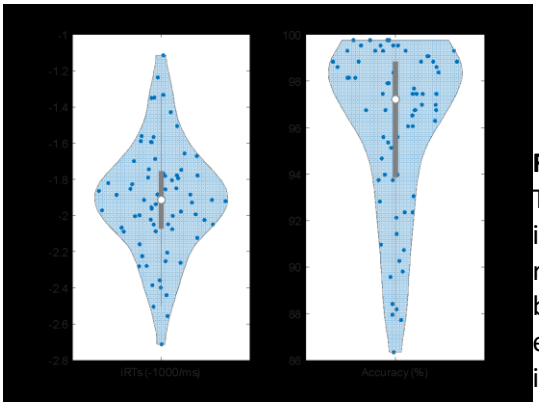

Figure A.2. Participants' overall performance.
The violin plots show the distribution of the participants' mean iRTs (left panel) and accuracy (right panel). The boxplots represent the median values (white dot at the center of the box), interquartile ranges (box), and dispersion outside the extreme quartiles (whiskers indicating 1.5 times the interquartile range).

A.3. Descriptive statistics

See the "Descriptive statistics" section in the ManyStroopScript.m file.

Table A.1. Descriptive statistics

	Peripheral		Perifoveal		Navon		Figure-Ground		Flanker		Saliency	
	M	SD	M	SD	M	SD	M	SD	M	SD	M	SD
Accuracy												
C	99%	3%	98%	4%	99%	2%	99%	2%	99%	2%	98%	2%
I	90%	9%	90%	11%	96%	6%	94%	8%	95%	7%	96%	6%
Stroop	9%	8%	8%	9%	3%	6%	5%	8%	4%	7%	3%	5%
RT												
C	586	158	529	169	544	114	500	90	523	124	490	105
I	716	214	658	219	615	140	579	90	586	108	523	108
Stroop	130	87	129	78	71	47	79	29	63	31	32	28
lnRT												
C	6.32	0.23	6.21	0.26	6.27	0.19	6.19	0.16	6.23	0.19	6.16	0.19
I	6.52	0.26	6.42	0.28	6.38	0.21	6.34	0.14	6.35	0.16	6.23	0.18
Stroop	0.19	0.09	0.21	0.09	0.11	0.06	0.15	0.05	0.12	0.06	0.07	0.05
iRT												
C	-1.87	0.39	-2.10	0.47	-1.96	0.34	-2.10	0.32	-2.03	0.34	-2.17	0.37
I	-1.55	0.38	-1.71	0.43	-1.77	0.35	-1.79	0.24	-1.78	0.24	-2.02	0.33
Stroop	0.32	0.14	0.39	0.14	0.19	0.10	0.31	0.12	0.25	0.12	0.15	0.10

Notes: C, congruent; I, incongruent.

Table A.2. Stroop effects

	GLM					LMM					RCA				
	M	**SD**	**t**	**d**	**Dom**	**M**	**SD**	**t**	**d**	**Dom**	**M**	**SD**	**t**	**d**	**Dom**
iRT															
Peripheral	0.324	0.137	20.08	2.366	100	0.343	0.113	25.65	3.023	100	0.345	0.143	20.47	2.412	100
Perifoveal	0.391	0.141	23.48	2.767	100	0.415	0.129	27.25	3.212	100	0.410	0.155	22.43	2.644	100
Navon	0.188	0.096	16.66	1.963	95.8	0.197	0.070	23.98	2.826	100	0.197	0.099	16.94	1.996	95.8
FG	0.307	0.120	21.75	2.563	100	0.320	0.100	27.20	3.205	100	0.319	0.121	22.45	2.646	100
Flanker	0.252	0.120	17.74	2.091	98.6	0.262	0.104	21.43	2.526	98.6	0.262	0.119	18.68	2.202	98.6
Saliency	0.152	0.097	13.38	1.577	91.7	0.157	0.064	20.84	2.456	100	0.156	0.099	13.34	1.572	91.7
lnRT															
Peripheral	0.195	0.093	17.74	2.090	100	0.205	0.086	20.38	2.402	100	0.205	0.099	17.65	2.080	100
Perifoveal	0.213	0.086	20.98	2.473	100	0.223	0.069	27.38	3.227	100	0.223	0.091	20.88	2.460	100
Navon	0.111	0.061	15.54	1.831	98.6	0.109	0.048	19.36	2.282	100	0.110	0.061	15.29	1.802	97.2
FG	0.153	0.053	24.61	2.900	100	0.160	0.035	38.77	4.570	100	0.161	0.051	26.73	3.151	100
Flanker	0.125	0.056	19.00	2.239	95.8	0.131	0.041	27.36	3.224	98.6	0.131	0.053	21.10	2.486	97.2
Saliency	0.069	0.047	12.43	1.465	91.7	0.075	0.026	24.54	2.892	100	0.073	0.046	13.49	1.589	93.1
RT															
Peripheral	129.8	86.7	12.70	1.497	100	129.5	79.7	13.79	1.625	100	133.2	92.9	12.17	1.434	98.6
Perifoveal	129.3	78.1	14.06	1.657	100	127.7	65.0	16.67	1.964	100	126.6	76.8	13.98	1.648	98.6
Navon	71.0	47.0	12.82	1.510	98.6	65.4	31.9	17.38	2.049	100	64.3	42.0	12.99	1.531	97.2
FG	78.9	29.5	22.73	2.678	100	82.8	15.0	46.82	5.518	100	83.1	27.5	25.67	3.025	100
Flanker	63.1	30.5	17.53	2.066	95.8	68.0	14.3	40.40	4.761	100	67.5	25.5	22.46	2.646	98.6
Saliency	32.3	27.6	9.92	1.169	87.5	35.1	13.4	22.29	2.627	100	33.7	26.2	10.93	1.288	93.1

Notes: Dom, percentage of participants showing a positive raw Stroop effect, FG, Figure-Ground task.

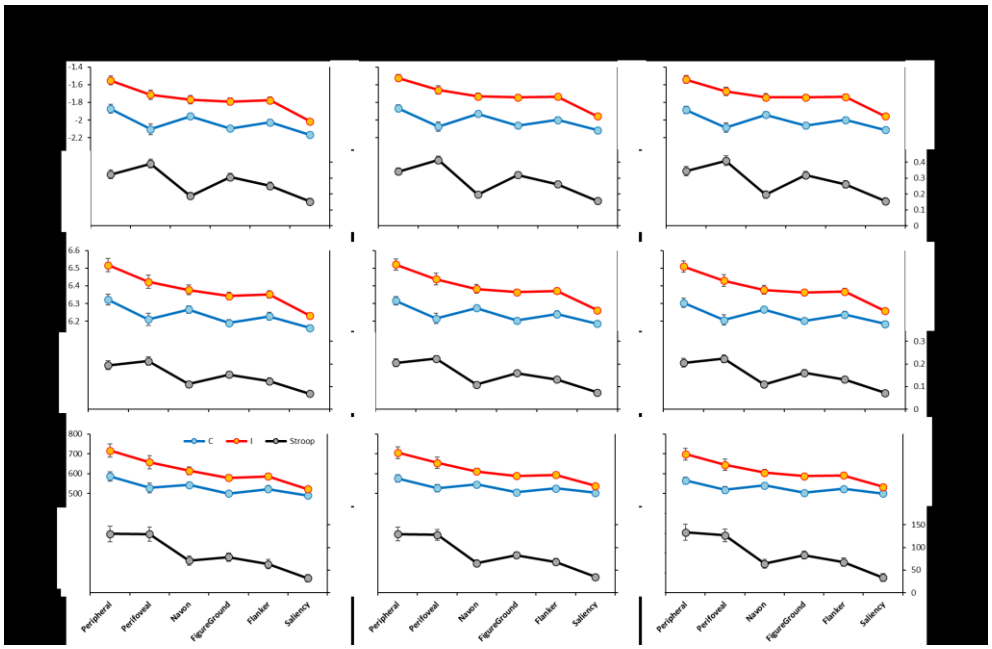

Figure A.3. Participants' response times.
The figure shows the participants' mean response times in the congruent (C, blue line, left y axis) and incongruent (I, red line, left y axis) conditions, as well as the corresponding Stroop effects (black line, right y axis), as a function of the analytical approaches (GLM, LMM, RCA, in columns) and the response time transformation (RTs, lnRTs, iRTs, in rows). The error bars indicate the within-subjects 95% confidence interval.

A.4. GLM

A.4.1. GLM on iRTs

See the "ManyStroop_iRT.omv" Jamovi file

A.4.2. GLM on lnRTs

See the "ManyStroop_lnRT.omv" Jamovi file

A.4.3. GLM on RTs

See the "ManyStroop_RT.omv" Jamovi file

A.4.4. GLM on accuracy

See the "ManyStroop_ACC.omv" Jamovi file

A.5. LMM

A.5.1. LMM on iRTs

A.5.1.1. Results

See the "LMM - iRT - Model building & test" section in the ManyStroopScript.m file.

Table A.3. LMM results, coefficients statistics

Coefficient	*Estimate*	*SE*	*t*	*DF*	*p*
(Intercept)	-1.8681	0.0396	-47.23	72.20	< .0001
Block	-0.0310	0.0053	-5.88	192.7	< .0001
Trial	-0.0421	0.0016	-27.01	28887	< .0001
preRT	0.0669	0.0024	28.27	28950	< .0001
$TASK_{Perifov}$	-0.2068	0.0307	-6.73	70.33	< .0001
$TASK_{Navon}$	-0.0621	0.0277	-2.24	71.77	0.0279
$TASK_{FG}$	-0.1948	0.0267	-7.30	69.50	< .0001
$TASK_{Flanker}$	-0.1294	0.0278	-4.65	72.21	< .0001
$TASK_{Saliency}$	-0.2463	0.0254	-9.68	71.44	< .0001
hResp	-0.0326	0.0031	-10.58	28862	< .0001
vResp	-0.0598	0.0031	-19.38	28859	< .0001
postERR	0.1747	0.0084	20.91	29124	< .0001
$CONG_{Inc}$	0.3425	0.0164	20.93	72.40	< .0001
Trial:Block	0.0074	0.0015	4.81	28868	< .0001
$CONG_{Inc}$:$TASK_{Perifov}$	0.0729	0.0148	4.93	73.62	< .0001
$CONG_{Inc}$:$TASK_{Navon}$	-0.1454	0.0175	-8.30	76.15	< .0001
$CONG_{Inc}$:$TASK_{FG}$	-0.0222	0.0217	-1.02	71.92	0.3088
$CONG_{Inc}$:$TASK_{Flanker}$	-0.0807	0.0202	-4.00	74.51	< .0001
$CONG_{Inc}$:$TASK_{Saliency}$	-0.1851	0.0186	-9.97	72.72	< .0001

Notes: preRT, iRT at the previous trial; Perifov, Perifoveal; FG, Figure-Ground; hResp, horizontal coding of the response (i.e., the responding hand: right vs left); vResp, vertical coding of the response (i.e., the responding finger: middle vs index); postERR, post-error trials; CONG, Congruency; Inc, Incongruent trials; DF, degrees of freedom. P values are computed using the Satterthwaite's approximation.

A.5.1.2. Residual analysis

See the "LMM – iRT – Inspect fit" section in the ManyStroopScript.m file

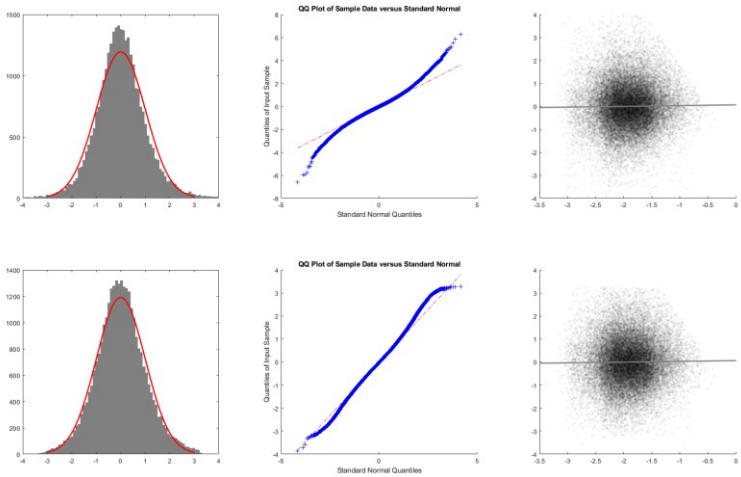

Figure A.4. Inspection of residuals for the LMM analysis on iRTs.
The figure shows the results of the analysis of the residuals for the LMM analysis on iRTs for the final model both before (upper panels) and after (bottom panels) excluding observations with absolute standardized residuals greater than 3. Left: histogram of the standardized residuals; the superimposed red curve represents the normal density function fitted to the data. Middle: quantile-quantile plot for the standardized residuals. Right: scatterplot of the fitted data (x) vs. the standardized residuals (y) for the visual inspection of the homoscedasticity; the gray line represents the corresponding linear regression line.

A.5.1.3. Post-hoc

See the "LMM – iRT – Post-hoc comparisons" section in the ManyStroopScript.m file

Table A.4. LMM on iRTs, post-hoc pairwise comparisons of Stroop effects between tasks

Task1	Task2	F	DF1	DF2	p
Peripheral	**Perifoveal**	24.35	1	73.62	< .0001
Peripheral	**Navon**	68.95	1	76.15	< .0001
Peripheral	**FigureGround**	1.05	1	71.92	0.3088
Peripheral	**Flanker**	15.99	1	74.51	0.0001
Peripheral	**Saliency**	99.31	1	72.72	< .0001
Perifoveal	**Navon**	144.26	1	74.75	< .0001
Perifoveal	**FigureGround**	19.94	1	73.04	< .0001
Perifoveal	**Flanker**	49.32	1	71.67	< .0001
Perifoveal	**Saliency**	174.62	1	71.93	< .0001
Navon	**FigureGround**	51.74	1	78.12	< .0001
Navon	**Flanker**	15.18	1	81.12	0.0002
Navon	**Saliency**	8.49	1	100.15	0.0044
FigureGround	**Flanker**	21.53	1	118.14	< .0001
FigureGround	**Saliency**	144.69	1	78.83	< .0001
Flanker	**Saliency**	56.38	1	80.02	< .0001

Notes: p values are computed using the Satterthwaite's approximation.

A.5.1.4. Stroop effects comparison, LMM vs GLM

See the "Compare GLM- and LMM-based Stroop effects - iRT" section in the ManyStroopScript.m file

Table A.5. Comparison of Stroop effects between LMM and GLM

Task	r	$t_{(71)}$	p	d
Peripheral	0.948	3.415	0.0011	0.402
Perifoveal	0.956	4.872	< .0001	0.574
Navon	0.817	1.421	0.1596	0.168
FigureGround	0.930	2.409	0.0186	0.284
Flanker	0.917	1.767	0.0814	0.208
Saliency	0.840	0.765	0.4467	0.090

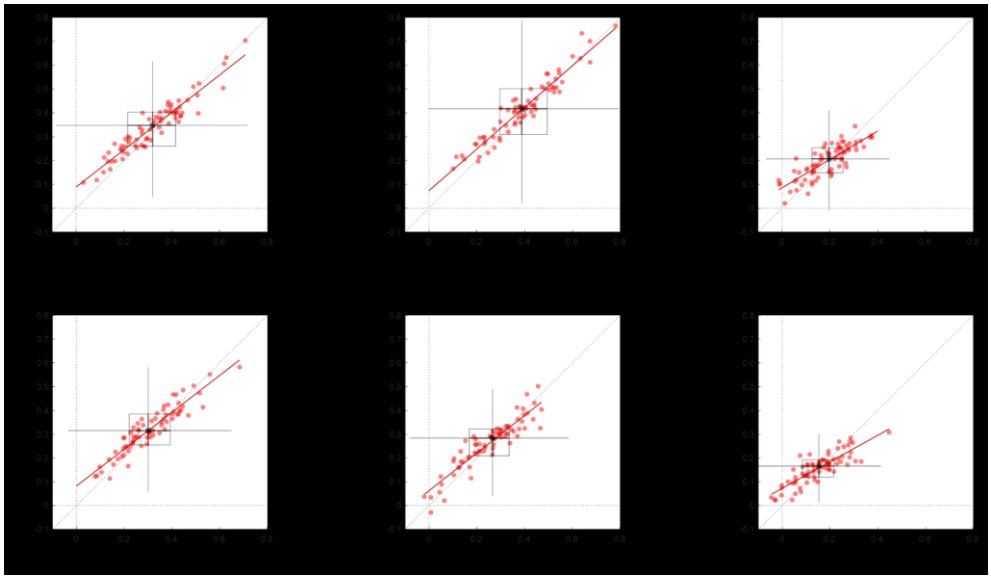

Figure A.5. Comparison of Stroop effects between LMM and GLM.
Each scatterplot shows the participants' Stroop effects (red circles) yielded by the LMM (y axis) and GLM (x axis) analytical approaches. The two-dimensional boxplot represents the corresponding median values (black square at the center of the box), interquartile ranges (height and width of the box, respectively), and dispersion outside the extreme quartiles (vertical and horizontal whiskers, respectively, indicating 1.5 times the interquartile range). The red solid line represents the corresponding linear regression line. The diagonal dotted line represents the equivalent line.

Table A.6. Comparison of Stroop effects between LMM and GLM – regression analysis, intercept vs 0

Task	Estimate	SE	$t_{(70)}$	p
Peripheral	0.088	0.011	7.97	< .0001
Perifoveal	0.073	0.013	5.50	< .0001
Navon	0.085	0.011	8.06	< .0001
FigureGround	0.082	0.012	6.81	< .0001
Flanker	0.063	0.011	5.52	< .0001
Saliency	0.073	0.008	9.36	< .0001

Table A.7. Comparison of Stroop effects between LMM and GLM – regression analysis, slope vs 1

Task	Estimate	SE	$t_{(70)}$	p
Peripheral	0.785	0.032	-6.80	< .0001
Perifoveal	0.875	0.032	-3.92	0.0002
Navon	0.596	0.050	-8.04	< .0001
FigureGround	0.775	0.037	-6.15	< .0001
Flanker	0.789	0.041	-5.13	< .0001
Saliency	0.557	0.043	-10.31	< .0001

A.5.2. LMM on lnRTs

A.5.2.1. Results

See the "LMM – lnRT – Model test

Table A.8. LMM results, ANOVA table

Effect	F	DF1	DF2	p
Block	35.4	1	191.39	< .0001
Trial	769.3	1	28740	< .0001
postERR	373.2	1	28979	< .0001
preRT	794.9	1	29000	< .0001
hResp	102.8	1	28721	< .0001
vResp	357.6	1	28718	< .0001
Trial:Block	32.0	1	28727	< .0001
Cong	1275.1	1	72.59	< .0001
Task	46.4	5	71.17	< .0001
Cong:Task	57.8	5	86.62	< .0001

Notes: see Table A.2 for conventions

Table A.9. LMM results, coefficients statistics

Effect	*Estimate*	*SE*	*t*	*DF*	*p*
(Intercept)	6.3152	0.0229	275.65	72.08	< .0001
Block	-0.0172	0.0029	-5.95	191.4	< .0001
Trial	-0.0238	0.0009	-27.74	28741	< .0001
preRT	0.0368	0.0013	28.19	29000	< .0001
$TASK_{Perifov}$	-0.1001	0.0179	-5.58	70.35	< .0001
$TASK_{Navon}$	-0.0409	0.0173	-2.37	71.72	0.0206
$TASK_{FG}$	-0.1111	0.0163	-6.80	69.49	< .0001
$TASK_{Flanker}$	-0.0754	0.0175	-4.31	71.79	0.0001
$TASK_{Saliency}$	-0.1291	0.0156	-8.28	70.70	< .0001
hResp	-0.0172	0.0017	-10.14	28721	< .0001
vResp	-0.0321	0.0017	-18.91	28718	< .0001
postERR	0.0898	0.0046	19.32	28979	< .0001
$CONG_{Inc}$	0.2055	0.0114	18.01	71.81	< .0001
Trial:Block	0.0048	0.0008	5.66	28727	< .0001
$CONG_{Inc}$:$TASK_{Perifov}$	0.0178	0.0089	2.01	69.62	0.0488
$CONG_{Inc}$:$TASK_{Navon}$	-0.0967	0.0122	-7.95	73.28	< .0001
$CONG_{Inc}$:$TASK_{FG}$	-0.0453	0.0140	-3.24	71.91	0.0018
$CONG_{Inc}$:$TASK_{Flanker}$	-0.0742	0.0138	-5.39	72.25	< .0001
$CONG_{Inc}$:$TASK_{Saliency}$	-0.1304	0.0123	-10.58	72.45	< .0001

Notes: see Table A.2 for conventions

A.5.2.2. Residual analysis

See the "LMM – lnRT – Inspect fit" section in the ManyStroopScript.m file

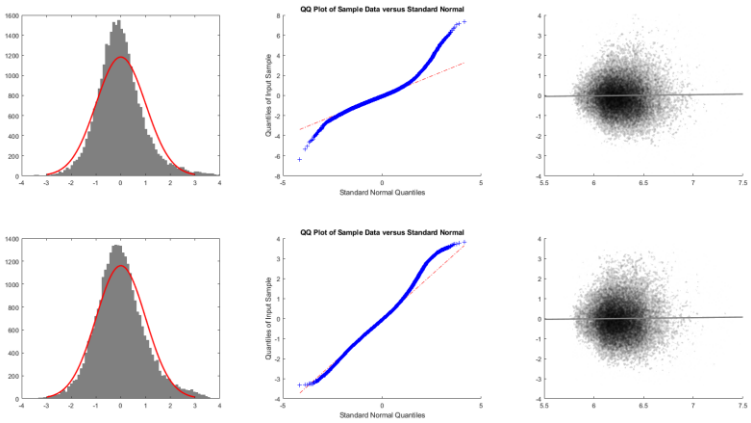

Figure A.6. Inspection of residuals for the LMM analysis on lnRTs.
The figure shows the results of the analysis of the residuals for the LMM analysis on lnRTs for the final model both before (upper panels) and after (bottom panels) excluding observations with absolute standardized residuals greater than 3.
Left: histogram of the standardized residuals; the superimposed red curve represents the normal density function fitted to the data. Middle: quantile-quantile plot for the standardized residuals. Right: scatterplot of the fitted data (x) vs. the standardized residuals (y) for the visual inspection of the homoscedasticity; the gray line represents the corresponding linear regression line.

A.5.2.3. Post-hoc

See the "LMM – lnRT – Post-hoc comparisons" section in the ManyStroopScript.m file

Table A.10. LMM on lnRTs, post-hoc pairwise comparisons of Stroop effects between tasks

Task1	Task2	F	DF1	DF2	p
Peripheral	**Perifoveal**	4.02	1	69.62	0.0488
Peripheral	**Navon**	63.25	1	73.28	< .0001
Peripheral	**FigureGround**	10.47	1	71.91	0.0018
Peripheral	**Flanker**	29.05	1	72.25	< .0001
Peripheral	**Saliency**	111.84	1	72.45	< .0001
Perifoveal	**Navon**	115.72	1	74.77	< .0001
Perifoveal	**FigureGround**	27.20	1	73.32	< .0001
Perifoveal	**Flanker**	55.06	1	71.51	< .0001
Perifoveal	**Saliency**	163.42	1	71.45	< .0001
Navon	**FigureGround**	29.83	1	81.09	< .0001
Navon	**Flanker**	5.72	1	80.34	0.0192
Navon	**Saliency**	16.40	1	88.88	0.0001
FigureGround	**Flanker**	19.06	1	153.12	< .0001
FigureGround	**Saliency**	149.40	1	91.81	< .0001
Flanker	**Saliency**	61.74	1	79.10	< .0001

Notes: p values are computed using the Satterthwaite's approximation.

A.5.2.4. Stroop effects comparison, LMM vs GLM

See the "Compare GLM- and LMM-based Stroop effects - lnRT" section in the ManyStroopScript.m file

Table A.11. Comparison of Stroop effects between LMM and GLM

Task	r	$t_{(71)}$	p	d
Peripheral	0.944	2.955	0.0042	0.348
Perifoveal	0.958	3.184	0.0022	0.375
Navon	0.825	-0.625	0.5343	-0.074
FigureGround	0.868	2.090	0.0402	0.246
Flanker	0.878	2.001	0.0492	0.236
Saliency	0.831	1.831	0.0714	0.216

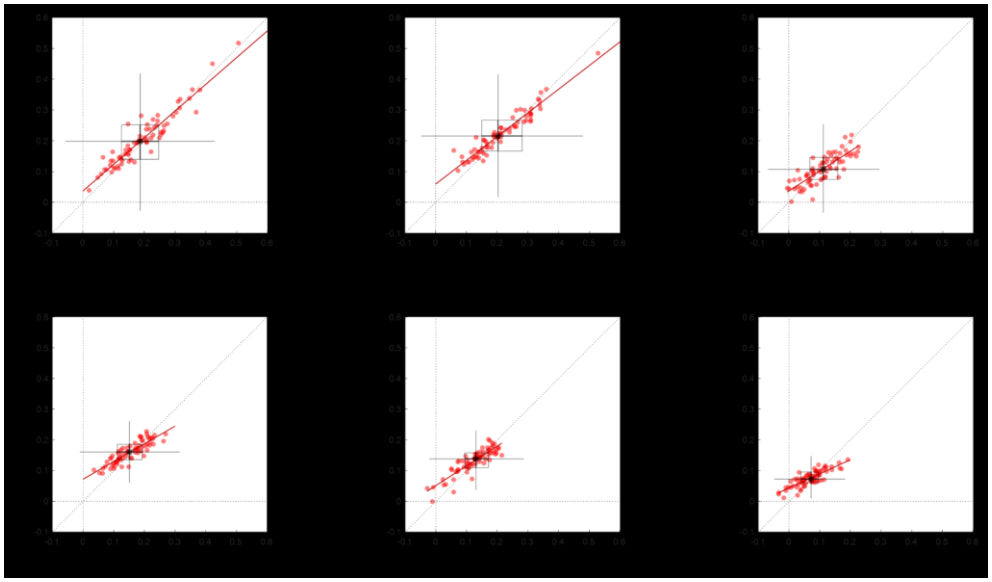

Figure A.7. Comparison of Stroop effects between LMM and GLM.
Each scatterplot shows the participants' Stroop effects (red circles) yielded by the LMM (y axis) and GLM (x axis) analytical approaches. The two-dimensional boxplot represents the corresponding median values (black square at the center of the box), interquartile ranges (height and width of the box, respectively), and dispersion outside the extreme quartiles (vertical and horizontal whiskers, respectively, indicating 1.5 times the interquartile range). The red solid line represents the corresponding linear regression line. The diagonal dotted line represents the equivalent line.

Table A.12. Comparison of Stroop effects between LMM and GLM – regression analysis, intercept vs 0

Task	Estimate	SE	$t_{(70)}$	p
Peripheral	0.037	0.008	4.70	< .0001
Perifoveal	0.059	0.006	9.43	< .0001
Navon	0.037	0.007	5.48	< .0001
FigureGround	0.072	0.006	11.28	< .0001
Flanker	0.051	0.006	8.98	< .0001
Saliency	0.043	0.003	14.23	< .0001

Table A.13. Comparison of Stroop effects between LMM and GLM – regression analysis, slope vs 1

Task	Estimate	SE	$t_{(70)}$	p
Peripheral	0.867	0.036	-3.68	0.0005
Perifoveal	0.771	0.027	-8.36	< .0001
Navon	0.647	0.053	-6.66	< .0001
FigureGround	0.576	0.039	-10.77	< .0001
Flanker	0.642	0.042	-8.56	< .0001
Saliency	0.459	0.037	-14.70	< .0001

A.5.3. LMM on RTs

A.5.3.1. Results

See the "LMM – RT – Model test" section in the ManyStroopScript.m file

Table A.14. LMM results, ANOVA table.

Effect	F	DF1	DF2	p
Block	23.5	1	199.57	< .0001
Trial	739.7	1	28626	< .0001
postERR	342.3	1	28870	< .0001
preRT	660.5	1	28805	< .0001
hResp	88.7	1	28604	< .0001
vResp	310.0	1	28603	< .0001
Trial:Block	37.3	1	28611	< .0001
Cong	718.4	1	71.61	< .0001
Task	34.5	5	70.94	< .0001
Cong:Task	49.0	5	85.21	< .0001

Notes: see Table A.2 for conventions

Table A.15. LMM results, coefficients statistics

Effect	*Estimate*	*SE*	*t*	*DF*	*p*
(Intercept)	577.37	15.70	36.78	71.90	< .0001
Block	-7.94	1.64	-4.85	199.6	< .0001
Trial	-14.26	0.52	-27.20	28626	< .0001
preRT	20.50	0.80	25.70	28805	< .0001
$TASK_{Perifov}$	-49.99	11.97	-4.18	70.29	0.0001
$TASK_{Navon}$	-31.38	13.20	-2.38	71.57	0.0201
$TASK_{FG}$	-70.28	12.41	-5.67	70.08	< .0001
$TASK_{Flanker}$	-50.52	13.24	-3.82	71.45	0.0003
$TASK_{Saliency}$	-73.54	12.12	-6.07	70.61	< .0001
hResp	-9.74	1.03	-9.42	28604	< .0001
vResp	-18.24	1.04	-17.61	28603	< .0001
postERR	52.57	2.84	18.50	28870	< .0001
$CONG_{Inc}$	129.50	9.94	13.03	70.30	< .0001
Trial:Block	3.16	0.52	6.11	28611	< .0001
$CONG_{Inc}$:$TASK_{Perifov}$	-1.84	8.20	-0.22	66.79	0.8231
$CONG_{Inc}$:$TASK_{Navon}$	-64.12	9.96	-6.44	70.74	< .0001
$CONG_{Inc}$:$TASK_{FG}$	-46.66	10.86	-4.29	70.76	0.0001
$CONG_{Inc}$:$TASK_{Flanker}$	-61.54	10.70	-5.75	70.01	< .0001
$CONG_{Inc}$:$TASK_{Saliency}$	-94.41	10.06	-9.39	70.75	< .0001

A.5.3.2. Residual analysis

See the "LMM – RT – Inspect fit" section in the ManyStroopScript.m file

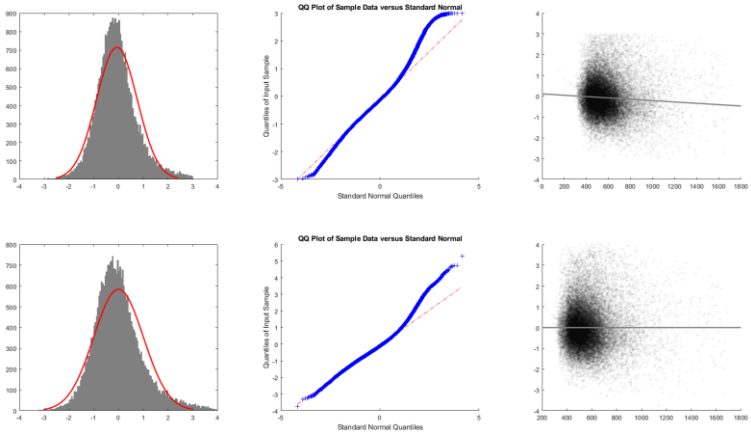

Figure A.8. Inspection of residuals for the LMM analysis on RTs.
The figure shows the results of the analysis of the residuals for the LMM analysis on RTs for the final model both before (upper panels) and after (bottom panels) excluding observations with absolute standardized residuals greater than 3.
Left: histogram of the standardized residuals; the superimposed red curve represents the normal density function fitted to the data. Middle: quantile-quantile plot for the standardized residuals. Right: scatterplot of the fitted data (x) vs. the standardized residuals (y) for the visual inspection of the homoscedasticity; the gray line represents the corresponding linear regression line.

A.5.3.3. Post-hoc

See the "LMM – RT – Post-hoc comparisons" section in the ManyStroopScript.m file

Table A.16. LMM on lnRTs, post-hoc pairwise comparisons of Stroop effects between tasks

Task1	Task2	F	DF1	DF2	p
Peripheral	**Perifoveal**	0.05	1	66.79	0.8231
Peripheral	**Navon**	41.41	1	70.74	< .0001
Peripheral	**FigureGround**	18.45	1	70.76	0.0001
Peripheral	**Flanker**	33.08	1	70.01	< .0001
Peripheral	**Saliency**	88.11	1	70.75	< .0001
Perifoveal	**Navon**	50.66	1	70.56	< .0001
Perifoveal	**FigureGround**	24.48	1	71.23	< .0001
Perifoveal	**Flanker**	40.44	1	70.34	< .0001
Perifoveal	**Saliency**	104.72	1	70.34	< .0001
Navon	**FigureGround**	9.66	1	83.71	0.0026
Navon	**Flanker**	0.21	1	81.33	0.6517
Navon	**Saliency**	34.30	1	85.76	< .0001
FigureGround	**Flanker**	14.02	1	175.37	0.0002
FigureGround	**Saliency**	143.55	1	122.96	< .0001
Flanker	**Saliency**	69.51	1	76.18	< .0001

Notes: p values are computed using the Satterthwaite's approximation.

A.5.3.4. Stroop effects comparison, LMM vs GLM

See the "Compare GLM- and LMM-based Stroop effects - RT" section in the ManyStroopScript.m file

Table A.17. Comparison of Stroop effects between LMM and GLM

Task	r	$t_{(71)}$	p	d
Peripheral	0.934	-0.089	0.9292	-0.011
Perifoveal	0.953	-0.562	0.5759	-0.066
Navon	0.810	-1.700	0.0935	-0.200
FigureGround	0.769	1.628	0.1080	0.192
Flanker	0.712	1.828	0.0718	0.215
Saliency	0.779	1.225	0.2248	0.144

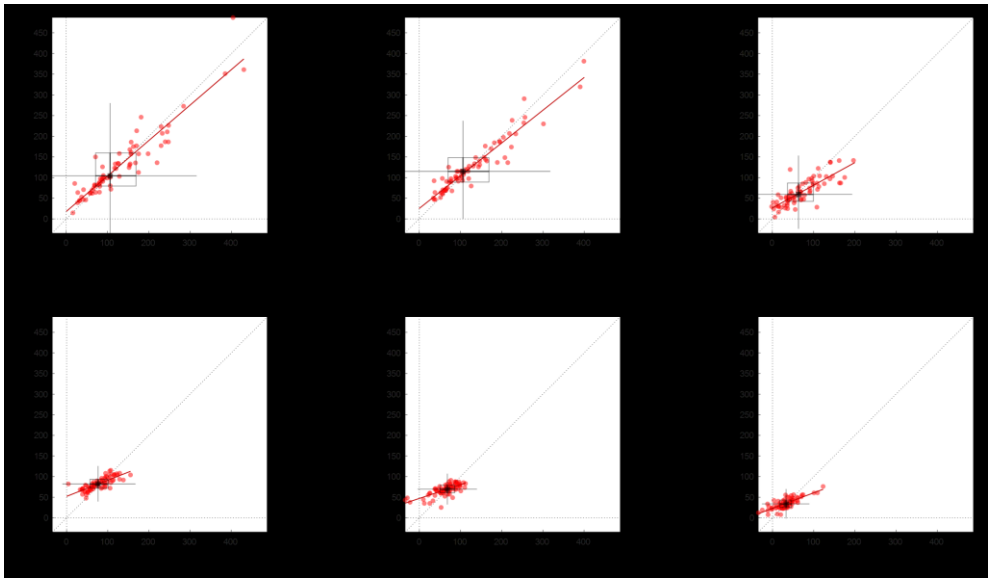

Figure A.9. Comparison of Stroop effects between LMM and GLM.
Each scatterplot shows the participants' Stroop effects (red circles) yielded by the LMM (y axis) and GLM (x axis) analytical approaches. The two-dimensional boxplot represents the corresponding median values (black square at the center of the box), interquartile ranges (height and width of the box, respectively), and dispersion outside the extreme quartiles (vertical and horizontal whiskers, respectively, indicating 1.5 times the interquartile range). The red solid line represents the corresponding linear regression line. The diagonal dotted line represents the equivalent line.

Table A.18. Comparison of Stroop effects between LMM and GLM – regression analysis, intercept vs 0

Task	Estimate	SE	$t_{(70)}$	p
Peripheral	18.092	6.100	2.97	0.0041
Perifoveal	25.072	4.554	5.51	< .0001
Navon	26.323	4.040	6.52	< .0001
FigureGround	51.925	3.277	15.84	< .0001
Flanker	46.950	2.745	17.10	< .0001
Saliency	22.928	1.537	14.92	< .0001

Table A.19. Comparison of Stroop effects between LMM and GLM – regression analysis, slope vs 1

Task	Estimate	SE	$t_{(70)}$	p
Peripheral	0.858	0.039	-3.62	0.0005
Perifoveal	0.793	0.030	-6.85	< .0001
Navon	0.550	0.048	-9.48	< .0001
FigureGround	0.392	0.039	-15.63	< .0001
Flanker	0.333	0.039	-17.00	< .0001
Saliency	0.376	0.036	-17.22	< .0001

A.5.4. Control analysis, reduced (i.e., minimal) LMM on iRTs

A.5.4.1. Results

See the "LMM - iRT - Control analysis (without confounders)" section in the ManyStroopScript.m file.

Table A.20. LMM results, coefficients statistics

Coefficient	*Estimate*	*SE*	*t*	*DF*	*p*
(Intercept)	-1.8769	0.0466	-40.25	71.98	< .0001
$TASK_{Perifov}$	-0.2271	0.0371	-6.13	71.71	< .0001
$TASK_{Navon}$	-0.0852	0.0333	-2.56	72.04	0.0126
$TASK_{FG}$	-0.2226	0.0337	-6.61	71.94	< .0001
$TASK_{Flanker}$	-0.1543	0.0330	-4.67	71.99	< .0001
$TASK_{Saliency}$	-0.2925	0.0321	-9.12	71.94	< .0001
$CONG_{Inc}$	0.3243	0.0157	20.71	72.68	< .0001
$CONG_{Inc}$:$TASK_{Perifov}$	0.0712	0.0145	4.92	75.73	< .0001
$CONG_{Inc}$:$TASK_{Navon}$	-0.1374	0.0168	-8.17	80.11	< .0001
$CONG_{Inc}$:$TASK_{FG}$	-0.0173	0.0205	-0.84	72.04	0.4019
$CONG_{Inc}$:$TASK_{Flanker}$	-0.0721	0.0196	-3.69	75.83	0.0004
$CONG_{Inc}$:$TASK_{Saliency}$	-0.1734	0.0175	-9.91	73.51	< .0001

Notes: Perifov, Perifoveal; FG, Figure-Ground; CONG, Congruency; Inc, Incongruent trials; DF, degrees of freedom. P values are computed using the Satterthwaite's approximation.

A.5.4.2. Residual analysis

See the “LMM - iRT - Control analysis (without confounders)” section in the ManyStroopScript.m file

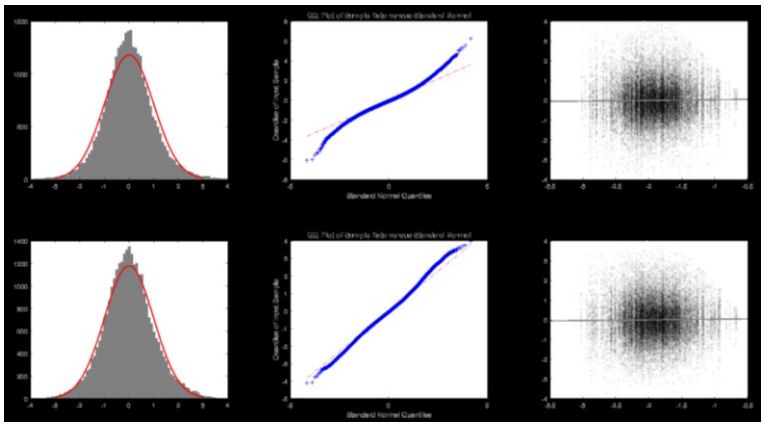

Figure A.10. Inspection of residuals for the control LMM analysis (with the reduced model) on iRTs.
The figure shows the results of the analysis of the residuals for the LMM analysis on iRTs for the reduced model both before (upper panels) and after (bottom panels) excluding observations with absolute standardized residuals greater than 3.
Left: histogram of the standardized residuals; the superimposed red curve represents the normal density function fitted to the data. Middle: quantile-quantile plot for the standardized residuals. Right: scatterplot of the fitted data (x) vs. the standardized residuals (y) for the visual inspection of the homoscedasticity; the gray line represents the corresponding linear regression line.

A.5.4.3. Stroop effects comparison, full vs reduced LMM

See the “LMM - iRT - Control analysis (without confounders)” section in the ManyStroopScript.m file

Table A.21. Comparison of Stroop effects between LMM and GLM

Task	r	$t_{(71)}$	p	d
Peripheral	0.992	9.676	< .0001	1.140
Perifoveal	0.997	13.321	< .0001	1.570
Navon	0.989	7.614	< .0001	0.897
FigureGround	0.996	10.586	< .0001	1.248
Flanker	0.993	6.497	< .0001	0.766
Saliency	0.984	4.209	< .0001	0.496

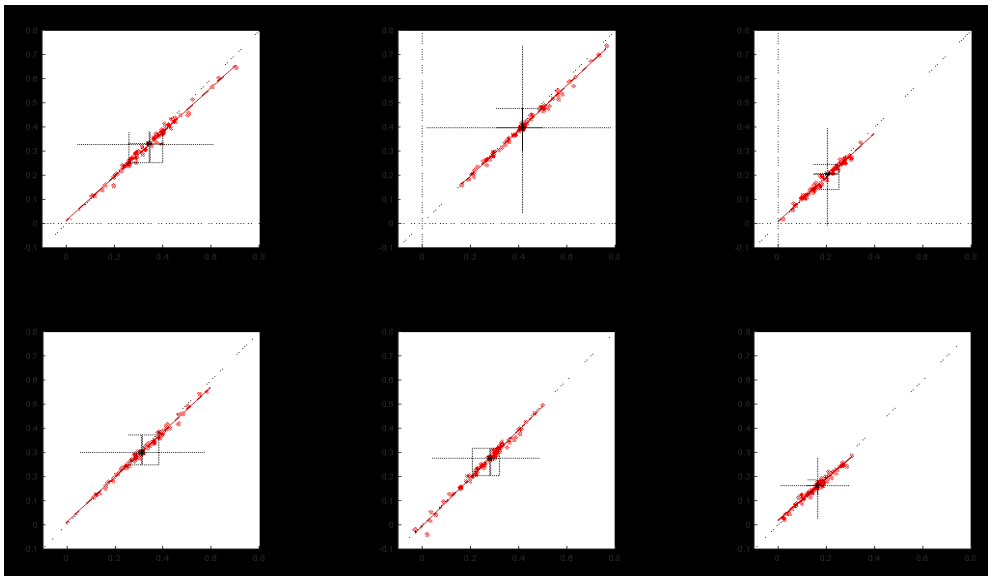

Figure A.11. Comparison of Stroop effects between full and reduced LMM.
Each scatterplot shows the participants' Stroop effects (red circles) yielded by the reduced (y axis) and full LMM (x axis) analytical approaches. The two-dimensional boxplot represents the corresponding median values (black square at the center of the box), interquartile ranges (height and width of the box, respectively), and dispersion outside the extreme quartiles (vertical and horizontal whiskers, respectively, indicating 1.5 times the interquartile range). The red solid line represents the corresponding linear regression line. The diagonal dotted line represents the equivalent line.

A.6. RCA

A.6.1. RCA on iRTs

A.6.1.1. Results

See the "RCA - iRT" section in the ManyStroopScript.m file.

Table A.22. RCA results, coefficients statistics

Effect	*Estimate*	*SE*	*t*	*DF*	*p*
(Intercept)	-1.8855	0.0397	-47.49	71	< .0001
Trial	-0.0416	0.0037	-11.26	71	< .0001
preRT	0.0624	0.0042	14.69	71	< .0001
$TASK_{Perifov}$	-0.1999	0.0316	-6.33	71	< .0001
$TASK_{Navon}$	-0.0539	0.0280	-1.92	71	0.0586
$TASK_{FG}$	-0.1780	0.0287	-6.21	71	< .0001
$TASK_{Flanker}$	-0.1133	0.0282	-4.01	71	0.0001
$TASK_{Saliency}$	-0.2283	0.0267	-8.54	71	< .0001
hResp	-0.0299	0.0079	-3.76	71	0.0003
vResp	-0.0620	0.0075	-8.27	71	< .0001
postERR	0.1980	0.0170	11.62	71	< .0001
$CONG_{Inc}$	0.3453	0.0169	20.47	71	< .0001
$CONG_{Inc}$:$TASK_{Perifov}$	0.0647	0.0159	4.08	71	0.0001
$CONG_{Inc}$:$TASK_{Navon}$	-0.1486	0.0180	-8.27	71	< .0001
$CONG_{Inc}$:$TASK_{FG}$	-0.0260	0.0219	-1.19	71	0.2396
$CONG_{Inc}$:$TASK_{Flanker}$	-0.0838	0.0205	-4.08	71	< .0001
$CONG_{Inc}$:$TASK_{Saliency}$	-0.1893	0.0189	-10.01	71	< .0001

Notes: see Table A.2 for conventions

A.6.1.2. Residual analysis

See the "RCA – iRT – Inspect fit" section in the ManyStroopScript.m file

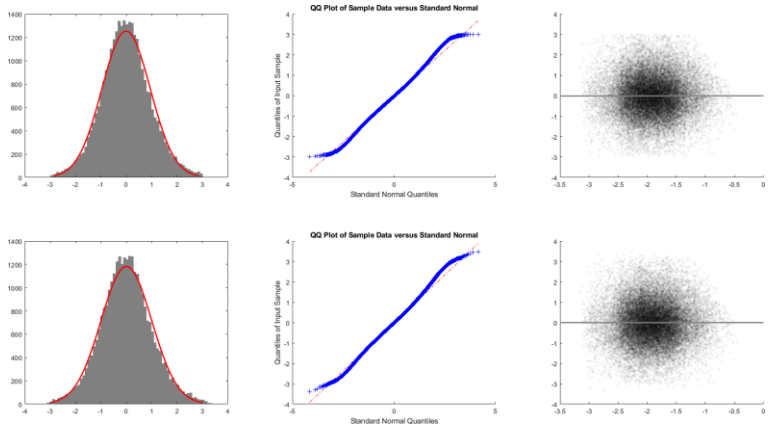

Figure A.12. Inspection of residuals for the RCA analysis on iRTs.
The figure shows the results of the analysis of the residuals for the RCA analysis on iRTs for the final model both before (upper panels) and after (bottom panels) excluding observations with absolute standardized residuals greater than 3.
Left: histogram of the standardized residuals; the superimposed red curve represents the normal density function fitted to the data. Middle: quantile-quantile plot for the standardized residuals. Right: scatterplot of the fitted data (x) vs. the standardized residuals (y) for the visual inspection of the homoscedasticity; the gray line represents the corresponding linear regression line.

A.6.1.3. Post-hoc

See the "RCA – iRT – Post-hoc comparisons" section in the ManyStroopScript.m file

Table A.23. RCA on iRTs, post-hoc pairwise comparisons of Stroop effects between tasks

Task1	Task2	F	DF1	DF2	p
Peripheral	**Perifoveal**	16.61	1	71	0.0001
Peripheral	**Navon**	68.36	1	71	< .0001
Peripheral	**FigureGround**	1.41	1	71	0.2396
Peripheral	**Flanker**	16.64	1	71	0.0001
Peripheral	**Saliency**	100.19	1	71	< .0001
Perifoveal	**Navon**	131.03	1	71	< .0001
Perifoveal	**FigureGround**	18.41	1	71	0.0001
Perifoveal	**Flanker**	46.55	1	71	< .0001
Perifoveal	**Saliency**	155.67	1	71	< .0001
Navon	**FigureGround**	51.31	1	71	< .0001
Navon	**Flanker**	15.96	1	71	0.0002
Navon	**Saliency**	8.67	1	71	0.0044
FigureGround	**Flanker**	29.98	1	71	< .0001
FigureGround	**Saliency**	150.01	1	71	< .0001
Flanker	**Saliency**	57.46	1	71	< .0001

Notes: p values are computed using the Satterthwaite's approximation.

A.6.1.4. Stroop effects comparison, RCA vs GLM

See the "Compare GLM- and RCA-based Stroop effects - iRT" section in the ManyStroopScript.m file

Table A.24. Comparison of Stroop effects between RCA and GLM

Task	r	$t_{(71)}$	p	d
Peripheral	0.985	7.298	< .0001	0.860
Perifoveal	0.977	4.611	< .0001	0.543
Navon	0.967	3.042	0.0033	0.359
FigureGround	0.982	4.514	< .0001	0.532
Flanker	0.990	4.813	< .0001	0.567
Saliency	0.965	1.169	0.2463	0.138

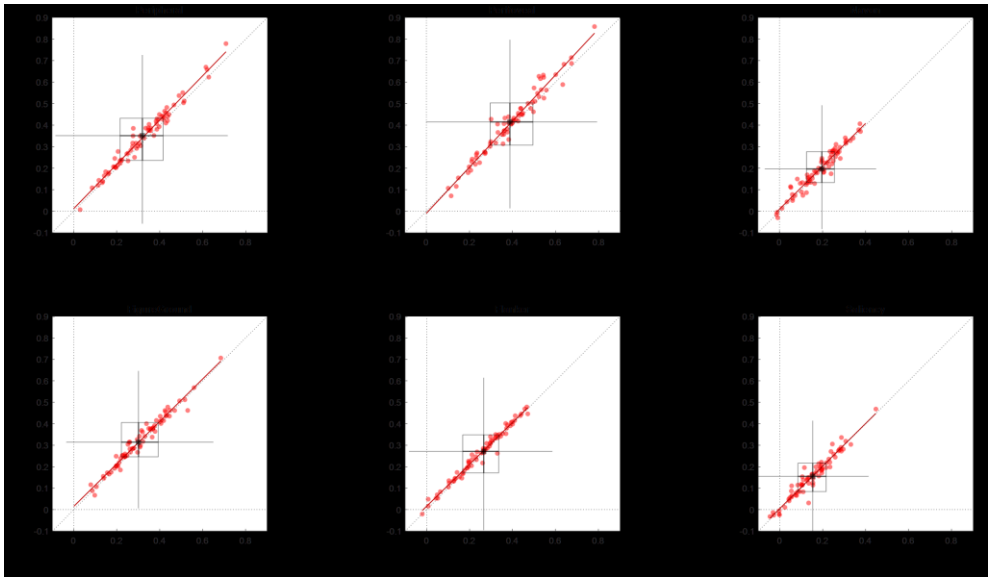

Figure A.13. Comparison of Stroop effects between RCA and GLM.
Each scatterplot shows the participants' Stroop effects (red circles) yielded by the RCA (y axis) and GLM (x axis) analytical approaches. The two-dimensional boxplot represents the corresponding median values (black square at the center of the box), interquartile ranges (height and width of the box, respectively), and dispersion outside the extreme quartiles (vertical and horizontal whiskers, respectively, indicating 1.5 times the interquartile range). The red solid line represents the corresponding linear regression line. The diagonal dotted line represents the equivalent line.

Table A.25. Comparison of Stroop effects between RCA and GLM – regression analysis, intercept vs 0

Task	Estimate	SE	$t_{(70)}$	p
Peripheral	0.012	0.008	1.53	0.1300
Perifoveal	-0.009	0.012	-0.82	0.4144
Navon	0.010	0.007	1.46	0.1487
FigureGround	0.015	0.007	2.09	0.0405
Flanker	0.016	0.005	3.35	0.0013
Saliency	0.005	0.006	0.87	0.3898

Table A.26. Comparison of Stroop effects between RCA and GLM – regression analysis, slope vs 1

Task	Estimate	SE	$t_{(70)}$	p
Peripheral	1.031	0.022	1.42	0.1592
Perifoveal	1.072	0.028	2.59	0.0116
Navon	0.997	0.031	-0.11	0.9140
FigureGround	0.989	0.022	-0.50	0.6197
Flanker	0.976	0.017	-1.41	0.1639
Saliency	0.991	0.032	-0.29	0.7717

A.6.1.5. Stroop effects comparison, LMM vs RCA

See the "Compare RCA- and LMM-based Stroop effects - iRT" section in the ManyStroopScript.m file

Table A.27. Comparison of Stroop effects between LMM and RCA

Task	r	$t_{(71)}$	p	d
Peripheral	0.954	-0.485	0.6291	-0.057
Perifoveal	0.950	0.875	0.3846	0.103
Navon	0.839	0.056	0.9551	0.007
FigureGround	0.934	0.176	0.8606	0.021
Flanker	0.912	0.051	0.9598	0.006
Saliency	0.842	0.209	0.8352	0.025

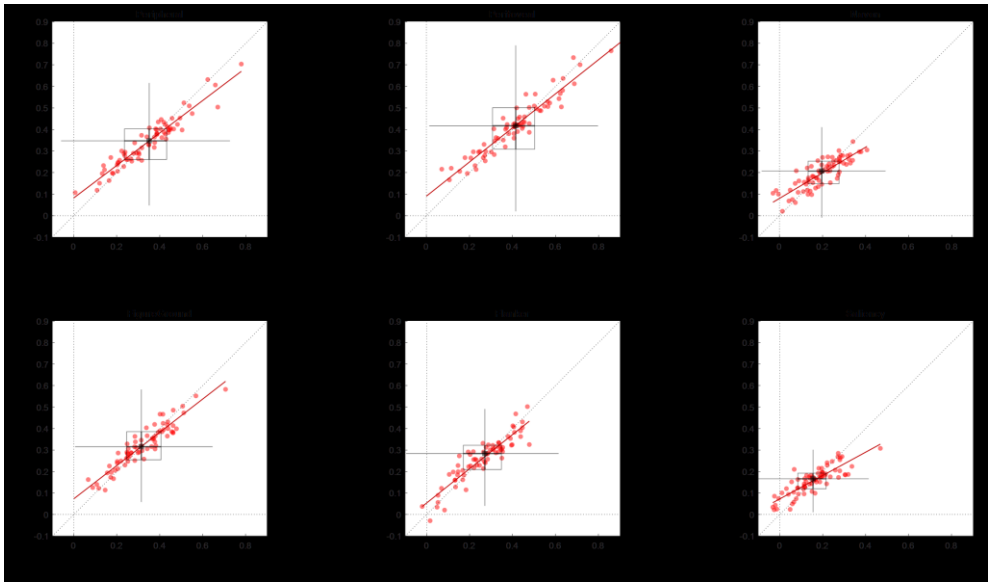

Figure A.14. Comparison of Stroop effects between LMM and RCA.
Each scatterplot shows the participants' Stroop effects (red circles) yielded by the LMM (y axis) and RCA (x axis) analytical approaches. The two-dimensional boxplot represents the corresponding median values (black square at the center of the box), interquartile ranges (height and width of the box, respectively), and dispersion outside the extreme quartiles (vertical and horizontal whiskers, respectively, indicating 1.5 times the interquartile range). The red solid line represents the corresponding linear regression line. The diagonal dotted line represents the equivalent line.

Table A.28. Comparison of Stroop effects between LMM and RCA – regression analysis, intercept vs 0

Task	Estimate	SE	$t_{(70)}$	p
Peripheral	0.082	0.011	7.72	< .0001
Perifoveal	0.091	0.014	6.62	< .0001
Navon	0.080	0.010	7.94	< .0001
FigureGround	0.073	0.012	6.08	< .0001
Flanker	0.054	0.012	4.37	< .0001
Saliency	0.073	0.008	9.44	< .0001

Table A.29. Comparison of Stroop effects between LMM and RCA – regression analysis, slope vs 1

Task	Estimate	SE	$t_{(70)}$	p
Peripheral	0.755	0.028	-8.63	< .0001
Perifoveal	0.792	0.031	-6.66	< .0001
Navon	0.594	0.046	-8.83	< .0001
FigureGround	0.773	0.035	-6.41	< .0001
Flanker	0.796	0.043	-4.77	< .0001
Saliency	0.544	0.042	-10.95	< .0001

Table A.30. Meng's test comparing LMM-GLM vs RCA-GLM correlations of Stroop effects

Task	z	p
Peripheral	5.269	< .0001
Perifoveal	2.905	0.0037
Navon	6.927	< .0001
FigureGround	5.774	< .0001
Flanker	8.498	< .0001
Saliency	6.234	< .0001

A.6.2. RCA on lnRTs

A.6.2.1. Results

See the "RCA - lnRT" section in the ManyStroopScript.m file.

Table A.31. RCA results, coefficients statistics

Effect	*Estimate*	*SE*	*t*	*DF*	*p*
(Intercept)	6.3040	0.0231	273.12	71	< .0001
Trial	-0.0241	0.0022	-11.17	71	< .0001
preRT	0.0357	0.0028	12.64	71	< .0001
$TASK_{Perifov}$	-0.0973	0.0184	-5.28	71	< .0001
$TASK_{Navon}$	-0.0374	0.0168	-2.22	71	0.0295
$TASK_{FG}$	-0.1025	0.0173	-5.91	71	< .0001
$TASK_{Flanker}$	-0.0677	0.0175	-3.87	71	0.0002
$TASK_{Saliency}$	-0.1193	0.0159	-7.50	71	< .0001
hResp	-0.0167	0.0043	-3.89	71	0.0002
vResp	-0.0335	0.0042	-8.04	71	< .0001
postERR	0.1173	0.0117	10.00	71	< .0001
$CONG_{Inc}$	0.2054	0.0116	17.65	71	< .0001
$CONG_{Inc}$:$TASK_{Perifov}$	0.0175	0.0095	1.85	71	0.0679
$CONG_{Inc}$:$TASK_{Navon}$	-0.0954	0.0124	-7.70	71	< .0001
$CONG_{Inc}$:$TASK_{FG}$	-0.0444	0.0140	-3.17	71	0.0023
$CONG_{Inc}$:$TASK_{Flanker}$	-0.0741	0.0135	-5.48	71	< .0001
$CONG_{Inc}$:$TASK_{Saliency}$	-0.1328	0.0125	-10.61	71	< .0001

Notes: see Table A.2 for conventions

A.6.2.2. Residual analysis

See the "RCA – lnRT – Inspect fit" section in the ManyStroopScript.m file

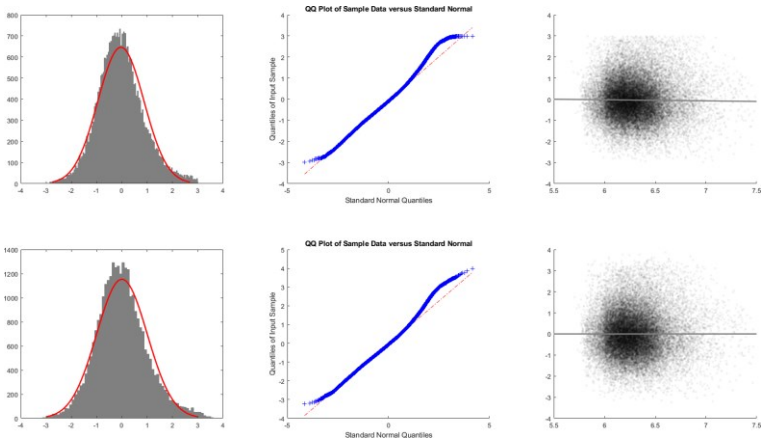

Figure A.15. Inspection of residuals for the RCA analysis on lnRTs.
The figure shows the results of the analysis of the residuals for the RCA analysis on lnRTs for the final model both before (upper panels) and after (bottom panels) excluding observations with absolute standardized residuals greater than 3. Left: histogram of the standardized residuals; the superimposed red curve represents the normal density function fitted to the data. Middle: quantile-quantile plot for the standardized residuals. Right: scatterplot of the fitted data (x) vs. the standardized residuals (y) for the visual inspection of the homoscedasticity; the gray line represents the corresponding linear regression line.

A.6.2.3. Post-hoc

See the "RCA – lnRT – Post-hoc comparisons" section in the ManyStroopScript.m file

Table A.32. RCA on lnRTs, post-hoc pairwise comparisons of Stroop effects between tasks

Task1	Task2	F	DF1	DF2	p
Peripheral	**Perifoveal**	3.44	1	71	0.0679
Peripheral	**Navon**	59.30	1	71	< .0001
Peripheral	**FigureGround**	10.03	1	71	0.0023
Peripheral	**Flanker**	30.01	1	71	< .0001
Peripheral	**Saliency**	112.58	1	71	< .0001
Perifoveal	**Navon**	97.75	1	71	< .0001
Perifoveal	**FigureGround**	23.84	1	71	< .0001
Perifoveal	**Flanker**	49.87	1	71	< .0001
Perifoveal	**Saliency**	145.70	1	71	< .0001
Navon	**FigureGround**	29.74	1	71	< .0001
Navon	**Flanker**	5.21	1	71	0.0254
Navon	**Saliency**	22.58	1	71	< .0001
FigureGround	**Flanker**	28.13	1	71	< .0001
FigureGround	**Saliency**	196.59	1	71	< .0001
Flanker	**Saliency**	71.04	1	71	< .0001

Notes: p values are computed using the Satterthwaite's approximation.

A.6.2.4. Stroop effects comparison, RCA vs GLM

See the "Compare GLM- and RCA-based Stroop effects - lnRT" section in the ManyStroopScript.m file

Table A.33. Comparison of Stroop effects between RCA and GLM

Task	r	$t_{(71)}$	p	d
Peripheral	0.973	3.930	0.0002	0.463
Perifoveal	0.974	4.165	0.0001	0.491
Navon	0.951	-0.571	0.5701	-0.067
FigureGround	0.955	4.272	0.0001	0.503
Flanker	0.965	3.882	0.0002	0.458
Saliency	0.956	2.387	0.0196	0.281

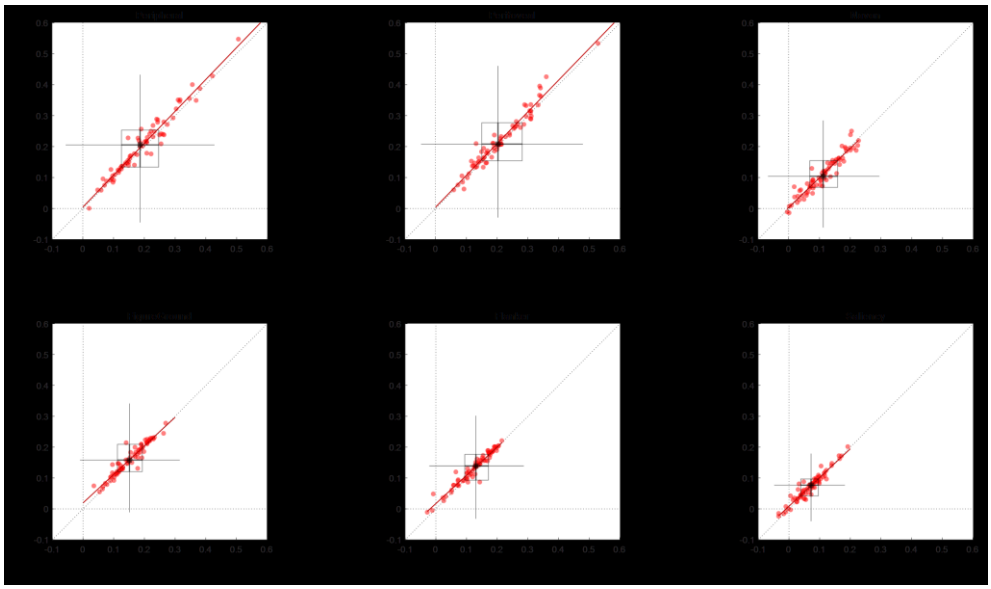

Figure A.16. Comparison of Stroop effects between RCA and GLM.
Each scatterplot shows the participants' Stroop effects (red circles) yielded by the RCA (y axis) and GLM (x axis) analytical approaches. The two-dimensional boxplot represents the corresponding median values (black square at the center of the box), interquartile ranges (height and width of the box, respectively), and dispersion outside the extreme quartiles (vertical and horizontal whiskers, respectively, indicating 1.5 times the interquartile range). The red solid line represents the corresponding linear regression line. The diagonal dotted line represents the equivalent line.

Table A.34. Comparison of Stroop effects between RCA and GLM – regression analysis, intercept vs 0

Task	Estimate	SE	$t_{(70)}$	p
Peripheral	0.005	0.006	0.72	0.4714
Perifoveal	0.005	0.007	0.71	0.4820
Navon	0.004	0.005	0.79	0.4326
FigureGround	0.019	0.006	3.51	0.0008
Flanker	0.017	0.004	4.25	0.0001
Saliency	0.009	0.003	3.04	0.0033

Table A.35. Comparison of Stroop effects between RCA and GLM – regression analysis, slope vs 1

Task	Estimate	SE	$t_{(70)}$	p
Peripheral	1.031	0.029	1.07	0.2895
Perifoveal	1.026	0.028	0.91	0.3666
Navon	0.955	0.037	-1.21	0.2310
FigureGround	0.924	0.034	-2.21	0.0305
Flanker	0.916	0.030	-2.84	0.0059
Saliency	0.931	0.034	-2.02	0.0468

A.6.2.5. Stroop effects comparison, LMM vs RCA

See the "Compare RCA- and LMM-based Stroop effects - lnRT" section in the ManyStroopScript.m file

Table A.36. Comparison of Stroop effects between LMM and RCA

Task	r	$t_{(71)}$	p	d
Peripheral	0.974	0.022	0.9827	0.003
Perifoveal	0.956	0.104	0.9175	0.012
Navon	0.871	-0.347	0.7294	-0.041
FigureGround	0.868	-0.279	0.7811	-0.033
Flanker	0.858	-0.036	0.9713	-0.004
Saliency	0.834	0.731	0.4674	0.086

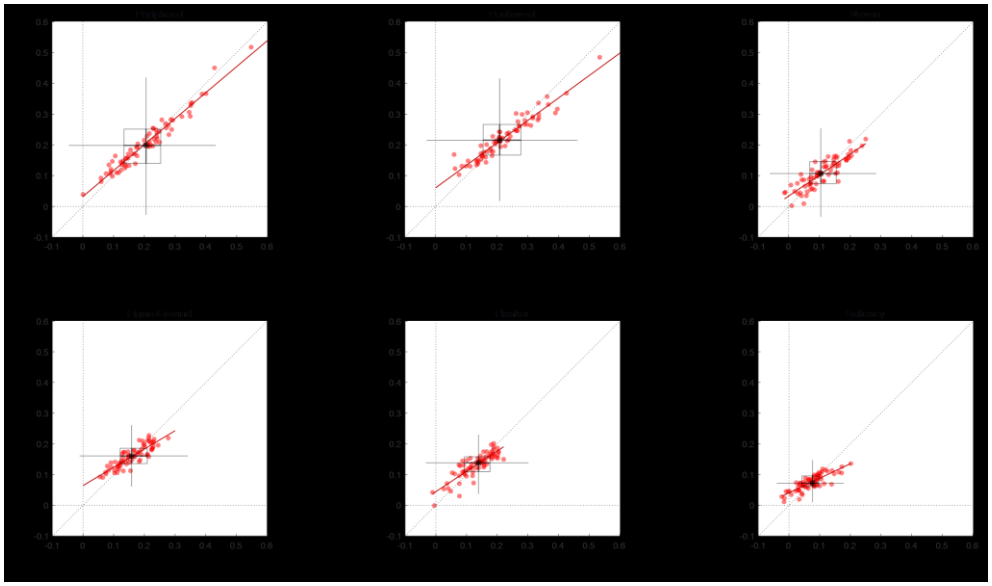

Figure A.17. Comparison of Stroop effects between LMM and RCA.
Each scatterplot shows the participants' Stroop effects (red circles) yielded by the LMM (y axis) and RCA (x axis) analytical approaches. The two-dimensional boxplot represents the corresponding median values (black square at the center of the box), interquartile ranges (height and width of the box, respectively), and dispersion outside the extreme quartiles (vertical and horizontal whiskers, respectively, indicating 1.5 times the interquartile range). The red solid line represents the corresponding linear regression line. The diagonal dotted line represents the equivalent line.

Table A.37. Comparison of Stroop effects between LMM and RCA – regression analysis, intercept vs 0

Task	Estimate	SE	$t_{(70)}$	p
Peripheral	0.032	0.005	6.06	< .0001
Perifoveal	0.060	0.006	9.43	< .0001
Navon	0.034	0.006	5.90	< .0001
FigureGround	0.064	0.007	9.36	< .0001
Flanker	0.044	0.007	6.64	< .0001
Saliency	0.041	0.003	12.68	< .0001

Table A.38. Comparison of Stroop effects between LMM and RCA – regression analysis, slope vs 1

Task	Estimate	SE	$t_{(70)}$	p
Peripheral	0.844	0.023	-6.70	< .0001
Perifoveal	0.730	0.027	-10.11	< .0001
Navon	0.680	0.046	-6.98	< .0001
FigureGround	0.595	0.041	-9.95	< .0001
Flanker	0.661	0.047	-7.17	< .0001
Saliency	0.474	0.037	-14.06	< .0001

Table A.39. Meng's test comparing LMM-GLM vs RCA-GLM correlations of Stroop effects

Task	z	p
Peripheral	3.158	0.0016
Perifoveal	2.146	0.0319
Navon	5.227	< .0001
FigureGround	4.548	< .0001
Flanker	5.204	< .0001
Saliency	5.522	< .0001

A.6.3. RCA on RTs

A.6.3.1. Results

See the "RCA - RT" section in the ManyStroopScript.m file.

Table A.40. RCA results, coefficients statistics

Effect	*Estimate*	*SE*	*t*	*DF*	*p*
(Intercept)	565.36	14.49	39.01	71	< .0001
Trial	-14.79	1.46	-10.10	71	< .0001
preRT	20.89	2.10	9.96	71	< .0001
$TASK_{Perifov}$	-46.81	11.28	-4.15	71	0.0001
$TASK_{Navon}$	-24.44	11.18	-2.19	71	0.0322
$TASK_{FG}$	-60.83	11.29	-5.39	71	< .0001
$TASK_{Flanker}$	-41.36	12.01	-3.44	71	0.0010
$TASK_{Saliency}$	-64.67	10.64	-6.08	71	< .0001
hResp	-9.55	2.58	-3.70	71	0.0004
vResp	-19.62	2.72	-7.21	71	< .0001
postERR	74.44	9.58	7.77	71	< .0001
$CONG_{Inc}$	133.24	10.95	12.17	71	< .0001
$CONG_{Inc}$:$TASK_{Perifov}$	-6.63	9.17	-0.72	71	0.4722
$CONG_{Inc}$:$TASK_{Navon}$	-68.90	10.97	-6.28	71	< .0001
$CONG_{Inc}$:$TASK_{FG}$	-50.16	11.42	-4.39	71	< .0001
$CONG_{Inc}$:$TASK_{Flanker}$	-65.72	11.48	-5.73	71	< .0001
$CONG_{Inc}$:$TASK_{Saliency}$	-99.53	10.89	-9.14	71	< .0001

Notes: see Table A.2 for conventions

A.6.3.2. Residual analysis

See the "RCA – RT – Inspect fit" section in the ManyStroopScript.m file

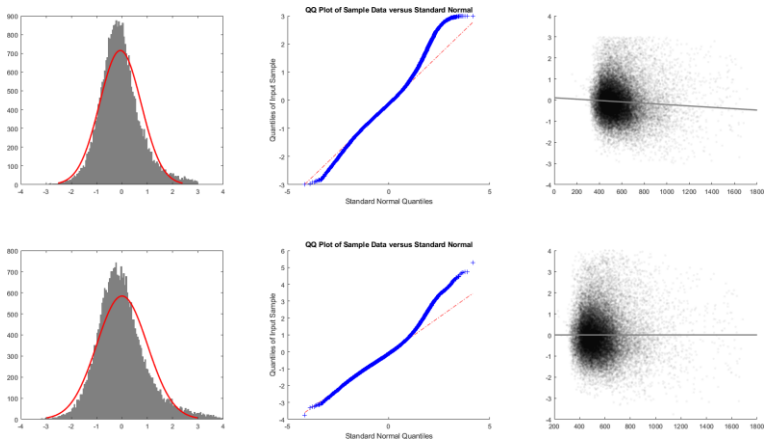

Figure A.18. Inspection of residuals for the RCA analysis on RTs.
The figure shows the results of the analysis of the residuals for the RCA analysis on RTs for the final model both before (upper panels) and after (bottom panels) excluding observations with absolute standardized residuals greater than 3.
Left: histogram of the standardized residuals; the superimposed red curve represents the normal density function fitted to the data. Middle: quantile-quantile plot for the standardized residuals. Right: scatterplot of the fitted data (x) vs. the standardized residuals (y) for the visual inspection of the homoscedasticity; the gray line represents the corresponding linear regression line.

A.6.3.3. Post-hoc

See the "RCA – RT – Post-hoc comparisons" section in the ManyStroopScript.m file

Table A.41. RCA on RTs, post-hoc pairwise comparisons of Stroop effects between tasks

Task1	Task2	F	DF1	DF2	p
Peripheral	**Perifoveal**	0.52	1	71	0.4722
Peripheral	**Navon**	39.43	1	71	< .0001
Peripheral	**FigureGround**	19.31	1	71	< .0001
Peripheral	**Flanker**	32.78	1	71	< .0001
Peripheral	**Saliency**	83.46	1	71	< .0001
Perifoveal	**Navon**	44.31	1	71	< .0001
Perifoveal	**FigureGround**	22.53	1	71	< .0001
Perifoveal	**Flanker**	36.53	1	71	< .0001
Perifoveal	**Saliency**	96.62	1	71	< .0001
Navon	**FigureGround**	10.98	1	71	0.0015
Navon	**Flanker**	0.33	1	71	0.5683
Navon	**Saliency**	34.95	1	71	< .0001
FigureGround	**Flanker**	22.54	1	71	< .0001
FigureGround	**Saliency**	209.56	1	71	< .0001
Flanker	**Saliency**	75.26	1	71	< .0001

Notes: p values are computed using the Satterthwaite's approximation.

A.6.3.4. Stroop effects comparison, RCA vs GLM

See the "Compare GLM- and RCA-based Stroop effects - RT" section in the ManyStroopScript.m file

Table A.42. Comparison of Stroop effects between RCA and GLM

Task	r	$t_{(71)}$	p	d
Peripheral	0.958	1.082	0.2829	0.128
Perifoveal	0.956	-1.002	0.3199	-0.118
Navon	0.937	-3.420	0.0010	-0.403
FigureGround	0.871	2.407	0.0187	0.284
Flanker	0.866	2.466	0.0161	0.291
Saliency	0.942	1.277	0.2058	0.150

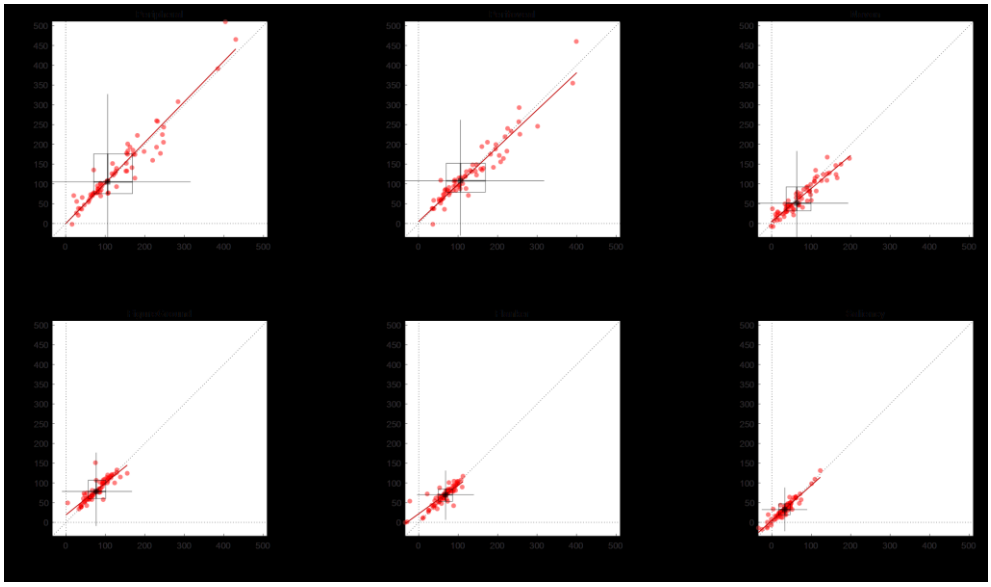

Figure A.19. Comparison of Stroop effects between RCA and GLM.
Each scatterplot shows the participants' Stroop effects (red circles) yielded by the RCA (y axis) and GLM (x axis) analytical approaches. The two-dimensional boxplot represents the corresponding median values (black square at the center of the box), interquartile ranges (height and width of the box, respectively), and dispersion outside the extreme quartiles (vertical and horizontal whiskers, respectively, indicating 1.5 times the interquartile range). The red solid line represents the corresponding linear regression line. The diagonal dotted line represents the equivalent line.

Table A.43. Comparison of Stroop effects between RCA and GLM – regression analysis, intercept vs 0

Task	Estimate	SE	$t_{(70)}$	p
Peripheral	0.05	5.74	0.01	0.9931
Perifoveal	4.96	5.23	0.95	0.3461
Navon	4.91	3.18	1.54	0.1274
FigureGround	19.03	4.61	4.13	0.0001
Flanker	21.89	3.50	6.25	< .0001
Saliency	4.89	1.61	3.04	0.0033

Table A.44. Comparison of Stroop effects between RCA and GLM – regression analysis, slope vs 1

Task	Estimate	SE	$t_{(70)}$	p
Peripheral	1.026	0.037	0.70	0.4832
Perifoveal	0.941	0.035	-1.71	0.0909
Navon	0.837	0.037	-4.36	< .0001
FigureGround	0.811	0.055	-3.44	0.0010
Flanker	0.723	0.050	-5.53	< .0001
Saliency	0.892	0.038	-2.85	0.0057

A.6.3.5. Stroop effects comparison, LMM vs RCA

See the "Compare RCA- and LMM-based Stroop effects - RT" section in the ManyStroopScript.m file

Table A.45. Comparison of Stroop effects between LMM and RCA

Task	r	$t_{(71)}$	p	d
Peripheral	0.983	-1.534	0.1295	-0.181
Perifoveal	0.973	0.436	0.6643	0.051
Navon	0.841	0.382	0.7034	0.045
FigureGround	0.767	-0.110	0.9125	-0.013
Flanker	0.633	0.187	0.8520	0.022
Saliency	0.776	0.650	0.5178	0.077

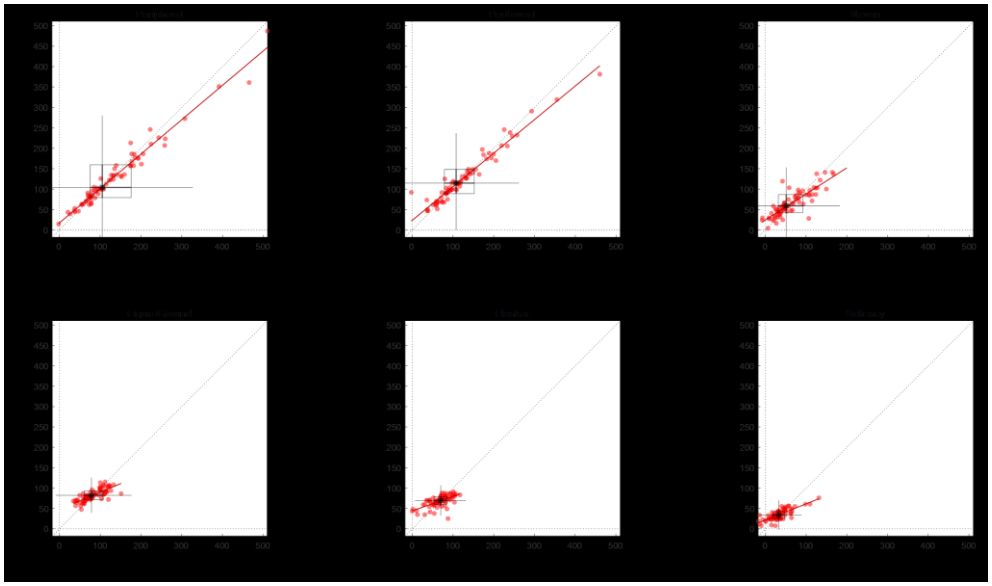

Figure A.20. Comparison of Stroop effects between LMM and RCA.
Each scatterplot shows the participants' Stroop effects (red circles) yielded by the LMM (y axis) and RCA (x axis) analytical approaches. The two-dimensional boxplot represents the corresponding median values (black square at the center of the box), interquartile ranges (height and width of the box, respectively), and dispersion outside the extreme quartiles (vertical and horizontal whiskers, respectively, indicating 1.5 times the interquartile range). The red solid line represents the corresponding linear regression line. The diagonal dotted line represents the equivalent line.

Table A.46. Comparison of Stroop effects between LMM and RCA – regression analysis, intercept vs 0

Task	Estimate	SE	$t_{(70)}$	p
Peripheral	17.21	3.06	5.62	< .0001
Perifoveal	23.46	3.44	6.81	< .0001
Navon	24.26	3.76	6.45	< .0001
FigureGround	48.02	3.67	13.10	< .0001
Flanker	44.04	3.73	11.80	< .0001
Saliency	21.73	1.64	13.27	< .0001

Table A.47. Comparison of Stroop effects between LMM and RCA – regression analysis, slope vs 1

Task	Estimate	SE	$t_{(70)}$	p
Peripheral	0.843	0.019	-8.32	< .0001
Perifoveal	0.823	0.023	-7.60	< .0001
Navon	0.639	0.049	-7.36	< .0001
FigureGround	0.419	0.042	-13.85	< .0001
Flanker	0.354	0.052	-12.48	< .0001
Saliency	0.396	0.038	-15.70	< .0001

Table A.48. Meng's test comparing LMM-GLM vs RCA-GLM correlations of Stroop effects

Task	z	p
Peripheral	1.984	0.0472
Perifoveal	0.293	0.7695
Navon	4.564	< .0001
FigureGround	2.544	0.0110
Flanker	3.250	0.0012
Saliency	5.466	< .0001

A.6.4. Control analysis, reduced (i.e., minimal) RCA on iRTs

A.6.4.1. Results

See the "RCA - iRT - Control analysis (without confounders)" section in the ManyStroopScript.m file.

Table A.49. RCA results, coefficients statistics

Effect	*Estimate*	*SE*	*t*	*DF*	*p*
(Intercept)	-1.8796	0.0469	-40.11	71	< .0001
$TASK_{Perifov}$	-0.2291	0.0368	-6.22	71	< .0001
$TASK_{Navon}$	-0.0825	0.0331	-2.49	71	0.0152
$TASK_{FG}$	-0.2214	0.0336	-6.59	71	< .0001
$TASK_{Flanker}$	-0.1495	0.0331	-4.52	71	< .0001
$TASK_{Saliency}$	-0.2905	0.0322	-9.03	71	< .0001
$CONG_{Inc}$	0.3261	0.0163	20.00	71	< .0001
$CONG_{Inc}$:$TASK_{Perifov}$	0.0691	0.0156	4.42	71	< .0001
$CONG_{Inc}$:$TASK_{Navon}$	-0.1385	0.0175	-7.91	71	< .0001
$CONG_{Inc}$:$TASK_{FG}$	-0.0165	0.0209	-0.79	71	0.4325
$CONG_{Inc}$:$TASK_{Flanker}$	-0.0746	0.0196	-3.81	71	< .0001
$CONG_{Inc}$:$TASK_{Saliency}$	-0.1754	0.0176	-9.96	71	< .0001

Notes: see Table A.2 for conventions

A.6.1.2. Residual analysis

See the "RCA - iRT - Control analysis (without confounders)" section in the ManyStroopScript.m file.

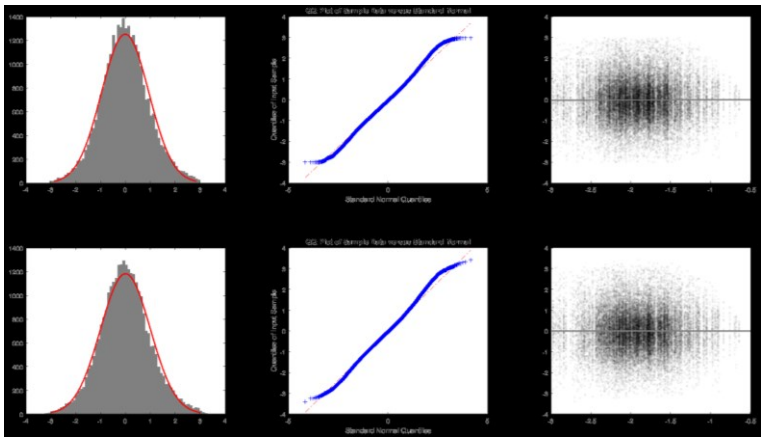

Figure A.21. Inspection of residuals for the control RCA analysis (with the reduced model) on iRTs.
The figure shows the results of the analysis of the residuals for the RCA analysis on iRTs for the reduced model both before (upper panels) and after (bottom panels) excluding observations with absolute standardized residuals greater than 3.
Left: histogram of the standardized residuals; the superimposed red curve represents the normal density function fitted to the data. Middle: quantile-quantile plot for the standardized residuals. Right: scatterplot of the fitted data (x) vs. the standardized residuals (y) for the visual inspection of the homoscedasticity; the gray line represents the corresponding linear regression line.

A.6.4.3. Stroop effects comparison, full vs reduced RCA

See the "RCA - iRT - Control analysis (without confounders)" section in the ManyStroopScript.m file.

Table A.50. Comparison of Stroop effects between RCA and GLM

Task	r	$t_{(71)}$	p	d
Peripheral	0.9869	6.999	< .0001	0.825
Perifoveal	0.9885	5.313	< .0001	0.626
Navon	0.9767	3.636	0.0005	0.428
FigureGround	0.9900	4.815	< .0001	0.567
Flanker	0.9924	5.746	< .0001	0.677
Saliency	0.9814	2.296	0.0246	0.271

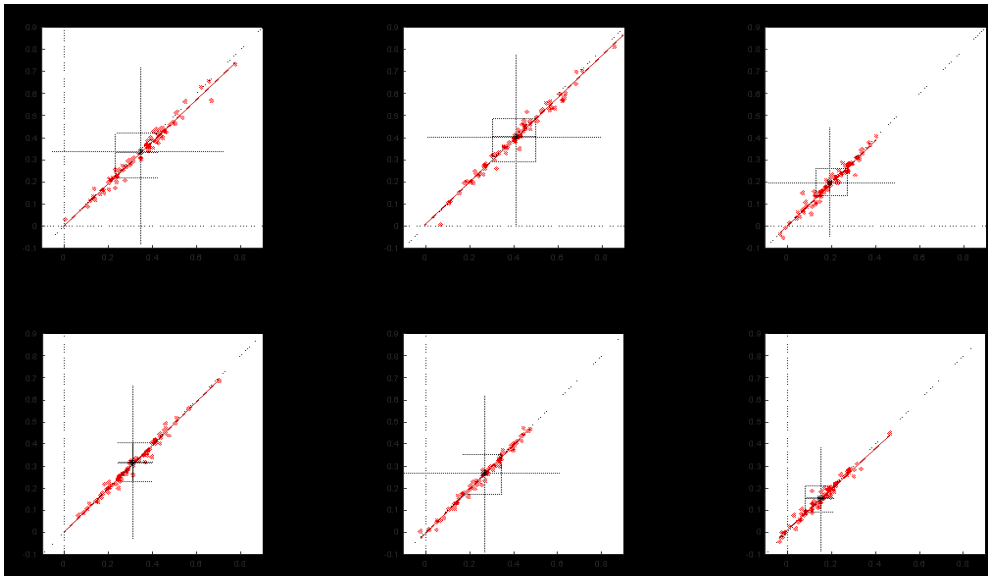

Figure A.22. Comparison of Stroop effects between full and reduced RCA.
Each scatterplot shows the participants' Stroop effects (red circles) yielded by the reduced (y axis) and full RCA (x axis) analytical approaches. The two-dimensional boxplot represents the corresponding median values (black square at the center of the box), interquartile ranges (height and width of the box, respectively), and dispersion outside the extreme quartiles (vertical and horizontal whiskers, respectively, indicating 1.5 times the interquartile range). The red solid line represents the corresponding linear regression line. The diagonal dotted line represents the equivalent line.

A.7. Correlational analysis, Stroop effects

A.7.1. GLM

See the "Across-tasks Stroop correlations - GLM" section in the ManyStroopScript.m file.

Table A.51. Between-tasks correlations of Stroop effects for each RT transformation

	Periph	Perifov	Navon	FG	Flanker	Saliency
iRT						
1 - Peripheral		0.627	0.264	0.052	0.149	0.198
2 - Perifoveal	6.734		0.260	0.139	0.092	0.156
3 - Navon	2.290	2.252		0.200	0.255	0.304
4 - FigureGround	0.438	1.171	1.704		0.720	0.491
5 - Flanker	1.263	0.769	2.210	8.688		0.443
6 - Saliency	1.694	1.318	2.674	4.713	4.137	
lnRT						
1 - Peripheral		0.655	0.224	-0.156	-0.078	0.089
2 - Perifoveal	7.253		0.149	-0.086	-0.152	-0.065
3 - Navon	1.924	1.260		0.053	0.091	0.263
4 - FigureGround	-1.324	-0.725	0.447		0.628	0.418
5 - Flanker	-0.656	-1.285	0.766	6.753		0.324
6 - Saliency	0.748	-0.548	2.277	3.848	2.864	
RT						
1 - Peripheral		0.612	0.231	-0.148	-0.173	0.156
2 - Perifoveal	6.473		0.155	-0.013	-0.195	-0.007
3 - Navon	1.983	1.309		0.066	-0.015	0.301
4 - FigureGround	-1.251	-0.109	0.553		0.499	0.402
5 - Flanker	-1.473	-1.661	-0.125	4.822		0.241
6 - Saliency	1.326	-0.058	2.642	3.677	2.078	

Notes: for each RT transformation, the upper triangles show the correlation coefficient, the lower triangles show the corresponding t values. The cells with a darker and lighter gray shade indicate significant correlations that did and did not survive the FDR correction for multiple correlations, respectively.

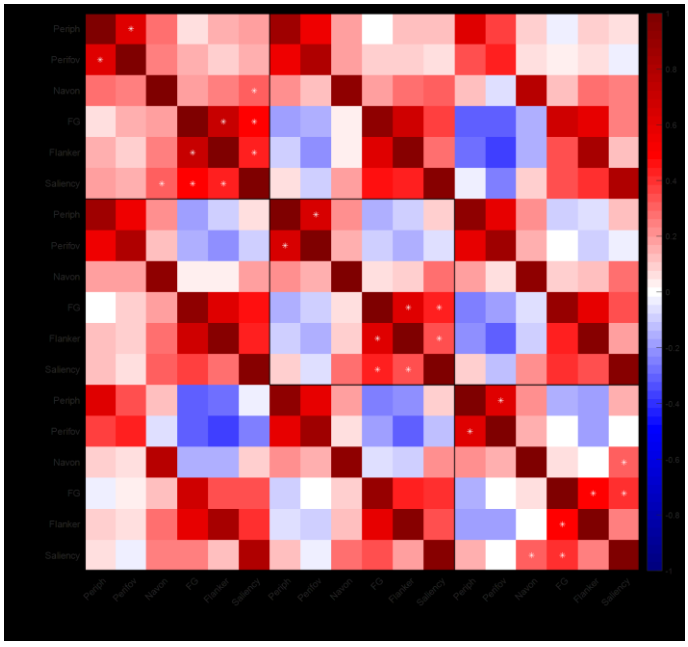

Figure A.23. Stroop effects correlations. The figure shows the correlation matrix for the Stroop effects across the six tasks and the three RT transformations. The white asterisks indicate the FDR-corrected significant correlations between task pairs within each RT transformation.

A.7.2. LMM

See the "Across-tasks Stroop correlations - LMM" section in the ManyStroopScript.m file.

Table A.52. Between-tasks correlations of Stroop effects for each RT transformation

	Periph	Perifov	Navon	FG	Flanker	Saliency
iRT						
1 - Peripheral		0.860	0.398	0.079	0.208	0.261
2 - Perifoveal	14.084		0.482	0.223	0.187	0.335
3 - Navon	3.634	4.608		0.212	0.304	0.472
4 - FigureGround	0.666	1.914	1.813		0.878	0.860
5 - Flanker	1.778	1.594	2.674	15.340		0.802
6 - Saliency	2.260	2.977	4.477	14.096	11.236	
lnRT						
1 - Peripheral		0.854	0.290	-0.282	-0.187	0.104
2 - Perifoveal	13.720		0.349	-0.222	-0.189	-0.110
3 - Navon	2.534	3.117		-0.051	0.046	0.246
4 - FigureGround	-2.461	-1.903	-0.426		0.809	0.718
5 - Flanker	-1.593	-1.611	0.389	11.517		0.693
6 - Saliency	0.872	-0.927	2.123	8.639	8.040	
RT						
1 - Peripheral		0.699	0.294	-0.215	-0.192	0.238
2 - Perifoveal	8.181		0.247	-0.097	-0.329	-0.048
3 - Navon	2.578	2.135		-0.044	-0.179	0.282
4 - FigureGround	-1.845	-0.819	-0.365		0.550	0.602
5 - Flanker	-1.637	-2.914	-1.519	5.509		0.567
6 - Saliency	2.054	-0.399	2.455	6.305	5.766	

Notes: for each RT transformation, the upper triangles show the correlation coefficient, the lower triangles show the corresponding t values. The cells with a darker and lighter gray shade indicate significant correlations that did and did not survive the FDR correction for multiple correlations, respectively.

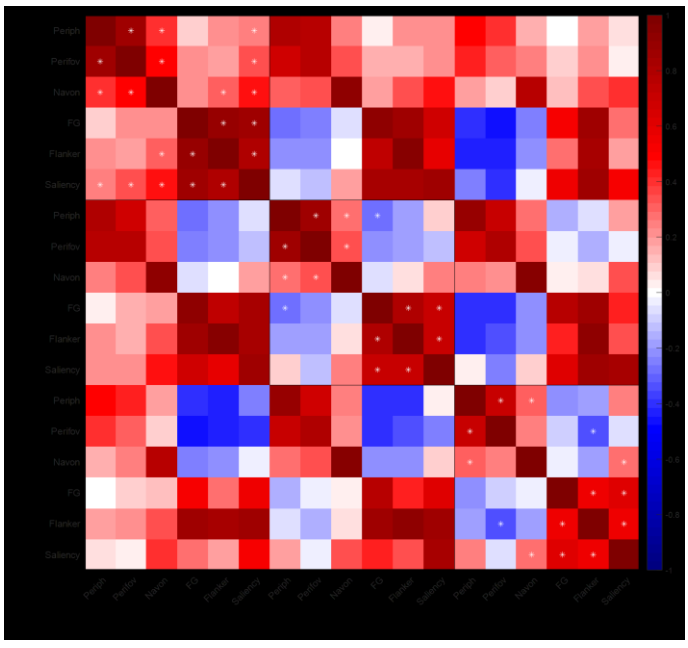

Figure A.24. Stroop effects correlations. The figure shows the correlation matrix for the Stroop effects across the six tasks and the three RT transformations. The white asterisks indicate the FDR-corrected significant correlations between task pairs within each RT transformation.

A.7.3. RCA

See the "Across-tasks Stroop correlations - RCA" section in the ManyStroopScript.m file.

Table A.53. Between-tasks correlations of Stroop effects for each RT transformation

	Periph	Perifov	Navon	FG	Flanker	Saliency
iRT						
1 - Peripheral		0.594	0.246	0.016	0.124	0.162
2 - Perifoveal	6.183		0.287	0.172	0.110	0.132
3 - Navon	2.127	2.503		0.133	0.208	0.296
4 - FigureGround	0.132	1.464	1.127		0.720	0.485
5 - Flanker	1.046	0.923	1.783	8.679		0.425
6 - Saliency	1.370	1.112	2.594	4.635	3.923	
lnRT						
1 - Peripheral		0.644	0.201	-0.174	-0.059	0.062
2 - Perifoveal	7.048		0.230	-0.080	-0.116	-0.105
3 - Navon	1.717	1.974		0.004	0.034	0.244
4 - FigureGround	-1.482	-0.671	0.035		0.582	0.393
5 - Flanker	-0.499	-0.977	0.283	5.992		0.286
6 - Saliency	0.522	-0.881	2.103	3.577	2.501	
RT						
1 - Peripheral		0.595	0.222	0.001	-0.042	0.159
2 - Perifoveal	6.188		0.212	0.143	-0.084	0.039
3 - Navon	1.902	1.814		0.093	0.094	0.236
4 - FigureGround	0.012	1.208	0.785		0.451	0.419
5 - Flanker	-0.355	-0.702	0.791	4.225		0.182
6 - Saliency	1.349	0.330	2.028	3.858	1.546	

Notes: for each RT transformation, the upper triangles show the correlation coefficient, the lower triangles show the corresponding t values. The cells with a darker and lighter gray shade indicate significant correlations that did and did not survive the FDR correction for multiple correlations, respectively.

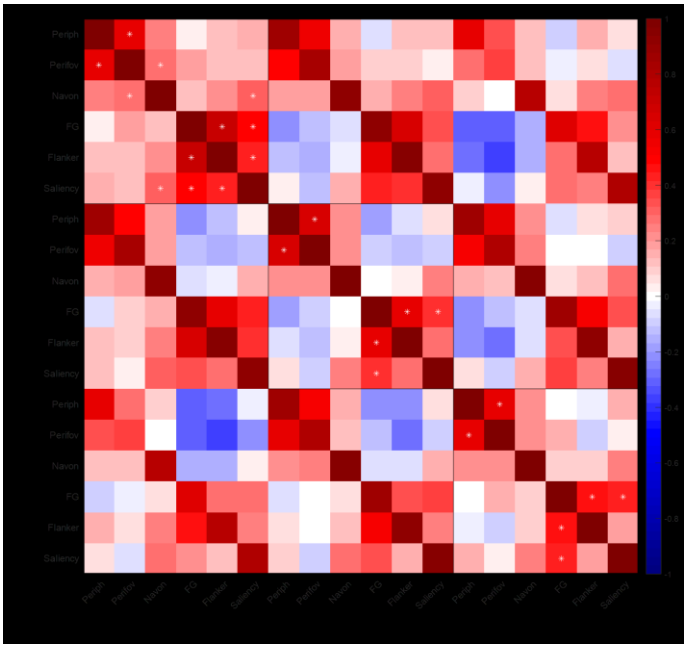

Figure A.25. Stroop effects correlations. The figure shows the correlation matrix for the Stroop effects across the six tasks and the three RT transformations. The white asterisks indicate the FDR-corrected significant correlations between task pairs within each RT transformation.

A.7.4. Exploratory factor analysis on Stroop effects

See the "ManyStroop_IC_EFA.omv" Jamovi file

Table A.54. Exploratory factor analyses on Stroop effects

	GLM		LMM		RCA	
Task	**F1**	**F2**	**F1**	**F2**	**F1**	**F2**
Peripheral	-0.02	**0.85**	-0.04	**0.88**	-0.04	**0.79**
Perifoveal	0.01	**0.73**	0.01	**0.97**	0.04	**0.74**
Navon	0.26	0.30	0.24	**0.43**	0.19	**0.33**
FigureGround	**0.88**	-0.05	**0.97**	-0.09	**0.89**	-0.05
Flanker	**0.81**	0.01	**0.90**	-0.01	**0.79**	0.02
Saliency	**0.55**	0.15	**0.89**	0.13	**0.53**	0.14

Notes: Factor loadings greater than .3 (in absolute terms) are indicated in bold.

A.8. Internal reliability of the Stroop effects

See the "Split-half reliability" section in the ManyStroopScript.m file.

Table A.55. Spearman-Brown-corrected split-half correlations

	GLM			LMM			RCA		
	Median	95%CI_l	95%Ci_u	Median	95%CI_l	95%Ci_u	Median	95%CI_l	95%Ci_u
iRT									
Peripheral	0.720	0.598	0.809	0.812	0.715	0.876	0.768	0.679	0.839
Perifoveal	0.649	0.482	0.773	0.814	0.699	0.884	0.726	0.594	0.814
Navon	0.392	0.129	0.584	0.762	0.558	0.864	0.470	0.227	0.638
FigureGround	0.747	0.644	0.822	0.927	0.864	0.966	0.754	0.651	0.835
Flanker	0.776	0.676	0.849	0.950	0.907	0.980	0.785	0.694	0.857
Saliency	0.445	0.228	0.606	0.767	0.570	0.867	0.515	0.286	0.668
lnRT									
Peripheral	0.733	0.595	0.824	0.838	0.736	0.897	0.785	0.693	0.853
Perifoveal	0.664	0.502	0.781	0.805	0.686	0.880	0.740	0.600	0.827
Navon	0.460	0.236	0.623	0.773	0.606	0.867	0.534	0.315	0.686
FigureGround	0.598	0.420	0.724	0.814	0.656	0.903	0.600	0.404	0.735
Flanker	0.644	0.454	0.763	0.900	0.748	0.958	0.658	0.467	0.776
Saliency	0.395	0.154	0.578	0.560	0.122	0.777	0.460	0.212	0.633
RT									
Peripheral	0.793	0.671	0.873	0.876	0.771	0.931	0.835	0.735	0.896
Perifoveal	0.769	0.612	0.855	0.851	0.728	0.923	0.803	0.652	0.883
Navon	0.541	0.328	0.699	0.787	0.588	0.884	0.612	0.393	0.750
FigureGround	0.475	0.132	0.665	0.319	-0.375	0.861	0.475	0.134	0.682
Flanker	0.417	-0.104	0.661	0.728	-0.282	0.941	0.453	-0.110	0.687
Saliency	0.414	0.146	0.617	0.100	-0.597	0.696	0.473	0.161	0.653

Notes: 95%CI_l and 95%CI_u, lower and upper bound of the non-parametric 95% confidence interval.

Table A.56. Spearman-Brown-corrected split-half correlations for the reduced LMM and RCA models on iRTs

	LMM			RCA		
	Median	95%CI$_l$	95%Ci$_u$	Median	95%CI$_l$	95%Ci$_u$
iRT						
Peripheral	0.750	0.645	0.828	0.718	0.606	0.798
Perifoveal	0.769	0.642	0.854	0.642	0.488	0.755
Navon	0.708	0.440	0.830	0.383	0.141	0.584
FigureGround	0.903	0.833	0.947	0.738	0.639	0.818
Flanker	0.933	0.872	0.966	0.768	0.670	0.841
Saliency	0.684	0.400	0.834	0.444	0.228	0.611

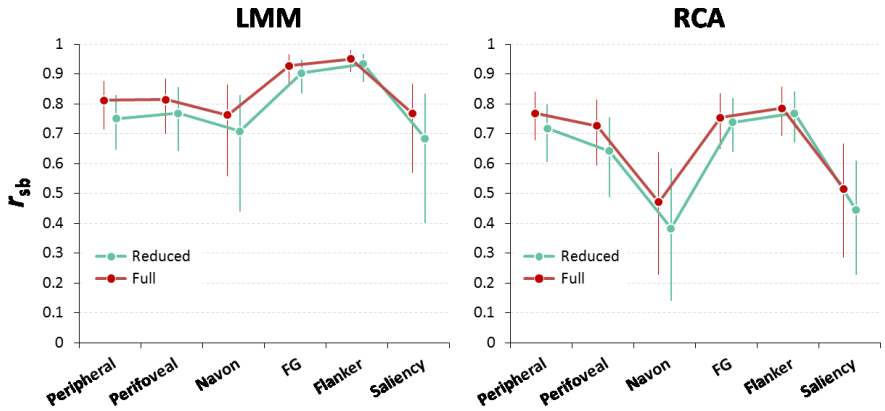

Figure A.26. Internal reliability of the iRT Stroop effects estimated by the multilevel approaches – Reduced vs full models.

The plot shows the median internal reliability estimates (r_{sb}) of the Stroop effects for each task (x axis) as a function of both the analytical approach (left panel: LMM, linear mixed-effect model; right panel: RCA, random coefficient analysis) and models (Reduced/minimal model not including the trial-level confounding predictors, in green, vs Full model, in red; see main text for details). The error bars represent the nonparametric 95% confidence interval.

APPENDIX B:

Supplementary Materials for Chapter 4

B.1. Experiment 1 – Peripheral Stroop task

B.1.1. Distributional analysis

See the "Distributional analysis" section in the PeripheralAnalysis.m file

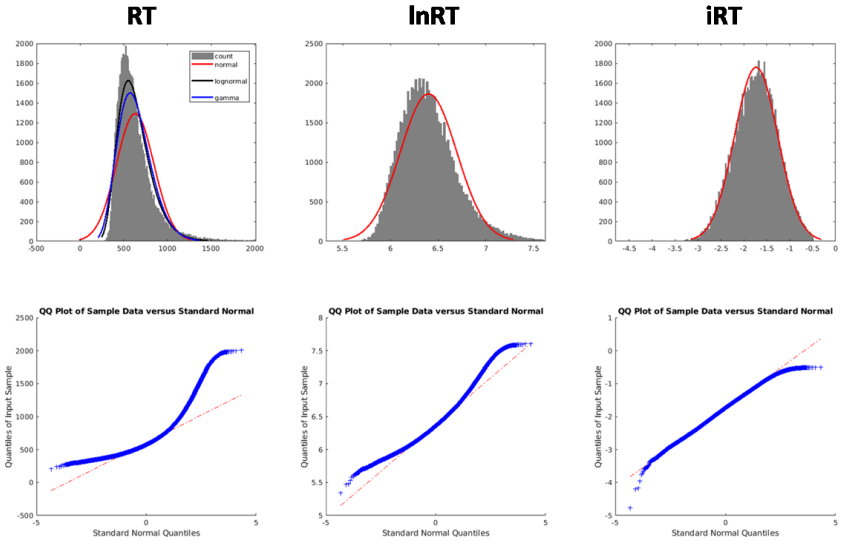

Figure B.1. Distributional analysis of participants' response times.
The top row shows the histograms of untransformed RT values (left panel), natural log-transformed RTs (lnRT, middle panel), and inverse-transformed RTs (iRT, right panel), computed as -1000/RT. The superimposed red curves represent the normal density function fitted to the data. The black and blue curves for the RT distribution represent the lognormal and gamma density functions fitted to the data, respectively. The number of bins was determined using the Freedman-Diaconis rule as implemented in the Matlab *histcounts* function. The bottom row shows the corresponding Q-Q plots.

B.1.2. Compliance checking

See the "Check for SS compliance" section in the PeripheralAnalysis.m file

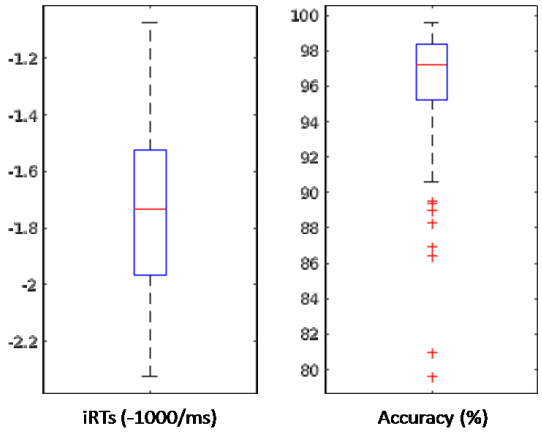

Figure B.2. Participants' overall performance.
The Figure shows the distribution of the participants' mean iRTs (left panel) and accuracy (right panel). The boxplots represent the median values (red line at the center of the box), interquartile ranges (box), and dispersion outside the extreme quartiles (whiskers indicating 1.5 times the interquartile range).

B.1.3. Descriptive statistics

See the "Descriptive statistics" section in the PeripheralAnalysis.m file.

Table B.1. Descriptive statistics and Stroop effects

	C		I		Stroop					
	M	***SD***	***M***	***SD***	***M***	***SD***	***t***	***p***	***d***	***Dom***
iRT	-1.934	0.314	-1.557	0.279	0.376	0.105	35.50	< .0001	3.586	100%
lnRT	6.279	0.172	6.500	0.190	0.221	0.063	34.98	< .0001	3.534	100%
RT	552.2	101.1	693.2	140.7	140.9	56.6	24.66	< .0001	2.491	100%
Acc	99.17%	1.66%	93.05%	6.33%	6.12%	5.58%	10.86	< .0001	1.097	100%

Notes: C, congruent; I, incongruent.

B.1.4. Results

B.1.4.1. LMM on iRTs, Continuous full model

See the "LMM" section in the PeripheralAnalysis.m file (the continuous full model is coded as "cFull" there).

Table B.2. LMM results, continuous full model (cFull), coefficients statistics

Coefficient	***Estimate***	***SE***	***t***	***DF***	***p***	d_s	d_r
(Intercept)	-1.9439	0.0350	-55.559	145.60	< .0001		
TrialTOT	-0.0923	0.0023	-40.030	1967.43	< .0001		
CON_0	0.3521	0.0123	28.620	179.86	< .0001	2.134	3.674
iRTpre	0.0551	0.0012	47.190	57392.28	< .0001		
hS	-0.0104	0.0028	-3.700	12850.75	0.0002		
vS	-0.0791	0.0027	-29.056	19753.88	< .0001		
hR	-0.0351	0.0026	-13.381	34201.64	< .0001		
vR	-0.1013	0.0026	-39.379	39671.65	< .0001		
LWb	-0.0086	0.0104	-0.825	97.51	0.4112		
ISb	-0.0135	0.0074	-1.827	435.59	0.0684		
PRSb	-0.0207	0.0059	-3.497	48890.40	0.0005		
PRb	-0.1234	0.0133	-9.256	49487.44	< .0001		
CON_0:LWb	0.0651	0.0081	8.071	101.81	< .0001	0.800	1.273
CON_0:ISb	0.0162	0.0102	1.590	939.28	0.1121	0.052	0.622
LWb:ISb	-0.0123	0.0109	-1.132	97.28	0.2606		
CON_0:LWb:ISb	0.0140	0.0120	1.167	94.08	0.2461	0.120	0.159

Notes: iRTpre, iRT at the previous trial; hS, horizontal coding of the stimulus position (i.e., the horizontal visual hemispace: right vs left); vS, vertical coding of the stimulus position (i.e., the vertical visual hemispace: upper vs lower); hR, horizontal coding of the response (i.e., the responding hand: right vs left); vR, vertical coding of the response (i.e., the responding finger: middle vs index); CON_0, Congruency (Incongruent trials); DF, degrees of freedom; d_s, effect size computed using the Satterthwaite's approximation of degrees of freedom; d_r, effect size computed using the by-participant random slopes. P values are computed using the Satterthwaite's approximation of degrees of freedom.

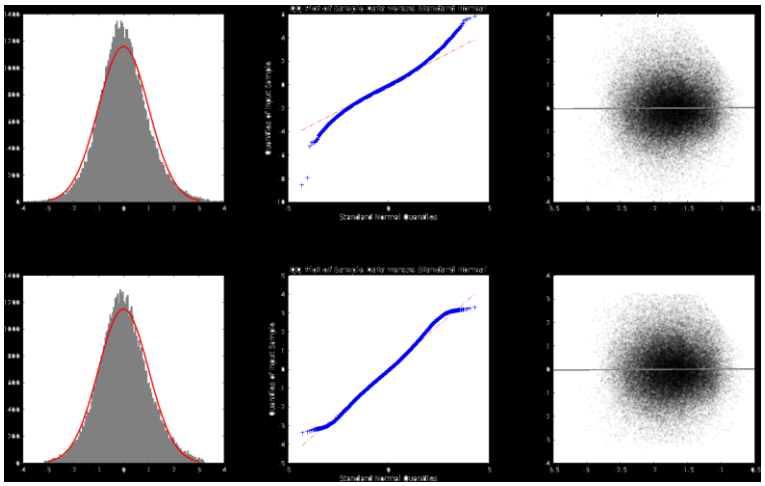

Figure B.3. Inspection of residuals for the LMM analysis on iRTs (cFull model).
The Figure shows the results of the analysis of the residuals for the LMM analysis on iRTs for the cFull model both before (upper panels) and after (bottom panels) excluding observations with absolute standardized residuals greater than 3. Left: histogram of the standardized residuals; the superimposed red curve represents the normal density function fitted to the data. Middle: quantile-quantile plot for the standardized residuals. Right: scatterplot of the fitted data (x) vs. the standardized residuals (y) for the visual inspection of the homoscedasticity; the gray line represents the corresponding linear regression line.

B.1.4.2. LMM on lnRTs, Continuous full model

See the "LMM" section in the PeripheralAnalysis.m file (the continuous full model is coded as "cFull" there).

Table B.3. LMM results on lnRTs, continuous full model (cFull), coefficients statistics

Coefficient	*Estimate*	*SE*	*t*	*DF*	*p*	d_s	d_r
(Intercept)	6.2634	0.0191	327.216	160.00	< .0001		
TrialTOT	-0.0577	0.0014	-40.422	3150.18	< .0001		
CON_0	0.2003	0.0075	26.732	178.26	< .0001	2.002	3.419
iRTpre	0.0320	0.0007	45.550	57092.80	< .0001		
hS	-0.0030	0.0017	-1.769	15133.95	0.0769		
vS	-0.0419	0.0016	-25.491	22846.55	< .0001		
hR	-0.0216	0.0016	-13.604	36158.54	< .0001		
vR	-0.0611	0.0016	-39.375	41378.18	< .0001		
LWb	-0.0022	0.0061	-0.366	95.07	0.7154		
ISb	-0.0008	0.0041	-0.196	631.69	0.8447		
PRSb	-0.0170	0.0036	-4.748	48361.30	< .0001		
PRb	-0.0725	0.0080	-9.027	48329.83	< .0001		
CON_0:LWb	0.0385	0.0052	7.373	101.52	< .0001	0.732	1.085
CON_0:ISb	0.0031	0.0060	0.512	1111.24	0.6090	0.015	0.262
LWb:ISb	-0.0039	0.0059	-0.659	97.91	0.5114		
CON_0:LWb:ISb	0.0065	0.0071	0.915	94.28	0.3626	0.094	0.125

Notes: iRTpre, iRT at the previous trial; hS, horizontal coding of the stimulus position (i.e., the horizontal visual hemispace: right vs left); vS, vertical coding of the stimulus position (i.e., the vertical visual hemispace: upper vs lower); hR, horizontal coding of the response (i.e., the responding hand: right vs left); vR, vertical coding of the response (i.e., the responding finger: middle vs index); CON_0, Congruency (Incongruent trials); DF, degrees of freedom; d_s, effect size computed using the Satterthwaite's approximation of degrees of freedom; d_r, effect size computed using the by-participant random slopes. P values are computed using the Satterthwaite's approximation of degrees of freedom.

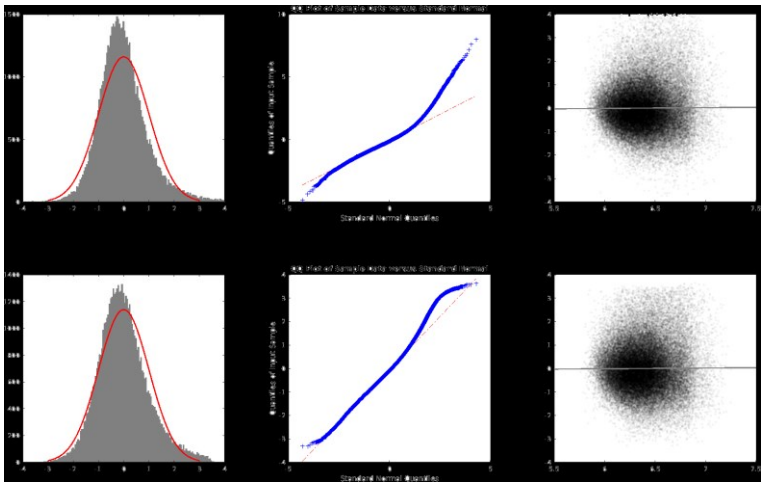

Figure B.4. Inspection of residuals for the LMM analysis on lnRTs (cFull model).
The Figure shows the results of the analysis of the residuals for the LMM analysis on lnRTs for the cFull model both before (upper panels) and after (bottom panels) excluding observations with absolute standardized residuals greater than 3. Left: histogram of the standardized residuals; the superimposed red curve represents the normal density function fitted to the data. Middle: quantile-quantile plot for the standardized residuals. Right: scatterplot of the fitted data (x) vs. the standardized residuals (y) for the visual inspection of the homoscedasticity; the gray line represents the corresponding linear regression line.

B.1.4.3. LMM on RTs, Continuous full model

See the "LMM" section in the PeripheralAnalysis.m file (the continuous full model is coded as "cFull" there).

Table B.4. LMM results on RTs, continuous full model (cFull), coefficients statistics

Coefficient	*Estimate*	*SE*	*t*	*DF*	*p*	d_s	d_r
(Intercept)	541.8439	11.2164	48.308	187.90	< .0001		
TrialTOT	-36.3878	0.9514	-38.248	3528.74	< .0001		
CON_0	120.7666	6.0678	19.903	143.52	< .0001	1.661	2.321
iRTpre	19.4817	0.4653	41.870	56834.53	< .0001		
hS	-0.2332	1.1315	-0.206	15404.27	0.8367		
vS	-22.7110	1.0912	-20.813	23250.47	< .0001		
hR	-14.0414	1.0531	-13.334	36887.48	< .0001		
vR	-38.6166	1.0301	-37.488	41978.78	< .0001		
LWb	0.1224	3.8316	0.032	92.35	0.9746		
ISb	1.4289	2.6167	0.546	888.66	0.5852		
PRSb	-11.3229	2.3731	-4.771	46616.23	< .0001		
PRb	-40.9244	5.3215	-7.690	48159.52	< .0001		
CON_0:LWb	24.9990	4.2554	5.875	99.34	< .0001	0.589	0.741
CON_0:ISb	0.3573	4.0392	0.088	1016.33	0.9295	0.003	0.036
LWb:ISb	-1.0189	3.5808	-0.285	98.10	0.7766		
CON_0:LWb:ISb	2.8321	4.8406	0.585	95.19	0.5599	0.060	0.079

Notes: iRTpre, iRT at the previous trial; hS, horizontal coding of the stimulus position (i.e., the horizontal visual hemispace: right vs left); vS, vertical coding of the stimulus position (i.e., the vertical visual hemispace: upper vs lower); hR, horizontal coding of the response (i.e., the responding hand: right vs left); vR, vertical coding of the response (i.e., the responding finger: middle vs index); CON_0, Congruency (Incongruent trials); DF, degrees of freedom; d_s, effect size computed using the Satterthwaite's approximation of degrees of freedom; d_r, effect size computed using the by-participant random slopes. P values are computed using the Satterthwaite's approximation of degrees of freedom.

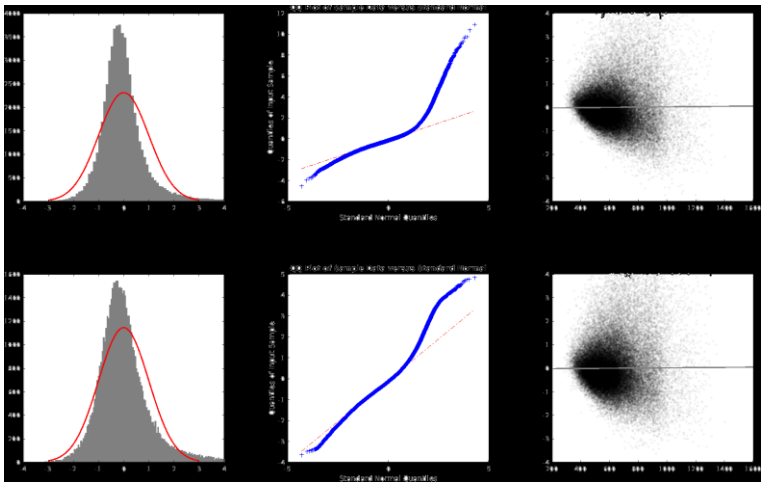

Figure B.5. Inspection of residuals for the LMM analysis on RTs (cFull model).
The Figure shows the results of the analysis of the residuals for the LMM analysis on RTs for the cFull model both before (upper panels) and after (bottom panels) excluding observations with absolute standardized residuals greater than 3. Left: histogram of the standardized residuals; the superimposed red curve represents the normal density function fitted to the data. Middle: quantile-quantile plot for the standardized residuals. Right: scatterplot of the fitted data (x) vs. the standardized residuals (y) for the visual inspection of the homoscedasticity; the gray line represents the corresponding linear regression line.

B.1.4.4. LMM on iRTs, Discrete full model

See the "LMM" section in the PeripheralAnalysis.m file (the discrete full model is coded as "dFull" there).

Table B.5. LMM results, discrete full model (dFull), coefficients statistics

Coefficient	*Estimate*	*SE*	*t*	*DF*	*p*	d_s	d_r
(Intercept)	-1.8315	0.0319	-57.425	99.93	< .0001		
TrialTOT	-0.0918	0.0021	-42.878	2918.74	< .0001		
CON_0	0.4334	0.0137	31.670	202.59	< .0001	2.225	4.232
iRTpre	-0.0133	0.0070	-1.916	98.62	0.0582		
hS	-0.0550	0.0073	-7.525	910.87	< .0001		
vS	0.0415	0.0062	6.693	57112.79	< .0001		
hR	-0.0124	0.0012	-10.441	57020.74	< .0001		
vR	0.0566	0.0012	48.610	57375.88	< .0001		
LW	-0.0115	0.0030	-3.833	7427.13	0.0001		
IS	-0.0751	0.0029	-25.995	10310.76	< .0001		
PRS	-0.0335	0.0027	-12.510	27690.24	< .0001		
PR	-0.1007	0.0026	-38.239	30089.41	< .0001		
CON_0:LW	0.0530	0.0055	9.702	111.35	< .0001	0.919	1.652
CON_0:IS	0.0801	0.0102	7.851	1577.83	< .0001	0.198	3.631
LWb:IS	0.0024	0.0074	0.321	97.96	0.7488		
CON_0:LW:IS	-0.0049	0.0081	-0.601	97.43	0.5490	-0.061	-0.078

Notes: iRTpre, iRT at the previous trial; hS, horizontal coding of the stimulus position (i.e., the horizontal visual hemispace: right vs left); vS, vertical coding of the stimulus position (i.e., the vertical visual hemispace: upper vs lower); hR, horizontal coding of the response (i.e., the responding hand: right vs left); vR, vertical coding of the response (i.e., the responding finger: middle vs index); CON_0, Congruency (Incongruent trials); DF, degrees of freedom; d_s, effect size computed using the Satterthwaite's approximation of degrees of freedom; d_r, effect size computed using the by-participant random slopes. P values are computed using the Satterthwaite's approximation of degrees of freedom.

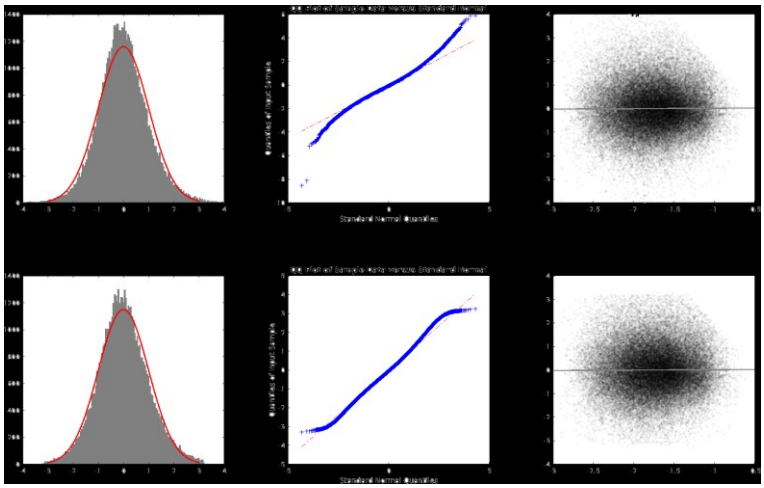

Figure B.6. Inspection of residuals for the LMM analysis on iRTs (dFull model).
The Figure shows the results of the analysis of the residuals for the LMM analysis on iRTs for the dFull model both before (upper panels) and after (bottom panels) excluding observations with absolute standardized residuals greater than 3. Left: histogram of the standardized residuals; the superimposed red curve represents the normal density function fitted to the data. Middle: quantile-quantile plot for the standardized residuals. Right: scatterplot of the fitted data (x) vs. the standardized residuals (y) for the visual inspection of the homoscedasticity; the gray line represents the corresponding linear regression line.

B.1.4.5. LMM on iRTs, Continuous reduced model

See the "LMM" section in the PeripheralAnalysis.m file (the continuous reduced model is coded as "cRedu" there).

Table B.6. LMM results, continuous reduced model (cRedu), coefficients statistics

Coefficient	*Estimate*	*SE*	*t*	*DF*	*p*	d_s	d_r
(Intercept)	-1.9301	0.0317	-60.952	97.99	< .0001		
CON_0	0.3129	0.0128	24.403	181.34	< .0001	1.812	3.169
LWb	-0.0256	0.0159	-1.611	97.84	0.1104		
ISb	0.0273	0.0079	3.478	422.23	0.0006		
PRSb	-0.0612	0.0062	-9.832	53301.98	< .0001		
CON_0:LWb	0.0412	0.0091	4.537	97.74	< .0001	0.459	0.709
CON_0:ISb	-0.0303	0.0112	-2.698	676.59	0.0071	-0.104	-0.795
LWb:ISb	-0.0073	0.0159	-0.458	97.62	0.6482		
CON_0:LWb:ISb	-0.0025	0.0144	-0.177	94.82	0.8602	-0.018	-0.022

Notes: CON_0, Congruency (Incongruent trials); DF, degrees of freedom; d_s, effect size computed using the Satterthwaite's approximation of degrees of freedom; d_r, effect size computed using the by-participant random slopes.
P values are computed using the Satterthwaite's approximation of degrees of freedom.

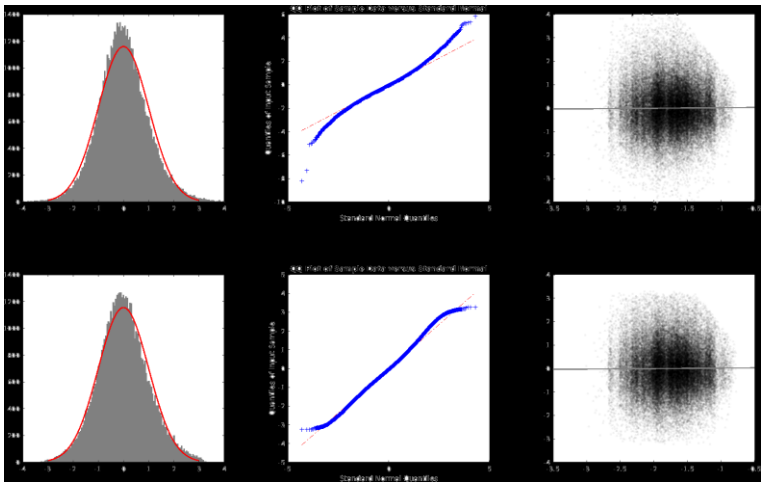

Figure B.7. Inspection of residuals for the LMM analysis on iRTs (cRedu model).
The Figure shows the results of the analysis of the residuals for the LMM analysis on iRTs for the cRedu model both before (upper panels) and after (bottom panels) excluding observations with absolute standardized residuals greater than 3. Left: histogram of the standardized residuals; the superimposed red curve represents the normal density function fitted to the data. Middle: quantile-quantile plot for the standardized residuals. Right: scatterplot of the fitted data (x) vs. the standardized residuals (y) for the visual inspection of the homoscedasticity; the gray line represents the corresponding linear regression line.

B.1.4.6. LMM on iRTs, Continuous full 2-way model

See the "LMM" section in the PeripheralAnalysis.m file (the continuous full 2-way model is coded as "c2way" there).

Table B.7. LMM results, continuous 2-way model (c2way), coefficients statistics

Coefficient	*Estimate*	*SE*	*t*	*DF*	*p*	d_s	d_r
(Intercept)	-1.9532	0.0346	-56.450	145.31	< .0001		
TrialTOT	-0.0930	0.0023	-40.273	2206.40	< .0001		
CON_0	0.3572	0.0118	30.229	200.95	< .0001	2.132	3.845
iRTpre	0.0543	0.0012	46.250	57494.81	< .0001		
hS	-0.0130	0.0026	-5.083	38849.99	< .0001		
vS	-0.0800	0.0025	-31.719	41096.27	< .0001		
hR	-0.0344	0.0025	-13.516	55455.85	< .0001		
vR	-0.1005	0.0025	-40.014	55685.56	< .0001		
LWb	-0.0092	0.0105	-0.872	97.23	0.3855		
ISb	-0.0146	0.0077	-1.908	368.83	0.0572		
PRSb	-0.0207	0.0059	-3.521	52849.48	0.0004		
PRb	-0.1287	0.0132	-9.770	57095.70	< .0001		
LWb:ISb	0.0659	0.0077	8.543	101.87	< .0001	0.846	1.403
CON_0:LWb:ISb	0.0173	0.0103	1.687	744.89	0.0920	0.062	0.499

Notes: iRTpre, iRT at the previous trial; hS, horizontal coding of the stimulus position (i.e., the horizontal visual hemispace: right vs left); vS, vertical coding of the stimulus position (i.e., the vertical visual hemispace: upper vs lower); hR, horizontal coding of the response (i.e., the responding hand: right vs left); vR, vertical coding of the response (i.e., the responding finger: middle vs index); CON_0, Congruency (Incongruent trials); DF, degrees of freedom; d_s, effect size computed using the Satterthwaite's approximation of degrees of freedom; d_r, effect size computed using the by-participant random slopes. P values are computed using the Satterthwaite's approximation of degrees of freedom.

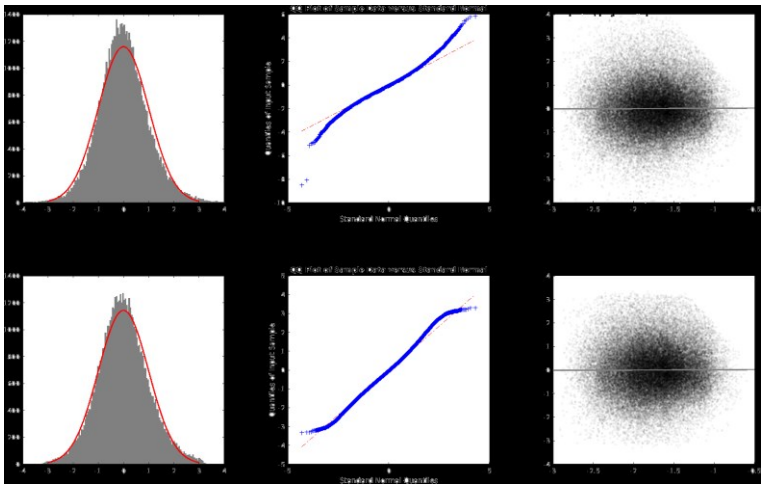

Figure B.8. Inspection of residuals for the LMM analysis on iRTs (c2way model).
The Figure shows the results of the analysis of the residuals for the LMM analysis on iRTs for the c2way model both before (upper panels) and after (bottom panels) excluding observations with absolute standardized residuals greater than 3.
Left: histogram of the standardized residuals; the superimposed red curve represents the normal density function fitted to the data. Middle: quantile-quantile plot for the standardized residuals. Right: scatterplot of the fitted data (x) vs. the standardized residuals (y) for the visual inspection of the homoscedasticity; the gray line represents the corresponding linear regression line.

B.1.4.7. RCA on iRTs, Continuous full model

See the "RCA" section in the PeripheralAnalysis.m file (the continuous full model is coded as "cFull" there).

Table B.8. RCA results, continuous full model (cFull), coefficients statistics

Coefficient	*Estimate*	*SE*	*t*	*DF*	*p*	d_r
(Intercept)	-1.9069	0.0516	-36.972	97	< .0001	-3.735
TrialTOT	-0.0887	0.0090	-9.855	97	< .0001	-0.996
CON_0	0.3291	0.0143	22.958	97	< .0001	2.319
iRTpre	0.0564	0.0029	19.657	97	< .0001	1.986
hS	-0.0101	0.0060	-1.675	97	0.0971	-0.169
vS	-0.0793	0.0081	-9.835	97	< .0001	-0.993
hR	-0.0366	0.0067	-5.461	97	< .0001	-0.552
vR	-0.1032	0.0081	-12.796	97	< .0001	-1.293
LWb	-0.0174	0.0112	-1.560	97	0.1221	-0.158
ISb	-0.0028	0.0086	-0.325	97	0.7462	-0.033
PRSb	-0.0338	0.0086	-3.941	97	0.0002	-0.398
PRb	-0.0991	0.0333	-2.979	97	0.0037	-0.301
CON_0:LWb	0.0661	0.0078	8.497	97	< .0001	0.858
CON_0:ISb	0.0011	0.0130	0.082	97	0.9344	0.008
LWb:ISb	-0.0365	0.0099	-3.673	97	0.0004	-0.371
CON_0:LWb:ISb	0.0405	0.0118	3.435	97	0.0009	0.347

Notes: iRTpre, iRT at the previous trial; hS, horizontal coding of the stimulus position (i.e., the horizontal visual hemispace: right vs left); vS, vertical coding of the stimulus position (i.e., the vertical visual hemispace: upper vs lower); hR, horizontal coding of the response (i.e., the responding hand: right vs left); vR, vertical coding of the response (i.e., the responding finger: middle vs index); CON_0, Congruency (Incongruent trials); DF, degrees of freedom; d_r, effect size computed using the by-participant random slopes.

B.1.4.8. Control analysis, LMM on iRTs, Continuous full model without PRSb

See the "Control analyses" section in the PeripheralAnalysis.m file (the continuous full model without PRSb is coded as "cFullNoPRS" there).

Table B.9. LMM results, continuous full model (cFull), coefficients statistics

Coefficient	*Estimate*	*SE*	*t*	*DF*	*p*	d_s
(Intercept)	-1.9483	0.0349	-55.758	145.41	< .0001	
TrialTOT	-0.0931	0.0023	-40.481	2025.86	< .0001	
CON_0	0.3744	0.0105	35.563	97.05	< .0001	3.610
iRTpre	0.0554	0.0012	47.604	57384.25	< .0001	
hS	-0.0108	0.0028	-3.834	12845.78	0.0001	
vS	-0.0790	0.0027	-29.008	19680.45	< .0001	
hR	-0.0347	0.0026	-13.261	33582.63	< .0001	
vR	-0.1012	0.0026	-39.341	39242.63	< .0001	
LWb	-0.0098	0.0104	-0.942	97.34	0.3485	
ISb	-0.0323	0.0051	-6.321	98.93	< .0001	
PRb	-0.1279	0.0133	-9.628	50405.84	< .0001	
CON_0:LWb	0.0676	0.0080	8.430	100.52	< .0001	0.841
CON_0:ISb	0.0456	0.0058	7.853	102.04	< .0001	0.777
LWb:ISb	-0.0122	0.0109	-1.123	97.30	0.2641	
CON_0:LWb:ISb	0.0159	0.0119	1.338	93.55	0.1840	0.138

Notes: iRTpre, iRT at the previous trial; hS, horizontal coding of the stimulus position (i.e., the horizontal visual hemispace: right vs left); vS, vertical coding of the stimulus position (i.e., the vertical visual hemispace: upper vs lower); hR, horizontal coding of the response (i.e., the responding hand: right vs left); vR, vertical coding of the response (i.e., the responding finger: middle vs index); CON_0, Congruency (Incongruent trials); DF, degrees of freedom; d_r, effect size computed using the by-participant random slopes.

B.1.4.9. Control analysis, RCA on iRTs, Continuous full model without PRSb

See the "Control analyses" section in the PeripheralAnalysis.m file (the continuous full model without PRSb is coded as "cFullNoPRS" there).

Table B.10. LMM results, continuous full model (cFull), coefficients statistics

Coefficient	*Estimate*	*SE*	*t*	*DF*	*p*	d_r
(Intercept)	-1.9135	0.0517	-36.978	97	< .0001	-3.74
TrialTOT	-0.0904	0.0090	-10.037	97	< .0001	-1.01
CON_0	0.3643	0.0111	32.676	97	< .0001	3.30
iRTpre	0.0569	0.0029	19.767	97	< .0001	2.00
hS	-0.0106	0.0060	-1.766	97	0.0806	-0.18
vS	-0.0794	0.0080	-9.974	97	< .0001	-1.01
hR	-0.0364	0.0066	-5.477	97	< .0001	-0.55
vR	-0.1034	0.0080	-12.966	97	< .0001	-1.31
LWb	-0.0193	0.0111	-1.739	97	0.0852	-0.18
ISb	-0.0329	0.0048	-6.867	97	< .0001	-0.69
PRb	-0.1072	0.0332	-3.232	97	0.0017	-0.33
CON_0:LWb	0.0710	0.0075	9.436	97	< .0001	0.95
CON_0:ISb	0.0477	0.0058	8.174	97	< .0001	0.83
LWb:ISb	-0.0381	0.0098	-3.886	97	0.0002	-0.39
CON_0:LWb:ISb	0.0444	0.0114	3.902	97	0.0002	0.39

Notes: iRTpre, iRT at the previous trial; hS, horizontal coding of the stimulus position (i.e., the horizontal visual hemispace: right vs left); vS, vertical coding of the stimulus position (i.e., the vertical visual hemispace: upper vs lower); hR, horizontal coding of the response (i.e., the responding hand: right vs left); vR, vertical coding of the response (i.e., the responding finger: middle vs index); CON_0, Congruency (Incongruent trials); DF, degrees of freedom; d_s, effect size computed using the Satterthwaite's approximation of degrees of freedom.
P values are computed using the Satterthwaite's approximation of degrees of freedom.

B.1.4.10. Internal reliability

See the "Split-half reliability" section in the PeripheralAnalysis.m file.

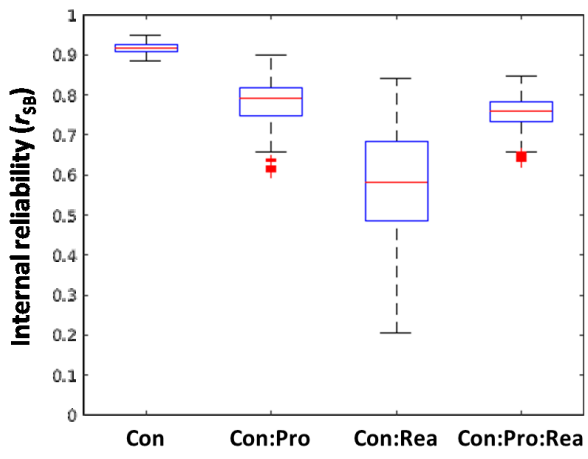

Figure B.9. Internal reliability of the Stroop effect and its modulations estimated by the LMM. The boxplots shows the distribution of the internal reliability estimates (r_{sb}) of the Stroop effect (Con) and its modulation by the Proactive (Con:Pro) and Reactive control (Con:Rea) and the interaction between them (Con:Pro:Rea), as estimated by the cFull LMM model. The boxplots represent the median values (red line at the center of the box), interquartile ranges (box), and dispersion outside the extreme quartiles (whiskers indicating 1.5 times the interquartile range).

B.2. Experiment 2 – Perifoveal Stroop task

B.2.1. Distributional analysis

See the "Distributional analysis" section in the PerifovealAnalysis.m file

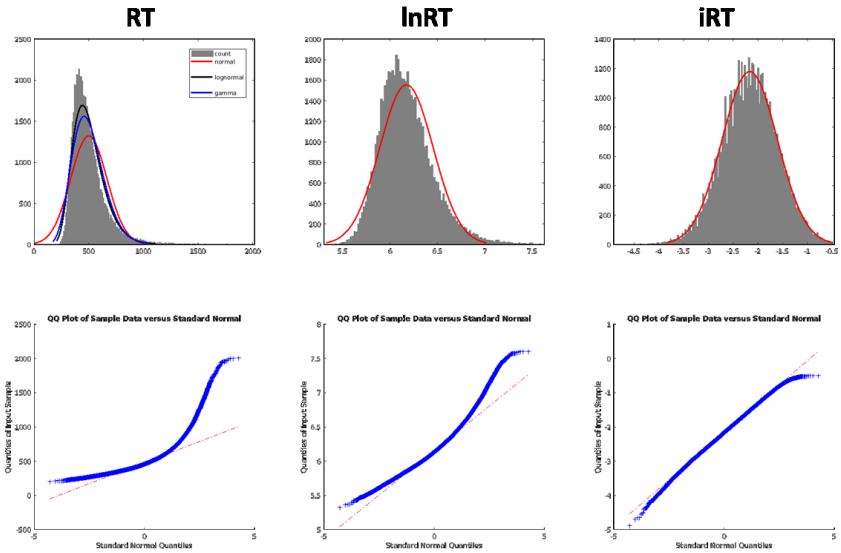

Figure B.10. Distributional analysis of participants' response times.
The top row shows the histograms of untransformed RT values (left panel), natural log-transformed RTs (lnRT, middle panel), and inverse-transformed RTs (iRT, right panel), computed as -1000/RT. The superimposed red curves represent the normal density function fitted to the data. The black and blue curves for the RT distribution represent the lognormal and gamma density functions fitted to the data, respectively. The number of bins was determined using the Freedman-Diaconis rule as implemented in the Matlab *histcounts* function. The bottom row shows the corresponding Q-Q plots.

B.2.2. Compliance checking

See the "Check for SS compliance" section in the PerifovealAnalysis.m file

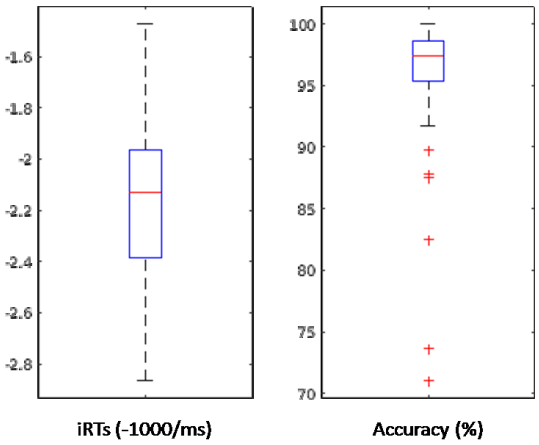

Figure B.11. Participants' overall performance.
The Figure shows the distribution of the participants' mean iRTs (left panel) and accuracy (right panel). The boxplots represent the median values (red line at the center of the box), interquartile ranges (box), and dispersion outside the extreme quartiles (whiskers indicating 1.5 times the interquartile range).

B.2.3. Descriptive statistics

See the "Descriptive statistics" section in the PerifovealAnalysis.m file.

Table B.11. Descriptive statistics and Stroop effects

	C		I		Stroop					
	M	***SD***	***M***	***SD***	***M***	***SD***	***t***	***p***	***d***	***Dom***
iRT	-2.407	0.337	-1.950	0.338	0.458	0.121	33.43	< .0001	3.785	100%
lnRT	6.055	0.149	6.274	0.185	0.219	0.069	28.06	< .0001	3.178	100%
RT	439.1	70.7	552.3	111.4	113.2	52.0	19.22	< .0001	2.176	100%
Acc	99.33%	0.94%	92.72%	9.43%	6.61%	9.08%	6.43	< .0001	0.729	100%

Notes: C, congruent; I, incongruent.

B.2.4. Results

B.2.4.1. LMM on iRTs, Continuous full model

See the "LMM" section in the PerifovealAnalysis.m file (the continuous full model is coded as "cFull" there).

Table B.2.2. LMM results, continuous full model (cFull), coefficients statistics

Coefficient	***Estimate***	***SE***	***t***	***DF***	***p***	d_s	d_r
(Intercept)	-2.4845	0.0448	-55.449	128.21	< .0001		
TrialTOT	-0.1018	0.0034	-29.687	2686.32	< .0001		
CON_0	0.3729	0.0177	21.059	138.27	< .0001	1.791	3.008
iRTpre	0.0586	0.0017	35.077	45622.01	< .0001		
hS	-0.0080	0.0039	-2.072	4301.02	0.0383		
vS	0.0110	0.0038	2.888	3793.44	0.0039		
hR	-0.0608	0.0038	-16.143	31342.78	< .0001		
vR	-0.0723	0.0037	-19.484	29671.40	< .0001		
LWb	-0.0002	0.0145	-0.012	78.89	0.9907		
lSb	-0.0025	0.0112	-0.223	262.95	0.8238		
PRSb	-0.0516	0.0085	-6.062	40688.90	< .0001		
PRb	-0.1572	0.0189	-8.300	39539.08	< .0001		
CON_0:LWb	0.0668	0.0119	5.606	77.49	< .0001	0.637	0.992
CON_0:lSb	-0.0066	0.0157	-0.416	422.46	0.6774	-0.020	-0.109
LWb:lSb	-0.0311	0.0149	-2.085	78.49	0.0403		
CON_0:LWb:lSb	0.0454	0.0204	2.226	78.29	0.0289	0.252	0.311

Notes: iRTpre, iRT at the previous trial; hS, horizontal coding of the stimulus position (i.e., the horizontal visual hemispace: right vs left); vS, vertical coding of the stimulus position (i.e., the vertical visual hemispace: upper vs lower); hR, horizontal coding of the response (i.e., the responding hand: right vs left); vR, vertical coding of the response (i.e., the responding finger: middle vs index); CON_0, Congruency (Incongruent trials); DF, degrees of freedom; d_s, effect size computed using the Satterthwaite's approximation of degrees of freedom; d_r, effect size computed using the by-participant random slopes. P values are computed using the Satterthwaite's approximation of degrees of freedom.

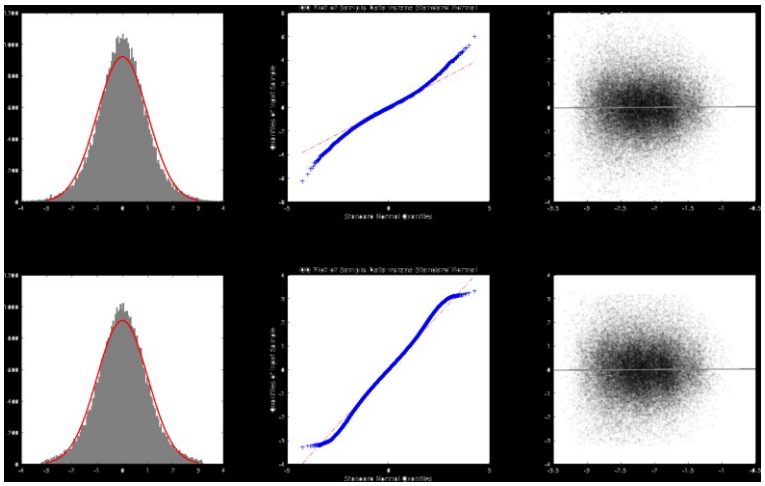

Figure B.12. Inspection of residuals for the LMM analysis on iRTs (cFull model).
The Figure shows the results of the analysis of the residuals for the LMM analysis on iRTs for the cFull model both before (upper panels) and after (bottom panels) excluding observations with absolute standardized residuals greater than 3. Left: histogram of the standardized residuals; the superimposed red curve represents the normal density function fitted to the data. Middle: quantile-quantile plot for the standardized residuals. Right: scatterplot of the fitted data (x) vs. the standardized residuals (y) for the visual inspection of the homoscedasticity; the gray line represents the corresponding linear regression line.

B.2.4.2. LMM on lnRTs, Continuous full model

See the "LMM" section in the PerifovealAnalysis.m file (the continuous full model is coded as "cFull" there).

Table B.12. LMM results, continuous full model (cFull), coefficients statistics

Coefficient	*Estimate*	*SE*	*t*	*DF*	*p*	d_s	d_r
(Intercept)	6.0108	0.0201	298.560	136.96	< .0001		
TrialTOT	-0.0512	0.0017	-30.905	3962.77	< .0001		
CON_0	0.1697	0.0089	19.075	129.08	< .0001	1.679	2.645
iRTpre	0.0277	0.0008	34.978	45420.67	< .0001		
hS	-0.0005	0.0019	-0.286	6383.25	0.7746		
vS	0.0081	0.0018	4.400	5840.48	< .0001		
hR	-0.0304	0.0018	-16.923	33066.77	< .0001		
vR	-0.0375	0.0018	-21.238	31239.69	< .0001		
LWb	-0.0042	0.0074	-0.559	77.86	0.5777		
ISb	0.0109	0.0049	2.238	380.87	0.0258		
PRSb	-0.0307	0.0041	-7.578	41445.15	< .0001		
PRb	-0.0745	0.0090	-8.289	39718.29	< .0001		
CON_0:LWb	0.0366	0.0074	4.964	74.24	< .0001	0.576	0.708
CON_0:ISb	-0.0171	0.0071	-2.394	568.52	0.0170	-0.100	-0.855
LWb:ISb	-0.0124	0.0064	-1.942	78.16	0.0558		
CON_0:LWb:ISb	0.0210	0.0095	2.199	77.50	0.0309	0.250	0.310

Notes: iRTpre, iRT at the previous trial; hS, horizontal coding of the stimulus position (i.e., the horizontal visual hemispace: right vs left); vS, vertical coding of the stimulus position (i.e., the vertical visual hemispace: upper vs lower); hR, horizontal coding of the response (i.e., the responding hand: right vs left); vR, vertical coding of the response (i.e., the responding finger: middle vs index); CON_0, Congruency (Incongruent trials); DF, degrees of freedom; d_s, effect size computed using the Satterthwaite's approximation of degrees of freedom; d_r, effect size computed using the by-participant random slopes. P values are computed using the Satterthwaite's approximation of degrees of freedom.

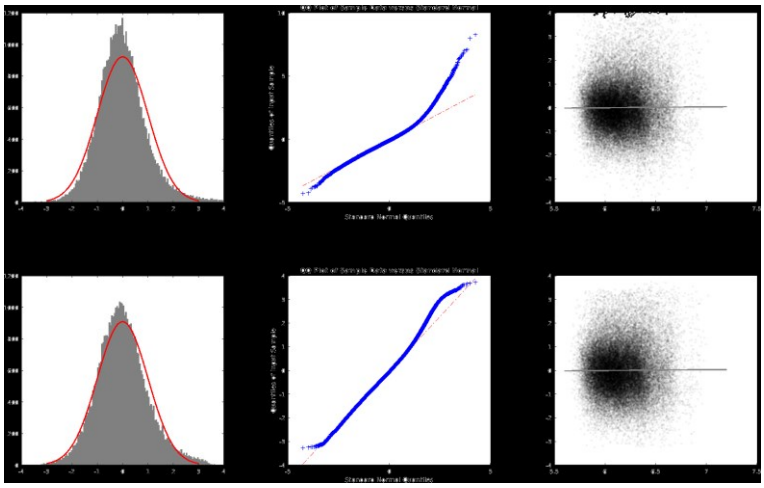

Figure B.13. Inspection of residuals for the LMM analysis on lnRTs (cFull model).
The Figure shows the results of the analysis of the residuals for the LMM analysis on lnRTs for the cFull model both before (upper panels) and after (bottom panels) excluding observations with absolute standardized residuals greater than 3. Left: histogram of the standardized residuals; the superimposed red curve represents the normal density function fitted to the data. Middle: quantile-quantile plot for the standardized residuals. Right: scatterplot of the fitted data (x) vs. the standardized residuals (y) for the visual inspection of the homoscedasticity; the gray line represents the corresponding linear regression line.

B.2.4.3. LMM on RTs, Continuous full model

See the "LMM" section in the PerifovealAnalysis.m file (the continuous full model is coded as "cFull" there).

Table B.13. LMM results, continuous full model (cFull), coefficients statistics

Coefficient	*Estimate*	*SE*	*t*	*DF*	*p*	d_s	d_r
(Intercept)	418.8132	9.6152	43.557	154.90	< .0001		
TrialTOT	-26.1903	0.8681	-30.171	4683.08	< .0001		
CON_0	80.2266	5.5982	14.331	107.00	< .0001	1.385	1.841
iRTpre	13.6985	0.4111	33.319	45263.25	< .0001		
hS	0.8766	0.9852	0.890	8866.71	0.3736		
vS	4.8119	0.9683	4.970	8360.65	< .0001		
hR	-15.8045	0.9358	-16.889	32588.14	< .0001		
vR	-20.1868	0.9197	-21.950	30499.11	< .0001		
LWb	-2.5775	3.9762	-0.648	77.11	0.5188		
ISb	10.5945	2.3712	4.468	569.86	< .0001		
PRSb	-18.5594	2.1121	-8.787	40904.89	< .0001		
PRb	-33.6575	4.6726	-7.203	38472.09	< .0001		
CON_0:LWb	18.4681	4.4584	4.142	74.78	0.0001	0.479	0.549
CON_0:ISb	-14.4628	3.6776	-3.933	607.04	0.0001	-0.160	-1.443
LWb:ISb	-4.9362	2.8871	-1.710	77.70	0.0913		
CON_0:LWb:ISb	8.6872	4.8850	1.778	76.36	0.0793	0.204	0.251

Notes: iRTpre, iRT at the previous trial; hS, horizontal coding of the stimulus position (i.e., the horizontal visual hemispace: right vs left); vS, vertical coding of the stimulus position (i.e., the vertical visual hemispace: upper vs lower); hR, horizontal coding of the response (i.e., the responding hand: right vs left); vR, vertical coding of the response (i.e., the responding finger: middle vs index); CON_0, Congruency (Incongruent trials); DF, degrees of freedom; d_s, effect size computed using the Satterthwaite's approximation of degrees of freedom; d_r, effect size computed using the by-participant random slopes. P values are computed using the Satterthwaite's approximation of degrees of freedom.

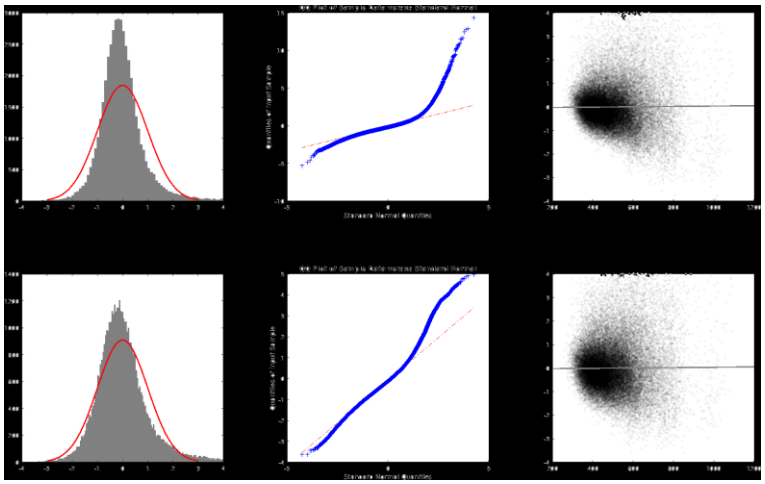

Figure B.14. Inspection of residuals for the LMM analysis on RTs (cFull model).
The Figure shows the results of the analysis of the residuals for the LMM analysis on RTs for the cFull model both before (upper panels) and after (bottom panels) excluding observations with absolute standardized residuals greater than 3. Left: histogram of the standardized residuals; the superimposed red curve represents the normal density function fitted to the data. Middle: quantile-quantile plot for the standardized residuals. Right: scatterplot of the fitted data (x) vs. the standardized residuals (y) for the visual inspection of the homoscedasticity; the gray line represents the corresponding linear regression line.

B.2.4.4. LMM on iRTs, Discrete full model

See the "LMM" section in the PerifovealAnalysis.m file (the discrete full model is coded as "dFull" there).

Table B.14. LMM results, discrete full model (dFull), coefficients statistics

Coefficient	*Estimate*	*SE*	*t*	*DF*	*p*	d_s	d_r
(Intercept)	-2.3200	0.0413	-56.162	79.76	< .0001		
TrialTOT	-0.1056	0.0031	-33.606	3618.57	< .0001		
CON_0	0.4446	0.0213	20.827	142.07	< .0001	1.747	2.954
iRTpre	-0.0072	0.0099	-0.735	79.40	0.4648		
hS	-0.0408	0.0116	-3.515	384.45	0.0005		
vS	0.0115	0.0089	1.287	45287.63	0.1980		
hR	-0.0109	0.0017	-6.385	45342.87	< .0001		
vR	0.0599	0.0017	35.968	45621.15	< .0001		
LW	-0.0080	0.0040	-1.998	2236.29	0.0458		
IS	0.0151	0.0040	3.805	1586.68	0.0001		
PRS	-0.0594	0.0038	-15.465	27973.58	< .0001		
PR	-0.0746	0.0038	-19.537	23624.22	< .0001		
CON_0:LW	0.0574	0.0082	7.007	85.23	< .0001	0.759	1.253
CON_0:IS	0.0527	0.0157	3.350	643.37	0.0009	0.132	0.900
LWb:IS	-0.0086	0.0114	-0.752	77.87	0.4546		
CON_0:LW:IS	0.0176	0.0153	1.150	77.47	0.2538	0.131	0.149

Notes: iRTpre, iRT at the previous trial; hS, horizontal coding of the stimulus position (i.e., the horizontal visual hemispace: right vs left); vS, vertical coding of the stimulus position (i.e., the vertical visual hemispace: upper vs lower); hR, horizontal coding of the response (i.e., the responding hand: right vs left); vR, vertical coding of the response (i.e., the responding finger: middle vs index); CON_0, Congruency (Incongruent trials); DF, degrees of freedom; d_s, effect size computed using the Satterthwaite's approximation of degrees of freedom; d_r, effect size computed using the by-participant random slopes. P values are computed using the Satterthwaite's approximation of degrees of freedom.

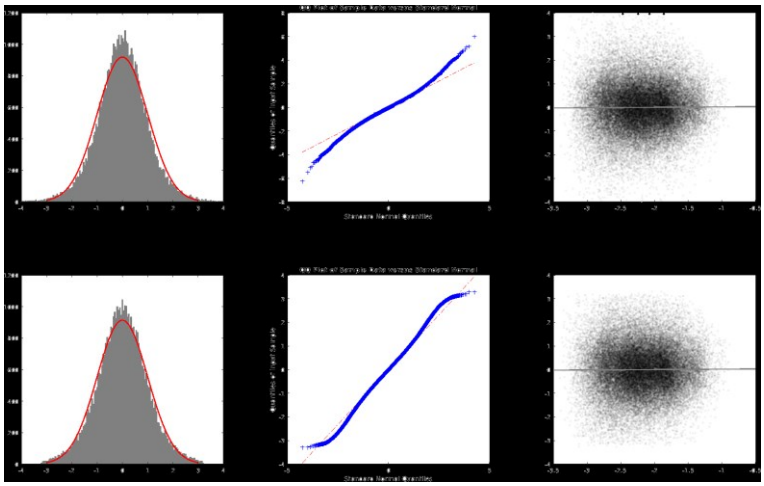

Figure B.15. Inspection of residuals for the LMM analysis on iRTs (dFull model).
The Figure shows the results of the analysis of the residuals for the LMM analysis on iRTs for the dFull model both before (upper panels) and after (bottom panels) excluding observations with absolute standardized residuals greater than 3. Left: histogram of the standardized residuals; the superimposed red curve represents the normal density function fitted to the data. Middle: quantile-quantile plot for the standardized residuals. Right: scatterplot of the fitted data (x) vs. the standardized residuals (y) for the visual inspection of the homoscedasticity; the gray line represents the corresponding linear regression line.

B.2.4.5. LMM on iRTs, Continuous reduced model

See the "LMM" section in the PerifovealAnalysis.m file (the continuous reduced model is coded as "cRedu" there).

Table B.15. LMM results, continuous reduced model (cRedu), coefficients statistics

Coefficient	*Estimate*	*SE*	*t*	*DF*	*p*	d_s	d_r
(Intercept)	-2.3823	0.0395	-60.335	77.96	< .0001		
CON_0	0.3288	0.0180	18.262	138.49	< .0001	1.552	2.618
LWb	-0.0445	0.0198	-2.252	78.25	0.0271		
ISb	0.0383	0.0115	3.323	261.97	0.0010		
PRSb	-0.0974	0.0086	-11.258	41527.96	< .0001		
CON_0:LWb	0.0378	0.0124	3.053	73.65	0.0032	0.356	0.528
CON_0:ISb	-0.0526	0.0163	-3.234	407.73	0.0013	-0.160	-0.828
LWb:ISb	-0.0378	0.0165	-2.293	77.47	0.0246		
CON_0:LWb:ISb	0.0335	0.0225	1.491	78.10	0.1399	0.169	0.202

Notes: CON_0, Congruency (Incongruent trials); DF, degrees of freedom; d_s, effect size computed using the Satterthwaite's approximation of degrees of freedom; d_r, effect size computed using the by-participant random slopes.
P values are computed using the Satterthwaite's approximation of degrees of freedom.

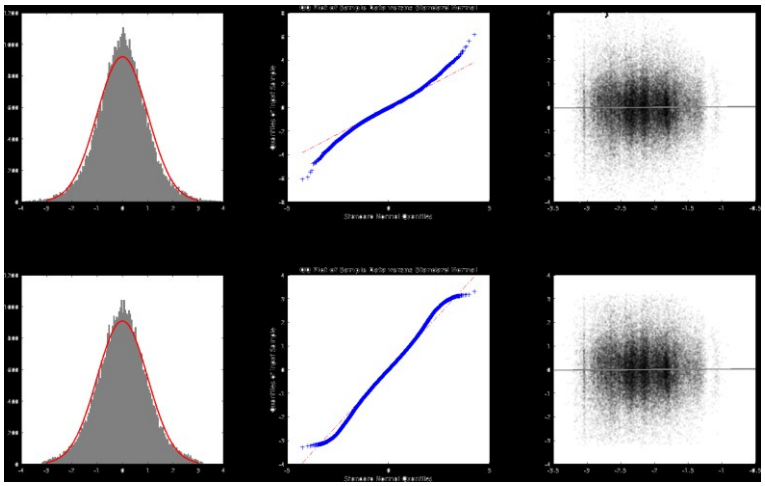

Figure B.16. Inspection of residuals for the LMM analysis on iRTs (cRedu model).
The Figure shows the results of the analysis of the residuals for the LMM analysis on iRTs for the cRedu model both before (upper panels) and after (bottom panels) excluding observations with absolute standardized residuals greater than 3.
Left: histogram of the standardized residuals; the superimposed red curve represents the normal density function fitted to the data. Middle: quantile-quantile plot for the standardized residuals. Right: scatterplot of the fitted data (x) vs. the standardized residuals (y) for the visual inspection of the homoscedasticity; the gray line represents the corresponding linear regression line.

B.2.4.6. LMM on iRTs, Continuous 2-way model

See the "LMM" section in the PerifovealAnalysis.m file (the continuous 2-way model is coded as "c2way" there).

Table B.16. LMM results, continuous 2-way model (c2way), coefficients statistics

Coefficient	*Estimate*	*SE*	*t*	*DF*	*p*	d_s	d_r
(Intercept)	-2.5041	0.0437	-57.328	129.48	< .0001		
TrialTOT	-0.1032	0.0034	-30.105	2990.24	< .0001		
CON_0	0.3866	0.0158	24.515	176.70	< .0001	1.844	3.619
iRTpre	0.0582	0.0017	34.751	45692.46	< .0001		
hS	-0.0079	0.0037	-2.161	25881.28	0.0307		
vS	0.0091	0.0036	2.528	28109.26	0.0115		
hR	-0.0585	0.0036	-16.025	39564.33	< .0001		
vR	-0.0728	0.0036	-20.291	41438.36	< .0001		
LWb	0.0028	0.0145	0.191	78.68	0.8494		
ISb	-0.0060	0.0118	-0.511	225.59	0.6100		
PRSb	-0.0538	0.0084	-6.412	41568.60	< .0001		
PRb	-0.1649	0.0186	-8.859	44953.82	< .0001		
LWb:ISb	0.0663	0.0115	5.785	78.58	< .0001	0.653	1.069
CON_0:LWb:ISb	-0.0078	0.0158	-0.491	365.94	0.6239	-0.026	-0.113

Notes: iRTpre, iRT at the previous trial; hS, horizontal coding of the stimulus position (i.e., the horizontal visual hemispace: right vs left); vS, vertical coding of the stimulus position (i.e., the vertical visual hemispace: upper vs lower); hR, horizontal coding of the response (i.e., the responding hand: right vs left); vR, vertical coding of the response (i.e., the responding finger: middle vs index); CON_0, Congruency (Incongruent trials); DF, degrees of freedom; d_s, effect size computed using the Satterthwaite's approximation of degrees of freedom; d_r, effect size computed using the by-participant random slopes. P values are computed using the Satterthwaite's approximation of degrees of freedom.

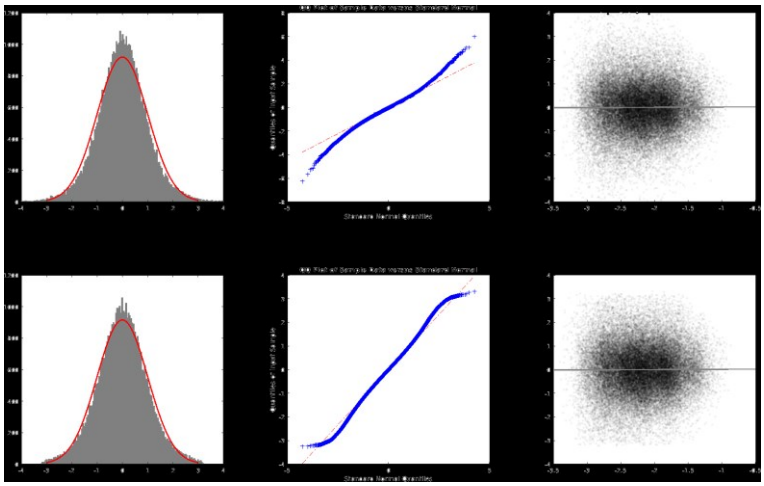

Figure B.17. Inspection of residuals for the LMM analysis on iRTs (c2way model).
The Figure shows the results of the analysis of the residuals for the LMM analysis on iRTs for the c2way model both before (upper panels) and after (bottom panels) excluding observations with absolute standardized residuals greater than 3.
Left: histogram of the standardized residuals; the superimposed red curve represents the normal density function fitted to the data. Middle: quantile-quantile plot for the standardized residuals. Right: scatterplot of the fitted data (x) vs. the standardized residuals (y) for the visual inspection of the homoscedasticity; the gray line represents the corresponding linear regression line.

B.2.4.7. RCA on iRTs, Continuous full model

See the "RCA" section in the PerifovealAnalysis.m file (the continuous full model is coded as "cFull" there).

Table B.17. RCA results, continuous full model (cFull), coefficients statistics

Coefficient	*Estimate*	*SE*	*t*	*DF*	*p*	d_r
(Intercept)	-2.4711	0.0670	-36.906	77	< .0001	-4.179
TrialTOT	-0.1019	0.0114	-8.970	77	< .0001	-1.016
CON_0	0.3643	0.0198	18.412	77	< .0001	2.085
iRTpre	0.0612	0.0040	15.446	77	< .0001	1.749
hS	-0.0104	0.0077	-1.360	77	0.1778	-0.154
vS	0.0121	0.0066	1.828	77	0.0714	0.207
hR	-0.0608	0.0127	-4.784	77	< .0001	-0.542
vR	-0.0758	0.0109	-6.937	77	< .0001	-0.785
LWb	0.0147	0.0130	1.129	77	0.2622	0.128
ISb	-0.0011	0.0148	-0.072	77	0.9430	-0.008
PRSb	-0.0533	0.0128	-4.183	77	0.0001	-0.474
PRb	-0.1513	0.0413	-3.661	77	0.0005	-0.415
CON_0:LWb	0.0658	0.0124	5.299	77	< .0001	0.600
CON_0:ISb	-0.0075	0.0207	-0.363	77	0.7178	-0.041
LWb:ISb	-0.0395	0.0135	-2.922	77	0.0046	-0.331
CON_0:LWb:ISb	0.0578	0.0162	3.580	77	0.0006	0.405

Notes: iRTpre, iRT at the previous trial; hS, horizontal coding of the stimulus position (i.e., the horizontal visual hemispace: right vs left); vS, vertical coding of the stimulus position (i.e., the vertical visual hemispace: upper vs lower); hR, horizontal coding of the response (i.e., the responding hand: right vs left); vR, vertical coding of the response (i.e., the responding finger: middle vs index); CON_0, Congruency (Incongruent trials); DF, degrees of freedom; d_r, effect size computed using the by-participant random slopes.

B.2.4.8. Control analysis, LMM on iRTs, Continuous full model without PRSb

See the "Control analyses" section in the PerifovealAnalysis.m file (the continuous full model without PRSb is coded as "cFullNoPRS" there).

Table B.18. LMM results, continuous full model (cFull), coefficients statistics

Coefficient	*Estimate*	*SE*	*t*	*DF*	*p*	d_s
(Intercept)	-2.4971	0.0448	-55.707	127.56	< .0001	
TrialTOT	-0.1037	0.0034	-30.385	2711.29	< .0001	
CON_0	0.4262	0.0154	27.602	77.94	< .0001	3.127
iRTpre	0.0589	0.0017	35.341	45614.71	< .0001	
hS	-0.0089	0.0039	-2.296	4210.96	0.0217	
vS	0.0116	0.0038	3.054	3699.02	0.0023	
hR	-0.0592	0.0038	-15.746	30903.41	< .0001	
vR	-0.0725	0.0037	-19.537	29178.67	< .0001	
LWb	-0.0045	0.0145	-0.310	78.74	0.7574	
ISb	-0.0486	0.0083	-5.834	77.22	< .0001	
PRb	-0.1709	0.0188	-9.079	40315.52	< .0001	
CON_0:LWb	0.0747	0.0116	6.434	75.90	< .0001	0.739
CON_0:ISb	0.0653	0.0103	6.308	79.15	< .0001	0.709
LWb:ISb	-0.0329	0.0148	-2.221	78.47	0.0293	
CON_0:LWb:ISb	0.0524	0.0203	2.581	77.79	0.0117	0.293

Notes: iRTpre, iRT at the previous trial; hS, horizontal coding of the stimulus position (i.e., the horizontal visual hemispace: right vs left); vS, vertical coding of the stimulus position (i.e., the vertical visual hemispace: upper vs lower); hR, horizontal coding of the response (i.e., the responding hand: right vs left); vR, vertical coding of the response (i.e., the responding finger: middle vs index); CON_0, Congruency (Incongruent trials); DF, degrees of freedom; d_r, effect size computed using the by-participant random slopes.

B.2.4.9. Control analysis, RCA on iRTs, Continuous full model without PRSb

See the "Control analyses" section in the PerifovealAnalysis.m file (the continuous full model without PRSb is coded as "cFullNoPRS" there).

Table B.19. LMM results, continuous full model (cFull), coefficients statistics

Coefficient	*Estimate*	*SE*	*t*	*DF*	*p*	d_r
(Intercept)	-2.4863	0.0670	-37.082	77	< .0001	-4.20
TrialTOT	-0.1042	0.0114	-9.184	77	< .0001	-1.04
CON_0	0.4201	0.0139	30.241	77	< .0001	3.42
iRTpre	0.0617	0.0040	15.448	77	< .0001	1.75
hS	-0.0109	0.0078	-1.392	77	0.1678	-0.16
vS	0.0132	0.0066	1.983	77	0.0509	0.22
hR	-0.0600	0.0128	-4.703	77	< .0001	-0.53
vR	-0.0766	0.0110	-6.959	77	< .0001	-0.79
LWb	0.0108	0.0129	0.839	77	0.4042	0.09
ISb	-0.0473	0.0080	-5.908	77	< .0001	-0.67
PRb	-0.1673	0.0410	-4.083	77	0.0001	-0.46
CON_0:LWb	0.0754	0.0121	6.241	77	< .0001	0.71
CON_0:ISb	0.0648	0.0099	6.515	77	< .0001	0.74
LWb:ISb	-0.0401	0.0133	-3.002	77	0.0036	-0.34
CON_0:LWb:ISb	0.0624	0.0158	3.955	77	0.0002	0.45

Notes: iRTpre, iRT at the previous trial; hS, horizontal coding of the stimulus position (i.e., the horizontal visual hemispace: right vs left); vS, vertical coding of the stimulus position (i.e., the vertical visual hemispace: upper vs lower); hR, horizontal coding of the response (i.e., the responding hand: right vs left); vR, vertical coding of the response (i.e., the responding finger: middle vs index); CON_0, Congruency (Incongruent trials); DF, degrees of freedom; d_s, effect size computed using the Satterthwaite's approximation of degrees of freedom.
P values are computed using the Satterthwaite's approximation of degrees of freedom.

B.2.4.10. Internal reliability

See the "Split-half reliability" section in the PerifovealAnalysis.m file.

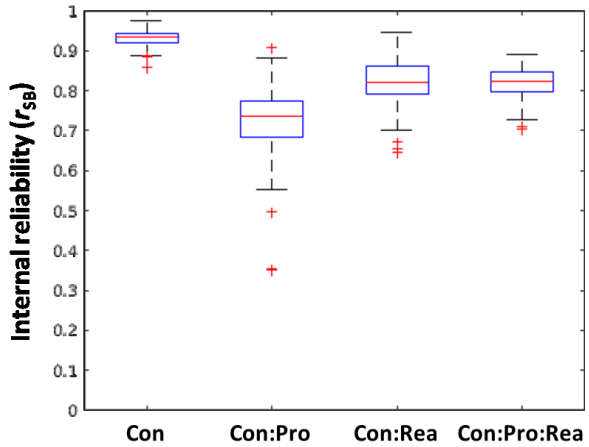

Figure B.18. Internal reliability of the Stroop effect and its modulations estimated by the LMM. The boxplots shows the distribution of the internal reliability estimates (r_{sb}) of the Stroop effect (Con) and its modulation by the Proactive (Con:Pro) and Reactive control (Con:Rea) and the interaction between them (Con:Pro:Rea), as estimated by the cFull LMM model. The boxplots represent the median values (red line at the center of the box), interquartile ranges (box), and dispersion outside the extreme quartiles (whiskers indicating 1.5 times the interquartile range).

B.3. Between-experiments analysis

B.3.1. Distributional analysis

See the "Distributional analysis" section in the BtwExpAnalysis.m file

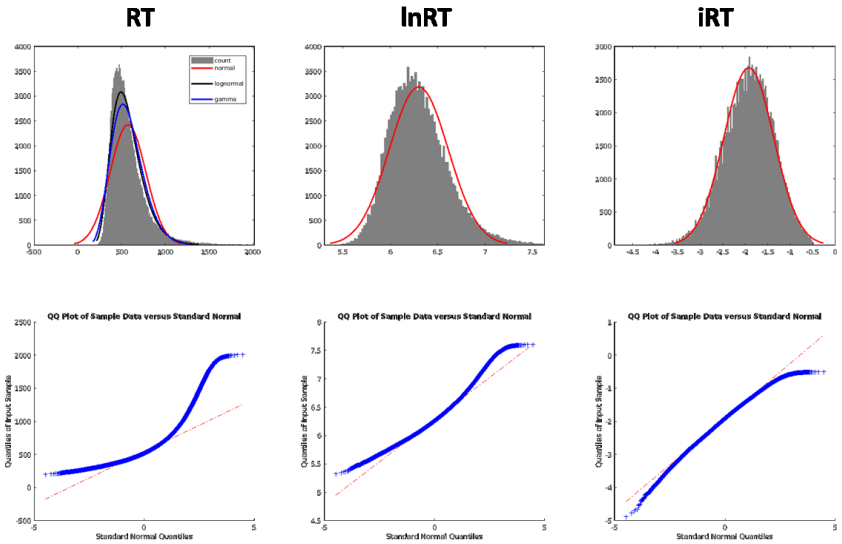

Figure B.19. Distributional analysis of participants' response times.
The top row shows the histograms of untransformed RT values (left panel), natural log-transformed RTs (lnRT, middle panel), and inverse-transformed RTs (iRT, right panel), computed as -1000/RT. The superimposed red curves represent the normal density function fitted to the data. The black and blue curves for the RT distribution represent the lognormal and gamma density functions fitted to the data, respectively. The number of bins was determined using the Freedman-Diaconis rule as implemented in the Matlab *histcounts* function. The bottom row shows the corresponding Q-Q plots.

B.3.2. Compliance checking

See the "Check for SS compliance" section in the BtwExpAnalysis.m file

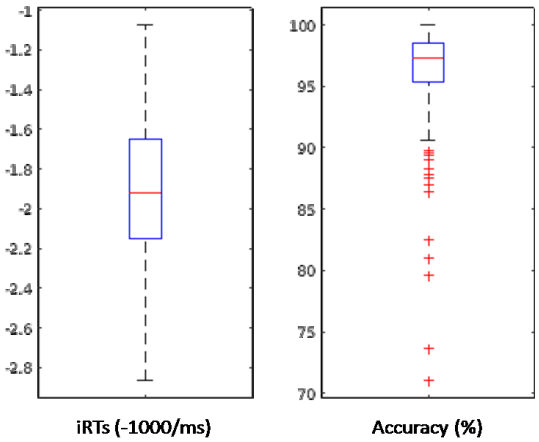

Figure B.20. Participants' overall performance.
The Figure shows the distribution of the participants' mean iRTs (left panel) and accuracy (right panel). The boxplots represent the median values (red line at the center of the box), interquartile ranges (box), and dispersion outside the extreme quartiles (whiskers indicating 1.5 times the interquartile range).

B.3.3. Results

B.3.3.1. LMM on iRTs, Continuous full_btw4 model

See the "LMM" section in the BtwExpAnalysis.m file (the continuous full_btw4 model is coded as "cFull4" there).

Table B.20. LMM results, continuous full_btw4 model (cFull4), coefficients statistics

Coefficient	*Estimate*	*SE*	*t*	*DF*	*p*	d_s	d_r
(Intercept)	-2.2047	0.0278	-79.283	273.83	< .0001		
TrialTOT	-0.0967	0.0020	-48.617	5495.30	< .0001		
CON_0	0.3622	0.0105	34.584	313.90	< .0001	1.952	3.326
iRTpre	0.0569	0.0010	58.197	102922.32	< .0001		
hS	-0.0103	0.0023	-4.427	17405.20	< .0001		
vS	-0.0331	0.0023	-14.489	20722.45	< .0001		
hR	-0.0463	0.0022	-20.993	72277.05	< .0001		
vR	-0.0899	0.0022	-41.515	74407.23	< .0001		
LWb	-0.0050	0.0087	-0.575	176.33	0.5663		
ISb	-0.0074	0.0064	-1.152	663.76	0.2498		
PRSb	-0.0363	0.0050	-7.263	91171.13	< .0001		
PRb	-0.1335	0.0111	-11.974	92379.92	< .0001		
CON_0:LWb	0.0654	0.0069	9.459	177.88	< .0001	0.709	1.150
CON_0:ISb	0.0049	0.0089	0.546	1212.21	0.5849	0.016	0.118
LWb:ISb	-0.0230	0.0090	-2.548	176.10	0.0117		
CON_0:LWb:ISb	0.0299	0.0114	2.627	174.35	0.0094	0.199	0.253
Exp	-0.5031	0.0499	-10.084	177.35	< .0001		
hS:Exp	-0.0098	0.0041	-2.382	18495.32	0.0172		
vS:Exp	0.1042	0.0041	25.578	22528.57	< .0001		
PRSb:Exp	-0.0362	0.0099	-3.665	94964.00	0.0002		
CON_0:Exp	0.0148	0.0209	0.708	309.70	0.4792		
LWb:Exp	0.0104	0.0174	0.597	174.50	0.5511		
ISb:Exp	0.0123	0.0128	0.960	650.27	0.3375		
CON_0:LWb:Exp	-0.0058	0.0137	-0.425	170.55	0.6713		
CON_0:ISb:Exp	-0.0223	0.0178	-1.252	1190.82	0.2110		
LWb:ISb:Exp	-0.0224	0.0180	-1.245	175.49	0.2147		
CON_0:LWb:ISb:Exp	0.0322	0.0228	1.415	174.01	0.1588		

Notes: iRTpre, iRT at the previous trial; hS, horizontal coding of the stimulus position (i.e., the horizontal visual hemispace: right vs left); vS, vertical coding of the stimulus position (i.e., the vertical visual hemispace: upper vs lower); hR, horizontal coding of the response (i.e., the responding hand: right vs left); vR, vertical coding of the response (i.e., the responding finger: middle vs index); CON_0, Congruency (Incongruent trials); Exp, Experiment (Exp1, Peripheral, vs Exp 2, Perifoveal); DF, degrees of freedom; d_s, effect size computed using the Satterthwaite's approximation of degrees of freedom; d_r, effect size computed using the by-participant random slopes.
P values are computed using the Satterthwaite's approximation of degrees of freedom.

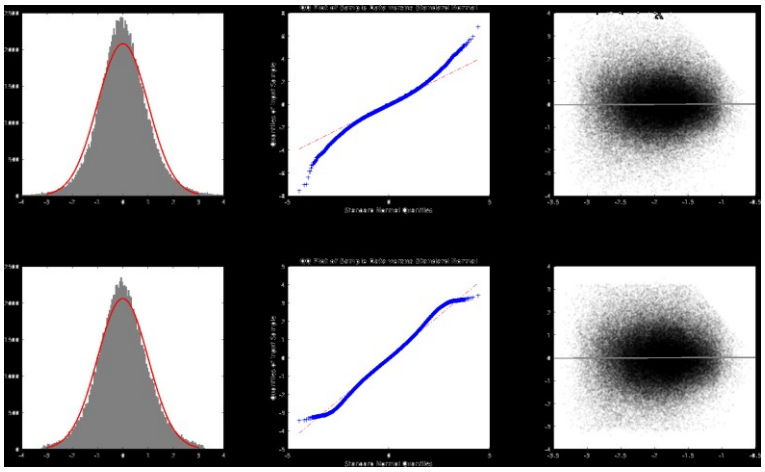

Figure B.21. Inspection of residuals for the LMM analysis on iRTs (cFull_btw4 model).
The Figure shows the results of the analysis of the residuals for the LMM analysis on iRTs for the cFull4 model both before (upper panels) and after (bottom panels) excluding observations with absolute standardized residuals greater than 3. Left: histogram of the standardized residuals; the superimposed red curve represents the normal density function fitted to the data. Middle: quantile-quantile plot for the standardized residuals. Right: scatterplot of the fitted data (x) vs. the standardized residuals (y) for the visual inspection of the homoscedasticity; the gray line represents the corresponding linear regression line.

B.3.3.2. LMM on iRTs, Continuous full_btw model

See the "LMM Model2" section in the BtwExpAnalysis.m file (the continuous full_btw model is coded as "cFull" there).

Table B.21. LMM results, continuous full model (cFull), coefficients statistics

Coefficient	*Estimate*	*SE*	*t*	*DF*	*p*	d_s	d_r
(Intercept)	-2.2029	0.0278	-79.225	273.92	< .0001		
TrialTOT	-0.0967	0.0020	-48.649	5466.32	< .0001		
CON_0	0.3612	0.0105	34.470	311.05	< .0001	1.954	3.283
iRTpre	0.0568	0.0010	58.150	102923.55	< .0001		
hS	-0.0103	0.0023	-4.394	17358.21	< .0001		
vS	-0.0330	0.0023	-14.442	20631.10	< .0001		
hR	-0.0463	0.0022	-21.001	72402.04	< .0001		
vR	-0.0899	0.0022	-41.542	74362.37	< .0001		
LWb	-0.0057	0.0087	-0.653	175.99	0.5144		
ISb	-0.0083	0.0064	-1.291	656.11	0.1972		
PRSb	-0.0356	0.0050	-7.152	91065.10	< .0001		
PRb	-0.1335	0.0111	-11.977	92613.89	< .0001		
CON_0:LWb	0.0658	0.0069	9.590	177.58	< .0001	0.720	1.159
CON_0:ISb	0.0063	0.0089	0.708	1198.54	0.4792	0.020	0.151
LWb:ISb	-0.0214	0.0090	-2.389	175.94	0.0180		
CON_0:LWb:Isb	0.0279	0.0113	2.458	174.02	0.0150	0.186	0.235
Exp	-0.4712	0.0448	-10.523	182.63	< .0001		
hS:Exp	-0.0098	0.0041	-2.376	17548.36	0.0175		
vS:Exp	0.1047	0.0041	25.703	22145.14	< .0001		
PRSb:Exp	-0.0229	0.0053	-4.357	336.10	< .0001		

Notes: iRTpre, iRT at the previous trial; hS, horizontal coding of the stimulus position (i.e., the horizontal visual hemispace: right vs left); vS, vertical coding of the stimulus position (i.e., the vertical visual hemispace: upper vs lower); hR, horizontal coding of the response (i.e., the responding hand: right vs left); vR, vertical coding of the response (i.e., the responding finger: middle vs index); CON_0, Congruency (Incongruent trials); Exp, Experiment (Exp1, Peripheral, vs Exp 2, Perifoveal); DF, degrees of freedom; d_s, effect size computed using the Satterthwaite's approximation of degrees of freedom; d_r, effect size computed using the by-participant random slopes.
P values are computed using the Satterthwaite's approximation of degrees of freedom.

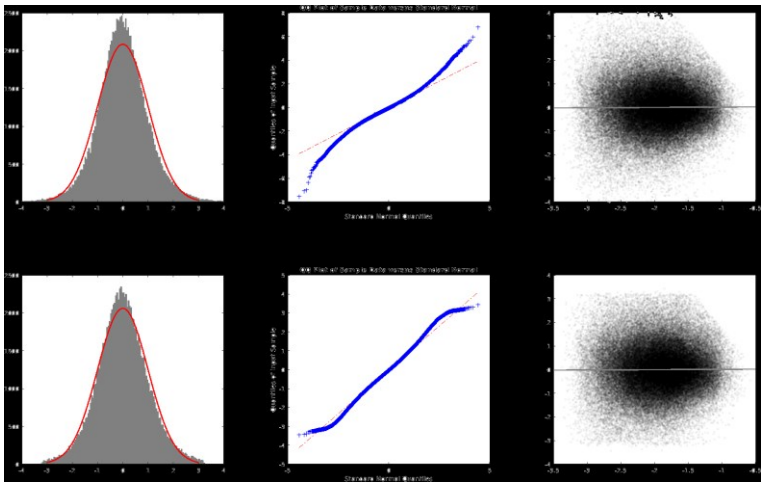

Figure B.22. Inspection of residuals for the LMM analysis on iRTs (cFull_btw model).
The Figure shows the results of the analysis of the residuals for the LMM analysis on iRTs for the cFull model both before (upper panels) and after (bottom panels) excluding observations with absolute standardized residuals greater than 3. Left: histogram of the standardized residuals; the superimposed red curve represents the normal density function fitted to the data. Middle: quantile-quantile plot for the standardized residuals. Right: scatterplot of the fitted data (x) vs. the standardized residuals (y) for the visual inspection of the homoscedasticity; the gray line represents the corresponding linear regression line.

B.3.3.3. RCA on iRTs, Continuous full_btw model

See the "RCA" section in the BtwExpAnalysis.m file (the continuous full_btw model is coded as "cFull" there).

Table B.22. RCA results, continuous full model (cFull), coefficients statistics

Coefficient	*Estimate*	*SE*	*t*	*DF*	*p*	d_r
(Intercept)	-2.1570	0.0463	-46.582	175	< .0001	-3.511
TrialTOT	-0.0946	0.0071	-13.318	175	< .0001	-1.004
CON_0	0.3447	0.0119	28.977	175	< .0001	2.184
iRTpre	0.0586	0.0024	24.654	175	< .0001	1.858
hS	-0.0102	0.0048	-2.151	175	0.0328	-0.162
vS	-0.0388	0.0064	-6.110	175	< .0001	-0.461
hR	-0.0474	0.0068	-6.964	175	< .0001	-0.525
vR	-0.0911	0.0067	-13.664	175	< .0001	-1.030
LWb	-0.0032	0.0085	-0.375	175	0.7080	-0.028
ISb	-0.0020	0.0081	-0.251	175	0.8024	-0.019
PRSb	-0.0424	0.0074	-5.728	175	< .0001	-0.432
PRb	-0.1223	0.0261	-4.693	175	< .0001	-0.354
CON_0:LWb	0.0660	0.0070	9.448	175	< .0001	0.712
CON_0:ISb	-0.0027	0.0116	-0.235	175	0.8147	-0.018
LWb:ISb	-0.0378	0.0081	-4.652	175	< .0001	-0.351
CON_0:LWb:Isb	0.0482	0.0097	4.964	175	< .0001	0.374

Notes: iRTpre, iRT at the previous trial; hS, horizontal coding of the stimulus position (i.e., the horizontal visual hemispace: right vs left); vS, vertical coding of the stimulus position (i.e., the vertical visual hemispace: upper vs lower); hR, horizontal coding of the response (i.e., the responding hand: right vs left); vR, vertical coding of the response (i.e., the responding finger: middle vs index); CON_0, Congruency (Incongruent trials); DF, degrees of freedom; d_r, effect size computed using the by-participant random slopes.

Table B.23. RCA results, continuous full model (cFull), between-Experiment comparisons (Exp1 vs Exp2)

Effect	*M*	*SD*	*t(174)*	*p*	*d*
CON_0	-0.0352	0.1573	-1.474	0.1422	-0.224
CON_0:LWb	0.0006	0.1858	0.020	0.9837	0.003
CON_0:ISb	0.0172	0.3096	0.365	0.7154	0.055
CON_0:LWb:Isb	-0.0693	0.5156	-0.885	0.3772	-0.134

Notes: CON_0, Congruency (Incongruent trials); d, Cohen's d effect size.

B.3.3.4. LMM on iRTs, Continuous full_btw No_PRS model

See the "Control analyses" section in the BtwExpAnalysis.m file (the continuous full_btw No_PRS model is coded as "cFullNoPRS" there).

Table B.24. LMM results, continuous full model without PRS (cFullNoPRS), coefficients statistics

Coefficient	*Estimate*	*SE*	*t*	*DF*	*p*	d_s	d_r
(Intercept)	-2.2029	0.0278	-79.225	273.92	< .0001		
TrialTOT	-0.0967	0.0020	-48.649	5466.32	< .0001		
CON_0	0.3612	0.0105	34.470	311.05	< .0001	1.954	3.283
iRTpre	0.0568	0.0010	58.150	102923.55	< .0001		
hS	-0.0103	0.0023	-4.394	17358.21	< .0001		
vS	-0.0330	0.0023	-14.442	20631.10	< .0001		
hR	-0.0463	0.0022	-21.001	72402.04	< .0001		
vR	-0.0899	0.0022	-41.542	74362.37	< .0001		
LWb	-0.0057	0.0087	-0.653	175.99	0.5144		
ISb	-0.0083	0.0064	-1.291	656.11	0.1972		
PRb	-0.1335	0.0111	-11.977	92613.89	< .0001		
CON_0:LWb	0.0658	0.0069	9.590	177.58	< .0001	0.720	1.159
CON_0:ISb	0.0063	0.0089	0.708	1198.54	0.4792	0.020	0.151
LWb:ISb	-0.0214	0.0090	-2.389	175.94	0.0180		
CON_0:LWb:Isb	0.0279	0.0113	2.458	174.02	0.0150	0.186	0.235
Exp	-0.4712	0.0448	-10.523	182.63	< .0001		
hS:Exp	-0.0098	0.0041	-2.376	17548.36	0.0175		
vS:Exp	0.1047	0.0041	25.692	21931.87	< .0001		

Notes: iRTpre, iRT at the previous trial; hS, horizontal coding of the stimulus position (i.e., the horizontal visual hemispace: right vs left); vS, vertical coding of the stimulus position (i.e., the vertical visual hemispace: upper vs lower); hR, horizontal coding of the response (i.e., the responding hand: right vs left); vR, vertical coding of the response (i.e., the responding finger: middle vs index); CON_0, Congruency (Incongruent trials); Exp, Experiment (Exp1, Peripheral, vs Exp 2, Perifoveal); DF, degrees of freedom; d_s, effect size computed using the Satterthwaite's approximation of degrees of freedom; d_r, effect size computed using the by-participant random slopes.
P values are computed using the Satterthwaite's approximation of degrees of freedom.

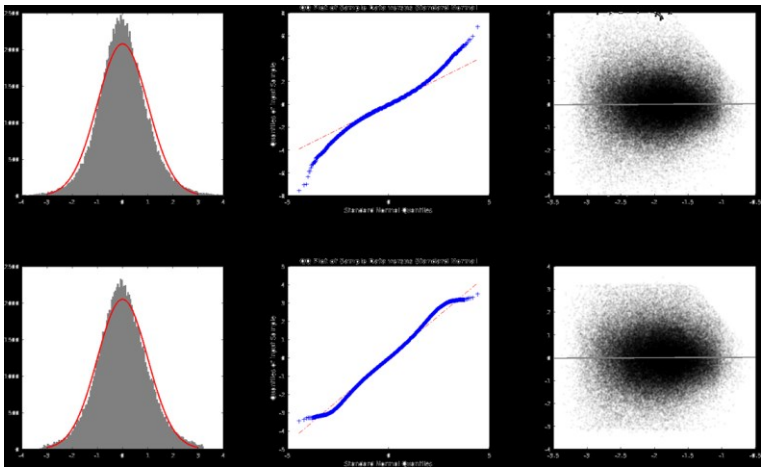

Figure B.22. Inspection of residuals for the LMM analysis on iRTs (cFull_btw No_PRS model).
The Figure shows the results of the analysis of the residuals for the LMM analysis on iRTs for the cFullNoPRS model both before (upper panels) and after (bottom panels) excluding observations with absolute standardized residuals greater than 3. Left: histogram of the standardized residuals; the superimposed red curve represents the normal density function fitted to the data. Middle: quantile-quantile plot for the standardized residuals. Right: scatterplot of the fitted data (x) vs. the standardized residuals (y) for the visual inspection of the homoscedasticity; the gray line represents the corresponding linear regression line.

B.3.3.5. RCA on iRTs, Continuous full_btw No_PRS model

See the "RCA" section in the BtwExpAnalysis.m file (the continuous full_btw No_PRS model is coded as "cFullNoPRS" there).

Table B.25. RCA results, continuous full model without PRS (cFullNoPRS), coefficients statistics

Coefficient	*Estimate*	*SE*	*t*	*DF*	*p*	d_r
(Intercept)	-2.1673	0.0465	-46.573	175	0.0000	-3.511
TrialTOT	-0.0965	0.0071	-13.594	175	0.0000	-1.025
CON_0	0.3890	0.0090	43.392	175	0.0000	3.271
iRTpre	0.0590	0.0024	24.721	175	0.0000	1.863
hS	-0.0107	0.0048	-2.235	175	0.0267	-0.168
vS	-0.0384	0.0063	-6.052	175	0.0000	-0.456
hR	-0.0469	0.0068	-6.896	175	0.0000	-0.520
vR	-0.0915	0.0067	-13.754	175	0.0000	-1.037
LWb	-0.0059	0.0085	-0.701	175	0.4845	-0.053
ISb	-0.0393	0.0045	-8.810	175	0.0000	-0.664
PRb	-0.1339	0.0259	-5.163	175	0.0000	-0.389
CON_0:LWb	0.0729	0.0068	10.760	175	0.0000	0.811
CON_0:ISb	0.0553	0.0055	10.055	175	0.0000	0.758
LWb:ISb	-0.0389	0.0080	-4.855	175	0.0000	-0.366
CON_0:LWb:Isb	0.0524	0.0094	5.553	175	0.0000	0.419

Notes: iRTpre, iRT at the previous trial; hS, horizontal coding of the stimulus position (i.e., the horizontal visual hemispace: right vs left); vS, vertical coding of the stimulus position (i.e., the vertical visual hemispace: upper vs lower); hR, horizontal coding of the response (i.e., the responding hand: right vs left); vR, vertical coding of the response (i.e., the responding finger: middle vs index); CON_0, Congruency (Incongruent trials); DF, degrees of freedom; d_r, effect size computed using the by-participant random slopes.